

# **Myofibroblast Differentiation in Human Fetal Membranes**

Thesis submitted for the degree of

**Doctor of Philosophy**

University of Leicester

by

**Penny Clare McParland**

B Med Sci, MB BS

Department of Obstetrics & Gynaecology

University of Leicester

December 2002

UMI Number: U170461

All rights reserved

INFORMATION TO ALL USERS

The quality of this reproduction is dependent upon the quality of the copy submitted.

In the unlikely event that the author did not send a complete manuscript and there are missing pages, these will be noted. Also, if material had to be removed, a note will indicate the deletion.



UMI U170461

Published by ProQuest LLC 2013. Copyright in the Dissertation held by the Author.  
Microform Edition © ProQuest LLC.

All rights reserved. This work is protected against  
unauthorized copying under Title 17, United States Code.



ProQuest LLC  
789 East Eisenhower Parkway  
P.O. Box 1346  
Ann Arbor, MI 48106-1346

## **Acknowledgments**

This research was carried out in the Department of Obstetrics & Gynaecology, University of Leicester, whilst employed as a Clinical Research Fellow, between 1996-2000. It was generously supported by grants from WellBeing, during the period from December 1996 to December 1997, and the Tommy's Campaign from September 1998 to August 2000.

I would like to acknowledge the invaluable help and support of my supervisors Professor Stephen Bell and Dr Howard Pringle, and of the Head of the Department of Obstetrics & Gynaecology, Professor David Taylor. I would also like to thank present and former colleagues Dr Tony Taylor and Dr John McLaren for their scientific advice and moral support. I am grateful for the expert technical assistance provided by Susan Spurling, Jill Ashmore, Balu Webb and Reshma Bharkhada of the Department of Obstetrics & Gynaecology, and for the technical advice of Angie Gillies of the Department of Pathology. I would like to thank Stephanie Moutrey, Zoe Wilson and Lisa Boulton for secretarial support, and in particular Lisa for her assistance with the preparation of this thesis. I would also like to thank the staff of the Directorate of Womens and Perinatal Health in the UHL Trust for their invaluable assistance during my research.

Finally I would like to thank my family for all their help, and Steve for his continuous encouragement, support and patience, without which this work would not have been possible.

# **Myofibroblast differentiation in human fetal membranes**

**Penny Clare McParland**

## **Abstract**

The occurrence of fetal membrane rupture is a key event in the process of parturition, and may be the initiator of labour at term and preterm. The structural integrity of the fetal membrane sac is therefore vital for the successful maintenance of pregnancy. Previous evidence suggested the presence of a region of altered fetal membrane morphology within the rupture line following term labour and delivery, which if present prior to the onset of labour may represent a region of structural weakness, predisposing the fetal membranes at that site to subsequent rupture.

This study has demonstrated the presence of extreme altered morphology in a restricted region of the fetal membranes overlying the cervix prior to, and during, labour at term. This was associated with myofibroblast differentiation as evidenced by expression of  $\alpha$ -smooth muscle actin. It was also associated with expression of the matricellular proteins tenascin-C and osteonectin within the connective tissue layer of the chorion, the reticular layer.

The expression of  $\alpha$ -smooth muscle actin, tenascin-C and osteonectin in the reticular layer was stimulated *in vitro* by either removal of the cellular layers of the fetal membrane, or by addition of TGF- $\beta_1$ . The differentiated myofibroblast phenotype, restricted in its expression within the gestation sac at term, was detected throughout the gestation sac in the first and second trimesters. At this stage of pregnancy it was associated with expression of osteonectin, but not of tenascin-C.

It is proposed that myofibroblast differentiation within the fetal membrane sac, and the associated expression of matricellular proteins, is required for the remodelling of the extracellular matrix of the fetal membranes in order to accommodate the growing fetus. The temporal and regional patterns of myofibroblast differentiation, and its property of contractility, suggests that it plays a key role in protecting the unsupported fetal membrane from untimely rupture.

## Table of Contents

<b>List of Figures</b> .....	<b>i</b>
<b>List of Tables</b> .....	<b>iv</b>
<b>Abbreviations</b> .....	<b>v</b>
<b>Chapter 1 General Introduction</b> .....	<b>1</b>
1.1. Parturition and fetal membrane rupture .....	1
1.1.1. Parturition.....	1
1.1.2. Term parturition .....	2
1.1.3. Preterm parturition .....	2
1.2. Development and structure of the fetal membranes.....	5
1.2.1. Embryological origin and development of the fetal membranes .....	5
1.2.2. Structure of the fetal membranes.....	8
1.2.2.1. Amniotic epithelium .....	8
1.2.2.2. Amniotic basement membrane .....	11
1.2.2.3. Compact layer.....	11
1.2.2.4. Fibroblast layer .....	11
1.2.2.5. Spongy layer .....	12
1.2.2.6. Cellular layer .....	12
1.2.2.7. Reticular layer.....	12
1.2.2.8. Pseudobasement membrane.....	13
1.2.2.9. Cytotrophoblast layer .....	14
1.2.2.10. Decidua.....	15
1.3. Fetal membrane behaviour and properties .....	15
1.3.1. Biophysical properties of the fetal membranes .....	15
1.3.2. Biochemical properties of the fetal membranes.....	17
1.3.3. The endocrine functions of the fetal membranes .....	18
1.4. Physiological fetal membrane rupture .....	19
1.4.1. Labour associated.....	20
1.4.2. Pre-labour .....	21
1.5. The 'Wound Response' Hypothesis.....	23
1.5.1. The 'wound response' hypothesis as a mechanism for fetal membrane rupture .....	23
1.5.2. The myofibroblast .....	24
1.5.2.1. Myofibroblast ultrastructure .....	25
1.5.2.2. Intermediate filament phenotype .....	25
1.5.2.3. Myofibroblast function.....	26
1.6. Plan of the current investigation .....	28
1.6.1. Aim.....	28
1.6.2. Objectives.....	28
<b>Chapter 2 Materials and Methods</b> .....	<b>29</b>
2.1. Tissue collection .....	29
2.1.1. Term fetal membranes.....	29
2.1.1.1. Patient groups .....	29
2.1.1.2. Sampling technique .....	30
2.1.1.3 Fetal membrane 'maps' .....	30
2.1.1.4. Dissected fetal membranes .....	31
2.1.2. Preterm fetal membranes.....	31
2.1.3. First and second trimester fetal membranes.....	31
2.1.4. First trimester decidua.....	34

2.2. Tissue processing and preparation of sections.....	34
2.2.1. Paraffin-embedded tissue sections.....	34
2.2.2. Cryostat tissue sections.....	34
2.2.3. Haematoxylin and eosin staining.....	34
2.2.4. Diagnosis of histological chorioamnionitis.....	35
2.3. Immunohistochemistry.....	35
2.3.1. Antibodies.....	35
2.3.2. Single labelling immunohistochemistry technique.....	35
2.3.3. Controls.....	37
2.3.4. Modifications of the immunohistochemistry technique.....	38
2.3.4.1. Pepsin digestion.....	38
2.3.4.2. Microwave pre-treatment.....	38
2.3.4.3. Cryostat tissue sections.....	38
2.3.4.4. Osteonectin monoclonal antibody N50.....	38
2.3.5. Standardisation of technique for quantification.....	39
2.4. Western blotting.....	39
2.4.1. Tissue homogenisation.....	39
2.4.2. Bradford assay.....	39
2.4.3. SDS-PAGE.....	40
2.4.4. Western blotting.....	41
2.4.5. Immunodetection.....	41
2.4.6. Standardisation of technique for quantification.....	43
2.4.7. Analysis of blots.....	43
2.5. Reverse Transcriptase - Polymerase Chain Reaction.....	43
2.5.1. Tissue homogenisation.....	43
2.5.2. RNA extraction.....	44
2.5.3. Primer design.....	46
2.5.4. Reverse transcriptase reaction.....	48
2.5.5. Polymerase chain reaction.....	48
2.5.6. Agarose gel electrophoresis.....	48
2.5.7. DNase treatment of RNA.....	50
2.5.8. Standardisation of technique for quantification.....	50
2.6. <i>In situ</i> hybridisation.....	52
2.6.1. Cell culture.....	52
2.6.2. mRNA extraction from cells.....	52
2.6.3. PCR production of template.....	53
2.6.4. Labelling of <i>in situ</i> hybridisation probes.....	53
2.6.4.1. Asymmetric PCR.....	53
2.6.4.2. Testing of <i>in situ</i> hybridisation probes.....	54
2.6.5. <i>In situ</i> hybridisation.....	54
2.7. Organ culture.....	57
2.7.1. Fetal membrane biopsy technique.....	57
2.7.2. Fetal membrane culture.....	57
2.7.2.1. Culture media.....	57
2.7.2.2. Culture technique.....	58
2.7.2.3. Additives.....	58
2.8. Image analysis.....	58
2.8.1. Histological and immunohistochemical image analysis.....	58
2.8.1.1. Morphology measurements.....	60
2.8.1.2. Cell counting.....	60
2.8.1.3. Quantification of extracellular matrix staining.....	61
2.8.2. Analysis of Western blots.....	61

2.9. Statistical analysis.....	61
<b>Chapter 3 Cellular populations of the connective tissue layers.....</b>	<b>63</b>
3.1. Introduction.....	63
3.2. Aims.....	64
3.3. Materials and Methods.....	64
3.3.1. Fetal membrane samples.....	64
3.3.2. Immunohistochemistry.....	65
3.3.3. SDS-PAGE and Western blotting.....	65
3.3.4. Image analysis.....	65
3.3.5. RT-PCR.....	65
3.3.6. Statistical analysis.....	65
3.4. Results.....	66
3.4.1. Fetal membrane morphology.....	66
3.4.2. Cellular phenotyping.....	69
3.4.2.1. Vimentin.....	69
3.4.2.2. Desmin.....	69
3.4.2.3. $\alpha$ -smooth muscle actin.....	69
3.4.2.4. $\gamma$ -smooth muscle actin.....	74
3.4.2.5. Smooth muscle myosin.....	80
3.4.2.6. CD68.....	80
3.4.2.7. Cellular phenotypes.....	80
3.4.3. Regional differences in cellular phenotype.....	86
3.4.3.1. Total cell count.....	86
3.4.3.2. 'VD' cells.....	86
3.4.3.3. 'VDA' and 'VA' cells.....	86
3.4.3.4. 'VDAG' cells.....	89
3.4.4. Macrophages.....	92
3.4.5. Cellular proportions.....	92
3.4.6. Relationship between cellular phenotype and fetal membrane morphology.....	98
3.5. Discussion.....	98
3.6. Conclusions.....	102
<b>Chapter 4 Mapping of morphological changes and myofibroblast differentiation in fetal membranes prior to the onset of labour.....</b>	<b>104</b>
4.1. Introduction.....	104
4.2. Aims.....	105
4.3. Materials and Methods.....	105
4.3.1. Tissue samples.....	105
4.3.2. Immunohistochemistry.....	106
4.3.3. Image analysis.....	106
4.3.4. Statistical analysis.....	106
4.4. Results.....	106
4.4.1. Fetal membrane morphology.....	106
4.4.2. 'Mucus-associated' fetal membrane morphology.....	115
4.4.2. $\alpha$ -sma expression.....	119
4.4.2.1. Chorion.....	119
4.4.2.2. Amnion.....	126
4.5. Discussion.....	126
4.6. Conclusions.....	132

<b>Chapter 5 Tenascin-C expression in human fetal membranes.....</b>	<b>134</b>
5.1. Introduction.....	134
5.1.1. Tenascin-C structure.....	134
5.1.2. Tenascin-C function.....	134
5.1.3. Alternative splicing of tenascin-C.....	136
5.1.4. Tenascin-C in pregnancy.....	136
5.2. Aims.....	137
5.3. Materials and Methods.....	138
5.3.1. Tissue samples.....	138
5.3.2. Immunohistochemistry.....	138
5.3.3. SDS-PAGE and Western blotting.....	138
5.3.4. RT-PCR.....	138
5.3.5. <i>In situ</i> hybridisation.....	139
5.3.6. Image analysis.....	139
5.3.7. Statistical analysis.....	139
5.4. Results.....	139
5.4.1. Tenascin-C protein expression.....	139
5.4.1.1. Tenascin-C immunolocalisation.....	139
5.4.1.2. Regional differences in tenascin-C immunolocalisation.....	141
5.4.1.3. Relationship to $\alpha$ -sma expression.....	146
5.4.1.4. Tenascin-C immunoreactivity on a fetal membrane map.....	149
5.4.1.5. Characterisation of tenascin-C protein.....	149
5.4.1.6. Regional differences in levels of extracted tenascin-C.....	149
5.4.2. Tenascin-C mRNA expression.....	153
5.4.2.1. Localisation and distribution of mRNA positive cells.....	153
5.4.2.2. Tenascin-C mRNA quantification.....	160
5.4.2.3. Tenascin-C mRNA isoforms.....	160
5.5. Discussion.....	165
5.6. Conclusions.....	170
<b>Chapter 6 Osteonectin expression in human fetal membranes.....</b>	<b>172</b>
6.1. Introduction.....	172
6.1.1. Osteonectin protein.....	172
6.1.2. Expression and function of osteonectin.....	173
6.2. Aims.....	174
6.3. Materials and Methods.....	174
6.3.1. Tissue samples.....	174
6.3.2. Immunohistochemistry.....	174
6.3.3. SDS-PAGE and Western blotting.....	175
6.3.4. RT-PCR.....	175
6.3.5. <i>In situ</i> hybridisation.....	175
6.3.6. Image analysis.....	175
6.3.7. Statistical analysis.....	176
6.4. Results.....	176
6.4.1. Osteonectin protein expression.....	176
6.4.1.1. Osteonectin immunolocalisation.....	176
6.4.1.2. Regional differences in immunoreactive cell numbers.....	181
6.4.1.3. Relationship to $\alpha$ -SMA expression.....	186
6.4.1.4. Osteonectin immunoreactivity on a fetal membrane map.....	188
6.4.1.5. Relationship to tenascin-C expression.....	188
6.4.1.6. Characterisation of osteonectin protein in fetal membranes.....	191
6.4.1.7. Regional differences in extracted osteonectin by Western blotting.....	191

6.4.2. Osteonectin mRNA expression .....	191
6.4.2.1. Localisation and distribution of mRNA positive cells .....	191
6.4.2.2. Regional differences in mRNA expression .....	198
6.4.2.3. Quantification of mRNA by RT-PCR .....	198
6.5. Discussion .....	198
6.6. Conclusions .....	204

**Chapter 7 Induction of myofibroblast differentiation, osteonectin and tenascin expression in an organ culture model .....206**

7.1. Introduction .....	206
7.1.1. Regulation of $\alpha$ -sma expression .....	206
7.1.2. Regulation of tenascin-C expression .....	207
7.1.3. Regulation of osteonectin expression .....	207
7.1.4. Fetal membrane organ culture model .....	207
7.2. Aims .....	209
7.3. Materials and Methods .....	209
7.3.1. Fetal membrane samples .....	209
7.3.2. Organ culture .....	209
7.3.3. Immunohistochemistry .....	209
7.3.4. Image analysis .....	209
7.3.5. Statistical analysis .....	210
7.4. Results .....	210
7.4.1. Behaviour of fetal membrane discs in culture .....	210
7.4.2. Effects of fetal bovine serum .....	214
7.4.2. Hypoxia .....	217
7.4.3. Removal of decidual layer .....	217
7.4.4. Removal of decidual and cytotrophoblast layers .....	217
7.4.5. 'Edge' effects .....	222
7.4.6. Addition of cytokines/additives .....	222
7.4.6.1. Response to TGF- $\beta_1$ in culture .....	226
7.4.6.2. Time course of TGF- $\beta_1$ response .....	229
7.4.6.3. Dose-response for TGF- $\beta_1$ .....	229
7.5. Discussion .....	229
7.6. Conclusions .....	232

**Chapter 8 Myofibroblast differentiation, osteonectin and tenascin expression during fetal membrane development .....233**

8.1. Introduction .....	233
8.2. Aims .....	233
8.3. Materials and Methods .....	234
8.3.1. Tissue samples .....	234
8.3.2. Immunohistochemistry .....	234
8.3.3. <i>In situ</i> hybridisation .....	234
8.3.4. Image analysis .....	234
8.3.5. Statistical analysis .....	234
8.4. Results .....	234
8.4.1. Fetal membrane morphology .....	234
8.4.2. Fetal membrane cellularity .....	239
8.4.3. Cellular phenotype .....	242
8.4.3.1. Amnion .....	242
8.4.3.2. Chorion .....	246
8.5. Discussion .....	256
8.6. Conclusions .....	260

<b>Chapter 9 General Discussion.....</b>	<b>261</b>
9.1. The Zone of Altered Morphology and its generation .....	261
9.1.1. Appearance prior to labour.....	261
9.1.2. Connective tissue layers .....	263
9.1.3. Generation of extreme altered morphology .....	265
9.2. Myofibroblast phenotype in term fetal membranes .....	266
9.2.1. What is a myofibroblast?.....	267
9.2.2. Ultrastructural features of fetal membrane fibroblasts/myofibroblasts.....	268
9.2.3. Intermediate filament phenotype of fetal membrane myofibroblasts .....	270
9.3. Functions of differentiated myofibroblasts in the fetal membranes at term .....	273
9.3.1. Contractility .....	273
9.3.2. Secretion of matricellular proteins .....	274
9.3.3. Matrix degradation .....	275
9.3.4. Matrix synthesis .....	276
9.4. Myofibroblast differentiation during gestation.....	276
9.5. Myofibroblast function during gestation .....	280
9.6. Regulation of myofibroblast differentiation in the fetal membranes.....	284
9.6.1. Regulation of myofibroblast differentiation.....	284
9.6.2. Regulation of tenascin-C expression.....	289
9.6.3. Regulation of osteonectin expression.....	289
9.6.4. TGF- $\beta_1$ in the fetal membranes .....	290
9.6.5. Integrated model of myofibroblast differentiation in the fetal membranes....	291
9.7. Myofibroblast differentiation and fetal membrane rupture.....	293
9.8. Future research.....	294
<b>Appendix Publications arising from this thesis.....</b>	<b>296</b>
<b>References.....</b>	<b>298</b>

#### **Addenda**

1. Reprint of paper: McParland P. C., D. J. Taylor and S. C. Bell (2000). Placenta 21: 44-53
2. Reprint of paper: McParland P. C., S. C. Bell, J. H. Pringle and D. J. Taylor (2001). Molecular Human Reproduction 5: 463-474

# List of Figures

## Chapter 1

Figure 1.1.....	3
1.2.....	4
1.3.....	7
1.4.....	9
1.5.....	10

## Chapter 2

Figure 2.1.....	32
2.2.....	33
2.3.....	45
2.4.....	51
2.5.....	55

## Chapter 3

Figure 3.1.....	67
3.2.....	71
3.3.....	72
3.4.....	73
3.5.....	75
3.6.....	76
3.7.....	77
3.8.....	78
3.9.....	79
3.10.....	81
3.11.....	82
3.12.....	83
3.13.....	84
3.14.....	85
3.15.....	90
3.16.....	91
3.17.....	93
3.18.....	95
3.19.....	96
3.20.....	97
3.21.....	99

## Chapter 4

Figure 4.1.....	107
4.2.....	110
4.3.....	111
4.4.....	112
4.5.....	113
4.6.....	117
4.7.....	118
4.8.....	121
4.9.....	122
4.10.....	123
4.11.....	124

4.12.....	125
4.13.....	127
4.14.....	128
4.15.....	130

**Chapter 5**

Figure 5.1.....	135
5.2.....	140
5.3.....	142
5.4.....	144
5.5.....	145
5.6.....	147
5.7.....	148
5.8.....	150
5.9.....	151
5.10.....	152
5.11.....	154
5.12.....	155
5.13.....	159
5.14.....	161
5.15.....	162
5.16.....	163
5.17.....	164
5.18.....	166
5.19.....	167

**Chapter 6**

Figure 6.1.....	177
6.2.....	179
6.3.....	180
6.4.....	182
6.5.....	187
6.6.....	189
6.7.....	190
6.8.....	192
6.9.....	193
6.10.....	194
6.11.....	195
6.12.....	199
6.13.....	200
6.14.....	201
6.15.....	202

**Chapter 7**

Figure 7.1.....	211
7.2.....	212
7.3.....	213
7.4.....	215
7.5.....	216
7.6.....	218
7.7.....	220
7.8.....	221
7.9.....	223

7.10.....	224
7.11.....	225
7.12.....	227
7.13.....	228
7.14.....	230

**Chapter 8**

Figure 8.1.....	236
8.2.....	237
8.3.....	238
8.4.....	240
8.5.....	244
8.6.....	247
8.7.....	250
8.8.....	251
8.9.....	252
8.10.....	253
8.11.....	254
8.12.....	255
8.13.....	257

**Chapter 9**

Figure 9.1.....	264
9.2.....	271
9.3.....	277
9.4.....	279
9.5.....	281
9.6.....	283
9.7.....	286
9.8.....	292

**List of Tables**

Table 2.1..... 36  
2.2..... 42  
2.3..... 47  
2.4..... 49  
2.5..... 59  
3.1..... 68  
3.2..... 70  
3.3..... 70  
3.4..... 87  
3.5..... 88  
3.6..... 94  
4.1..... 114  
4.2..... 116  
4.3..... 120  
6.1..... 184  
6.2..... 185  
8.1..... 241  
8.2..... 243  
8.3..... 245  
8.4..... 248

## Abbreviations

A	$\alpha$ -smooth muscle actin
$\alpha$ -sma	$\alpha$ -smooth muscle actin
AMPS	Ammonium persulphate
BCIP	5-Bromo-4-chloro-3 indolyl phosphate
BPAS	British Pregnancy Advisory Service
BSA	Bovine serum albumin
dH <sub>2</sub> O	Distilled water
CAPS	3-[cyclohexylamino]-1-propane-sulfonic acid
COX	Cyclo-oxygenase
D	Desmin
dATP	Deoxyadenosine triphosphate
dCTP	Deoxycytosine triphosphate
DEPC	Diethylene pyrocarbonate
dGTP	Deoxyguanosine triphosphate
dH <sub>2</sub> O	Distilled water
DMEM	Dulbecco's Modified Eagles Medium
DNA	Deoxyribonucleic acid
DNase	Deoxyribonuclease
dTTP	Deoxythymidine triphosphate
ECL	Enhanced chemiluminescence
EDTA	Ethylenediaminetetra-acetic acid
EGF	Epidermal Growth Factor
EGTA	Ethyleneglycoltetra-acetic acid
EMBL	European Molecular Biology Laboratory
FBS	Fetal bovine serum
FMMI	Fetal membrane morphometric index
Fn-III	Fibronectin type III-like
G	$\gamma$ -smooth muscle actin
$\gamma$ -sma	$\gamma$ -smooth muscle actin
HRP	Horseradish peroxidase
Ig	Immunoglobulin
IMS	Industrial Methylated Spirits
LDH	Lactate dehydrogenase

M	Smooth muscle myosin
MMP	Matrix metalloproteinase
mRNA	Messenger ribonucleic acid
NBT	Nitro blue tetrazolium
NRS	Normal Rabbit Serum
PAGE	Polyacrylamide gel electrophoresis
PAI	Plasminogen activator inhibitor
PBS	Phosphate-buffered saline
PCR	Polymerase chain reaction
PDGH	Prostaglandin dehydrogenase
PMSF	Phenylmethanesulfonyl fluoride
PROM	Pre-labour rupture of the membranes
PPROM	Preterm pre-labour rupture of the membranes
RNA	Ribonucleic acid
RT	Reverse transcriptase
SDS	Sodium dodecyl sulphate
TAE	Tris-acetate EDTA
TBS	Tris-buffered saline
TEMED	N, N, N', N'-Tetramethylethylenediamine
TGF- $\beta_1$	Transforming growth factor- $\beta_1$
TIMP	Tissue inhibitor of metalloproteinase
Tn-C	Tenascin-C
t-PA	Tissue type plasminogen activator
UHL	University Hospitals of Leicester
u-PA	Urokinase type plasminogen activator
UPH <sub>2</sub> O	Ultrapure water
V	Vimentin
ZAM	Zone of Altered Morphology

# **Chapter 1**

## **General Introduction**

### **1.1. Parturition and fetal membrane rupture**

#### **1.1.1. Parturition**

Parturition is the physiological process by which the fetus, placenta, and fetal membranes are expelled from the mother's reproductive tract, and occurs on average at 280 days from the first day of the last menstrual period in the human. Labour is the occurrence of regular involuntary uterine contractions, which result in dilatation of the cervix, and delivery of the fetus, placenta and membranes from the uterus (Moore & Persaud, 1998). Clinically, labour is considered to consist of three stages (Beazley, 1995):

1. During the first stage of labour, regular myometrial contractions lead to dilatation of the cervix.
2. The second stage of labour occurs once full dilatation of the cervix has occurred. The fetus is expelled from the uterus.
3. The placenta and fetal membranes are then expelled from the uterus during the third stage of labour.

Prior to the onset of clinically apparent contractions, a number of processes occur in preparation for the onset of labour. The lower segment of the uterus, derived from the uterine isthmus, develops during the third trimester (Morrison, 1972). Prior to the onset of labour, 'ripening' of the cervix occurs, with clinical detection of effacement, softening, and dilatation, arising from underlying changes in the collagen cross-linking and glycosaminoglycan content of the cervix (Turnbull & Lopez Bernal, 1994). The myometrium remains largely quiescent during pregnancy, with development of irregular uterine activity, Braxton Hicks contractions, predominantly from 32 weeks onwards (Turnbull & Lopez Bernal, 1994). The onset of regular co-ordinate uterine contractions marks the onset of labour.

These processes are considered by Casey & MacDonald to be part of parturition, the onset of which they distinguish from the onset of labour. Phase 0, 'quiescence', extends for the majority of pregnancy. This is followed by a state of 'activation' of the uterus, phase 1, in response to uterotropins, which defines the onset of parturition. Cervical ripening and formation of the lower uterine segment occur at this time. The primed uterus then may undergo 'stimulation', phase 2, with occurrence of uterine contractions, and lastly 'involution' of the uterus following delivery corresponds to phase 3 (Casey & MacDonald, 1993). The relationship between these phases of parturition and the clinical stages of labour is illustrated in **Figure 1.1**.

### **1.1.2. Term parturition**

Term parturition is defined as that occurring between 37 and 42 completed weeks (259 to 294 days) from the first day of the last menstrual period.

The usual fate of the fetal membranes in term labour is to rupture during the first or second stage of labour. In the majority of women in labour at term, the fetal membranes rupture during the latter part of labour, at 9 cm dilatation or greater (**Figure 1.2**) (Romero *et al.*, 1999). In approximately 5-10% of term births, however, the fetal membranes rupture prior to the onset of labour (Duff, 1996); this is termed pre-labour rupture of the fetal membranes (PROM). Over 90% of women will labour within 24 hours of PROM at term (Egan & O'Herlihy, 1988). A latency period of greater than 24 hours following term PROM is associated with an increased risk of the development of intrauterine infection (Duff, 1996). The greater the latency period, the greater the risk of intrauterine infection (Mead, 1980). Thus infection appears to be a consequence rather than a precursor of PROM at term. The timing of membrane rupture at term, either prior to or during labour, therefore appears to be part of a continuum, rather than a pathological process.

### **1.1.3. Preterm parturition**

Preterm parturition is defined as that occurring prior to 37 completed weeks (259 days) from the first day of the last menstrual period (Kaltreider & Kohl, 1980). It occurs in 7-10% of pregnancies, and despite medical advances, rates are increasing (Yan & Yin, 1990; Creasy, 1993). Preterm delivery is responsible for significant neonatal morbidity and mortality, and accounts for 85% of the deaths of normally formed infants (Copper *et al.*, 1993). Preterm deliveries may arise as a consequence of three (approximately equally

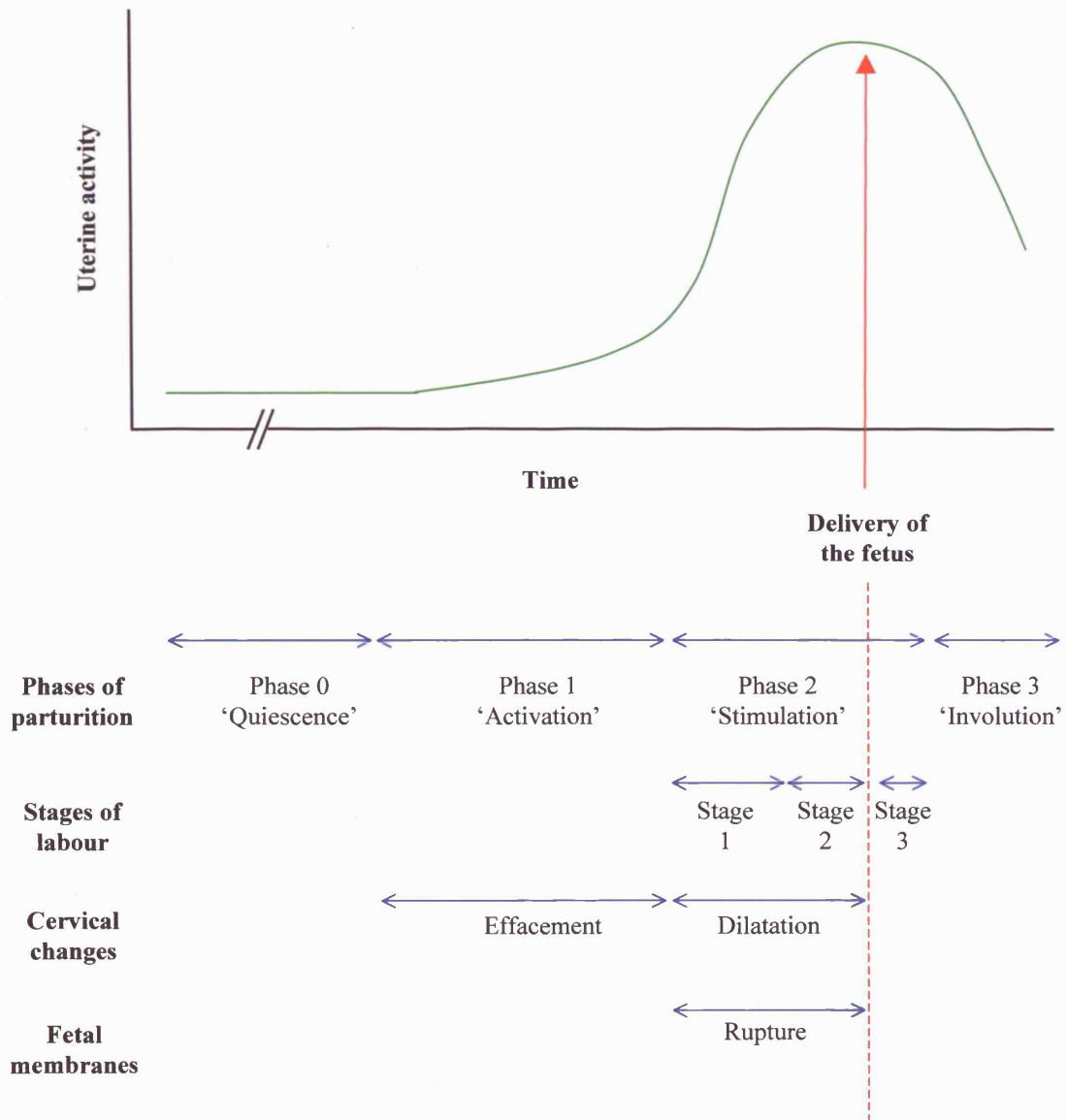


**Figure 1.1.** The relationship between the phases of parturition defined by Casey & MacDonald (1993), the clinically defined stages of labour, the effacement and dilatation of the cervix, and the rupture of the fetal membranes.

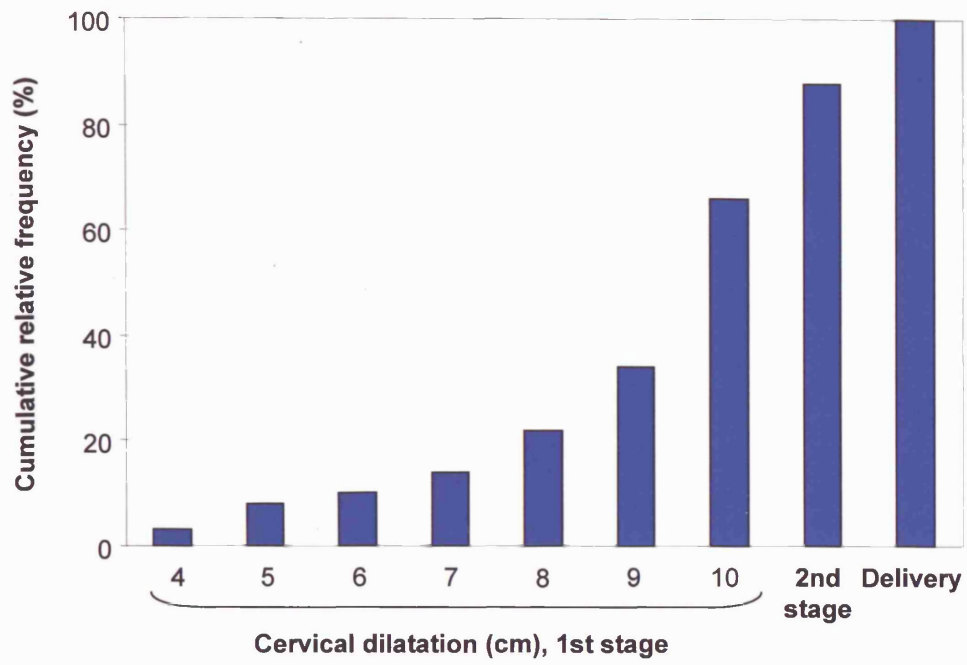


**Figure 1.2.** The cumulative relative frequency at which spontaneous fetal membrane rupture occurred during labour (from 4cm dilatation to delivery). (Drawn from data obtained from Romero *et al*, 1999).

proportioned) precursors (Gomez *et al.*, 1997): medically indicated deliveries; preterm labour; and preterm pre-labour rupture of the membranes (PPROM).

Preterm pre-labour rupture of the fetal membranes occurs in 1-2% of all pregnancies, and precedes approximately 30% of preterm births (Major & Garite, 1997). Although numerous epidemiological and clinical associations with PPRM have been described, multivariate analysis isolates just three significant predictors (Harger *et al.*, 1990): smoking; gestational bleeding; and previous preterm birth. Intrauterine infection has been described as both a precursor and a consequence of PPRM. Approximately 25% of women presenting with PPRM will have positive amniotic fluid cultures at presentation, compared to 75% at the onset of labour at the end of the latency period (Romero *et al.*, 1988). The length of the latency period prior to the onset of labour following PPRM is inversely related to the gestation (Lewis *et al.*, 1992; Savitz *et al.*, 1997).

The occurrence of fetal membrane rupture is a key event in the process of parturition, and may be the initiator of labour at term and preterm. The structural integrity of the fetal membrane sac is therefore vital for the successful maintenance of pregnancy. In order to understand this essential function of the fetal membranes, we need to understand the nature of the tissues of the fetal membranes, and the basis for their inherent strength, and the changes that they undergo during pregnancy.

## **1.2. Development and structure of the fetal membranes**

Embryologically, the true fetal membranes consist of the amnion fused to the chorion laeve. However, immediately following labour and delivery a cleavage plane develops within the decidua parietalis, and thus the 'fetal membranes' expelled following labour and delivery consist of the amniochorion, with an attached layer of decidua parietalis. In order to understand the structure of the membranes, it is first necessary to understand how they have arisen and developed.

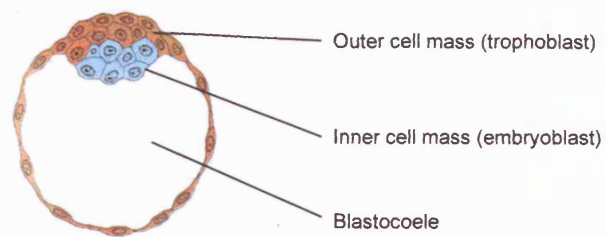
### **1.2.1. Embryological origin and development of the fetal membranes**

Following fertilisation, the human ovum undergoes a series of cell divisions to form a ball of cells, the morula. It is the morula that enters the endometrial cavity approximately three days after fertilisation. The internal cells of the morula (the inner cell mass) will ultimately

give rise to the tissues of the embryo, yolk sac, amnion and connective tissue layer of the chorion (Sadler, 1985; Moore & Persaud, 1998; Benirschke & Kaufmann, 2000) (**Figure 1.3a**). The outer cell mass gives rise to the trophoblast. Following formation of a fluid space (blastocoele), the embryo is known as a blastocyst, and undergoes implantation into the wall of the uterus approximately six days following fertilisation (Sadler, 1985; Moore & Persaud, 1998).

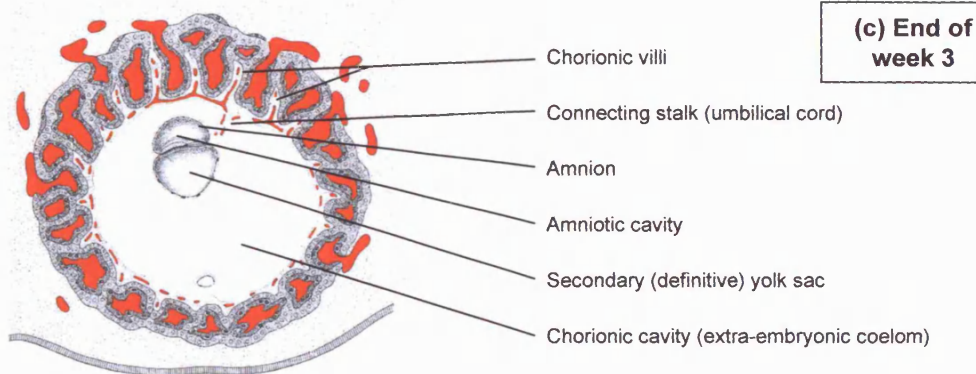
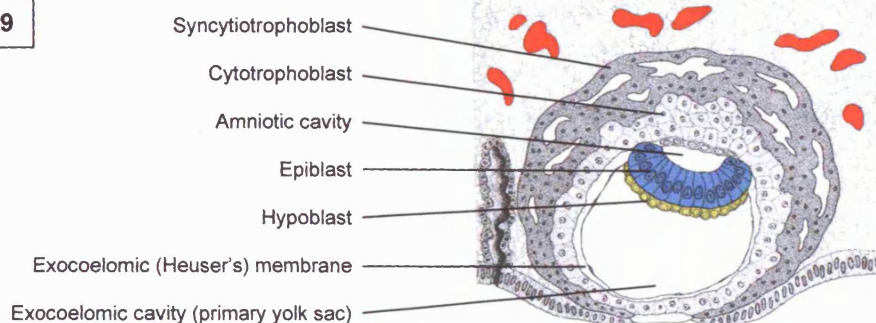
The inner cell mass differentiates into two layers (hypoblast and epiblast) to form the bilaminar germ disc. The amniotic cavity appears as a slit-like cavity either within the epiblast (Sadler, 1985; Moore & Persaud, 1998), or between the epiblast and trophoblast (Bourne, 1962; Schmidt, 1992; Benirschke & Kaufmann, 2000). Thus the amnioblasts which form the membrane (amnion) surrounding the amniotic cavity have been reported to differentiate solely from the epiblast (Sadler, 1985; Schmidt, 1992; Moore & Persaud, 1998), solely from the cytotrophoblast (Bourne, 1962; Benirschke & Kaufmann, 2000), or from both populations of cells (Hoyes, 1975). The inner surface of the cytotrophoblast becomes lined by Heuser's membrane, formed by cells deriving from the hypoblast, and the cavity (formerly the blastocoele) is known as the exocoelomic cavity (or primary yolk sac) (**Figure 1.3b**). Cells derived from the trophoblast then form a loose connective tissue layer (extra-embryonic mesoderm) between the inner surface of the cytotrophoblast and the lining of the exocoelomic cavity. Formation of a fluid cavity within the extra-embryonic mesoderm occurs, forming the extra-embryonic coelom. The primary yolk sac decreases in size, and the smaller secondary yolk sac is formed (Moore & Persaud, 1998).

By thirteen days following fertilisation the bilaminar germ disc, with the amniotic cavity and secondary yolk sac adjacent to the disc, lies within the extra-embryonic coelom (the chorionic cavity) attached by the connecting stalk (extra-embryonic mesoderm) to the surrounding trophoblast shell (Sadler, 1985). As the bilaminar germ disc undergoes gastrulation and forms a trilaminar disc and folds, the amniotic cavity formerly on one side of the disc surrounds the embryo. The connecting stalk becomes the umbilical cord, connecting the embryo to the placenta. The trophoblast shell surrounding the pregnancy implants within the endometrium, and is entirely covered with villi (**Figure 1.3c**). As the pregnancy expands, the chorionic villi on the embryonic pole proliferate, giving rise to the chorion frondosum (the placenta). The villi, and overlying decidua, at the abembryonic pole degenerate, forming the chorion laeve and decidua capsularis (Sadler, 1985; Moore & Persaud, 1998; Benirschke & Kaufmann, 2000) (**Figure 1.3d**).



**(a) Day 4**

**(b) Day 9**



**(c) End of week 3**

**(d) Beginning of 2nd month**

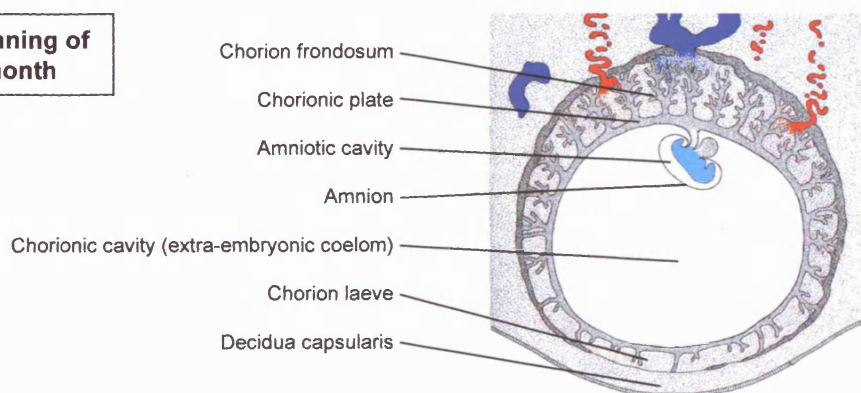


**Figure 1.3.** The development of the fetal membranes, placenta and embryo up to the beginning of the 2nd month after fertilisation. (Redrawn from Sadler (1985), with permission).

As the pregnancy progresses, the amniotic sac enlarges faster than the chorionic sac, the amnion and chorion fuse, and the extra-embryonic coelom is obliterated (**Figure 1.4a&b**). The amnion then covers the surface of the umbilical cord, and the surface of the placenta. This process has been reported to be completed by the twelfth week post-conception (Benirschke & Kaufmann, 2000). The amniochorion, with overlying decidua capsularis, reaches and fuses with the decidua parietalis, reported at 15-20 weeks post-conception (Benirschke & Kaufmann, 2000) and at 22-24 weeks gestation (Moore & Persaud, 1998), thus obliterating the uterine cavity (**Figure 1.4c**). The formation of the chorio-decidual interface of the fetal membranes in mid-pregnancy has been suggested to occur as a process analogous to formation of anchoring villi at placental implantation (Bell & Malak, 1994). This region is rich in onco-fetal fibronectin (Lockwood *et al.*, 1991), which has been suggested to act as a trophoblast 'glue', stabilising the interface (Feinberg *et al.*, 1991).

Thus the amniotic epithelium is derived from the trophoblast (outer cell mass), epiblast (from the inner cell mass) or both. The underlying amniotic connective tissue layers from the extra-embryonic mesoderm (derived from the hypoblast from the inner cell mass), the spongy layer from the obliteration of the extra-embryonic coelom, and the connective tissue layer of the chorion from the extra-embryonic mesoderm.

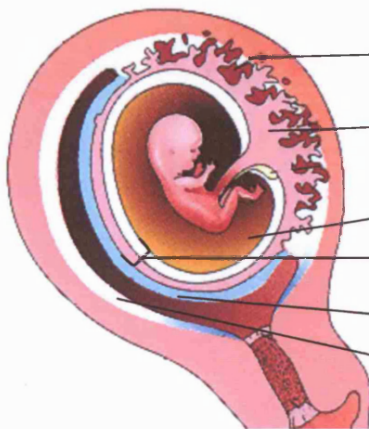
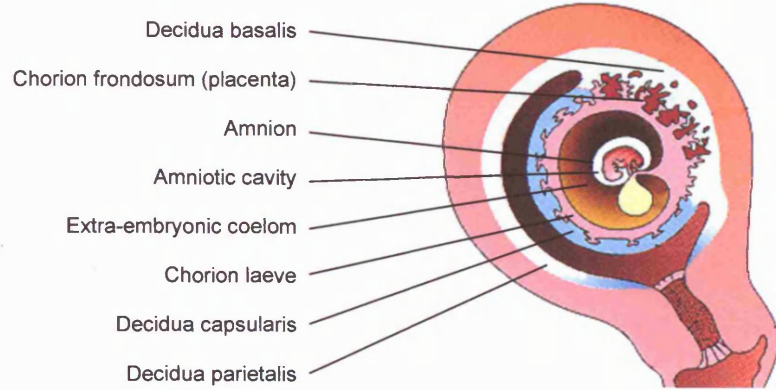
### **1.2.2. Structure of the fetal membranes**

The fetal membranes have been reported to consist of 9 or 10 layers. The amniotic epithelium, amniotic basement membrane, compact layer, fibroblast layer, spongy layer, reticular layer, pseudobasement membrane, cytotrophoblast layer and attached decidua parietalis have all been consistently described, and are illustrated in **Figure 1.5** (Bourne, 1962; Schmidt, 1992). Additionally a further layer has also been described between the spongy and reticular layers, termed the cellular layer (Bourne, 1962).

#### **1.2.2.1. Amniotic epithelium**

The amniotic epithelium is a simple cuboidal epithelium. The cells are tightly opposed to each other connected by desmosomes, and exhibit numerous microvilli on the apical and lateral borders (Hoyes, 1975; van Herendael *et al.*, 1978). At the bases, cell processes extend into the underlying basement membrane (van Herendael *et al.*, 1978).

**(a) Prior to 12 weeks of gestation**



**(b) Week 12-15 of gestation**

Decidua basalis  
Chorion frondosum (placenta)  
Amniotic cavity  
Amnio-chorion  
Decidua capsularis  
Decidua parietalis

**(c) After 24 weeks of gestation**

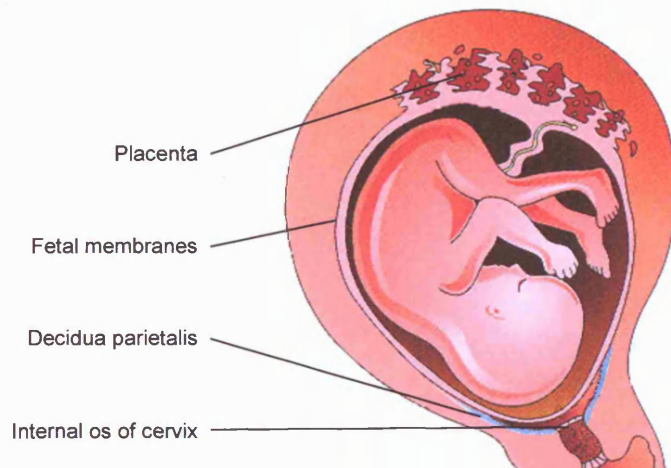


**Figure 1.4.** The stages of fusion of the components of the fetal membranes. Prior to 12 weeks of gestation the amnion and chorion are free (a). After 12 weeks of gestation the amnion and chorion exist as the fused amniochorion (b). Fusion of the amniochorion with the decidua parietalis has been reported to occur between 15-24 weeks gestation. It has certainly occurred by 24 weeks gestation (c). In this diagram the amniochorion in the lower part of the uterus is shown as unfused with the decidua parietalis, although the literature does not clarify whether this is correct. Redrawn from Moore & Persaud (1998), with permission

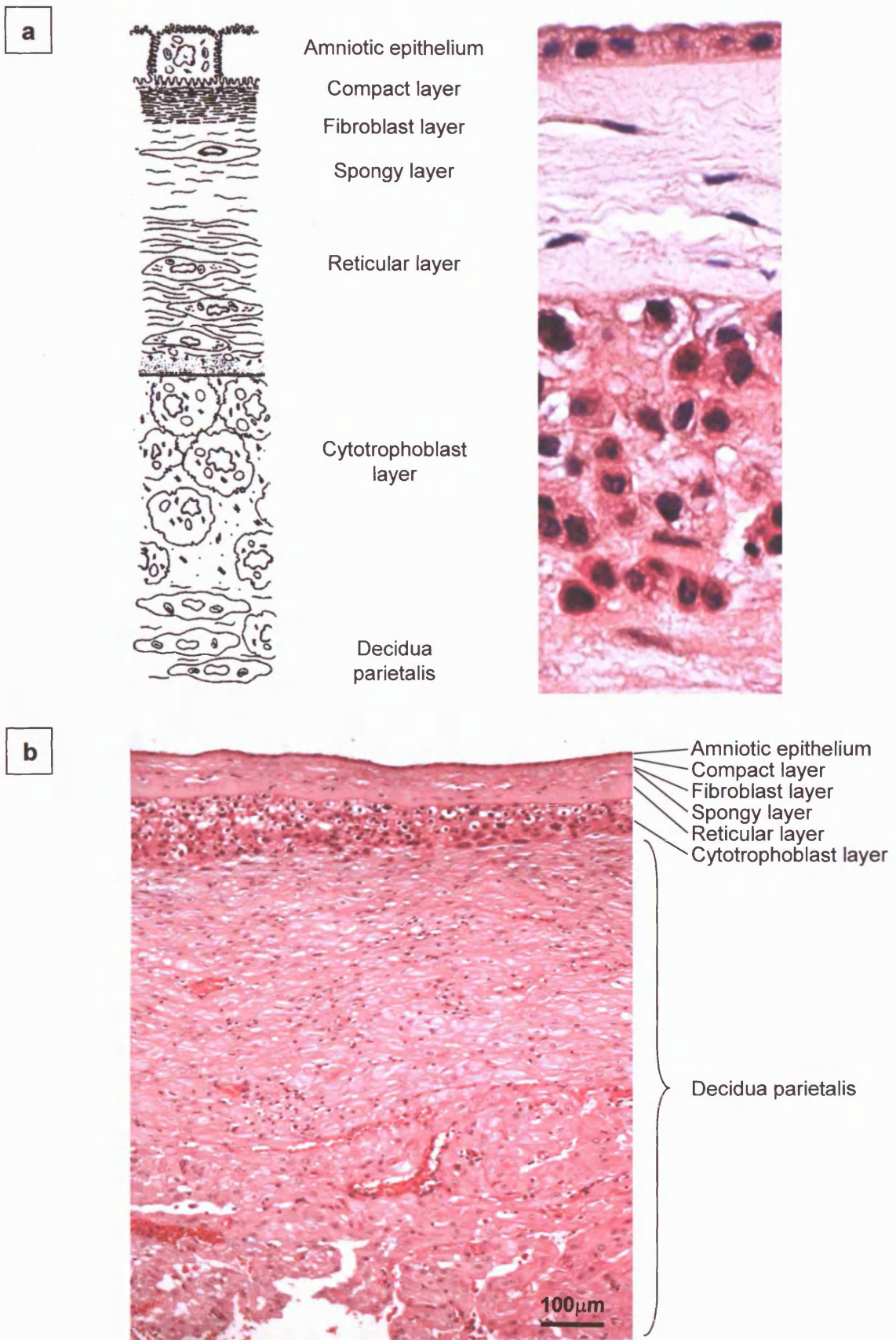


**Figure 1.5.** Diagrammatic representation and haematoxylin and eosin stained section of term fetal membrane, demonstrating the constituent layers of the amnion (amniotic epithelium, compact layer, fibroblast layer), the spongy layer, the chorion (reticular layer and cytotrophoblast layer) and attached decidua parietalis (a). (Line diagram redrawn from Malak & Bell (1994) with permission). The full thickness of the fetal membranes, and constituent layers, is illustrated in (b).

#### **1.2.2.2. Amniotic basement membrane**

Beneath the amniotic epithelium lies the amniotic basement membrane, rich in collagen types IV and V (Modesti *et al.*, 1989; Schmidt, 1992; Malak *et al.*, 1993), fibronectin and laminin (Schmidt, 1992). The basement membrane is anchored to the underlying stroma by a fibrillar network containing collagen types V and VII (Modesti *et al.*, 1984; Keene *et al.*, 1987; Modesti *et al.*, 1989; Malak & Bell, 1996) and fibrillin (Malak & Bell, 1994a).

#### **1.2.2.3. Compact layer**

The acellular compact layer lies immediately adjacent to the amniotic basement membrane to which it is densely adherent (Bourne, 1962). It contains collagen types I (Malak *et al.*, 1993), III (Malak *et al.*, 1993), V (Malak *et al.*, 1993), VI (Malak *et al.*, 1993) and VII (Keene *et al.*, 1987), as well as small amounts of collagen IV (Malak *et al.*, 1993). Non-collagenous components of this extracellular matrix layer include fibrillin (Malak & Bell, 1994a), fibronectin (Aplin *et al.*, 1985), and elastin fibres (Hieber *et al.*, 1997). The elastin fibres within this, and the other layers of the fetal membrane, are very fine, just 1% the diameter of those occurring in the aorta (Hieber *et al.*, 1997). Ultrastructural examination reveals densely packed collagen fibrils (Aplin *et al.*, 1985; Malak *et al.*, 1993; Fawthrop & Ockleford, 1994).

#### **1.2.2.4. Fibroblast layer**

The fibroblast layer lies beneath the compact layer. It comprises a diffuse network of fusiform and stellate cells lying within an irregular network of fibrils (Bourne, 1962). The cellular populations have been reported to be mainly fibroblasts (Bourne, 1962; Schmidt, 1992), with a second population of cells described as macrophages (Bulmer & Johnson, 1984), ultrastructurally typical Hofbauer cells (Bourne, 1962; Hoyes, 1975) or 'histiocytic connective tissue cells' (Schmidt, 1992). The 'fibroblastic' population of cells have been described as containing moderately well formed endoplasmic reticulum, and large glycogen deposits (Bourne, 1962; Hoyes, 1975; Schmidt, 1992). However, intracellular bundles of microfibrils which also project from the cell surface in places have been described (Bourne, 1962), and bundles of filaments with dense bodies noted to be analogous to those normally observed in smooth muscle cells (Hoyes, 1975). The cells have, however, been considered to be fibroblasts. The second, non-fibroblast, population of cells express CD68 (Schmidt, 1992), HLA-DR (Sutton *et al.*, 1983; Bulmer & Johnson,

1984), and CD14 (Bulmer & Johnson, 1984; Malak, 1995). They are fetal cells (Sutton *et al.*, 1983), which have been described as macrophages (Bulmer & Johnson, 1984) or dendritic cells (Sutton *et al.*, 1983). They have been suggested to differentiate from macrophages (Hoyes, 1975), or from fibroblasts (Schmidt, 1992).

The extracellular matrix comprises collagen types I (Malak *et al.*, 1993), III (Malak *et al.*, 1993), V (Malak *et al.*, 1993), VI (Malak *et al.*, 1993) and IV (Malak *et al.*, 1993), fibrillin (Malak & Bell, 1994a), fibronectin (Lockwood *et al.*, 1991), and elastin fibres (Hieber *et al.*, 1997). The layer contains micro-trabeculae containing type IV collagen, laminin and nidogen, and are of uncertain origin and function (Ockleford *et al.*, 1993a).

#### **1.2.2.5. Spongy layer**

The spongy layer, also known as the intermediate layer, lies between the connective tissue layers of the amnion and chorion, and represents a condensation of the extra-embryonic coelom (Bourne, 1962; Schmidt, 1992). When the amnion and chorion are separated following delivery, the spongy layer may adhere to either amnion or chorion (Schmidt, 1992). It is fluid rich, containing proteoglycans (Bourne, 1962; Schmidt, 1992). It also contains collagen types I (Malak *et al.*, 1993), III (Malak *et al.*, 1993), IV (Malak *et al.*, 1993), V (Malak *et al.*, 1993) and VI (Malak *et al.*, 1993), fibronectin (Lockwood *et al.*, 1991), and elastin fibres (Hieber *et al.*, 1997). The spongy layer may swell considerably and is believed to permit movement of the amnion over the underlying chorion (Bourne, 1962). Coiled fibrous structures detected within the spongy layer are believed to facilitate this movement (Ockleford *et al.*, 1993a). The sparse cells within the layer are believed to comprise fibroblasts and macrophages (Schmidt, 1992) or Hofbauer cells (Bourne, 1962).

#### **1.2.2.6. Cellular layer**

The cellular layer has been reported to be difficult to visualise in all fetal membrane specimens, and comprises a single layer of fibroblasts lying between the spongy layer and reticular layer (Bourne, 1962).

#### **1.2.2.7. Reticular layer**

The reticular layer is the connective tissue layer of the chorion. It is in continuum with the chorionic plate of the placenta, although the reticular layer of the chorion laeve is

avascular. It contains collagen types I (Malak *et al.*, 1993), III (Aplin & Campbell, 1985; Malak *et al.*, 1993), IV (Malak *et al.*, 1993), V (Malak *et al.*, 1993) and VI (Malak *et al.*, 1993), fibrillin (Malak & Bell, 1994a), fibronectin (Aplin & Campbell, 1985; Lockwood *et al.*, 1991), elastin fibres (Hieber *et al.*, 1997), and proteoglycans.

The cellular population of the reticular layer has been reported to be solely fibroblasts (Schmidt, 1992), or to consist of fibroblasts and macrophages (or Hofbauer cells) (Bourne, 1962; Nehemiah *et al.*, 1981). The fibroblastic cells have ultrastructural features including dilated endoplasmic reticulum and glycogen granules (Schmidt, 1992). However, cells with indented nuclei, bundles of myofilaments with dense bodies, thickened areas of plasma membrane, and discontinuous basement-membrane-like material on the cell surface have been described (Wang & Schneider, 1983; Malak, 1995). Invaginations of the cell surface similar to the caveolae of the smooth muscle cell membrane, and intercellular communicating channels have also been observed (Bartels & Wang, 1983). These are ultrastructural features associated with smooth muscle cells, and therefore these cells have thus been considered to be myofibroblasts (Bartels & Wang, 1983; Wang & Schneider, 1983; Malak, 1995). Studies of these cells throughout gestation demonstrated highly developed rough endoplasmic reticulum, glycogen deposits, and groups of fine filaments with localised electron-dense areas in the first trimester (Hoyes, 1971). The frequency of detection of the fine filaments decreased with increasing gestation. The reticular layer cells also express intermediate filaments vimentin and desmin (Khong *et al.*, 1986; Ockleford *et al.*, 1993b), and dipeptidyl peptidase IV (Imai *et al.*, 1994; Malak, 1995; Kohnen *et al.*, 1996).

The non-fibroblast population of the layer are fetal in origin (Sutton *et al.*, 1983). Their nature is uncertain. They have been considered as tissue macrophages on the basis of their expression of leucocyte-common antigen and CD14 (Bulmer & Johnson, 1984; Malak, 1995), or as dendritic cells based on their expression of HLA-DR (Sutton *et al.*, 1983; Bulmer & Johnson, 1984), and factor XIIIa (Trimble *et al.*, 1992).

#### **1.2.2.8. Pseudobasement membrane**

This is the basement membrane of the trophoblast, to which it is firmly adherent. It comprises collagen IV (Schmidt, 1992; Malak *et al.*, 1993) and III (Aplin & Campbell,

1985), fibronectin (Aplin & Campbell, 1985), laminin (Schmidt, 1992) and merosin (Malak & Bell, 1996).

#### **1.2.2.9. Cytotrophoblast layer**

The cytotrophoblast layer of the chorion consists of 2-10 layers of round/polygonal cells (Bourne, 1962), and is considered the epithelial layer of the chorion. Two subpopulations have been described (Yeh *et al.*, 1989): 1) A population of vacuolated cells adjacent to the pseudobasement membrane which express placental alkaline phosphatase but are negative for human placental lactogen; 2) A population of eosinophilic cytotrophoblast cells adjacent to the decidua which are positive for human placental lactogen, and weakly positive for placental alkaline phosphatase. These populations have been designated the basal and superficial cytotrophoblast respectively (Malak & Bell, 1996). The basal cytotrophoblast cells are tightly packed (Malak & Bell, 1996). The vacuolated appearance of the basal cytotrophoblast cells may be due to their content of soluble glycogen (Schmidt, 1992; Bell & Malak, 1997). Within the cytotrophoblast layer lie degenerate villi, remnants of chorionic villi consisting of evaginations of the reticular layer down into the cytotrophoblast layer (Bourne, 1962). These structures are observed more frequently in the fetal membranes adjacent to the placenta (Schmidt, 1992; Malak, 1995).

The extracellular matrix surrounding the cytotrophoblast cells comprises collagen types IV (Aplin & Campbell, 1985; Malak *et al.*, 1993), V (Malak *et al.*, 1993), III (Aplin & Campbell, 1985) and VI, fibrillin (Malak & Bell, 1994a), soluble elastin (Hieber *et al.*, 1997), laminin (Aplin & Campbell, 1985; Schmidt, 1992), and fibronectin (Schmidt, 1992). Collagen type I has been described by some authors (Aplin & Campbell, 1985), but noted to be absent by others (Malak *et al.*, 1993). Malak *et al.* described collagen type II between the superficial cytotrophoblast cells, but not the basal cytotrophoblast cells (Malak *et al.*, 1993).

The interface between the cytotrophoblast layer and decidua parietalis is typically indistinct, with superficial cytotrophoblast cells often interspersed with decidual cells (Bourne, 1962; Schmidt, 1992; Malak & Bell, 1996). The cytotrophoblast-decidual interface is rich in onco-fetal fibronectin (Lockwood *et al.*, 1991). A layer of fibrinoid material is often observed at this interface (Schmidt, 1992).

#### **1.2.2.10. Decidua**

The layer of decidua attached to the shed fetal membranes is decidua parietalis (Benirschke & Kaufmann, 2000). It contains decidual cells, macrophages (Nehemiah *et al.*, 1981; Bulmer & Johnson, 1984), blood vessels (Benirschke & Kaufmann, 2000), and occasional degenerate glands. The decidual cells are surrounded by basement membrane-like material containing collagen IV (Malak *et al.*, 1993) and laminin (Benirschke & Kaufmann, 2000). The matrix also contains collagen types I (Malak *et al.*, 1993), II, III (Aplin & Campbell, 1985; Malak *et al.*, 1993) and V (Malak *et al.*, 1993), fibronectin (Aplin & Campbell, 1985) and soluble elastin (Hieber *et al.*, 1997).

### **1.3. Fetal membrane behaviour and properties**

The structural integrity of the fetal membranes is vital for the successful maintenance of the pregnancy to term. The behaviour of the fetal membranes during pregnancy must allow the expansion and growth of the sac and its contents, yet remain intact to permit the continuation of the pregnancy. The understanding of these functions, which can be considered in terms of biophysical properties, and biochemical and endocrine functions, will assist in the understanding of underlying basis of the integrity of the membranes.

#### **1.3.1. Biophysical properties of the fetal membranes**

The biophysical properties of the fetal membranes have been examined in depth, to determine possible mechanisms of fetal membrane rupture, and examine for evidence for generalised structural weakness. The molecular and cellular basis of the structural stability of the fetal membranes relies on the collagens, and their structural arrangement within the amnion and chorion. The collagens form the major structural components of the fetal membranes. Interstitial collagens, types I and III are found throughout the amniochorion (Malak *et al.*, 1993). In the amnion both amniotic epithelial cells (Aplin *et al.*, 1985) and mesenchymal cells (Casey & MacDonald, 1996) have been demonstrated to synthesise the interstitial collagens. Anchoring fibrils of collagen V extend into the underlying stroma, binding the basement membrane to the interstitial collagens (Modesti *et al.*, 1984; Modesti *et al.*, 1989). The compact layer comprises densely packed collagen fibrils arranged parallel to the amniotic epithelium. The basement membrane, compact layer, fibroblast layer are held together by 'rivets' of collagen VII (Ockleford *et al.*, 1997). Collagens types IV (generally associated with basement membranes) and VI are found throughout the

amnion and chorion, suggesting a significant structural role (Malak *et al.*, 1993). Fibres crossing the spongy layer, from reticular layer to fibroblast layer, were observed, and have been suggested to function as 'guy-ropes', limiting the degree of movement permitted of amnion upon chorion. Demonstration of complementary gyri and sulci with a helical substructure on the opposing surfaces of the fibroblast and reticular layers facing the spongy layer suggests a mechanism for permitting movement of amnion upon chorion whilst still maintaining structural integrity (Fawthrop & Ockleford, 1994). The fetomaternal interface appears to be stabilised by onco-fetal fibronectin (Feinberg *et al.*, 1991; Lockwood *et al.*, 1991).

The fetal membranes are visco-elastic in behaviour. They extend under deformation (elasticity), but only the elastic component will recover, thus the membrane does not return completely to its original state: properties termed 'elastic extension' (the recoverable component) and 'creep extension' (the non-recoverable viscous component) (Lavery & Miller, 1977; Lavery & Miller, 1979; Alger & Pupkin, 1986). The elastic properties of the fetal membranes had been attributed to the presence of fibrillin microfibrils, due to the absence of demonstrable elastin fibres (Malak & Bell, 1994a). Subsequent work, however, has demonstrated the presence of very thin elastic fibres and sheets, 1% the size of those isolated from the aorta (Hieber *et al.*, 1997). Thus the fetal membranes recoil following their expulsion from the uterus. It has been estimated that the internal surface area of the uterus at term is 2.1 times (Parry-Jones & Priya, 1976) greater than the surface area of the gestational sac following delivery.

The strength of the fetal membranes, upon biomechanical testing, is such that they are unlikely to rupture during physiological contractions (French & McGregor, 1996). Studies indicate that the main tensile strength of the amniochorion lies in the thinner of the two main components, the amnion (Meudt & Meudt, 1967), which requires more pressure to burst, and has 5 times the ability to withstand stress than the choriodecidua (Polishuk *et al.*, 1962). However, the integrity of the amniochorion appears vital, with the combined strength of the membranes being greater if the amnion and chorion are not delaminated (French & McGregor, 1996). The amniochorion obtained prior to labour and delivery demonstrate biomechanical properties of a single membrane, exhibiting greater strength than those obtained following labour and delivery, which typically demonstrated evidence of functional amnio-chorial separation (Helmig *et al.*, 1993). It has been demonstrated that

a 'two-phase' rupture of the fetal membranes commonly occurs, with the chorion rupturing prior to the amnion (Meudt & Meudt, 1967; Schmidt, 1992).

It has been noted that during labour the contraction during which fetal membrane rupture occurred was not the strongest contraction in 86% of cases (Topozada *et al.*, 1970). Fetal membranes subjected to repeated stretching (analogous to uterine activity) require less pressure to rupture than prior to the repeat stretching, an observation suggested to be due to the phenomenon of 'strain-hardening' (Topozada *et al.*, 1970). It has therefore been suggested that repetitive stress from contractions causes gradual thinning of the fetal membranes, due to creep extension, and further strain hardening would cause the membranes to become brittle, and rupture at a stress level below that expected (Alger & Pupkin, 1986; Polzin & Brady, 1991; French & McGregor, 1996).

This complex biophysical behaviour is reinforced by the observation that fetal membranes obtained following preterm pre-labour rupture of the membranes, which logically may be expected to be 'weak' have been demonstrated to have a bursting pressure greater than term fetal membranes (Alger & Pupkin, 1986). These properties and evidence mitigate against a generalised weakness of the fetal membranes leading directly to fetal membrane rupture.

### **1.3.2. Biochemical properties of the fetal membranes**

Following a period of growth of the fetal membranes in the first half of pregnancy, it is believed that the increase in size of the gestational sac during the second half of pregnancy is due to stretch. This was suggested by a lack of mitotic activity in the fetal membranes in the second half of pregnancy (Alger & Pupkin, 1986). The greatest capacity for collagen synthesis and cross-linking by lysyl oxidase occurs in the first part of pregnancy, up to 16 weeks gestation (Casey & MacDonald, 1996). A decrease in the collagen content of the amnion has been demonstrated over the last 8 weeks of pregnancy (Skinner *et al.*, 1981).

The extracellular matrix of the fetal membranes undergoes continuous turnover and remodelling. The synthesis of the strength-giving matrix components must be balanced by the degradative enzymes. The key degradative enzymes are the matrix metalloproteinase (MMP) family, their modifiers (tissue inhibitors of metalloproteinases, TIMPs), the plasminogen activators (tissue-type plasminogen activator, t-PA, and urokinase-type plasminogen activator, u-PA) and their inhibitors (plasminogen activator inhibitors, PAI-1

and PAI-2). The MMPs have specific substrates, and are secreted as latent forms, activated by other MMPs or plasmin, and inhibited by the TIMPs. The collagenases (MMP-1 and MMP-8) degrade collagen types I and III. The gelatinases (MMP-2 and MMP-9) degrade collagens IV, V and VII, fibronectin and elastin. The stromelysins (MMP-3, MMP-7 and MMP-10) exhibit broader specificity including proteoglycans, fibronectins and collagens (Woessner, 1991; Mignatti *et al.*, 1996; Hulboy *et al.*, 1997). Within the fetal membranes, MMP-9 and MMP-1 have been localised primarily to the amniotic epithelium and cytotrophoblast layer, as well as to the fibroblast layer (Vadillo-Ortega *et al.*, 1995; Fortunato *et al.*, 1997; Hulboy, 1997 #85), and MMP-2 to the amniotic epithelium and cytotrophoblast layer (Fortunato *et al.*, 1997). Members of the TIMP family have been demonstrated throughout the fetal membranes (Fortunato *et al.*, 1997). Relaxin, produced by the decidua, has been demonstrated to modify activity of the MMP family, with upregulation of MMP-1, MMP-3 and MMP-9 (Bogic *et al.*, 1997).

### **1.3.3. The endocrine functions of the fetal membranes**

The fetal membranes can be considered not only in terms of biochemical and biophysical function but also in terms of their endocrine properties. They have been demonstrated to play a role in the synthesis and regulation of a number of regulators of parturition, including prostaglandins, cytokines and oxytocin. Their role in the degradation of the uterotonic agents prostaglandins, oxytocin, and endothelin may act to maintain myometrial quiescence.

Prostaglandin E<sub>2</sub> and prostaglandin F<sub>2α</sub> have been demonstrated to play a role in uterine activity: blockage of their synthesis inhibits uterine activity, and administration of exogenous prostaglandins to the pregnant woman stimulates myometrial contraction (Casey & MacDonald, 1993). Prostaglandins are synthesised from arachidonic acid by cyclo-oxygenase type 1 and type 2 (COX-1 and COX-2, also known as prostaglandin endoperoxide synthase type 1 and type 2), and metabolised to biologically inactive metabolites by prostaglandin dehydrogenase (PDGH) (Smith & DeWitt, 1996). COX-1 has been demonstrated to be constitutively expressed throughout the fetal membranes. COX-2 expression, however, has been demonstrated within the amniotic epithelium, fibroblast layer, reticular layer and decidua (Slater *et al.*, 1995). Upregulation of COX-2 mRNA in amnion, and to a lesser extent in choriodecidua and myometrium has been demonstrated with the onset of labour (Slater *et al.*, 1995). Thus increased levels of prostaglandins, derived from the fetal membranes, are detected within amniotic fluid with labour (Mitchell

*et al.*, 1995). PGDH has been localised to the cytotrophoblast layer, where it has been hypothesised to function to prevent active prostaglandins produced by the amnion from reaching the myometrium (Keirse & Turnbull, 1975; Cheung *et al.*, 1992). Reduction in PGDH activity occurs with labour (Sangha *et al.*, 1994). Prostaglandin production may be stimulated by cytokines, especially by interleukin-1 $\beta$  and tumour necrosis factor- $\alpha$  which upregulate COX-2 within amniotic epithelial cells (Trautman *et al.*, 1996). Glucocorticoids have a complex action on prostaglandin production. They appear to upregulate COX-2 in the mesenchymal cells of the amnion, but to inhibit it in the amniotic epithelium (Economopoulos *et al.*, 1996).

The amnion, chorion, and decidua are also sites of production of oxytocin. Oxytocin is a powerful uterotonic, but the role of oxytocin in the physiological onset of labour is unclear (Challis *et al.*, 2000). It is produced by the posterior pituitary, but also in a number of peripheral sites where it is postulated to have a paracrine action (Zingg, 2001). Levels of oxytocin gene expression by the choriodecidua increase with parturition (Chibbar *et al.*, 1993). Oxytocin receptors are localised to the decidua and myometrium, and are upregulated in the latter stage of pregnancy prior to parturition (Challis *et al.*, 2000). Oxytocinase, which degrades oxytocin, is detected at high levels in the chorion laeve (Germain *et al.*, 1994).

The fetal membranes also produce a third uterotonic, endothelin-1. It is produced by amniotic epithelial cells and is detected in high levels in amniotic fluid (Casey & MacDonald, 1993). It usually acts in a paracrine manner (Germain *et al.*, 1997). High levels of activity of enkephalinase, which degrades the endothelin-1, have been detected within the chorion laeve (Germain *et al.*, 1994).

#### **1.4. Physiological fetal membrane rupture**

Physiological fetal membrane rupture occurs most commonly at the end of the first stage of term labour, although it occurs prior to labour in approximately 10% of term deliveries (1.1.2.). The normal functions of the fetal membranes, and the factors that confer strength have been discussed. A number of different potential underlying mechanisms of fetal membrane rupture may be considered. Fetal membrane rupture may be considered a purely passive process, due to the 'bursting of a balloon', from the increased intrauterine pressure generated by uterine activity, or alternatively considered as an active process within the

membranes due to biochemical changes, predisposing to rupture. Additionally, processes may be considered as generalised, affecting the whole gestational sac, or as localised, occurring in one region of the sac only. Each of these processes may occur in association with labour, or prior to the onset of labour. Considerable overlap exists between the evidence for each of these concepts. Initially these will be divided according to pre-labour or labour associated processes, however within these groups, active and passive, and generalised and localised phenomena may be identified.

#### **1.4.1. Labour associated**

The biophysical properties of the fetal membranes (1.3.1.), and in particular the phenomenon of strain-hardening (Topozada *et al.*, 1970) may permit the rupture of the fetal membranes in response to uterine contractions, and occur as a purely passive process. This may be a generalised process, affecting the whole sac, or may be a localised process, acting only on the fetal membranes directly overlying the cervix, once the support of the cervix has been removed when cervical dilatation occurs.

The repeated stretching of the fetal membranes due to contractions may also induce active degradative processes within the fetal membranes. Mechanical stretch has been demonstrated *in vitro* to increase production of prostaglandin E2 (Kanayama & Fukamizu, 1989) by amniotic epithelial cells, and interleukin 8 expression (El Maradny *et al.*, 1996; Maehara *et al.*, 1996) and collagenase (MMP-1) activity (El Maradny *et al.*, 1996) by the amniochorion. Interleukin-8 is a chemoattractant, and activator of neutrophils, but also induces release of MMPs from neutrophils and cervical fibroblasts (El Maradny *et al.*, 1994; El Maradny *et al.*, 1996).

Considerable additional evidence exists to suggest that extracellular matrix degradation in the fetal membranes occurs in association with the onset of labour. Activation of the MMP cascade has been demonstrated in, and has been proposed to play a causal role in the loss of integrity of the fetal membranes leading to rupture. Increased gene expression of MMP-1, -2, -3 and -9, relaxin, t-PA and TIMP-1 in the fetal membranes have been demonstrated (Bryant-Greenwood & Yamamoto, 1995; Hulboy *et al.*, 1997), and increased levels of MMP-9 protein and activity also occurs in association with labour (Vadillo-Ortega *et al.*, 1995).

Localised changes in uterotonin production have been described in association with labour, by examination of the contents of the amniotic fluid of the forebag compared to the hindbag. However, a higher concentration in a number of prostanoids, including prostaglandin E<sub>2</sub> and prostaglandin F<sub>2α</sub>, occurs in amniotic fluid obtained from the forebag (in front of the fetal head) compared to the hindbag, during labour (MacDonald & Casey, 1993; Romero *et al.*, 1994). PDGH activity within the cytotrophoblast layer is decreased in fetal membranes obtained from the lower uterine pole during labour at term, compared to distal sites (Van Meir *et al.*, 1997), and would decrease prostaglandin degradation in this region, permitting prostaglandins to reach the underlying myometrium. Increased expression of IL-1β mRNA occurs in the decidua parietalis adjacent to the forebag during labour, compared to the hindbag (MacDonald *et al.*, 1991). These phenomena may be a result of the process of labour, secondary to the process of stretching of the membranes over the cervix, local release of cytokines, local application of bacteria and toxins from the vagina (Cox *et al.*, 1993; Romero *et al.*, 1994), and the stripping of the decidua parietalis from the fetal membranes and resultant hypoxia (MacDonald *et al.*, 1991). However the localised increased concentration of prostaglandins in the forebag amniotic fluid may play a role in fetal membrane rupture at that site.

#### **1.4.2. Pre-labour**

Alternatively it may be considered that significant changes occur in the uterus, and in the fetal membranes, in order to prepare for labour and programme for fetal membrane rupture, as part of Phase 1 of parturition as described by Casey and MacDonald (Casey & MacDonald, 1993). During this phase, upregulation of a cassette of genes including connexin-43, prostaglandins, and oxytocin receptor occurs in the uterus, in preparation for the onset of labour (Challis & Gibb, 1996).

The lower uterine segment develops from the isthmus of the cervix, from approximately 28 weeks gestation (Morrison, 1972). Effacement of the cervix may also occur prior to clinically apparent labour. It has been estimated that at term, the cervix of the nullipara is 70% effaced, and that of multipara 61% effaced, in association with a mean cervical dilatation of 2cm (although with a wide standard deviation of 0.75cm) on the day prior to labour (Hendricks *et al.*, 1970). The release of onco-fetal fibronectin into the cervico-vaginal secretions in the 2-3 weeks prior to the clinical onset of labour occurs (Lockwood *et al.*, 1991), presumably due to the disruption of the feto-maternal interface due to these changes in the lower segment in late pregnancy.

Other changes prior to the onset of clinically apparent labour have been described. Regional differences in the fetal membranes prior to the onset of labour at term have also been noted and could be considered as local and active processes. The fetal membranes overlying the cervix contain higher levels of MMP-9, albeit of the latent form, compared to membranes from distal sites (McLaren *et al.*, 1997). This may contribute to a local structural weakness predisposing to fetal membrane rupture.

In the absence of evidence for generalised structural weakness as a precursor of fetal membrane rupture, extensive investigation has been undertaken to search for localised factors that may predispose to rupture. Bourne demonstrated in 1962 that the most common site of fetal membrane rupture, is in the membranes overlying the internal os of the cervix (which he termed the 'dependent' membranes) (Bourne, 1962). He identified this area of membrane by insertion of blue dye through the cervix prior to membrane rupture, and demonstrated that the rupture tear always passed through this area of membrane, which usually appeared towards one end of the rupture tear, suggesting transmission of the tear away from the point of initial rupture. Malak *et al* identified structural changes within fetal membranes in a restricted area of the rupture line, commonly towards one end of the rupture line, an area he termed the 'zone of altered morphology', or ZAM, which affected an area of fetal membranes of 4-12cm diameter (Malak & Bell, 1994b). The ZAM was characterised by an increased thickness of the connective tissue layers of both the amnion and chorion, and a decrease in the thickness of the cytotrophoblast and decidual layers. A marked increase in the thickness of the spongy layer was noted, with physical separation of amnion and chorion. Ultrastructural and immunohistochemical studies demonstrated a decrease in the lateral and basal processes of the amniotic epithelial cells, with a reduction of the number of desmosomes and hemidesmosomes (Malak & Bell, 1996; Bell & Malak, 1997). A significant decrease in immunoreactive collagen was observed in the connective tissue layers, with disruption and disorganisation of the collagen fibres and filaments demonstrated by electron microscopy (Malak & Bell, 1996; Bell & Malak, 1997). The reduction in the thickness of the cellular layers of the fetal membranes was attributed in part to loss of superficial trophoblast cells, rather than a physical change in the cleavage plane of the fetal membrane from the underlying decidua, since decidual cells remained present overlying the cytotrophoblast layer (Malak & Bell, 1994b). The structural changes observed in the ZAM have been hypothesised to be consistent with structural weakness (Malak & Bell, 1994b).

Structural changes had previously been noted in the fetal membranes adjacent to the rupture line, with dispersal of connective tissue in the fibroblast and spongy layers (Bou-Resli *et al.*, 1981), and associated with reduction in collagen content of the fetal membranes at the same site (Al-Zaid *et al.*, 1986). Similar structural changes to those observed in the ZAM have also been observed in the 'dependent' fetal membranes, overlying the cervix prior to the onset of labour at term, by Bourne (Bourne, 1962) and Ibrahim *et al.* (Ibrahim *et al.*, 1983). It is therefore hypothesised that the ZAM described following labour and delivery, is equivalent to the 'dependent' membranes, and is present prior to the onset of labour in a restricted region of the fetal membranes overlying the cervix. This region of the fetal membranes, exhibiting features consistent with structural weakness, is therefore potentially 'programmed' for fetal membrane rupture.

## **1.5. The 'Wound Response' Hypothesis**

### **1.5.1. The 'wound response' hypothesis as a mechanism for fetal membrane rupture**

The features of the regional structural changes in the fetal membranes described following spontaneous labour and delivery at term include extracellular matrix synthesis and degradation, and share many similarities with the classical 'wound response'. The soft tissue wound response has a number of overlapping stages: inflammation (early and late phases); granulation tissue formation and re-epithelialisation; and extracellular matrix formation and remodelling. Soft tissue injury causes vascular damage, activation of the coagulation cascade, and platelet aggregation. Thrombin release induces platelet degranulation, and the consequent cytokine release attracts macrophages and neutrophils, which clear cell debris. The fibrin clot provides a provisional matrix, and a basis for granulation tissue formation. Fibroblasts and macrophages lay down extracellular matrix, the key components of which are collagen, fibronectin and tenascin-C. In the last phase of the wound response, the granulation tissue is remodelled, and replaced with a more organised matrix. Proteases break down the granulation tissue, and new matrix is laid down. Fibroblasts differentiate into myofibroblasts, which cause wound contraction. The final repair is generally characterised by fibrosis and scar formation. The last stage in the wound response is apoptosis of the cells that effected the final repair, the myofibroblasts. Throughout the wound response, not only is matrix synthesis occurring, but also matrix degradation and remodelling (Clark, 1996).

Several of the key features of the wound response have been observed in association with the fetal membranes derived from the 'dependent' membranes:

- The mesenchymal cells of the reticular layer of the chorion are considered by some authors to be typical of myofibroblasts (Wang & Schneider, 1983; Malak, 1995), the key cell in the wound response.
- Preliminary evidence suggests an increase in immunoreactive tenascin-C in the reticular layer of the fetal membranes in the ZAM (Malak, 1995).
- Increased expression of MMP-9 is detected in the 'dependent' membranes overlying the cervix prior to labour at term (McLaren *et al.*, 1997).
- Disruption and disorganisation of the collagen fibrils within the extracellular matrix, consistent with degradation and remodelling (Malak & Bell, 1996).
- Increased content of cytokines derived from the fetal membranes, in the amniotic fluid of the forebag during labour (MacDonald *et al.*, 1991; MacDonald & Casey, 1993; Romero *et al.*, 1994).

Thus the ZAM exhibits a number of features characteristic of a wound response. This has led to the hypothesis that the net effect of this process may be structural weakness, resulting in an area of the fetal membrane 'programmed' with increased susceptibility to rupture due to the subsequent uterine contractions during labour (Bell & Malak, 1997). As a key cell in the 'wound response', the myofibroblast would therefore also be predicted to play a major role in the fetal membranes.

### **1.5.2. The myofibroblast**

The myofibroblast plays a key role in the wound response. It is a cell with morphological and biological properties intermediate between fibroblasts and smooth muscle cells (Sappino *et al.*, 1990). It was first described by Gabbiani in 1971, when he discovered that granulation tissue fibroblasts displayed ultrastructural features of smooth muscle cells (Gabbiani *et al.*, 1971), and subsequently that these cells exhibited contractile functions similar to smooth muscle cells (Majno *et al.*, 1971; Gabbiani *et al.*, 1972). Since that time,

myofibroblasts have been studied extensively. They are defined in terms of their ultrastructure (1.5.2.1.), and may be described in terms of their intermediate filament phenotype (1.5.2.2.), and biochemical function (1.5.2.3.).

#### **1.5.2.1. Myofibroblast ultrastructure**

Numerous sources agree that the ultimate definition of a cell as a myofibroblast is based on ultrastructure. The key features are the presence of stress fibres, cell-stroma attachment sites (fibronexi) and intercellular intermediate and gap junctions. Additional features described include an indented nucleus, prominent rough endoplasmic reticulum, and the presence of an incomplete layer of basal lamina on the cell surface (Sappino *et al.*, 1990; Schmitt-Graff *et al.*, 1994). Bundles of stress fibres with interspersed dense bodies lie parallel to the long axis of the cell, often beneath the cell membrane. These are believed to represent bundles of actin myofilaments. They connect to extracellular fibronectin fibrils at attachment points on the cell membrane termed fibronexi (Singer *et al.*, 1984; Eyden, 1993).

#### **1.5.2.2. Intermediate filament phenotype**

The cytoskeleton of cells is composed of three filamentous systems: microfilaments (e.g. actin (A), myosin (M)); intermediate filaments (e.g. vimentin (V), desmin (D)); and microtubules (e.g. tubulin) (Schmitt-Graff *et al.*, 1994). Mesenchymal cells express vimentin, and muscle cells express desmin (Osborn & Weber, 1982). The myofibroblast has been described and classified with respect to microfilament and intermediate filament expression. Thus four main types of myofibroblast were described: 'V' cells, 'VD' cells, 'VA' cells, and 'VAD' cells (Skalli *et al.*, 1989; Sappino *et al.*, 1990). Granulation tissue myofibroblasts are 'VA' cells (Darby *et al.*, 1990; Sappino *et al.*, 1990; Gabbiani, 1992). Subsequently expression of  $\gamma$ -smooth muscle actin (G) (Kohnen *et al.*, 1996) and smooth muscle myosin (Schmitt-Graff *et al.*, 1994; Kohnen *et al.*, 1996) by myofibroblasts has been described. Sequential acquisition of  $\alpha$ -smooth muscle actin,  $\gamma$ -smooth muscle actin and smooth muscle myosin, with development of increasing ultrastructural features of myofibroblast differentiation has been described in placental villi and the umbilical cord. They have therefore been proposed as sequential markers of increasing myofibroblast differentiation approaching the phenotype of true smooth muscle cells (Kohnen *et al.*, 1996; Nanaev *et al.*, 1997).

Almost all myofibroblast populations *in vivo* express  $\alpha$ -sma (Schmitt-Graff *et al.*, 1994; Desmouliere & Gabbiani, 1996), as described by immunohistochemistry with a specific monoclonal antibody against  $\alpha$ -sma (Skalli *et al.*, 1986). Expression of desmin (as expressed by cells of the reticular layer of the fetal membranes) occurs in a minority of myofibroblasts, and is of unknown significance (Sappino *et al.*, 1990). Expression of  $\alpha$ -sma been considered a key marker of myofibroblast differentiation (Sappino *et al.*, 1990; Schmitt-Graff *et al.*, 1994).

### **1.5.2.3. Myofibroblast function**

One of the first described properties of myofibroblasts is that of contractility (Majno *et al.*, 1971). Myofibroblasts connect to each other via gap junctions (Gabbiani *et al.*, 1978; Spanakis *et al.*, 1998), and to the extracellular matrix at the fibronexus which allows connection of the intracellular actin filaments to the extracellular matrix (Eyden, 1993). These connections permit contractility. The contractile function of the myofibroblast plays a role in the contraction of wounds, and produces skin retraction around tumours (Seemayer *et al.*, 1979). Expression of  $\alpha$ -smooth muscle actin is critical for force generation (Darby *et al.*, 1990), although expression of smooth muscle myosin is not required (Sappino *et al.*, 1990).

Although originally described in granulation tissue, myofibroblasts have been demonstrated in other tissues, in association with tissue remodelling or tissue retraction and tension (Sappino *et al.*, 1990; Schmitt-Graff *et al.*, 1994): normal tissues, fibrotic diseases, and neoplasia.

Within normal tissues they play a role in organogenesis and morphogenesis, through mesenchymal-epithelial interactions. Cells demonstrating myofibroblastic features have been described in a number of sites, including the intestines, theca externa of the ovary, reticular cells of lymph nodes and spleen, testicular stroma, hepatic perisinusoidal cells, lung septa, bone marrow stroma, intestinal pericryptal cells, adrenal gland capsule and periodontal ligament (Sappino *et al.*, 1990; Schmitt-Graff *et al.*, 1994).

In wound healing myofibroblasts are involved in the formation and repair of the extracellular matrix through production of degradative enzymes and synthesis of new matrix components, and in generation of epithelium and vasculature. The disappearance of

myofibroblasts at the end of the wound response, with formation of the scar, is thought to be due to apoptosis (Darby *et al.*, 1990; Desmouliere *et al.*, 1995). Myofibroblasts are found not only in granulation tissue, but also in pathological fibrotic conditions, such as Dupuytren's contracture (Berndt *et al.*, 1994), and renal (Muchaneta-Kubara & Nahas, 1997; Roberts *et al.*, 1997), cardiac (Campbell & Katwa, 1997), hepatic (Blazejewski *et al.*, 1995) and pulmonary (Zhang *et al.*, 1996) fibrosis.

Although myofibroblasts may rarely undergo neoplastic transformation, they are also found in the desmoplastic stromal response to neoplasia (Taccagni *et al.*, 1997). They are commonly found associated with invasive and metastatic carcinomas, with retraction and fixation to adjacent tissues (Seemayer *et al.*, 1979). They have been described in association with many tumours, including those of the breast, colon, stomach and lung, as well as in association with lymph node metastases (Seemayer *et al.*, 1979; Balazs & Kovacs, 1982). The retraction phenomena associated with these tumours have been attributed to the contractile properties of the myofibroblast (Seemayer *et al.*, 1979). Although it was initially considered that the desmoplastic reaction around tumours may serve to limit tumour spread (Schurch *et al.*, 1981; Seemayer *et al.*, 1982), it has more recently been suggested that protease secretion by myofibroblasts may act to promote tumour invasion (Basset *et al.*, 1990; Nielsen *et al.*, 1996).

Myofibroblasts have numerous functions in the wound response, including the production of growth factors, synthesis of prostaglandins through expression of both COX-1 and COX-2. They also play a key role in cell-matrix interactions (Clark, 1996; Desmouliere & Gabbiani, 1996). A key role for myofibroblasts in the latter stages of the wound response is synthesis of new extracellular matrix. They have been demonstrated to produce the 'anti-adhesive' proteins tenascin-C (Berndt *et al.*, 1994) and osteonectin (Blazejewski *et al.*, 1997), as well as collagen, laminin and fibronectin (Berndt *et al.*, 1994). Both tenascin-C and osteonectin play a key role in cell-matrix interactions, and in cell migration and motility, and thus in tissue remodelling. They have both been demonstrated to induce expression of metalloproteinases (Tremble *et al.*, 1993; Tremble *et al.*, 1994; Khan & Falcone, 1997; Shankavaram *et al.*, 1997), and thus may play a direct role in the degradation of extracellular matrix and structural weakness.

## **1.6. Plan of the current investigation**

### **1.6.1. Aim**

The aim of this thesis is to test the hypotheses that:

The ZAM detected in the fetal membranes following labour and delivery is present prior to the onset of labour, and is located in the fetal membranes within the lower uterine pole **and** that myofibroblast differentiation, and expression of the key matricellular proteins tenascin-C and osteonectin, is associated with the structural changes characteristic of the ZAM in the connective tissue layers of the fetal membranes.

### **1.6.2. Objectives**

- To determine whether the structural changes in the fetal membranes described within the rupture line at term (in the ZAM) are present prior to and during labour at term.
- To determine whether the ‘altered morphology’ in the fetal membranes before, during and after labour at term, is associated with differences in the phenotype of the cellular populations of the connective tissue layers, in particular the intermediate filament phenotype of the mesenchymal cell populations.
- To confirm the previous detection of tenascin-C in the connective tissue layers of the extracellular matrix, to determine whether the related ‘anti-adhesive’ matricellular protein osteonectin is expressed in the fetal membranes, and to relate the expression of both proteins to the presence of ‘altered morphology’ in the fetal membranes.
- To develop *in vitro* models to mimic the changes detected within the connective tissue layers of the fetal membranes analogous to those involved in the wound response and to examine the control mechanisms involved.
- To investigate the ontogeny of the development of fetal membrane altered morphology, tenascin-C expression, and the mesenchymal cellular phenotype during gestation.

## **Chapter 2**

### **Materials and Methods**

The materials and methods used in this thesis are described in this chapter. All reagents were obtained from Sigma (Poole, UK) unless stated otherwise.

#### **2.1. Tissue collection**

Fetal membranes were collected from Leicester Royal Infirmary Women's Hospital, University Hospitals of Leicester (UHL) NHS Trust, according to guidance from Leicestershire Health Authority Ethics Committee, and from the British Pregnancy Advisory Service (BPAS) Blackdown Clinic, Leamington Spa, with approval from the BPAS Ethics Committee. First trimester decidua and fetal membranes were collected from Leicester Royal Infirmary, UHL NHS Trust, according to guidance from Leicestershire Health Authority Ethics Committee.

##### **2.1.1. Term fetal membranes**

###### **2.1.1.1. Patient groups**

Fetal membranes were collected at term from three groups of women:

Pre-labour. Women undergoing elective Caesarean section at term, for breech presentation or previous Caesarean section. All women had an uncomplicated antenatal course, and had intact fetal membranes and no clinical signs of labour at the time of Caesarean section. A total of 27 fetal membranes were collected from this group.

Labour. Women established in labour (with regular uterine contractions and documented cervical change), at term, undergoing Caesarean section for fetal distress, failure to progress in labour, or breech presentation. Eleven fetal membranes were collected from this group.

Post-labour. Women with spontaneous onset of labour and spontaneous rupture of membranes, at term. All women had an uncomplicated antenatal course, and a vaginal delivery. Sixteen fetal membranes were collected from this group.

### **2.1.1.2. Sampling technique**

In women undergoing Caesarean section, whether pre-labour or in labour, the area of fetal membranes overlying the internal os of the cervix was identified by the application of a Babcock tissue forceps following delivery of the baby, but prior to delivery of the placenta and membranes. Fetal membrane biopsies were then taken from two sites:

‘Cervical’ fetal membranes. Within 5cm of the site of the Babcock, avoiding tissue directly traumatised by the instrument.

Midzone fetal membranes. At least 12cm from the site of the ‘cervical’ membrane biopsy, on the longest axis from the ‘cervical’ biopsy to the placental edge, and at least 3cm from the placental edge.

In women who had a vaginal delivery, biopsies were taken from:

Rupture line fetal membranes. The rupture line of the fetal membranes was identified. As the ZAM has been reported to be commonly found at one end of the rupture line (Malak & Bell, 1994b), biopsies were taken from 3 sites along the rupture line (both ends, and from the middle). The biopsy with the most extreme altered morphology was used for subsequent work. This method should obtain fetal membrane within the ZAM, although may not obtain fetal membrane with the most extreme altered morphology present.

Midzone fetal membranes. At least 12cm from the rupture line, on the longest axis from the rupture line to the placental edge, and at least 3cm from the placental edge.

Fetal membrane biopsies were collected in all cases for formalin-fixation (2.2.1.), and in selected cases snap-frozen to obtain cryostat sections (2.2.2.), snap frozen for protein extraction (2.4.1.) or homogenised for RNA extraction (2.5.1.).

### **2.1.1.3 Fetal membrane ‘maps’**

Ten fetal membranes obtained prior to delivery at term were subjected to a detailed mapping technique. The membranes were obtained with the ‘cervical’ area identified with a Babcock tissue forceps as above. Sequential 3 x 1cm biopsies were taken radiating away from the site of the Babcock along four axes. Additional biopsies were taken in the lower

uterine segment. An example of such a map obtained is shown in **Figure 2.1**. All biopsies were formalin-fixed (**2.2.1.**).

#### **2.1.1.4. Dissected fetal membranes**

Paired midzone and 'cervical' fetal membranes were obtained from pre-labour Caesarean section (n=5), and the cellular layers (cytotrophoblast and decidua) removed by scraping with a glass microscope slide. The remaining tissue (amnion, spongy layer and reticular layer) was used for RNA extraction and RT-PCR (**2.5.**), and protein extraction and Western blotting (**2.4.**). Midzone fetal membranes were similarly dissected to obtain tissue for selected organ culture experiments (**2.7.**). A piece of each tissue was formalin-fixed and wax-embedded (**2.2.1.**), and a haematoxylin and eosin stained section (**2.2.3.**) obtained, to confirm the removal of the cytotrophoblast layer and decidua (**Figure 2.2**).

#### **2.1.2. Preterm fetal membranes**

Fetal membranes were obtained from prelabour Caesarean sections at 25-36 weeks gestation, being performed for pre-eclampsia (n=10), intrauterine growth restriction (n=4), placenta praevia (n=2), complications of maternal diabetes (n=2), Rhesus isoimmunisation (n=1), and severe maternal back pain (n=1). As many of these Caesarean sections were technically difficult, placement of a Babcock tissue forceps to identify the fetal membranes overlying the internal os of the cervix was not possible. A minimum of two random fetal membrane biopsies were therefore taken, formalin-fixed and wax-embedded (**2.2.1.**). Haematoxylin and eosin stained sections were prepared (**2.2.3.**), and morphology examined. A single random biopsy exhibiting typical midzone morphology from each fetal membrane was used for further study.

#### **2.1.3. First and second trimester fetal membranes**

First and second trimester fetal membranes from 8-20 weeks gestation were obtained from surgical termination of pregnancy (n=12). Fetal membranes were identified from the products of conception obtained. As many random biopsies as possible were taken (1-6) from the membranes identified, and formalin-fixed (**2.2.1.**). The nature of the membrane obtained (amnion, chorion, or amniochorion) was later established by microscopic assessment of a haematoxylin and eosin stained tissue section (**2.2.3.**).

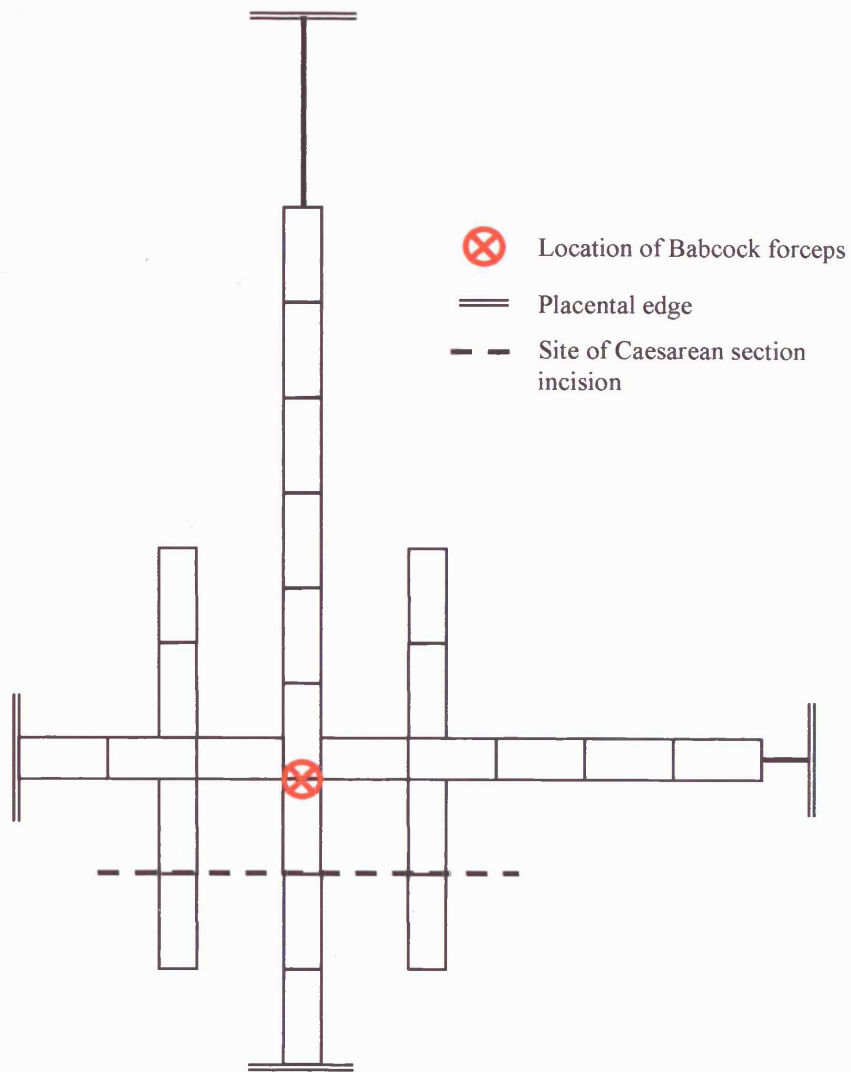


**Figure 2.1.** Example of a fetal membrane map. A two dimensional representation of each membrane map was drawn. Each biopsy is 3 x 1 cm. The location of the Babcock tissue forceps, the Caesarean section incision, and the placental edge are shown.

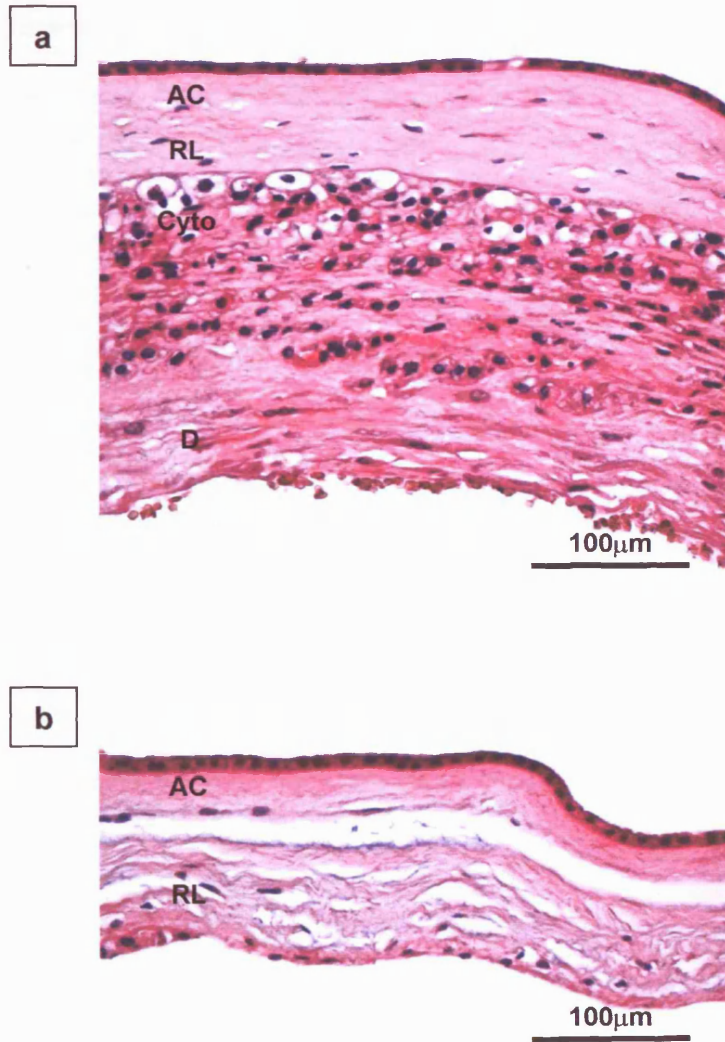


**Figure 2.2.** Haematoxylin stained sections of whole fetal membrane (a), and of an adjacent biopsy of the same fetal membrane from which the cytotrophoblast and decidua layers were removed by scraping with a glass slide (b). The connective tissue layers of the amnion (AC), the reticular layer (RL) and cytotrophoblast layer (Cyto) of the chorion, and the decidua parietalis (D) are indicated.

#### **2.1.4. First trimester decidua**

Decidua parietalis was collected from surgical termination of pregnancy. Tissue was formalin-fixed (2.2.1.), wax embedded, and confirmation of tissue identity made by microscopic assessment of a haematoxylin and eosin stained section (2.2.3.).

## **2.2. Tissue processing and preparation of sections**

### **2.2.1. Paraffin-embedded tissue sections**

Fetal membrane biopsies of approximately 3 x 1cm were rolled, placed in a tissue cassette, and fixed in 10% formal saline at room temperature for 48 hours. Formalin-fixed tissue was subjected to automated processing overnight in a Shandon Hypercentre XP (ThermoShandon, Runcorn, UK), with dehydration through seven serial grades of ethyl alcohol from 70% to 100%, and washing twice in xylene before transferring to hot wax at 60°C. Paraffin embedding was carried out with the membrane rolls embedded 'end-on' to ensure a cross-section of membrane was obtained on subsequent tissue sectioning.

Tissue sections of 4µm were cut on a Leica RM2135 microtome (Leica Microsystems (UK) Ltd, Milton Keynes, UK) onto silane-coated slides (dipped in 3% 3-aminopropyl-triethoxy-silane in methanol for 5 seconds, rinsed twice in UPH<sub>2</sub>O and dried overnight). Cut sections were dried in an oven overnight at 37°C.

### **2.2.2. Cryostat tissue sections**

Fetal membrane biopsies of approximately 3 x 1cm were rolled, and snap-frozen in isopentane that had been pre-cooled in liquid nitrogen. The snap-frozen tissue was stored in liquid nitrogen until use.

Tissue sections of 10µm were cut on a Shandon cryostat onto slides pre-coated with 3-aminopropyl-triethoxy-silane, and slides stored in containers at -80°C for up to 5 days before use.

### **2.2.3. Haematoxylin and eosin staining**

Sections of paraffin-embedded tissues processed in a Jung Autostainer XL (Leica Microsystems (UK) Ltd) automated machine. They were dried at 65°C, de-waxed and rehydrated through two changes of xylene and two changes of 99% alcohol, and washed in

water. They were then stained in Mayers haematoxylin, washed, and stained in eosin, and dehydrated through 4 changes of 99% alcohol and two changes of xylene, prior to mounting.

#### **2.2.4. Diagnosis of histological chorioamnionitis**

Haematoxylin and eosin stained sections from all tissue biopsies obtained were examined carefully under a microscope at 20x magnification in order to exclude chorioamnionitis. Chorioamnionitis was defined as described by Romero et al (Romero *et al.*, 1992), and any membrane demonstrating polymorphonuclear infiltration (cluster of at least 5 cells) within the chorion or amnion was excluded from subsequent study. Two fetal membranes obtained prior to labour, six obtained during labour, and eight obtained following labour were excluded in this manner.

### **2.3. Immunohistochemistry**

#### **2.3.1. Antibodies**

Antibodies were stored in aliquots at -20°C to avoid the use of repeated freeze-thaw cycles. Thawed aliquots were stored at 4°C and used within 7 days. Primary antibodies used within this thesis are summarised in **Table 2.1**.

#### **2.3.2. Single labelling immunohistochemistry technique**

Immunohistochemistry was performed using an avidin-biotin complex technique. The following technique is for formalin-fixed paraffin-embedded tissue, and assumes a mouse monoclonal primary antibody, with modifications given for use with a rabbit polyclonal primary antibody:

1. Tissue sections were de-waxed through three steps of xylene, rehydrated through 99%, 99% and 90% IMS and washed in dH<sub>2</sub>O (3 minutes per step).
2. Pre-treatment with pepsin digestion or microwave pre-treatment was carried out if required.
3. Endogenous peroxidase was inhibited by incubating in fresh 6% H<sub>2</sub>O<sub>2</sub> (Fisher Scientific, Loughborough, UK) for 10 minutes.
4. Sections were washed in running tap water for 5 minutes.

Primary antibody against	Clone name	Antibody type	Pre-treatment	Working conc. ( $\mu\text{g/ml}$ )	Incubation	Source
$\alpha$ -sma	1A4	Mouse monoclonal IgG2a kappa	None	1.90	1 hour, 37°C	Dako Ltd.
CD68	PG-M1	Mouse monoclonal IgG3 kappa	Pepsin digestion	3.60	Overnight, 4°C	Dako Ltd.
Cytokeratin (5, 6, 8, 17 & 19)	MNF116	Mouse monoclonal IgG1 kappa	Pepsin digestion	0.93	1 hour, 37°C	Dako Ltd.
Desmin	D33	Mouse monoclonal IgG1 kappa	None	4.50	1 hour, 37°C	Dako Ltd.
$\gamma$ -sma	B4	Mouse monoclonal IgG1 kappa	Microwave	* 1:2000 dilution	Overnight, 4°C	ICN
Osteonectin	N50	Mouse monoclonal IgG1	None	7.50	1 hour, 37°C, in 2mM CaCl <sub>2</sub>	Biodesign International Kennebunk, USA
Osteonectin	BON-I	Rabbit polyclonal antiserum	Microwave	Dilution of 1:4000	Overnight, 4°C	**
Smooth muscle myosin	SMMS-1	Mouse monoclonal IgG1 kappa	Microwave	4.26	Overnight, 4°C	Dako Ltd.
Tenascin, EGF-like repeat region	BC24	Mouse monoclonal IgG1	Pepsin digestion	1.87	1 hour, 37°C	Sigma
Tenascin	TN2	Mouse monoclonal	Pepsin digestion	* 1:2000 dilution	1 hour, 37°C	Gibco BRL, Paisley, UK
Tenascin	T2H5	Mouse monoclonal IgG1	None	11.30	1 hour, 37°C	Biogenesis, Poole, UK
Tenascin, fibronectin repeat B	$\alpha$ IIIB	Mouse monoclonal IgG1 kappa	None	4.0	Overnight, room temp.	Chemicon, Hants, UK
Tenascin		Polyclonal	Pepsin digestion	Dilution of	1 hour, 37°C	Gibco BRL
Vimentin	V9	Mouse monoclonal IgG1	None	3.87	Overnight, 4°C	Sigma

**Table 2.1.** Primary antibodies used for immunohistochemistry in this thesis.

\* Immunoglobulin concentration not available from supplier.

\*\* Gift from Dr L. W. Fisher (Fisher *et al.*, 1995).

5. Sections were then incubated in TBS-BSA buffer (58mM Tris, 145mM NaCl, 4mM MgCl<sub>2</sub>, 0.01% BSA, pH 7.6) for 5 minutes.
6. Tissue sections were then covered in 100µl of 10% Normal Rabbit Serum (Dako Ltd, Ely, UK) (NRS, diluted in TBS-BSA). (If the primary antibody was a rabbit polyclonal antiserum, then Normal Swine Serum (Dako Ltd) was used instead).
7. Excess NRS was removed, and sections were covered in 100µl primary antibody at required dilution (diluted in TBS), and incubated for the optimal time (Table 2.1). Slides were then washed in TBS-BSA for 20 minutes
8. Sections were incubated in biotinylated rabbit anti-mouse Ig secondary antibody (Dako Ltd; diluted to 2.5µg/ml in TBS-BSA) for 20 minutes at room temperature. (For a rabbit polyclonal primary antibody, biotinylated swine anti-rabbit Ig secondary antibody (Dako Ltd) at 1.4µg/ml was used).
9. Slides were washed for 20 minutes in TBS-BSA.
10. They were then incubated in Vectastain ABC Elite (Vector Laboratories, Peterborough, UK) for 30 minutes at room temperature. The ABC solution was prepared at least 30 minutes before use, to allow the formation of the avidin-biotin complexes.
11. Sections were washed twice in PBS (137mM NaCl, 8mM Na<sub>2</sub>HPO<sub>4</sub>, 1.5mM KH<sub>2</sub>PO<sub>4</sub>, pH 7.6) for 15 minutes each.
12. Sections were incubated with diaminobenzidine substrate (Vector Laboratories) for 5 minutes, and washed in running tap water for 5 minutes.
13. Counterstaining was carried out with Mayers haematoxylin (Sigma, Poole, UK) for 30 seconds, followed by washing in tap water.
14. Sections were rehydrated through graded IMS, cleared in xylene, and mounted using XAM mountant (BDH, Poole, UK).

A small number of experiments were carried out using ABC-Alkaline Phosphatase (Step 10), and developed using BCIP/NBT (Sigma) liquid substrate (Step 12).

### **2.3.3. Controls**

Negative controls included omission of primary antibody (slides incubated with TBS-BSA only), and replacement of primary antibody with equivalent concentration of mouse immunoglobulin (for mouse monoclonal primary antibodies) or rabbit serum (for rabbit polyclonal primary antibodies). Positive control tissues were determined for each individual antibody, and included in each experiment.

## **2.3.4. Modifications of the immunohistochemistry technique**

### **2.3.4.1. Pepsin digestion**

Enzyme pre-treatment may unmask antigens (Polak & Van Noorden, 1997). Pepsin digestion was carried out using 0.4% pepsin (Sigma) in 0.1M HCl for 30 minutes at 37°C. Sections were then washed in running tap water for 5 minutes.

### **2.3.4.2. Microwave pre-treatment**

Microwave pre-treatment of tissue sections has been demonstrated to unmask epitopes, or enhance staining (Polak & Van Noorden, 1997). Sections were immersed in 10mM citric acid buffer, pH 6, and microwaved at 700W for 30 minutes, ensuring the buffer level covered the tissue sections at all times. Slides were left immersed in buffer, until it had cooled to room temperature, before continuing with the immunohistochemistry protocol.

### **2.3.4.3. Cryostat tissue sections**

Immunohistochemistry was carried out on 10µm cryostat tissue sections for selected antibodies, using the following technique:

1. Cryostat tissue sections were thawed and air-dried for 30 minutes at room temperature.
2. Sections were fixed in ice cold acetone (or in 10% formal saline) for 15 minutes, air dried, and rinsed in tap water for 5 minutes.
3. Sections were incubated in 3% H<sub>2</sub>O<sub>2</sub> for 10 minutes, and rinsed in tap water for 5 minutes.
4. Sections were then incubated in TBS-BSA for 5 minutes.
5. Steps 6-14 of the protocol for formalin-fixed wax-embedded tissue (2.3.2.) were then carried out.

### **2.3.4.4. Osteonectin monoclonal antibody N50**

The buffer used in steps 5-7 of the basic immunohistochemistry technique (2.3.2.) was 20mM Hepes, 150mM NaCl, 2mM CaCl<sub>2</sub>, pH 7.4 as recommended by the supplier of the osteonectin monoclonal antibody clone N50 (Biodesign International, Kennebunk, USA).

### **2.3.5. Standardisation of technique for quantification**

The titre of each antibody used was optimised in order to confirm that the maximum number of immunoreactive cells was being detected without incurring non-specific background staining. All slides under direct comparison were included in a single experiment. The use of positive control slides assured standardisation of results, to permit comparison between different experiments.

## **2.4. Western blotting**

### **2.4.1. Tissue homogenisation**

Fetal membrane samples of approximately 3 x 3cm were snap frozen in liquid nitrogen, and stored at -80°C for later use. Samples were subsequently thawed on ice, weighed, and rinsed in PBS. A 50% (w/v) homogenate was prepared in a Heidolph RZR50 glass-glass homogeniser (Heidolph Instruments, Schwabach, Germany). The tissue was homogenised until smooth, in burst of 2-3 seconds at a time to prevent heating. All reagents were kept ice cold, and the homogenate was cooled on ice intermittently during homogenisation. For preparations for immunoblotting for tenascin-C homogenisation was carried out in an alkaline buffer of 0.2M 3-[cyclohexylamino]-1-propane-sulfonic acid (CAPS) pH 11.5, 150mM NaCl, 1mM EDTA and 1mM PMSF (McCachren & Lightner, 1992). All other preparations were carried out in 50mM Tris HCl pH 7.2, 150mM NaCl, 0.5% Igepal CA630, 100IU/ml aprotinin and 5µg/ml PMSF. The homogenates were centrifuged at 100,000g at 4°C in a Centrikon T-2070 ultracentrifuge (Kontron Instruments, Zurich, Switzerland). The supernatant was stored at -80°C until used.

### **2.4.2. Bradford assay**

The protein concentrations in the tissue extracts (2.4.1.) were determined by Bradford assay. Dye reagent (Bio-Rad, Hemel Hempstead, UK) was diluted 1:4 with dH<sub>2</sub>O for use. Tissue extracts were then diluted 1:20 in the prepared dye reagent, and optical density read at 595nm within 30 minutes. A standard curve was constructed using known concentrations (0 – 0.6mg/ml) of human serum albumin solution, and protein concentration of the tissue extracts read from the standard curve. The total protein yield per gram wet weight of tissue was also calculated.

### 2.4.3. SDS-PAGE

Electrophoresis conditions were optimised according to the molecular weight of the protein of interest, and was performed using Bio-Rad mini-gel equipment as follows:

1. The electrophoresis plates and spacers were cleaned with alcohol and assembled.
2. 6% (for tenascin-C blotting) or 10% (for osteonectin and  $\alpha$ -sma) resolving gel was prepared by mixing, in order:

	<u>6%</u>	<u>10%</u>
dH <sub>2</sub> O	5.3ml	4ml
30% acrylamide mix*	2ml	3.3ml
2M Tris pH 8.8	2.5ml	2.5ml
10% SDS	100 $\mu$ l	100 $\mu$ l
10% AMPS	100 $\mu$ l	100 $\mu$ l
TEMED	8 $\mu$ l	8 $\mu$ l

\* (30:0.8 w/v acrylamide:bisacrylamide (Protogel), (National Diagnostics, Hull, UK))

3. Reagents were mixed, poured between the gel plates, and overlaid with dH<sub>2</sub>O.

Stacking gel was prepared:

dH <sub>2</sub> O	6.8ml
30% acrylamide mix	1.7ml
1M Tris pH 6.8	1.25ml
10% SDS	100 $\mu$ l
10% AMPS	100 $\mu$ l
TEMED	10 $\mu$ l

4. The dH<sub>2</sub>O was poured off the polymerised resolving gel, an appropriate comb cleaned in alcohol and inserted between the plates, and stacking gel poured over the resolving gel.
5. Tissue extracts were mixed 1:1 with sample buffer containing 100mM Tris HCl pH 6.8, 0.2% bromophenol blue, 20% glycerol, 4% SDS and 10%  $\beta$ -mercaptoethanol, and denatured by boiling for 3 minutes prior to SDS-PAGE.

6. After polymerisation of the stacking gel, the comb was removed, the wells rinsed with dH<sub>2</sub>O, and the gel mounted in the electrophoresis apparatus.
7. Samples were loaded, and running buffer (25mM Tris, 250mM glycine (Fisher Scientific), 0.1% SDS buffer) poured into inner and outer reservoirs of tank.
8. Gels were run at 120V for 1 hour (10% gels to identify ~40kDa proteins) to 2 hours (6% gels to identify ~200kDa proteins). Biotinylated molecular weight markers (Sigma) were run in one lane.

#### **2.4.4. Western blotting**

Blotting conditions were optimised according to the molecular weight of the protein of interest. Western blotting was performed using a Biorad 3000Xi system as follows:

1. A piece of Hybond-C nitrocellulose (Amersham Pharmacia Biotech, Little Chalfont, UK) was trimmed to the size of the gel, and soaked in deionised water, followed by transfer buffer (25mM Tris, 192mM glycine, 0.02% SDS and 5% methanol at 100V). Two pieces of 3MM paper (Whatman, Maidstone, UK) were trimmed to size.
2. The blot was assembled on the transfer frame: Scotch pad, 3MM paper, gel, nitrocellulose, 3MM paper, Scotch pad. Care was taken not to trap any bubbles.
3. The frame was assembled in the tank, and filled with transfer buffer.
4. Transfer was performed at 100V for 1 hour for 10% gels for osteonectin and  $\alpha$ -sma, and at 80V for 2 hour and 15 minutes for 6% gels for tenascin-C. The tank was kept cool on ice, and the buffer within the tank stirred, throughout transfer.
5. After transfer the nitrocellulose blot was removed, carefully orientated at all times, and rinsed in dH<sub>2</sub>O.

#### **2.4.5. Immunodetection**

1. The resultant blot was blocked in 5% powdered milk solution in TBS-Tween (50mM Tris, 150mM NaCl, 0.1% Tween 20 (Sigma)) for 30 minutes, and washed for 30 minutes in 3 changes of TBS-Tween.
2. The blot was incubated in primary antibody (**Table 2.2**) in 5% powdered milk in TBS-Tween overnight at 4°C, and washed for 30 minutes in 3 changes of TBS-Tween.
3. It was then incubated with secondary antibody (**Table 2.2**) in TBS-Tween for 1 hour at room temperature, washed for 30 minutes in 3 changes of TBS-Tween.

<b>Primary antibody against</b>	<b>Clone name</b>	<b>Concentration used (<math>\mu\text{g/ml}</math>)</b>	<b>Secondary antibody</b>	<b>Concentration used (<math>\mu\text{g/ml}</math>)</b>
$\alpha$ -sma	IA4	0.04	Peroxidase conjugated sheep anti-mouse IgG (Amersham)	* 1:5000 dilution
Tenascin-C	T2H5	2.26	Biotinylated rabbit anti mouse IgG (Dako Ltd)	0.1
Osteonectin	N50	5.4	Peroxidase conjugated sheep anti-mouse IgG (Amersham)	* 1:5000 dilution
Osteonectin polyclonal antiserum	BON-I	* 1:4000 dilution	Peroxidase conjugated donkey anti-rabbit IgG (Amersham)	0.5

\* Antibody concentration unavailable

**Table 2.2.** Antibodies used for Western blotting in this thesis. Suppliers for primary antibodies as in Table 2.1.

4. For tenascin-C immunodetection only, the blot was then incubated in pre-complexed HRP conjugated avidin-biotin (ABC-Elite, Vector Laboratories) for 30 minutes at room temperature and washed for 30 minutes in 3 changes of TBS-Tween.
5. Detection was carried out with enhanced luminescence (ECL, Amersham Pharmacia Biotech). ECL reagents were brought to room temperature, mixed 1:1, pipetted over the surface of the blot for 1 minute, and drained off.
6. Blots were sealed in a plastic bag, taped into an x-ray cassette, and exposed to x-ray film (Kodak Biomax ML) for 15-120 seconds to obtain appropriate signal strength. X-ray films were processed in an Agfa Curix 60 (Agfa Gevaert Ltd, Brentford, UK), automatic processor.

Control blots were carried out by replacing primary antibody with an equal concentration of mouse IgG, and by omission of primary antibody.

#### **2.4.6. Standardisation of technique for quantification**

Titration of selected samples was performed, and the relative densities of bands plotted (2.8.2.). This confirmed that the results obtained were within the linear part of the resulting sigmoid curve, to ensure that quantification of bands was valid i.e. that bands were not saturated, and that the blotting technique was sufficiently sensitive. Where possible all samples to be directly compared were run on the same gel. Where this was not possible, the inclusion of a single sample on each gel acted as a control for standardisation of results.

#### **2.4.7. Analysis of blots**

The molecular weight of the bands obtained by Western blotting were calculated by reference to the molecular weight markers, and construction of a curve plotting the distance migrated against the logarithm of the molecular weight.

### **2.5. Reverse Transcriptase - Polymerase Chain Reaction**

#### **2.5.1. Tissue homogenisation**

Tissue to be processed for RNA extraction (approximately 100mg wet weight) was weighed and transferred to Tri-Reagent (Sigma) on ice (maximum 10% w/v) as soon as possible after collection. This was then homogenised using an Ultraturrax T25 homogeniser (Janke and Kunkel, Staufen, Germany), in short bursts of a few seconds,

keeping the homogenate on ice throughout. The homogenate was stored at -80°C for up to 1 month before RNA extraction. All processing was carried out within 1 hour of collection of tissue.

### **2.5.2. RNA extraction**

RNA extraction was carried out as per the Tri-Reagent RNA extraction protocol as follows:

1. The frozen homogenate was thawed on ice, and centrifuged in a Sanyo/MSE MicroCentaur microfuge at 13,000 rpm at 4°C for 10 minutes to precipitate insoluble material, and left to stand at room temperature for 5 minutes.
2. The supernatant was transferred to new tube, chloroform added (0.2ml per 1ml Tri-Reagent used), and shaken vigorously. This was left to stand for 10 minutes at room temperature, and centrifuged at 13,000rpm at 4°C for 15 minutes.
3. The upper, aqueous, phase containing the RNA was transferred to new tube, isopropanol added (0.5ml per 1ml Tri-Reagent used), shaken, and left to stand for 10 minutes at room temperature. This was then centrifuged at 13,000rpm at 4°C for 10 minutes.
4. The supernatant was removed, and the RNA pellet was washed in 75% ethanol in DEPC water, air dried, and dissolved in 100µl DEPC water at 4°C overnight.

RNA quality was examined by separation in an agarose gel. 1% agarose (Roche Molecular Biochemicals, Lewes, UK) was prepared in TAE/DEPC (40mM Tris-acetate, 1mM EDTA pH 8.3, prepared with DEPC water) containing 5µl/100ml ethidium bromide (Sigma). 5µl RNA was mixed with 2µl 10X loading buffer (220mM Tris-acetate, 55mM EDTA, 65% glycerol, 0.1% bromophenol blue) and 13µl DEPC water, and denatured at 65°C for 5 minutes prior to loading into gel. Gels were run in TAE/DEPC containing 5µl/100ml ethidium bromide at 85V for 1 hour. Gels were examined on an ultraviolet transilluminator, and image captured using a as a TIF file using a gel documentation system (UltraViolet Products Ltd, Cambridge, UK). Good quality RNA preparations demonstrated 28S and 18S bands, with no evidence of degradation (**Figure 2.3**).

Optical density of a 1:20 dilution of RNA in DEPC water was measured at 260nm and 280nm using a Unicam 5625 spectrophotometer (ATI Unicam, Cambridge, UK). RNA

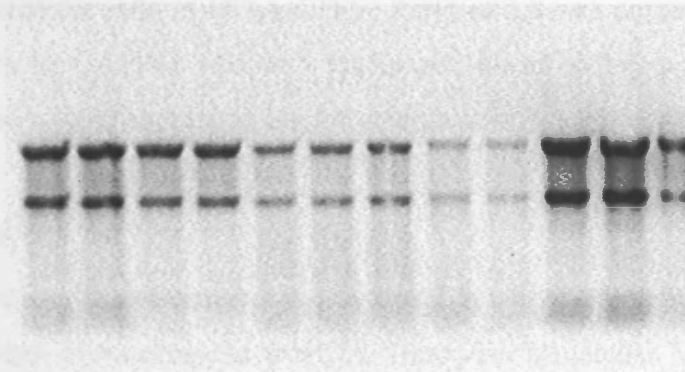


**Figure 2.3.** An example of an RNA gel, demonstrating good quality RNA preparations with 28S and 18S bands and minimal degradation.

concentration was calculated from the optical density at 260nm. The RNA quality was assessed by calculated the ratio of OD<sub>260</sub>/OD<sub>280</sub>. Ratio of 1.8 was considered optimal. RT-PCR using primers to GAPDH was also performed on all samples, with and without reverse transcriptase to confirm that no DNA contamination was present.

### 2.5.3. Primer design

Primers for polymerase chain reaction were designed to osteonectin and  $\alpha$ -smooth muscle actin. Gene sequences were obtained from the European Molecular Biology Laboratory (EMBL) database, accessed via the Sequence Retrieval Service of the European Bioinformatics Institute (<http://srs.ebi.ac.uk>), and checked against the published literature. The gene sequences for  $\alpha$ -sma (Kamada & Kakunaga, 1989; Reddy *et al.*, 1990) (EMBL Accession Number X13839) and osteonectin (Lankat-Buttgereit *et al.*, 1988) (EMBL Accession Number Y00755) were identified. The gene sequences were entered into the Primer3 primer design program (<http://www-genome.wi.mit.edu/cgi-bin/primer/primer3-www.cgi>) and 18-20 base pair primers designed to amplify a 200-300 base pair sequence. The Fasta3 program was accessed via the European Bioinformatics Institute (<http://www.ebi.ac.uk/fasta33/index.html>), and the primer sequences entered, to search for homologous sequences. This ensured that the primers designed did not share significant homology with genes other than that of interest. For  $\alpha$ -sma care was taken to avoid areas of the gene sharing homology with other members of the actin family (Miwa *et al.*, 1988). It was possible to design only one primer within a unique sequence of the gene. However the use of one unique primer together with one primer with homology to other genes allowed specific amplification of  $\alpha$ -sma. Primers to specific exons of the tenascin-C gene were synthesised, using published sequences (Bell *et al.*, 1999). This allowed amplification of specific isoforms of tenascin-C. All primers were synthesised by Sigma-Genosys (Cambridgeshire, UK), and sequences are shown in **Table 2.3**.

Optimal conditions for PCR with each primer pair was determined by carrying out RT-PCR on a positive control RNA sample (RNA extracted from SK-MEL 28 cells) at a range of annealing temperatures either side of that recommended.

Gene/exon	Primer	Sequence
$\beta$ -actin forward	ACT-F	5'-GGAGACAAGCTTGCTCATCACCATTGGCAATGAGCG-3'
$\beta$ -actin reverse	ACT-R	5'-GCGAATTCGAGCTCTAGAAGCATTGCGGTGGACG-3'
GAPD forward	GAPD-F	5'-AGAACATCATCCCTGCCTC-3'
GAPD reverse	GAPD-R	5'-GCCAAATTCGTTGTCATACC-3'
$\alpha$ -sma forward	SMA-F	5'-CATCAGGAAGGACCTCTATGC-3'
$\alpha$ -sma reverse	SMA-R	5'-CAGAGAGGAGCAGGAAAGTG-3'
Osteonectin forward	ON-F	5'-GCTCCACCTGGACTACATCG-3'
Osteonectin reverse	ON-R	5'-GGAGAGGTACCCGTCAATGG-3'
Tn-C EGF rpts forward	T-EGF-F	5'-TCCTGCTGACTGTCACAATC-3'
Tn-C EGF rpts reverse	T-EGF-R	5'-TGCTCACATACACATTTGCC-3'
Tn-C exon 8 forward	T8F	5'-CAATCCAGCGACCATCAACG-3'
Tn-C exon 9 forward	T9F	5'-AGAAAGGCAGACACAAGAGC-3'
Tn-C exon 9 reverse	T11R	5'-ACGACCTCTCCCAAATTGGG-3'
Tn-C exon 14 forward	T14F	5'-TCTGGTGCTGAACGAACTGC-3'
Tn-C exon 14 reverse	T14R	5'-GTTTCGTTTCAGCACCAGAGAT-3'
Tn-C exon 18 reverse	T18R	5'-CGTCCACAGTTACCATGGAG-3'
Tn-C exon 25 forward	T25F	5'-TGAACAAAATCACAGCCCAG-3'
Tn-C exon 27 reverse	T27R	5'-CAGTGAACCAGTTAACGCC-3'

**Table 2.3.** Primers used in this thesis.

#### **2.5.4. Reverse transcriptase reaction**

cDNA was prepared from 0.5mg RNA as follows:

1. The RNA was heated to 70°C with 15pmol oligo d(T) 12-18 (Amersham Pharmacia Biotech) in a total volume of 10µl for 5 minutes and cooled.
2. Reactions were then prepared in RT buffer (50mM Tris-HCl pH8.3, 50mM KCl, 10mM MgCl<sub>2</sub>, 10mM dithiothreitol, 0.5mM spermidine (Promega, Southampton, UK)), with 1mM dNTPs (Roche Molecular Biochemicals), 25IU RNasin™ ribonuclease inhibitor (Promega), and 5IU AMV reverse transcriptase (Promega) in a total volume of 25µl.
3. The reaction was incubated at 42°C for 1 hour. Control reactions were prepared in the absence of AMV reverse transcriptase.
4. The cDNA was stored at 4°C until use.

#### **2.5.5. Polymerase chain reaction**

Polymerase chain reaction was carried out in a Techne Genius™ thermal cycler (Techne, Cambridge, UK) as follows:

1. Reactions were performed with 1µl of prepared cDNA (2.5.4.) in 45mM Tris-HCl pH8.8, 11mM (NH<sub>4</sub>)<sub>2</sub>SO<sub>4</sub>, 4.5mM MgCl<sub>2</sub>, 800µM dNTPs, 110µg/ml bovine serum albumin, 6.7mM β-mercaptoethanol, 4.4µM EDTA pH8.0 and 10pmol of forward and reverse primers in a reaction volume of 50µl.
2. The cDNA was denatured at 98°C for 5 minutes, and held at the annealing temperature during the addition of 1IU *Taq* polymerase (Promega), and heated to 72°C for 1 minute.
3. The following cycle profile was used: 98°C for 1 minute, annealing temperature for 45 seconds, 72°C for 1 minute. The temperature was held at 72°C for 10 minutes at the end of the amplification. The optimal annealing temperatures and cycle numbers used for each primer pair are given in Table 2.4.

#### **2.5.6. Agarose gel electrophoresis**

PCR products (18µl) were mixed with 2µl loading buffer (as in 2.5.2.) and denatured at 65°C for 5 minutes. They were loaded onto a 3% agarose (Roche Molecular Biochemicals)

Primer pair	Annealing temperature (°C)	Cycle number
ACT-F/ACT-R	58	*
GAPD-F/GAPD-R	60	32
SMA-F/SMA/R	60	35
ON-F/ON-R	62	34, *
T8F/T14R	58	40
T8F/T18R	58	40
T9F/T11R	58	*
T14F/T18R	58	40, *
TEGF-F/T-EGF-R	58	*
T25F/T27R	58	*

\* 25 cycles used for production of template for probe for *in situ* hybridisation.

**Table 2.4.** Optimal annealing temperature and cycle number for primer pairs used for PCR in this thesis.

gel prepared in TAE buffer containing 15µg/100ml ethidium bromide, with 100 base pair ladder (Life Technologies, Paisley, UK) in one lane as a size marker, and run at 100V for 2 hours. Gels were visualised on an ultraviolet transilluminator, and images captured as TIF files using a gel documentation system.

### **2.5.7. DNase treatment of RNA**

RNA prepared from dissected connective tissue layers of fetal membranes (2.1.1.4.), and subjected to RT-PCR, consistently demonstrated bands in the negative control reactions prepared in the absence of reverse transcriptase. This did not occur in any other tissue preparations, and was attributed to the presence of contaminating DNA, and presumed to be secondary to the technique of scraping the fetal membranes firmly with a glass slide to remove the cellular layers of tissue. The RNA preparations obtained from these tissues were treated with RNase-free DNase as follows:

1. Reactions were prepared containing 2µg RNA, 1µl RQ1 DNase 10X reaction buffer (400mM Tris-HCl pH8.0, 100mM MgSO<sub>4</sub>, 10mM CaCl<sub>2</sub>) (Promega), 2 units RQ1 RNase-free DNase (Promega), 25IU RNasin™ ribonuclease inhibitor (Promega) and DEPC water to a total volume of 10µl.
2. The reaction was incubated at 37°C for 30 minutes, and 1µl RQ1 DNase Stop solution (20mM EGTA pH 8.0) (Promega) added.
3. The reaction was then incubated at 65°C for 10 minutes.

Control reactions were prepared in the absence of RNase-free DNase. 5µl of the reaction (containing 1µg RNA) was then used immediately in a reverse transcriptase reaction (2.5.4.), with control reactions in the absence of reverse transcriptase. PCR for GAPDH was performed, and the products run on an agarose gel and visualised. The absence of a band in the –RT control lane that had been subjected to DNase treatment confirmed the success of the reaction (Figure 2.4).

### **2.5.8. Standardisation of technique for quantification**

Selected RNA samples were subject to PCR at a range of cycle numbers for each pair of primers used for quantitative techniques. The resultant band densities (2.8.2.) were plotted against cycle number, and the cycle number was selected to be within the linear part of the

2.4.1. *GAPDH RT-PCR*

	-	-	+	+	-	-	+	+	<b>RT</b>
	-	+	-	+	-	+	-	+	<b>DNase</b>

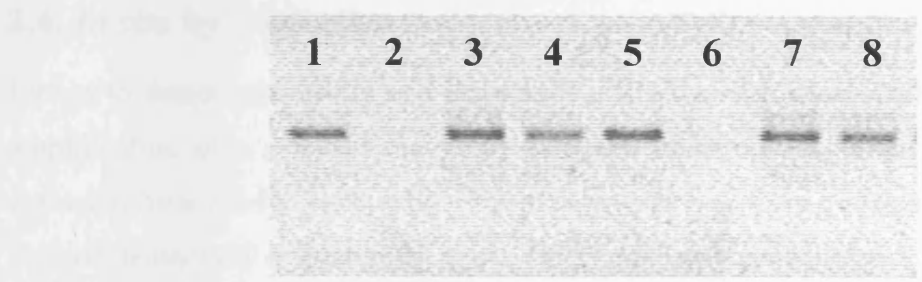


**Figure 2.4.** GAPDH RT-PCR performed on RNA obtained from dissected fetal membranes (from which the cytotrophoblast and decidua layers were removed). Control reactions in the absence of reverse transcriptase, and in the absence of DNase treatment (Lanes 1 and 5), reveal the presence of bands, suggestive of DNA contamination. However, following treatment with DNase, no band is present (Lanes 2 and 6).

curve. All samples being directly compared were analysed in a single experiment, and run on a single agarose gel.

## **2.6. *In situ* hybridisation**

Probes to detect osteonectin and tenascin-C mRNA *in situ* were synthesised by RT-PCR amplification of a selected region of the gene under investigation, employing mRNA extracted from SK-MEL-28 cells. This cell line derived from a melanoma produces large isoform tenascin-C (Carnemolla *et al.*, 1992), and was demonstrated by PCR to produce osteonectin. The template produced was then used in an 'asymmetric' PCR reaction incorporating digoxigenin to produce a single stranded antisense DNA probe. The resultant probe was used to detect mRNA *in situ* in formalin-fixed paraffin-embedded tissue sections.

### **2.6.1. Cell culture**

Human melanoma cell line SK-MEL-28 was obtained from the American Type Culture Collection (Rockville, MD, USA). Cells were grown in  $\alpha$ -minimal essential medium containing 10% v/v fetal calf serum (Life Technologies) to 90% confluence. Media was aspirated, cells washed in sterile PBS (Life Technologies) and were harvested by incubation with 0.25% trypsin-EDTA (Life Technologies) at 37°C for approximately 5 minutes (monitored intermittently under an inverted microscope). Culture media containing 10% FBS (Life Technologies) was added to the flask to stop the trypsin digestion, and the media/cells aspirated from the flask and centrifuged at 200g for 10 minutes.

### **2.6.2. mRNA extraction from cells**

mRNA was harvested from SK-MEL-28 cells as follows:

1. The harvested cells from one 25cm<sup>2</sup> flask were lysed in 1ml of 100mM Tris-HCl pH 8.0, 500mM LiCl, 10mM EDTA pH 8.0, 1% SDS and 5mM dithiothreitol, with repeated pipetting to shear the DNA.
2. 40 $\mu$ l Oligo d(T)<sub>25</sub> Dynabeads™ (Dynal, Merseyside, UK), was added, and incubated at room temperature for 10 minutes.

3. This was pelleted in a microfuge, and washed in 200µl washing buffer (10mM Tris-HCl pH 8.0, 0.15M LiCl, 1mM EDTA) with 0.1% SDS, and then three times in washing buffer without SDS.
4. The resulting pellet was resuspended in 20µl DEPC water.

SK-MEL-28 cDNA was prepared using 10µl SK-MEL-28 mRNA as in steps 2-3 of 2.5.4. The cDNA was stored at 4°C until use.

### **2.6.3. PCR production of template**

A DNA template for later production of probe was synthesised by PCR amplification of 1µl SK-MEL-28 cDNA using primer pairs to the specific gene or isoform of interest. Amplification was carried out as in 2.5.5., using biotinylated forward primer and non-biotinylated reverse primer, at optimal annealing temperature (Table 2.4), for 25 cycles. PCR product was run on an agarose gel as in 2.5.6. to confirm satisfactory amplification.

### **2.6.4. Labelling of *in situ* hybridisation probes**

#### **2.6.4.1. Asymmetric PCR**

One µl of PCR product (2.6.3.) was used as a template for production of a probe for *in situ* hybridisation. Reactions were performed in 45mM Tris-HCl pH 8.8, 11mM (NH<sub>4</sub>)<sub>2</sub>SO<sub>4</sub>, 4.5mM MgCl<sub>2</sub>, 200µM dATP, 200µM dCTP, 200µM dGTP, 130µM dTTP, 110µg/ml bovine serum albumin, 6.7mM β-mercaptoethanol, 4.4µM EDTA pH 8.0 with 100pmol reverse primer and 70µM digoxigenin-11-dUTP (Roche Molecular Biochemicals). One IU *Taq* polymerase was added after an initial denaturation to 98°C, and amplification carried out for 20 cycles at optimal annealing temperature (Table 2.4.). Any double-stranded contaminant would be labelled with biotin, due to the initial production of template using biotinylated forward primer. This was removed by incubation with Streptavidin-Dynabeads™ (Dyna) to give a single-stranded digoxigenin labelled probes. Beads were pelleted in a Magnetic Particle Concentrator® (Dyna), and supernatant removed. The beads were prepared by resuspending in Bind and Wash buffer (10mM Tris HCl pH 7.5, 1mM EDTA, 2M NaCl), pelleted and supernatant removed. This process was repeated twice, before resuspending the Dynabeads in Bind and Wash buffer. 45µl asymmetric PCR product was incubated with 2µl prepared Dynabeads and incubated at room temperature for 15 minutes. The beads were pelleted on a Magnetic Particle Concentrator® (Dyna),

and the supernatant containing the probe removed. The labelled probe was aliquoted and stored at -20°C until use. Antisense probes were synthesised in this manner to  $\beta$ -actin (positive control), osteonectin, all isoforms of tenascin-C (primers T25F/T27R and TEGF-F/TEGF-R) and large isoforms of tenascin-C (primer pairs T9F/T11R and T14F/T18R). Primer sequences are in **Table 2.3**. Sense probes were also synthesised, for use as negative controls.

#### **2.6.4.2. Testing of *in situ* hybridisation probes**

Digoxigenin labelling of probes was assessed by production of a test strip:

1. Starting probe concentration was assumed to be 20ng/ml (J. H. Pringle, personal communication). Serial dilutions of probe from 100pg/ml down to 0.01pg/ml were made in 900mM NaCl, 90mM trisodium citrate dihydrate, 0.2mg/ml prepared salmon sperm DNA (an initial 10mg/ml solution of salmon sperm DNA was sonicated for 30x 30-second bursts, denatured at 100°C for 10 minutes, and aliquots frozen at -20°C for subsequent dilution and use).
2. 1 $\mu$ l of each probe dilution was spotted onto a sheet of nitrocellulose (unbranded), air dried and baked at 80°C for 2 hours.
3. The nitrocellulose was blocked in TBS-BT (TBS containing 3% BSA with 0.1% Triton-X) for 20 minutes, baked at 80°C for 20 minutes and left overnight.
4. It was then rehydrated in TBS-BT for 10 minutes at room temperature.
5. It was incubated in alkaline phosphate conjugated anti-digoxigenin Fab fragments 1.25U/ml (Roche Molecular Biochemicals) for 30 minutes, washed twice for 5 minutes each in TBS, and rinsed in UPH<sub>2</sub>O.
6. It was incubated in 100mM Tris pH 9.5, 100mM MgCl<sub>2</sub>, 0.5M NaCl for 5 minutes, and developed in BCIP/NBT (Sigma) for 2 hours in the dark.

Adequate labelling was considered to have occurred if probe was detected at 1pg/ml (**Figure 2.5**).

#### **2.6.5. *In situ* hybridisation**

*In situ* hybridisation was carried out on formalin-fixed, wax-embedded tissue sections, using methodology modified from Pringle (Pringle, 1995). All glass slides used were silane coated (dipped in 1.7% 3-aminopropyltriethoxy-silane in acetone for 5 seconds, rinsed in

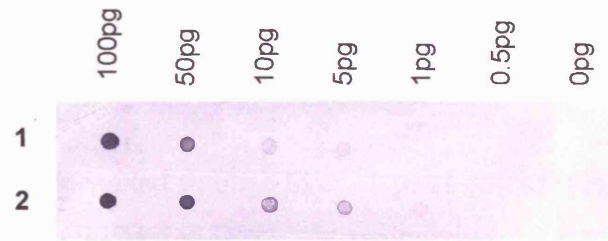


**Figure 2.5.** Example of a test strip, demonstrating labelling of probes for *in situ* hybridisation. Probe 1 is detected at 5pg, and probe 2 at 1pg.

acetone and twice in UPH<sub>2</sub>O and dried overnight) and all coverslips siliconised (dipped in 2% dimethyldichlorosilane (BDH) in chloroform for 5 seconds, rinsed twice in UPH<sub>2</sub>O and dried overnight). All solutions used up to and including the hybridisation step were prepared using DEPC H<sub>2</sub>O.

1. Tissue sections were de-waxed through three steps of xylene, rehydrated through 99%, 99% and 90% IMS and washed in DEPC H<sub>2</sub>O (3 minutes per step).
2. Pre-treatment with proteinase K (Roche Molecular Biochemicals) (2-10µg/ml in 50mM Tris HCl pH 7.6) was carried out for 1 hour at 37°C.
3. The slides were then washed for 10 minutes in three changes of DEPC H<sub>2</sub>O.
4. Slides were incubated in prehybridisation buffer (0.6M NaCl, 1 x PE (50mM Tris HCl pH 7.5, 5mM EDTA, 2.2mM tetrasodium pyrophosphate, 0.2% polyvinyl pyrrolidone, 0.2% Ficoll), 10% dextran sulphate, 50% ultrapure formamide (Life Technologies), and 150µg/ml pre-treated salmon sperm DNA (2.6.4.2. step 1) (boiled for 5 minutes)), for 1 hour at 37°C.
5. Prehybridisation solution was drained from the slides, and labelled probe diluted in prehybridisation solution (25µl) was applied and covered with a siliconised coverslip. Slides were incubated overnight at 37°C.
6. The coverslips were removed, and the slides washed in 50% formamide (BDH) and 2x SSC (0.3M NaCl, 30mM trisodium citrate dihydrate) twice, each for 10 minutes. They were then incubated in TBS-BT for 5 minutes at room temperature.
7. Slides were incubated in 1.25U/ml alkaline phosphate conjugated anti-digoxigenin Fab fragments (Roche Molecular Biochemicals) for 30 minutes at room temperature, and washed twice in TBS pH 7.6 for 5 minutes each. Slides were rinsed in dH<sub>2</sub>O.
8. Detection was carried out by incubation with BCIP/NBT (Sigma) in the dark for 6 hours.
9. Slides were washed in running tap water for 5 minutes, and mounted with Aquamount (BDH).

The technique required optimisation for each tissue block used, and for each probe used. Optimal proteinase K concentration required was determined for each tissue block used, by control *in situ* hybridisation experiments with β-actin probe. Concentrations of 2-10µg/ml were used. Probe concentration was also optimised. Initial dilution of 1:40 v/v was made. Optimal probe concentration for use was determined by *in situ* hybridisation and titration

of probe on a positive control tissue (umbilical cord) to obtain good signal strength without non-specific background staining. Negative controls included hybridisation with a sense probe, and pre-treatment of the tissue section with RNase (0.1mg/ml RNase (pancreatic RNase, Sigma) in 50mM Tris pH 7.5, 50mM MgCl<sub>2</sub> was added to the slide following step 3, incubated at 37°C for 1 hour, and washed in UPH<sub>2</sub>O before proceeding to step 4).

## **2.7. Organ culture**

### **2.7.1. Fetal membrane biopsy technique**

Fetal membranes for culture were obtained from the midzone of the fetal membranes from elective Caesarean section prior to the onset of labour at term, performed for breech presentation or for previous Caesarean section. Cultures were performed on whole fetal membranes, 'scraped' fetal membranes, and 'superscraped' fetal membranes. 'Scraped' fetal membranes were scraped with a glass microscope slide to remove the majority of the decidua. 'Superscraped' fetal membranes were prepared as in 2.1.1.4. in order to remove decidua and cytotrophoblast, confirmed histologically. 8mm diameter biopsies were obtained using biopsy punches (Stiefel Laboratories, Bucks., UK).

### **2.7.2. Fetal membrane culture**

All manipulation of fetal membranes and reagents for culture were performed using sterile technique in a class II cabinet. Membrane discs were cultured at 37°C in 5% CO<sub>2</sub>. Selected experiments were performed in the presence of 1% O<sub>2</sub> and 9-13% CO<sub>2</sub> (created with Anaerogen AN25 sachet (Oxoid Ltd, Basingstoke, UK) in a 2.5 litre sealed chamber).

#### **2.7.2.1. Culture media**

Culture media was prepared at the beginning of each culture and stored at 4°C. Culture media was Dulbecco's Modified Eagles Medium with Glutamax-I (DMEM, Life Technologies) containing 100U/ml penicillin, 100µg/ml streptomycin and 0.25µg/ml amphotericin B (Life Technologies), with and without 10% fetal bovine serum (Life Technologies).

### **2.7.2.2. Culture technique**

8mm fetal membrane discs were washed in prepared culture media. Day 0 discs were formalin-fixed. Discs were cultured in 1ml culture media in 24 well plates. Minimally duplicate, and more commonly triplicate, discs were cultured. Media was changed daily. Discs were removed every 2 days, formalin-fixed and wax-embedded (2.2.1.). Discs were cut in half, and embedded in wax 'end-on' so that the fetal membrane cross section across the maximum diameter of the disc would be obtained when the tissue block was sectioned. Cultures were carried out for 6 days. Formalin-fixed wax-embedded tissue sections were used for haematoxylin and eosin staining (2.2.3.), and for immunohistochemistry (2.3.).

### **2.7.2.3. Additives**

Additives used in cultures are in Table 2.5. Media was prepared fresh daily. The concentration of each additive used was determined from the available literature, for induction of  $\alpha$ -sma, Tn-C or osteonectin expression *in vitro*. Negative control discs were cultured for each additive used, with the additive diluent only added to the culture media. All cultures performed with the additives in Table 2.5 were performed without the addition of fetal bovine serum.

## **2.8. Image analysis**

### **2.8.1. Histological and immunohistochemical image analysis**

Image analysis for immunohistochemistry slides was performed by visualising slides on a Zeiss Axioplan microscope, capturing images using an attached Sony Model DXC-151P video camera and Scion Image™ software on an IBM-compatible personal computer.

All histochemical and immunohistochemical image analysis was performed on systematically captured random fields examined at 40x magnification. For fetal membrane rolls, fields were captured along the axes 12 o'clock to 6 o'clock and 9 o'clock to 3 o'clock. Only fields with true cross sections of fetal membrane (not oblique cuts) were used, as assessed by the finding of a single layer of amniotic epithelial cells. Ten fields per biopsy were examined. Subsequent re-analysis of the data within Chapter 3 revealed that all significant differences would have also been detected by examining 5 fields per biopsy. Therefore 5 fields per biopsy were analysed for the large quantity of biopsies examined in the fetal membrane maps within Chapter 4. For tissues not in rolls (predominantly first and

<b>Additive</b>	<b>Concentration used</b>	<b>Diluent (Final concentration in media)</b>
TGF- $\beta_1$ (Promega)	10ng/ml (Rettig <i>et al.</i> , 1994; Jester <i>et al.</i> , 1996; Tamm <i>et al.</i> , 1996; Matthey <i>et al.</i> , 1997)	0.012% acetonitrile, 0.0001% trifluoroacetic acid
TNF- $\alpha$ (R&D Systems, Abingdon, UK)	10ng/ml (Matthey <i>et al.</i> , 1997)	0.1% PBS, 0.0001% BSA
IL-1 $\beta$ (R&D Systems)	1ng/ml (Rettig <i>et al.</i> , 1994)	0.1% PBS, 0.0001% BSA
Endothelin-1 (ICN)	10 <sup>-7</sup> M (Valentich <i>et al.</i> , 1997)	1% dH <sub>2</sub> O
IL-4 (R&D Systems)	1ng/ml (Matthey <i>et al.</i> , 1997)	0.02% PBS, 0.00002% BSA
bFGF (R&D Systems)	10ng/ml (Jester <i>et al.</i> , 1996; Matthey <i>et al.</i> , 1997)	0.1% PBS, 0.0001% BSA, 1nM dithiothreitol
GM-CSF (R&D Systems)	100ng/ml (Bussolino <i>et al.</i> , 1991)	2% PBS, 0.002% BSA
Angiotensin II (Calbiochem, Notts, UK)	10 <sup>-7</sup> M (Mackie <i>et al.</i> , 1992; Campbell & Katwa, 1997)	0.0005% acetic acid

**Table 2.5.** Additives used in fetal membrane organ culture, with working concentrations used, and the diluent for each additive, with which the negative control cultures are performed. The references from which the concentration of the additives are derived are shown.

second trimester fetal membrane), ten random fields evenly spaced along the length of the biopsy were examined.

#### **2.8.1.1. Morphology measurements**

The thickness of the connective tissue layers (amniotic connective tissue, spongy layer, reticular layer) of the fetal membranes was measured using captured images of haematoxylin and eosin stained sections. Sections immunohistochemically stained with anti-cytokeratin were used for measurement of the cytotrophoblast and decidual layers, to allow clear distinction between the cell types. All measurements were performed using the Straight-Line tool in Scion Image™. The scale was calibrated by previous measurements of captured images of a graticule, allowing direct measurements in  $\mu\text{m}$  to be performed. Ten fields per fetal membrane biopsy were examined (five fields per biopsy for mapping biopsies in Chapter 4). The fetal membrane morphometric index (FMMI) was calculated as the ratio of the total connective tissue thickness (amniotic connective tissue, spongy and reticular layers) to the total cellular tissue thickness (cytotrophoblast and decidual layers).

The diameter of fetal membrane discs used in organ culture measurements was measured in a similar fashion. In order to allow for any distortion and folding of the discs when processed for histology, measurements were made by drawing along the pseudobasement membrane using the freehand drawing tool, and measuring the length of the line.

#### **2.8.1.2. Cell counting**

Immunoreactive cells were counted in each layer of the fetal membrane per computer screen width ( $176\mu\text{m}$ ) in 10 fields per fetal membrane biopsy (5 fields per biopsy for mapping biopsies in Chapter 4). For cell density measurement, the thickness of the relevant layer of the fetal membrane was measured on the same field as the cells counted, allowing calculation of the density per cross sectional area of the fetal membrane for each field.

The same technique was used for counting mRNA-positive cells detected by *in situ* hybridisation.

### **2.8.1.3. Quantification of extracellular matrix staining**

The immunoreactivity obtained with antibodies against Tn-C was confined to the extracellular matrix. A methodology to quantify the staining obtained with monoclonal antibody BC24 was developed. Slides used for this technique were not counterstained with haematoxylin. Ten systematically chosen fields were examined (2.8.1.) in each fetal membrane roll. Images were captured as TIF files, and viewed using Scion Image™ software. The layer under examination (amniotic connective tissue layers or reticular layer) was outlined using the freehand drawing tool, and area measured. Images were converted to black and white, and a threshold set to differentiate immunoreactivity. The function ‘analyse particles’ was used to measure the area of all immunoreactivity above the defined threshold within the layer. The area of immunoreactivity was expressed as a percentage of the area of the layer of the fetal membranes for each field examined. The threshold was chosen to best differentiate between the varying degrees of immunoreactivity apparent by visual inspection of all fetal membranes examined. The technique was standardised by the inclusion of three fetal membrane biopsies expressing high, medium and low BC24 immunoreactivity within the reticular layer in each immunohistochemistry experiment.

### **2.8.2. Analysis of Western blots**

Western blots were scanned on a Umax Astra 1220P flatbed scanner, and saved as TIF files. Band density was assessed by measuring the area under the curve using the GelPlot2 macro in Scion Image™. This allows a box to be drawn around the specific bands on the image, and a lane profile plot to be drawn. The area under the curve for each lane was measured. Where possible all samples being compared were on the same Western blot. If this was not possible, then a single sample was repeated on each blot, to act as an internal control for standardisation.

Band intensity of RT-PCR products was assessed using the same technique.

## **2.9. Statistical analysis**

Prior to analysis of data, Shapiro-Wilk test was applied to each data set to test for evidence of deviation from a normal distribution (StatsDirect™ statistical software). Only where no evidence of deviation from normality was demonstrated was a parametric statistical test applied. 5% significance level was used for all statistical analysis.

Correlation between sets of data (e.g. correlating  $\alpha$ -sma expression with fetal membrane morphology) was assessed using linear regression analysis (parametric), or Spearman Rank Correlation (non-parametric), using Statview™ statistical software. Comparison between two sets of data for evidence of significant differences (e.g. comparing Western blot densitometry values between ‘cervical’ and midzone biopsies) was made using Student t-test (parametric) or Mann-Whitney U test (non-parametric) using Statview™. Paired t-test was used where pairs of data from each biopsy were being compared. Multiple comparisons (e.g. comparing  $\alpha$ -sma expression between physiological groups and between biopsy sites) were made using two-way analysis of variance with post-hoc analysis (Scheffe’s test) using Statview™. Physiological groups (i.e. pre-labour, labour, post-labour) and biopsy site (‘cervical’/rupture line, midzone) were set as independent factors in the analysis.

Determination of an apparent ‘threshold’ in decidual thickness for prediction of  $\alpha$ -sma expression in the fetal membranes (Chapter 4) was made using receiver-operating-curve (ROC) analysis using StatsDirect™.  $\alpha$ -sma positivity was determined by measuring the maximum area under the curve, and the decidual thickness which best predicted this calculated.

Areas of fetal membrane affected by morphological change, and by immunoreactivity to antibodies, were calculated. The length of the long and short axes were measured (the length of each biopsy was 3cm), and halved to calculate the long (a) and short (b) radius. The area was then calculated by the formula to calculate the area of an ellipse:

$$\text{Area} = \pi ab$$

## **Chapter 3**

### **Cellular populations of the connective tissue layers**

#### **3.1. Introduction**

The cellular population of the connective tissue layers of the fetal membrane have been the subject of controversy, as discussed in Chapter 1. The fibroblast layer of the amnion contains fibroblasts (vimentin positive, or V cells) and macrophage-like cells (1.2.2.4.). It has been suggested that these exist in approximately 60:40 ratio (Malak, 1995). The reticular layer of the chorion contains desmin-positive cells and macrophage-like cells (1.2.2.7.), again in approximately 60:40 ratio. The 'fibroblastic' reticular layer cells are believed to be myofibroblasts (1.2.2.7.).

Regional differences in fetal membrane structure have been observed following labour and delivery at term (1.4.2.). A 'Zone of Altered Morphology' (ZAM) associated with a restricted area of the rupture line following labour, membrane rupture, and delivery at term, exhibits a marked increase in thickness in the connective tissue layers of both the amnion and chorion, and a decrease in thickness of the cellular layers of the membrane. This is in comparison to fetal membrane biopsies obtained distal to this site ('midzone') (Malak & Bell, 1994b). The features of altered morphology are associated with an increase in overall cellularity of the reticular layer, and a change in the cellular populations within this layer. Thus within the ZAM the reticular layer contains 20% macrophages (no change in the absolute number of cells), and 80% 'VD' cells (Malak, 1995). Although the ZAM exhibits a number of features characteristic of a 'wound response', and ultrastructurally the 'fibroblastic' 'VD' cell population of the reticular layer appear to be myofibroblasts, they have been reported as negative for  $\alpha$ -sma (Malak, 1995), a marker considered characteristic of the myofibroblast of the 'wound response' (1.5.2.2.).

The hypothesis was therefore developed that the ZAM, which exhibits features of a 'wound response', may be generated during labour, or be present prior to the onset of labour, and may exhibit structural weakness and represent the site of initial membrane rupture. The usual site of fetal membrane rupture is in the membranes directly overlying

the internal os of the cervix (Bourne, 1962), and this is proposed as the likely site of structural alterations in the fetal membranes if present prior to the onset of labour.

### **3.2. Aims**

- To determine whether regional structural changes are present prior to and during labour at term associated with the fetal membranes overlying the cervix, by examining biopsies obtained from membranes overlying the cervix and from the midzone.
- To establish the phenotype of the cellular populations of the amnion and chorion, with particular reference to the macrophage population, and the fibroblast/myofibroblast cell phenotype defined by intermediate filament and myofilament expression.
- To determine whether alterations in the cellular populations and in the connective tissue layers of the amnion and chorion are associated with anatomically defined regions, and/or present prior to or during labour.
- To determine whether any changes in the cellular populations observed are associated with structural changes in the fetal membranes.

### **3.3. Materials and Methods**

#### **3.3.1. Fetal membrane samples**

Regional fetal membrane biopsies obtained prior to and during labour at term were examined. Regional fetal membrane biopsies obtained following labour and delivery at term were also included as a positive control, to confirm the previous results. As the ZAM has been reported to be commonly found at one end of the rupture line (Malak & Bell, 1994b), biopsies were obtained from each end and from the middle of the rupture line. The biopsy with the most extreme altered morphology was used for subsequent work. This method should obtain fetal membrane within the ZAM, although may not obtain fetal membrane with the most extreme altered morphology present.

Fetal membranes were obtained at term prior to labour (n=11), during labour (n=5), and following spontaneous labour and vaginal delivery (n=5) as previously described (2.1.1.).

### **3.3.2. Immunohistochemistry**

Immunohistochemistry was carried out on formalin-fixed wax-embedded fetal membrane samples using monoclonal antibodies to vimentin,  $\alpha$ -sma, desmin, CD-68,  $\gamma$ -sma, and smooth muscle myosin as previously described (2.3.). Immunohistochemistry for  $\alpha$ -sma was also carried out on acetone-fixed and formalin-fixed cryostat tissue sections (2.2.2.).

### **3.3.3. SDS-PAGE and Western blotting**

Fetal membrane extracts from paired 'superscraped' (2.1.1.4.) fetal membrane biopsies (n=5) were separated on 10% polyacrylamide gels and transferred to nitrocellulose as previously described (2.4.). Monoclonal antibody 1A4 was used to detect  $\alpha$ -sma using enhanced chemiluminescence (2.4.5.). The resultant bands were quantified using Scion Image™ (2.8.2.).

### **3.3.4. Image analysis**

The thickness of the constituent layers of the fetal membranes were measured (2.8.1.1.) and the numbers of cells immunoreactive to the monoclonal antibodies were counted (2.8.1.2.).

### **3.3.5. RT-PCR**

RT-PCR using primers to  $\alpha$ -sma and GAPDH was carried out (2.5.4. & 2.5.5.), and the band densities analysed using Scion Image™ (2.8.3.).

### **3.3.6. Statistical analysis**

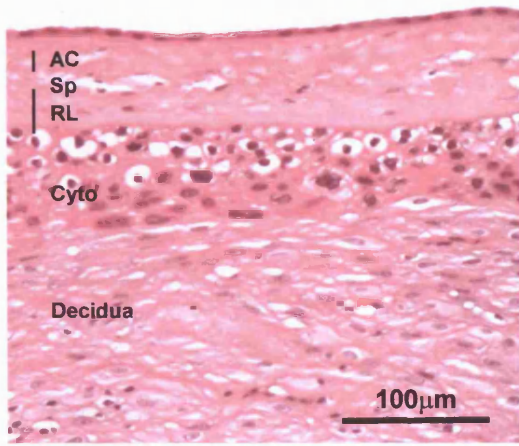
Statistical analyses used to compare thickness of layers of the fetal membranes, numbers of immunoreactive cells, Western blot and RT-PCR band densities, and to correlate parameters are described in 2.9.

## 3.4. Results

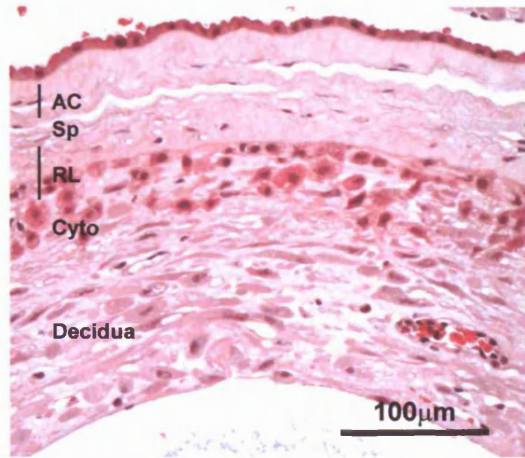
### 3.4.1. Fetal membrane morphology

A wide range of morphology of fetal membranes was observed. Examples are seen in **Figure 3.1**. The measurements of the individual layers of the fetal membranes prior to, during, and following labour at term are shown in **Table 3.1**. The thickness of each of the individual connective tissue layers of the fetal membrane is significantly greater in the post-labour rupture line biopsies compared to their midzones: amniotic connective tissue 75% greater ( $p=0.031$ ), spongy layer 138% greater ( $p=0.011$ ), reticular layer 85% greater ( $p=0.029$ ). The thickness of the decidua is significantly less in the post-labour rupture line biopsies compared to their midzones (85% reduction in thickness,  $p=0.0012$ ). These results are consistent with the previously published regional structural alterations in the fetal membranes obtained after labour at term (Malak & Bell, 1994b). Thus the fetal membrane morphometric index (FMMI) is significantly higher in the post-labour rupture line biopsies compared to their midzones (2.33 vs 0.28,  $p=0.019$ ) (**Table 3.1**). Within the pre-labour fetal membranes, the spongy layer was significantly thicker in the 'cervical' biopsies compared to the midzones (57% higher,  $p=0.028$ ). Although there were no significant differences in thickness of the other layers observed in group overall, significant differences in thickness were observed within individual patients: amniotic connective tissue (1 out of 5) and reticular layer (3 out of 5) thickness greater in 'cervical' compared to midzone; cytotrophoblast layer (2 out of 5) and decidua (3 out of 5) thickness reduced in 'cervical' compared to midzone; thus the FMMI was significantly greater in 'cervical' compared to midzone in 2 out of 5 patients. In the labour affected fetal membranes only the decidua thickness exhibited a significant difference between 'cervical' and midzone fetal membranes in the group as a whole (83% reduction in 'cervical' compared to midzone'  $p=0.035$ ). However on examination of fetal membrane pairs from individual patients, a number of significant differences in thickness were observed: amniotic connective tissue (2 out of 5), spongy layer (3 out of 5) and reticular layer (4 out of 5) thickness greater in 'cervical' compared to midzone; cytotrophoblast layer (3 out of 5) and decidua (4 out of 5) thickness reduced in 'cervical' compared to midzone. Thus in the group as a whole, the FMMI was significantly greater in 'cervical' compared to midzone biopsies (1.52 vs 0.38,  $p=0.012$ ).

a



b



c

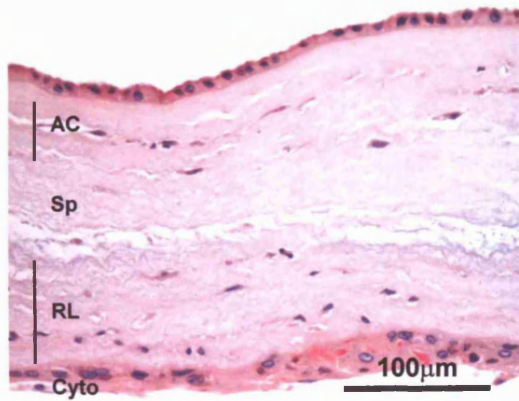


**Figure 3.1.** Haematoxylin and eosin stained sections of fetal membrane illustrating the range of morphology observed. Fetal membranes illustrated were from the midzone prior to labour (a), overlying the cervix prior to labour (b), and from the rupture line following labour and delivery (c). AC, amniotic connective tissue; Sp, spongy layer; RL, reticular layer; Cyto, cytotrophoblast layer; Decidua, decidua parietalis. Scale bar of 100µm is shown.

	Pre-labour (n=5)		Labour (n=5)		Post-labour (n=5)	
	Midzone	'Cervical'	Midzone	'Cervical'	Midzone	Rupture line
<b>Amnion connective tissue layers</b>	18.47 ±1.87	21.19 ±1.24	23.36 ±4.32	30.80 ±4.36	17.18 <sup>a</sup> ±2.52	30.04 <sup>a</sup> ±4.23
<b>Spongy layer</b>	11.54 <sup>b</sup> ±1.28	18.07 <sup>b</sup> ±2.08	14.91 ±2.73	28.91 ±5.62	12.10 <sup>c</sup> ±1.79	28.83 <sup>c</sup> ±4.76
<b>Reticular layer</b>	38.68 ±5.09	48.42 ±6.00	50.41 ±14.56	74.55 ±13.91	41.35 <sup>d</sup> ±6.53	76.36 <sup>d</sup> ±11.49
<b>Cyto layer</b>	81.66 ±6.75	75.04 ±11.84	75.24 ±13.67	57.27 ±6.39	70.06 ±9.27	50.86 ±6.07
<b>Decidua</b>	156.55 ±30.43	114.31 ±39.07	211.34 <sup>e</sup> ±67.87	36.80 <sup>e</sup> ±11.10	214.69 <sup>f</sup> ±36.40	31.41 <sup>f</sup> ±7.78
<b>FMMI</b>	0.35 ±0.07	0.55 ±0.06	0.38 <sup>g</sup> ±0.08	1.52 <sup>g</sup> ±0.35	0.28 <sup>h</sup> ±0.05	2.33 <sup>h</sup> ±0.88

**Table 3.1.** Thicknesses of the individual layer of fetal membrane biopsies obtained prior to, during, and following labour at term. All measurements are in  $\mu\text{m}$ . Ten fields per biopsy were examined. The mean value and standard error of the mean (derived from n=5 patients) are shown. Comparisons between biopsy sites and physiological group were using two way ANOVA and Scheffes test. Significant differences are highlighted: a, b, c, d, e, f, g & h, all  $p < 0.05$ .

### **3.4.2. Cellular phenotyping**

Immunohistochemistry was carried out to characterise the cellular populations, and intermediate filament and myofibrillar phenotype, of the connective tissue cells of the term fetal membrane. Five pairs of membrane biopsies were examined from each of 3 groups: prior to labour, during labour, and following labour at term. A summary of the results is given in **Tables 3.2 & 3.3**.

#### **3.4.2.1. Vimentin**

Vimentin immunoreactivity was observed within cells of the fibroblast layer and the reticular layer (**Figure 3.2**). No cells negative for vimentin were noted. The number of vimentin immunoreactive cells was therefore used to represent the total cell count within the fibroblast and reticular layers.

#### **3.4.2.2. Desmin**

Desmin immunoreactive cells were observed within the reticular layer as previously reported, but very rarely observed in the fibroblast layer (**Figure 3.3**).

#### **3.4.2.3. $\alpha$ -smooth muscle actin**

$\alpha$ -sma immunoreactive cells were detected in the fibroblast and reticular layers. Their distribution was restricted, in that they were detected in high numbers principally in the reticular layer of 'cervical' and rupture line biopsies, and only rarely in midzone biopsies (**Figure 3.4a**). In biopsies with lower numbers of immunoreactive cells, positive cells were detected toward the basal aspect of the reticular layer, adjacent to the cytotrophoblast layer (**Figure 3.4b**). In biopsies with higher numbers of immunoreactive cells, positive cells were distributed throughout the reticular layer (**Figure 3.4c & d**).

Cells immunoreactive for  $\alpha$ -sma were observed in the fibroblast layer of some, but not all, 'cervical' pre-labour and labour biopsies and rupture line post-labour biopsies (**Figure 3.4d**). They were not observed in the fibroblast layer of midzone biopsies (**Figure 3.4a**).

The  $\alpha$ -sma immunoreactivity observed within the fibroblast and reticular layer cells in this study conflicts with previously reported results (Malak, 1995). The work in the previous study was carried out on acetone fixed cryostat tissue sections. In order to investigate this,

	Pre-labour		Labour		Post-labour	
	Midzone	'Cervical'	Midzone	'Cervical'	Midzone	Rupture line
<b>Vimentin</b>	+	+	+	+	+	+
<b>Desmin</b>	-	-	-	-	-	-
<b><math>\alpha</math>-sma</b>	-	+/-	-	+/-	-	+/-
<b><math>\gamma</math>-sma</b>	-	-	-	-	-	+/-
<b>SMM</b>	-	-	-	-	-	-
<b>CD68</b>	+	+	+	+	+	+

**Table 3.2.** Summary of immunohistochemistry results for the fibroblast layer of regional fetal membrane biopsies obtained prior to, during, and following labour at term. The presence (+), absence (-), and inconsistent presence/absence (+/-) of immunoreactive cells is indicated.

	Pre-labour		Labour		Post-labour	
	Midzone	'Cervical'	Midzone	'Cervical'	Midzone	Rupture line
<b>Vimentin</b>	+	+	+	+	+	+
<b>Desmin</b>	+	+	+	+	+	+
<b><math>\alpha</math>-sma</b>	-	+/-	-	+	-	+
<b><math>\gamma</math>-sma</b>	-	+/-	-	+/-	-	+/-
<b>SMM</b>	-	-	-	-	-	-
<b>CD68</b>	+	+	+	+	+	+

**Table 3.3.** Summary of immunohistochemistry results for the reticular layer of regional fetal membrane biopsies obtained prior to, during, and following labour at term. The presence (+), absence (-), and inconsistent presence/absence (+/-) of immunoreactive cells is indicated.

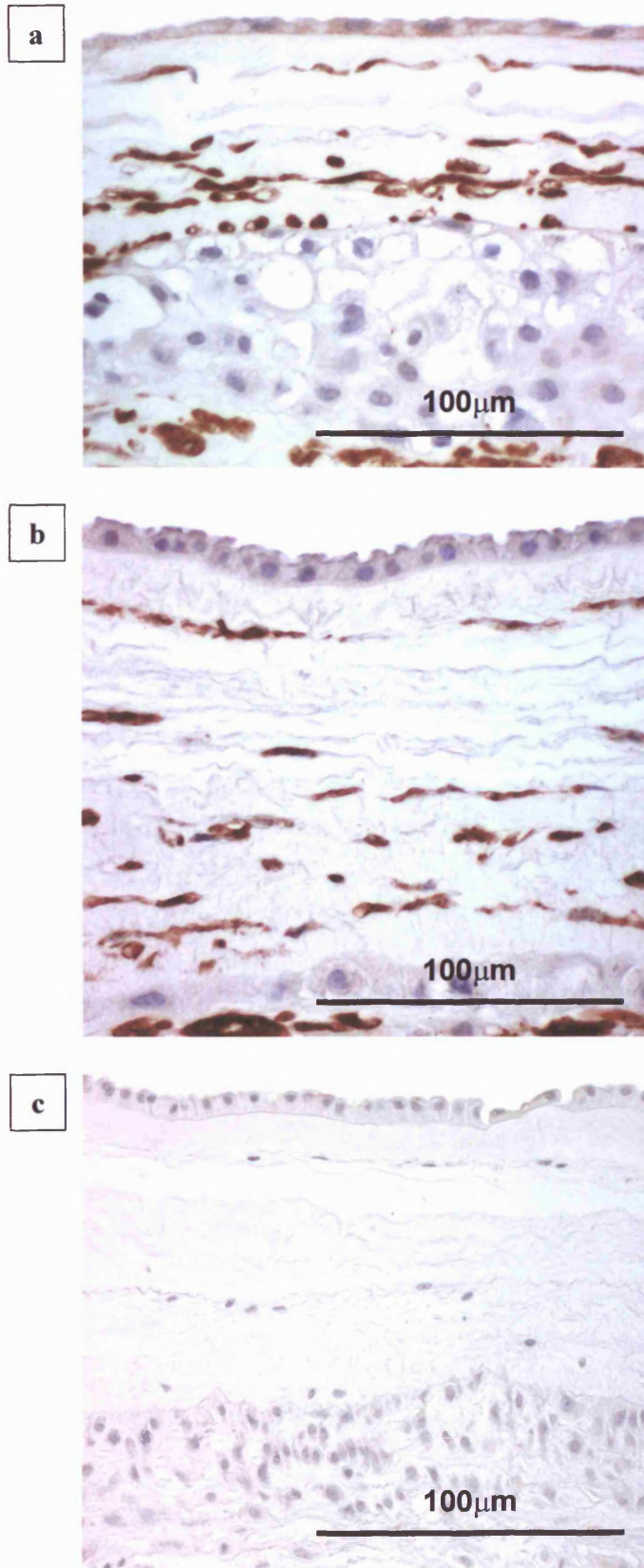
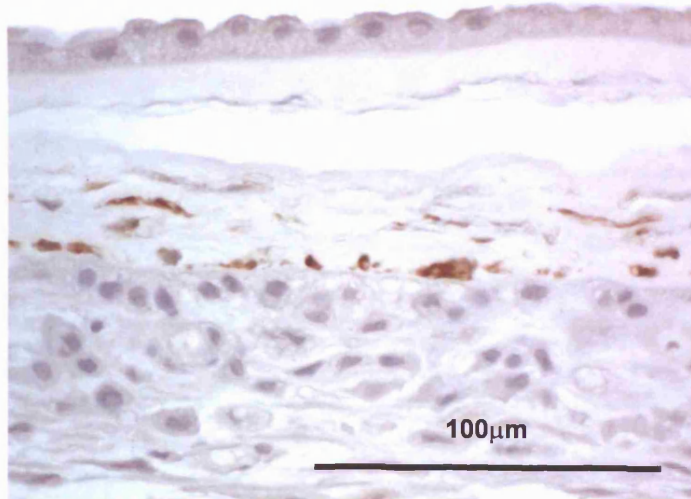


**Figure 3.2.** Vimentin immunohistochemistry on a midzone fetal membrane biopsy (a) and a fetal membrane biopsy exhibiting altered morphology (b). In both biopsies, immunoreactive cells are detected within the fibroblast layer and the reticular layer. No negative cells are observed within these layers. Decidual cells are also immunoreactive. Immunohistochemistry using mouse IgG does not demonstrate any immunoreactivity (c). Such negative control slides were included in every immunohistochemistry experiment within this thesis, using mouse IgG at concentration equivalent to the IgG concentration of the antibody being used. They were consistently negative.

a



b

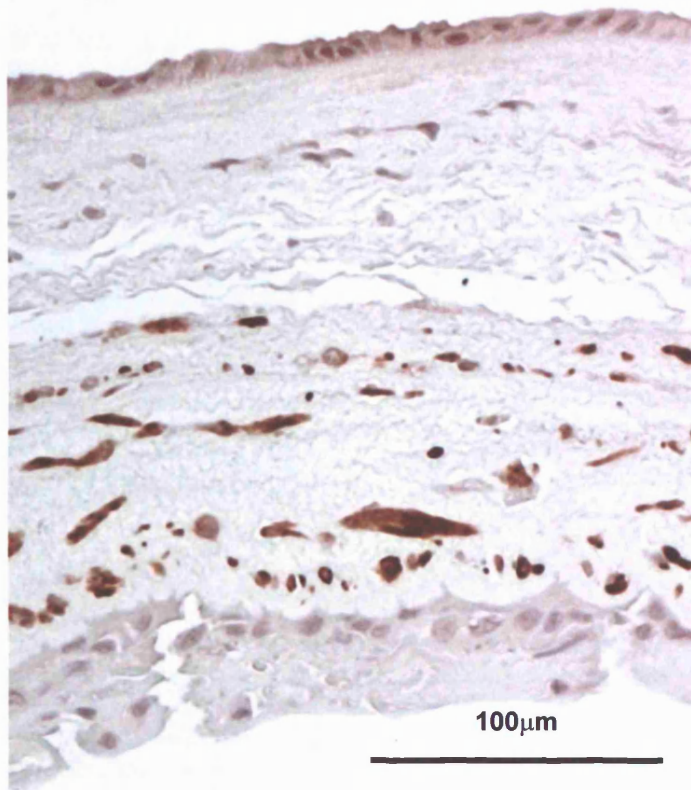


**Figure 3.3.** Desmin immunohistochemistry on a midzone fetal membrane biopsy (a) and a fetal membrane biopsy exhibiting altered morphology (b). In both biopsies, immunoreactive cells are detected within the the reticular layer only. No immunoreactive cells are detected within the fibroblast layer.

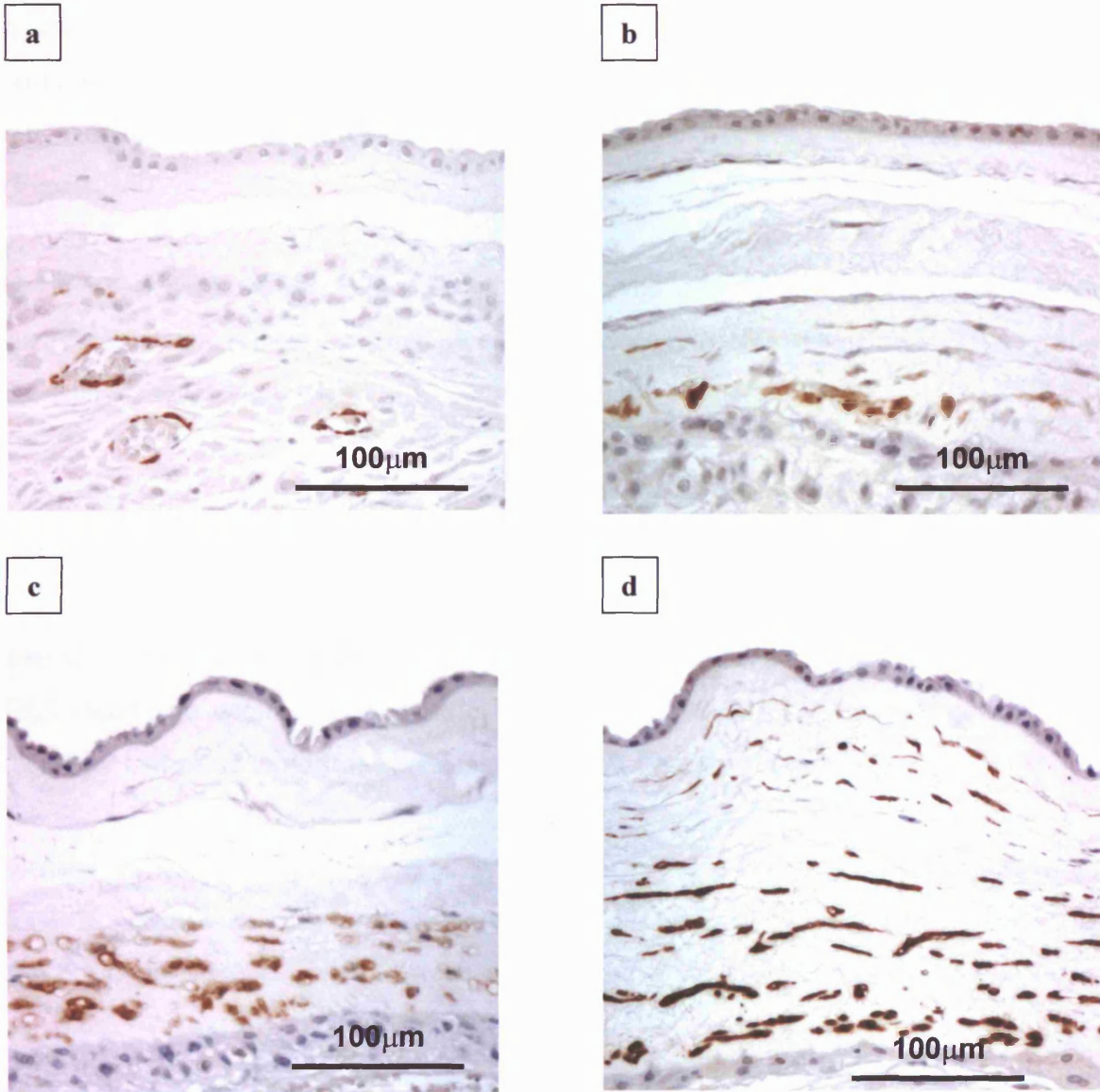


**Figure 3.4.** Immunohistochemistry for  $\alpha$ -sma on a midzone fetal membrane biopsy (**a**) and fetal membrane biopsies with altered morphology (**b-d**). In the midzone biopsy (**a**), no immunoreactive cells are detected within the reticular layer or the fibroblast layer. Immunoreactivity within smooth muscle cells around a decidual blood vessel serves as a positive control. A range of patterns of immunoreactivity is observed within the altered morphology biopsies. Immunoreactivity is observed within the reticular layer (**b-d**), and the fibroblast layer (**d**). Where low numbers of immunoreactive cells are detected in the reticular layer, they are usually situated adjacent to the pseudobasement membrane (**b**).

$\alpha$ -sma immunohistochemistry was carried out on cryostat fetal membrane tissue sections post-fixed in acetone and formalin. Immunoreactivity for  $\alpha$ -sma was observed in the reticular layer of both the formalin-fixed and acetone fixed 'cervical' fetal membrane (Figure 3.5).

In order to confirm that the immunoreactivity observed with monoclonal antibody 1A4 was specific to  $\alpha$ -sma, further confirmation of the presence of  $\alpha$ -sma protein and mRNA within the fetal membrane was sought.

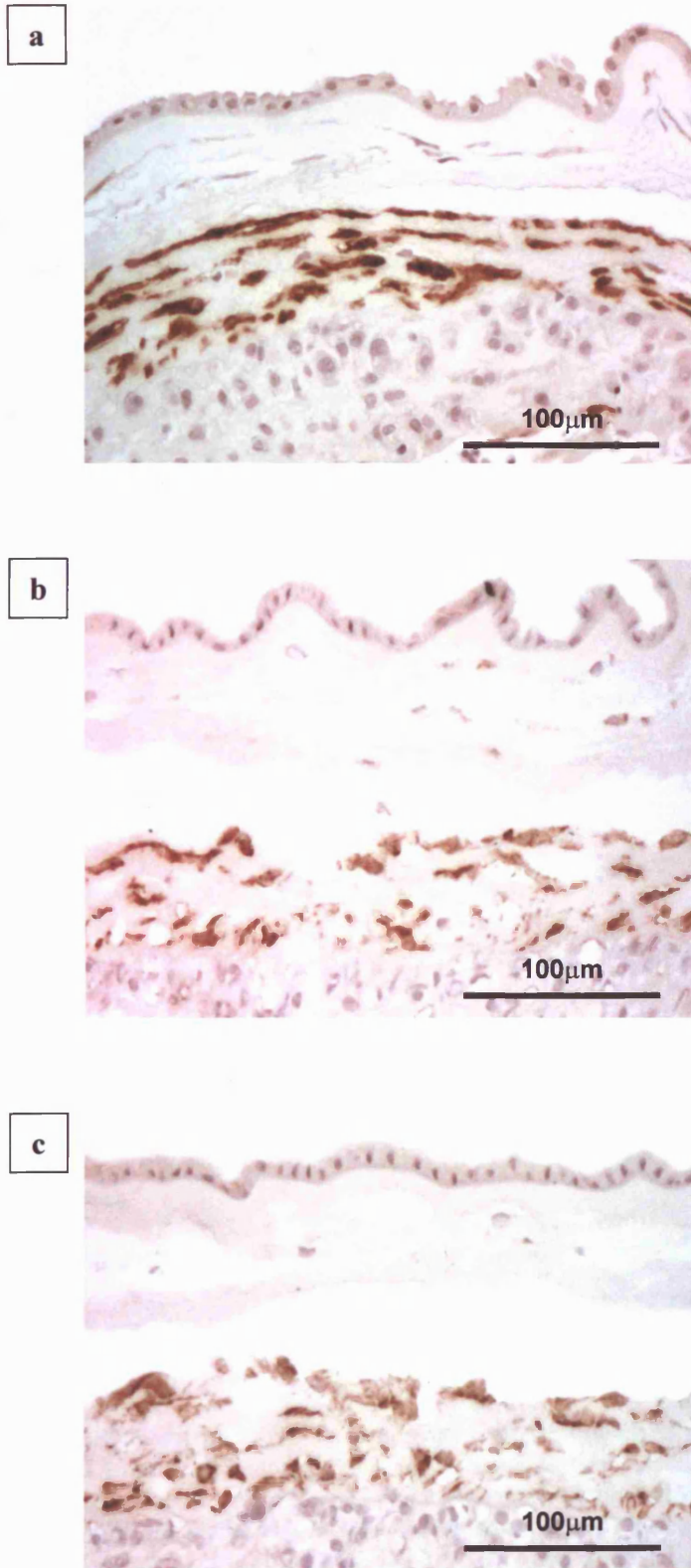
SDS-PAGE and Western blotting of extracts of the connective tissue layers of paired 'cervical' and midzone fetal membrane biopsies using monoclonal antibody to  $\alpha$ -sma, 1A4 was carried out. A single band at 40kDa was demonstrated, consistent with the reported size of  $\alpha$ -sma (Figure 3.6a&b). Densitometry of the band produced by blotting 5 pairs of fetal membrane demonstrated significantly higher amounts of  $\alpha$ -sma in extracts from 'cervical' compared to midzone biopsies ( $p=0.0278$ , Figure 3.6c&d).

$\alpha$ -SMA mRNA was demonstrated in the connective tissue layers of fetal membranes by RT-PCR (Figure 3.7). However densitometry of the resultant bands, relative to GAPDH, was not significantly different between 'cervical' and midzone biopsies (Figure 3.8).

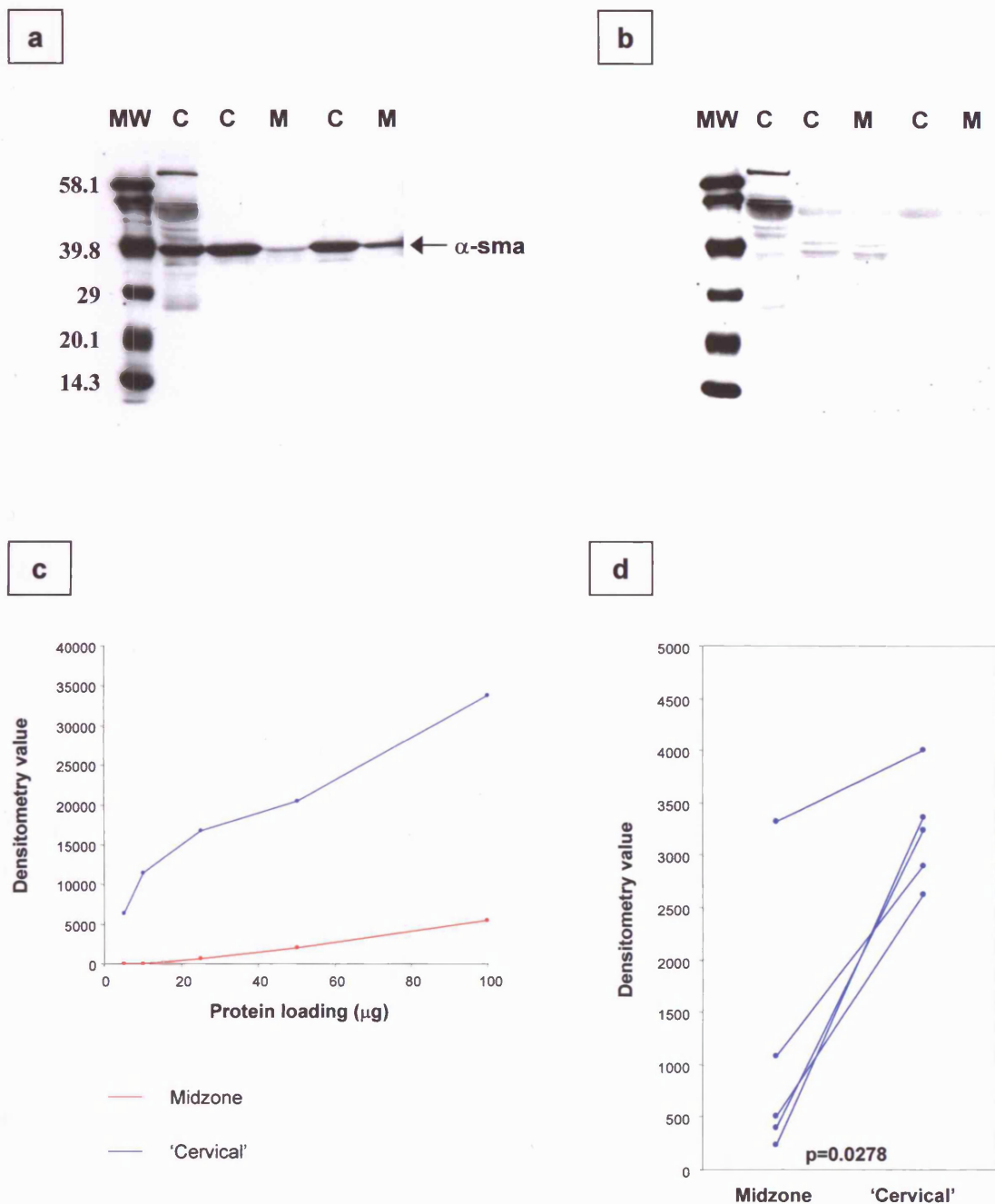
Attempts to design a probe for *in situ* hybridisation to look for further evidence of  $\alpha$ -sma mRNA expression did not succeed due to the high degree of homology between  $\alpha$ -sma and other actin genes.

#### 3.4.2.4. $\gamma$ -smooth muscle actin

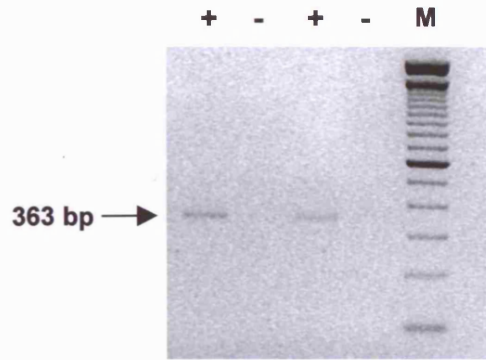
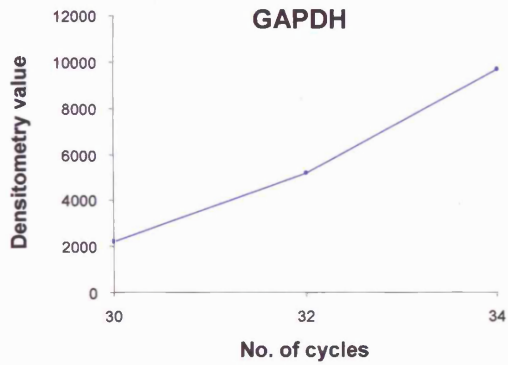
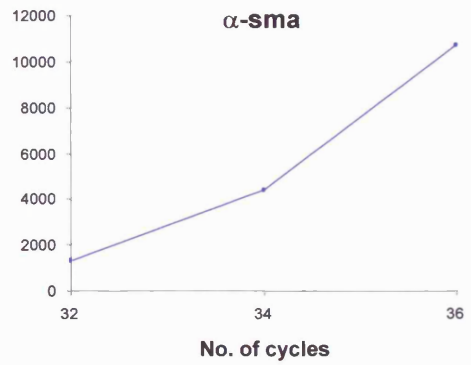
Cells immunoreactive for  $\gamma$ -sma were detected within the reticular layer of some 'cervical' and rupture line fetal membrane biopsies (Figure 3.9b & c). Where low numbers of immunoreactive cells were present, they tended to be located towards the upper aspect of the reticular layer, adjacent to the spongy layer (Figure 3.9b), although where higher numbers of immunoreactive cells were present, they were distributed throughout the layer (Figure 3.9c). Immunoreactive cells were noted within the fibroblast layer in one rupture line biopsy. No immunoreactive cells were observed within the connective tissue layers of midzone biopsies (Figure 3.9a). Positive cells were noted in the smooth muscle cells around blood vessels in the decidua.



**Figure 3.5.** Immunohistochemistry for  $\alpha$ -sma on adjacent biopsies from the same fetal membrane. Formalin-fixed wax-embedded tissue (a), and cryostat sections post-fixed in formalin (b) and in acetone (c) all exhibit the same pattern of  $\alpha$ -sma immunoreactivity.

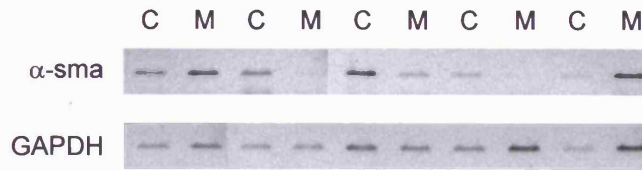


**Figure 3.6.** Western blot of 'superscraped' fetal membrane biopsies obtained prior to labour at term using monoclonal antibody 1A4 against  $\alpha$ -sma, demonstrating a single band at approximately 40kDa (a). (C, 'cervical' fetal membrane biopsies; M, midzone fetal membrane biopsies; MW, molecular weight marker, with sizes indicated in kDa). A paired blot incubated with an equivalent concentration of IgG confirms the specificity of the band identified (b). The protein loading was titred using a pair of 'cervical' and midzone protein extracts, to determine the optimal protein loading. Protein loading of 50 $\mu$ g is in the linear part of the curve obtained, and was used for quantitative experiments (c). Densitometry values of bands obtained from 'cervical' fetal membrane biopsies are significantly greater than those obtained from midzone fetal membranes biopsies (d)(Mann-Whitney U test). Lines connect the data points from the paired biopsies from individual patients.

**a****b****c**

**Figure 3.7.** RT-PCR using primers to  $\alpha$ -sma on RNA extracted from fetal membrane amplifies a 363 base pair band. No band is detected in control reactions prepared in the absence (-) of reverse transcriptase (a). 100 base pair ladder is in lane M. Titration curves to optimise the number of cycles of amplification for GAPDH (b) and  $\alpha$ -sma (c). 32 cycles were subsequently used for GAPDH, and 35 cycles for  $\alpha$ -sma.

**a**



**b**

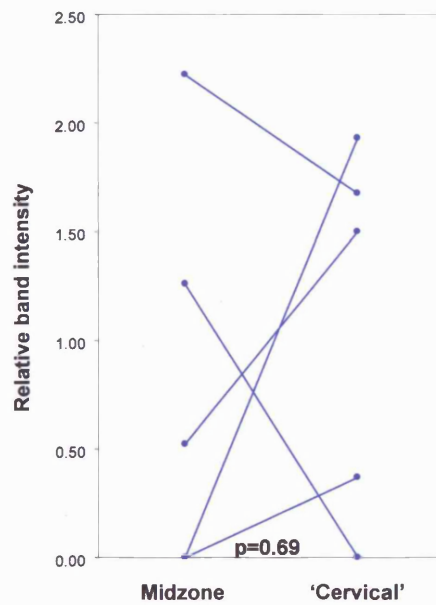


**Figure 3.8.** RT-PCR for  $\alpha$ -sma of paired 'superscraped' fetal membrane biopsies obtained prior to labour at term (a). (C, 'cervical' fetal membrane biopsies; M, midzone fetal membrane biopsies). (All samples were run on a single gel, although on several rows of lanes, therefore images cut and paste to align lanes from the same samples). Relative densitometry values (as a ratio of GAPDH densitometry value) of bands obtained from 'cervical' fetal membrane biopsies are no different to those obtained from midzone fetal membranes biopsies (b)(Mann-Whitney U test). Lines connect the data points from the paired biopsies from individual patients.

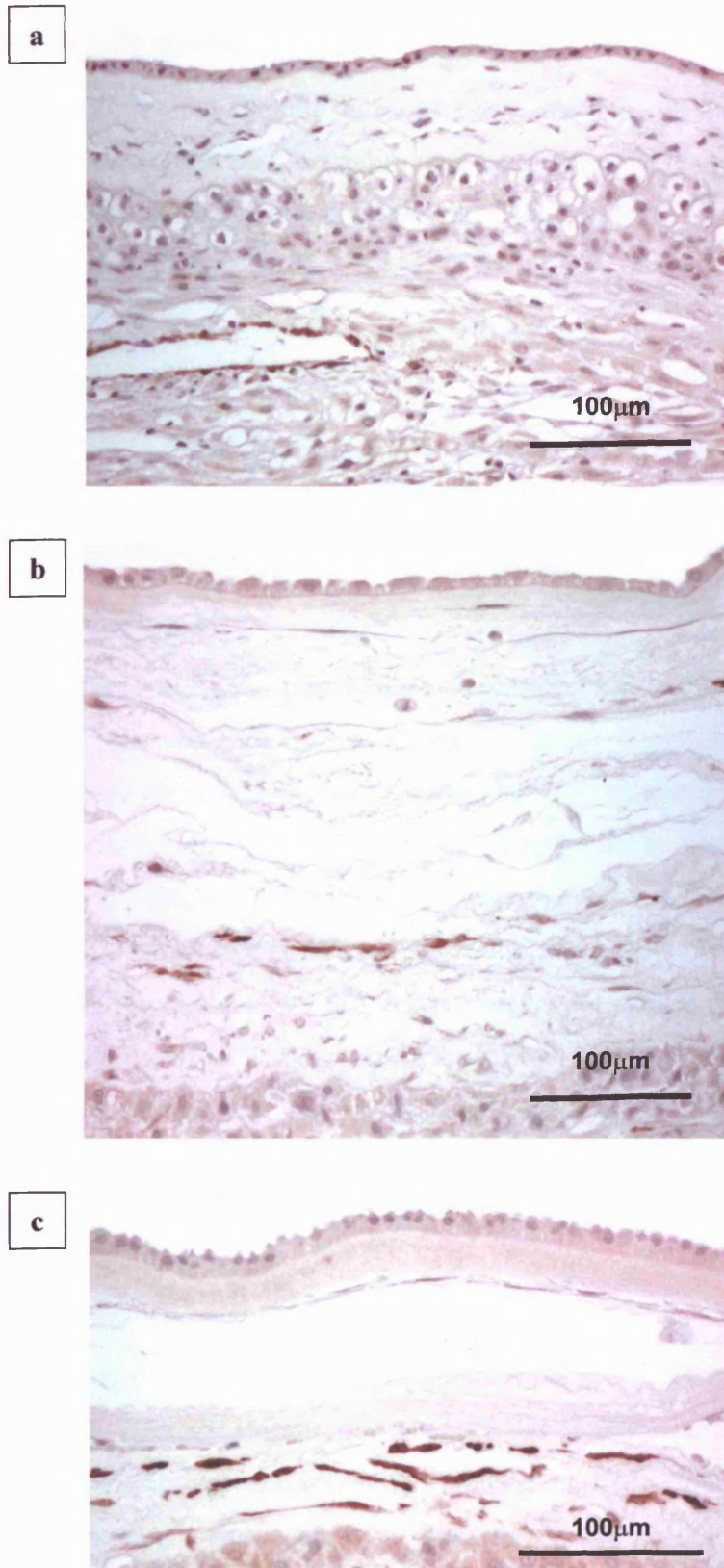


**Figure 3.9.** Immunohistochemistry for  $\gamma$ -sma on a midzone fetal membrane biopsy (a), and on fetal membrane biopsies with altered morphology (b&c). No immunoreactive cells are observed in the fibroblast or reticular layers of the midzone biopsy (a). Immunoreactivity in the smooth muscle cells around a decidual blood vessel acts as a positive control. Immunoreactive cells are observed within the reticular layer of fetal membrane biopsies exhibiting altered morphology (b&c). Where only a small number of immunoreactive cells are present within the reticular layer, they are usually observed at the upper aspect of the layer (b).

#### **3.4.2.5. Smooth muscle myosin**

No cells immunoreactive for smooth muscle myosin were identified in the connective tissue layers of the amnion or the chorion in any fetal membrane biopsy. Immunoreactive cells in the smooth muscle coat in blood vessels in the decidua were identified, acting as an internal positive control (**Figure 3.10**).

#### **3.4.2.6. CD68**

Cells immunoreactive for CD68 were identified within the fibroblast layer and the reticular layer (**Figure 3.11**).

#### **3.4.2.7. Cellular phenotypes**

The cellular markers used for immunohistochemistry identified a number of cell phenotypes. All cells in the reticular layer were vimentin immunoreactive. Immunohistochemistry on serial sections demonstrated that both desmin immunoreactive cells and CD68 positive cells co-express vimentin (**Figure 3.12**). Immunohistochemistry on serial sections of fetal membranes demonstrated that desmin immunoreactivity and CD68 immunoreactivity occurred in different populations of cells within the reticular layer (**Figure 3.12b&c**). Examination of serial sections demonstrated that  $\alpha$ -sma immunoreactive cells represent a subgroup of the desmin-positive cells (**Figure 3.13**). A number of rupture line and 'cervical' fetal membrane biopsies also contained  $\gamma$ -sma positive cells, a subpopulation of  $\alpha$ -sma cells (**Figure 3.14**). The reticular layer therefore contains 'macrophages' (CD68 positive), and 'myofibroblastic' cells (VD, VDA, and VDAG cells).

Within the amnion, two principle cellular populations are found: CD68 positive cells and CD68 negative cells. Sporadic desmin-positive cells are found within the CD68 negative cells. In a number of 'cervical' and rupture line fetal membrane biopsies, a proportion of CD68 negative cells were  $\alpha$ -sma positive, and within a single rupture line biopsy, rare  $\gamma$ -sma positive cells occurred. The fibroblast layer of the amnion therefore contains 'macrophages' (CD68 positive), and 'fibroblastic' cells (V cells). It also contains rare VA and VAG cells in 'cervical' and rupture line fetal membrane biopsies.

Based on the qualitative immunohistochemistry results, numbers of cells immunoreactive

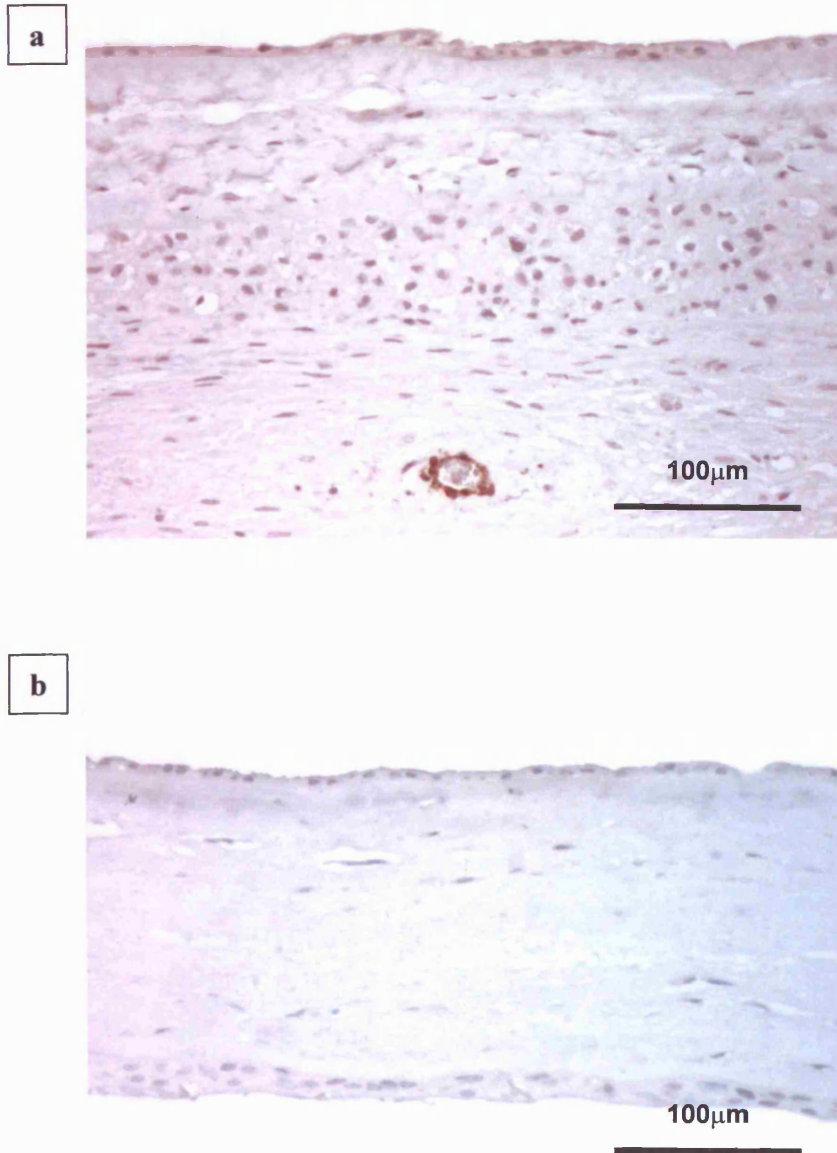
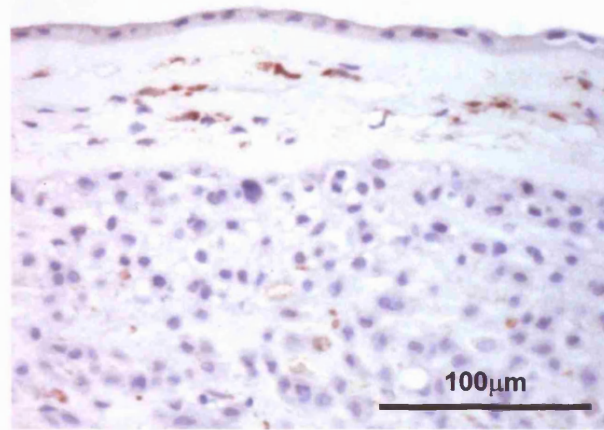


**Figure 3.10.** Immunohistochemistry for smooth muscle myosin on a midzone fetal membrane biopsy (a), and on a fetal membrane biopsy with altered morphology (b). No immunoreactive cells are observed in the fibroblast or reticular layers of either biopsy. Immunoreactivity in the smooth muscle cells around a decidual blood vessel acts as a positive control.

**a**



**b**

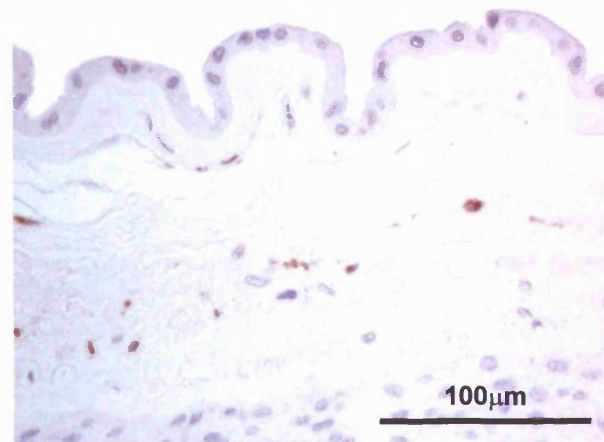


**Figure 3.11.** Immunohistochemistry for CD68 on a midzone fetal membrane biopsy (**a**), and on a fetal membrane biopsy with altered morphology (**b**). Immunoreactive cells are detected in the fibroblast and reticular layers of both biopsies.

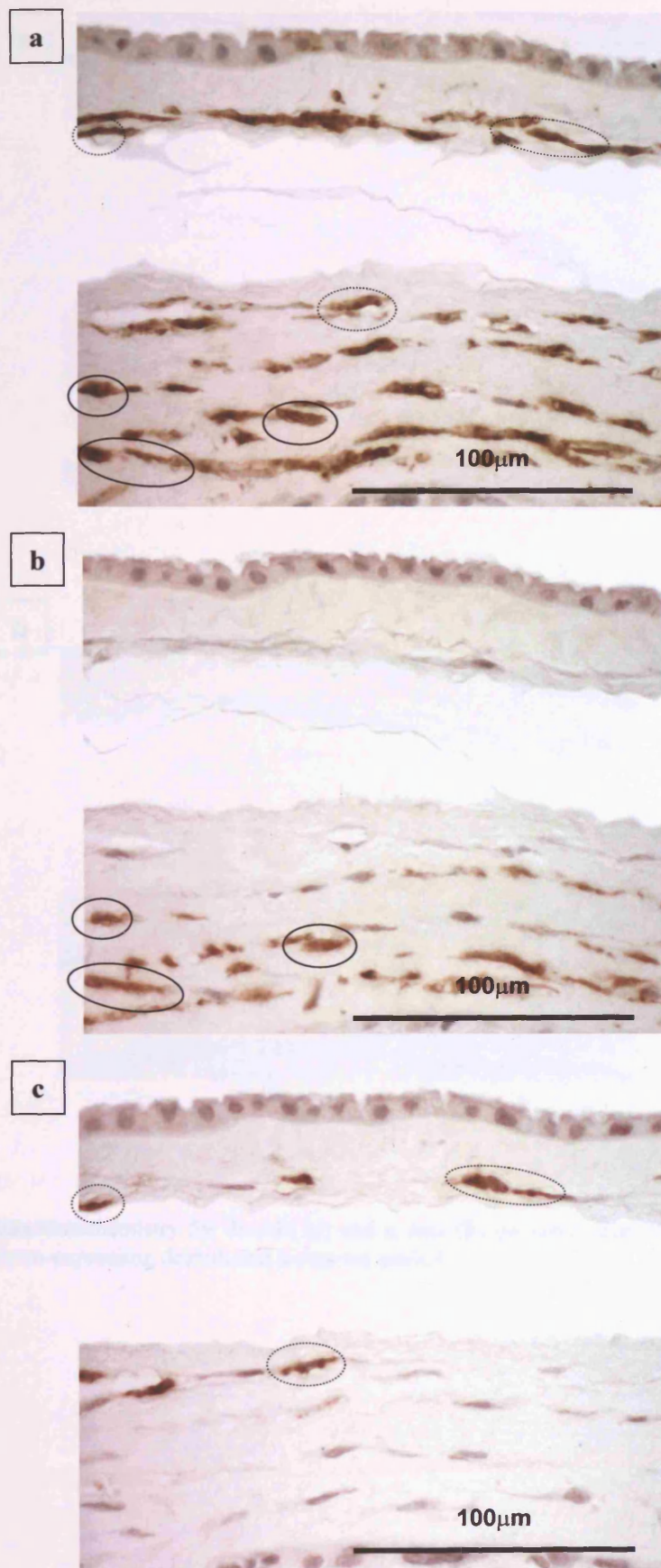


**Figure 3.12.** Immunohistochemistry for vimentin (a), desmin (b) and CD68 (c) on serial sections of a fetal membrane biopsy. Representative cells co-expressing vimentin and desmin are highlighted with a circle with a continuous line (a&b), and representative cells co-expressing vimentin and CD-68 highlighted with a circle with a dotted line (a&c). Co-expression of desmin and CD-68 was not observed.

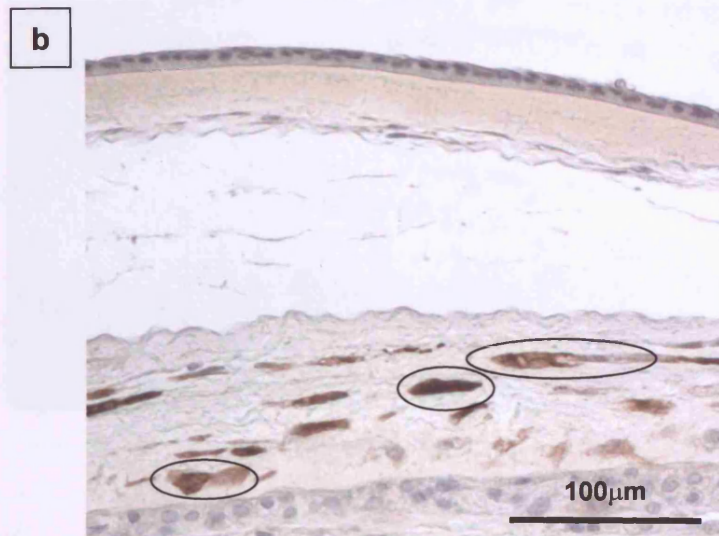
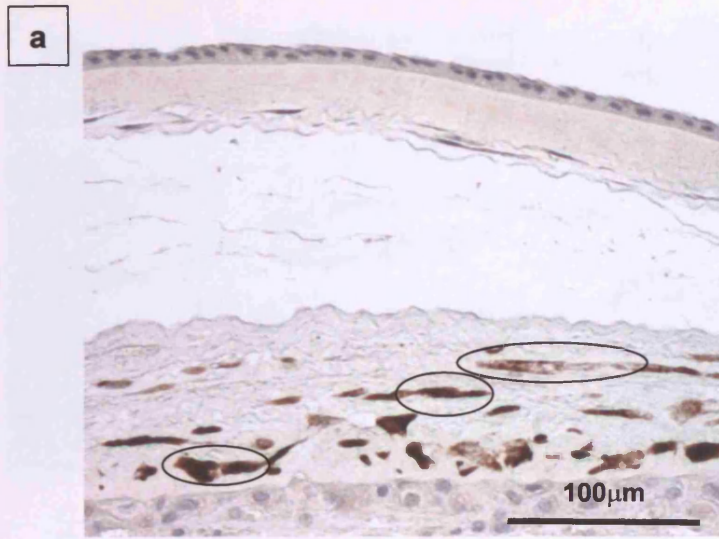


**Figure 3.13.** Immunohistochemistry for desmin (a) and  $\alpha$ -sma (b) on serial sections of fetal membrane. Representative cells co-expressing desmin and  $\alpha$ -sma are circled.

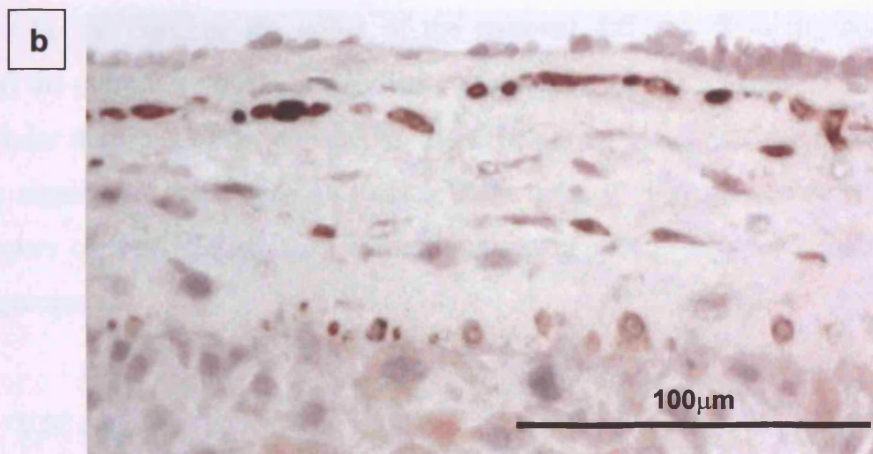
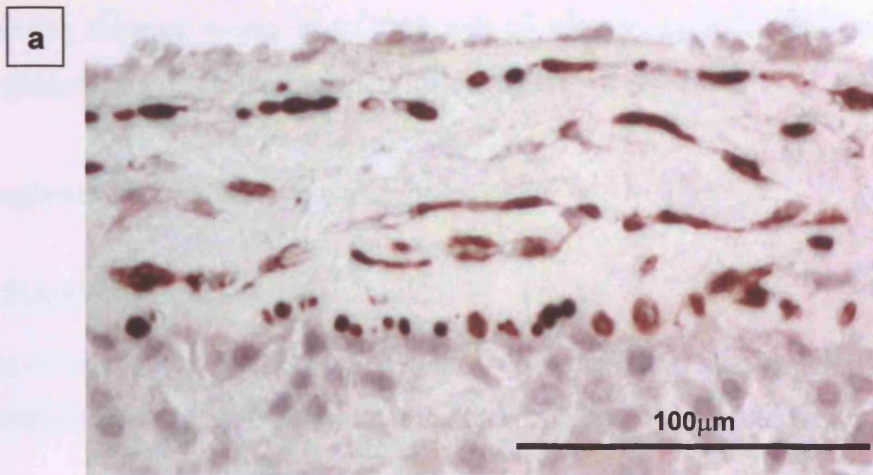


**Figure 3.14.** Immunohistochemistry for  $\alpha$ -sma (a) and  $\gamma$ -sma (b) on serial sections of fetal membrane. The  $\gamma$ -sma positive cells represent a sub-population of the  $\alpha$ -sma positive cells. (Some separation of the amnion and chorion has occurred, therefore only the reticular layer and cytotrophoblast layer are illustrated, with red blood cells adherent to the superficial surface of the reticular layer).

for vimentin, desmin,  $\alpha$ -sma and CD68 will be used to explore differences in regional cellular phenotype prior to, during, and following labour at term.

### **3.4.3. Regional differences in cellular phenotype**

#### **3.4.3.1. Total cell count**

Numbers of vimentin immunoreactive cells within the fibroblast layer and reticular layer were counted to give a representation of the total cell count within each layer.

There were no significant changes in the numbers of vimentin positive cells in the connective tissue layers between sites within any patient group, or between patient groups (Table 3.4). To examine the effect of the regional differences in the connective tissue layers on the cellularity of the layers, the cellular density of the layers was examined. The total cellular densities of the connective tissue layers are demonstrated in Table 3.4. There were no significant differences in total cellular density of either the amniotic connective tissue layers or the reticular layer either between patient groups, or between sites within patient groups.

#### **3.4.3.2. 'VD' cells**

Desmin immunoreactive cells were commonly observed in the reticular layer, and rarely in the fibroblast layer (Figure 3.3). Only 6 out of 30 fetal membrane biopsies contained desmin immunoreactive cells within the fibroblast layer, accounting for 1.4 - 11.9% (range) of the cells within the layer in these six biopsies. There were no significant differences between numbers or percentages of desmin immunoreactive cells either between patient groups, or between biopsy sites within patient groups (Table 3.5).

There were significantly higher numbers and percentages of desmin immunoreactive cells in the reticular layer of the post-labour rupture line biopsies compared to their midzone biopsies (Table 3.5) (2.2-fold higher,  $p=0.01$ ; 1.5-fold higher,  $p=0.025$  respectively).

#### **3.4.3.3. 'VDA' and 'VA' cells**

Cells immunoreactive for  $\alpha$ -sma were identified in the reticular layer of 'cervical' and rupture line fetal membrane biopsies. The numbers of  $\alpha$ -sma immunoreactive cells in the

	Pre-labour		Labour		Post-labour	
	Midzone	'Cervical'	Midzone	'Cervical'	Midzone	Rupture line
<b>Amnion cell no.</b>	4.80 ±0.55	6.06 ±0.81	6.02 ±0.61	5.92 ±1.14	4.94 ±0.40	8.28 ±1.61
<b>Chorion cell no.</b>	26.08 ±1.85	25.50 ±1.47	22.42 ±1.10	30.78 ±4.79	24.64 ±2.28	36.96 ±8.90
<b>Amnion density</b>	16.07 ±1.60	16.59 ±1.12	15.00 ±2.25	10.38 ±1.80	18.96 ±4.18	15.45 ±3.00
<b>Chorion density</b>	42.43 ±5.69	29.60 ±4.43	33.63 ±6.76	25.69 ±5.56	41.09 ±8.03	30.13 ±5.05

**Table 3.4.** Numbers and densities of vimentin immunoreactive cells in the connective tissue layers of the amnion and chorion, of regional fetal membrane biopsies obtained prior to, during, and following labour at term. The mean derived from 10 fields from each biopsy, and SEM derived from 5 patients per group are shown. Numbers are expressed as immunoreactive cells per computer screen width (176 $\mu$ m). Densities are expressed immunoreactive cells per 0.01mm<sup>2</sup> of the cross sectional area of the layer. Comparisons between biopsy sites and physiological group were using two-way ANOVA and Scheffes test. All comparisons between physiological groups and between biopsy sites were non-significant.

	Pre-labour		Labour		Post-labour	
	Midzone	'Cervical'	Midzone	'Cervical'	Midzone	Rupture line
<b>Amnion cell no.</b>	0.06 ±0.04	0.02 ±0.02	0.00 ±0.00	0.14 ±0.14	0.00 ±0.00	0.08 ±0.05
<b>Chorion cell no.</b>	8.96 ±1.36	13.00 ±2.05	11.98 ±2.66	21.86 ±5.34	13.10 <sup>a</sup> ±1.15	29.14 <sup>a</sup> ±4.64
<b>Amnion cell %</b>	1.4 ±0.9	0.3 ±0.3	0.0 ±0.0	2.4 ±2.4	0.0 ±0.0	0.8 ±0.5
<b>Chorion cell %</b>	34.9 ±5.6	52.1 ±9.6	53.1 ±10.7	67.3 ±6.7	54.5 <sup>b</sup> ±5.3	83.9 <sup>b</sup> ±9.3

**Table 3.5.** Numbers and percentages of desmin immunoreactive cells in the connective tissue layers of the amnion and chorion, of regional fetal membrane biopsies obtained prior to, during, and following labour at term. The mean derived from 10 fields from each biopsy, and SEM derived from 5 patients per group are shown. Numbers are expressed as immunoreactive cells within the layer per computer screen width (176µm). Percentages are the number of immunoreactive cells within the layer for each biopsy, expressed as a percentage of the vimentin immunoreactive cell count, and are derived from the mean values for each biopsy. Comparisons between biopsy sites and physiological group were using two-way ANOVA and Scheffes test. Significant differences are highlighted: a & b,  $p < 0.05$ .

reticular layer, per unit length of membrane, were 17-fold higher in the reticular layer of 'cervical' biopsies compared to midzone biopsies in the labour affected group ( $p=0.041$ ), and 50-fold higher in the rupture line biopsies compared to midzone biopsies obtained following labour and delivery ( $p=0.002$ ) (Figure 3.15). When expressed as a percentage of the total vimentin immunoreactive cell population, in the reticular layer of midzone biopsies only 2-5% of cells were  $\alpha$ -sma positive. In the labour affected 'cervical' biopsies 49% of cells were  $\alpha$ -sma positive (9.8-fold higher than midzone,  $p=0.0031$ ), and in the rupture line biopsies following labour and delivery 69% of cells were  $\alpha$ -sma positive (34.5-fold higher than midzone,  $p<0.0001$ ) (Figure 3.16). There were no significant differences between the numbers and percentages of  $\alpha$ -sma positive cells in the reticular layer between midzone and 'cervical' biopsies in the pre-labour patient group. However, within this group, two patients exhibited significantly higher numbers and percentages of  $\alpha$ -sma immunoreactive cells within the reticular layer compared to their midzone biopsy (Figures 3.15 & 3.16). These are the same two patients in whom the FMMI of the 'cervical' fetal membrane biopsy was significantly higher compared to the respective midzone biopsy (section 3.4.1).

In the fibroblast layer of the amnion, a significant difference in the number of  $\alpha$ -sma immunoreactive cells between the 'cervical' and midzone biopsies was noted in the labour affected group ( $p=0.04$ ) (Figure 3.15). Significantly higher percentages of  $\alpha$ -sma immunoreactive cells were noted in the labour affected 'cervical' biopsies compared to their respective midzones ( $p=0.026$ ) (Figure 3.16).

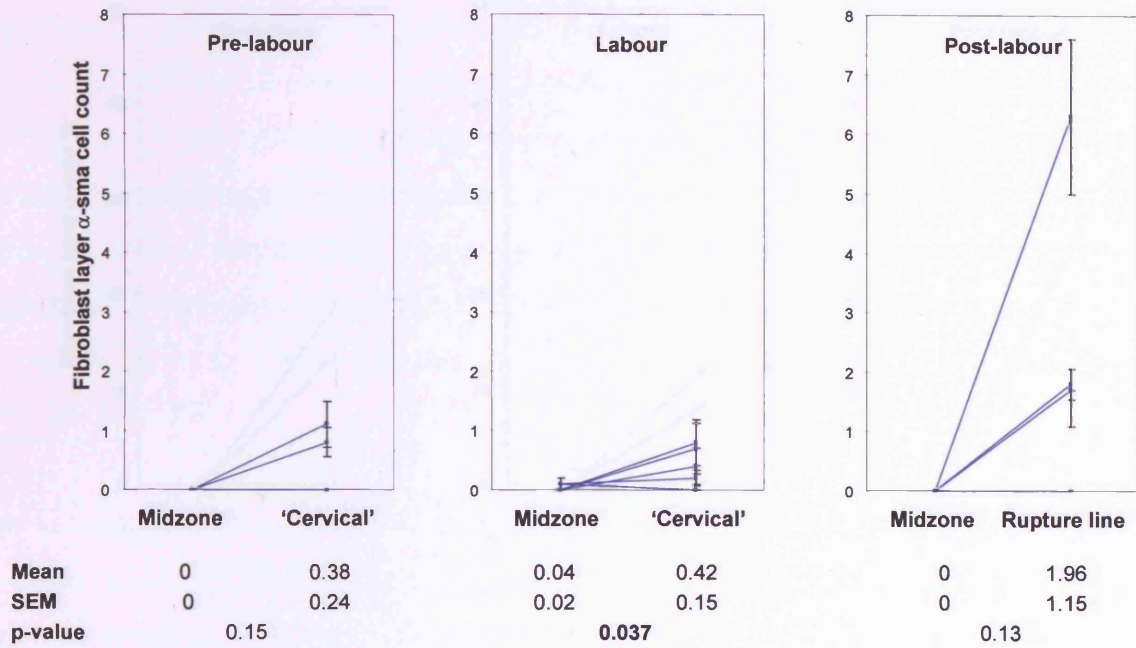
The percentage of  $\alpha$ -sma immunoreactive cells within the fibroblast layer correlated significantly with the percentage of  $\alpha$ -sma immunoreactive cells within the reticular layer (Spearman  $r=0.574$ ,  $p=0.002$ ).

#### 3.4.3.4. 'VDAG' cells

Cells immunoreactive for  $\gamma$ -sma were identified in the reticular layer of some 'cervical' and rupture line biopsies. Four pre-labour and one labour 'cervical' biopsy did not contain any  $\gamma$ -sma immunoreactive cells within the reticular layer. Cells immunoreactive for  $\gamma$ -sma were not identified in the reticular layer of any midzone biopsy. Examining the mean number of immunoreactive cells within the groups, significantly greater numbers of immunoreactive cells were identified in the rupture line biopsies following labour and

**a**

**Fibroblast layer**



**b**

**Reticular layer**

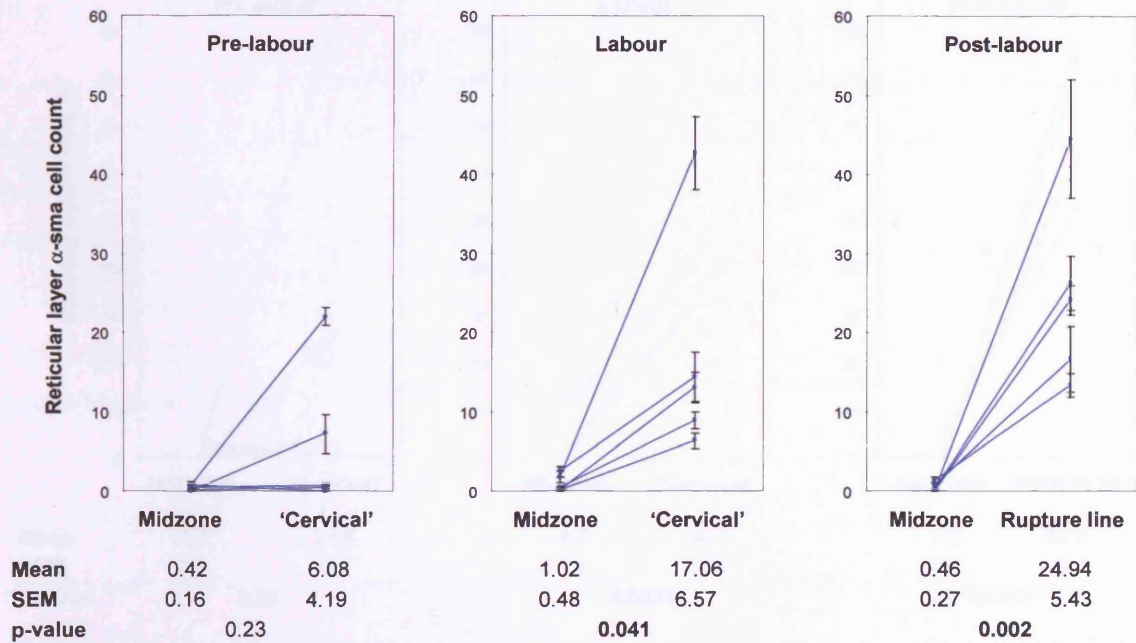
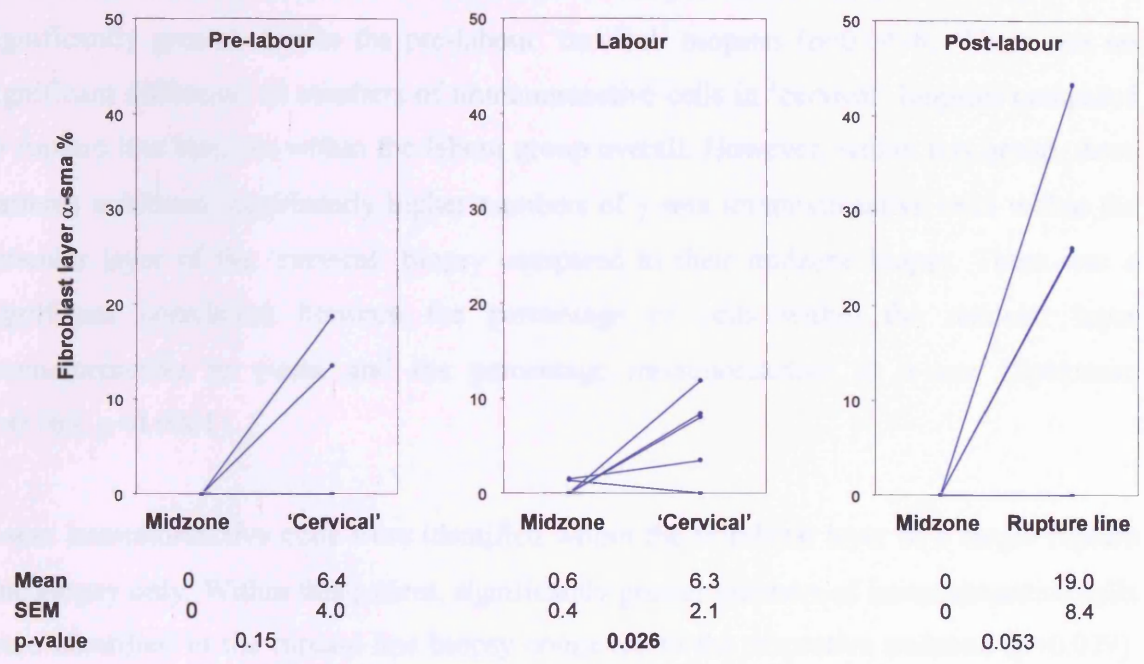


**Figure 3.15.** Numbers of  $\alpha$ -sma immunoreactive cells in the fibroblast (a) and the reticular (b) layers of regional fetal membrane biopsies obtained prior to, during and after labour at term. The graphs show the mean and SEM derived from 10 fields from each biopsy, with lines connecting the data points from individual patients. The mean and SEM (derived from n=5 patients per group) for each group are shown beneath the graphs. Comparisons between biopsy sites and physiological group were using two way ANOVA and Scheffes test. All comparisons between physiological groups were non-significant. Significant p-values are shown in bold.

**a**

**Fibroblast layer**



**b**

**Reticular layer**

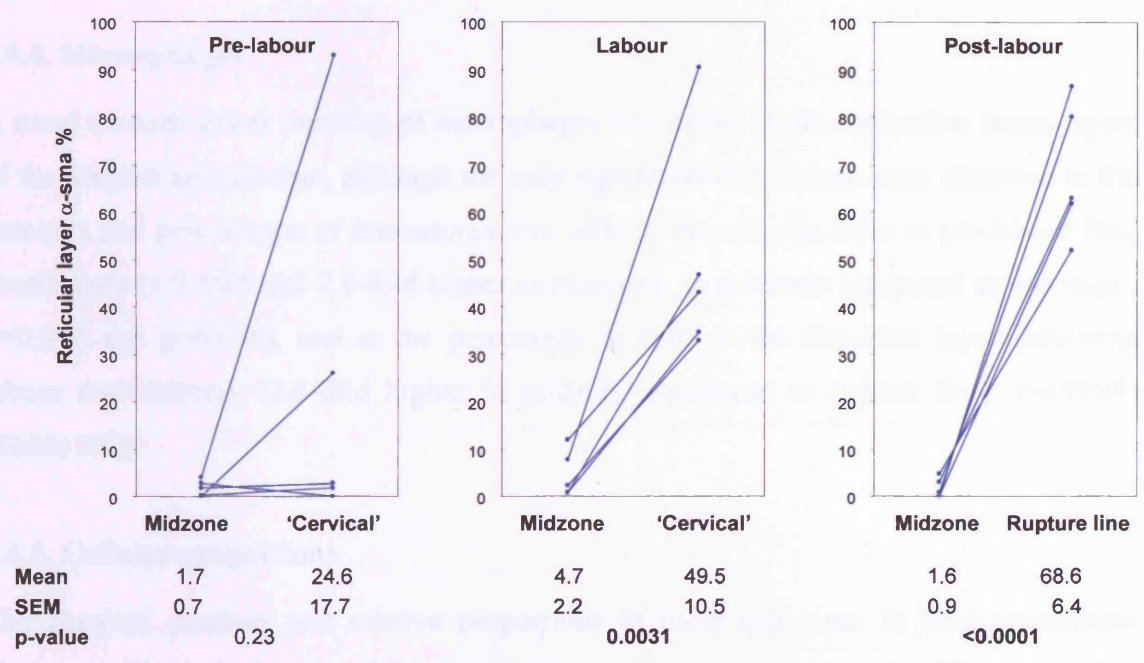


**Figure 3.16.** Percentages of  $\alpha$ -sma immunoreactive cells in the fibroblast (a) and the reticular (b) layers of regional fetal membrane biopsies obtained prior to, during and after labour at term. The graphs show the mean derived from 10 fields from each biopsy, with lines connecting the data points from individual patients. The percentages are the number of immunoreactive cells for each biopsy, expressed as a percentage of the vimentin immunoreactive cell count, and are derived from the mean values from the biopsy. (Therefore there is no SEM for the mean percentage for each biopsy). The mean and SEM (derived from n=5 patients per group) for each group are shown beneath the graphs. Comparisons between biopsy sites and physiological group were using two way ANOVA and Scheffes test. All comparisons between physiological groups were non-significant. Significant p-values are shown in bold.

delivery compared to the midzone biopsies ( $p=0.037$ ; **Figure 3.17**). The number of immunoreactive cells within the reticular layer of the post-labour rupture line biopsies was significantly greater than in the pre-labour 'cervical' biopsies ( $p=0.0498$ ). There was no significant difference in numbers of immunoreactive cells in 'cervical' biopsies compared to rupture line biopsies within the labour group overall. However, within this group, three patients exhibited significantly higher numbers of  $\gamma$ -sma immunoreactive cells within the reticular layer of the 'cervical' biopsy compared to their midzone biopsy. There was a significant correlation between the percentage of cells within the reticular layer immunoreactive to  $\gamma$ -sma and the percentage immunoreactive to  $\alpha$ -sma (Spearman  $r=0.763$ ,  $p<0.0001$ ).

$\gamma$ -sma immunoreactive cells were identified within the fibroblast layer of a single rupture line biopsy only. Within this patient, significantly greater numbers of immunoreactive cells were identified in the rupture line biopsy compared to the respective midzone ( $p=0.029$ ). This patient also exhibited the greatest number and percentage of  $\alpha$ -sma immunoreactive cells within the fibroblast layer (**3.4.3.3.**, **Figure 3.15** & **Figure 3.16**).

#### **3.4.4. Macrophages**

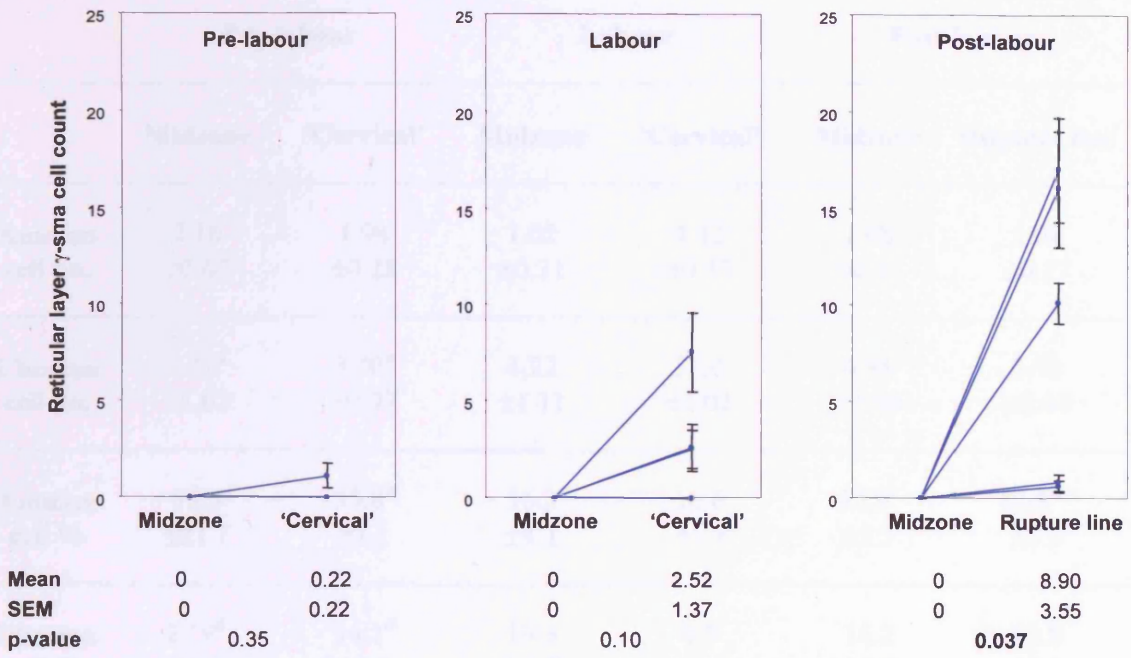
A trend towards lower numbers of macrophages was noted in the connective tissue layers of the amnion and chorion, although the only significant differences were observed in the numbers and percentages of immunoreactive cells in the reticular layer in pre-labour fetal membranes (1.9-fold and 2.0-fold higher respectively in midzone compared to 'cervical',  $p=0.041$  and  $p=0.036$ ), and in the percentage of cells in the fibroblast layer following labour and delivery (2.6-fold higher in midzone compared to rupture line,  $p=0.0098$ ) (**Table 3.6**).

#### **3.4.5. Cellular proportions**

The absolute numbers and relative proportions of these cell types in fetal membranes obtained prior to, during, and following labour at term are demonstrated in **Figures 3.18** & **3.19**.

VDA myofibroblasts represent 3.1-8.1% of the desmin positive myofibroblast population in midzone fetal membrane biopsies (**Figure 3.20**). VDA myofibroblasts represent 72.8% of desmin positive myofibroblasts in labour affected 'cervical' fetal membranes (9.0-fold

**a**



**b**

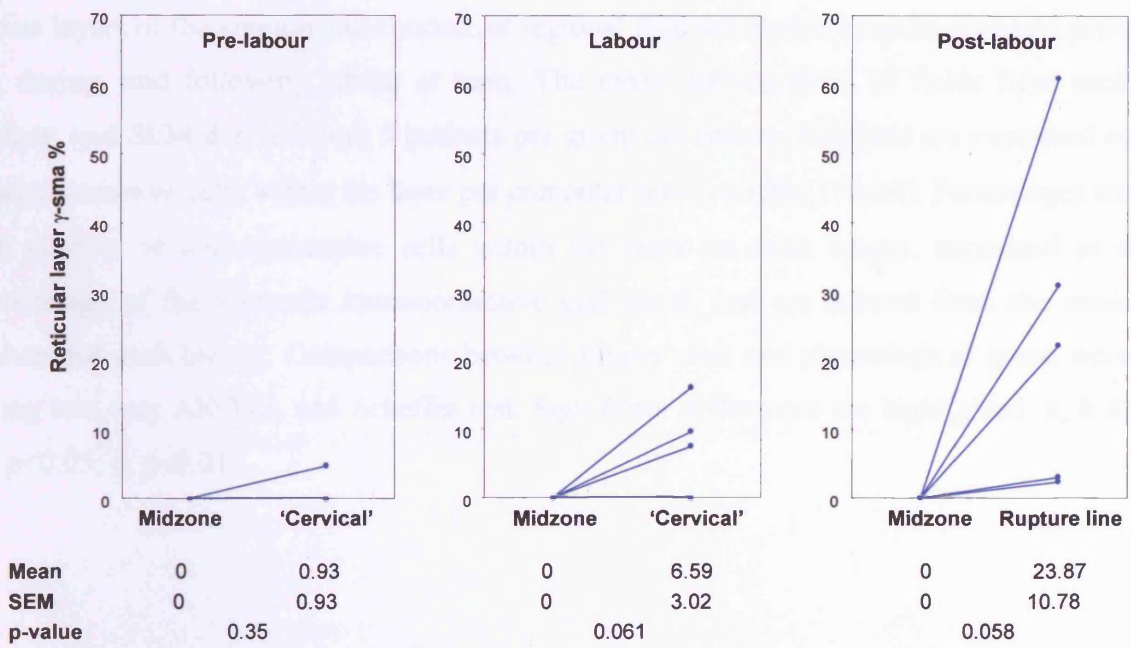


**Figure 3.17.** Numbers (a) and percentages (b) of  $\gamma$ -sma immunoreactive cells in the reticular layer of regional fetal membrane biopsies obtained prior to, during and after labour at term. (a) The graphs show the mean and SEM derived from 10 fields from each biopsy, with lines connecting the data points from individual patients. (b) The percentages are the number of immunoreactive cells for each biopsy, expressed as a percentage of the vimentin immunoreactive cell count, and are derived from the mean values from the biopsy. (Therefore there is no SEM for the mean percentage for each biopsy). The mean and SEM (derived from n=5 patients per group) for each group are shown beneath the graphs. Comparisons between biopsy sites and physiological group were using two way ANOVA and Scheffes test.

	Pre-labour		Labour		Post-labour	
	Midzone	'Cervical'	Midzone	'Cervical'	Midzone	Rupture line
<b>Amnion cell no.</b>	2.16 ±0.67	1.98 ±0.28	1.02 ±0.31	1.12 ±0.57	1.68 ±0.37	1.02 ±0.17
<b>Chorion cell no.</b>	7.12 <sup>a</sup> ±1.02	3.70 <sup>a</sup> ±0.97	4.22 ±1.11	3.10 ±1.01	4.34 ±1.58	3.78 ±1.44
<b>Amnion cell %</b>	51.5 ±21.7	35.8 <sup>b</sup> ±7.1	16.2 ±4.1	16.6 ±5.5	32.9 <sup>c</sup> ±5.7	12.8 <sup>b, c</sup> ±1.5
<b>Chorion cell %</b>	27.9 <sup>d</sup> ±4.4	14.1 <sup>d</sup> ±3.3	19.3 ±5.2	9.9 ±3.4	16.2 ±4.9	10.8 ±4.5

**Table 3.6.** Numbers and percentages of CD68 immunoreactive cells in the connective tissue layers of the amnion and chorion, of regional fetal membrane biopsies obtained prior to, during, and following labour at term. The mean derived from 10 fields from each biopsy, and SEM derived from 5 patients per group are shown. Numbers are expressed as immunoreactive cells within the layer per computer screen width (176µm). Percentages are the number of immunoreactive cells within the layer for each biopsy, expressed as a percentage of the vimentin immunoreactive cell count, and are derived from the mean values for each biopsy. Comparisons between biopsy sites and physiological group were using two way ANOVA and Scheffes test. Significant differences are highlighted: **a, b & d, p<0.05; c, p<0.01.**

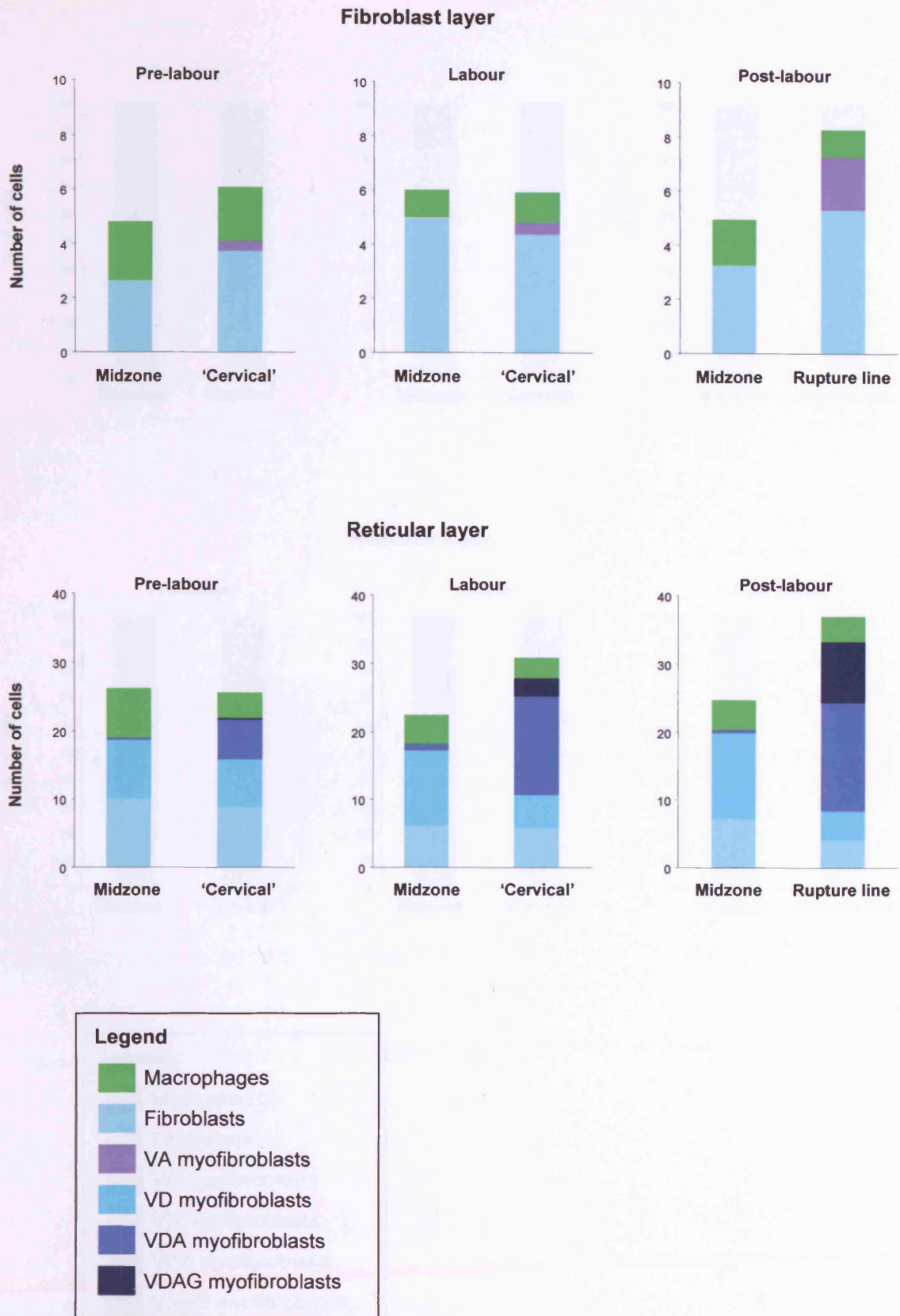


**Figure 3.18.** Numbers of cells (per 176µm computer screen width) immunoreactive for markers to macrophages (CD68), desmin,  $\alpha$ -sma and  $\gamma$ -sma in regional fetal membrane biopsies obtained prior to, during, and following labour at term.

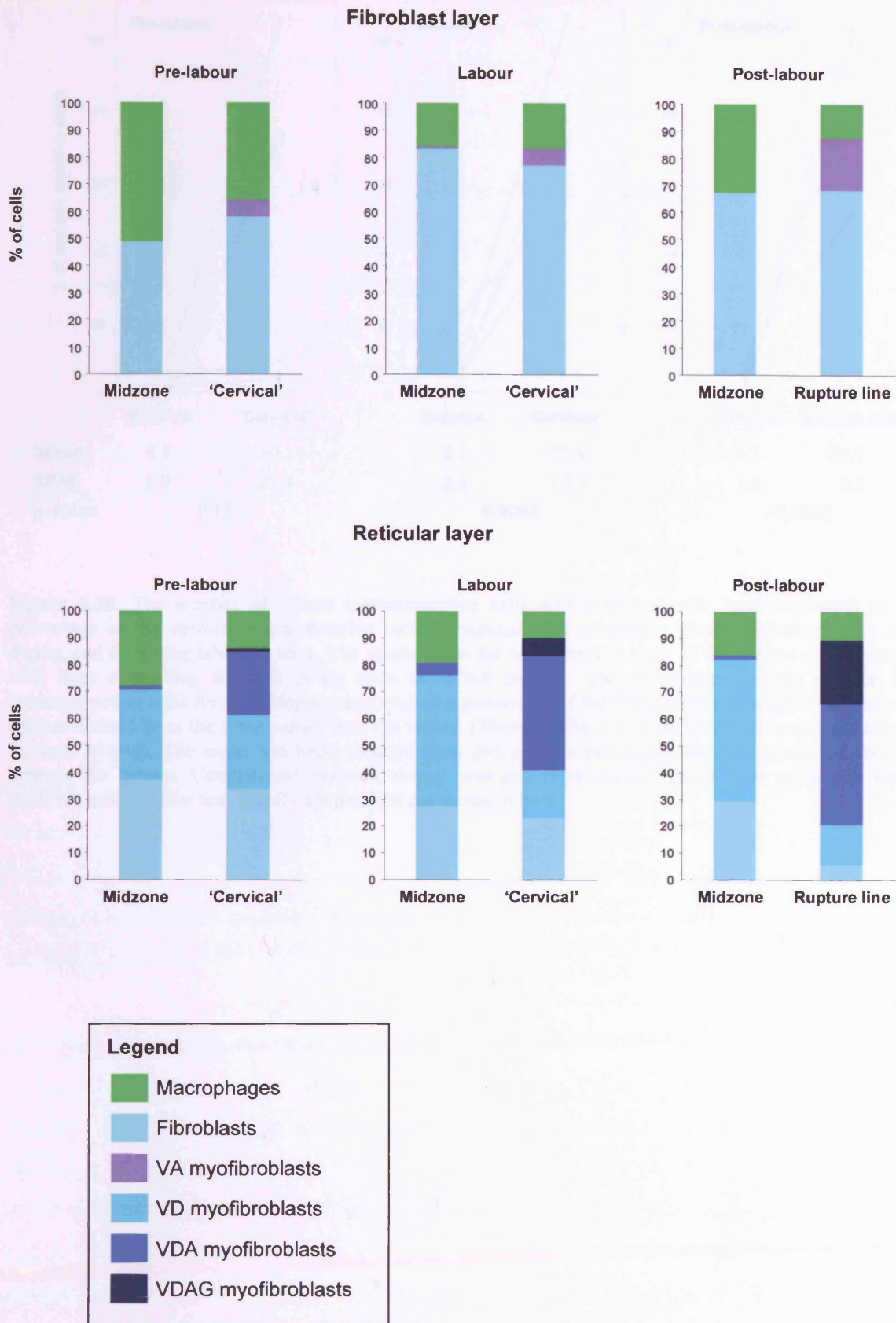


**Figure 3.19.** Proportions of cells immunoreactive for markers to macrophages (CD68), desmin,  $\alpha$ -sma and  $\gamma$ -sma in regional fetal membrane biopsies obtained prior to, during, and following labour at term.

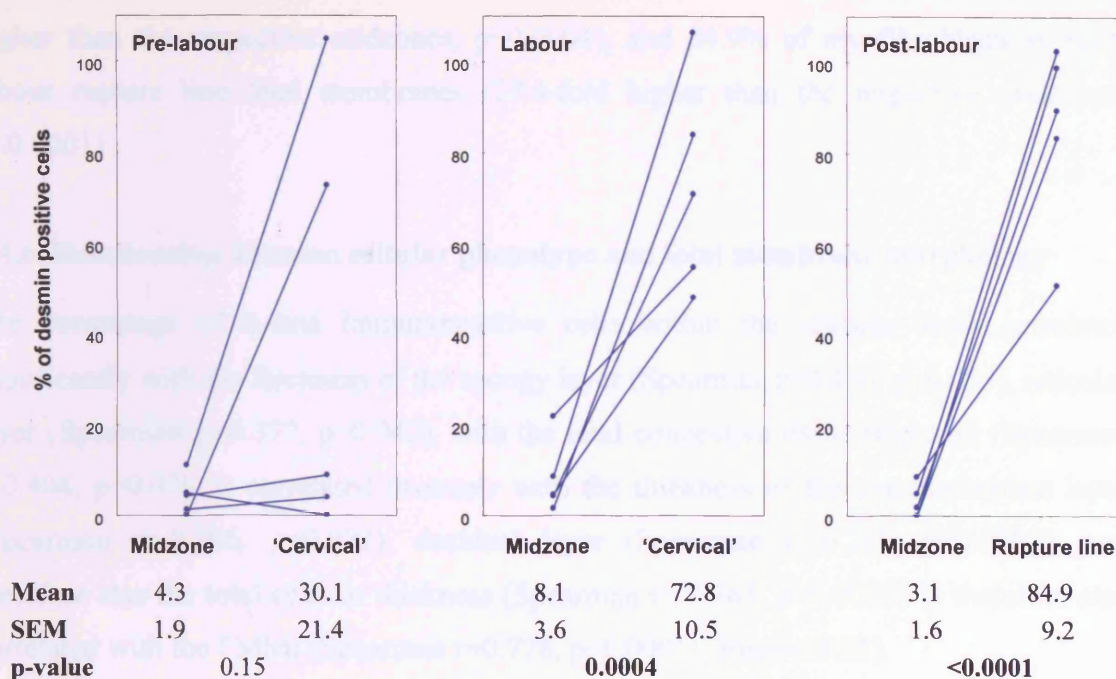


**Figure 3.20.** The number of  $\alpha$ -sma immunoreactive cells within the reticular layer expressed as a percentage of the desmin immunoreactive cells in regional fetal membrane biopsies obtained prior to, during, and following labour at term. The graphs show the mean derived from 10 fields from each biopsy, with lines connecting the data points from individual patients. The percentages are the number of immunoreactive cells for each biopsy, expressed as a percentage of the desmin immunoreactive cell count, and are derived from the mean values from the biopsy. (Therefore there is no SEM for the mean percentage for each biopsy). The mean and SEM (derived from n=5 patients per group) for each group are shown beneath the graphs. Comparisons between biopsy sites and physiological group were using two way ANOVA and Scheffes test. Significant p-values are shown in bold.

higher than the respective midzones,  $p=0.0004$ ), and 84.9% of myofibroblasts in post-labour rupture line fetal membranes (27.4-fold higher than the respective midzones,  $p<0.0001$ ).

#### **3.4.6. Relationship between cellular phenotype and fetal membrane morphology**

The percentage of  $\alpha$ -sma immunoreactive cells within the reticular layer correlated significantly with the thickness of the spongy layer (Spearman  $r=0.450$ ,  $p=0.015$ ), reticular layer (Spearman  $r=0.377$ ,  $p=0.042$ ), with the total connective tissue thickness (Spearman  $r=0.404$ ,  $p=0.03$ ). It correlated inversely with the thickness of the cytotrophoblast layer (Spearman  $r=-0.396$ ,  $p=0.033$ ), decidua layer (Spearman  $r=-0.749$ ,  $p<0.0001$ ), and therefore also the total cellular thickness (Spearman  $r=-0.761$ ,  $p<0.0001$ ). It therefore also correlated with the FMMI (Spearman  $r=0.778$ ,  $p<0.0001$ ) (Figure 3.21).

### **3.5. Discussion**

This work confirms the previous findings of regional altered morphology associated with the rupture line following labour and delivery at term (Malak & Bell, 1994b). However, altered morphology, as determined by significantly increased FMMI compared to the midzone biopsy, was also detected associated with fetal membranes overlying the cervix during labour, and in 2 out of 5 patients prior to the onset of labour. The degree of altered morphology varied widely between patients, especially in the pre-labour and labour groups, but also in the post-labour group where the rupture line FMMI varied between 1.1 and 5.8.

The detection of regional altered morphology prior to the onset of labour at term is consistent with descriptions of the fetal membranes in previous reports (Bourne, 1962; Ibrahim *et al.*, 1983), and with a recent publication on fetal membrane morphology (McLaren *et al.*, 1999a). Bourne had previously described features of the 'dependent' fetal membranes, defined as lying within 1 inch of the undilated internal cervical os (Bourne, 1962). These were biopsied at the commencement of induction of labour. He described the compact, fibroblast, and reticular layers as being thinner than usual, and the trophoblast as degenerate, and the decidua as thin or absent. His illustration of such membranes, however, demonstrates morphology typical of the 'Zone of Altered Morphology' (Malak & Bell, 1994b). Ibrahim described ultrastructural features of loosely and randomly arranged collagen fibrils in the compact, fibroblast and spongy layers in fetal membranes overlying

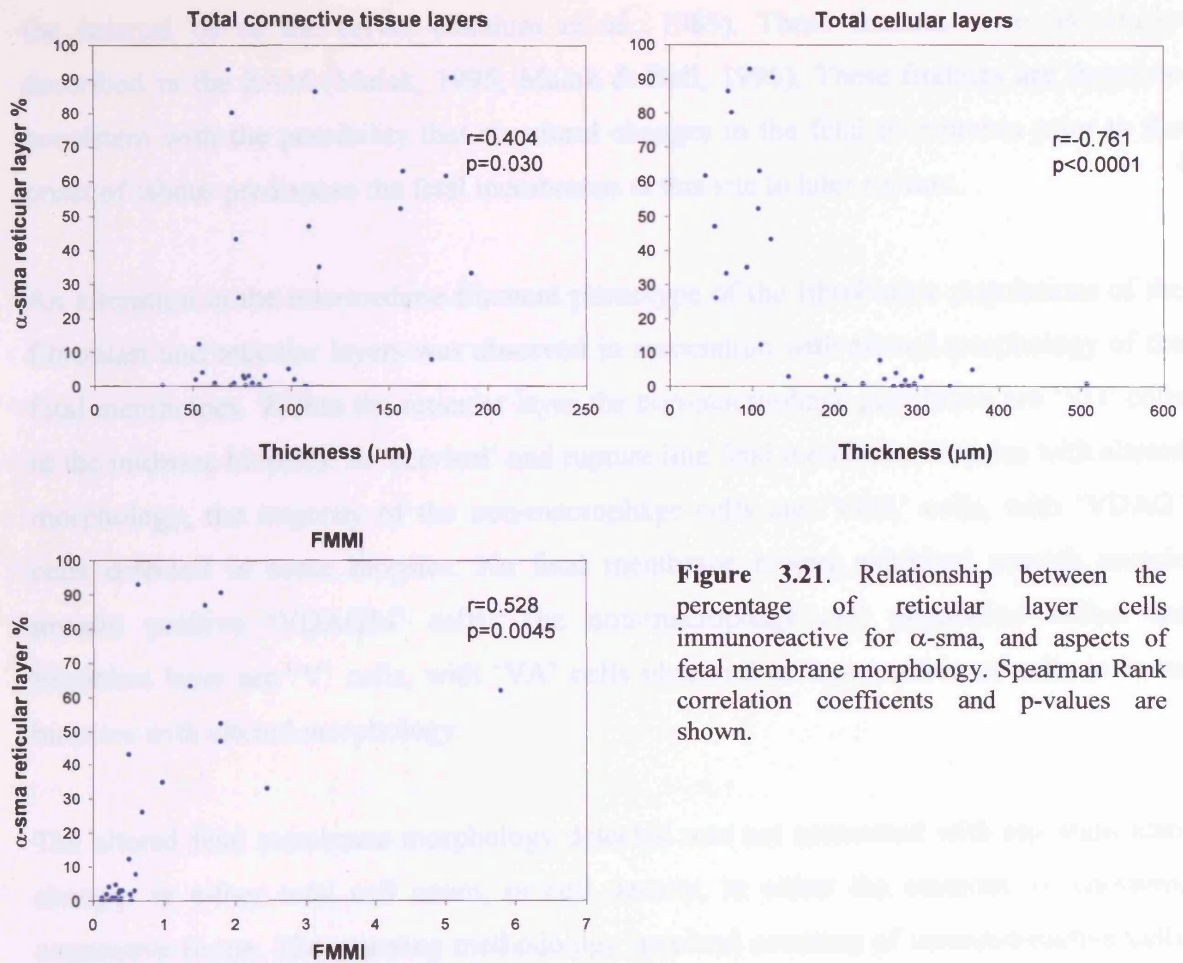


**Figure 3.21.** Relationship between the percentage of reticular layer cells immunoreactive for  $\alpha$ -sma, and aspects of fetal membrane morphology. Spearman Rank correlation coefficients and p-values are shown.

the internal os of the cervix (Ibrahim *et al.*, 1983). These features were previously described in the ZAM (Malak, 1995; Malak & Bell, 1996). These findings are therefore consistent with the possibility that structural changes in the fetal membranes prior to the onset of labour predispose the fetal membranes at this site to later rupture.

An alteration in the intermediate filament phenotype of the fibroblastic populations of the fibroblast and reticular layers was observed in association with altered morphology of the fetal membranes. Within the reticular layer the non-macrophage population are 'VD' cells in the midzone biopsies. In 'cervical' and rupture line fetal membrane biopsies with altered morphology, the majority of the non-macrophage cells are 'VDA' cells, with 'VDAG' cells detected in some biopsies. No fetal membrane biopsy exhibited smooth muscle myosin positive 'VDAGM' cells. The non-macrophage cell population within the fibroblast layer are 'V' cells, with 'VA' cells observed in a proportion of cells in some biopsies with altered morphology.

The altered fetal membrane morphology detected was not associated with any significant changes in either total cell count, or cell density, in either the amniotic or chorionic connective tissue. The counting methodology involved counting of immunoreactive cells. As the markers are expressed within the cytoplasm, then cell processes may be counted as a positive cell. The cell shapes mean that cell nuclei are not commonly encountered. Therefore counting cell nuclei was not used to count the total number of cells. Vimentin immunoreactivity was used as a surrogate for the total cell count. Vimentin is expressed in mesenchymal cells, and expression is therefore expected in fibroblastic cells (Osborn & Weber, 1982). No cells negative for vimentin were noted within the fibroblast and reticular layers in this study, and serial sections confirmed co-expression by cells expressing CD68. Co-expression of vimentin and CD-68 has been described previously (Adegboyega *et al.*, 2002).

The non-fibroblastic cells of the fibroblast and reticular layers have previously been suggested to be dendritic cells (Sutton *et al.*, 1983; Trimble *et al.*, 1992) or macrophages (Bulmer & Johnson, 1984; Malak, 1995). Expression of vimentin has previously been described in both dendritic cells (Narvaez *et al.*, 1996; Badouin *et al.*, 1997), and also in CD68-positive macrophages (Hotta *et al.*, 1998). The non-fibroblastic cells of the fibroblast and reticular layers were identified by immunoreactivity to CD68 in this study, as previously described (Schmidt, 1992; Hanssens *et al.*, 1995). They have previously been

demonstrated to express CD14 (Bulmer & Johnson, 1984; Malak, 1995), HLA-DR (Sutton *et al.*, 1983; Bulmer & Johnson, 1984) and factor XIIIa (Trimble *et al.*, 1992). It is likely, therefore that they are tissue macrophages, as dendritic cells do not usually express CD68 or CD14 (Steinman *et al.*, 1997).

The cellular populations within the connective tissue layers of the fetal membranes changed in association with altered morphology. A trend towards lower percentages of macrophages was identified in association with altered fetal membrane morphology, although this was only significant among the fibroblast layer of the post-labour group and the reticular layer of the pre-labour group. A trend towards an increase in the proportion of desmin-positive cells was also observed in association with altered morphology, although this only reached significance in the reticular layer in the post-labour group.

The detection of  $\alpha$ -sma within the reticular layer cells on both formalin-fixed wax-embedded tissue, and on acetone fixed cryostat sections, contradicts a previous report where  $\alpha$ -sma was not detected within fetal membrane biopsies with altered morphology (Malak, 1995). This anomaly was not resolved. The immunohistochemistry result was confirmed by immunoblotting of extracts obtained from the connective tissue layers of altered morphology and midzone biopsies, using the same monoclonal antibody, 1A4.

It was possible to detect mRNA for  $\alpha$ -sma within the fetal membranes by RT-PCR. However, semi-quantitative RT-PCR, relating the  $\alpha$ -sma RT-PCR products obtained in relation to GAPDH RT-PCR products, did not demonstrate any difference in mRNA level between altered morphology and midzone biopsies. This may be due to the limitations of the technology applied, or may reflect the true *in vivo* relationship between  $\alpha$ -sma mRNA and protein levels. The experiments were performed on mRNA extracted from the connective tissue layers of the fetal membranes only, as the inherent differences in cellular composition between fetal membranes with altered morphology and those from the midzone would invalidate work being carried out on whole fetal membranes. However, the technique of dissecting the connective tissue layers resulted in significant tissue damage, as demonstrated by the degree of DNA contamination of the resultant RNA preparations. It is thus possible that the RNA obtained may not accurately reflect the composition of the tissue. Also, the inherent inaccuracies in the technique of PCR limit its accuracy as a quantitative technique, and an alternative technique such as real-time PCR may have been more appropriate (Freeman *et al.*, 1999). The choice of GAPDH as the reference

housekeeping gene may also not have been appropriate. It is possible that the fetal membranes within the lower uterine segment, exhibiting altered morphology, with poor underlying decidua and undergoing stretch, are relatively hypoxic. Hypoxia is recognised to upregulate GAPDH expression (Lu *et al.*, 2002), and thus may have affected the results. The result may also, however, be a true reflection of the nature of  $\alpha$ -sma expression within the tissue studied. It is well recognised that mRNA expression need not represent protein expression, due to factors including mRNA stability, mRNA processing and nuclear export, translation, and protein degradation (Pradet-Balade *et al.*, 2001).

The inability to detect  $\alpha$ -sma mRNA by *in situ* hybridisation also appears to reflect technical difficulties. The  $\alpha$ -sma gene has a high degree of homology with other actin genes, and the probe designed for *in situ* hybridisation reacted to all cells within the biopsies tested, suggesting cross reactivity with  $\beta$ -actin or  $\gamma$ -actin (the  $\alpha$ -sma nucleotide sequence shares 82.6% homology with the  $\gamma$ -cytoplasmic actin nucleotide sequence, and 82.0% homology with the  $\beta$ -cytoplasmic actin nucleotide sequence (Miwa *et al.*, 1988)).

Altered fetal membrane morphology, and  $\alpha$ -sma expression within cells of the reticular layer was detected in 2 out of 5 pre-labour 'cervical' fetal membrane biopsies. There are a number of possible reasons for this. It may be that the altered morphology and  $\alpha$ -sma expression develop in the fetal membranes overlying the cervix over a period prior to labour, and their detection in a proportion of patients reflects this temporal development and indicates proximity to spontaneous labour. Alternatively, the altered morphology and  $\alpha$ -sma expression may be present overlying the cervix prior to labour at term in all patients, and the detection in 2 out of 5 studied in this chapter reflects inaccuracy in the biopsy technique. It may also be a combination of these, as increase in size of such an area would affect the probability of biopsying such an area accurately.

### 3.6. Conclusions

- Regional changes in fetal membrane morphology, characterised by increased connective tissue thickness and reduced cellular layer thickness, can be identified in fetal membrane biopsies obtained overlying the cervix following, and during labour, and in the rupture line following labour and delivery at term.

- Myofibroblasts in the reticular layer express the 'VD' phenotype. Expression of the 'VDA' and the 'VDAG' phenotypes were detected in association with regional altered morphology.
- Cells within the fibroblast layer have the 'V' phenotype, and rarely the 'VA' or 'VAG' phenotype.
- CD68-positive macrophages were detected in both the fibroblast layer and reticular layer

## **Chapter 4**

### **Mapping of morphological changes and myofibroblast differentiation in fetal membranes prior to the onset of labour**

#### **4.1. Introduction**

In Chapter 3, a regional increase in  $\alpha$ -sma expression in the reticular layer of the chorion was demonstrated, associated with altered morphology of the fetal membranes. Increased  $\alpha$ -sma expression within the reticular layer was observed in rupture line biopsies following labour at term, in 'cervical' fetal membrane biopsies obtained during labour, but in only 2 out of 5 'cervical' biopsies obtained prior to the onset of labour at term. Altered morphology in the fetal membranes as measured by increased FMMI was observed in rupture line biopsies following labour at term, 'cervical' fetal membrane biopsies obtained during labour, and in 2 out of 5 of the 'cervical' biopsies obtained prior to the onset of labour at term. There are two possible related explanations for these anomalies:

1. The altered morphology and  $\alpha$ -sma expression in the fetal membranes over the cervix develop in association with preparation for labour, in a fixed period prior to the onset of labour. The detection of these features in the 'cervical' fetal membrane biopsies obtained prior to labour at 38 weeks gestation may therefore depend on the proximity of the woman to spontaneous labour.

And/Or

2. The altered morphology and  $\alpha$ -sma expression in the fetal membranes over the cervix affects a limited area of membrane. This area may increase in size as labour approaches/occurs. The detection of increased  $\alpha$ -sma expression and altered morphology in all of the 'cervical' fetal membrane biopsies during labour (compared to 2 out of 5 prior to labour) would be consistent with a larger area being affected.

It is therefore possible that obtaining a single biopsy of fetal membrane overlying the cervix may not be sufficiently representative, and may be affected by variation in size and development of morphological changes and reticular layer  $\alpha$ -sma expression. It is also

possible that the morphological changes and  $\alpha$ -sma expression may occur independently, and affect different areas of fetal membrane, or have a different temporal onset. In order to test these hypotheses, a study examining the morphology and  $\alpha$ -sma expression in comprehensively mapped fetal membranes prior to the onset of labour at term was undertaken.

## **4.2. Aims**

- To determine the frequency of the occurrence, approximate size, and location of an area of altered morphology in fetal membranes obtained prior to the onset of labour at term.
- To determine the frequency of the occurrence, approximate size, and location of the area of  $\alpha$ -sma expression in the reticular layer of the fetal membranes prior to the onset of labour at term.
- To examine the relationship between individual features of altered morphology (increase in connective tissue thickness and decrease in thickness of cellular layers) and  $\alpha$ -sma expression in areas of fetal membrane prior to the onset of labour at term.

## **4.3. Materials and Methods**

### **4.3.1. Tissue samples**

Fetal membranes were obtained from elective Caesarean section carried out prior to labour at 38-39 weeks (n=10). Multiple 3cm biopsies were taken radially from the location of a Babcock tissue forceps, placed on the membranes over the internal os of the cervix by the surgeon, out towards the placental edge (2.1.1.3.). Additional biopsies were taken in the angles between the axes to assist with the accuracy of the mapping. When the membrane was placed flat, the location of the Babcock tissue forceps and the Caesarean section incision in the membranes allowed orientation of the membranes with respect to the uterus. Thus the longitudinal axis of biopsies corresponds to the sagittal plane of the uterus, and the transverse axis of biopsies to the coronal plane. Tissues were formalin-fixed and wax-embedded (2.2.1.).

### **4.3.2. Immunohistochemistry**

Immunohistochemistry was carried out using monoclonal antibodies to  $\alpha$ -sma, vimentin and cytokeratin as previously described (2.3.) in order to assess total cell number and myofibroblast phenotype, and to assist with morphology measurements.

### **4.3.3. Image analysis**

Fetal membrane morphology was examined by measuring the constituent layers of the fetal membranes (2.8.1.1.). Sections immunohistochemically stained with a monoclonal antibody to cytokeratin were used to identify and measure the cytotrophoblast layer. Counting of cells immunoreactive for  $\alpha$ -sma and vimentin was carried out (2.8.1.2.).

### **4.3.4. Statistical analysis**

The area of fetal membrane affected by morphological and other changes was calculated based upon the area of an ellipse (section 2.9.). ROC curve analysis was used to determine the decidual thickness which best predicted  $\alpha$ -sma immunoreactivity within the reticular layer. Statistical tests used to compare parameters between biopsies from different areas of the fetal membranes, and to correlate different parameters, are described in section 2.9.

## **4.4. Results**

### **4.4.1. Fetal membrane morphology**

The relationship between the changes in thickness of the different layers of the fetal membrane was examined by looking at graphical representations of the parameters along the longitudinal and transverse axes of the membrane maps. The results for a sample patient are shown in **Figures 4.1a&b.**

Decidual thinning was a consistent feature of the altered morphology in all ten membranes, affecting the widest area of the membrane (in comparison to the changes in the other parameters), and typically showing an abrupt change from 'thick' decidua to 'thin' decidua, over a maximal distance of one biopsy. Within the area of thin decidua, the membranes exhibited increased thickness of the individual connective layers (amniotic connective tissue, spongy and reticular layers), and thinning of the cytotrophoblast layers.

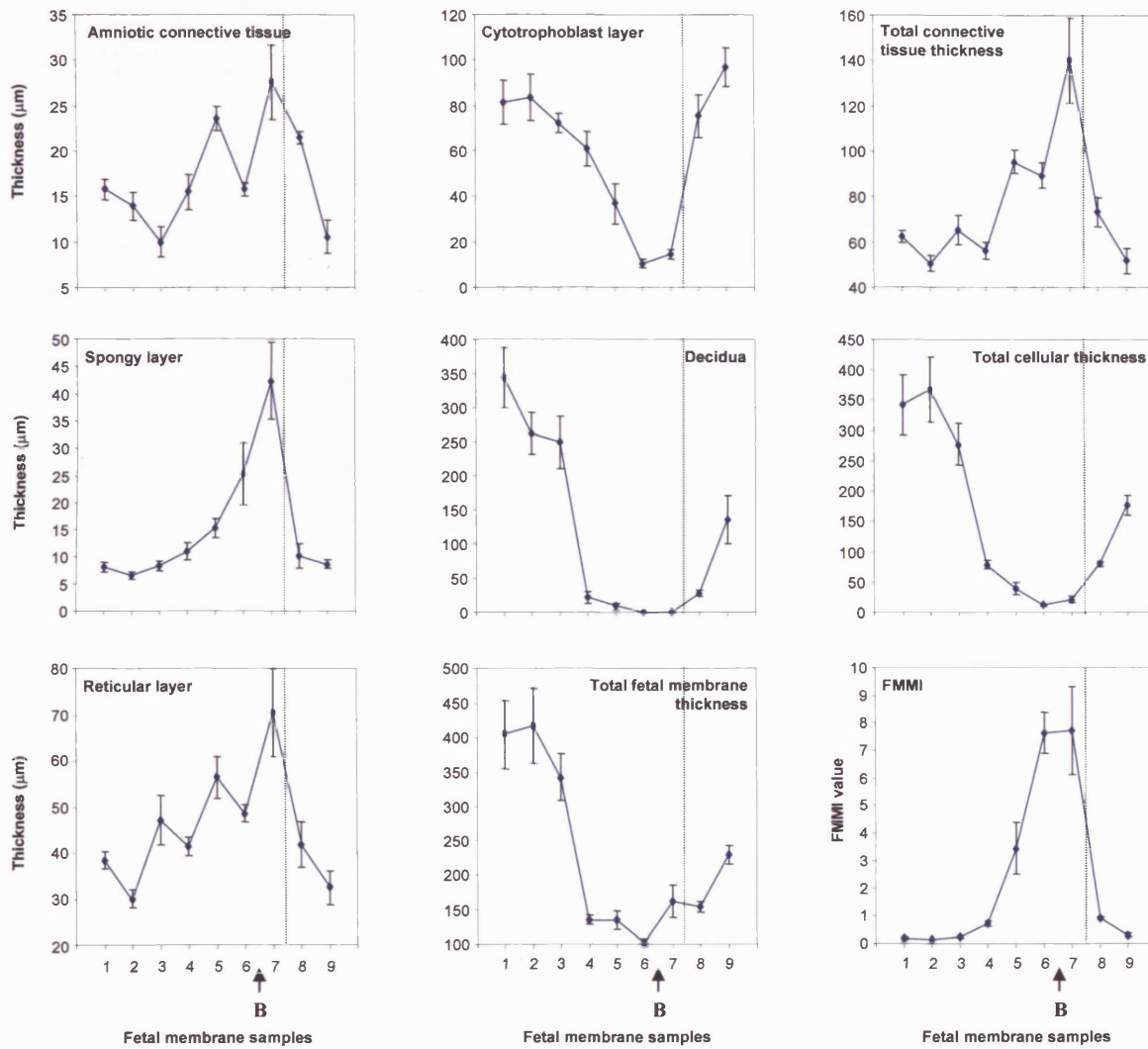


**Figure 4.1a.** The thickness ( $\mu\text{m}$ ) of the different layers of the fetal membrane samples, and the resultant FMMI, obtained from sequential fetal membrane biopsies along the longitudinal axis of a fetal membrane map (Patient 270). Each point represents the mean of 5 measurements, and the standard errors are also indicated. The location of the Babcock tissue forceps is shown (B). The dotted line marks the intersection with the transverse axis of the map (see Figure 4.1b).

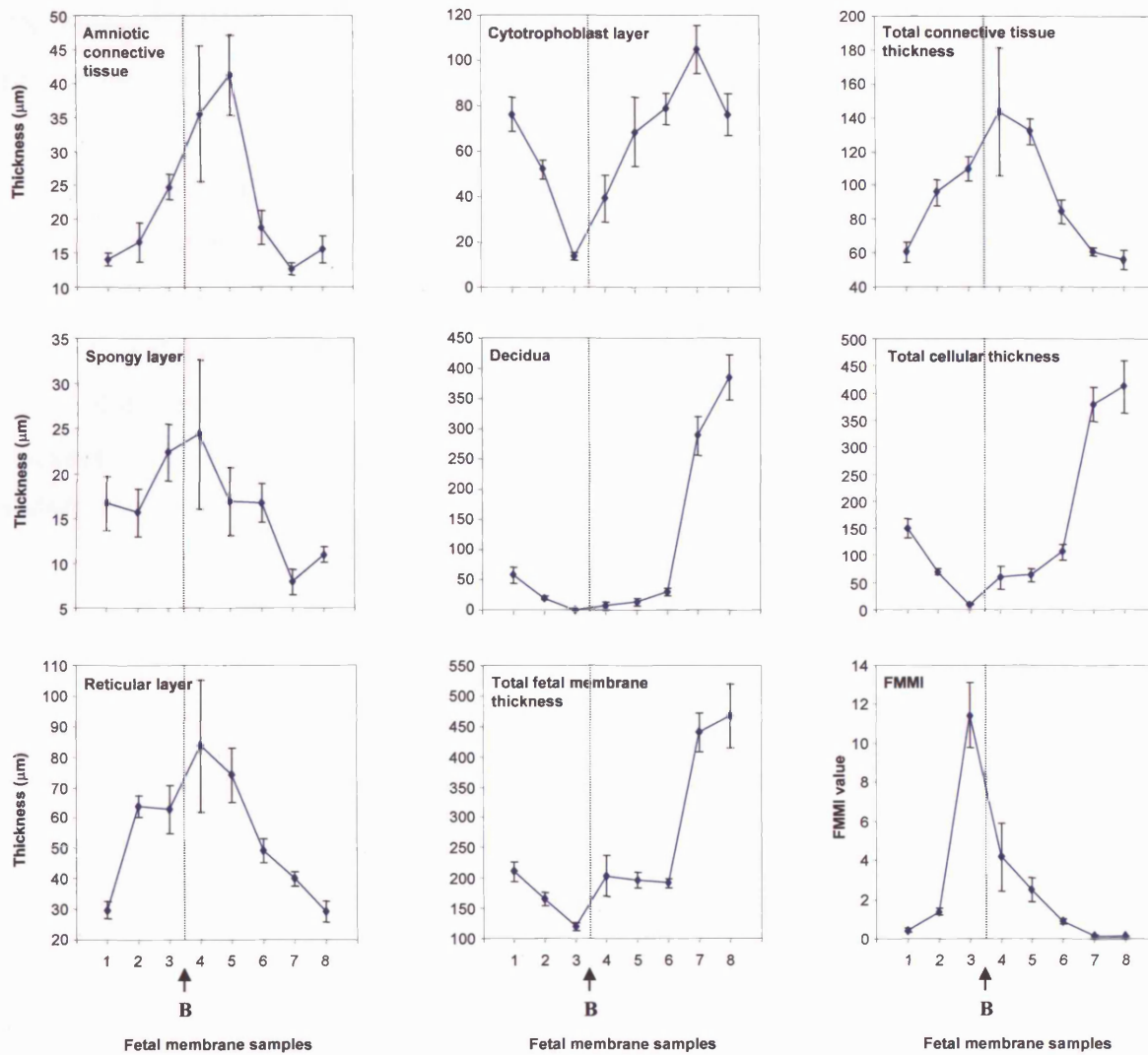


**Figure 4.1b.** The thickness ( $\mu\text{m}$ ) of the different layers of the fetal membrane samples, and the resultant FMMI, obtained from sequential fetal membrane biopsies along the transverse axis of a fetal membrane map (Patient 270). Each point represents the mean of 5 measurements, and the standard errors are also indicated. The location of the Babcock tissue forceps is shown (B). The dotted line marks the intersection with the longitudinal axis of the map (see Figure 4.1a).

The change in thickness of these layers was typically gradual, and confined within the area of thin decidua.

The degree of altered morphology and area affected varied between patients. Because of the variation in the thickness of the component layers between patients, it was not possible to define a 'normal' thickness for each layer which could be applied to membranes from all patients, and beyond which the morphology could be considered altered. The altered morphology was therefore described as the ratio of the total connective tissue layer thickness to total connective tissue thickness (the Fetal Membrane Morphometric Index, FMMI (Malak & Bell, 1994b)). The distribution of FMMI of the biopsies for a representative fetal membrane map is shown in **Figure 4.2**.

The maximal FMMI for each individual membrane map varied from 2.0 to 11.4. The changes in FMMI along the longitudinal and transverse axes of the ten fetal membrane maps are shown in **Figures 4.3 & 4.4**. (The area of altered morphology was eccentric to the Babcock in patient 276, and the 'secondary' longitudinal axis running through the region was used). There was not a consistent relationship between the area affected by the increase in thickness of the individual connective tissue layers and that of cytotrophoblast thinning. One membrane did not exhibit an increase in connective tissue thickness, it did however display thinning of the cytotrophoblast and decidua. Thus the FMMI was increased. One membrane did not have an area of thinned cytotrophoblast, but did have increased connective tissue thickness and thinning of the decidua, thus giving a raised FMMI. The area affected by elevated FMMI, which was in most fetal membranes affected significantly by the decidual thinning, was calculated for each individual fetal membrane, based on elevation of the FMMI above the baseline for the midzone for that membrane. Within this area an inner zone of 'extreme altered morphology', characterised by marked thinning of the connective tissue layers of the amnion and chorion, and thinning of the cytotrophoblast and decidual layers was identified. The area affected by elevated FMMI and 'extreme altered morphology' can be seen on the maps in **Figure 4.5**. The areas affected by elevated FMMI and 'extreme altered morphology', based on the axes of the maps and the area of an ellipse, are shown for individual patients in **Table 4.1**. The location of the area of extreme altered morphology with respect to the Babcock tissue forceps and the Caesarean section incision indicates that it is located in the membranes from the lower uterine segment, and is centred upon the internal os of the cervix.

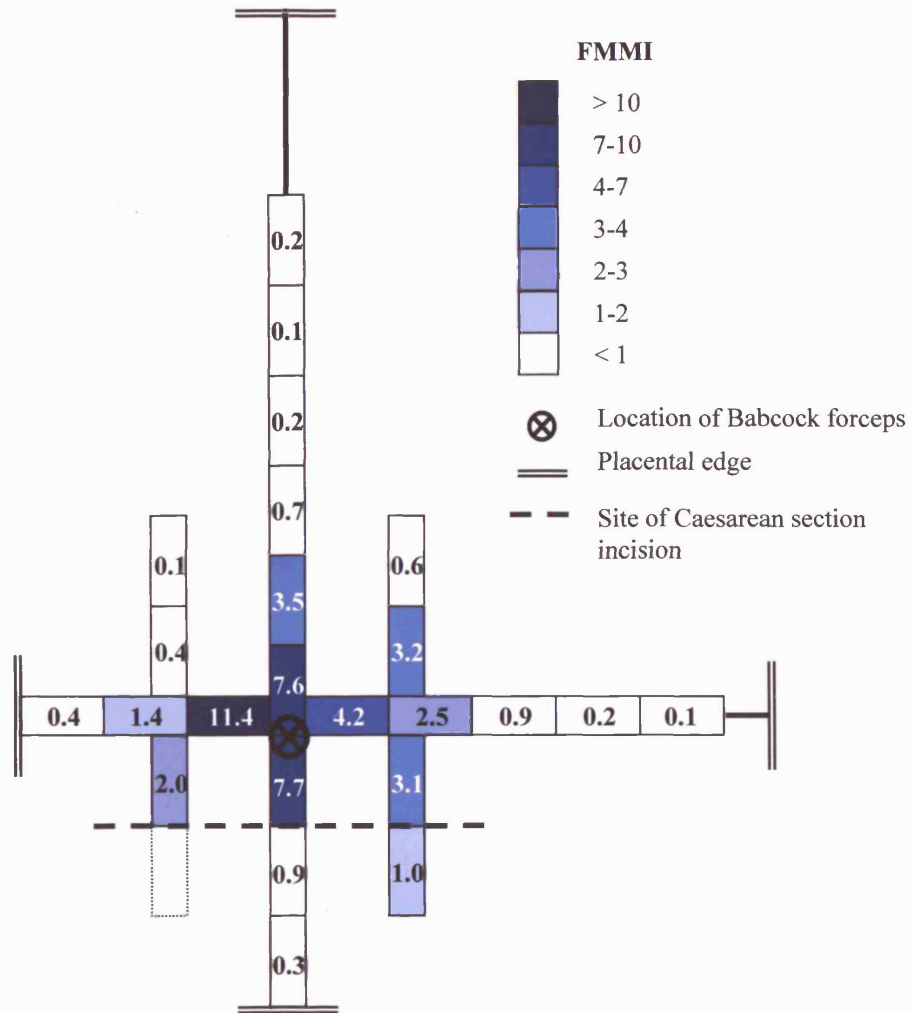


**Figure 4.2.** Diagrammatic representation of the FMMI of the fetal membrane biopsies for a fetal membrane map (Patient 270). The FMMI values for each individual biopsy are shown.

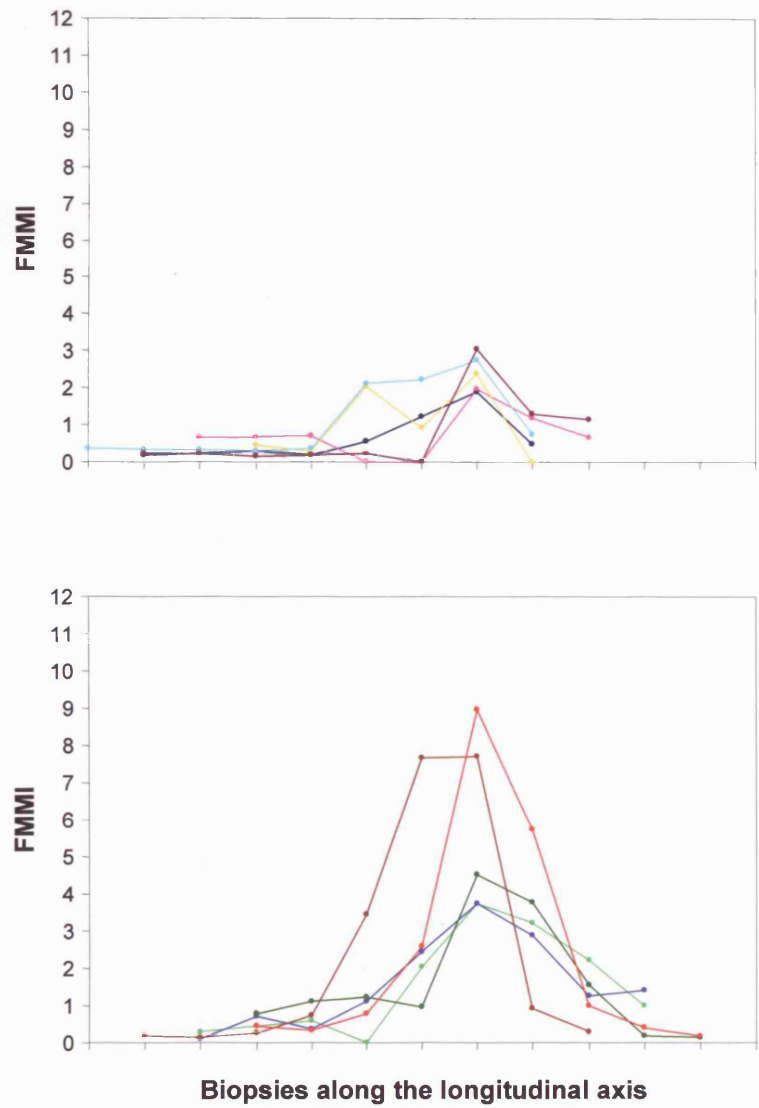


**Figure 4.3.** The FMMI values of the fetal membrane samples along the longitudinal axis of the maps obtained from 10 patients at term prior to the onset of labour. Each line represents a different patient, with the colour of the line representing the same patient as in Figures 4.4, 4.9 & 4.10. The data is spread across two graphs solely to assist in the clarity of reading.

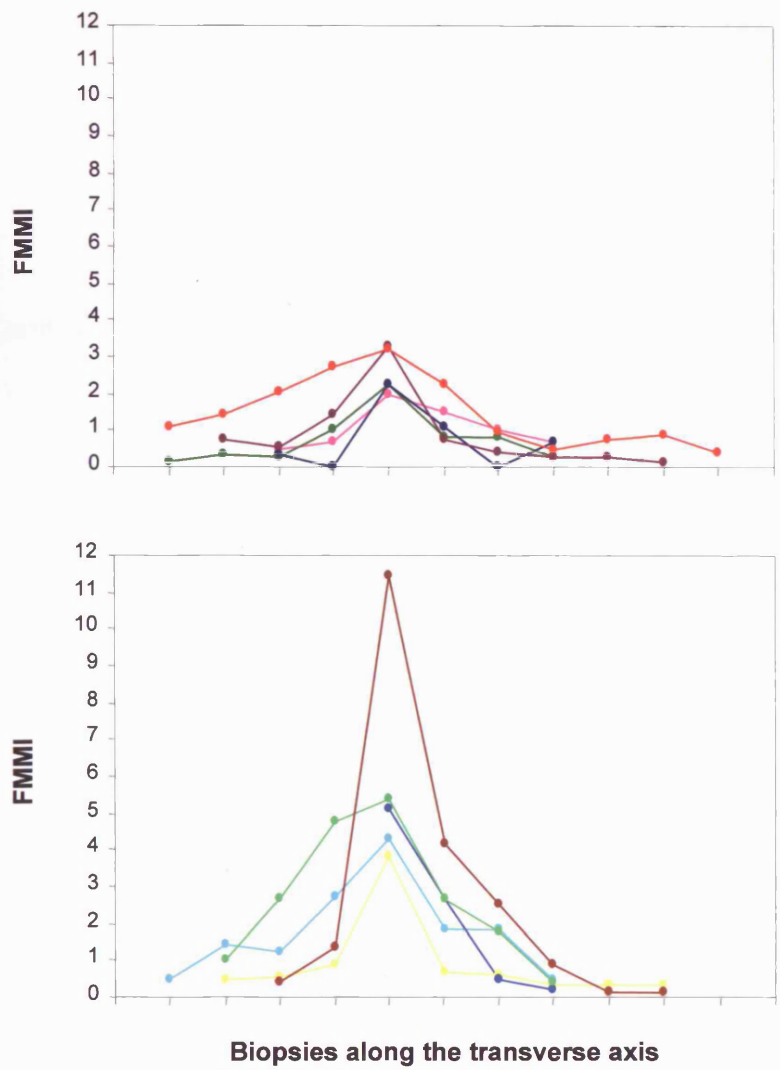


**Figure 4.4.** The FMMI values of the fetal membrane samples along the transverse axis of the maps obtained from 10 patients at term prior to the onset of labour. Each line represents a different patient, with the colour of the line representing the same patient as in Figures 4.3, 4.9 & 4.10. The data is spread across two graphs solely to assist in the clarity of reading.

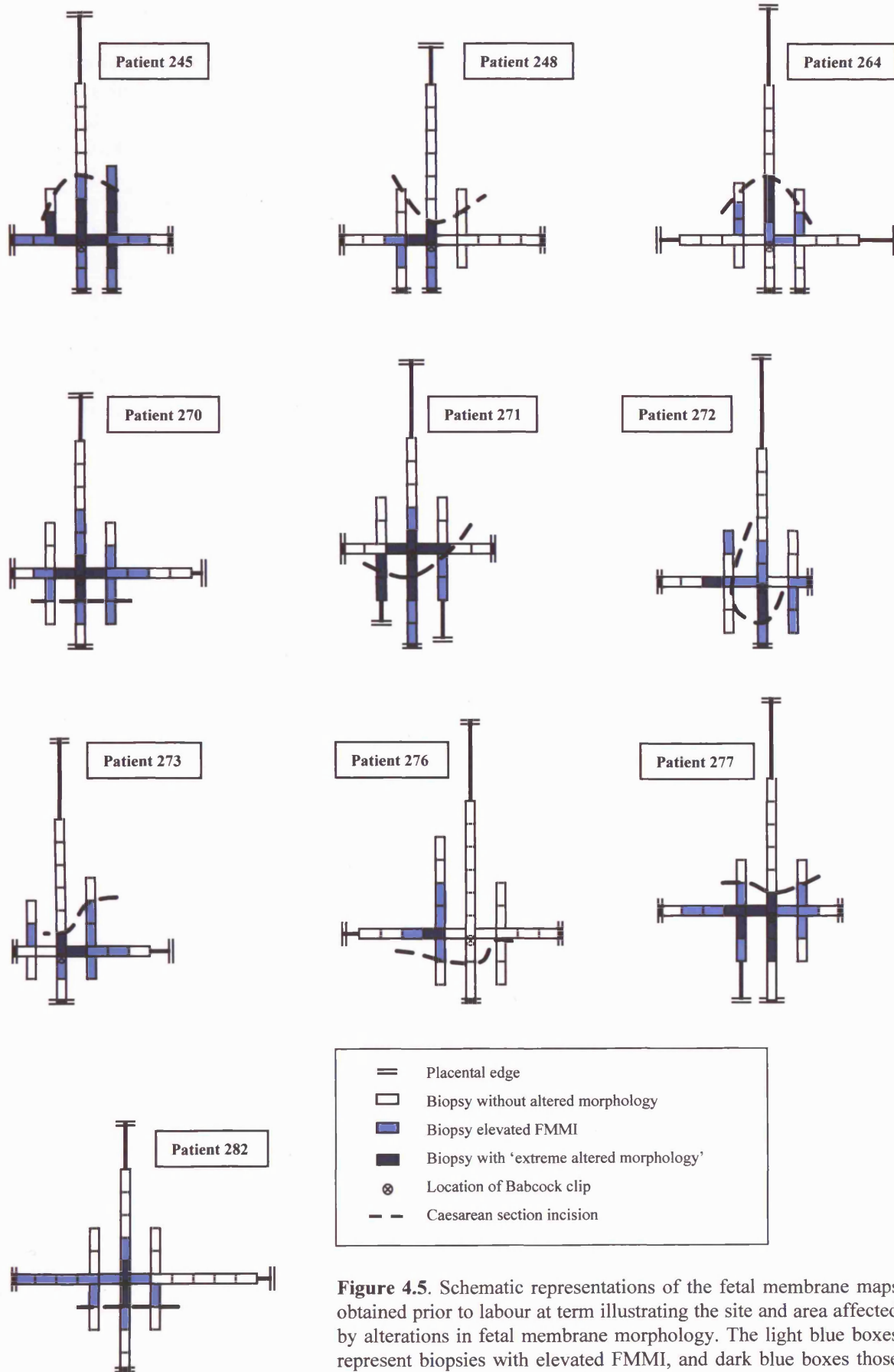


**Figure 4.5.** Schematic representations of the fetal membrane maps obtained prior to labour at term illustrating the site and area affected by alterations in fetal membrane morphology. The light blue boxes represent biopsies with elevated FMMI, and dark blue boxes those with 'extreme altered morphology'. Great variation between patients in the area of fetal membrane affected by altered morphology can be seen.

<b>Patient code</b>	<b>Area (cm<sup>2</sup>) with elevated FMMI</b>	<b>Area (cm<sup>2</sup>) with extreme altered morphology</b>	<b>Area (cm<sup>2</sup>) with <math>\alpha</math>-sma positivity</b>
<b>245</b>	223.8	33.0	113.1
<b>248</b>	49.5	9.4	70.7
<b>264</b>	28.3	4.7	49.5
<b>270</b>	188.5	33.0	176.7
<b>271</b>	127.2	63.6	141.4
<b>272</b>	153.9	3.9	121.0
<b>273</b>	78.5	9.4	70.7
<b>276</b>	47.1	2.4	47.1
<b>277</b>	127.2	49.5	70.7
<b>282</b>	169.6	4.7	70.7
<b>Mean</b>	119.4	21.4	93.1

**Table 4.1.** Estimated area affected by altered morphology (elevated FMMI), extreme altered morphology and  $\alpha$ -sma positivity in fetal membrane maps obtained prior to the onset of labour at term. The area is based on calculating the area of an ellipse.

The morphology measurements for the single biopsy exhibiting the most extreme altered morphology (as defined by the maximal FMMI within the fetal membrane map), and a single midzone biopsy (defined as the 5<sup>th</sup> biopsy along the longitudinal axis from the Babcock location, i.e. minimum 12cm from the Babcock forceps, as previously defined), per patient are shown in **Table 4.2**. The fetal membranes exhibiting extreme altered morphology demonstrated increased thickness of 48%, 84% and 81% of the amniotic connective tissue, spongy layer and reticular layer respectively compared to midzone biopsies. The cytotrophoblast layer and decidual layer had decreased thickness of 51% and 91% respectively compared to midzone fetal membranes. The fetal membranes exhibiting extreme altered morphology were therefore 47% thinner than midzone biopsies. All of these differences were highly significant (all  $p \leq 0.01$ ).

When the values for fetal membrane biopsies identified by the Babcock tissue forceps were compared to the midzone biopsies, similar increased thickness of the connective tissue layers was observed, although less extreme thinning of the cellular layers occurred (**Table 4.2**). When the data for individual patients is examined, it is apparent that 9 out of 10 'Babcock' biopsies exhibited some degree of altered morphology (in 8 out of 10, extreme altered morphology). In 7 out of the 9 membranes with a 'Babcock' biopsy with altered morphology, an alternative biopsy with more extreme altered morphology could be identified (**Figure 4.6**).

#### **4.4.2. 'Mucus-associated' fetal membrane morphology**

Six out of the ten patients had one or more fetal membrane biopsies with histologically identified mucoïd material adherent to the cellular surface of the fetal membrane (**Figure 4.7**). The biopsies with mucoïd material attached were in the middle of the area of extreme altered morphology, and the material is presumed to be mucus derived from the cervical glands. In four of the patients the mucoïd material was associated with part or all of a single fetal membrane biopsy. In the remaining two patients a number of adjacent biopsies had mucoïd material attached, covering an estimated area of 22cm<sup>2</sup>. These two patients had 1<sup>st</sup> and 2<sup>nd</sup> largest areas affected by elevated FMMI, and the 1<sup>st</sup> and 3<sup>rd</sup> highest peak FMMI values (5.4 and 11.4).

When compared to other membrane biopsies exhibiting extreme altered morphology (total 27 biopsies from 10 patients), the 'mucus-associated' biopsies (total 13 biopsies from 6 patients) had significantly thinner amniotic connective tissue, reticular layer,

	Extreme altered morphology			Midzone			p-value
	Mean	SEM	COV	Mean	SEM	COV	
<b>Amniotic connective tissue</b>	31.6	2.1	21.2	21.4	2.9	42.3	0.01
<b>Spongy layer</b>	25.7	4.2	51.3	14.0	2.3	52.4	0.01
<b>Reticular layer</b>	85.6	9.2	34.0	47.4	4.7	31.7	0.003
<b>Cytotrophoblast layer</b>	40.9	15.6	38.1	83.0	7.0	26.6	0.0002
<b>Decidua</b>	19.9	4.2	65.9	218.8	45.2	65.4	0.002
<b>Total connective tissue</b>	142.9	13.1	28.9	82.7	9.3	35.3	0.001
<b>Total cellular</b>	60.8	7.2	37.6	301.8	45.8	48.0	0.0006
<b>Total fetal membrane thickness</b>	203.7	16.8	26.1	384.6	45.2	37.2	0.006
<b>FMMI</b>	4.9	1.0	62.7	0.4	0.1	77.1	0.001

**Table 4.2.** Thickness measurements ( $\mu\text{m}$ ) of the component layers of the fetal membranes obtained prior to labour at term, in selected biopsies exhibiting extreme altered morphology (n=10) and midzone biopsies (n=10). The Fetal Membrane Morphometric Index (FMMI) represents the ratio between the total connective tissue thickness and total cellular thickness. The coefficient of variance (COV) gives a measure of the variation in the measurement values as a percentage of the mean. The ‘extreme altered morphology’ and midzone biopsy data are compared using a paired t-test, and the p-values shown on the table. All differences are highly significant.

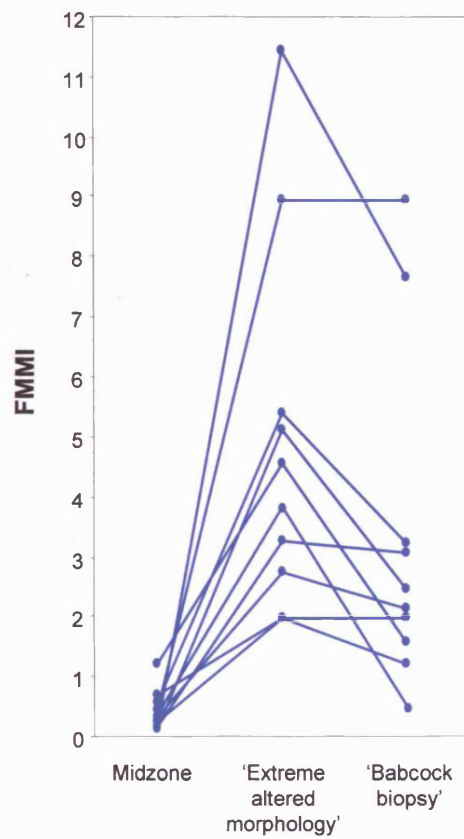
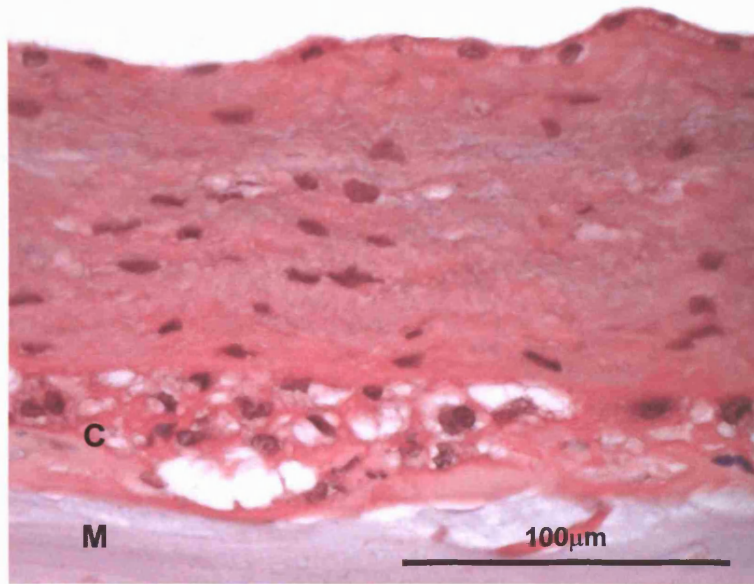


**Figure 4.6.** The fetal membrane morphometric index for selected biopsies from fetal membrane maps obtained from patients prior to the onset of labour at term. Each point represents the mean value of 10 fields measured. The lines connect the samples from individual patients. Midzone biopsies, selected 'extreme altered morphology' biopsies, and the biopsy marked by the Babcock tissue forceps are plotted.

a



b

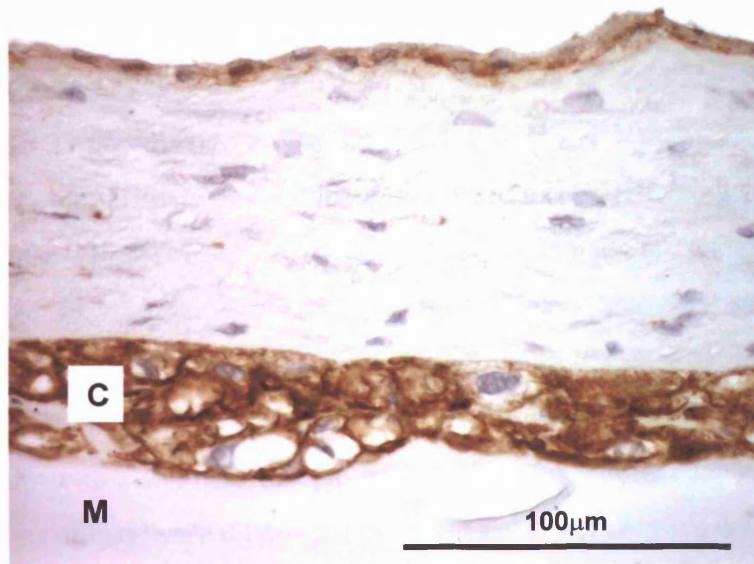


**Figure 4.7.** Serial sections of a 'mucus-associated' fetal membrane biopsy stained with haematoxylin and eosin (a), and immunohistochemistry for cytokeratin (b). Mucoïd maternal (M) is present immediately beneath the cytotrophoblast layer (C). Immunoreactivity for cytokeratin within the cytotrophoblast layer (b) highlights the absence of decidual cells.

cytotrophoblast layer, decidua and total fetal membrane thickness (**Table 4.3**). Indeed on a number of the biopsies no decidual cells were discernible at all (**Figure 4.7**). The reduction in thickness of the reticular layer did not however reach the values associated with midzone biopsies (77.4 $\mu$ m compared to 47.4 $\mu$ m in midzone biopsies,  $p=0.0027$ ), although the thickness of the amniotic connective tissue and spongy layers were not significantly different from that measured in midzone biopsies (29.0 $\mu$ m vs. 21.6 $\mu$ m,  $p=0.07$ ; and 19.8 $\mu$ m vs. 14.0 $\mu$ m,  $p=0.09$  respectively). Thus the total connective tissue thickness in the 'mucus-associated' biopsies was still significantly higher than in the midzone biopsies (122.5 $\mu$ m vs. 82.7 $\mu$ m,  $p=0.0059$ ) (**Tables 4.2, 4.3**). The extreme thinning of the cellular layers on these membranes gave a significantly higher FMMI (**Table 4.3, Figure 4.8**).

#### **4.4.2. $\alpha$ -sma expression**

##### **4.4.2.1. Chorion**

All fetal membranes examined exhibited a region of  $\alpha$ -sma expression within the reticular layer of the chorion. This was located within the area of decidual thinning previously described (4.4.1.). The change along the longitudinal and transverse axes from ' $\alpha$ -sma negative' to ' $\alpha$ -sma positive' was typically abrupt in onset, occurring over a maximum of one 3cm biopsy (**Figures 4.9 & 4.10**). The percentage of vimentin positive cells immunoreactive for  $\alpha$ -sma was 72.7% in the selected 'extreme altered morphology' biopsies (those defined with the maximum FMMI, as in **Table 4.2**) compared to 5.2% in the selected midzone biopsies (biopsies as in **Table 4.2**;  $p=0.000003$ ). The area of fetal membrane with  $\alpha$ -sma immunoreactive cells within the reticular layer (calculation based on the area of an ellipse) varied between patients (**Table 4.1, Figure 4.11**).

**Figure 4.12** compares the reticular layer  $\alpha$ -sma count in the selected midzone, 'extreme altered morphology' and 'Babcock' biopsy per membrane. Only 1 out of 10 'Babcock' biopsies failed to demonstrate  $\alpha$ -sma immunoreactive cells, and also did not exhibit altered morphology (**Figure 4.6**).

When data from all biopsies from all ten fetal membranes was combined, the numbers of  $\alpha$ -sma immunoreactive cells within the reticular layer correlated positively with the reticular layer thickness (Spearman  $r=0.459$ ,  $p<0.0001$ ), amniotic connective tissue thickness (Spearman  $r=0.421$ ,  $p<0.0001$ ) and total connective tissue thickness (Spearman

	<b>'Mucus-associated' biopsies (n=13)</b>			<b>Other extreme altered morphology biopsies (n=27)</b>			<b>t-test p value</b>
	<b>Mean</b>	<b>SEM</b>	<b>COV</b>	<b>Mean</b>	<b>SEM</b>	<b>COV</b>	
<b>Amniotic connective tissue</b>	29.0	2.8	33.5	41.6	2.0	31.3	0.0049
<b>Spongy layer</b>	19.8	2.3	40.6	28.2	3.5	78.6	0.21
<b>Reticular layer</b>	77.4	6.8	31.7	108.1	4.5	26.7	0.0022
<b>Cyto layer</b>	31.7	4.4	49.8	54.3	3.1	36.9	0.0010
<b>Decidua</b>	8.4	2.8	118.9	29.3	3.6	79.4	0.0037
<b>Total connective tissue</b>	122.5	8.9	25.2	177.9	7.6	27.2	0.00083
<b>Total cellular</b>	40.1	6.2	55.6	83.7	5.6	43.0	0.00029
<b>Total fetal membrane thickness</b>	153.2	14.1	33.2	261.5	9.1	22.5	0.000002
<b>FMMI</b>	5.2	0.7	49.4	3.5	0.2	43.0	0.015

**Table 4.3.** Thickness measurements ( $\mu\text{m}$ ) of the component layers of the fetal membranes obtained prior to labour at term, in all 'mucus-associated' fetal membrane biopsies compared to all other fetal membrane biopsies exhibiting extreme altered morphology. The Fetal Membrane Morphometric Index (FMMI) represents the ratio between the total connective tissue thickness and total cellular thickness. The coefficient of variance (COV) gives a measure of the variation in the measurement values as a percentage of the mean.

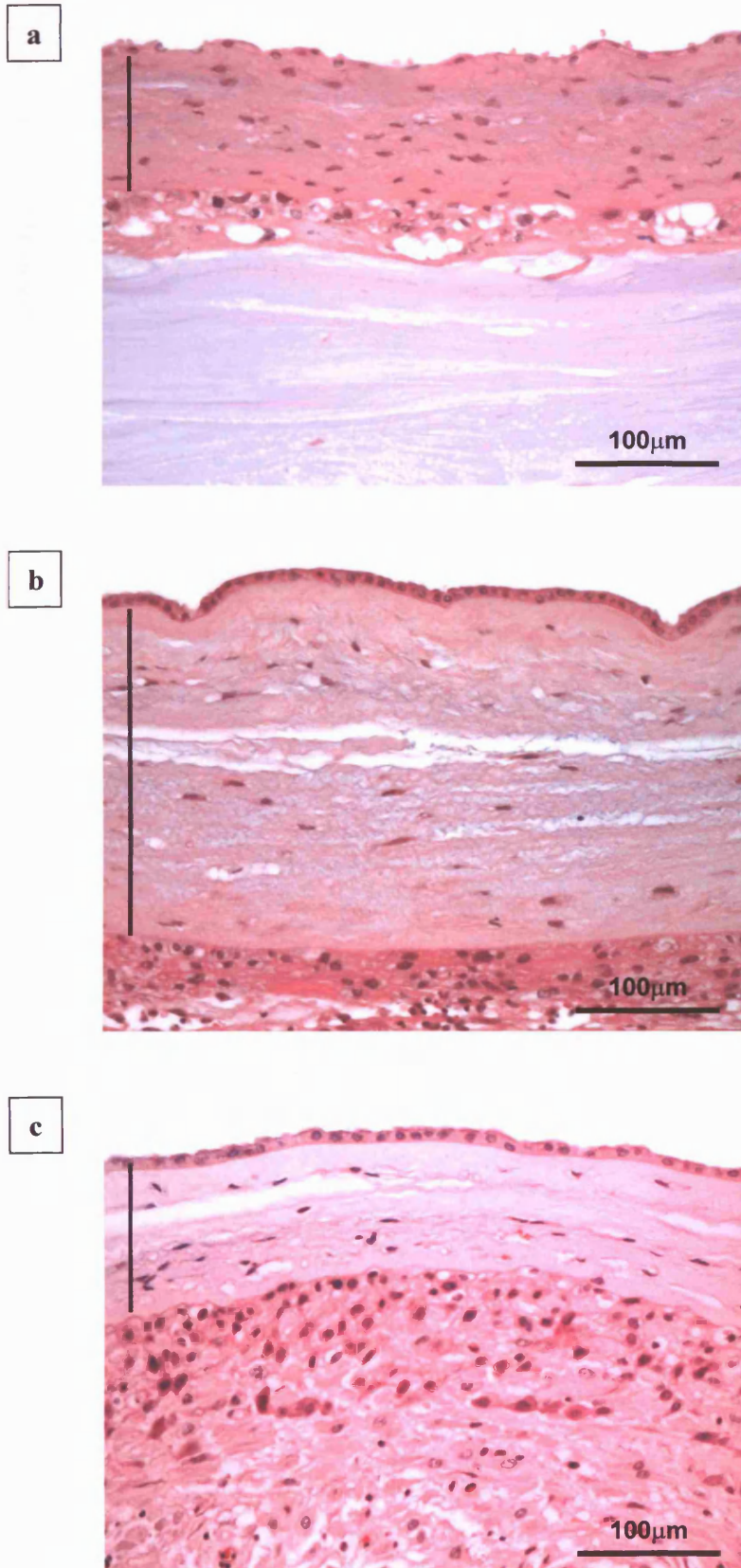


**Figure 4.8.** Haematoxylin and eosin stained sections of a 'mucus-associated' fetal membrane biopsy (a), a fetal membrane biopsy exhibiting extreme altered morphology (b), and a midzone fetal membrane biopsy (c). The vertical line highlights the thickness of the combined connective tissue layers of the amnion and chorion.

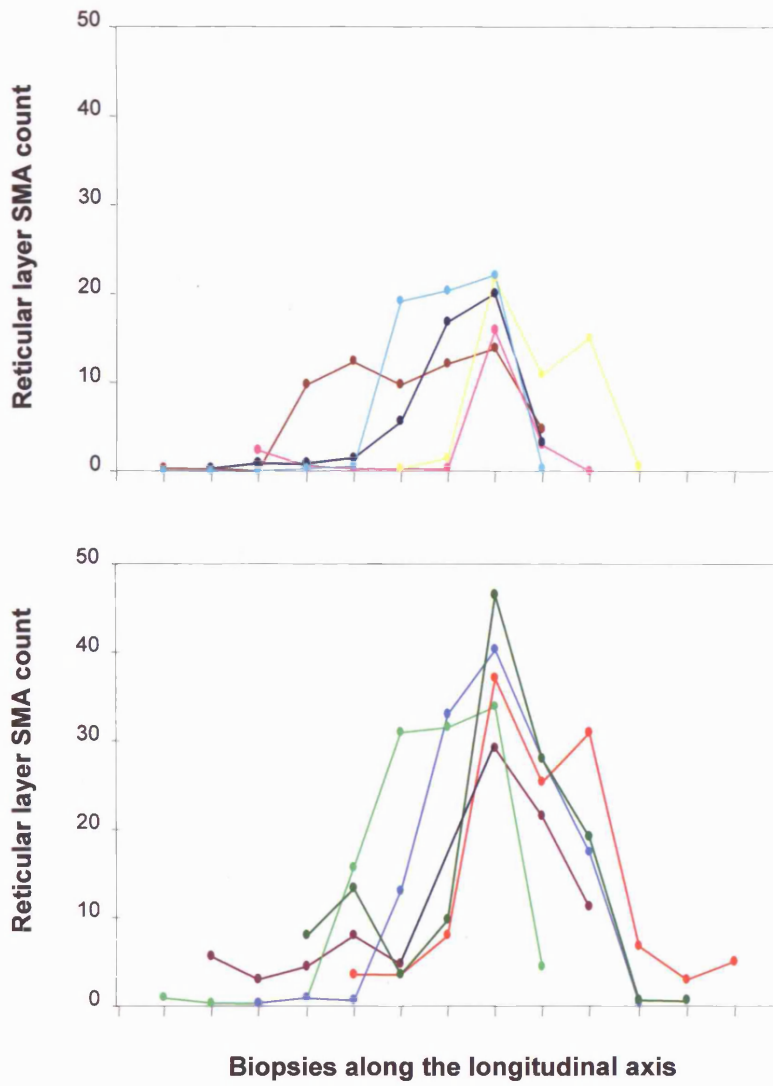


**Figure 4.9.** The reticular layer  $\alpha$ -SMA count of the fetal membrane samples along the longitudinal axis of the maps obtained from 10 patients at term prior to the onset of labour. Each line represents a different patient, with the colour of the line representing the same patient as in Figures 4.3, 4.4 & 4.10. The data is spread across two graphs solely to assist in the clarity of reading.

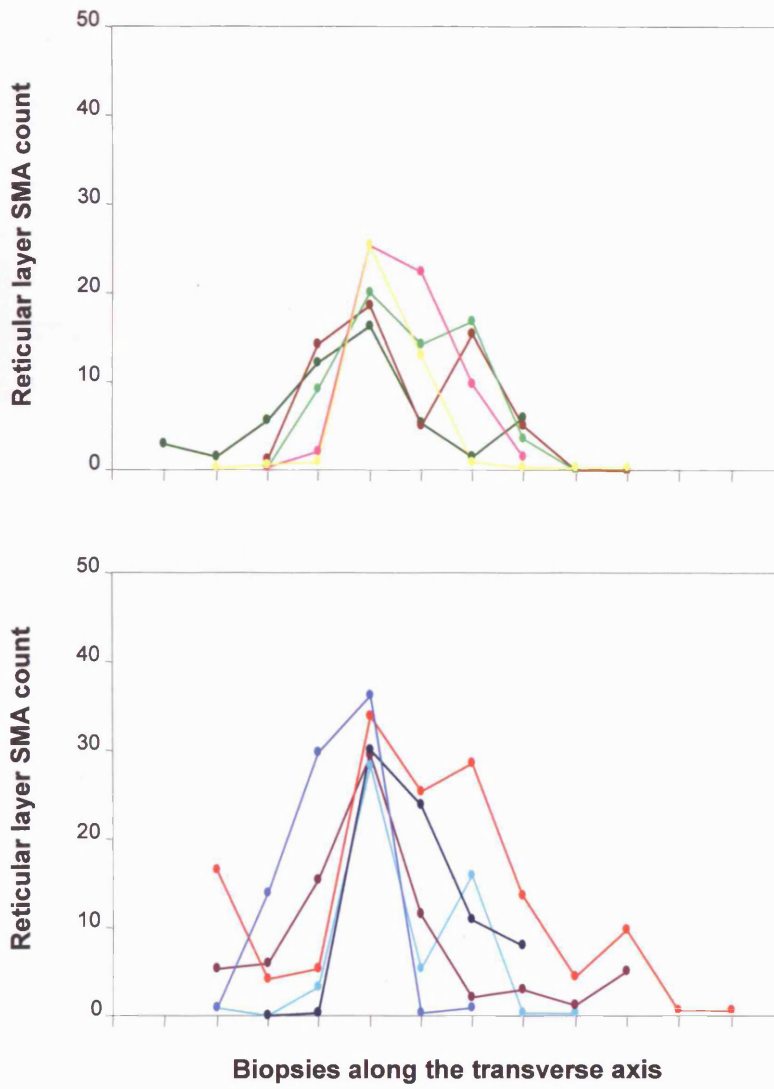


**Figure 4.10.** The reticular layer  $\alpha$ -sma counts of the fetal membrane samples along the transverse axis of the maps obtained from 10 patients at term prior to the onset of labour. Each line represents a different patient, with the colour of the line representing the same patient as in Figures 4.3, 4.4 & 4.9. The data is spread across two graphs solely to assist in the clarity of reading.

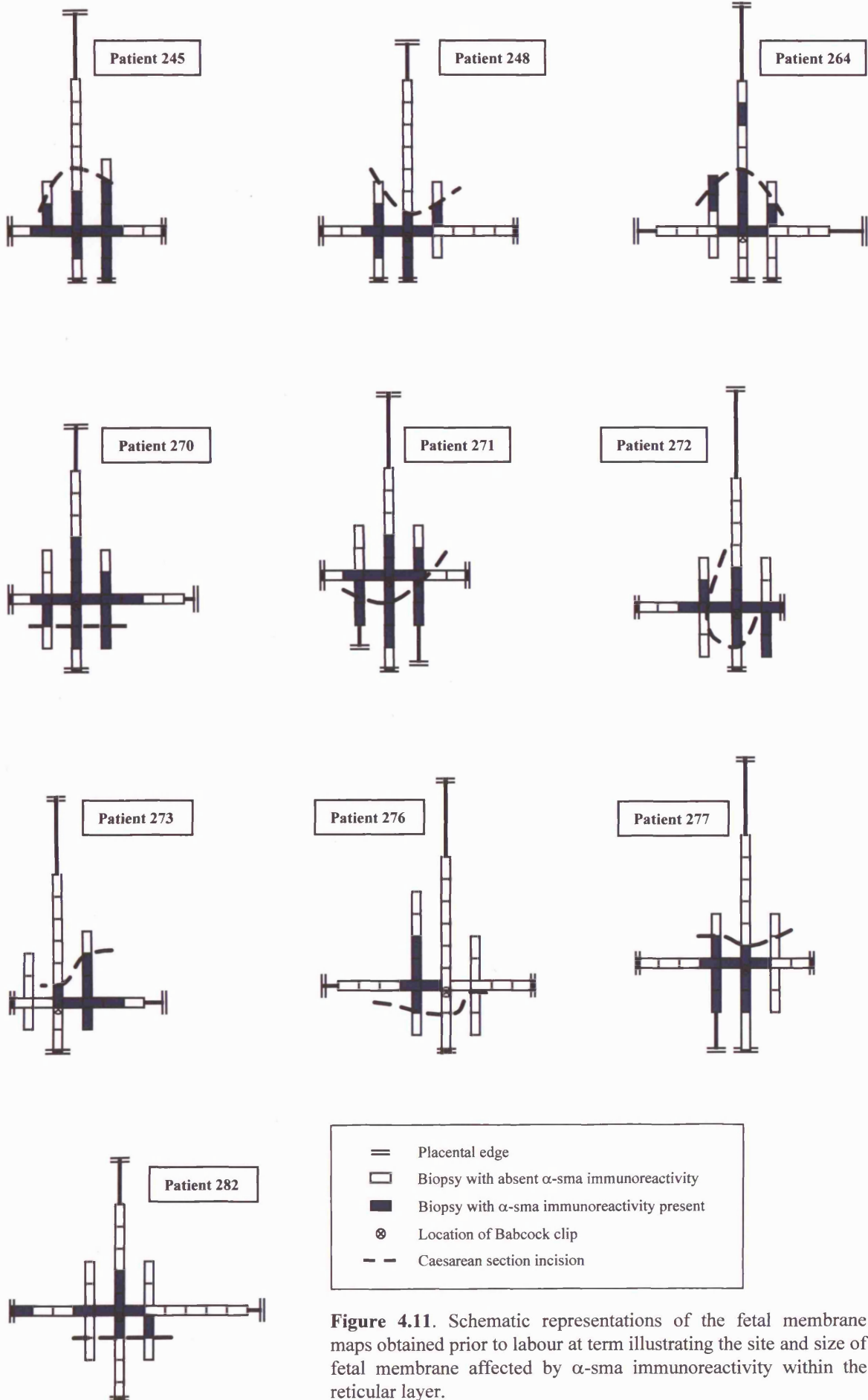


**Figure 4.11.** Schematic representations of the fetal membrane maps obtained prior to labour at term illustrating the site and size of fetal membrane affected by  $\alpha$ -sma immunoreactivity within the reticular layer.

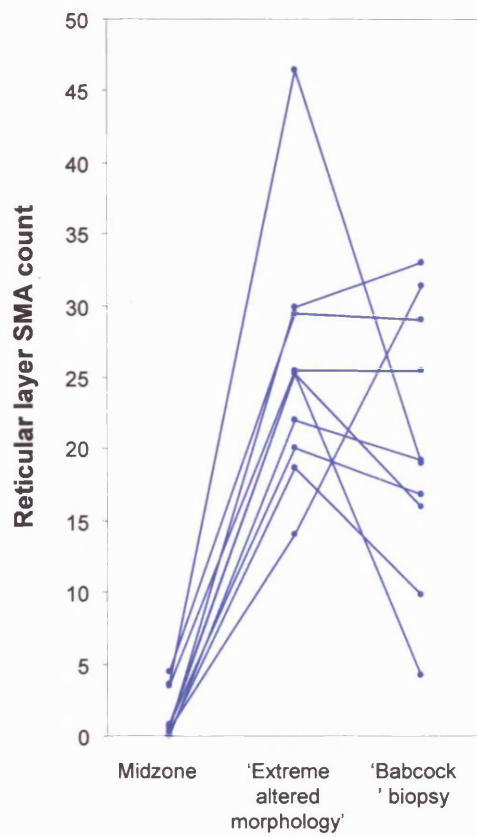


**Figure 4.12.** The reticular layer  $\alpha$ -sma count for selected biopsies from fetal membrane maps obtained from patients prior to the onset of labour at term. Each point represents the mean value of 10 fields measured. The lines connect the samples from individual patients. Midzone biopsies, selected 'extreme altered morphology' biopsies, and the biopsy marked by the Babcock tissue forceps are plotted.

$r=0.486$ ,  $p<0.0001$ ). It correlated inversely with the cytotrophoblast layer thickness (Spearman  $r=-0.489$ ,  $p<0.0001$ ), and correlated positively with the FMMI (Spearman  $r^2=0.731$ ,  $p<0.0001$ ). The relationship between decidual thickness and  $\alpha$ -sma immunoreactivity within the reticular layer appeared to exhibit a 'threshold' (Figure 4.13). ROC curve analysis demonstrated a maximum area under the curve for  $\alpha$ -sma immunoreactivity of 9 cells per field, which was best predicted by decidual thickness  $<45\mu\text{m}$ .

#### **4.4.2.2. Amnion**

Rare cells (average less than 1 immunoreactive cell per computer screen width) within the fibroblast layer of the amnion exhibited  $\alpha$ -sma immunoreactivity. However, two patients had significant numbers of  $\alpha$ -sma immunoreactive cells within the fibroblast layer, in a region of fetal membrane originating in the lower uterine segment, within the region of fetal membrane exhibiting extreme altered morphology. One of these is illustrated in Figure 4.14. This fetal membrane exhibited a large region of 'mucus-associated' altered morphology, but did not have any other distinctive features to correlate with the amniotic  $\alpha$ -sma expression.

### **4.5. Discussion**

All fetal membranes examined exhibited a region of extreme altered morphology located in the membranes originating in the lower uterine segment. The key features of extreme altered morphology were increased thickness of the connective tissue layers of the amnion and chorion, and thinning of the cytotrophoblast and decidual layers. The ratio of the connective tissue to cellular layers (Fetal Membrane Morphometric Index, FMMI) was therefore markedly increased.

The morphological parameter affecting the largest area was that of thinning of the maternal decidual layer. This resulted in a zone of fetal membrane with an elevated FMMI in comparison to the fetal membrane in the remainder of the sac. Within this zone there was a change to a more restricted area exhibiting all the features of extreme altered morphology i.e. thickened connective tissue layers of the amnion and the chorion, the compact, fibroblast, spongy and reticular layers, and thin cellular cytotrophoblast layers (Malak & Bell, 1994b). The changes in thickness of the individual component layers of the fetal

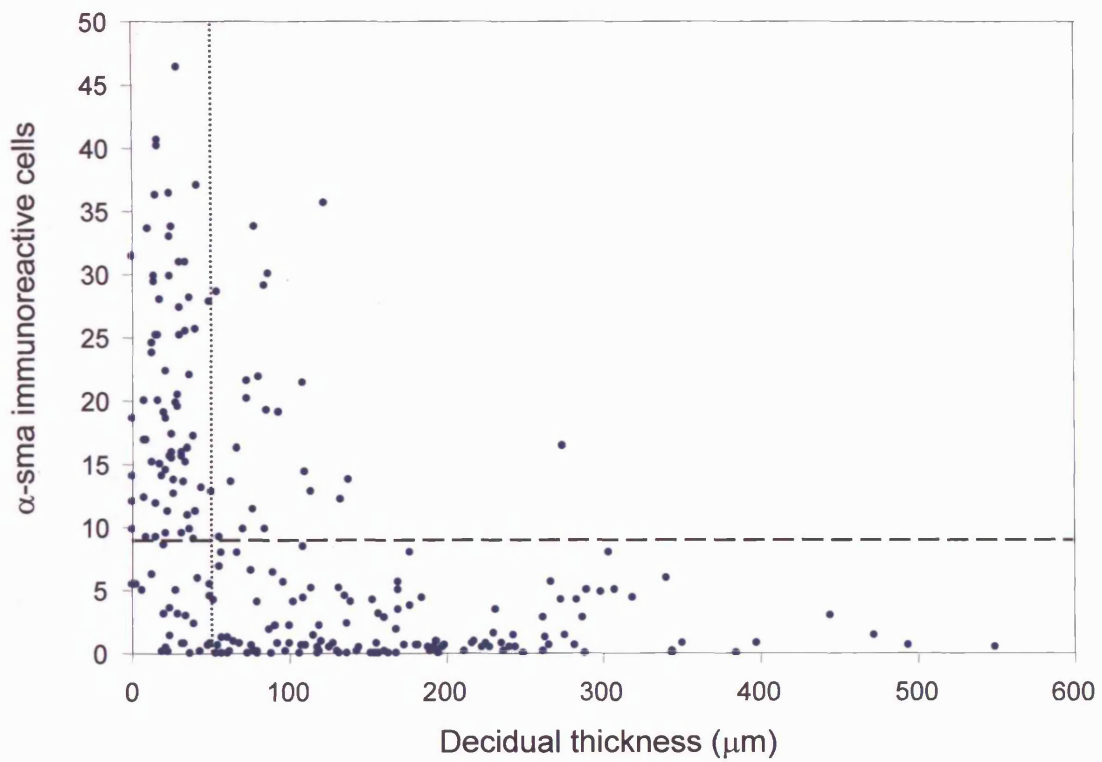


**Figure 4.13.** The relationship between the thickness of the maternal decidua and numbers of immunoreactive  $\alpha$ -smooth muscle actin cells in the reticular layer, in all biopsies ( $n=242$ ) obtained from fetal membranes obtained from 10 patients prior to labour at term. Decidual thickness of  $45\mu\text{m}$  (dotted line) was determined by ROC curve analysis to best predict  $\alpha$ -smooth muscle actin positivity (9 cells per field; dashed line) within the reticular layer.

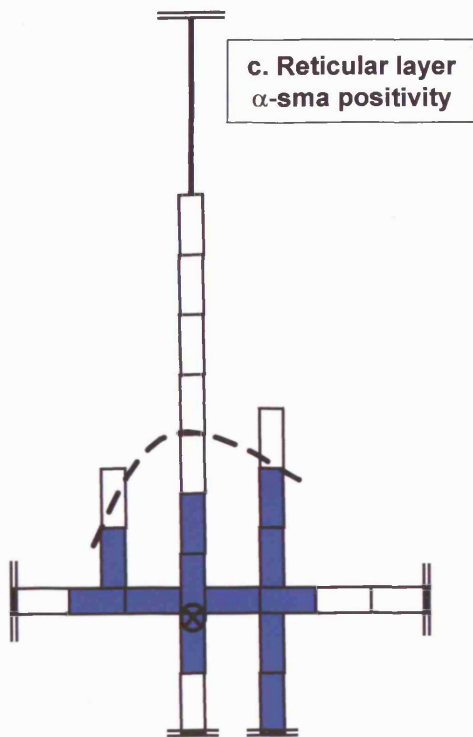
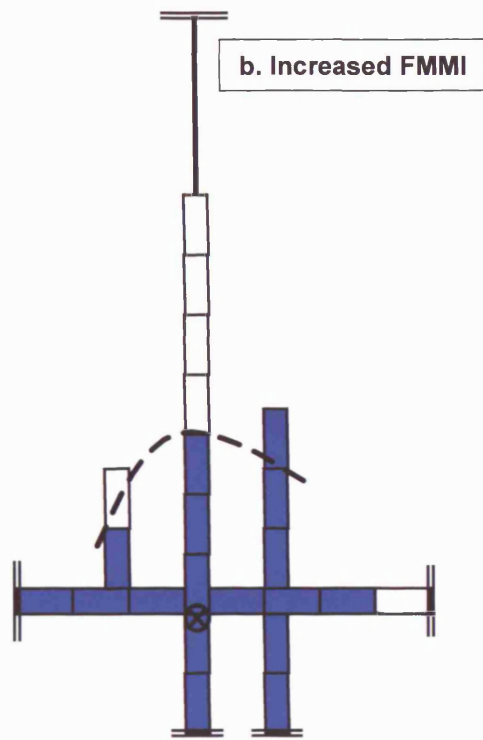
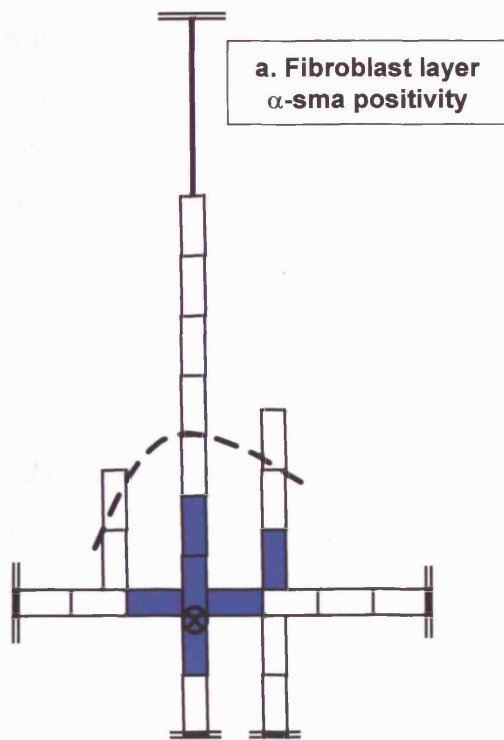


**Figure 4.14.** Maps demonstrating the region of fetal membrane exhibiting  $\alpha$ -sma immunoreactivity within the fibroblast layer in Patient 245 (a), in comparison to the region exhibiting altered morphology, and the region exhibiting reticular layer  $\alpha$ -sma positivity (c). These regions substantially overlap.

membranes were typically gradual, and affected widely varying areas of the fetal membrane sac (whilst still remaining within the area of decidual thinning, and always centred upon the same point, presumed to represent the site of the internal os of the cervix) (Figure 4.15). There was no fixed relationship between the area affected by the changes of thickness of the component layers of the fetal membranes (e.g. in some membranes the increased reticular layer thickness affected a wider area than reduction in cytotrophoblast layer thickness, and in some membranes *vice versa*). It was not possible to define thickness thresholds for each layer of the fetal membranes in order to define altered morphology, due to the biological variation between individual fetal membranes. The area of elevated FMMI represents an average of 10.7% of the surface area of the expelled fetal membranes, based on the published average total surface area of 1115cm<sup>2</sup> at term (Millar *et al.*, 2000). The area of extreme altered morphology, affected by changes in thickness of all component layers affected an average of 1.9% of the surface area. The size of the region of extreme altered morphology in this study is approximately comparable to that of the ZAM identified by Malak (described as 4-10cm diameter, equates to 12.5-78.5cm<sup>2</sup> (Malak & Bell, 1994b); compared to 2.4-63.6cm<sup>2</sup> in this study). The zones of elevated FMMI and extreme altered morphology appear to be anatomically centred upon the internal os of the cervix and, given their relationship with the site of the uterine incision, the former to extend over the lower uterine segment of the lower uterine pole.

Since the  $\alpha$ -smooth muscle actin-positive myofibroblastic phenotype of the chorionic reticular layer was found to be most closely associated with adjacent thin decidua this suggests that the cellular phenotype of the reticular layer may be dependent upon the functional thickness of the underlying maternal decidua mediated by decidual-derived paracrine factors. The region of extreme altered morphology is contained within a fraction of the area of thin decidua. This therefore suggests that other factors are required, albeit still requiring the presence of the differentiated myofibroblast phenotype in the chorion, to act to produce the structural changes. This may also apply to other features of the extreme morphology such as thinned cytotrophoblastic layer. It is possible that cervical effacement, with the potential direct apposition of the cervical glands upon this zone, could act to produce the extreme morphology. This may be supported by the observation that in six patients in the present study mucoid material, presumed to represent cervical gland-derived mucus, was adherent to the cellular surface of the fetal membranes of one or more biopsies and these were in the middle of the area of extreme altered morphology.

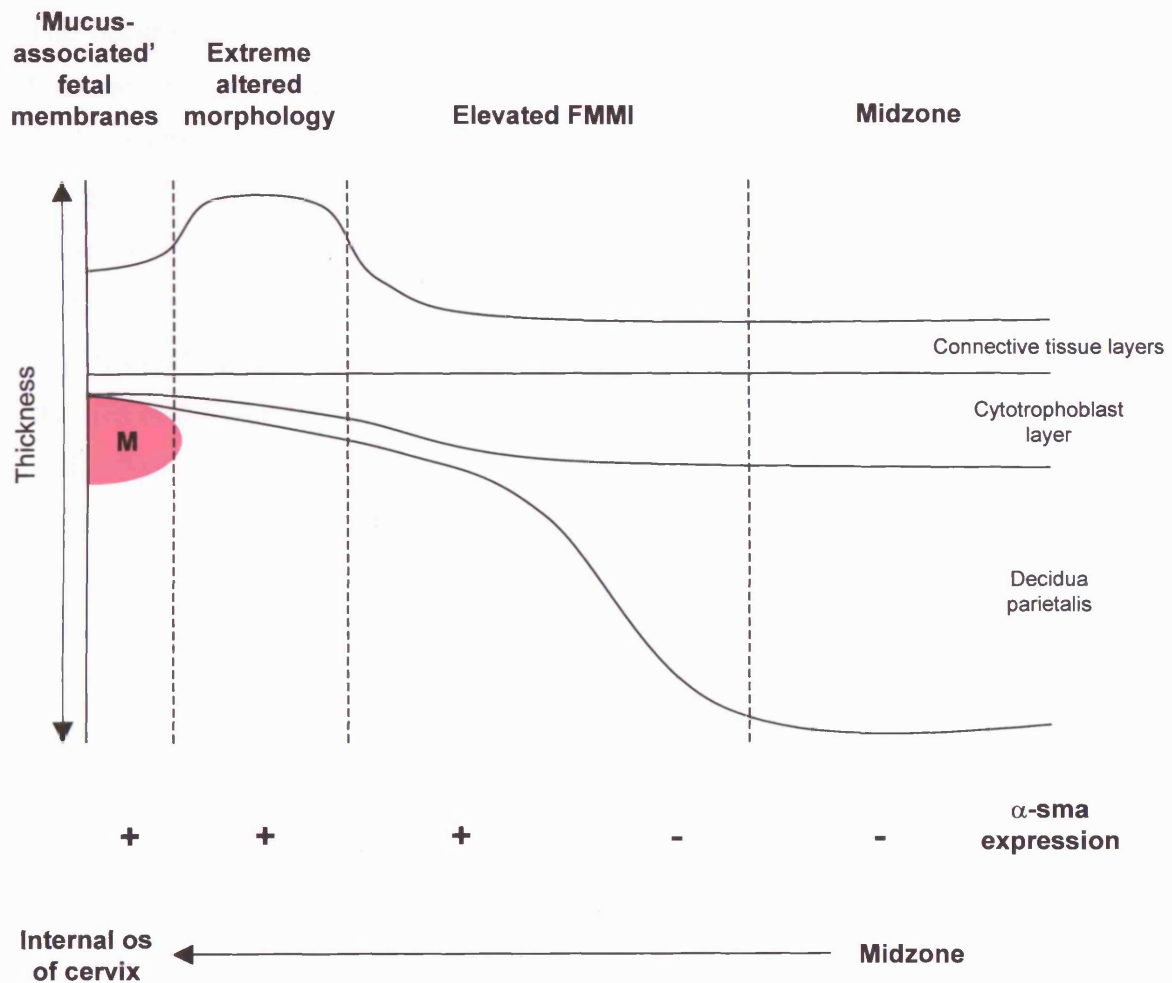


**Figure 4.15.** A diagrammatic representation of the changes in thickness of the fetal membrane layers along an axis from midzone fetal membrane towards the internal os of the cervix. The first change is a decrease in thickness of the decidua parietalis, leading to an elevation of the FMMI. This is followed by gradual reduction in the thickness of the cytotrophoblast layer and increase in thickness of the connective tissue layers (occurring in no defined order). A region of extreme altered morphology is defined where changes in thickness of all component layers has occurred. Within this region, 'mucus-associated' fetal membranes are present, with very thin cytotrophoblast layer, minimal/absent decidua parietalis, and a reduction in thickness of the connective tissue layers (although not to the thickness of the midzone fetal membranes) and attached layer of cervical mucus (**M**). Expression of  $\alpha$ -sma within the reticular layer is most closely associated with a reduction in thickness of the decidua parietalis to  $<45\mu\text{m}$ .

The occurrence of myofibroblast differentiation and extreme altered morphology in all fetal membranes examined in this chapter suggests that the variable results obtained from fetal membranes obtained prior to labour in Chapter 3 arose due to inaccuracy of the placement of the Babcock tissue forceps. The same technique in application of the Babcock forceps was applied to fetal membranes obtained during labour in Chapter 3, yet 100% of these membranes exhibited regional myofibroblast differentiation and some degree of altered morphology. Although this may have arisen by chance, it is possible that the area of the fetal membrane affected by these features is increased in size during labour, and is thus more likely to be sampled when a Babcock forceps is applied. However, since 90% of membrane biopsies adjacent to the Babcock forceps in this chapter exhibited myofibroblast differentiation and altered morphology, it also suggests that a 'learning curve' in the placement of the Babcock forceps may have occurred.

Questions as to the potential mechanisms by which regional differences in fetal membrane morphology and cellular phenotype, centred upon the internal os of the cervix, arise are raised by this study and it is most likely that these would be linked with differences in between the upper and lower uterine poles. The nature of the origin of the decidual thinning is unlikely to arise directly as a feature of the internal os of the cervix. It is unclear whether decidua is present directly over the internal os, and whether the amniochorion fuses with it (Sadler, 1985; Moore & Persaud, 1998; Benirschke & Kaufmann, 2000). However, the area represented by decidual thinning is substantially larger than the area affected by other features of extreme altered morphology. It is possible that development of the lower uterine segment by 38-39 weeks could have produced a shear plane in the upper decidua underlying the fetal membranes surrounding the internal os to produce the thin decidua. The areas of thicker decidua associated with the upper pole could have therefore represented a deeper cleavage plane artificially produced by the manual removal of the membranes at Caesarean section. However this zone could also reflect the situation *in vivo* with a differential thickness of the decidua parietalis in the upper and lower uterine poles, reflecting differential thickness in the endometrium from which the decidua arises, and with which the amniochorion fuses during mid-pregnancy.

The decreased thickness of the cytotrophoblast layer associated with fetal membranes with extreme altered morphology may arise either due to reduced proliferation of cells within this layer, or alternatively due to increased cell death. The fusion of the amniochorion to the underlying decidua parietalis, with proliferation of cytotrophoblast and attachment of

chorion to decidua, may be related to the nature of the underlying decidua and nutrition and paracrine factors obtained from it. The possibility that the decidua within the lower uterine segment may be thinner than that in the upper uterine pole has already been discussed. There is also evidence for a regional increase in apoptosis among cells of the cytotrophoblast layer prior to labour at term (McLaren *et al.*, 1999b).

It is possible that the regional myofibroblast differentiation and fetal membrane extreme altered morphology develops during late pregnancy as a consequence of lower segment development and cervical effacement. Distortion of the lower uterine segment may then lead to disruption of feto-maternal interface in lower segment, involution of the decidua parietalis, increased apoptosis of the cytotrophoblast and relative increased stretch of the fetal membranes in this region. This may predispose the membranes within this region to later rupture.

A region of extreme altered morphology and myofibroblast differentiation occurs in all fetal membranes examined at 38-39 weeks prior to labour at term. Therefore work in future chapters on prelabour fetal membranes will be carried out only on paired fetal membrane biopsies that exhibit myofibroblast differentiation as detected by  $\alpha$ -sma immunoreactivity within the reticular layer.

#### **4.6. Conclusions**

- All fetal membranes examined prior to the onset of labour at term exhibit a region of extreme altered morphology, localised to the area of membrane originating in the lower uterine segment, centred upon the internal os of the cervix, and exhibiting large variation in size. This may not be identified by a single 'cervical' biopsy.
- The characteristics of extreme altered morphology are increased thickness of the connective tissue layers, and decreased thickness of the cellular layers, giving rise to a marked increase in the Fetal Membrane Morphometric Index.
- Fetal membrane biopsies with attached cervical mucus were found in 6 out of 10 fetal membranes, located in the centre of the area of extreme altered morphology. The fetal

membrane biopsies with cervical mucus had significantly thinner connective tissue and cellular layers than the surrounding biopsies with extreme altered morphology.

- All fetal membranes examined prior to the onset of labour at term had a region of increased  $\alpha$ -sma expression within the cells of the chorion localised to the area of membrane originating in the lower uterine segment, and centred upon the internal os of the cervix.
- The number of  $\alpha$ -sma immunoreactive cells within the reticular layer of the chorion is inversely related to the thickness of the underlying decidua parietalis, particularly decidual thickness  $<45\mu\text{m}$ .

## **Chapter 5**

### **Tenascin-C expression in human fetal membranes**

#### **5.1. Introduction**

The results presented in Chapter 3 and Chapter 4 demonstrate regional changes in fetal membrane structure, present prior to, during, and following labour at term. These changes are associated with  $\alpha$ -sma expression in the reticular layer of the chorion, consistent with myofibroblast differentiation. It is known that in other organ systems myofibroblast differentiation in the wound response is associated with tenascin-C (Tn-C) expression (Carnemolla *et al.*, 1996).

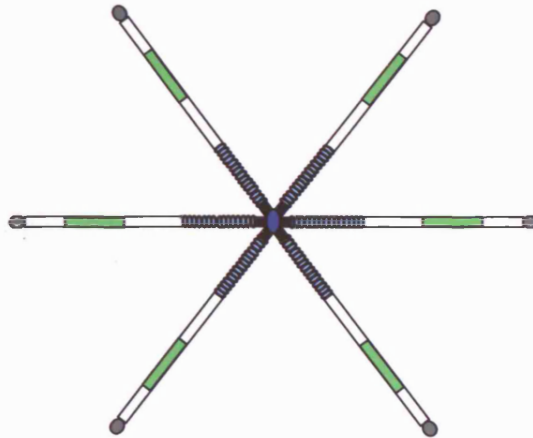
##### **5.1.1. Tenascin-C structure**

Tenascin-C is a high molecular weight hexameric glycoprotein (**Figure 5.1a**), also known as hexabrachion (Erickson & Taylor, 1987), cytotactin (Grumet *et al.*, 1985), J1 protein, neuronectin (Siri *et al.*, 1991), and myotendinous antigen (Erickson & Taylor, 1987). Each arm of the hexabrachion has a molecular weight from 190-300kDa (Jones & Copertino, 1996), and was originally described to consist of a cysteine-rich amino-terminal region, 14<sup>1/2</sup> EGF-like repeats, 8-15 fibronectin type III (Fn-III) domains, and a fibrinogen-like domain at the carboxy-terminal end (Nies *et al.*, 1991; Siri *et al.*, 1991). Two additional alternatively spliced Fn-III domains have subsequently been described, in association with Tn-C expression in malignancy, designated AD1 (Sriramarao & Bourdon, 1993) and AD2 (Mighell *et al.*, 1997) (**Figure 5.1b**). The gene encoding Tn-C is located on 9q32-q34 (Rocchi *et al.*, 1991). The relationship between the exons within the Tn-C gene and the protein domains is illustrated in **Figure 5.1c**.

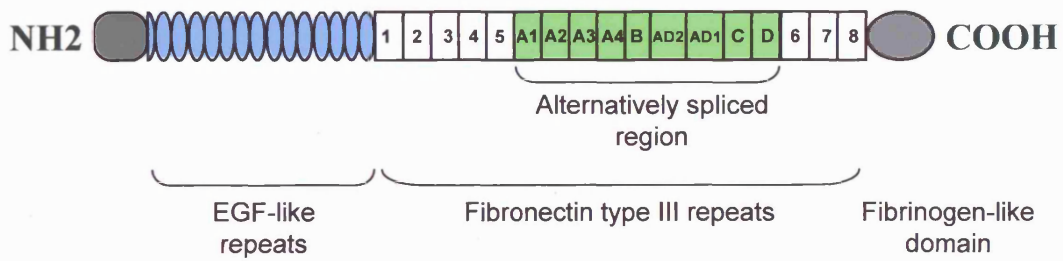
##### **5.1.2. Tenascin-C function**

Tenascin-C expression is highly restricted, and occurs during embryonic development, and in normal and pathological adult tissues in situations of tissue remodelling and epithelial-mesenchymal interaction (Koukoulis *et al.*, 1991; Natali *et al.*, 1991). Whilst it is considered a prototype of the anti-adhesive matricellular proteins, along with osteonectin and thrombospondin (Crossin, 1996), it has also had functions of promoting cell adhesion ascribed to it. Different functions of Tn-C have been ascribed to different domains of the

a



b



c



**Figure 5.1.** The tenascin-C hexamer is illustrated in (a). It comprises 6 protein monomers as in (b). The protein domains are encoded by 27 exons. The relationship between the fibronectin type III-like repeats (black numbers) and exons (blue numbers) is illustrated in (c).

protein, for instance the counteradhesive properties have been mapped to the EGF-like repeats, and the adhesive properties to the Fn-III repeats (Crossin, 1996). It may also promote cell motility and regulate cell migration (Bartsch, 1996). Tenascin-C has been demonstrated to induce expression of the MMP-1, MMP-3 (Tremble *et al.*, 1994) and MMP-9 (Tremble *et al.*, 1994; Khan & Falcone, 1997).

### **5.1.3. Alternative splicing of tenascin-C**

Alternative splicing of the Tn-C mRNA gives rise to different isoforms, by varying the number of Fn-III domains (**Figure 5.1b&c**). It was initially considered that two major isoforms of Tn-C existed: 'large isoform', with inclusion of all Fn-III domains, and 'small isoform', with exclusion of Fn-III domains A-D. However, molecular biology studies have demonstrated the occurrence of multiple different isoforms (Wilson *et al.*, 1996; Mighell *et al.*, 1997).

Expression of alternatively-spliced isoforms may be regulated by TGF- $\beta_1$ , which has been demonstrated to preferentially upregulate expression of small isoform Tn-C (Zhao & Young, 1995), and has also been demonstrated to be cell cycle (Borsi *et al.*, 1994) and pH dependent (Borsi *et al.*, 1995).

Splice variants of Tn-C may have specific functions, and are differentially expressed during development and adult life. Large isoforms of Tn-C are expressed in association with tissue remodelling (Kaplony *et al.*, 1991), wound healing (Carnemolla *et al.*, 1996), tumour invasion (Borsi *et al.*, 1992), and increased cell migration (Prieto *et al.*, 1990), and have been demonstrated to induce loss of focal adhesion and facilitate cell migration (Borsi *et al.*, 1994). Large isoforms of Tn-C are also more susceptible to degradation by MMP-2 and MMP-3, with digestion sites within the alternatively spliced region, although are resistant to digestion by MMP-9 (Siri *et al.*, 1995).

### **5.1.4. Tenascin-C in pregnancy**

Tenascin-C expression has been described in the mesenchyme of placental villi, tissue with the same embryological derivation as the mesenchyme of the fetal membranes. Within placental villi, Tn-C was localised beneath fibrin deposits, sites of villous wounding, and in the stroma adjacent to cytotrophoblast cell islands and anchoring villus cell columns, sites

of cellular proliferation and differentiation (Castellucci *et al.*, 1991; Damsky *et al.*, 1992). It has also been described in the stroma of placental villi that had been wounded *in vitro* (Watson *et al.*, 1996). Tenascin-C expression has been described within the reticular layer of the chorion, with a qualitative description suggesting an association with fetal membrane altered morphology (Malak, 1995). The cellular origin of this has not been described, although *in vitro* studies suggest that the amniotic epithelium is able to produce Tn-C (Linnala *et al.*, 1993), which may be detected in amniotic fluid (Linnala *et al.*, 1994).

The expression of Tn-C during wound healing, the association with myofibroblast differentiation, ability to upregulate MMP expression, and reports of expression within the reticular layer of the fetal membranes suggest a possible association between Tn-C expression and extreme altered morphology in the fetal membranes. If Tn-C expression were upregulated in association with altered morphology, the upregulation of specific isoforms, especially large isoforms, may suggest specific functions of Tn-C, in particular with respect to generation of altered morphology.

## **5.2. Aims**

- To establish whether tenascin-C mRNA and protein are expressed in term fetal membranes.
- To determine the distribution of tenascin-C protein and the nature of the cells producing mRNA in the fetal membranes.
- To determine whether regional changes in tenascin-C protein and mRNA expression exist.
- To determine whether large isoforms of tenascin-C mRNA are expressed in the fetal membranes, and to establish whether any regional patterns of isoform expression exist.
- To examine any association between tenascin-C protein and mRNA expression and  $\alpha$ -sma immunoreactivity.

## **5.3. Materials and Methods**

### **5.3.1. Tissue samples**

Fetal membrane samples were obtained at term prior to labour (n=19), during labour (n=5) and following labour and delivery (n=8) as previously described (2.1.1.). The restricted area of tissue taken, to ensure accurate mapping, meant that in some cases different tissue samples were used for different techniques. Following the results obtained in Chapter 4, which demonstrated that all pre-labour fetal membranes at term exhibited extreme altered morphology overlying the cervix in association with myofibroblast differentiation, only pre-labour ‘cervical’ fetal membrane biopsies exhibiting  $\alpha$ -sma immunoreactivity within the reticular layer were used in this chapter.

### **5.3.2. Immunohistochemistry**

Immunohistochemistry for tenascin-C was carried out on formalin-fixed wax-embedded tissue samples using monoclonal antibodies BC24 and TN2, and a polyclonal antiserum, and on cryostat tissue sections using monoclonal antibodies T2H5 and  $\alpha$ IIIB (2.3.). Immunohistochemistry for  $\alpha$ -sma (clone 1A4) and endothelial marker anti-CD31 (clone JC/70A) was carried out to assist with the identification of cell types (2.3.).

### **5.3.3. SDS-PAGE and Western blotting**

Fetal membrane extracts from paired whole fetal membrane biopsies obtained prior to (n=3), during (n=3), and following (n=5) labour at term, and from paired ‘superscraped’ (2.1.1.4.) fetal membrane biopsies (n=5) were separated on 6% polyacrylamide gels and transferred to nitrocellulose as previously described (2.4.). Monoclonal antibody T2H5 was used to detect tenascin-C using enhanced chemiluminescence (2.4.5.). The resultant bands obtained with T2H5 were quantified using Scion Image™ (2.8.2.).

### **5.3.4. RT-PCR**

RNA was extracted from 5 paired ‘cervical’ and midzone fetal membrane biopsies obtained prior to labour at term, and from the connective tissue layers only from a further 5 pairs of ‘cervical’ and midzone prelabour fetal membrane biopsies (2.1.). The RNA was subjected to RT-PCR using primers to tenascin-C and to GAPDH at previously determined optimal cycle numbers (2.5.). The PCR products were separated on an agarose gel, and the bands on the captured image of the gel quantified using Scion Image™ (2.8.2.). For semi-

quantification of tenascin-C mRNA, the value obtained for the tenascin-C band was standardised with reference to the GAPDH value.

### **5.3.5. *In situ* hybridisation**

Probes to detect tenascin-C mRNA *in situ* were synthesised by RT-PCR amplification of defined regions of the tenascin-C gene, employing mRNA extracted from SK-MEL-28 cells. Templates were used in an 'asymmetric' PCR reaction incorporating digoxigenin to produce single stranded antisense DNA probes to detect all isoforms of tenascin-C, specific large isoforms, and the 'totally spliced' small isoform (2.6.3. & 2.6.4.). *In situ* hybridisation was carried out on formalin-fixed wax-embedded paired 'cervical' and midzone fetal membrane biopsies obtained prior to labour at term (n=5) as previously described (2.6.5.).

### **5.3.6. Image analysis**

The area of connective tissue expressing immunoreactivity to monoclonal antibody BC24 was measured in ten fields per fetal membrane biopsy, and expressed as a percentage of the total connective tissue area (2.8.1.3.). The numbers of mRNA positive cells in the reticular layer were counted in 10 fields per biopsy (2.8.1.2.).

### **5.3.7. Statistical analysis**

The methodology used to compare areas of tenascin-C immunoreactivity and numbers of *in situ* positive cells, to correlate different parameters, and to analyse data obtained from Western blots and by RT-PCR are described in section 2.9.

## **5.4. Results**

### **5.4.1. Tenascin-C protein expression**

#### **5.4.1.1. Tenascin-C immunolocalisation**

Examination of paired fetal membrane biopsies from 22 patients (9 pre-labour, 5 labour, 8 post-labour; 3 out of the 8 post-labour fetal membranes had the amnion missing) demonstrated tenascin-C immunoreactivity in a number of sites (Figure 5.2). The most prominent immunoreactivity was detected within the extracellular matrix of the reticular

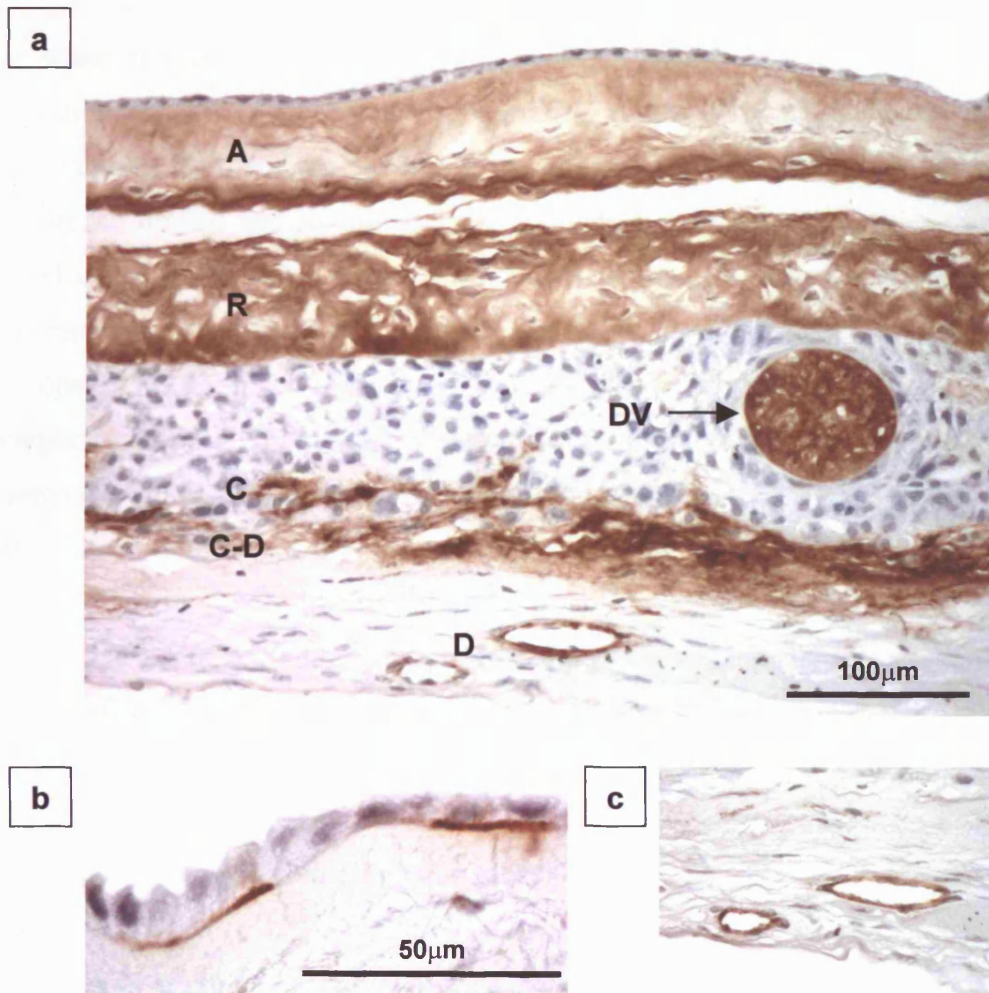


**Figure 5.2.** Tenascin-C immunoreactivity within the fetal membranes (a). The main sites of immunoreactivity are the reticular layer (R), amniotic connective tissue (A), degenerate villi (DV), between cytotrophoblast cells (C), at the cytotrophoblast-decidual interface (C-D), and around structures within the decidua (D). Occasionally patches of immunoreactivity are observed along the amniotic basement membrane (b). Immunohistochemistry with an endothelial cell marker on a serial section confirms that the Tn-C immunoreactive structures within the decidua are blood vessels (c).

layer, where it was detected to some degree in all biopsies examined. It varied from a single small patch, to diffuse patches, to intense staining throughout the layer along the whole length of the membrane biopsy. Immunoreactivity within this layer was commonly most intense toward the pseudobasement membrane. More rarely diffuse patches were detected within the amniotic connective tissue layers, the compact and fibroblast layers (it was completely absent in 10 out of 19 midzone biopsies, and 4 out of 19 'cervical'/rupture line biopsies). In 22 out of 38 biopsies it was detected as thin deposits along the amniotic basement membrane (**Figure 5.2b**). Immunoreactivity within the cytotrophoblast layer appeared as intense thin streaks between cells, horizontally along the membrane (observed in 40 out of 44 biopsies), and in the extracellular matrix of degenerate villi (in 20 out of 44 biopsies) (**Figure 5.2a**). Intense lines of immunoreactivity were detected within the decidua attached to the amniochorion, associated with the walls of sinusoidal vascular structures (identified by immunohistochemical staining of serial sections with the endothelial marker, against CD31; **Figure 5.2c**). More diffuse immunoreactivity was detected at the cytotrophoblastic-decidual interface associated with areas of fibrinoid deposits (25 out of 44 biopsies) (**Figure 5.2a**).

These patterns of immunoreactivity were detected with all 4 monoclonal antibodies (clones BC24, TN2, T2H5 and  $\alpha$ IIIB) and with polyclonal antiserum (**Figure 5.3a-e**). The occurrence of immunoreactivity with  $\alpha$ IIIB indicates the presence of tenascin-C isoforms containing protein encoded by alternatively spliced exon 14.

#### **5.4.1.2. Regional differences in tenascin-C immunolocalisation**

Subjective assessment of the tenascin-C immunoreactivity appeared to indicate regional variation in staining (**Figures 5.4 & 5.5**). A method of assessing the degree of immunoreactivity was therefore developed (**2.8.1.3**). Differences in staining intensity and in area affected were noted. The area of connective tissue positive above a threshold was used as an indirect method of assessing immunoreactivity. This was expressed as a percentage of the total area of the layer being examined (per computer screen width), as, by definition, thicker connective tissue layers may give larger immunoreactive areas.

Regional variation in the proportion of the reticular layer immunoreactive for tenascin-C was demonstrated. The percentage of the reticular layer immunoreactive was 2.0-fold higher in 'cervical' biopsies compared to midzone biopsies obtained prior to labour, 2.7-

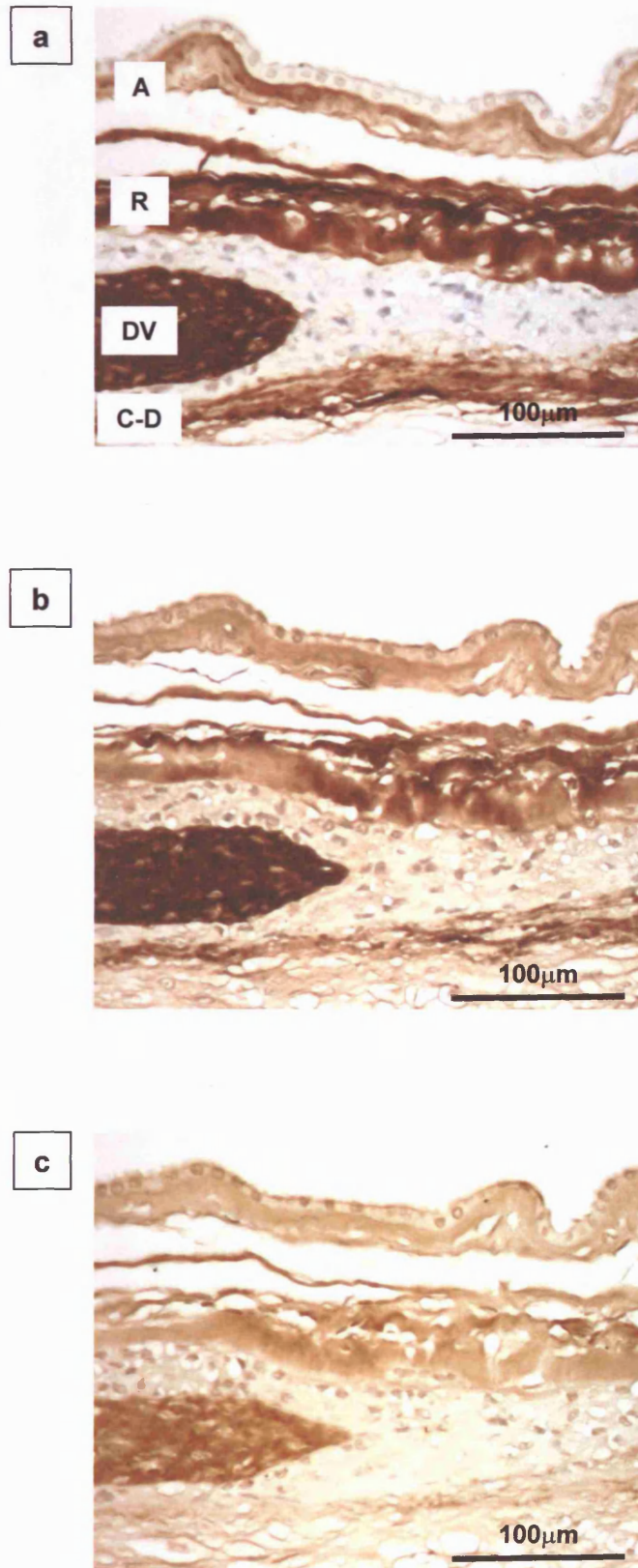


**Figure 5.3a-c.** Immunohistochemistry for tenascin-C on adjacent sections of formalin-fixed fetal membrane using monoclonal antibodies BC24 (a), and TN2 (b), and polyclonal antiserum (c). All three antibodies demonstrate immunoreactivity within the amniotic connective tissue (A), the reticular layer (R), the degenerate villus (DV) and the cytotrophoblast-decidual interface (C-D).

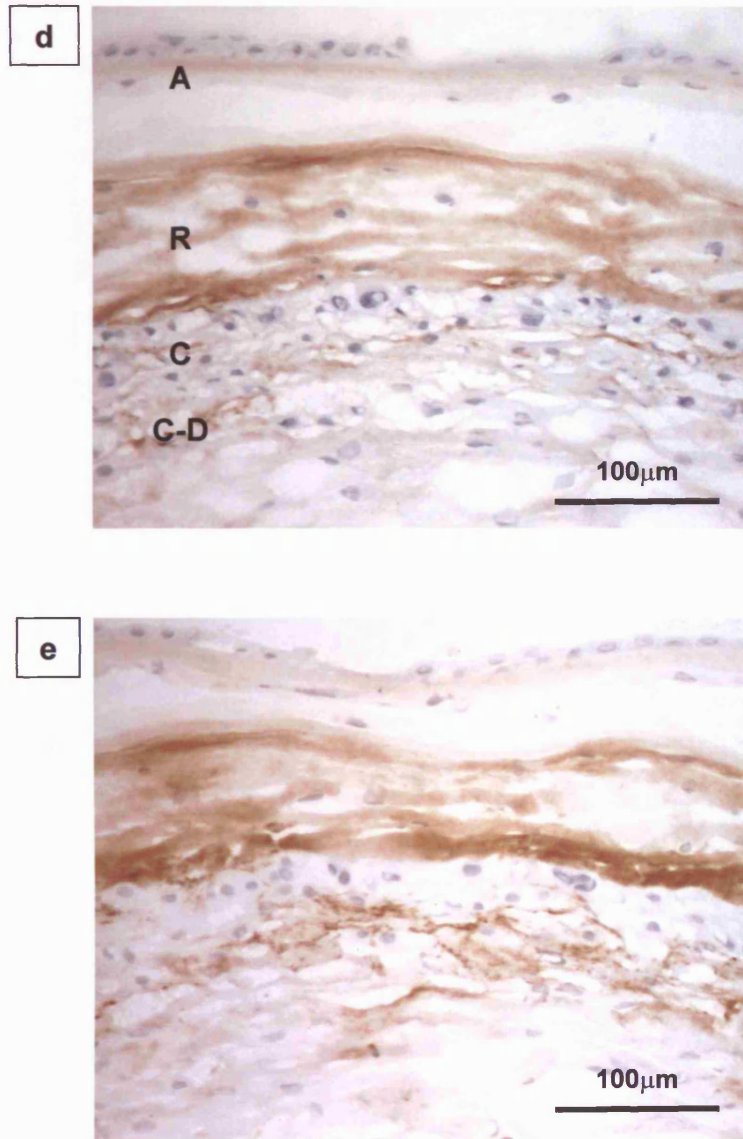


**Figure 5.3d-e.** Immunohistochemistry on cryostat sections of the same fetal membrane sample using monoclonal antibodies T2H5 (d), and  $\alpha$ IIIB (e). Both antibodies demonstrate immunoreactivity within the amniotic connective tissue (A), the reticular layer (R), between cytotrophoblast cells (C), and at the cytotrophoblast-decidual interface (C-D).

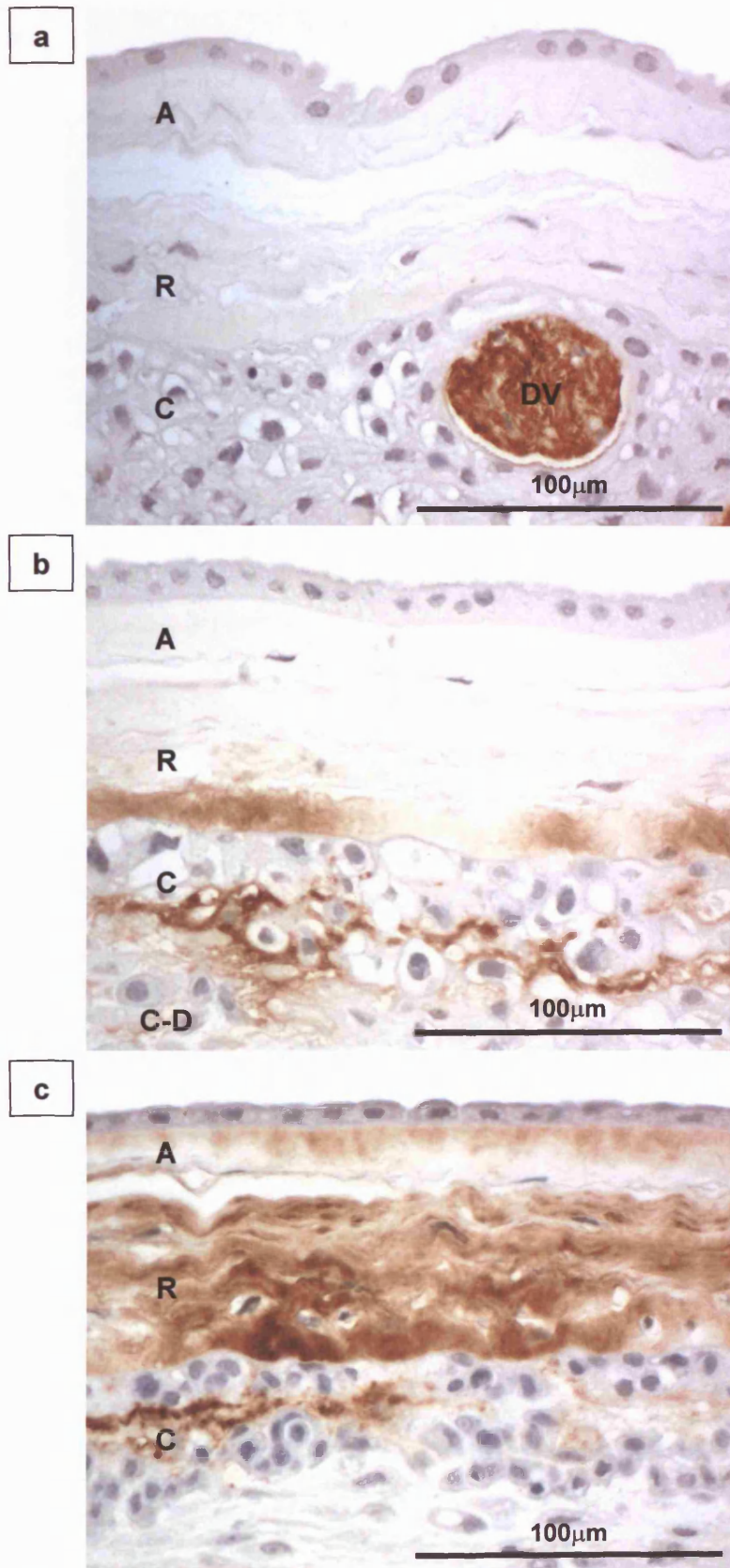


**Figure 5.4.** Tenascin-C immunohistochemistry on midzone fetal membranes, demonstrating the range of extent of reticular layer immunoreactivity (R), from absent/minimal (a), to patchy staining predominantly adjacent to the pseudobasement membrane (b), to intense immunoreactivity throughout the reticular layer (c). No biopsy was completely negative for Tn-C immunoreactivity within the reticular layer. Immunoreactivity is also observed within a degenerate villus (DV), within the amniotic connective tissue layers (A), between cytotrophoblast cells (C), and at the cytotrophoblast-decidual interface (C-D).

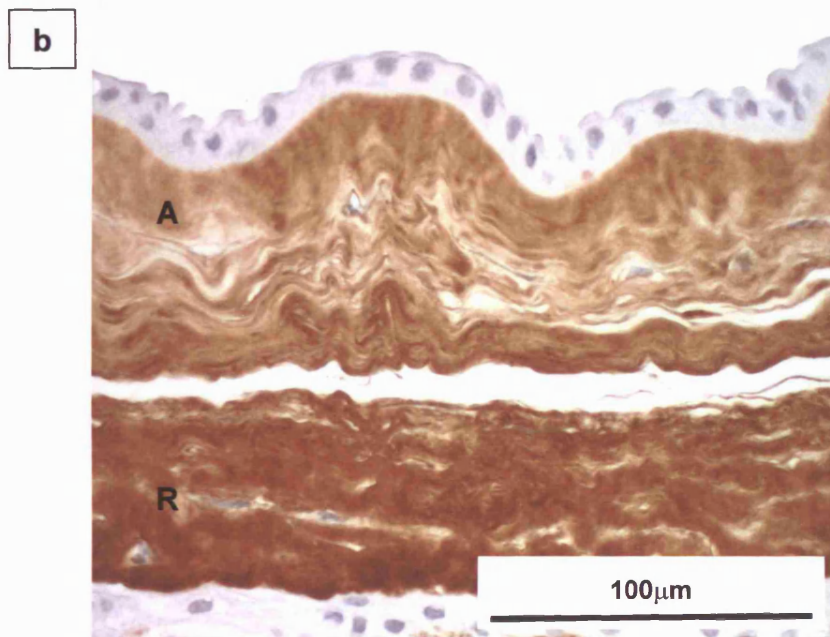
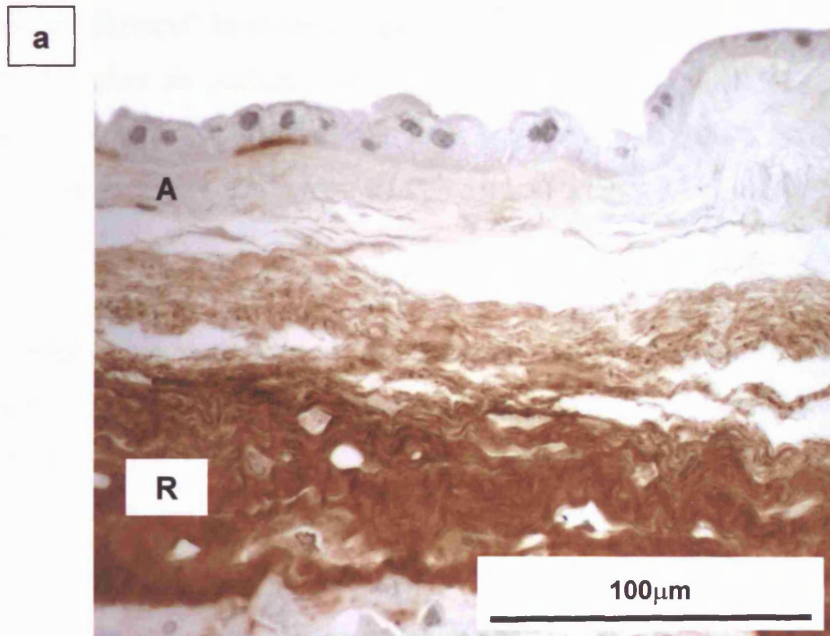


**Figure 5.5.** Tenascin-C immunoreactivity in fetal membranes with altered morphology. Uniform immunoreactivity within the reticular layer (R) is observed (a&b), with amniotic connective tissue (A) staining in some biopsies (b).

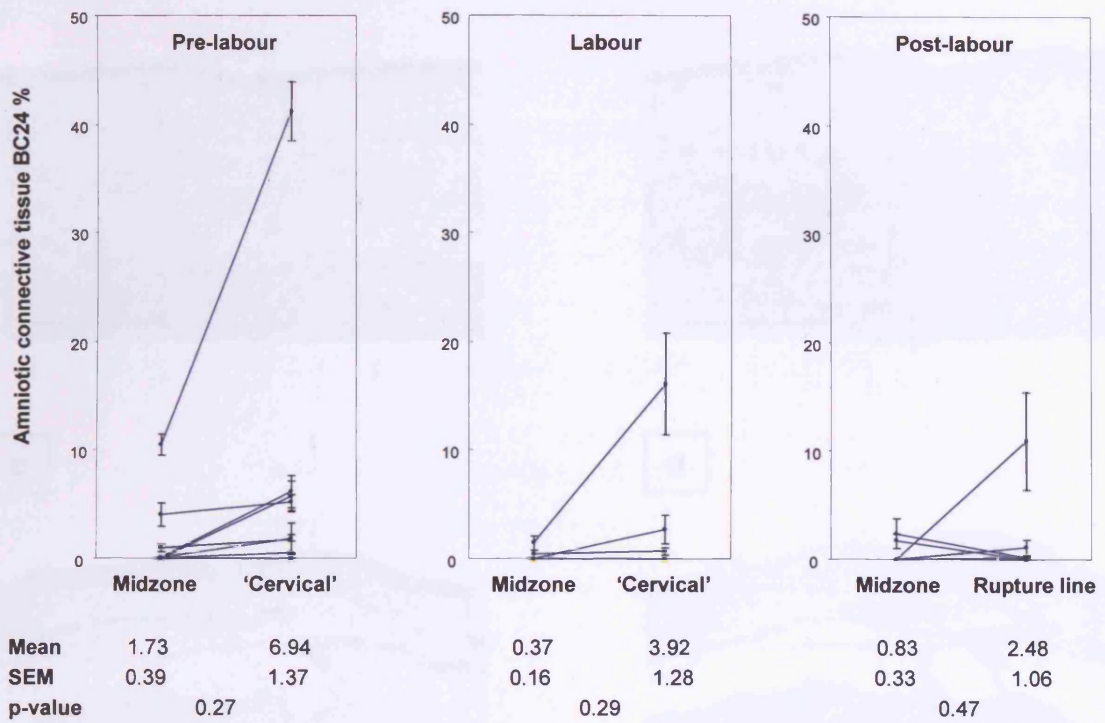
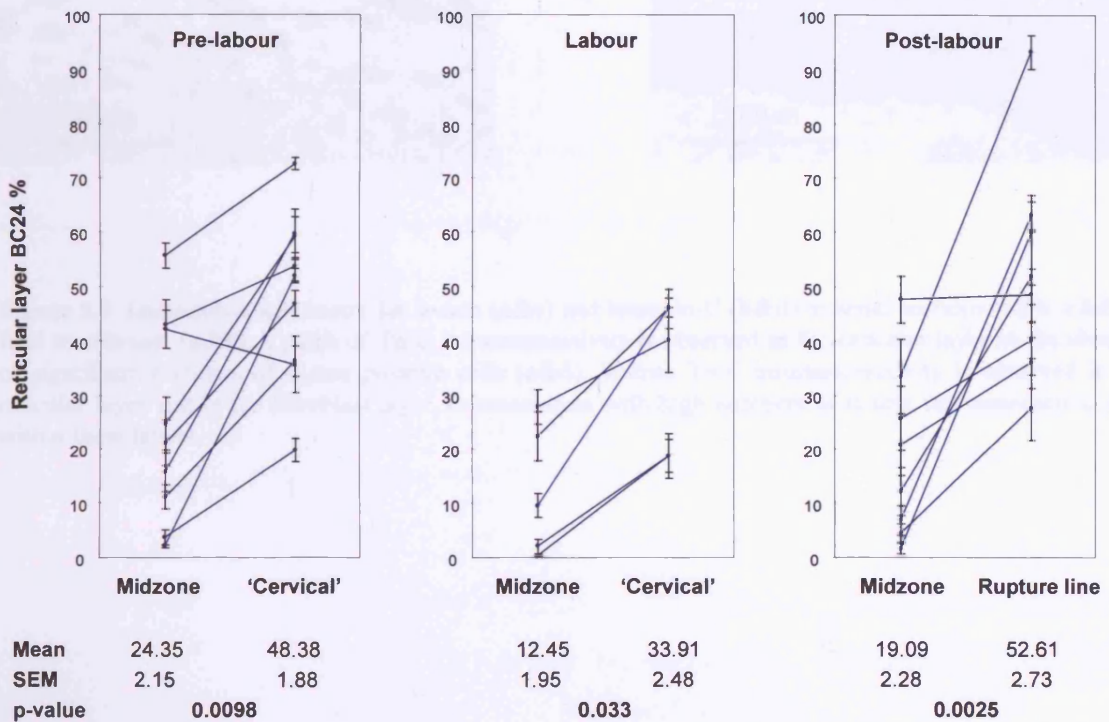
fold higher in 'cervical' biopsies compared to midzone biopsies obtained during labour, and 2.8-fold higher in rupture line biopsies compared to midzone biopsies obtained following labour and delivery. (Figure 5.6). There were no significant differences in the percentage immunoreactive area between physiological groups of patients in the respective biopsy sites.

When all biopsy data was grouped, the percentage of the reticular layer immunoreactive for tenascin-C positively correlated with the thickness of the reticular layer (Spearman  $r=0.552$ ,  $p=0.0001$ ), the total connective tissue thickness (Spearman  $r=0.596$ ,  $p=0.0003$ ), and inversely with the total thickness of the cellular layers of the fetal membrane (Spearman  $r=-0.530$ ,  $p=0.0005$ ).

Overall no significant differences in amniotic connective tissue immunoreactivity between regions or between patient groups were seen (Figure 5.6). Areas of immunoreactivity were low, with only 3 out of 19 patients with greater than 10% amniotic connective tissue immunoreactivity (in the 'cervical'/rupture line biopsy). However, 7 patients had significantly greater areas of immunoreactivity in the 'cervical' or rupture line biopsy compared to the midzone (5 out of 9 pre-labour, 1 out of 5 labour, 1 out of 5 post-labour), and only 1 had significantly greater area in the midzone compared to 'cervical'/rupture line (post-labour patient). The percentage amniotic connective tissue immunoreactivity correlated significantly with the percentage reticular layer immunoreactivity (Spearman  $r=0.748$ ,  $p<0.0001$ ) and with the amniotic connective tissue thickness (Spearman  $r=0.543$ ,  $p=0.001$ ).

#### **5.4.1.3. Relationship to $\alpha$ -sma expression**

Comparison of serial sections did not demonstrate an absolute association between areas of tenascin-C immunoreactivity and  $\alpha$ -sma immunoreactive cells in either the reticular layer or the amniotic connective tissue layers within individual biopsies. Although in many areas the two coincided, areas of tenascin-C immunoreactivity were seen in the absence of  $\alpha$ -sma immunoreactive cells, and  $\alpha$ -sma immunoreactive cells were seen in the absence of tenascin-C immunoreactivity. (Figure 5.7). However, biopsies with largest areas of tenascin-C immunoreactivity in the reticular layer were also those with highest numbers of  $\alpha$ -sma immunoreactive cells, as demonstrated by a significant correlation between the tenascin-C percentage immunoreactive area and the number of  $\alpha$ -sma immunoreactive

**a****Amniotic connective tissue****b****Reticular layer**

**Figure 5.6.** Percentage area immunoreactive for monoclonal antibody BC24 in the amniotic connective tissue (a) and reticular layer (b) in fetal membranes obtained before, during and after labour at term. The graphs show the mean and SEM derived from 10 fields from each biopsy, with lines connecting the data points from individual patients. The mean and SEM (derived from the total 50 observations) for each group are shown beneath the graphs. Comparisons between biopsy sites and physiological group were using two way ANOVA and Scheffes test. Significant p-values are in bold. All comparisons between physiological groups were non-significant.

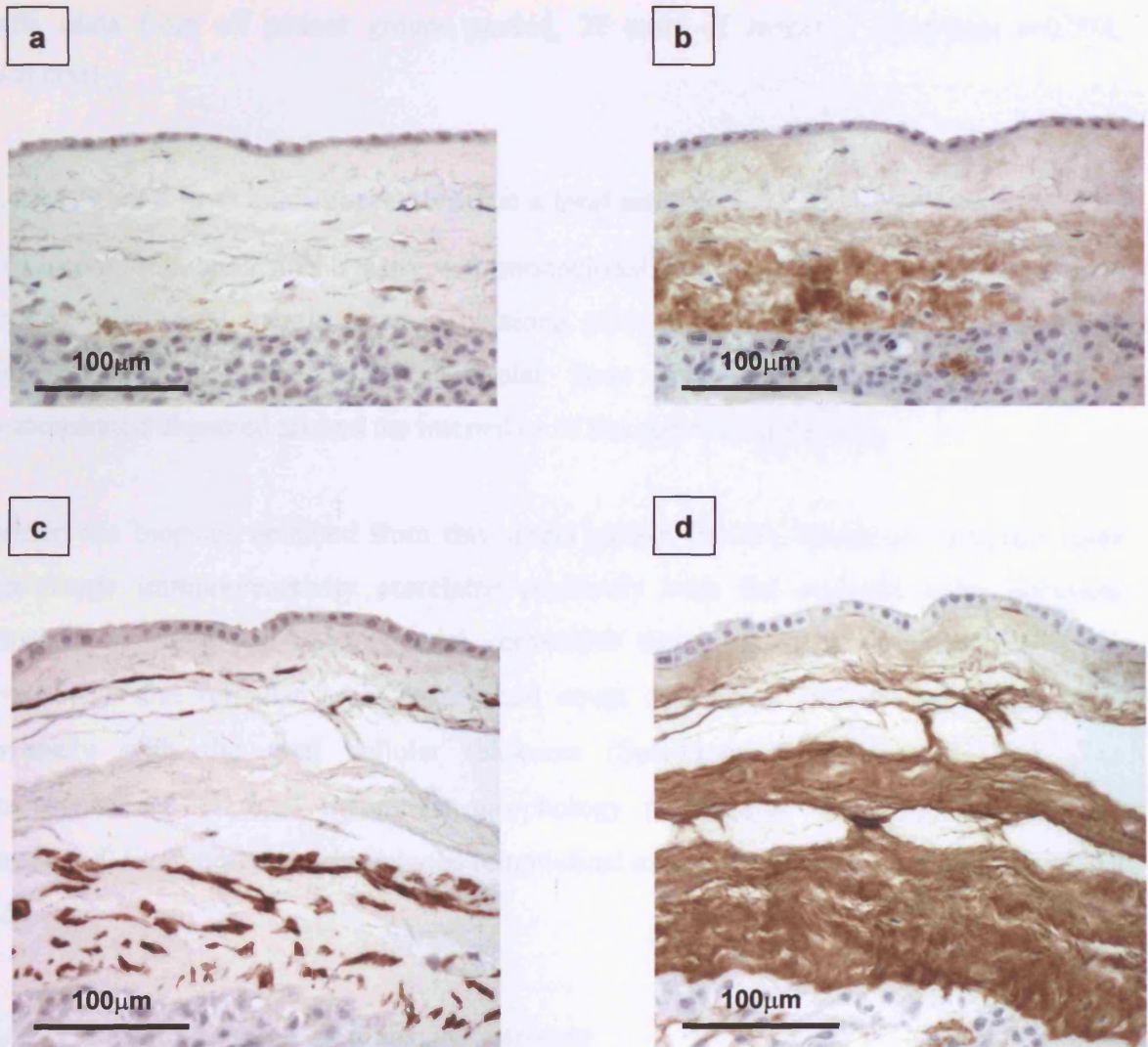


**Figure 5.7.** Immunohistochemistry for  $\alpha$ -sma (**a&c**) and tenascin-C (**b&d**) in serial sections (**a&b, c&d**) of fetal membrane. (**a&b**) A patch of Tn-C immunoreactivity is observed in the reticular layer in the absence of significant numbers of  $\alpha$ -sma positive cells (**c&d**). Intense Tn-C immunoreactivity is observed in the reticular layer and in the fibroblast layer, in association with high numbers of  $\alpha$ -sma immunoreactive cells within these layers.

cells (data from all patient groups pooled, 22 pairs of biopsies; Spearman  $r=0.774$ ,  $p<0.0001$ ).

#### **5.4.1.4. Tenascin-C immunoreactivity on a fetal membrane map**

Tenascin-C immunohistochemistry with monoclonal antibody BC24 was carried out on a representative fetal membrane map obtained prior to labour at term. Fetal membrane biopsies containing the highest reticular layer percentage immunoreactivity were demonstrated clustered around the internal os of the cervix (Figure 5.8).

Within the biopsies obtained from this single patient ( $n=28$ ), tenascin-C reticular layer percentage immunoreactivity correlated positively with the reticular layer thickness (Spearman  $r=0.689$ ,  $p=0.0003$ ), total connective tissue thickness (Spearman  $r=0.820$ ,  $p<0.0001$ ), and reticular layer  $\alpha$ -sma cell count (Spearman  $r=0.657$ ,  $p=0.0006$ ), and inversely with the total cellular thickness (Spearman  $r=-0.439$ ,  $p=0.0226$ ). The correspondence of fetal membrane morphology parameters,  $\alpha$ -sma cell count, and tenascin-C immunoreactivity along the longitudinal axis of this map is illustrated in Figure 5.9.

#### **5.4.1.5. Characterisation of tenascin-C protein**

Western blotting of extracts of whole fetal membranes ( $n=3$  paired pre-labour 'cervical' and midzone) using monoclonal antibody T2H5 demonstrated multiple bands, with major bands at 260-295 kDa, 210-220 kDa and 190-205 kDa, and minor bands at 225-260 kDa and 165-180 kDa (sizes derived from examination of 3 Western blots, Figure 5.10a). Examination of the banding patterns obtained from 'superscraped' fetal membranes ( $n=3$  paired pre-labour 'cervical' and midzone) demonstrated major bands at 270-280 kDa and 210-220 kDa and minor bands at 230-240 kDa and 170-180 kDa (three Western blots examined, Figure 5.10b). No consistent difference in banding patterns was noted in extracts from different anatomical sites and patient groups on examination of banding patterns of homogenates from both whole and 'superscraped' fetal membranes.

#### **5.4.1.6. Regional differences in levels of extracted tenascin-C**

Western blotting and densitometry of extracts of whole fetal membranes obtained prior to the onset of labour ( $n=3$ ), during labour ( $n=3$ ) and following spontaneous labour and

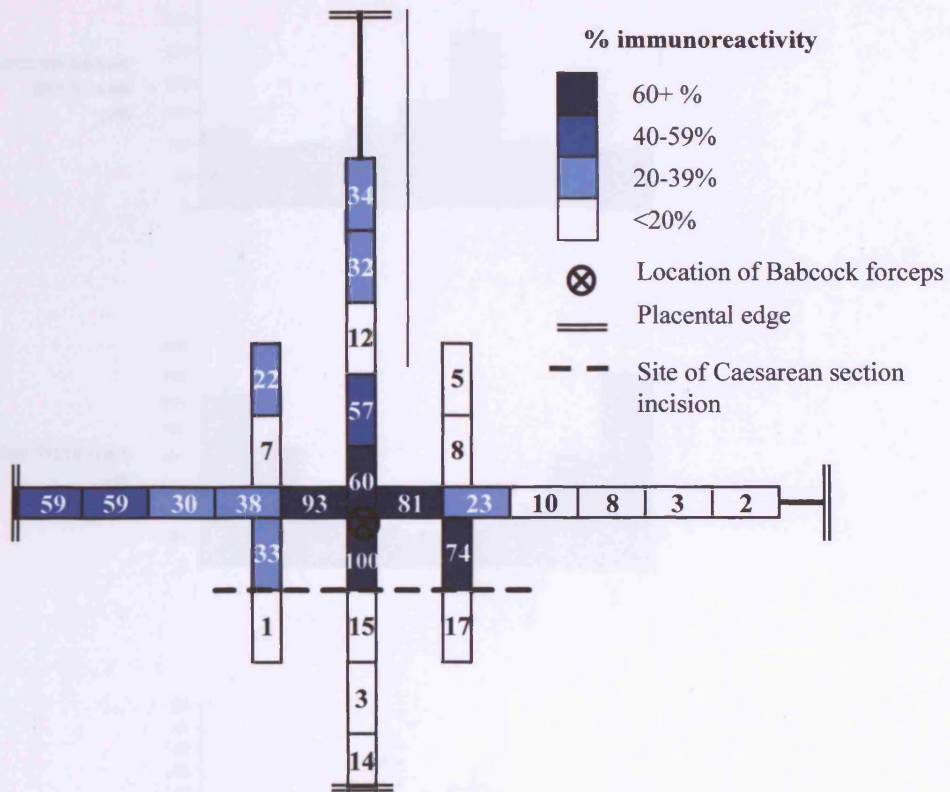


**Figure 5.8.** A representative fetal membrane map (patient 282), obtained prior to labour at term, with measured 3cm biopsies radiating out from the internal os of the cervix to the placental edge. The biopsies are shaded to demonstrate the distribution of the reticular layer percentage tenascin-C immunoreactivity, with the percentage immunoreactivity for each individual biopsy shown. The biopsies with the greatest immunoreactivity are centred upon the internal os of the cervix.

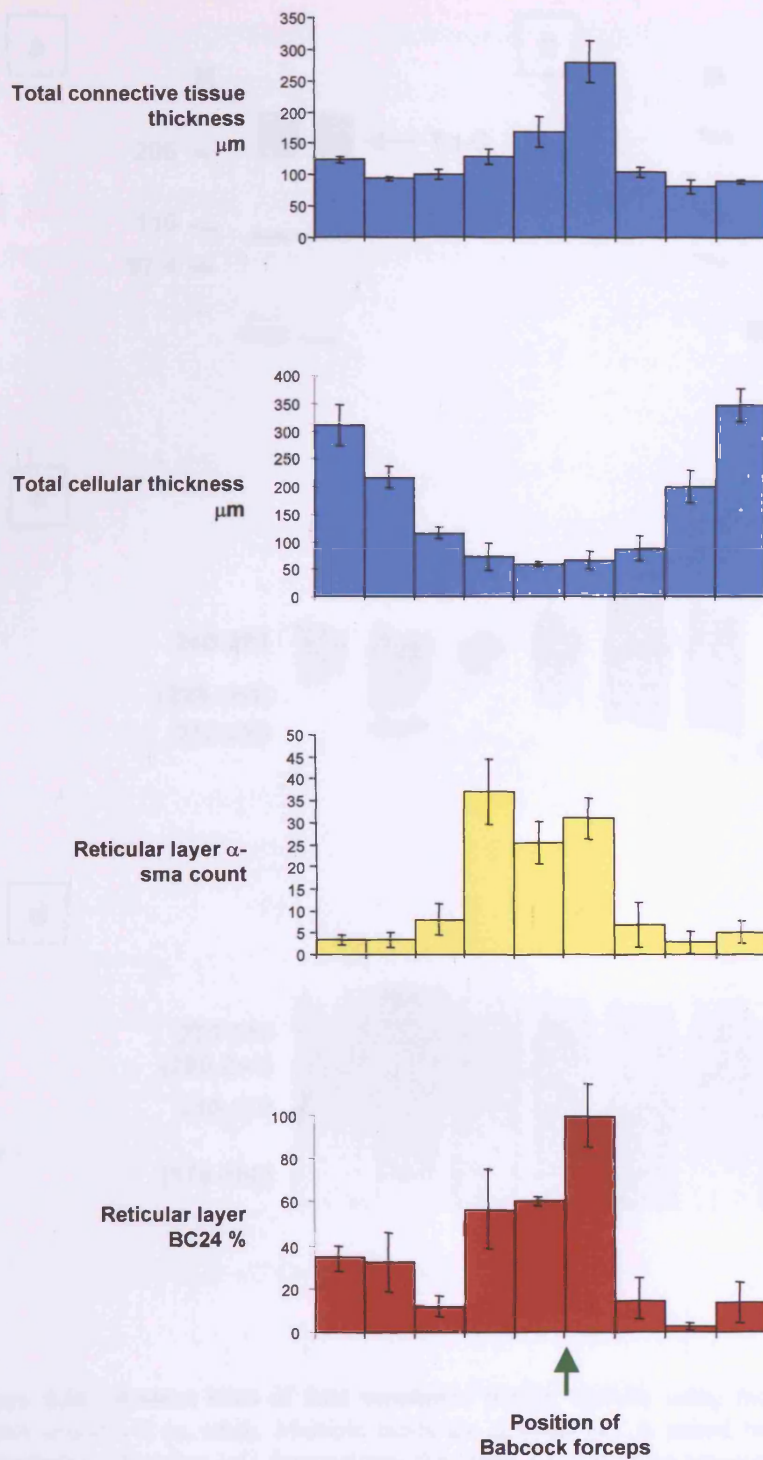


**Figure 5.9.** Graphs demonstrating fetal membrane morphology, reticular layer  $\alpha$ -sma count, and reticular layer tenascin-C percentage immunoreactivity in biopsies taken along the longitudinal axis of a fetal membrane map. (As in Figure 5.4). Maximal tenascin-C immunoreactivity is demonstrated in biopsies with the highest  $\alpha$ -sma cell count, greatest connective tissue thickness, and least cellular thickness. These biopsies cluster around the position of the Babcock tissue forceps.

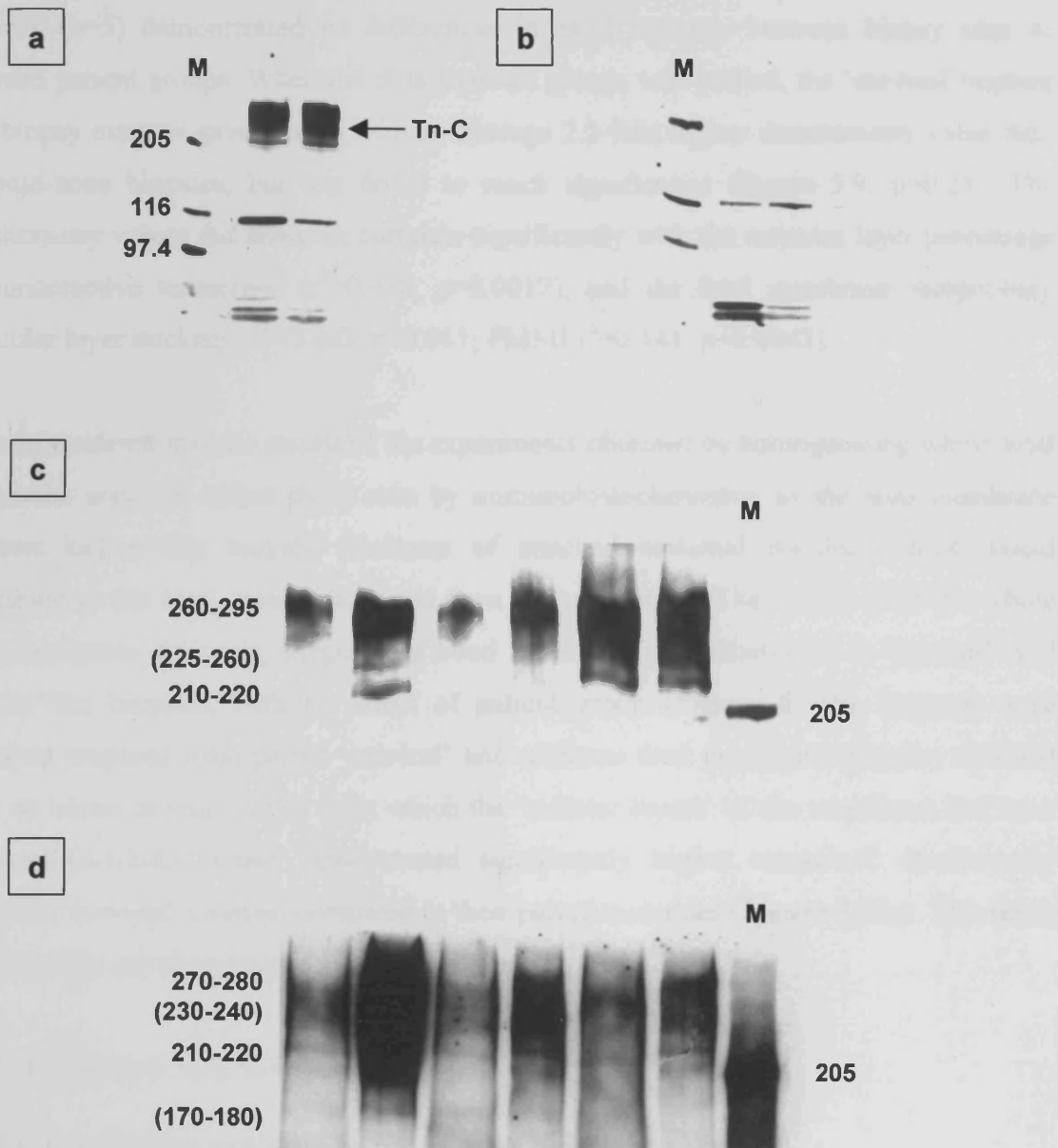


**Figure 5.10.** Western blots of fetal membrane protein extracts using monoclonal antibody clone T2H5 against tenascin-C (**a**, **c&d**). Multiple bands are detected (**a**). A paired blot incubated with an equivalent concentration of mouse IgG demonstrates the lower 3 bands to be non-specific (**b**). The group of specific Tn-C bands are marked (**a**). Multiple bands are detected in extracts from whole fetal membrane (**c**), and from the connective tissue layers only (**d**) (non specific bands cropped off images **c** & **d**). Sizes of bands (kDa) are indicated (minor band sizes in brackets). Not all bands detected are apparent in the blots shown. Lanes containing molecular weight markers (**M**) are included, and sizes shown.

delivery (n=5) demonstrated no differences in band intensity between biopsy sites or between patient groups. When the data from all groups was pooled, the 'cervical'/rupture line biopsy extracts gave a band with an average 2.5-fold higher densitometry value than the mid-zone biopsies, but this failed to reach significance (Figure 5.9, p=0.23). The densitometry values did however correlate significantly with the reticular layer percentage immunoreactive tenascin-C ( $r^2=0.418$ , p=0.0012), and the fetal membrane morphology (reticular layer thickness  $r^2=0.283$ , p=0.011; FMMI  $r^2=0.341$ , p=0.0043).

It was considered that the results of the experiments obtained by homogenising whole fetal membrane may not reflect those seen by immunohistochemistry, as the fetal membrane biopsies had widely varying thickness of attached maternal decidua, which would contribute to the total protein extracted from the membrane. The results from the whole fetal membrane, however, suggested a trend towards higher tenascin-C in 'cervical' and rupture line biopsies, with no effect of patient group (Figure 5.11b). Extracts were therefore prepared from paired 'cervical' and midzone fetal membrane biopsies obtained prior to labour at term (n=5), from which the 'cellular layers' of the membrane had been removed (2.1.1.4). These demonstrated significantly higher tenascin-C densitometry values in 'cervical' biopsies compared to their paired midzones (Figure 5.11c). This result is consistent with the immunohistochemistry results (5.4.1.2.).

## **5.4.2. Tenascin-C mRNA expression**

### **5.4.2.1. Localisation and distribution of mRNA positive cells**

Paired 'cervical' and midzone fetal membrane biopsies obtained prior to the onset of labour at term were examined employing probes to tenascin-C. Specificity was confirmed by the absence of signal when either sense probes were employed, or sections were pre-treated with RNase (Figure 5.12a-d). mRNA positive cells were identified within the reticular layer of the fetal membranes, particularly located toward the pseudobasement membrane (Figure 5.12 e-f), more rarely in the fibroblast layer, in the cores of degenerate villi, and in the walls of sinusoidal vascular structures within the decidua (Figure 5.12i-j).

Tenascin-C mRNA positive cells were always detected in, and embedded within, reticular layer areas and specimens exhibiting the highest intensity tenascin-C immunoreactive matrix (Figure 5.13). They were found in sections exhibiting high numbers of  $\alpha$ -sma positive cells within the reticular layer, and serial sections indicated that mRNA positive

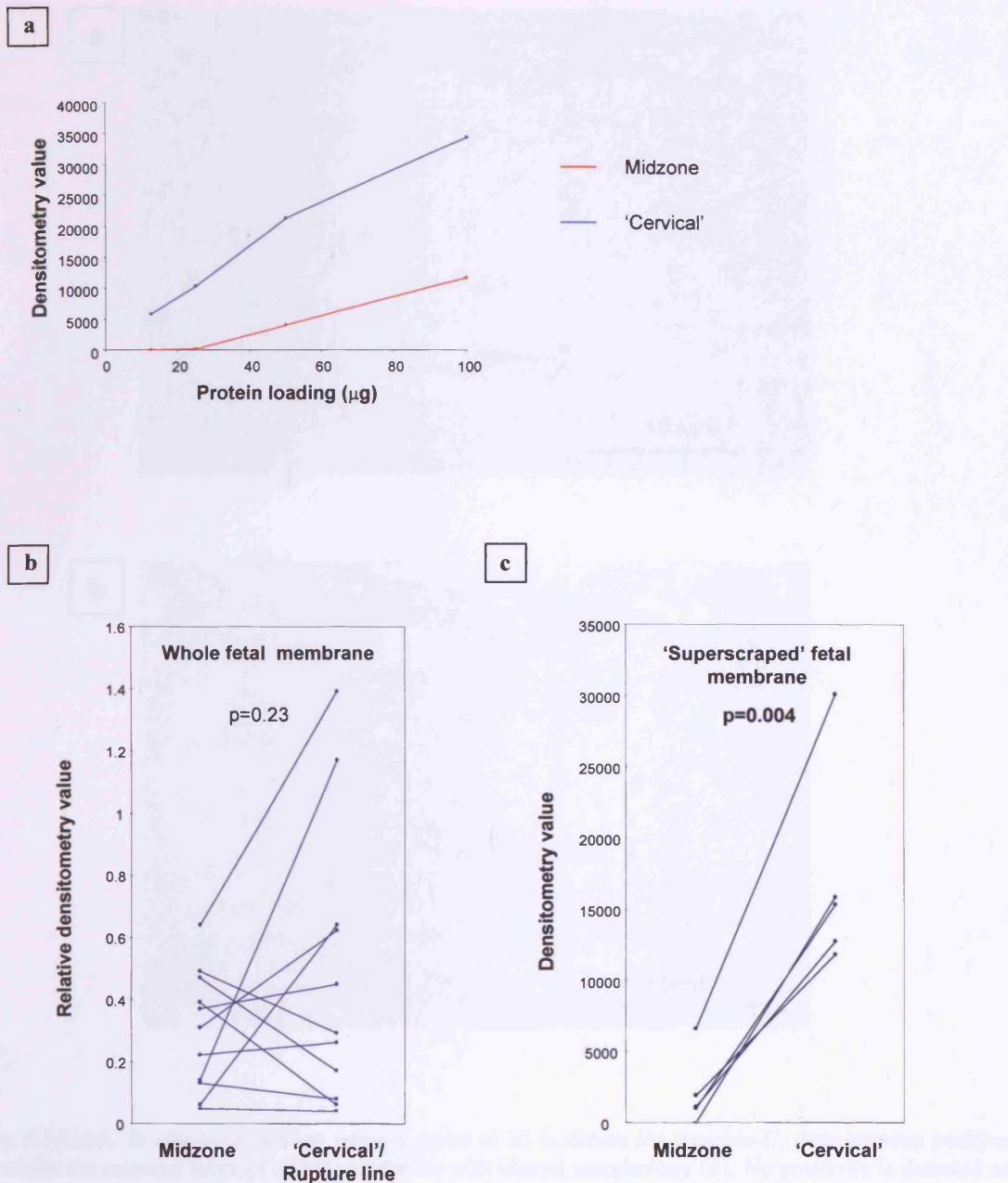


**Figure 5.11.** Relative densitometry values of immunoblotted tenascin-C from fetal membrane homogenates. (a) A titration curve of protein loading using a representative pair of fetal membranes. Protein loading of  $50\mu\text{g}$  was chosen for subsequent experiments, as it lay on the linear part of the curve. (b) Relative densitometry values of immunoblotted tenascin-C from homogenates of whole fetal membranes obtained prior to, during, and following labour at term (Data pooled from 2 Western blots. Densitometry values therefore expressed relative to a known standard on each blot). (c) Densitometry values of immunoblotted tenascin-C from homogenates of 'superscraped' fetal membranes obtained prior to labour at term (Data from a single blot, absolute densitometry values plotted). Lines join the data from paired membranes from an individual patient. Comparisons between biopsy sites and physiological group were using paired t-test (whole fetal membranes) and Mann-Whitney U test ('superscraped' fetal membranes). Significant p-values are shown in bold.

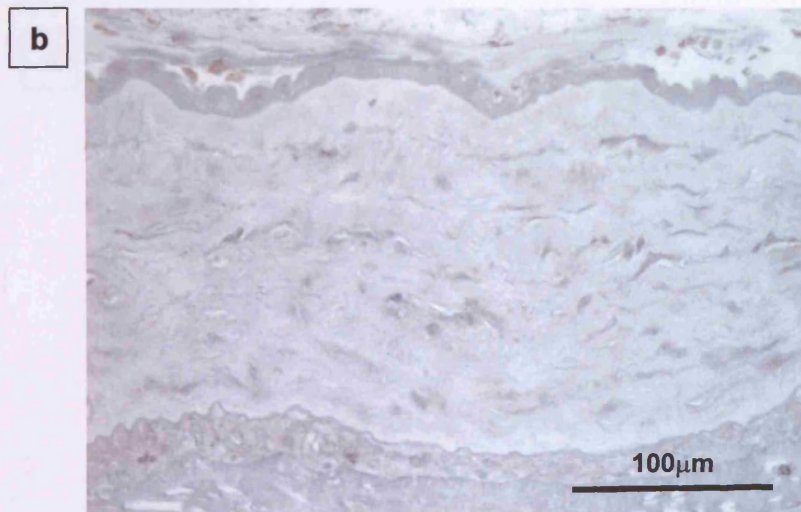
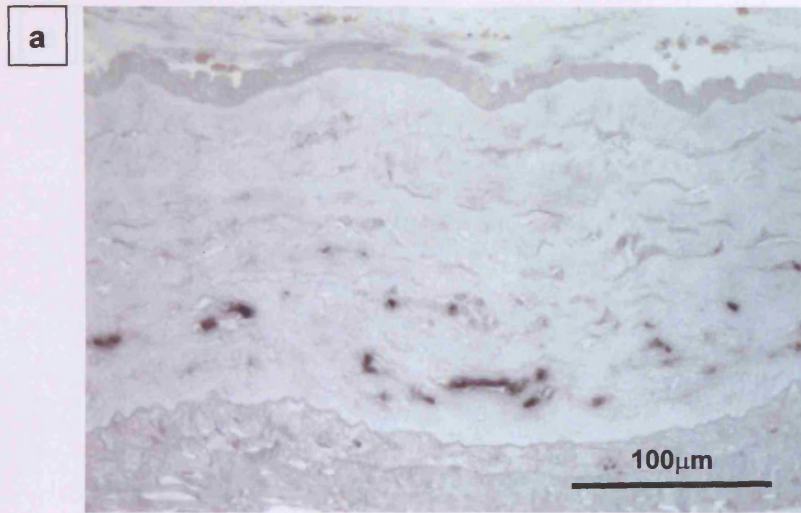


**Figure 5.12a&b.** *In situ* hybridisation using a probe to all isoforms for tenascin-C, demonstrates positive cells within the reticular layer of a fetal membrane with altered morphology (**a**). No positivity is detected in a serial section of the same fetal membrane incubated with a sense control probe (**b**).

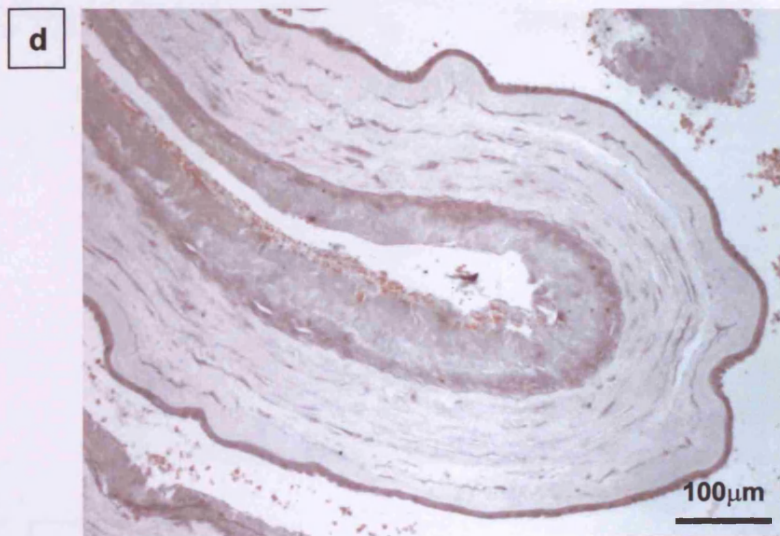
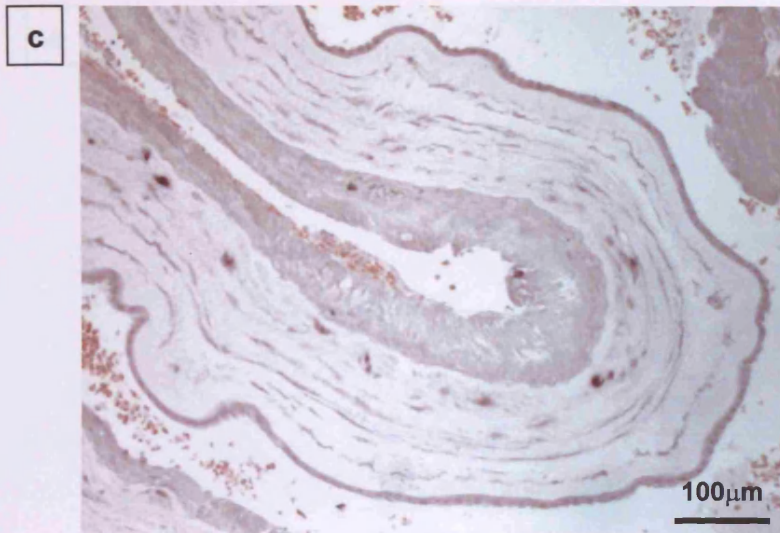
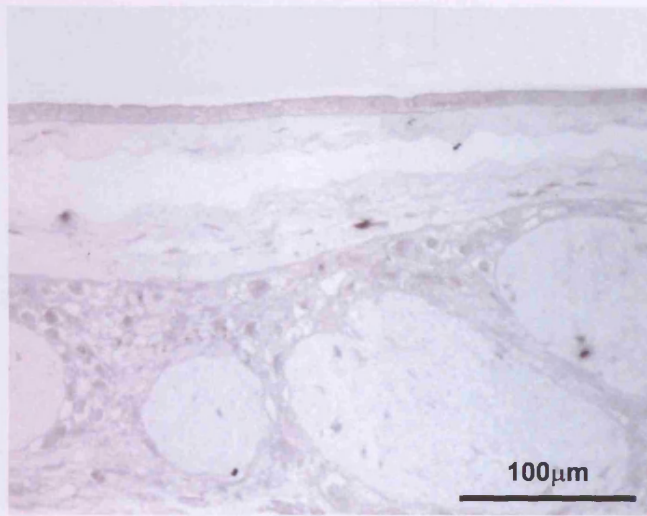
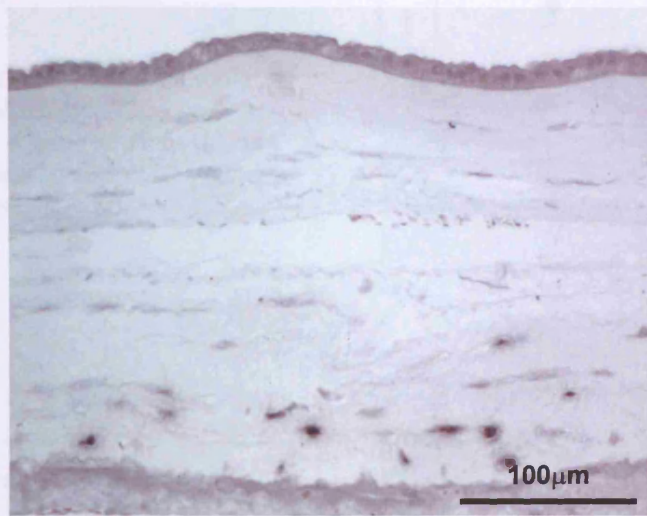


**Figure 5.12c&d.** *In situ* hybridisation using a probe to all isoforms of tenascin-C demonstrates positive cells within the reticular layer of a fetal membrane with altered morphology (c). No positive cells are identified on a serial section of the same fetal membrane pre-treated with RNase prior to incubation with the same probe (d).

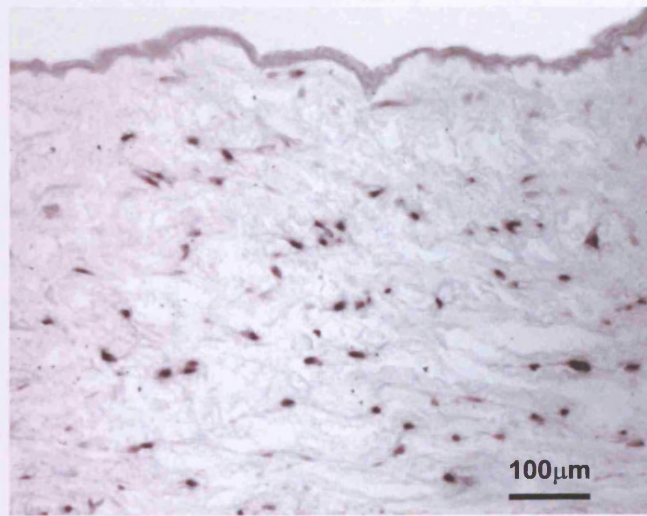
e



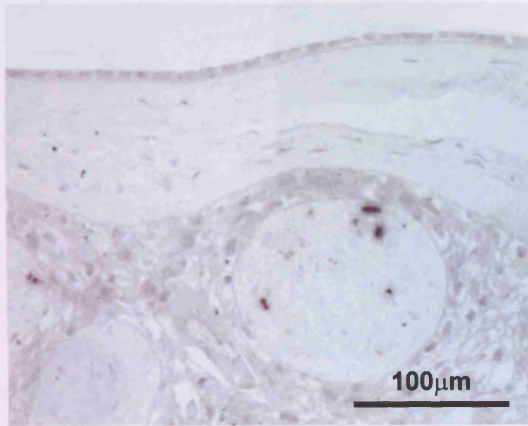
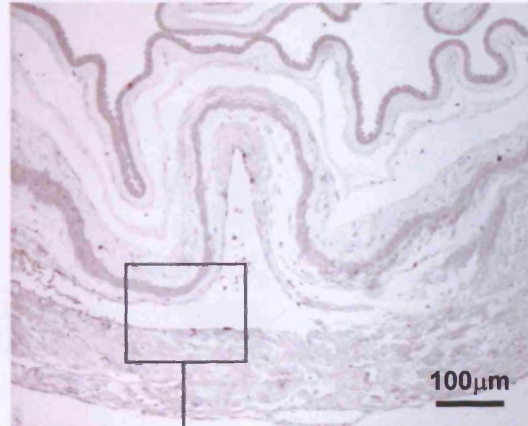
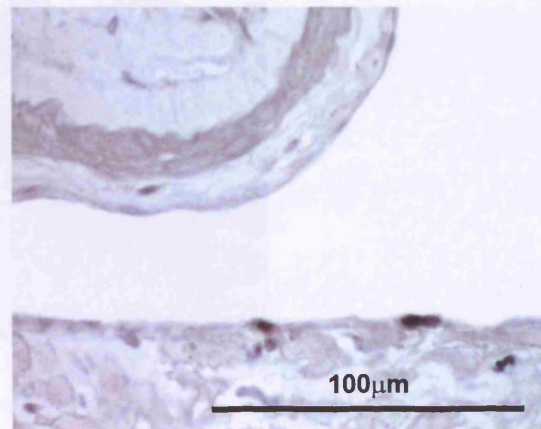
f



g



**Figure 5.12e-g.** *In situ* hybridisation using a probe to all isoforms of tenascin-C demonstrates rare positive cells within the reticular layer of a midzone fetal membrane (e), greater numbers of positive cells within the reticular layer of a fetal membrane with altered morphology (f), and numerous positive cells in the mesenchymal cells of the umbilical cord, used as a positive control tissue (g).

**h****i****j**

**Figure 5.12h-j.** *In situ* hybridisation using a probe to all isoforms of tenascin-C demonstrates positive cells within a degenerate villus (**h**), and within the wall of a vascular sinusoidal structure within the decidua parietalis (**i&j**).

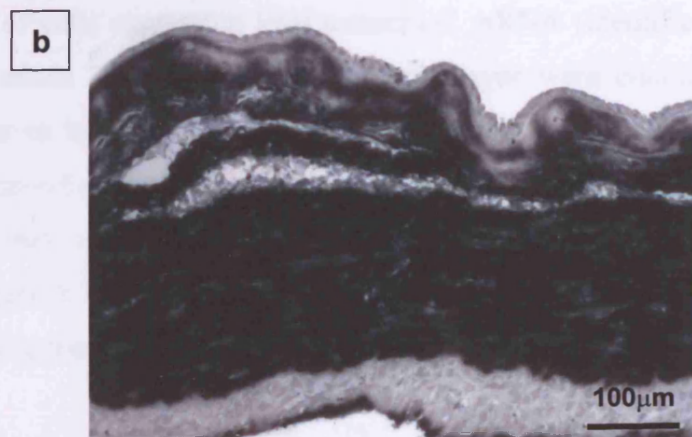
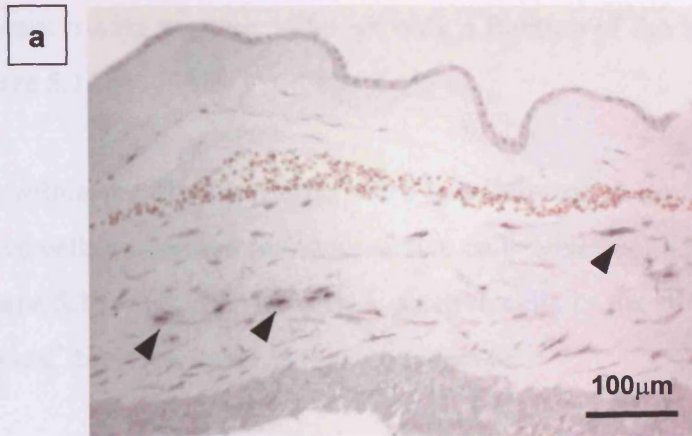


**Figure 5.13.** *In situ* hybridisation using a probe to all isoforms of tenascin-C (a) and immunohistochemistry for tenascin-C (b) on serial sections of fetal membrane. Numerous mRNA positive cells are present within the reticular layer (examples highlighted with arrowheads), and intense immunoreactivity is present throughout the matrix of the reticular, fibroblast and compact layers.

cells were always  $\alpha$ -sma positive, although only a fraction of the latter cells were mRNA positive (Figure 5.14).

Positive cells within the fibroblast layer were less frequent. A direct relationship between mRNA positive cells and  $\alpha$ -sma immunoreactive cells could not be demonstrated on serial sections (Figure 5.14). Tenascin-C mRNA positive cells in the fibroblast layer were only found in 'cervical' biopsies, never in midzone biopsies.

#### **5.4.2.2. Tenascin-C mRNA quantification**

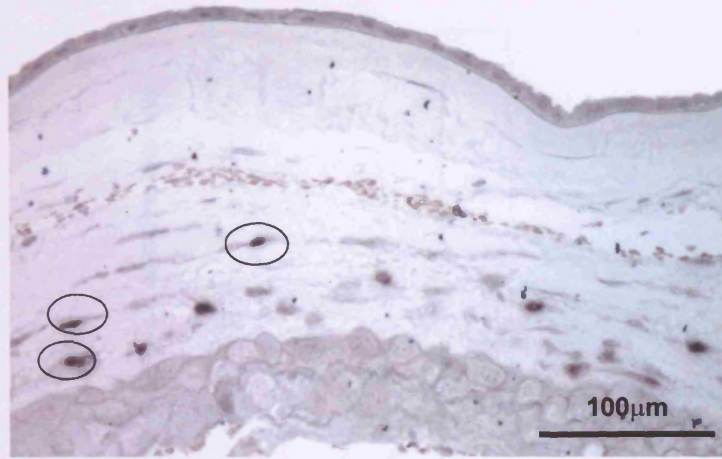
The number of cells expressing total tenascin-C mRNA (identified with a probe against exon 2 and exons 25-27) within the reticular layer were counted in fetal membranes obtained prior to labour at term (n=5). Significantly higher numbers of mRNA positive cells were identified within the reticular layer of 'cervical' fetal membrane biopsies compared to their paired midzone biopsies (1.8 vs. 0.06 cells per computer screen width,  $p=0.028$ , Figure 5.15). However, the proportion of vimentin immunoreactive cells in this layer expressing tenascin-C mRNA was low (5.7% vs. 0.23%).

As tenascin-C mRNA was predominantly observed within cells of the reticular layer, semi-quantitative RT-PCR of tenascin-C mRNA was carried out on RNA extracted from the connective tissue layers only of the fetal membranes (n=5). If RNA were extracted from the whole fetal membrane, the vast majority of the RNA would derive from the highly cellular cytotrophoblast and decidual layers, diluting the RNA of interest. Using primers to exons 25 and 27 to detect total tenascin-C mRNA, no difference was detected in band intensity between 'cervical' and midzone biopsies (Figures 5.16 & 5.17).

#### **5.4.2.3. Tenascin-C mRNA isoforms**

RT-PCR of 'cervical' and midzone RNA pairs using primers to exons 8-14, 14-18 and 8-18, to span the alternatively spliced exons, was performed on RNA extracted from the connective tissue layers of fetal membranes with and without altered morphology. However, RNA extracted from these membranes was heavily DNA contaminated, and required treatment with DNase (2.5.8.). RT-PCR of the resultant RNA preparations did not demonstrate the presence of any bands above the smallest possible for the reaction being performed. This was presumed to be due to insufficient quantities of RNA present, as the smallest PCR product would always be amplified preferentially, and with the greatest

**a**



**b**

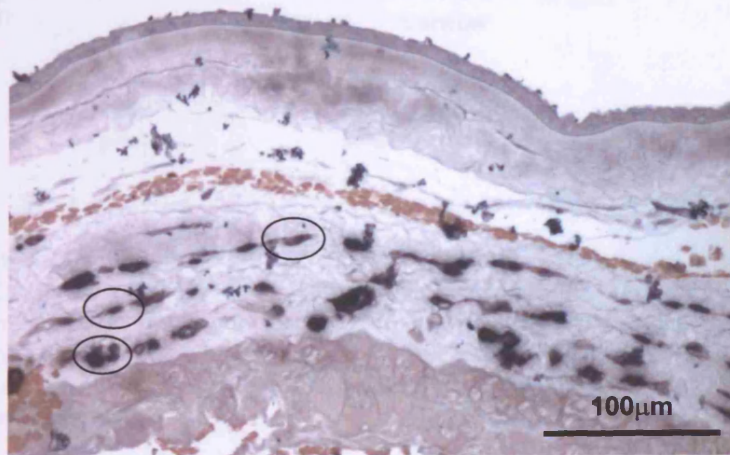
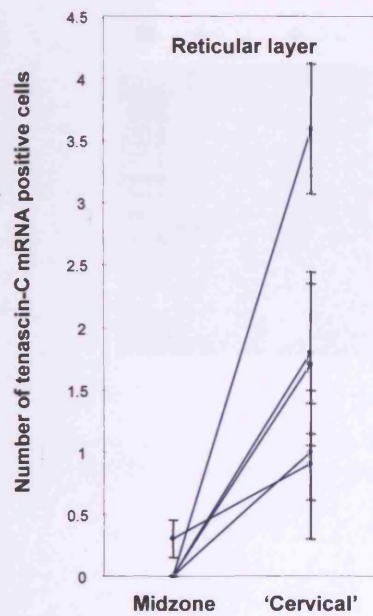


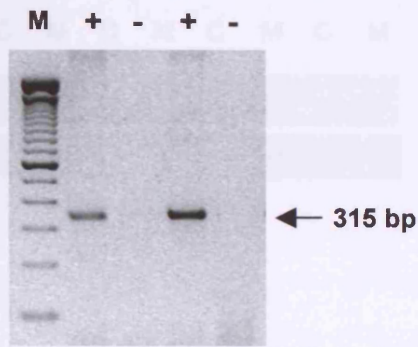
**Figure 5.14.** *In situ* hybridisation using a probe against all isoforms of tenascin-C (**a**) and immunohistochemistry for  $\alpha$ -sma (**b**) on serial sections of fetal membrane. The Tn-C mRNA positive cells are all  $\alpha$ -sma immunoreactive. Examples are highlighted with circles.



Mean	0.06	1.80
SEM	0.03	0.28
p-value	<b>0.028</b>	

**Figure 5.15.** Numbers of cells positive for total tenascin-C mRNA in the reticular layer of fetal membranes obtained prior to labour at term (expressed per computer screen width). The graphs show the mean and SEM derived from 10 fields from each biopsy, with lines connecting the data points from individual patients. The mean and SEM (derived from the total 50 observations) for each group are shown beneath the graphs. Comparisons are made between midzone and 'cervical' biopsies using paired t-test. Significant p-values are shown in bold.

**a**



**b**

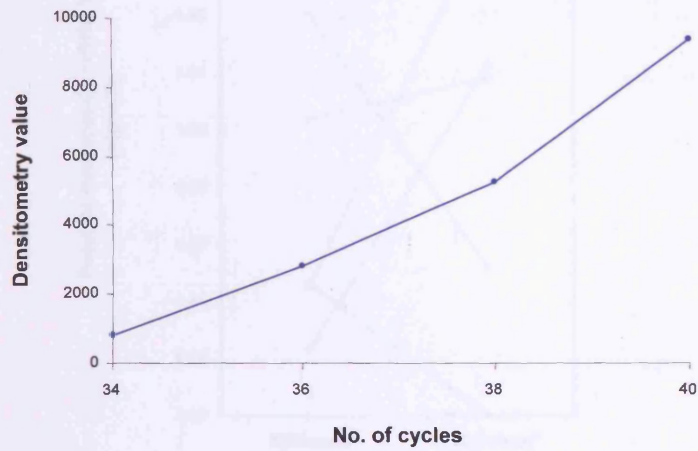
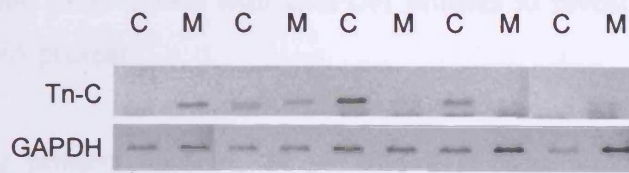


**Figure 5.16.** RT-PCR using primers against exons 25 and 27 of tenascin-C, to amplify all isoforms, on RNA extracted from fetal membranes. A band of 315 base pairs is amplified, and no band is detected in control reactions prepared in the absence (-) of reverse transcriptase (**a**). 100 base pair ladder is in lane **M**. A titration curve demonstrates increasing band intensity, with no evidence of a plateau as cycle number increases (**b**). Visual inspection of gels suggested that bands were frequently not visible at less than 40 cycles of amplification. 40 cycles were therefore used for subsequent experiments.

**a**



**b**

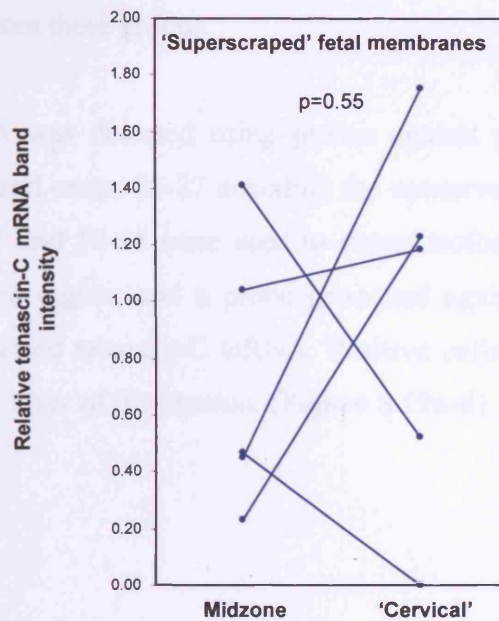


**Figure 5.17.** Densitometry values of total tenascin-C RT-PCR bands obtained using primers to exons 25 and 27, relative to GAPDH, using RNA extracted from 'superscraped' fetal membranes. Lines connect data from paired samples from a single patient. Comparison made using Mann-Whitney U test.

efficiency, when multiple isoforms are present. The RNA from these preparations required amplification for 33-35 cycles with GAPDH primers to reveal a band, again suggesting insufficient RNA present.

RT-PCR using primers to 8-14, 14-18, and 8-18 was similarly performed on RNA extracted from whole fetal membranes with and without altered morphology, and did not demonstrate any regional fetal membrane isoform pattern (Figure 5.18). However, the RNA extracted from these preparations may be considered to arise predominantly from different cell types due to the different underlying structure and cellular composition of the fetal membranes from these groups.

Tenascin-C mRNA was detected using probes against exon 2 encoding the conserved EGF-like repeats, and exons 25-27 encoding the conserved fibrinogen-like region. Probes against exons 9-11 and 14-18 were used to detect isoforms containing exons within the alternatively spliced region, and a probe generated against exons 8-18 to detect 'small isoform' totally spliced tenascin-C mRNA. Positive cells were identified with all probes within the reticular layer of the chorion. (Figure 5.19a-d).

## 5.5. Discussion

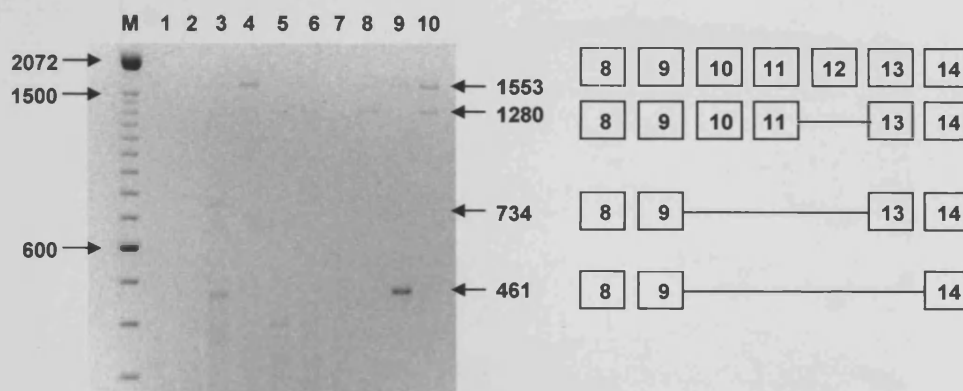
Tenascin-C was immunolocalised to the connective tissue layers of the amnion and chorion, with regional differences in expression, unrelated to the onset of labour, within the reticular layer of the chorion. Immunoreactive Tn-C was also detected between cytotrophoblast cells, along the amniotic basement membrane, at the chorio-decidual interface, and around blood vessels in the decidua, with no regional pattern of expression. The expression at the chorio-decidual interface commonly occurred in association with fibrin deposition, and may reflect a type of wound response. Immunoreactivity within degenerate villi, outgrowths of the reticular layer, is consistent with reported expression within wounded villi in the placenta (Castellucci *et al.*, 1991). Expression of Tn-C has previously been reported around blood vessels (Mackie *et al.*, 1992), and along the amniotic basement membrane, albeit on the chorionic plate of the placenta (Castellucci *et al.*, 1991).

The expression of lesser amounts of Tn-C within the connective tissue layers of the amnion compared to the reticular layer of the chorion may be related to the different nature of the

a. Primers to exons 8 and 18



b. Primers to exons 8 and 14



c. Primers to exons 14 and 18

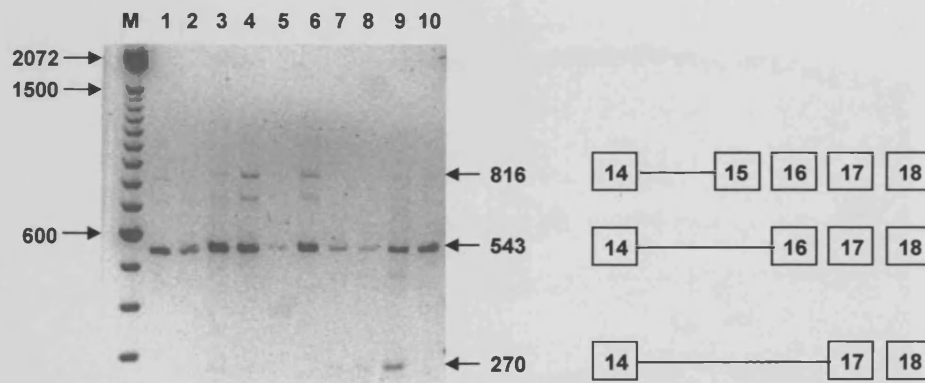


**Figure 5.18.** Agarose gel electrophoresis of reverse transcription polymerase chain reaction products from RNA preparations from whole fetal membranes obtained prior to labour at term. The exons contained within the products are shown in the diagrams to the right (from Bell et al, 2000). The shaded box represents inclusion of a partial exon (Bell et al, 2000). Primers to exons 8 and 18 were used to amplify across the whole alternatively spliced region. Only isoforms containing alternatively spliced exon 16 were demonstrated (a). However, using primers within the alternatively spliced regions, numerous other isoforms can be demonstrated (b, c). Lanes 1, 3, 5, 7 and 9 are from 'cervical' fetal membrane biopsies, and lanes 2, 4, 6, 8 and 10 from midzone fetal membrane biopsies. No consistent pattern of isoforms is seen associated with biopsy site. Lane M contains 100 base pair DNA markers.

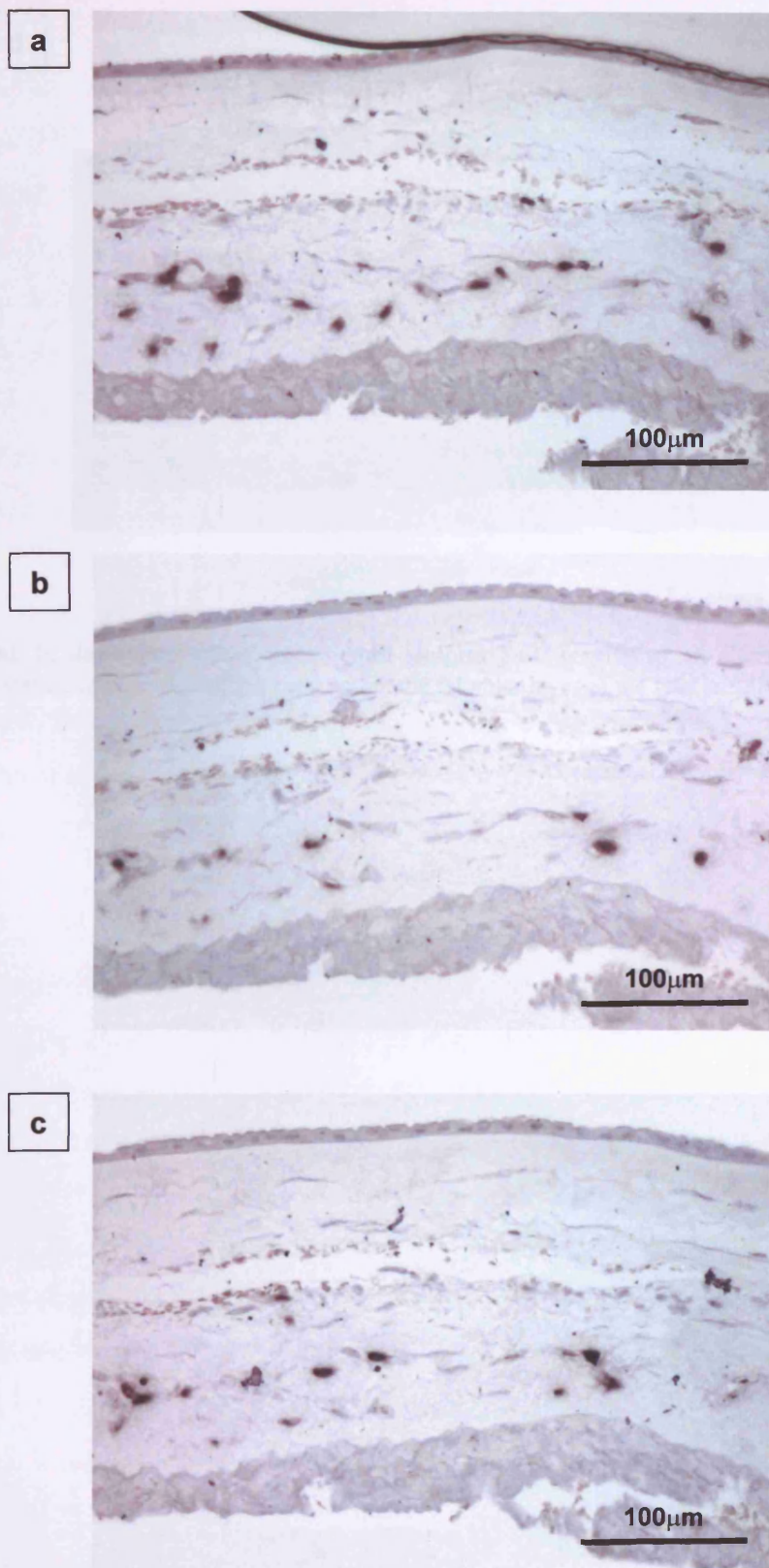


**Figure 5.19a-c.** *In situ* hybridisation to tenascin-C isoforms, using probes to all isoforms of Tn-C (a), and to large isoforms of Tn-C (exons 9-11 (b) and exons 14-18 (c)) on serial sections of fetal membrane.

d

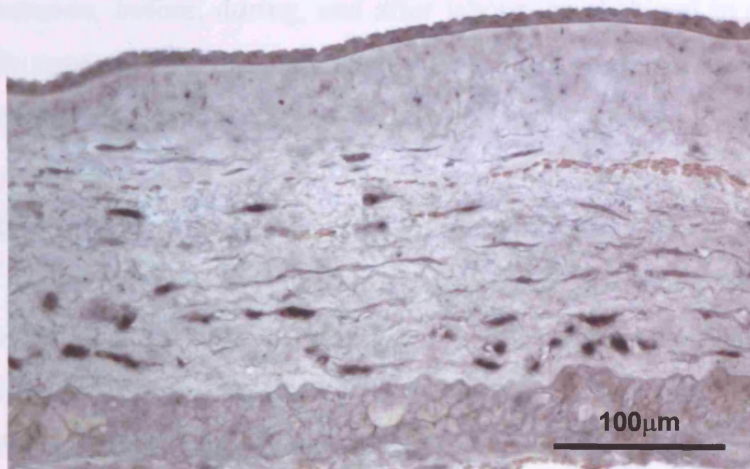


**Figure 5.19d.** In situ hybridisation against small isoform Tn-C (excluding all alternatively spliced Fn-III exons) demonstrating mRNA positive cells within the reticular layer of the fetal membrane.

cells, which are desmin-negative (Chapter 3). However, regional Tn-C expression may be induced in the amnion, before, during, and after labour, as observed in one patient from each group. This suggests that the cells have the ability to produce Tn-C, although may require greater stimulus to do so.

Tenascin-C mRNA production was detected in the fibroblasts of the amnion, and the myofibroblasts of the reticular layer. Production of Tn-C is a recognised feature of the myofibroblast in the wound response (Powell *et al.*, 1999). Rare mRNA positive cells were also detected around the blood vessels of the decidua, although they were not observed within cells of the cytotrophoblast layer.

Although regional differences in Tn-C protein expression were detected by immunohistochemistry and by Western blotting, and in mRNA expression by *in situ* hybridisation, no differences in mRNA expression were detected using RT-PCR. This may be due to technical difficulties, or may reflect the properties and expression pattern of the mRNA being examined. RT-PCR was performed on RNA extracted from the connective tissue layers only, to ensure that mRNA from comparable tissues were examined. A proportion of the cells present will be epithelial cells, which may affect the results. However, difficulties in the technique for RNA extraction from the connective tissue layers lead to reduction in the mRNA available for examination. The Tn-C PCR was performed at 40 cycles, at the limits of accuracy of the technique, and may not thus be considered quantitative. However, PCR amplification of RNA summates the RNA present in all cells, whereas *in situ* hybridisation only detects cells with mRNA above a threshold. Thus the presence of a large number of cells with lesser amounts of mRNA may not be detected by *in situ* hybridisation, but may give significant bands when amplified by PCR. Possible reasons for the lack of correspondence between mRNA and protein expression are as discussed with relation to  $\alpha$ -sma in Chapter 3 (3.5.).

Expression of different isoforms of Tn-C was examined by Western blotting, *in situ* hybridisation, and by RT-PCR. Early work on Tn-C suggested the presence of only two isoforms; 'large' isoform, and 'small' isoform, with expression of 'large' isoform associated with tissue wounding and remodelling. Subsequent molecular biology studies suggest a far more complex picture, with the presence of multiple different isoforms (Wilson *et al.*, 1996; Mighell *et al.*, 1997; Vollmer *et al.*, 1997; Bell *et al.*, 1999; Latijnhouwers *et al.*, 2000). A number of the alternatively spliced exons encode for regions

with specific functions, thus expression of different isoforms may have functional significance. Expression of larger isoforms of Tn-C has been associated with malignant compared to benign ovarian tumours (Wilson *et al.*, 1996), and expression of Tn-C containing exons 14 and 16 with invasive potential of breast tumours (Adams *et al.*, 2002). However, increased expression of Tn-C in psoriasis, epidermal tumours, and wounding was not associated with upregulation of specific isoforms (Latijnhouwers *et al.*, 2000). The major isoforms described within fetal membranes are those with complete exclusion of the alternatively spliced exons, inclusion of exon 16, and inclusion of exons 10-14 and 16, including or excluding exon 12 (Bell *et al.*, 1999). Exon 12 contains the site for susceptibility to cleavage by MMP-2 and MMP-3, thus providing potential functional significance (Siri *et al.*, 1995). Expression of small isoform Tn-C (excluding all alternatively spliced exons), and a number of large isoforms of Tn-C were detected in the connective tissue layers of the fetal membranes in this study. However, screening of the fetal membrane samples with and without altered morphology did not suggest upregulation of specific isoforms.

The amount of immunoreactive Tn-C detected correlated to the number of cells immunoreactive for  $\alpha$ -sma. However, there did not appear to be an absolute direct relationship between  $\alpha$ -sma and Tn-C protein expression when serial sections were examined. It is possible that this is related to temporal differences in expression and differences in degradation of proteins. The mRNA positive cells were not necessarily  $\alpha$ -sma positive cells. mRNA expression was not necessarily co-localised with protein expression, although this phenomenon is well recognised, and may be related to temporal differences in tenascin-C mRNA and protein expression. Alternatively  $\alpha$ -sma expression may not be required for production of Tn-C, but production of both proteins independently controlled, either by the same or by different regulatory factors.

## 5.6. Conclusions

- Tenascin-C protein has been demonstrated in the fetal membranes, and was primarily localised in the extracellular matrix of the connective tissue layer of the amnion and chorion, and was also demonstrated at the chorio-decidual interface, between cytotrophoblast cells, around blood vessels in the decidua, and rarely in patches along the amniotic basement membrane.

- **Tenascin-C mRNA is produced by myofibroblasts in the reticular layer of the chorion, and by fibroblasts in the amnion, as demonstrated by *in situ* hybridisation.**
- **Regional increased expression of tenascin-C protein and mRNA was demonstrated within the reticular layer in fetal membrane biopsies obtained from overlying the cervix prior to and during labour, and from the rupture line following labour and delivery at term.**
- **Tenascin-C protein expression was confirmed by Western blotting of fetal membrane protein extracts, and the regional increase in protein expression within the connective tissue layers in fetal membranes overlying the cervix prior to labour confirmed.**
- **Tenascin-C mRNA was amplified by RT-PCR, but this technique was unable to confirm the regional difference in mRNA expression in total RNA extracted from fetal membranes that had been demonstrated in tissue sections by *in situ* hybridisation.**
- **Expression of numerous isoforms of tenascin-C, both large and small, was confirmed by Western blotting, *in situ* hybridisation and RT-PCR. No regional pattern of isoform expression was observed.**

## Chapter 6

### Osteonectin expression in human fetal membranes

#### **6.1. Introduction**

The work presented in Chapter 3, demonstrated regional myofibroblast differentiation within the reticular layer of the fetal membranes. The expression of  $\alpha$ -sma by these cells is associated with structural changes within the fetal membranes, and expression of the matricellular protein tenascin-C (Chapter 5). Myofibroblast differentiation and tenascin-C expression are characteristic features of wound repair (Clark, 1996). A recent paper reported the expression of osteonectin by liver myofibroblasts during fibrosis (Blazejewski *et al.*, 1997). This matricellular protein is expressed by fibroblastic cells in the mid to late stages of wound repair (Reed *et al.*, 1993). It is expressed in tissues undergoing matrix remodelling and repair, and has been shown to regulate matrix metalloproteinases and the inhibitor plasminogen activator inhibitor-1 (Reed & Sage, 1996). It was therefore considered that it may be expressed in the fetal membranes, and indeed may play a key role in the development of the regional structural alterations previously described. Therefore this chapter examines the regional expression of osteonectin, and its relationship to myofibroblast differentiation and regional structural changes in the fetal membranes.

##### **6.1.1. Osteonectin protein**

Osteonectin is a matricellular protein, also known as SPARC (Secreted Protein Acidic and Rich in Cysteine), BM-40, and 43K protein. It was first isolated as a major noncollagenous constituent of bone (Termine *et al.*, 1981), and subsequently found to be identical to a 43K protein synthesised *in vitro* by endothelial cells and fibroblasts (Motamed *et al.*, 1996). The amino acid sequence predicts a protein with a mass of 32,517 Da, although glycosylation results in a secreted glycoprotein with an apparent size of 40-44 kDa by SDS-PAGE (Lane & Sage, 1994).

Osteonectin cDNA encodes a 286 amino acid  $\text{Ca}^{2+}$  binding protein (Lankat-Buttgereit *et al.*, 1988), with 4 functional domains. Domain I is highly acidic and binds  $\text{Ca}^{2+}$ , domain II is cysteine-rich and contains  $\text{Cu}^{2+}$  binding sites, domain III contains a protease sensitive

site, and domain IV contains a Ca<sup>2+</sup> binding site and mediates collagen binding (Lane & Sage, 1994; Motamed *et al.*, 1996).

Osteonectin is encoded by a single copy gene on chromosome 5q31-33 (Swaroop *et al.*, 1988). The gene has ten exons and exhibits a high degree of homology between species. There is no evidence for variants arising from alternative splicing (Lane & Sage, 1994; Motamed *et al.*, 1996). Protein domain I is encoded by exons 3 and 4, domain II by exons 5 and 6, domain III by exons 6 and 7, and domain IV by exon 9 (Lane & Sage, 1994; Motamed *et al.*, 1996).

### 6.1.2. Expression and function of osteonectin

Osteonectin is a collagen-binding glycoprotein with widespread expression in tissues undergoing morphogenesis, remodelling and repair (e.g. during fetal development, bone, and in wound repair) (Lane & Sage, 1994). Expression has been reported in a wide range of cells, including fibroblasts (Lane & Sage, 1994), myofibroblasts (Blazejewski *et al.*, 1997), macrophages (Lane & Sage, 1994), endothelial cells (Sage *et al.*, 1984), smooth muscle cells (Reed & Sage, 1996) and chondrocytes (Reed & Sage, 1996). It is also released during platelet degranulation (Lane & Sage, 1994). It is expressed in a wide variety of tumours, both by tumour cells and by reactive cells in the surrounding stroma (Porter *et al.*, 1995). Although osteonectin expression has been described in the chick chorio-allantoic membrane (Iruela-Arispe *et al.*, 1995), there are no reports of its expression in human fetal membranes.

Osteonectin induces the expression of matrix metalloproteases involved in matrix remodelling, MMP-1, -3, and -9 (Tremble *et al.*, 1993; Shankavaram *et al.*, 1997), and the inhibitor plasminogen activator inhibitor-1 (Lane *et al.*, 1992). It has thus been proposed to play a key role in extracellular matrix remodelling, and in facilitating cellular migration, such as that seen in tumour progression and metastasis (Reed & Sage, 1996). Osteonectin acts as an anti-adhesive protein in cell culture *in vitro*, promoting cell rounding, and inhibiting cell spreading (Lane & Sage, 1994; Motamed *et al.*, 1996). It has also been demonstrated to mediate focal adhesion disassembly in endothelial cells, with breakdown of actin-containing stress-fibres, and redistribution of actin toward the cell periphery (Motamed *et al.*, 1996).

## **6.2. Aims**

- To establish whether osteonectin, at both mRNA and protein level, is expressed in term fetal membranes.
- To determine the nature of cells expressing osteonectin protein and mRNA in the fetal membranes.
- To determine whether regional changes in osteonectin protein and mRNA expression exist.
- To examine any association between osteonectin expression and expression of  $\alpha$ -sma and of tenascin-C in the connective tissue layers of the fetal membranes.

## **6.3. Materials and Methods**

### **6.3.1. Tissue samples**

Fetal membrane samples were obtained at term prior to labour (n=15), during labour (n=5) and following labour and delivery (n=5) as previously described (2.1.1.). The restricted area of tissue taken, to ensure accurate mapping, meant that in some cases different tissue samples were used for different techniques. First trimester decidua (n=5) was obtained following suction termination of pregnancy (2.1.3.).

### **6.3.2. Immunohistochemistry**

Immunohistochemistry for osteonectin was carried out on formalin-fixed wax-embedded tissue samples using mouse monoclonal antibody clone N50 and rabbit polyclonal antiserum BON-I. Immunohistochemistry with monoclonal antibodies to vimentin (clone V9), CD68 (clone PGM1), cytokeratin (MNF116), and  $\alpha$ -sma (clone 1A4) was performed in order to assist in quantifying and to characterise the nature of cells within the fetal membrane found to be immunoreactive for osteonectin (2.3.).

### 6.3.3. SDS-PAGE and Western blotting

Fetal membrane extracts from paired whole fetal membrane biopsies obtained during and following labour at term (n=9), and from paired 'superscraped' (section 2.1.1.4.) fetal membrane biopsies (n=5) were separated on 10% polyacrylamide gels and transferred to nitrocellulose as previously described (2.4.). Monoclonal antibody N50 and polyclonal antiserum BON I were used to detect osteonectin using enhanced chemiluminescence (2.4.5.). The resultant bands were quantified using Scion Image™ (2.8.2.).

### 6.3.4. RT-PCR

RNA was extracted from 5 paired 'cervical' and midzone fetal membrane biopsies obtained prior to labour at term, and from the connective tissue layers only from a further 5 pairs of 'cervical' and midzone prelabour fetal membrane biopsies. The RNA was subjected to RT-PCR using primers to osteonectin and to GAPDH at previously determined optimal cycle number, and the PCR products were separated on an agarose gel (2.5.). The bands on the captured image of the gel were quantified using Scion Image™ (2.8.2.).

### 6.3.5. *In situ* hybridisation

A probe to detect osteonectin mRNA *in situ* was synthesised by RT-PCR amplification of a 325 base pair region of the osteonectin gene, employing mRNA extracted from SK-MEL-28 cells. This template was used in an 'asymmetric' PCR reaction incorporating digoxigenin to produce a single stranded antisense DNA probe (2.6.). *In situ* hybridisation was carried out on formalin-fixed wax-embedded paired 'cervical' and midzone fetal membrane biopsies obtained prior to labour at term (n=5) as previously described (2.6.5.).

### 6.3.6. Image analysis

Immunoreactivity to monoclonal antibody N50 was used to quantify the number of osteonectin immunoreactive cells in the constituent layers of the fetal membranes (2.8.1.2.). The numbers of mRNA positive cells by *in situ* hybridisation was similarly quantified.

### **6.3.7. Statistical analysis**

The methodology used to compare numbers of immunoreactive and mRNA positive cells, to correlate parameters, and to analyse data obtained from Western blots and by RT-PCR are described in **section 2.9**.

## **6.4. Results**

### **6.4.1. Osteonectin protein expression**

#### **6.4.1.1. Osteonectin immunolocalisation**

Osteonectin immunoreactive cells were identified in the amniotic epithelium, and in the fibroblast, reticular, and cytotrophoblast layers in fetal membrane biopsies obtained from all zones and all patient groups employing both monoclonal antibody N50 and polyclonal antiserum BON-I (**Figure 6.1a-e**). Immunoreactive cells were also identified within degenerate villi in the cytotrophoblast layer. No immunoreactive cells were detected in the decidua attached to the amniochorion with either antibody. Occasional immunoreactive cells were seen within the first trimester decidua (as described previously (Wewer *et al.*, 1988)) with both N50 and BON-I, although the previously reported extracellular matrix staining around decidual cells (Wewer *et al.*, 1988) was seen only with BON-I (**Figure 6.1c**).

Serial sections stained with an antibody CD68 confirmed that the positive cells within the fibroblast and reticular layers of the fetal membranes did not co-express this marker, and were thus fibroblastic/myofibroblastic in nature (**Figure 6.2**). Serial sections stained with an antibody to cytokeratin confirmed that the positive cells within the cellular layers of the fetal membranes were cytotrophoblast cells (**Figure 6.3a&b**). Osteonectin immunoreactive cells identified within the cellular layers of the fetal membranes were predominantly within the superficial maternal aspect of the cytotrophoblast layer (**Figure 6.3a**), although in membranes exhibiting significant thinning of the cytotrophoblast layer, immunoreactive cells were also seen adjacent to the pseudobasement membrane (**Figure 6.3c-e**).

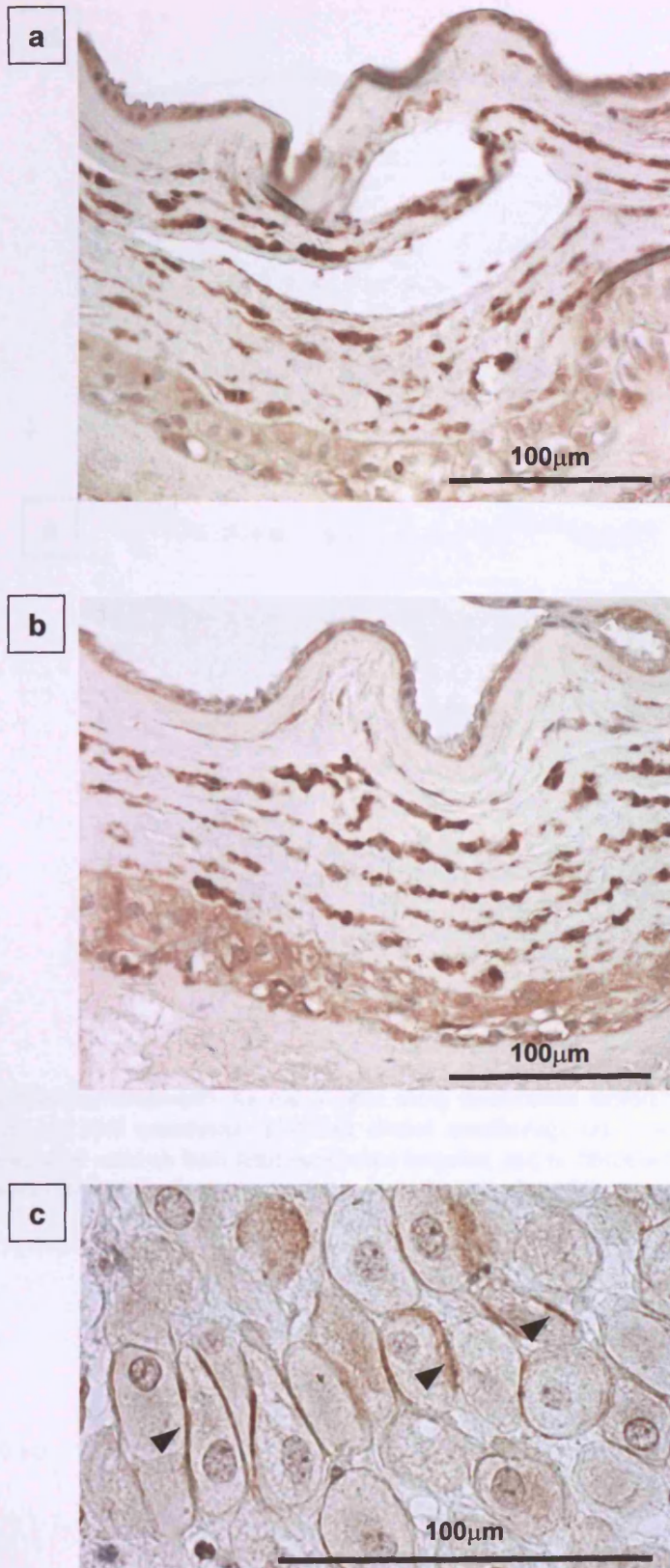
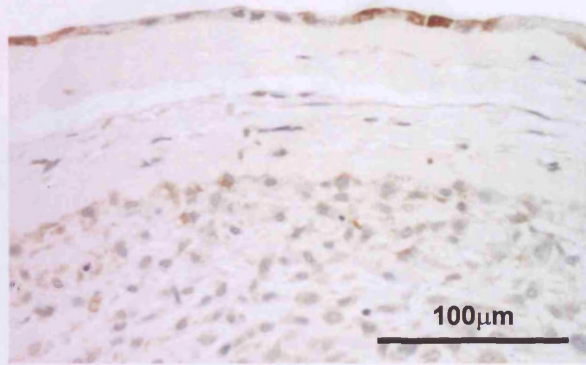


**Figure 6.1a-c.** Immunohistochemistry for osteonectin on sections of the same fetal membrane biopsy, using a polyclonal antiserum (a), and using monoclonal antibody N50 (b). Immunoreactive cells can be observed within the fibroblast layer, reticular layer and cytotrophoblast layer. Some lifting of the tissue section is seen in (a), due to the microwave pretreatment. (c) Immunohistochemistry for osteonectin using polyclonal antiserum on first trimester fetal membrane confirms the previously reported finding of immunoreactivity surrounding decidual cells (arrowheads).

d



e

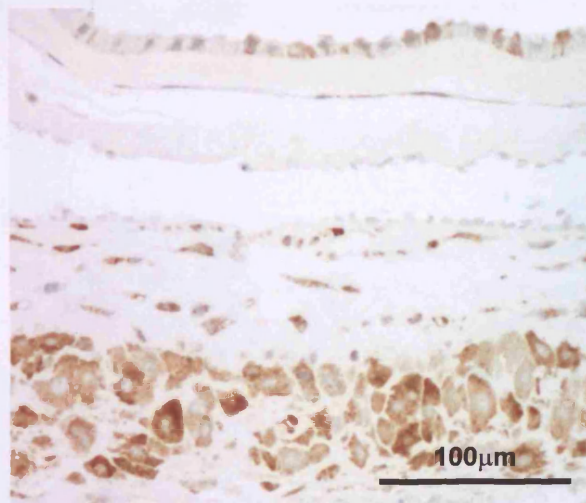
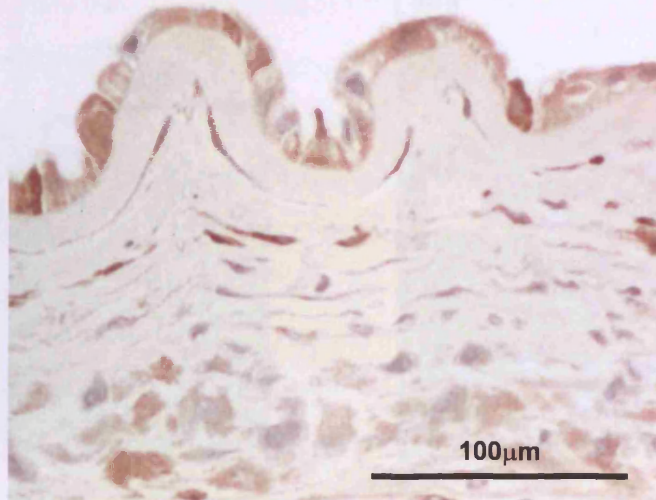


**Figure 6.1d-e.** Immunohistochemistry for osteonectin using monoclonal antibody clone N50, on midzone fetal membrane (d) and fetal membrane exhibiting altered morphology (e). Immunoreactivity is observed within amniotic epithelial cells on both fetal membrane biopsies, and in fibroblast layer, reticular layer and cytotrophoblast layer cells predominantly within the altered morphology biopsy (e).

a



b

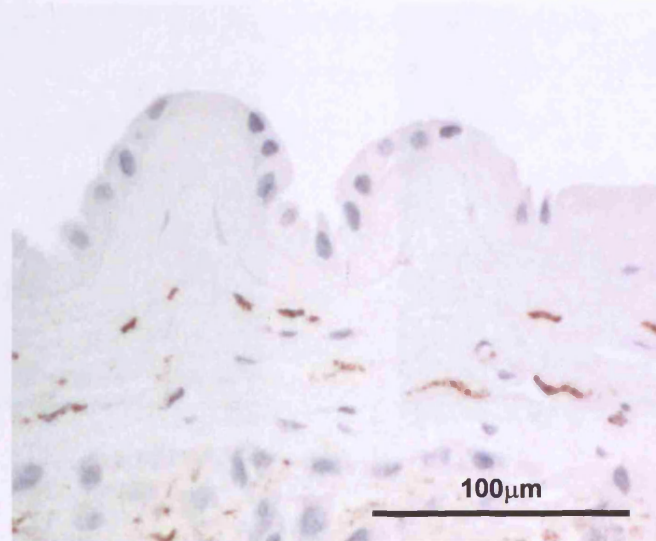


**Figure 6.2.** Immunohistochemistry for osteonectin (a) and macrophage marker CD68 (b) on serial sections of fetal membrane, demonstrating that the osteonectin immunoreactive cells within the fibroblast and reticular layers are negative for CD68.

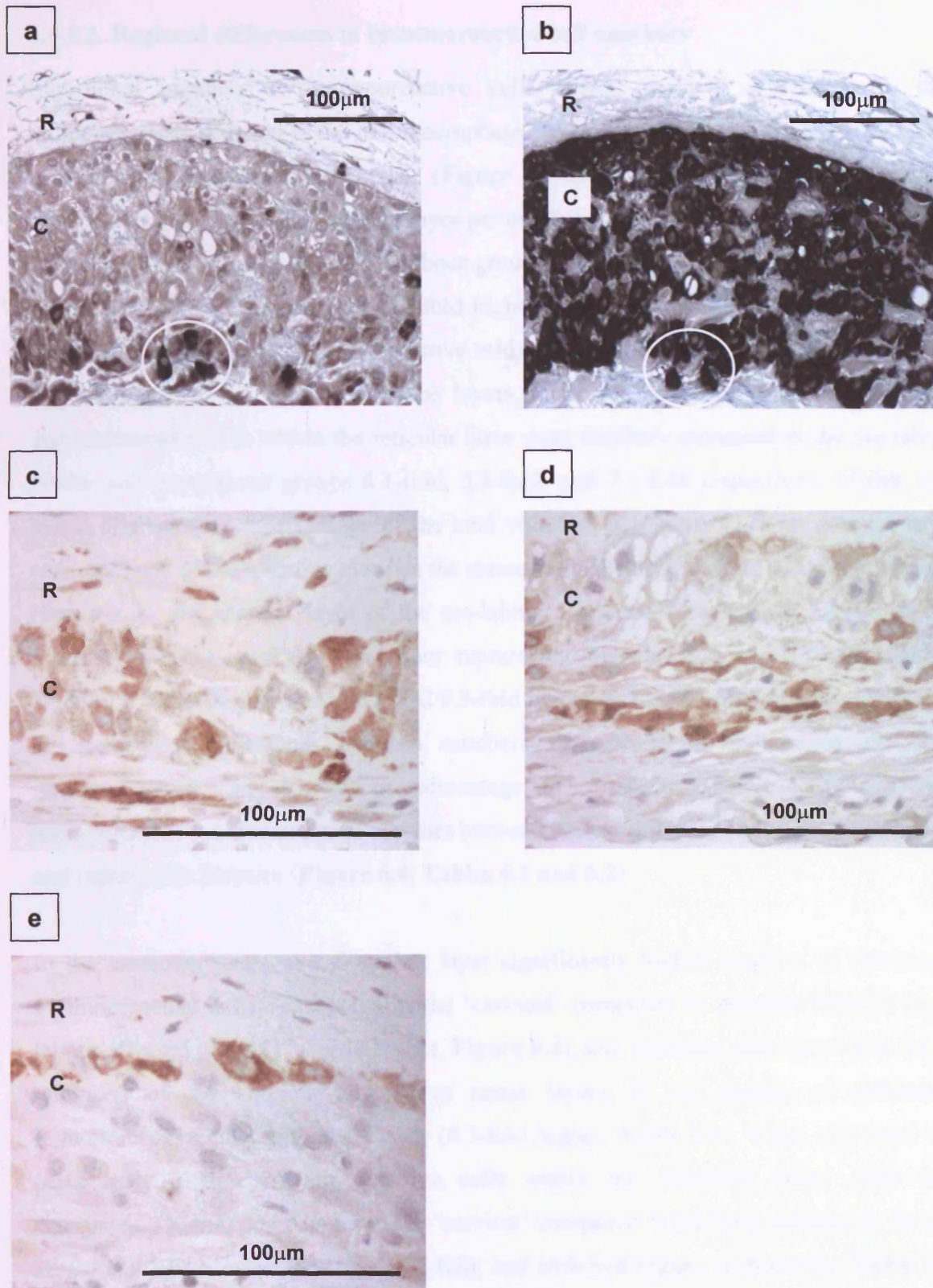


**Figure 6.3.** Immunohistochemistry for osteonectin using monoclonal antibody clone N50 on sections of fetal membrane. In midzone fetal membranes, cytotrophoblast layer immunoreactivity was less common, but where present was in the superficial cells within the layer (a). A serial section stained with a monoclonal antibody against cytokeratin confirms that the immunoreactive cells are cytotrophoblast and not decidua (b) (examples of co-expressing cells circled). A wide range of patterns of immunoreactivity was detected in the cytotrophoblast layer of fetal membranes exhibiting altered morphology (c-e). The reticular layer (R) and cytotrophoblast layer (C) are indicated.

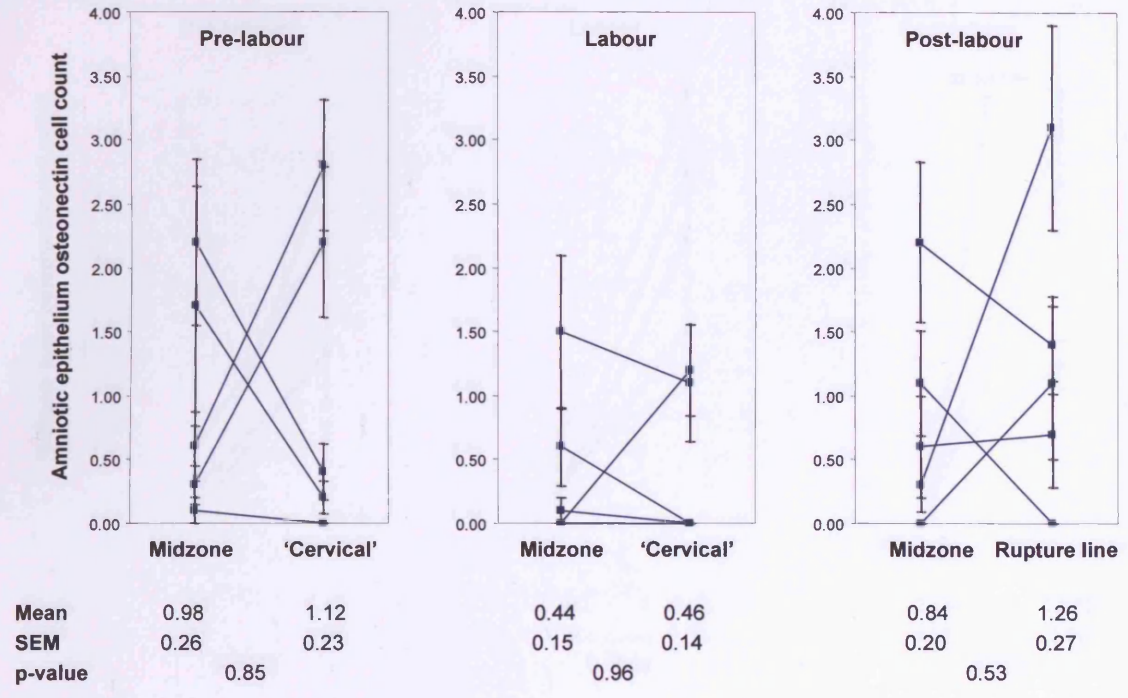
#### **6.4.1.2. Regional differences in immunoreactive cell numbers**

Significant numbers of immunoreactive cells, and/or regional differences in their incidence, were detected in the non-macrophage cells in the fibroblast and reticular layers, and in the cytotrophoblast cells. (Figure 6.4a-d). The numbers of osteonectin immunoreactive cells in the reticular layer per unit length of membrane was 6.5-fold higher in the 'cervical' biopsies in the pre-labour group, 10-fold higher in the 'cervical' biopsies in the labour affected group, and 12-fold higher in the rupture line biopsies in the post-labour group compared to their respective midzones. These changes were not affected by the thickness of the connective tissue layers, since the mean densities of osteonectin immunoreactive cells within the reticular layer were similarly increased in the pre-labour, labour and post-labour groups 6.1-fold, 5.3-fold, and 7.5-fold respectively (Table 6.1). When expressed as a percentage of the total vimentin positive population present, in the reticular layer of the midzone biopsies the means ranged from 3.51% to 4.03% (Table 6.2). However in the reticular layer of the pre-labour 'cervical' biopsies, the labour-affected 'cervical' biopsies, and the post-labour rupture line biopsies this was 7.1-fold higher at 24.85%, 8.2-fold higher at 33.00% and 9.3-fold higher at 33.00% respectively. There were no significant differences between numbers of osteonectin immunoreactive cells, immunoreactive cell density, or percentage of vimentin positive cells that were immunoreactive, in the midzone biopsies between patient groups, or between the 'cervical' and rupture line biopsies (Figure 6.4, Tables 6.1 and 6.2).

In the amniotic connective fibroblast layer significantly higher numbers of osteonectin immunoreactive cells were noted in the 'cervical' compared to midzone biopsies in the labour-affected group (12.7-fold higher, Figure 6.4), and similarly, after correction for the thickness of the amniotic connective tissue layers, in the density of osteonectin immunoreactive cells within the layer (8.3-fold higher, Table 6.1). When expressed as a percentage of the vimentin positive cells within the fibroblast layer, there were significantly higher percentages in the 'cervical' compared to midzone biopsies in the pre-labour and labour-affected groups (7.2-fold, and 16.6-fold higher, respectively, Table 6.2). The failure to detect a difference in the post-labour group appeared to be due to increased numbers of immunoreactive cells in the midzone biopsy from one patient (16.9%), bringing the average for the group to 4.46%, compared to 1.44% and 0.81% in the pre-labour and labour-affected groups (Table 6.2). Exclusion of the data for this patient

**a**

**Amniotic epithelium**



**b**

**Fibroblast layer**

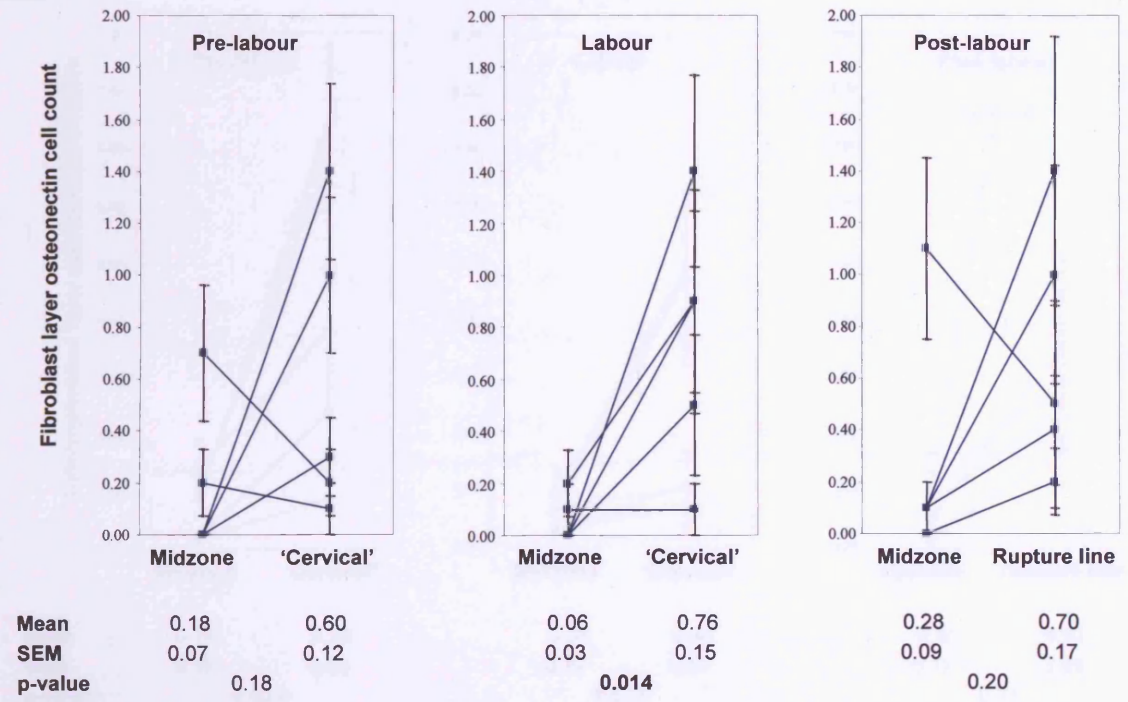
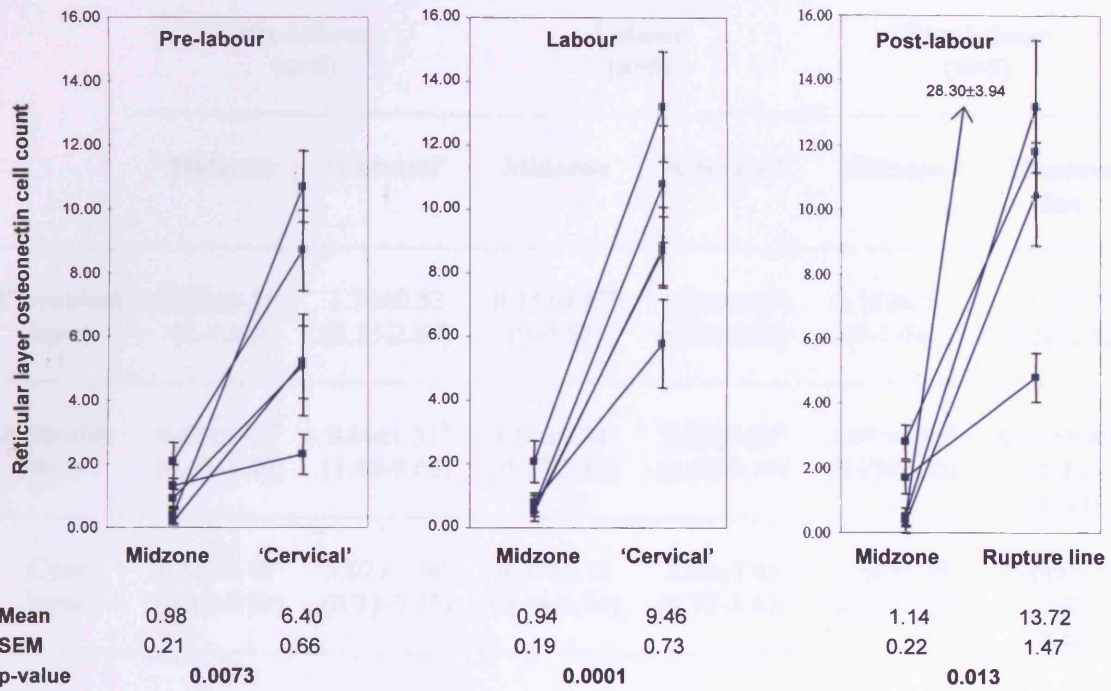


**Figure 6.4. a & b.** Numbers of osteonectin immunoreactive cells in the epithelial (a) and fibroblast (b) layers of the amnion, obtained prior to, during, and following labour at term. The graphs show the mean and SEM derived from 10 fields from each biopsy, with lines connecting the data points from individual patients. The mean and SEM (derived from the total 50 observations) for each group are shown beneath the graphs. Comparisons between biopsy sites and physiological group were using two way ANOVA and Scheffes test. Significant p-values are in bold. All comparisons between physiological groups were non-significant.

**c**

**Reticular layer**



**d**

**Cytotrophoblast layer**

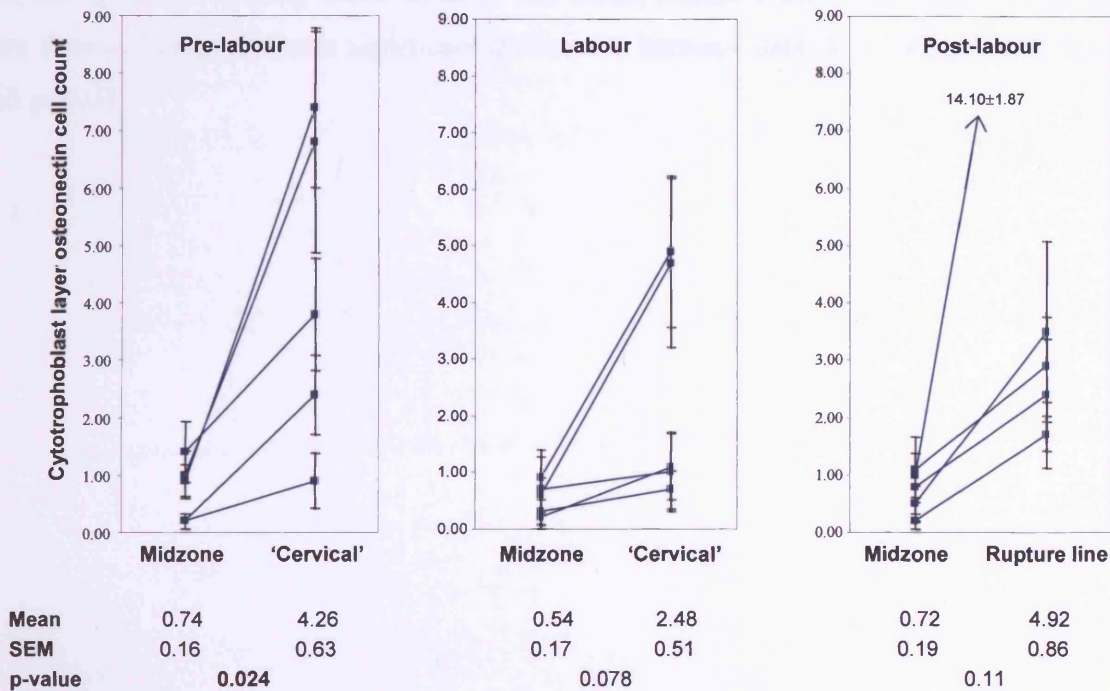


**Figure 6.4. c & d.** Numbers of osteonectin immunoreactive cells in the reticular (**c**) and cytotrophoblast (**d**) layers of the chorion, obtained prior to, during, and following labour at term. The graphs show the mean and SEM derived from 10 fields from each biopsy, with lines connecting the data points from individual patients. The mean and SEM (derived from the total 50 observations) for each group are shown beneath the graphs. Comparisons between biopsy sites and physiological group were using two way ANOVA and Scheffes test. Significant p-values are in bold. All comparisons between physiological groups were non-significant.

	Pre-labour (n=5)		Labour (n=5)		Post-labour (n=5)	
	Midzone	'Cervical'	Midzone	'Cervical'	Midzone	Rupture line
<b>Fibroblast layer</b>	0.27±0.17 (0-0.86)	1.34±0.53 (0.25-2.69)	0.15±0.11 <sup>a</sup> (0-0.57)	1.25±0.93 <sup>a</sup> (0.32-2.46)	0.73±0.51 (0-2.76)	1.13±0.27 (0.28-1.86)
<b>Reticular layer</b>	0.89±0.23 <sup>b</sup> (0.24-1.40)	5.44±1.31 <sup>b</sup> (1.48-9.65)	1.06±0.31 <sup>c</sup> (0.37-2.13)	5.64±0.25 <sup>c</sup> (4.68-6.10)	1.07±0.34 <sup>d</sup> (0.29-2.20)	8.05±1.89 <sup>d</sup> (4.22- 14.68)
<b>Cyto layer</b>	0.56±0.18 <sup>e</sup> (0.13-0.99)	5.02±1.74 <sup>e</sup> (0.71-9.45)	0.47±0.15 (0.18-0.94)	2.64±1.03 (0.72-5.63)	0.64±0.18 (0.21-1.12)	5.48±2.32 (2.05- 14.60)

**Table 6.1.** Density of osteonectin immunoreactive cells, expressed as cell number per  $10^{-8} \text{ m}^2$  cross-sectional area of the fetal membrane layer, in fetal membranes obtained prior to, during, and following labour at term. The mean, standard error, and range (in brackets) are shown. Letters indicate significant differences between data: a, e both  $p < 0.05$ ; b, c, d all  $p < 0.01$ .

	Pre-labour (n=5)		Labour (n=5)		Post-labour (n=5)	
	Midzone	'Cervical'	Midzone	'Cervical'	Midzone	Rupture line
<b>Fibroblast layer</b>	1.44±0.90 <sup>a</sup> (0-4.05)	10.36±3.49 <sup>a</sup> (1.22-16.67)	0.81±0.55 <sup>b</sup> (0-2.74)	13.43±3.89 <sup>b</sup> (3.23- 23.08)	4.46±3.14 (0-16.92)	8.32±1.88 (3.17- 14.49)
<b>Reticular layer</b>	3.51±1.10 <sup>c</sup> (0.81-6.56)	24.85±4.60 <sup>c</sup> (11.66- 38.91)	4.03±1.60 <sup>d</sup> (2.00- 10.40)	33.01±6.84 <sup>d</sup> (17.90- 50.00)	3.56±1.20 <sup>e</sup> (1.24-7.57)	33.02±5.42 <sup>e</sup> (12.66- 41.90)
<b>Cyto layer</b>	1.14±0.38 <sup>f</sup> (0-0.63)	10.10±3.61 <sup>f</sup> (0.52-10.26)	0.94±0.25 (0.43-1.67)	6.29±2.44 (1.32- 12.70)	1.38±0.36 <sup>g</sup> (0.50-2.38)	11.74±4.25 <sup>g</sup> (4.87- 28.03)

**Table 6.2.** Percentage of vimentin positive cells possessing osteonectin in the fibroblast and reticular layers, and of the cytokeratin positive cells possessing osteonectin in the cytotrophoblast layer, in fetal membranes obtained prior to, during, and following labour at term. The mean, standard error, and range (in brackets) are shown. Letters indicate significant differences between data: a, b, f, g all  $p < 0.05$ ; c, d, e all  $p < 0.01$ .

brings the average for the group to 1.34%, significantly lower than the rupture line biopsies, 8.32% ( $p=0.015$ ).

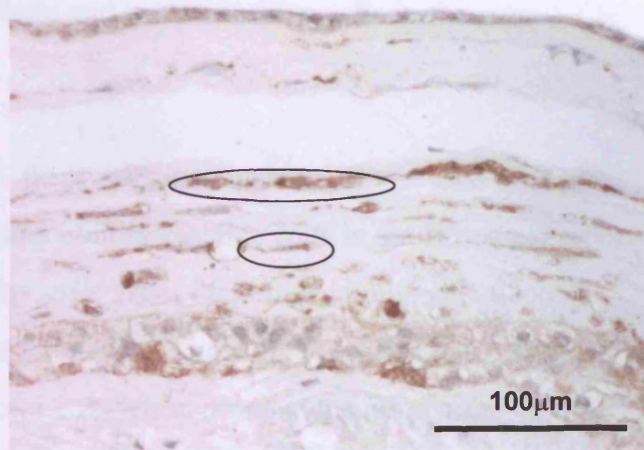
In the cytotrophoblast layer there were 5.8-fold, 4.6-fold and 6.8-fold higher numbers of immunoreactive cells in the 'cervical' biopsies in the pre-labour, labour-affected, and in the post-labour rupture line biopsies compared to their respective midzones, although this only achieved significance in the former group (Figure 6.4). The density of immunoreactive cells, correcting for the thickness of the cytotrophoblast layer, was similarly significantly higher in the pre-labour 'cervical' biopsies compared to the midzone (9.0-fold higher, Table 6.1). The percentage of cytotrophoblast cells immunoreactive for osteonectin was significantly higher in the pre-labour 'cervical' and post-labour rupture line biopsies, compared to their respective midzone biopsies (8.8-fold, and 8.5-fold respectively, Table 6.2).

When data from all biopsies were combined there was a significant positive correlation between the absolute numbers of osteonectin positive cells in the reticular layer and its thickness (Spearman  $r=0.753$ ,  $p<0.0001$ ), combined thickness of the amniotic and chorionic connective tissue layers (Spearman  $r=0.798$ ,  $p<0.0001$ ), the FMMI (Spearman  $r=0.873$ ,  $p<0.0001$ ), and a negative correlation with the total thickness of the cellular layers (Spearman  $r=-0.713$ ,  $p=0.0001$ ). There was also a significant positive correlation between the number of osteonectin positive cells in the fibroblast layer and in the reticular layer (Spearman  $r=0.749$ ,  $p<0.0001$ ). There were also significant correlations between the number of immunoreactive cells in the cytotrophoblast layer and the number of immunoreactive cells in the reticular layer (Spearman  $r=0.591$ ,  $p=0.0014$ ), and inverse correlation with the total thickness of the cellular layers (Spearman  $r=-0.691$ ,  $p=0.0005$ ).

#### **6.4.1.3. Relationship to $\alpha$ -SMA expression**

Serial sections demonstrated that the majority of immunoreactive osteonectin cells within the reticular layer were also  $\alpha$ -sma immunoreactive. However not all  $\alpha$ -sma immunoreactive cells contained immunoreactive osteonectin (Figure 6.5). For example, in the reticular layer of the post-labour rupture line biopsies  $57.7\pm 11.4\%$  (mean $\pm$ SEM) of  $\alpha$ -sma positive cells were immunoreactive for osteonectin. However, in midzone biopsies, where the numbers of osteonectin immunoreactive positive cells in the reticular layers were low, these exceeded the numbers of  $\alpha$ -sma immunoreactive cells. When the data from

a



b

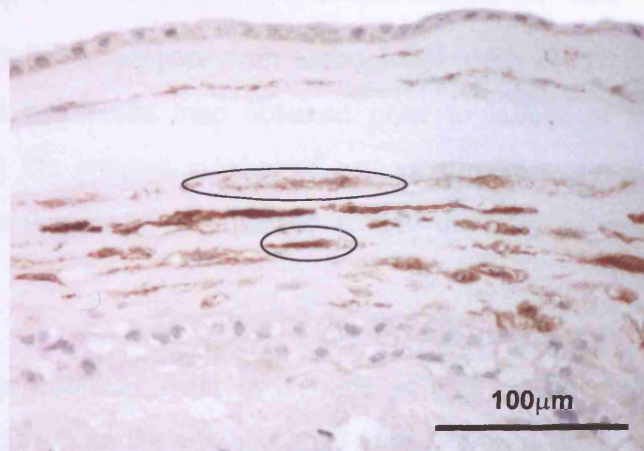


**Figure 6.5.** Immunohistochemistry for osteonectin (a) and  $\alpha$ -sma (b) on serial sections of fetal membrane. The majority of the osteonectin positive cells within the reticular layer are also  $\alpha$ -sma positive. Examples of co-expressing cells are circled. The relationship between osteonectin and  $\alpha$ -sma within the fibroblast layer is less clear.

all biopsies was combined there was a significant positive correlation between the absolute numbers of osteonectin and  $\alpha$ -sma positive cells in the reticular layer (Spearman  $r=0.813$ ,  $p<0.0001$ ).

On serial sections there was no apparent direct and consistent relationship between osteonectin and  $\alpha$ -sma immunoreactive cells in the fibroblast layer. Within 'cervical' and rupture line biopsies cells were identified immunoreactive for osteonectin only,  $\alpha$ -sma only, or both osteonectin and  $\alpha$ -sma. However when data from all biopsies was combined, there was a significant correlation between the numbers of osteonectin and  $\alpha$ -sma positive cells in the fibroblast layer (Spearman  $r=0.632$ ,  $p=0.0007$ ).

#### **6.4.1.4. Osteonectin immunoreactivity on a fetal membrane map**

Osteonectin immunohistochemistry with monoclonal antibody N50 was carried out on a representative fetal membrane map obtained prior to labour at term. Fetal membrane biopsies containing the greatest number of osteonectin immunoreactive cells within the reticular layer were demonstrated clustered around the internal os of the cervix (Figure 6.6).

Within the biopsies obtained from this single patient ( $n=28$ ), numbers of osteonectin immunoreactive cells within the reticular layer correlated positively with the reticular layer thickness (Spearman  $r=0.693$ ,  $p=0.0003$ ), total connective tissue thickness (Spearman  $r=0.736$ ,  $p=0.001$ ), and reticular layer  $\alpha$ -sma cell count (Spearman  $r=0.676$ ,  $p=0.0004$ ), and inversely with the total cellular thickness (Spearman  $r=-0.503$ ,  $p=0.0089$ ). The correspondence of fetal membrane morphology parameters,  $\alpha$ -sma cell count, and osteonectin immunoreactivity along the longitudinal axis of a representative map is demonstrated in Figure 6.7.

#### **6.4.1.5. Relationship to tenascin-C expression**

Fetal membrane biopsies with the most osteonectin immunoreactive cells had the greatest proportion of area immunoreactive for tenascin-C in the connective tissue layers of both the amnion and chorion (Spearman  $r=0.613$ ,  $p=0.001$ ; Spearman  $r=0.751$ ,  $p<0.0001$  respectively). However examination of serial sections demonstrated no direct relationship between the osteonectin immunoreactive cells and the intensity of tenascin-C

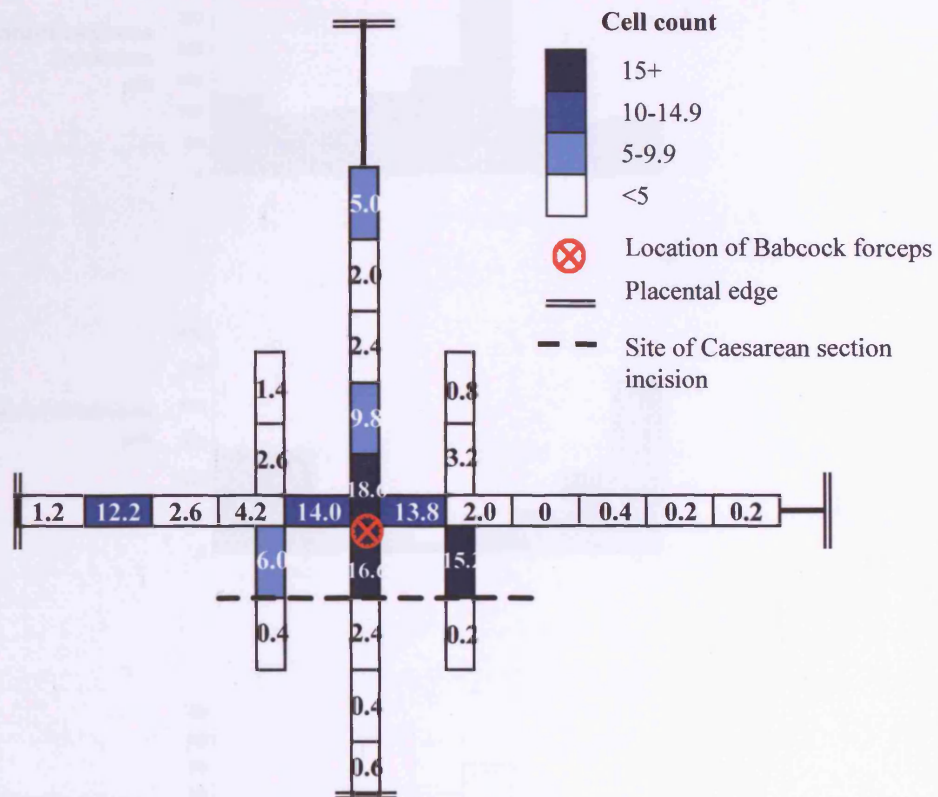
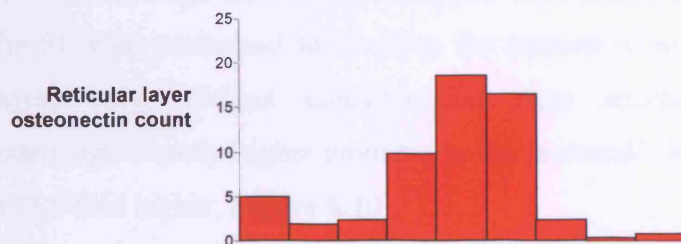
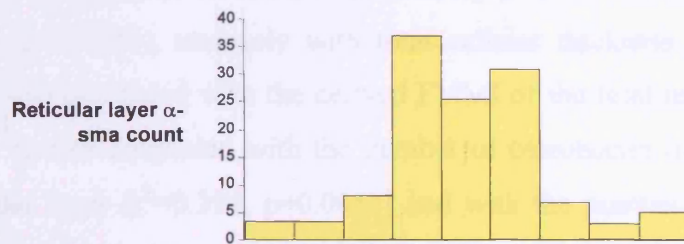
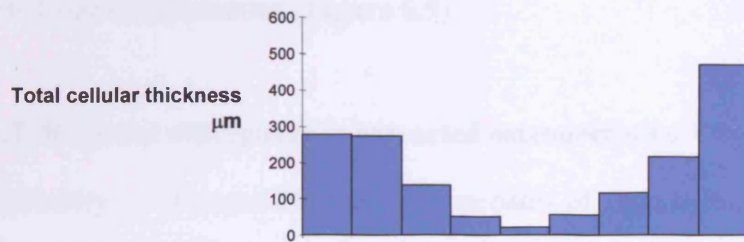
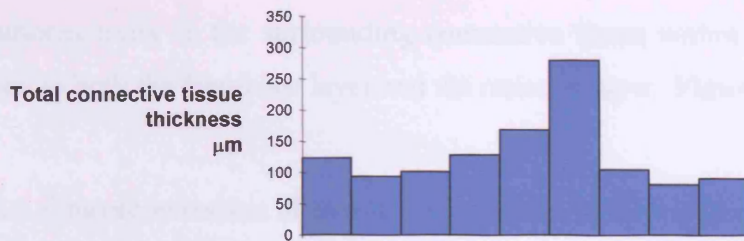


**Figure 6.6.** A representative fetal membrane map, obtained prior to labour at term, with measured 3cm biopsies radiating out from the internal os of the cervix to the placental edge. The biopsies are shaded to demonstrate the distribution of the numbers of osteonectin immunoreactive cells in the reticular layer (per computer screen width), with the biopsies with the greatest immunoreactivity centred upon the internal os of the cervix.



↑  
Internal os of  
the cervix

**Figure 6.7.** Graphs demonstrating fetal membrane morphology, reticular layer  $\alpha$ -sma count, and reticular layer osteonectin immunoreactive cell count in biopsies taken along the longitudinal axis of a fetal membrane map. (As in Figure 6.6). Maximal numbers of osteonectin immunoreactive cells are demonstrated in biopsies with the highest  $\alpha$ -sma cell count, greatest connective tissue thickness, and least cellular thickness. These biopsies cluster around in the internal os of the cervix.

immunoreactivity in the surrounding connective tissue within an individual biopsy. This applied to both the fibroblast layer and the reticular layer (Figure 6.8).

#### **6.4.1.6. Characterisation of osteonectin protein in fetal membranes**

Western blotting of fetal membrane extracts with monoclonal antibody N50 and polyclonal antiserum BON-I demonstrated a single band at approximately 40kDa, consistent with the reported size of osteonectin (Figure 6.9).

#### **6.4.1.7. Regional differences in extracted osteonectin by Western blotting**

Densitometry of Western blots of homogenates of fetal membranes obtained during and following labour (n=9) demonstrated significantly higher amounts of osteonectin protein in the 'cervical'/rupture line compared to the midzone samples (2.9-fold higher, Figure 6.10). The densitometry value correlated significantly with the total connective tissue thickness ( $r^2=0.403$ ,  $p=0.0046$ ), inversely with total cellular thickness ( $r^2=0.381$ ,  $p=0.0063$ ), and therefore also correlated with the derived FMMI of the fetal membrane biopsies ( $r^2=0.50$ ,  $p=0.001$ ). It also correlated with the number of osteonectin immunoreactive cells within the reticular layer ( $r^2=0.394$ ,  $p=0.0053$ ) and with the number of  $\alpha$ -sma immunoreactive cells within the reticular layer ( $r^2=0.25$ ,  $p=0.037$ ).

Western blots of homogenates of 'superscraped' fetal membranes obtained prior to labour at term (n=5) were performed to examine the amount of osteonectin in the connective tissue layers only, without contamination from attached decidua. Densitometry demonstrated significantly higher amounts in the 'cervical' fetal membranes compared to midzones (2.5-fold higher, Figure 6.10).

### **6.4.2. Osteonectin mRNA expression**

#### **6.4.2.1. Localisation and distribution of mRNA positive cells**

Osteonectin mRNA was detected in significant numbers of cells in both the reticular and fibroblast layers, and in smaller numbers of cells in the cytotrophoblast layer (Figure 6.11a-h).

As a group, the 'cervical' biopsies exhibiting the highest numbers of osteonectin immunoreactive cells in the reticular and fibroblast layers also exhibited the higher

**ORIENTATION  
OF PAGE IS AS  
PER THE  
ORIGINAL IN  
THE BOOK.**

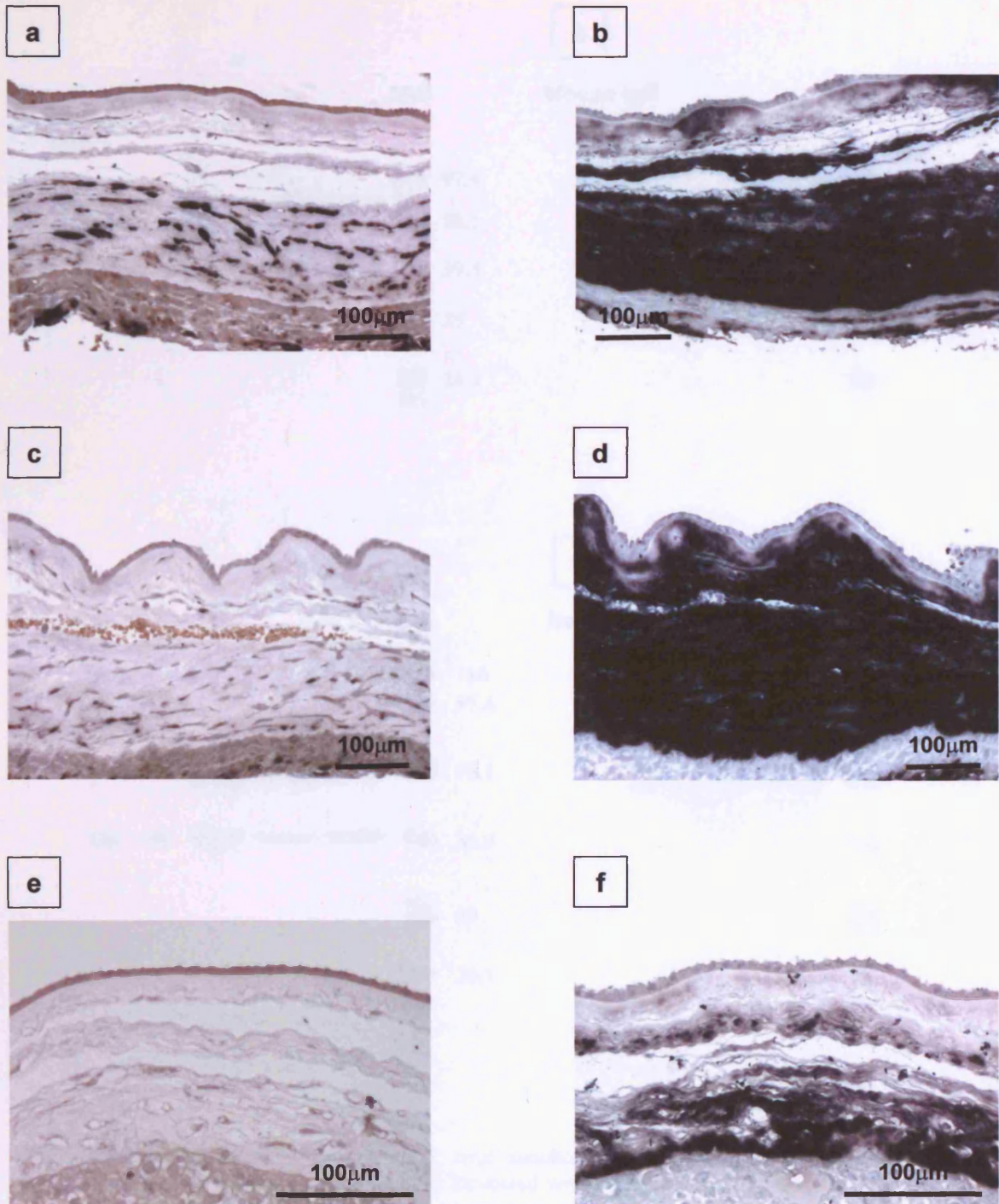


**Figure 6.8.** Immunohistochemistry for osteonectin (a, c & e) and tenascin-C (b, d, & f) on sections of fetal membrane. Large numbers of osteonectin immunoreactive cells are present within the reticular layer in a fetal membrane biopsy exhibiting extreme altered morphology (a), corresponding with intense tenascin-C immunoreactivity on an adjacent section of the same biopsy in the same layer (b). Yet elsewhere within the same membrane biopsy an area of fetal membrane with few osteonectin immunoreactive cells within the reticular layer is observed (c), although on an adjacent section of the same biopsy intense tenascin-C immunoreactivity is still present (d). Rare osteonectin immunoreactive cells are present within the reticular layer of a midzone fetal membrane biopsy (e), although an adjacent section of the same biopsy exhibits moderate tenascin-C immunoreactivity (f).

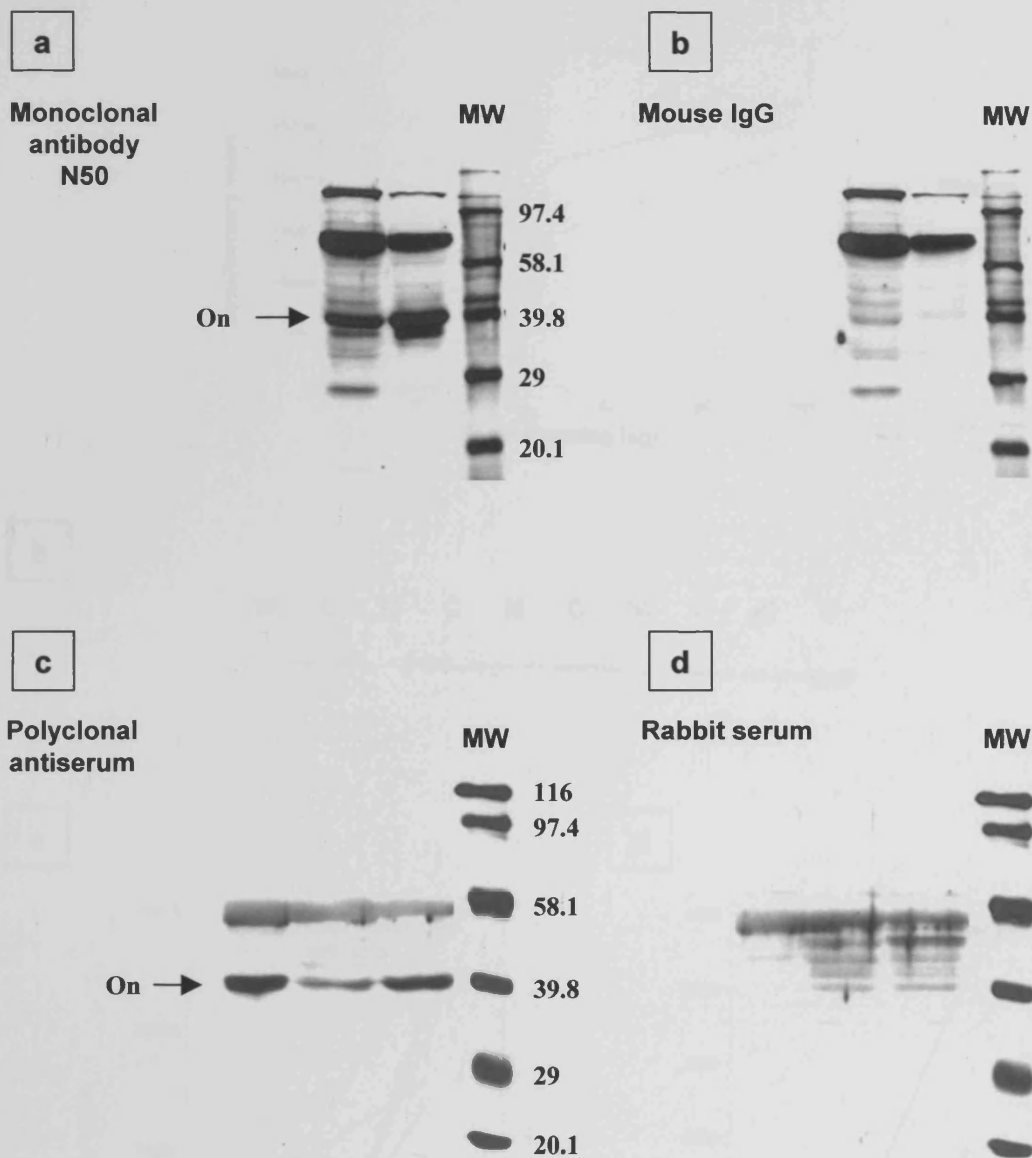


**Figure 6.9.** Western blots of 'superscraped' fetal membrane biopsies. (a) Incubated with osteonectin monoclonal antibody N50, and paired blot (b) incubated with a matched concentration of mouse IgG. (c) Incubated with polyclonal antiserum against osteonectin, and paired blot (d) incubated with a matched concentration of rabbit serum. Bands specific for osteonectin (On) and molecular weight marker lanes (MW) are indicated.

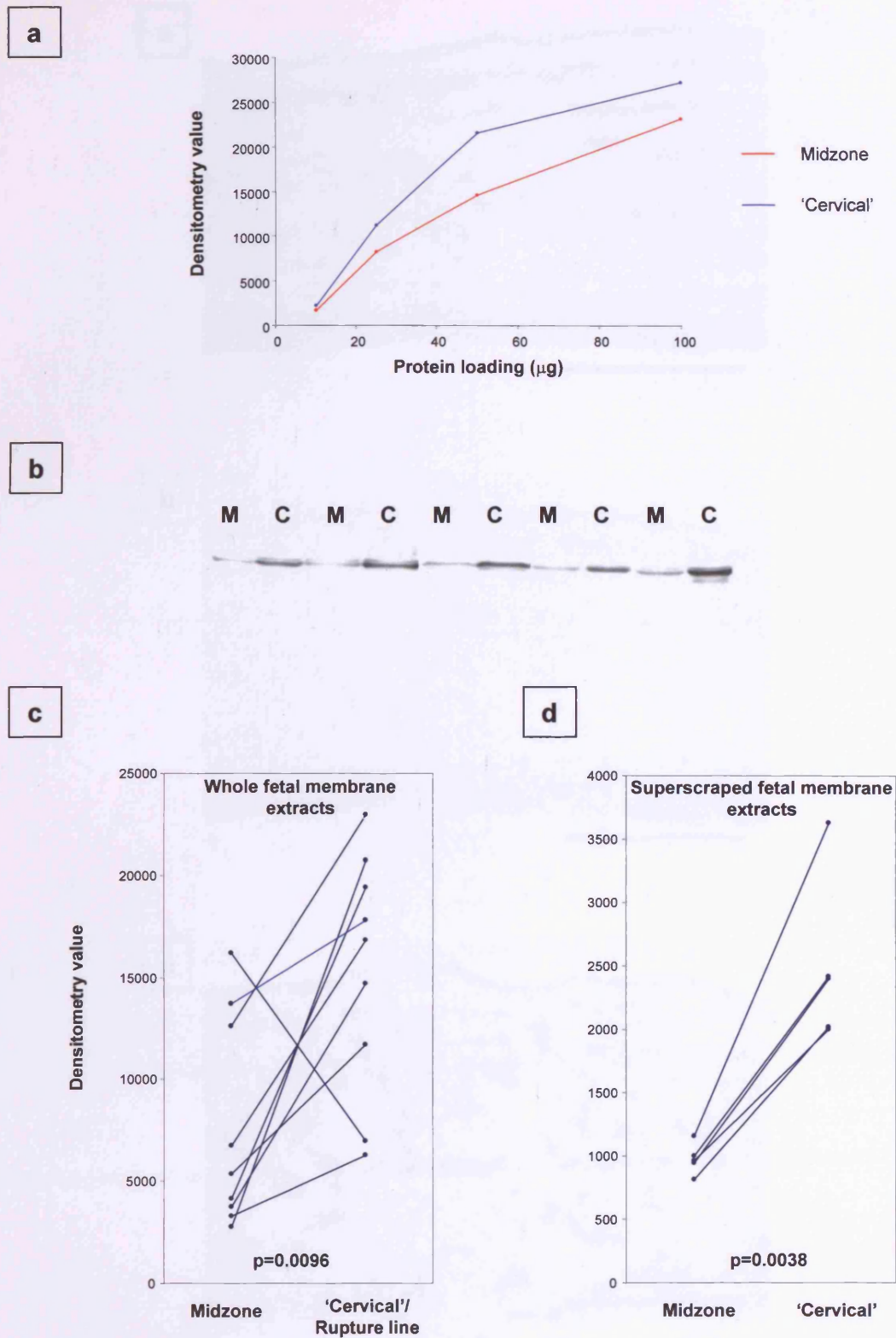


**Figure 6.10.** Western blotting of fetal membrane extracts with osteonectin (monoclonal antibody N50). The protein loading was titred using a pair of 'cervical' and midzone protein extracts, to determine the optimal protein loading. Protein loading of 50µg is in the linear part of the curve obtained, and was used for quantitative experiments (a). A Western blot of 5 pairs of 'superscraped' midzone (M) and 'cervical' (C) fetal membranes is shown (b). Non-specific bands have been cropped from this image. Densitometry values of immunoblotted osteonectin from whole (c) and 'superscraped' (d) fetal membrane homogenates. Lines join the data from paired membranes from an individual patient. Comparisons between data was made using paired t-test.

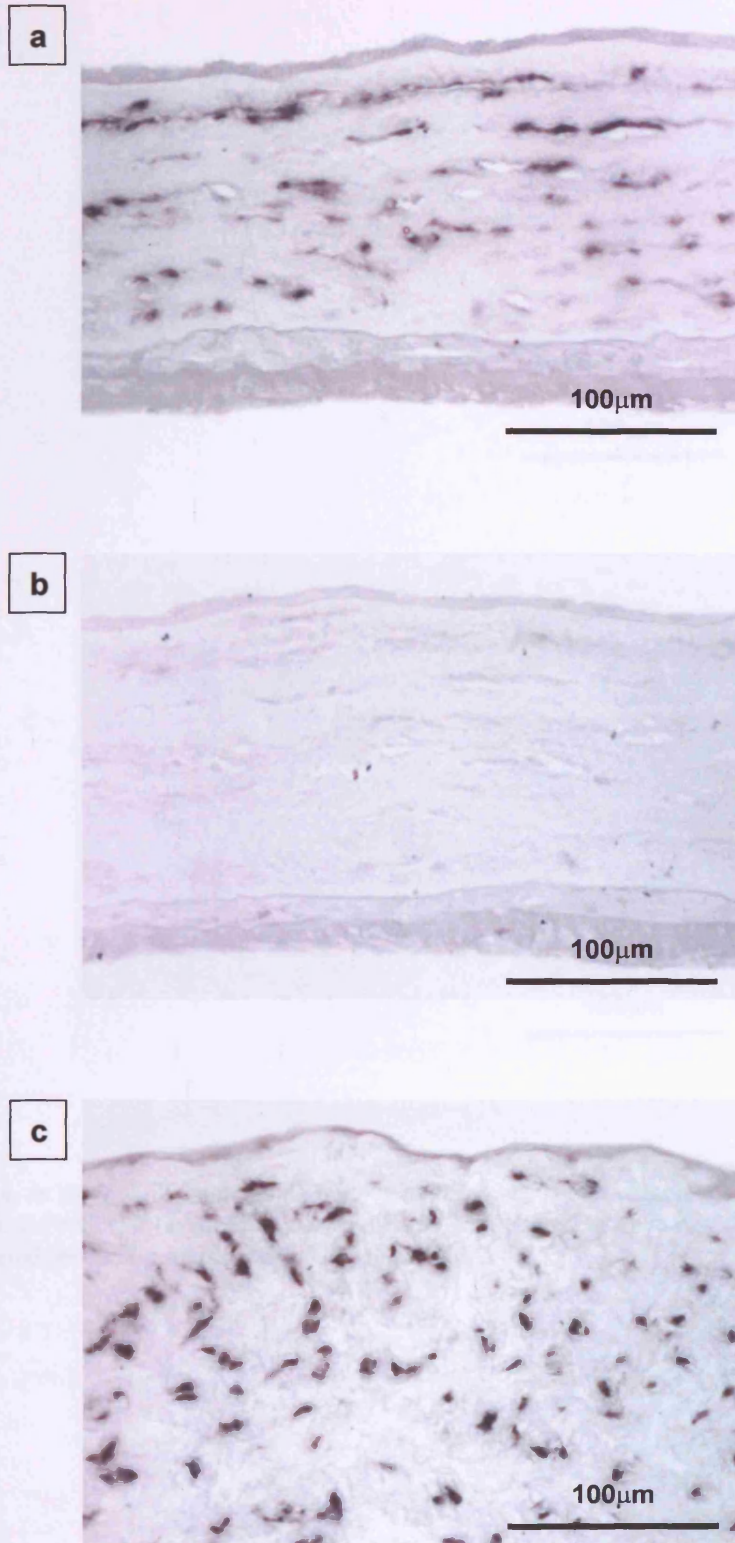
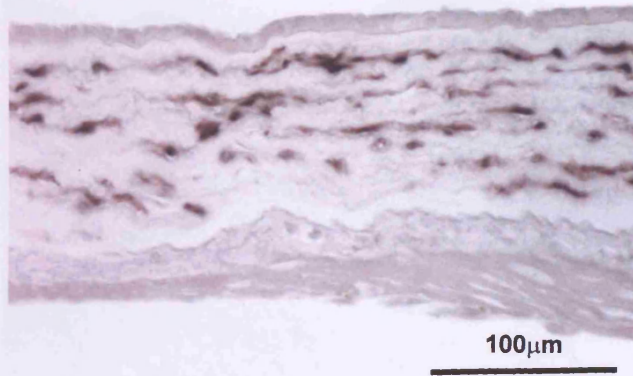


**Figure 6.11a-c.** *In situ* hybridisation using a probe against osteonectin. mRNA positive cells are detected in the fibroblast and reticular layer of a fetal membrane with altered morphology (a). No positive cells are detected in a serial section incubated with the sense control probe (b). Numerous positive cells are detected in the mesenchyme of the umbilical cord, used as a positive control (c).

d



e

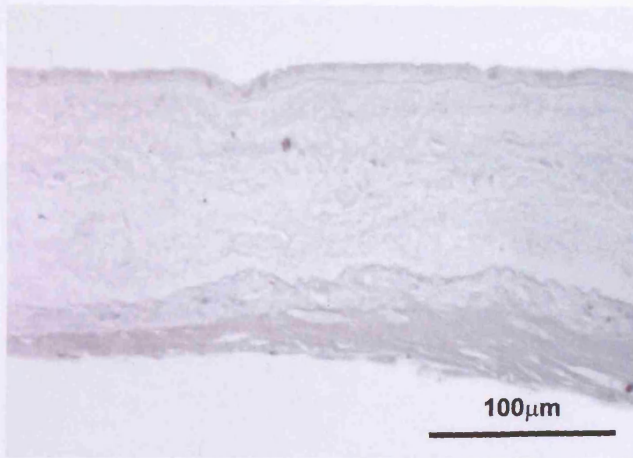


**Figure 6.11d&e.** *In situ* hybridisation using a probe against osteonectin demonstrates mRNA positive cells in the fibroblast and reticular layers of a fetal membrane with altered morphology (a). No positive cells are observed in a serial section pre-treated with RNase (b).

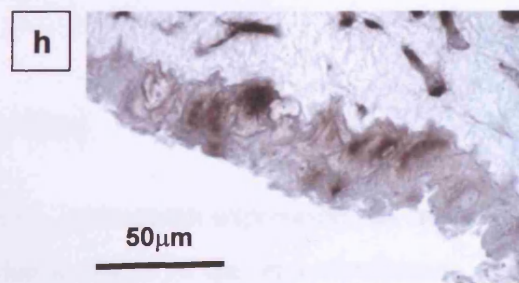
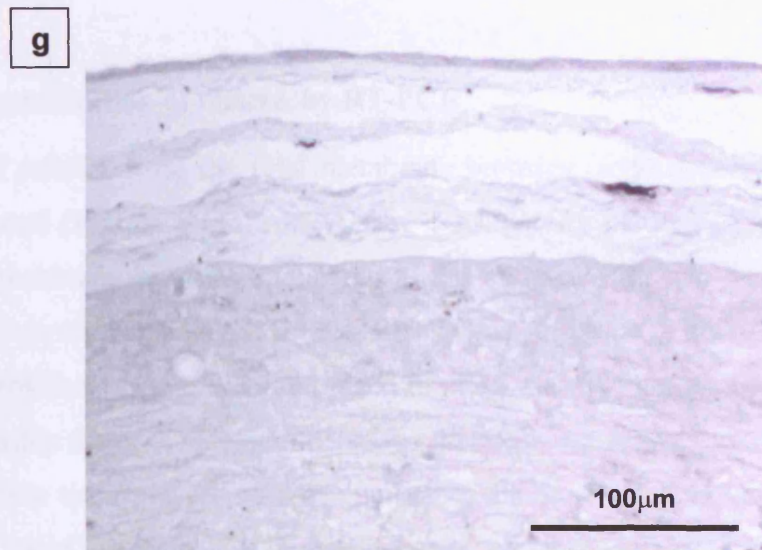
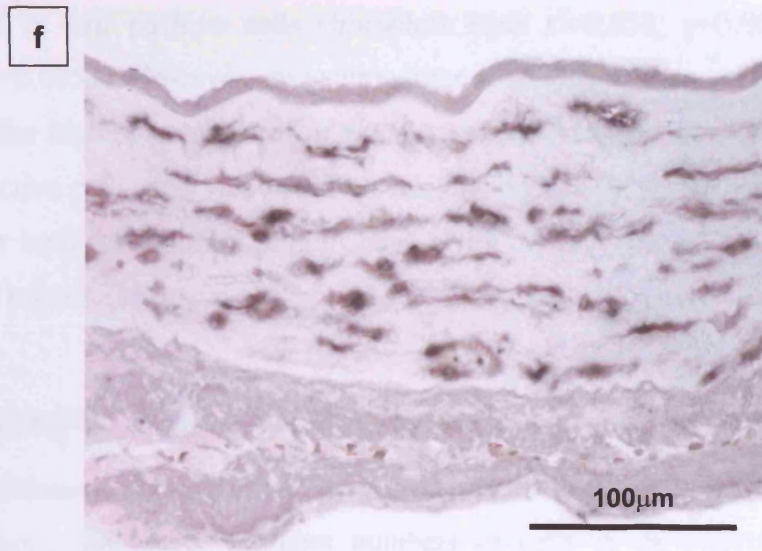


**Figure 6.11f-h.** *In situ* hybridisation using a probe against osteonectin demonstrates numerous mRNA positive cells in the fibroblast and reticular layers of a fetal membrane with altered morphology (f), and rare cells only in a midzone fetal membrane (g). mRNA positive cells were also detected in cytotrophoblast cells (h).

numbers of *in situ* positive cells (fibroblast layer  $r^2=0.658$ ,  $p=0.0044$ ; reticular layer  $r^2=0.645$ ,  $p=0.0051$ ). However, on examination of serial sections, areas of fetal membrane containing the highest numbers of *in situ* positive cells tended to contain low numbers of immunoreactive cells, and vice versa. Occasional areas of fetal membrane contained cells positive for both mRNA and protein, and a few cells were detected that co-expressed mRNA and protein (Figure 6.12).

#### **6.4.2.2. Regional differences in mRNA expression**

*In situ* hybridisation was performed on paired midzone and 'cervical' biopsies from 5 pre-labour patients. Significantly higher numbers of cells in the reticular layer expressed osteonectin mRNA in the 'cervical' biopsies compared to the midzone biopsies (10.7-fold higher, Figure 6.13).

#### **6.4.2.3. Quantification of mRNA by RT-PCR**

RT-PCR of mRNA from the fetal membrane biopsies ( $n=5$ ) demonstrated a single 325 base pair band (Figure 6.14). Analysis by densitometry of the bands obtained from the 'cervical' membrane biopsies, compared to the midzone biopsies, gave a non-significant difference ('cervical' bands 21% more intense than midzone, Figure 6.15). The different tissue composition of 'cervical' compared to midzone membrane biopsies was considered to be a possible factor. The experiment was therefore repeated using RNA extracted from the connective tissue layers of the membranes ( $n=5$ ). A slightly greater, but still non-significant trend towards more intense bands obtained by RT-PCR of the 'cervical' biopsies compared to the midzones was observed ('cervical' bands 42% more intense than midzone, Figure 6.15).

### **6.5. Discussion**

In this chapter, osteonectin expression has been demonstrated in mesenchymal cells in the connective tissue layers of the fetal membranes, and within cytotrophoblast cells, restricted to specific anatomical regions of membrane. It was particularly expressed by cells within the reticular layer of the chorion, where 25-33% of vimentin positive cells in rupture line and 'cervical' fetal membrane biopsies were immunoreactive for osteonectin, compared to 3-4% in midzone membrane biopsies. More mesenchymal cells within the fibroblast layer

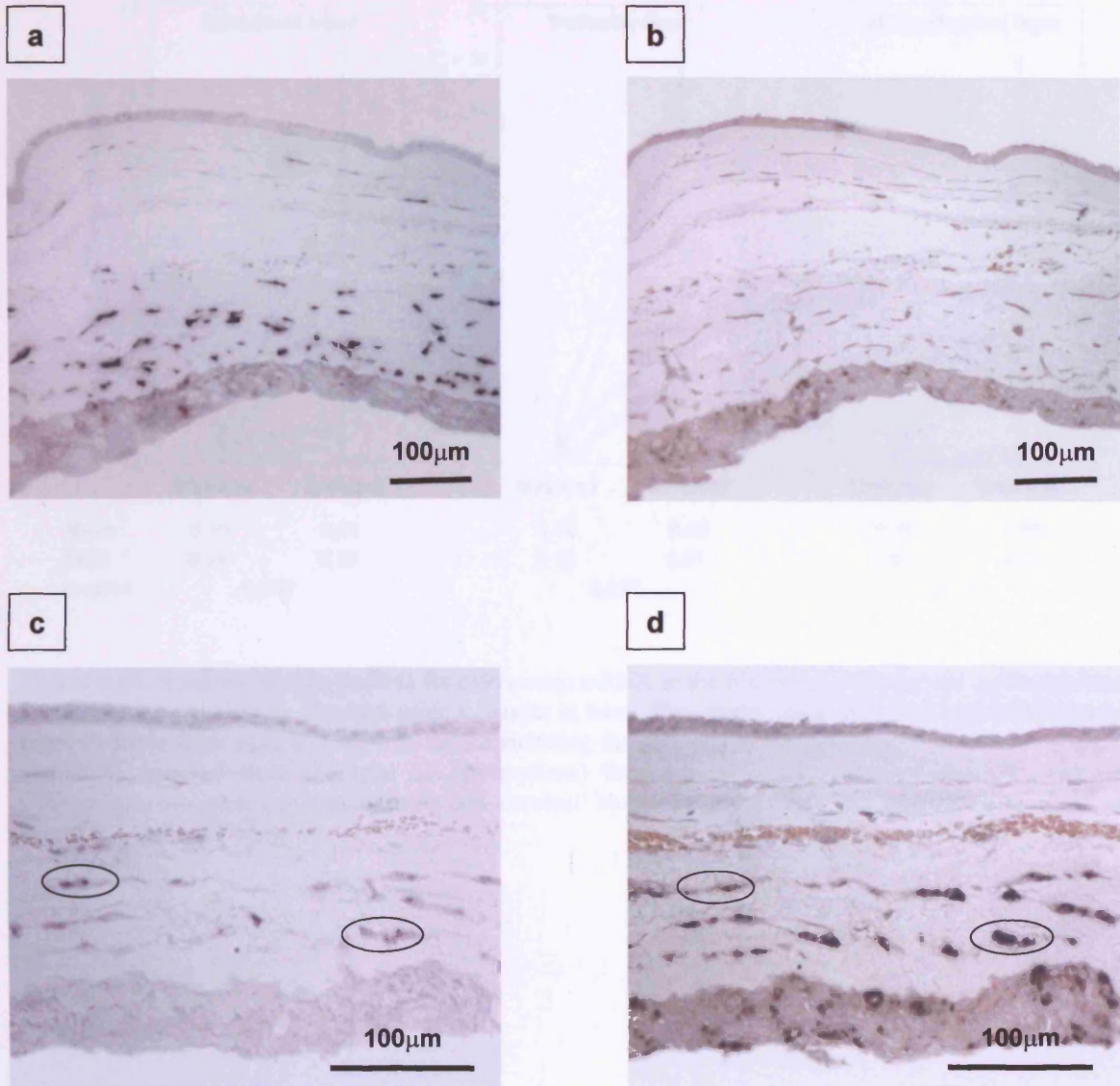


**Figure 6.12.** *In situ* hybridisation using a probe to osteonectin (**a&c**) and immunohistochemistry using a monoclonal antibody against osteonectin (**b&d**). Examination of serial sections demonstrates large numbers of mRNA positive cells in the reticular layer (**a**) and low numbers of immunoreactive cells (**b**), and *vice versa* (**c&d**). A few cells co-express mRNA and protein (circled).

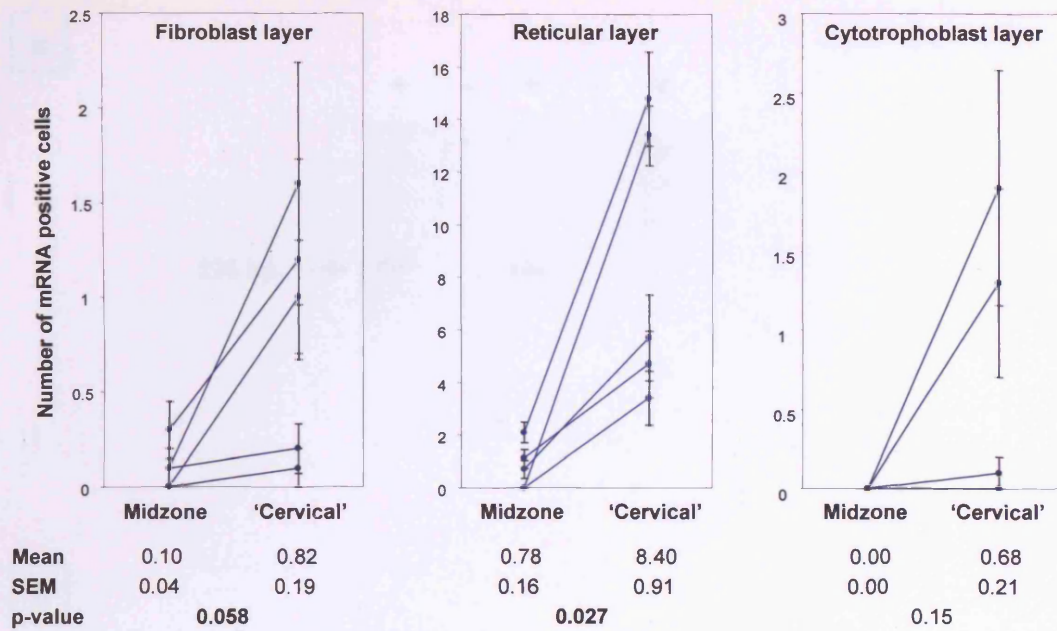
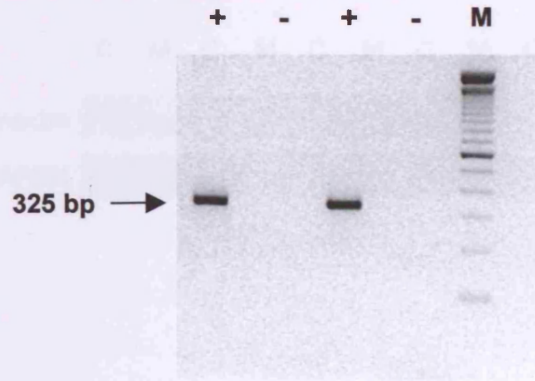


**Figure 6.13.** Numbers of cells positive for osteonectin mRNA in the fibroblast, reticular and cytotrophoblast layers of fetal membranes obtained prior to labour at term. The graphs show the mean and SEM derived from 10 fields from each biopsy, with lines connecting the data points from individual patients. The mean and SEM (derived from the total 50 observations) for each group are shown beneath the graphs. Comparisons are made between midzone and 'cervical' biopsies using paired t-test. Significant p-values are shown in bold.

**a**



**b**

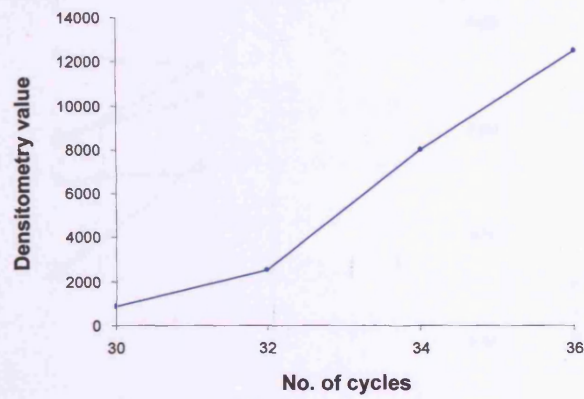
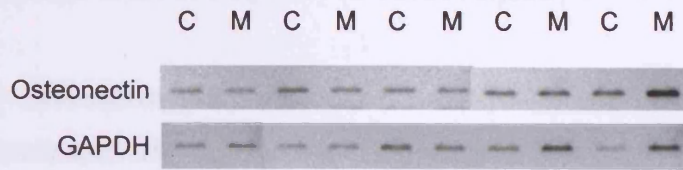
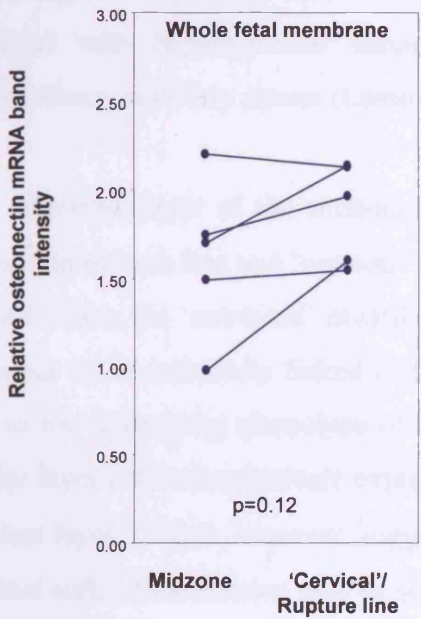


**Figure 6.14.** RT-PCR of fetal membrane RNA using primers to osteonectin amplifies a 325 base pair band. No band is apparent in reactions performed in the absence (-) of reverse transcriptase (a). 100 base pair ladder is in lane M. (b) Titration of the number of cycles of amplification carried out. Subsequent experiments were performed using 34 cycles, on the linear part of the titration curve.

**a**



**b**



**c**

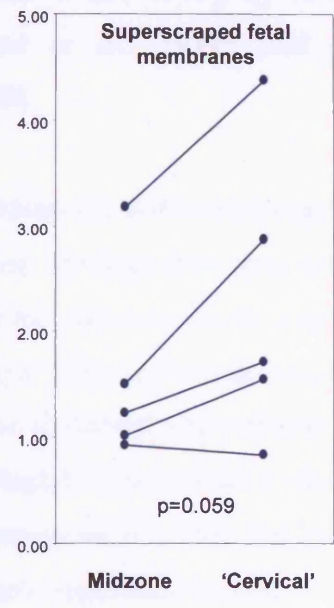


**Figure 6.15.** RT-PCR on pairs of 'superscraped' fetal membrane RNA samples using primers against osteonectin (a). (Samples all run on a single gel, but on several rows of lanes, therefore images cut and pasted to align bands from the same RNA sample). Densitometry values of osteonectin RT-PCR bands, relative to GAPDH, using RNA extracted from whole fetal membrane (b), and from 'superscraped' fetal membrane (c). Lines connect data from paired samples from a single patient.

of the amnion were immunoreactive in biopsies from the same sites, compared to midzone biopsies, although at lower frequency (8-13% compared to 3-4%).

Osteonectin immunoreactivity was not demonstrated within the macrophage population of the fetal membranes. The distribution of osteonectin immunoreactive cells corresponded to the distribution of  $\alpha$ -sma immunoreactive cells (Chapter 3). Within the reticular layer, the osteonectin immunoreactive cells appeared to represent a subgroup of the myofibroblasts. The majority of osteonectin immunoreactive cells within the reticular layer also co-expressed  $\alpha$ -sma. Osteonectin expression has previously been demonstrated in  $\alpha$ -sma positive myofibroblasts in liver fibrosis (Blazejewski *et al.*, 1997), by myofibroblasts associated with hepatocellular carcinoma (Le Bail *et al.*, 1999), and periductular myofibroblasts in biliary atresia (Lamireau *et al.*, 1999).

In the fibroblast layer of the amnion, osteonectin expression and  $\alpha$ -sma expression were increased in rupture line and 'cervical' fetal membranes, although they were not always co-localised. Thus the 'activated' myofibroblast phenotype and osteonectin expression does not appear to be intimately linked in cells of this layer. This differential expression may relate to the underlying phenotype of the cells of the fibroblast and reticular layers. The reticular layer cells constitutively express desmin (Chapter 3) in contrast to the cells of the fibroblast layer. It does, however, suggest that the expression of  $\alpha$ -sma and osteonectin by fibroblast cells of the amnion may be subject to the same regulatory factors.

Osteonectin expression was also detected within cytotrophoblast cells. In the midzone biopsies these cells were concentrated at the maternal-fetal interface. In the 'cervical' and rupture line biopsies 6-9 fold higher percentages, and a higher absolute number of cells of the cytotrophoblast layer expressed osteonectin. This localisation and differential expression may reflect differential attachment of the cytotrophoblast layer to the underlying decidua, and/or differential breakdown of the maternal-fetal interface.

Using both polyclonal and monoclonal antibodies, no osteonectin was detected in the extracellular matrix of the fetal membranes. This is consistent with previous reports of almost exclusive intracellular localisation (Porter *et al.*, 1995), although osteonectin was originally described as a protein secreted by a basement membrane tumour (Dziadek *et al.*, 1986), and has been described in the extracellular matrix surrounding decidual cells (Wewer *et al.*, 1988). This latter finding was confirmed in this study in first trimester

decidua. Recently the immunoreactive-negative basement membrane underneath the lens epithelium as been described as a 'virtual repository' for osteonectin, as revealed by immunoblotting of extracts (Yan & Sage, 1999). The failure to demonstrate extracellular osteonectin has been suggested to be due to extracellular degradation of osteonectin (Reed & Sage, 1996). Osteonectin is readily degraded into peptides, which have been demonstrated to have functional significance e.g. angiogenesis, and higher affinity collagen binding (Lane & Sage, 1994).

The regional difference in protein results was mirrored by a regional difference in osteonectin mRNA expression as demonstrated by *in situ* hybridisation. Significantly higher numbers of *in situ* positive cells in the fibroblast and reticular layers were noted in the 'cervical' fetal membrane biopsies compared to midzone biopsies. Although the biopsies containing highest numbers of immunoreactive cells also contained the highest numbers of *in situ* positive cells, serial sections demonstrated that mRNA and protein were rarely co-expressed. This suggests a transient increase in osteonectin transcription within the cells. There was, however, a failure to demonstrate a regional difference in mRNA expression by RT-PCR. Initially the technique was applied to RNA extracted from whole fetal membrane. Histology, however, readily demonstrates the different cellular compositions of 'cervical' and midzone fetal membranes, thus making this approach invalid. The technique was therefore applied to RNA extracted from 'superscraped' fetal membrane, that had the decidua and cytotrophoblast removed. Thus the tissue composition between 'cervical' membrane and midzone membrane should have been comparable. This approach demonstrated a non-significant trend toward higher amounts of osteonectin mRNA in 'cervical' fetal membranes. The possible reasons for the lack of correspondence between mRNA and protein expression are as discussed with relation to  $\alpha$ -sma in Chapter 3 (3.5.).

## 6.6. Conclusions

- Expression of osteonectin mRNA and protein was demonstrated in human fetal membranes, within myofibroblasts in the reticular layer of the chorion, fibroblast cells of the amnion, cytotrophoblast cells, and amniotic epithelium.
- Regional increased expression of osteonectin protein in the fetal membranes, within the myofibroblasts of the reticular layer, fibroblast cells of the amnion, and cytotrophoblast

cells was demonstrated, in fetal membranes obtained from overlying the cervix prior to and during labour, and from the rupture line following labour and delivery.

- Osteonectin protein was expressed by myofibroblasts within the reticular layer, although an absolute direct relationship between expression of  $\alpha$ -sma and osteonectin in individual cells was not observed.
- Osteonectin protein expression was confirmed by Western blotting, which also demonstrated regional increased protein expression in fetal membranes overlying the cervix prior to the onset of labour.
- Regional increased mRNA expression in amniotic fibroblasts and reticular layer myofibroblasts was demonstrated by *in situ* hybridisation in fetal membranes overlying the cervix prior to the onset of labour
- Osteonectin mRNA was amplified by RT-PCR, but this technique was unable to confirm the regional difference in mRNA expression that had been demonstrated by *in situ* hybridisation.

## **Chapter 7**

### **Induction of myofibroblast differentiation, osteonectin and tenascin expression in an organ culture model**

#### **7.1. Introduction**

The previous chapters have demonstrated changes in the cellular phenotype associated with extreme altered morphology of the fetal membranes at term, localised to fetal membranes overlying the cervix prior to delivery and a restricted region of the rupture line after delivery. The characteristics of this phenotype are expression of  $\alpha$ -sma, osteonectin and tenascin-C. These changes are associated with an increase in thickness of the connective tissue layers of the fetal membranes and a decrease in the thickness of the cellular layers of the fetal membranes. The elucidation of the factors involved in regulation of this phenotype may be critical for the understanding of the generation of the altered morphology of the fetal membranes.

##### **7.1.1. Regulation of $\alpha$ -sma expression**

Expression of  $\alpha$ -sma is considered a key feature of myofibroblast differentiation, and thus its regulation has been studied extensively *in vitro*. Fibroblasts in culture may acquire stress fibres and express  $\alpha$ -sma when cultured on plastic, without addition of any cytokines (Schmitt-Graff *et al.*, 1994). Of all growth factors studied, TGF- $\beta_1$  has been consistently demonstrated to induce  $\alpha$ -sma expression in myofibroblast and fibroblast cell cultures (Desmouliere *et al.*, 1993; Ronnov-Jessen & Petersen, 1993; Jester *et al.*, 1996; Zhang *et al.*, 1996). GM-CSF stimulates  $\alpha$ -sma expression by myofibroblasts in an *in vivo* rat model, apparently by induction of TGF- $\beta_1$  expression by macrophages (Xing *et al.*, 1997), but does not stimulate  $\alpha$ -sma expression *in vitro*. Angiotensin II, demonstrated to play a role in fibrosis, also acts to stimulate TGF- $\beta_1$  production (Campbell & Katwa, 1997). Interleukin-4 has also been reported to induce  $\alpha$ -sma expression in fibroblasts (Mattey *et al.*, 1997), and endothelin-1 to upregulate  $\alpha$ -sma in cultured vascular smooth muscle cells (Schmitt-Graff *et al.*, 1994) and bronchial fibroblasts (Sun *et al.*, 1997). Basic fibroblast growth factor has been reported to induce (Schmitt-Graff *et al.*, 1994), and to inhibit  $\alpha$ -sma expression (Jester *et al.*, 1996; Mattey *et al.*, 1997). TNF- $\alpha$ , PDGF (Desmouliere *et al.*,

1993), IL-1 and IL-6 (Mattey *et al.*, 1997) have all been demonstrated not to induce  $\alpha$ -sma expression by myofibroblasts and fibroblasts. Interferon- $\gamma$  decreases  $\alpha$ -sma expression by fibroblasts (Desmouliere *et al.*, 1992).

### **7.1.2. Regulation of tenascin-C expression**

Numerous factors have been studied *in vitro* with respect to induction of Tn-C expression. TGF- $\beta$  consistently upregulates Tn-C expression *in vitro*, in all cell types studied (Pearson *et al.*, 1988). Other factors identified which may upregulate Tn-C include serum (Chiquet-Ehrismann *et al.*, 1986; Pearson *et al.*, 1988), angiotensin II (Mackie *et al.*, 1992; Sharifi *et al.*, 1992; Hahn *et al.*, 1995), platelet derived growth factor (Mackie *et al.*, 1992), TNF- $\alpha$  (Harkonen *et al.*, 1995), interferon- $\gamma$  (Harkonen *et al.*, 1995), interleukin-1 (McCachren & Lightner, 1992) and acidic and basic fibroblast growth factor (Tucker *et al.*, 1993; Rettig *et al.*, 1994). Many of these growth factors have been demonstrated to upregulate Tn-C expression in specific cell types only and not in others. Expression of Tn-C may be suppressed by dexamethasone (Ekblom *et al.*, 1993; Talts *et al.*, 1995). Tenascin-C expression may also be upregulated by mechanical stress (Chiquet-Ehrismann *et al.*, 1994; Chiquet *et al.*, 1996), acting via a stress-response element in the Tn-C gene promoter (Chiquet-Ehrismann *et al.*, 1994).

### **7.1.3. Regulation of osteonectin expression**

Osteonectin regulation has also been studied *in vitro*. Upregulation of expression has been demonstrated by TGF- $\beta$  (Wrana *et al.*, 1991), platelet derived growth factor, insulin-like growth factor-1 and colony stimulating factor-1 (Motamed *et al.*, 1996).

### **7.1.4. Fetal membrane organ culture model**

Organ culture models for the maintenance of tissues *in vitro* have the advantage of maintaining the morphology and the autocrine and paracrine relationships within the tissue. A number of models have been described for the fetal membrane, and have been utilised for examination of the mechanisms involved in the cytokine response to inflammation (Fortunato *et al.*, 1994; Laham *et al.*, 1994), and for examination of mechanisms of induction of MMP-9 production (McLaren J, personal communication, subsequently published (McLaren *et al.*, 2000b)). These involve maintaining discs of amnio-chorio-decidua of 6-15mm diameter in culture, and allow the addition of agents, and subsequent examination of changes in the composite tissue, and of quantification of factors secreted

into the media. These models have been demonstrated to maintain normal morphology and steady RNA yield over 10 days in culture (Fortunato *et al.*, 1994), and to maintain 77-89% cell viability over 6 days in culture as measured by LDH secretion into the media (McLaren J, personal communication, subsequently published (McLaren *et al.*, 2000b)).

This model will be used to investigate the regulation of myofibroblast differentiation within the connective tissue layers of the fetal membranes.

Variables examined within this culture system will be:

1. Addition of Fetal Bovine Serum. This has been demonstrated to increase secretion of latent MMP-9 in the fetal membranes *in vitro* (McLaren J, personal communication, subsequently published (McLaren *et al.*, 2000b)). Increased levels of latent MMP-9 have been detected the fetal membranes overlying the cervix at term in association with extreme altered morphology (McLaren J, personal communication, subsequently published (McLaren *et al.*, 2000a)).
2. Partial and complete removal of the cytotrophoblast and decidual layers. Paracrine interaction between the different cell types in the different layers of the fetal membrane may also be important. Fetal membranes exhibiting extreme altered morphology are characterised by reduction in thickness of the cytotrophoblast and decidual layers, therefore partial and complete removal of these layers will be used to examine these relationships in culture.
3. Hypoxia. The fetal membranes within the lower uterine pole may be subject to relative hypoxia as the lower uterine segment develops, and potential nutritional support from the decidua lost.
4. Addition of cytokines and growth factors. The cytokines and factors chosen to investigate this will be those commonly reported to regulate myofibroblast differentiation (as observed by  $\alpha$ -sma expression), Tn-C and osteonectin expression *in vitro* in other models: TGF- $\beta_1$ , TNF- $\alpha$ , IL-1 $\beta$ , GM-CSF, endothelin-1, basic fibroblast growth factor, angiotensin II and IL-4.

## **7.2. Aims**

- To attempt to induce expression of  $\alpha$ -sma, osteonectin, and tenascin-C in myofibroblasts of the reticular layer in midzone fetal membranes in an organ culture system.
- To induce morphological changes in the fetal membranes in an organ culture system.

## **7.3. Materials and Methods**

### **7.3.1. Fetal membrane samples**

Fetal membrane samples were obtained following elective Caesarean section at term as previously described (section 2.1.1.2.). Midzone fetal membranes were used.

### **7.3.2. Organ culture**

8mm discs of midzone fetal membrane were cultured for 6 days (2.7.). Each experiment was performed at least twice in duplicate, and more commonly three times and using triplicate discs. Discs removed from culture were formalin-fixed and wax-embedded (2.2.1.).

### **7.3.3. Immunohistochemistry**

Immunohistochemistry for vimentin,  $\alpha$ -sma, osteonectin and tenascin-C was performed on formalin-fixed wax-embedded tissue sections (2.3.). All discs were screened with immunohistochemistry for  $\alpha$ -sma, with further immunohistochemistry performed on selected discs only.

### **7.3.4. Image analysis**

Measurements of the thickness of the component layers of the fetal membrane discs and of the diameter of the fetal membrane discs were carried out (2.8.1.1.). Five fields per 8mm-diameter disc were measured, excluding the edge portion of the disc (2 fields width, approximately 350 $\mu$ m, excluded). The disc diameters were measured in a similar way, with all measurements taken along the pseudobasement membrane, to control for any distortion of discs. Cell counting within both the central portion (5 fields per disc) and the edge portion (1 field at each edge of each disc) of each disc was also performed, on the full

thickness of each layer being examined in a fixed computer screen width (2.1.1.2.). Visual inspection of all  $\alpha$ -sma immunostained discs was performed. The majority of discs examined were negative for  $\alpha$ -sma within the connective tissue layers. The aim was to reproduce the 'activated' myofibroblast phenotype previously observed in *ex-in vivo* fetal membranes. Only slides where a minimum of 2  $\alpha$ -sma immunoreactive cells per field was present on visual screening were subject to formal cell counting. Fields within disc edges were subsequently classified as 'positive' or 'negative' for  $\alpha$ -sma, using a threshold of 5  $\alpha$ -sma immunoreactive cells in the reticular layer in the field. This threshold would not have detected any of the midzone fetal membrane biopsies examined in this thesis either prior to, during or following labour and delivery, and would have detected all extreme altered morphology membrane biopsies in these groups.

#### **7.3.5. Statistical analysis**

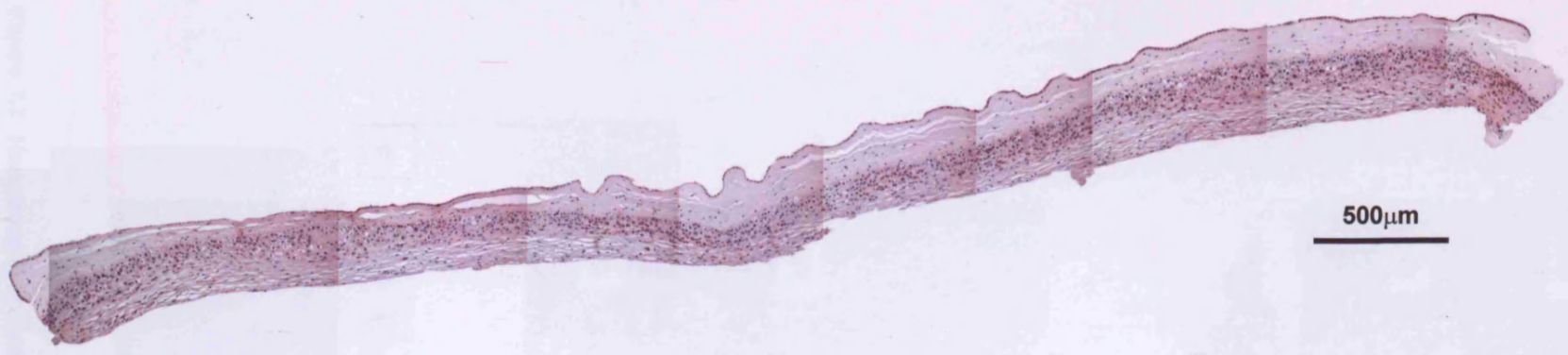
Comparison of data between and within experiments was carried out as described in section 2.9.

### **7.4. Results**

#### **7.4.1. Behaviour of fetal membrane discs in culture**

After 6 days in culture, the fetal membrane discs underwent significant morphological changes, and exhibited a number of consistent histological features (Figures 7.1, 7.2 & 7.3). Marked swelling and dispersal of the spongy layer was observed, occasionally associated with separation of amnion from choriodecidua. The edge of the amnion became infolded, with the amniotic epithelium curled around the edge of the compact and fibroblast layers and often made contact with the cytotrophoblast layer (Figures 7.1 & 7.3). In a proportion of discs the amniotic epithelium grew over the edge of the cytotrophoblast and decidual layers, effectively 'sealing' the edge of the disc (demonstrated by immunohistochemistry for cytokeratin in Figure 7.3). This phenomenon was observed in 10 out of 22 disc edges examined. The edges of the choriodecidua often had a 'pinched' appearance, with reticular layer, cytotrophoblast layer and decidua pinched together. The cells within the cytotrophoblast layer commonly became vacuolated (Figure 7.2b). Numerous small dense cell nuclei within the cytotrophoblast layer were observed (Figure 7.2b). A layer of decidua immediately beneath the cytotrophoblast layer became

a



b

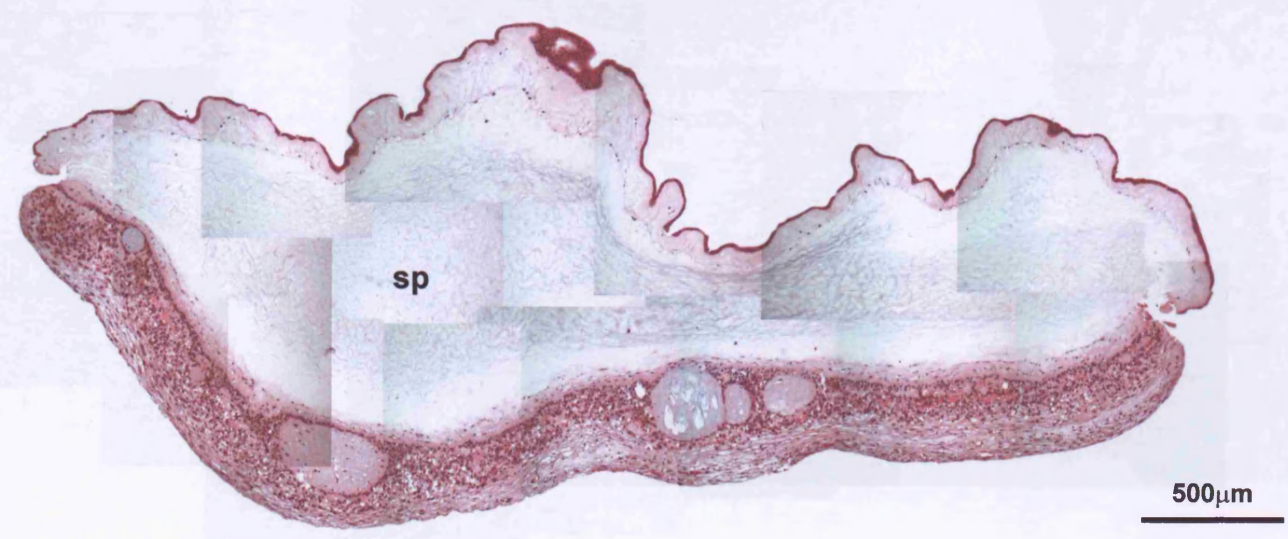


**Figure 7.1.** A composite picture of haematoxylin and eosin stained sections of a fetal membrane disc at Day 0, prior to organ culture (a), and following 6 days in culture (b). Distortion of the disc occurs after 6 days in culture, with marked dispersal of the spongy layer (sp).

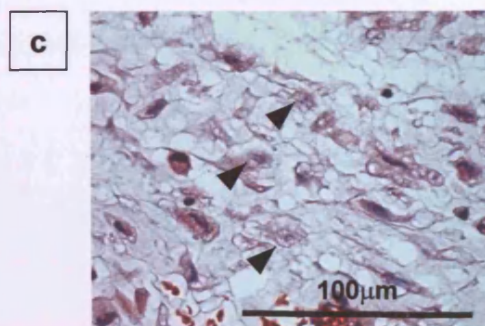
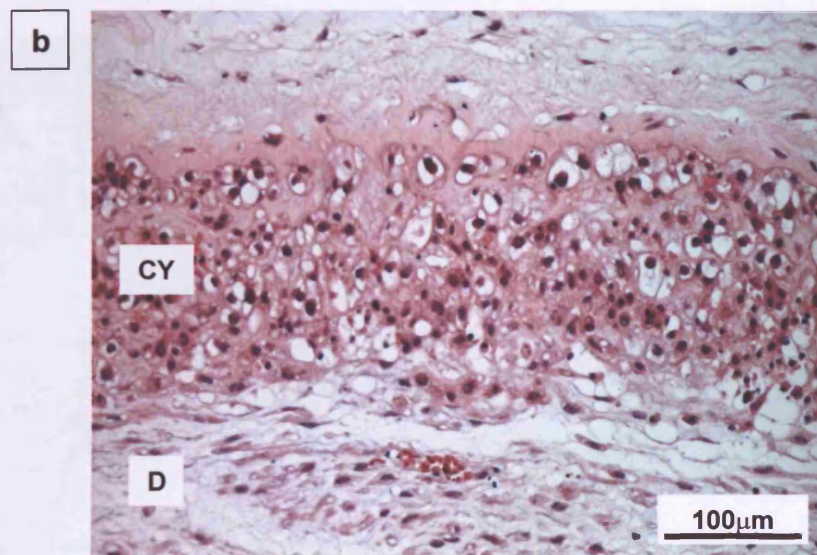
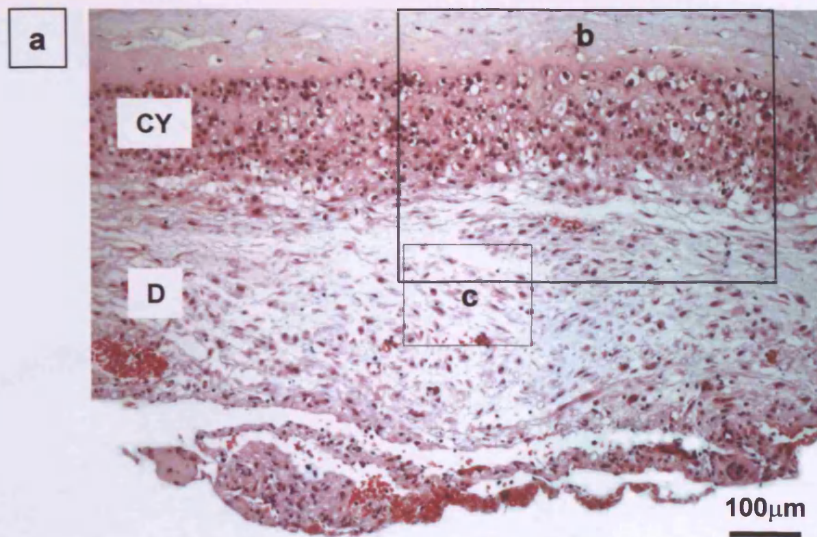


**Figure 7.2.** Haematoxylin and eosin stained section of fetal membrane disc following 6 days in culture. Large numbers of vacuolated cytotrophoblast cells are observed (**a&b**). Many decidua cells at the decidua-cytotrophoblast interface have pale nuclei (**b&c**) (arrowheads). The cytotrophoblast layer (**CY**) and decidua (**D**) are indicated.

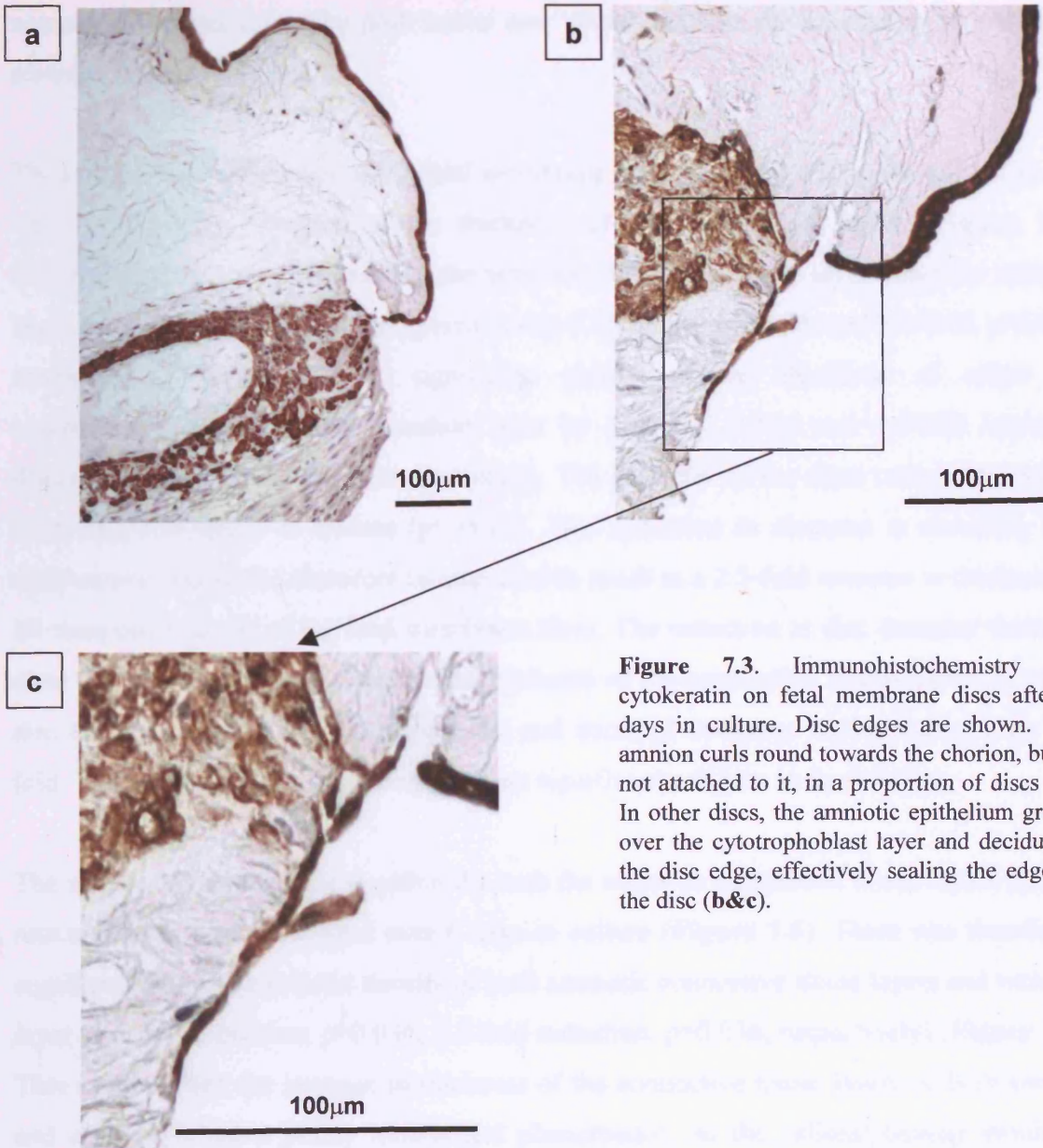


**Figure 7.3.** Immunohistochemistry for cytokeratin on fetal membrane discs after 6 days in culture. Disc edges are shown. The amnion curls round towards the chorion, but is not attached to it, in a proportion of discs (a). In other discs, the amniotic epithelium grows over the cytotrophoblast layer and decidua at the disc edge, effectively sealing the edge of the disc (b&c).

necrotic, as characterised by pink nuclei and 'ghost' cells on the haematoxylin and eosin sections (**Figure 7.2a&c**).

The morphological changes in the fetal membrane discs observed during the culture period were reflected in changes in the thickness of the component layers (**Figure 7.4**). Significantly increased thickness of the amniotic connective tissue layers, and the reticular layer were observed by day 6 compared to day 0 (3.7-fold,  $p=0.036$ ; and 2.8-fold,  $p=0.036$ , respectively). There was no significant change in the thickness of either the cytotrophoblast layer or the decidual layer by day 6 (1.5-fold and 1.2-fold increased thickness respectively, both non-significant). The diameter of the discs reduced by 31.1% from day 0 to day 6 in culture ( $p=0.011$ ). This reduction in diameter is occurring in 2 dimensions, and would therefore be expected to result in a 2.1-fold increase in thickness of all component layers of the fetal membrane discs. The reduction in disc diameter therefore does not explain the large increases in thickness of the connective tissue layers. It would also be expected that the cytotrophoblast and decidual thickness should increase by 2.1-fold. The absence of this occurring suggests significant cell loss in these layers.

The number of cells per field within the both the amniotic connective tissue layers and the reticular layer was unchanged over 6 days in culture (**Figure 7.5**). There was therefore a significant fall in the cellular density of both amniotic connective tissue layers and reticular layer (3.6-fold reduction,  $p=0.036$ ; 2.2-fold reduction,  $p=0.036$ , respectively) (**Figure 7.5**). This suggests that the increase in thickness of the connective tissue layers of both amnion and chorion is not a purely mechanical phenomenon, as the cellular density would be expected to remain constant if this were the case. The reduction in cellular densities observed in vitro are greater than those observed in the ex-in vivo 'cervical'/rupture line biopsies compared to their respective midzone biopsies (see Chapter 3, **Table 3.4**). The constant cell number per field in the fibroblast and reticular layers in culture over time, combined with a reduction in disc diameter, suggests an overall loss of cells from both the fibroblast and reticular layers.

#### **7.4.2. Effects of fetal bovine serum**

Discs of whole fetal membrane were cultured for 6 days in the presence and absence of 10% fetal bovine serum. No significant differences were observed in the thickness of any of the component layers of the fetal membranes (**Figure 7.4**), nor in the cellularity or cell density of the connective tissue layers (**Figure 7.5**), in comparison to those cultured in the

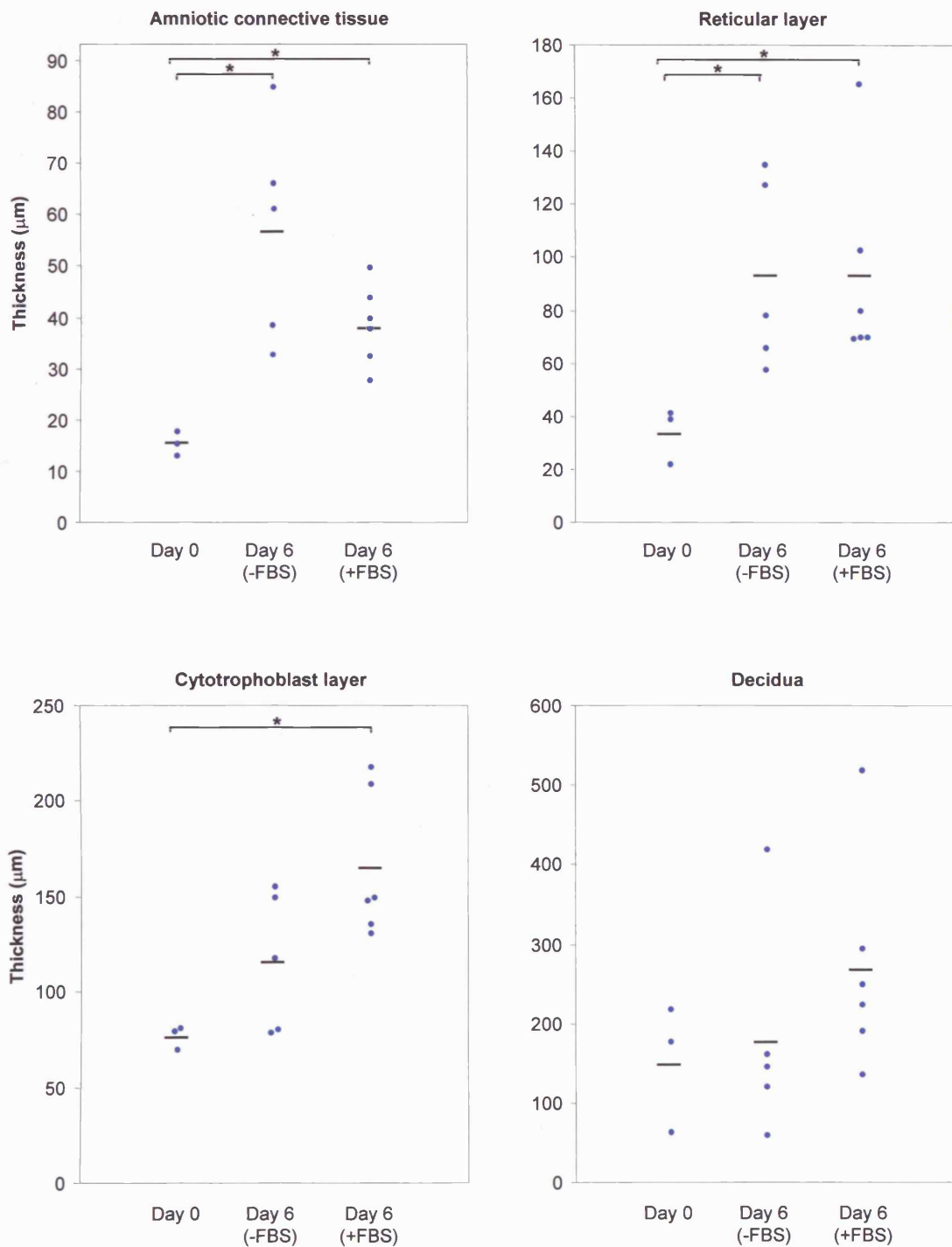


**Figure 7.4.** The thickness of the component layers of the fetal membranes at Day 0, and after 6 days in culture with (+FBS) and without (-FBS) the addition of 10% fetal bovine serum. Each dot represents the mean value of a fetal membrane roll (Day 0, n=10 fields measured) or fetal membrane disc (Day 6, n=5 fields measured). The horizontal bars represent the mean value of the points in each group.

Significant differences between data are indicated (\*, Mann Whitney U test  $p < 0.05$ ).

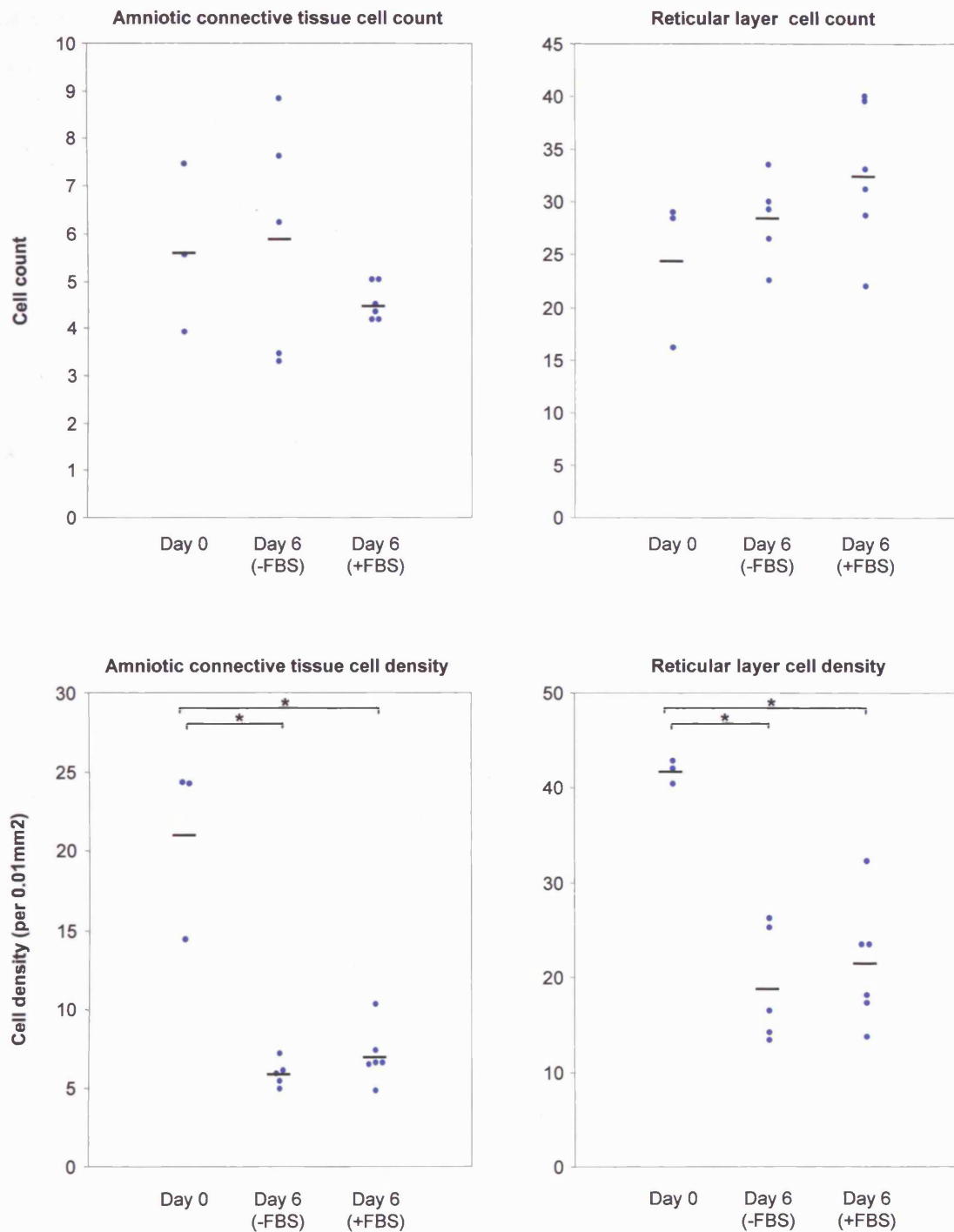


**Figure 7.5.** The total cell count and cellular density of the connective tissue layer of the amnion, and of the reticular layer at Day 0, and after 6 days in culture with (+FBS) and without (-FBS) the addition of 10% fetal bovine serum. The cell count was determined by counting vimentin immunoreactive cells within the relevant layer of the fetal membranes, and is expressed per computer screen width (176 $\mu$ m). Cell density represents the cell count per 0.01mm<sup>2</sup> cross sectional area of the relevant layer of the fetal membrane. Each dot represents the mean value of a fetal membrane roll (Day 0, n=10 fields measured) or fetal membrane disc (Day 6, n=5 fields measured). The horizontal bars represent the mean value of the points in each group. Significant differences between data are indicated (\*, Mann Whitney U test p<0.05).

absence of fetal bovine serum. However, the cytotrophoblast layer was significantly thicker in comparison to day 0 (2.2-fold,  $p=0.024$ ), and a non-significant increase in thickness of the decidual layer was observed in comparison to day 0 (1.8-fold) (Figure 7.4). These changes are comparable to the 2.1-fold increase in thickness expected due to the decrease in disc diameter, and may suggest that the presumed cellular loss detected within these layers when cultured in the absence of fetal bovine serum (7.4.1.) was not occurring when the fetal membrane discs were cultured in the presence of fetal bovine serum.

Visual inspection of  $\alpha$ -sma immunostained slides did not reveal any significant  $\alpha$ -sma immunostaining in either the fibroblast or reticular layer in either the presence or absence of 10% FBS (Figure 7.6).

These conditions, with and without the addition of 10% fetal bovine serum were then used in combination with other possible stimulatory factors.

#### **7.4.2. Hypoxia**

Duplicate experiments performed in the presence of 1% O<sub>2</sub> were performed. Screening by immunohistochemistry for  $\alpha$ -sma did not reveal any significant immunostaining in either the fibroblast or reticular layer in either the presence or absence of 10% FBS.

#### **7.4.3. Removal of decidual layer**

Fetal membrane discs with the majority of the decidua removed (by scraping the maternal surface of the fetal membrane with a glass microscope slide) were cultured in the presence/absence of 10% FBS for 6 days. Histological examination of the resultant fetal membrane discs, and image analysis, demonstrated that the decidual thickness was reduced by an average of 48% from 151.5 $\mu$ m to 79.2 $\mu$ m by this technique (difference not statistically significant). Screening by immunohistochemistry for  $\alpha$ -sma did not reveal any significant immunostaining in either the fibroblast or reticular layer in either the presence or absence of 10% FBS.

#### **7.4.4. Removal of decidual and cytotrophoblast layers**

A technique to remove all of the decidual and cytotrophoblast cells from the fetal membrane was developed and validated by examination of haematoxylin and eosin stained

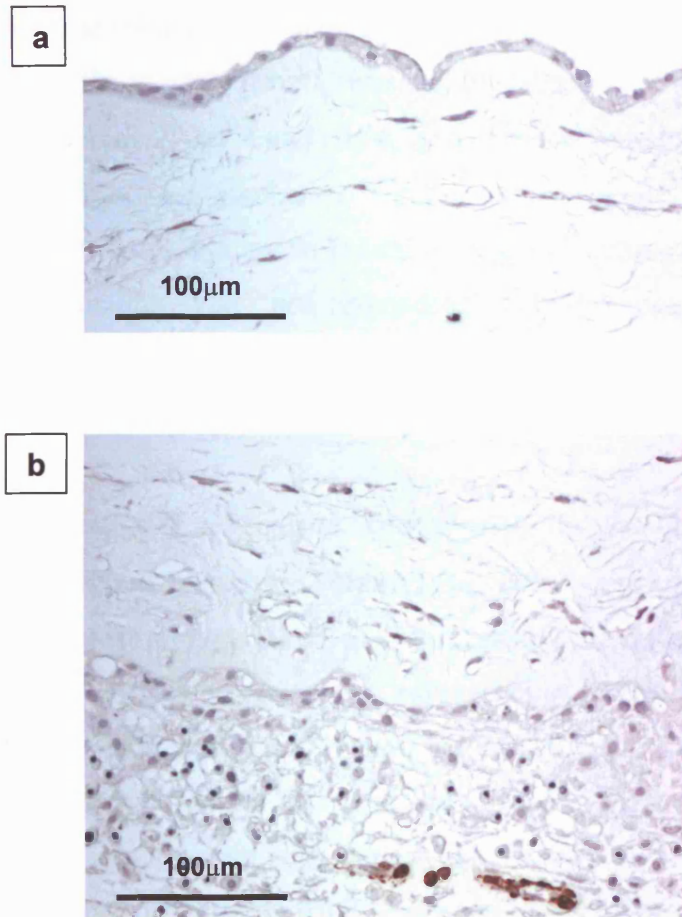


**Figure 7.6.** Immunohistochemistry for  $\alpha$ -sma on a fetal membrane disc following 6 days in culture. No immunoreactive cells are detected in the fibroblast layer (a) or reticular layer (b). Immunoreactive cells are detected around blood vessels in the decidua (b).

sections (2.1.1.4.). The resultant fetal membrane was cultured in the presence and absence of 10% FBS. Due to the variable results obtained, this experiment was performed 6 times, and discs removed on day 2, day 4 and day 6. Screening by immunohistochemistry for  $\alpha$ -sma demonstrated significant numbers of immunoreactive cells within the connective tissue layers of two cultures, but not in the remaining four cultures. Results are therefore given for the 'responding' and 'non-responding' cultures separately. No significant differences were observed in results for discs cultured in the presence or absence of fetal bovine serum, and the results were therefore pooled.

In the two 'responding' cultures,  $\alpha$ -sma immunoreactivity was observed in cells of the fibroblast layer and the reticular layer (Figure 7.7a). There were significantly more  $\alpha$ -sma immunoreactive cells within both the fibroblast layer and the reticular layer by Day 6 in culture, in the discs from the 'superscraped' culture compared to the control discs within the same cultures ( $p=0.035$  and  $p=0.0027$  respectively), (Figure 7.8), representing 21.5% of fibroblast layer cells and 64.2% of reticular layer cells. There were also significantly more osteonectin immunoreactive cells within the reticular layer of the 'superscraped' discs compared to control discs ( $p=0.017$ ), representing 13.7% of reticular layer cells (Figure 7.7b). Tenascin-C immunoreactivity was observed as deposits along the amniotic basement membrane, and as occasional haloes around reticular layer cells, visible above background matrix staining (Figure 7.7c).

Within the 'responding' cultures, there was no significant difference in the thickness of the connective tissue layers of the amnion or chorion between the 'superscraped' discs and the control discs after 6 days in culture (amniotic connective tissue  $58.1\pm 1.9\mu\text{m}$  and  $51.8\pm 4.9\mu\text{m}$  respectively, reticular layer  $96.1\pm 8.8\mu\text{m}$  and  $94.4\pm 3.2\mu\text{m}$  respectively). When comparing 'responding' cultures to 'non-responding' cultures, there was no significant difference in the thickness of the reticular layer after 6 days in culture ( $96.1\pm 8.8\mu\text{m}$  vs  $87.1\pm 4.7\mu\text{m}$ ). However, the amniotic connective tissue thickness was significantly greater in the 'non-responding' cultures compared to 'responding' cultures ( $95.2\pm 4.7\mu\text{m}$  vs  $58.1\pm 1.9\mu\text{m}$ ,  $p=0.00002$ ). The relevance of this is uncertain, although it may be related to a greater initial (though non-significant) thickness of the amniotic connective tissue layers in the 'non-responding' cultures ( $27.9\pm 2.0\mu\text{m}$  vs  $20.0\pm 3.3\mu\text{m}$ ,  $p=0.27$ ).

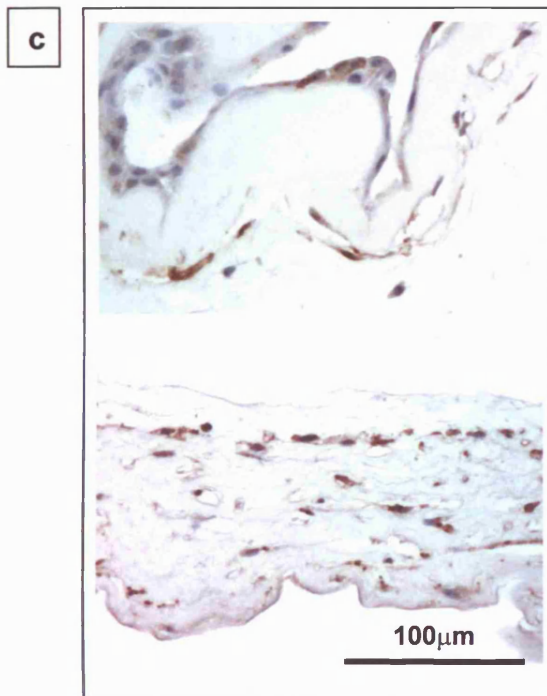
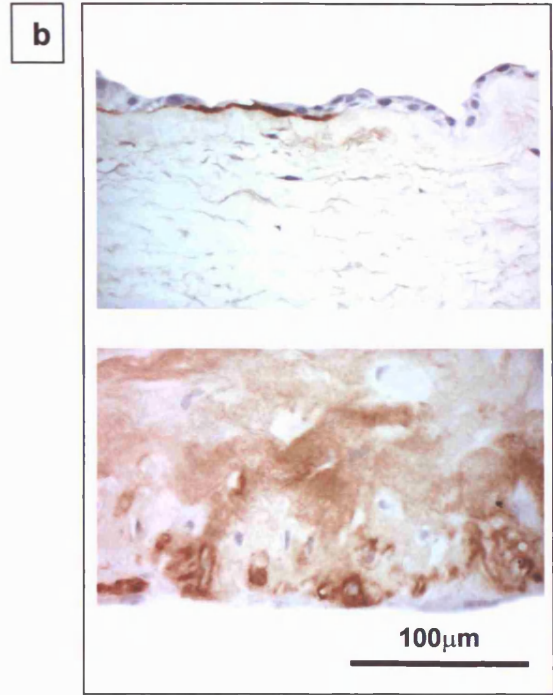
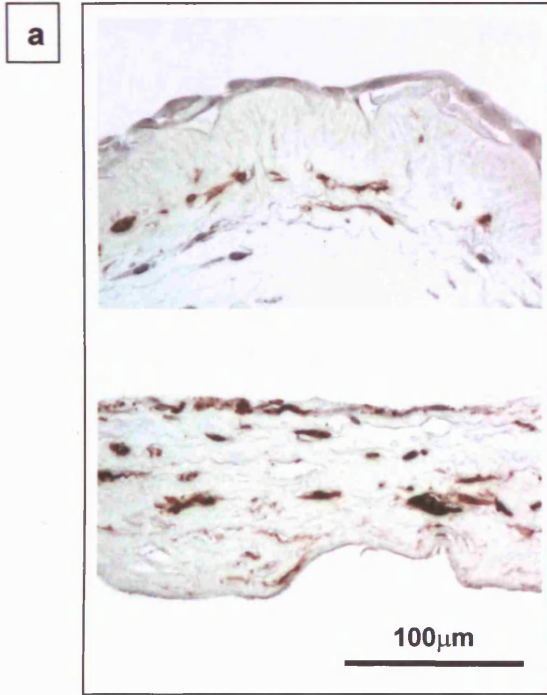


**Figure 7.7.** Immunohistochemistry for  $\alpha$ -sma (a), tenascin-C (b) and osteonectin (c) on 'superscraped' fetal membrane discs following 6 days in culture. The upper picture in each pair illustrates the amnion, the lower picture the reticular layer.

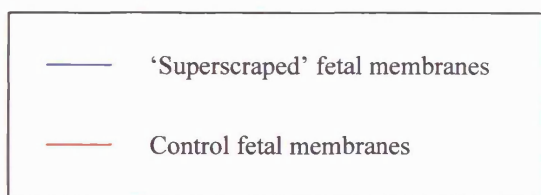
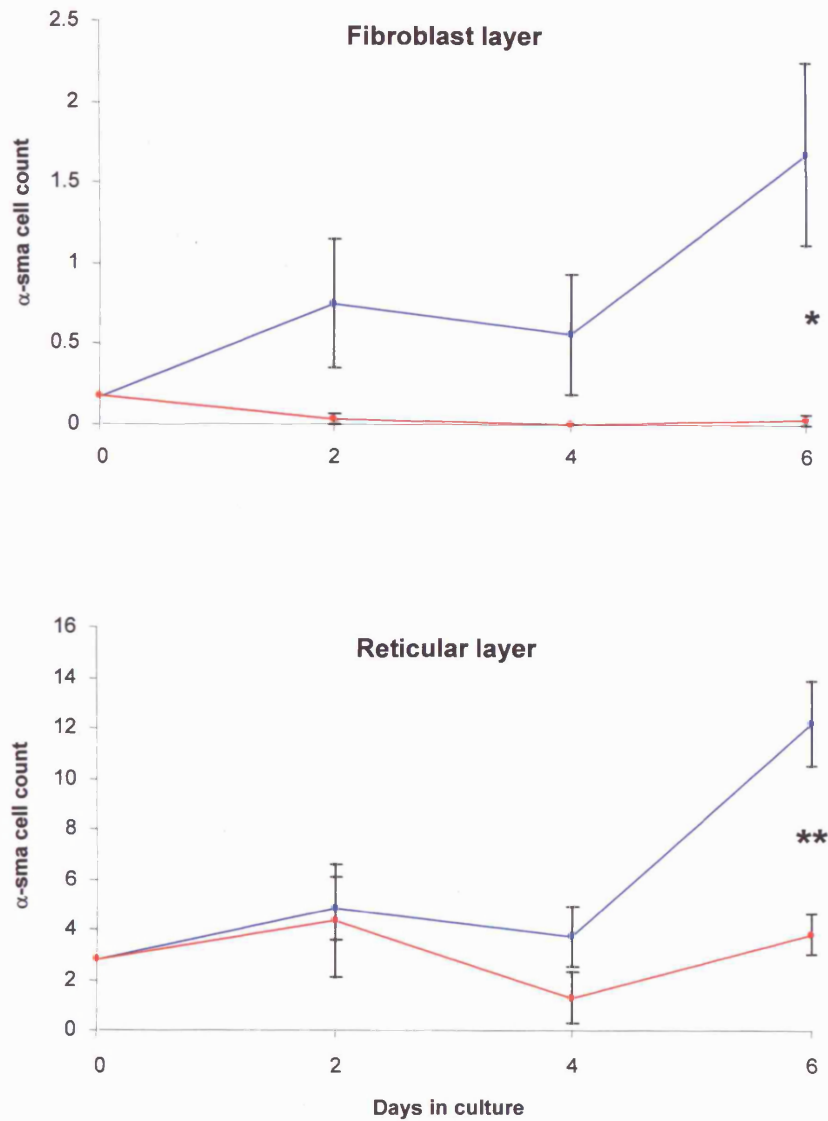


**Figure 7.8.** Numbers of  $\alpha$ -sma immunoreactive cells in the fibroblast and reticular layer prior to, and after 2, 4, and 6 days in culture. 'Superscraped' fetal membrane discs (decidua and cytotrophoblast layers removed) are compared to control membrane discs (decidua only removed). The mean  $\pm$  SEM  $\alpha$ -sma immunoreactive cell count is shown for all discs removed at each individual time point (n=5-9) from 2 culture experiments. The immunoreactive cell count is per computer screen width (176 $\mu$ m).

Significantly greater numbers of  $\alpha$ -sma immunoreactive cells in 'superscraped' fetal membrane discs:

\*  $p < 0.05$

\*\*  $p < 0.01$

The reason for the lack of  $\alpha$ -sma immunoreactivity in the 'non-responding' cultures appeared to be cell death within the reticular layer of the chorion (**Figure 7.9**). The reticular layer total cell count, as assessed by vimentin immunoreactivity, was significantly lower in the 'non-responding' compared to the 'responding' cultures after 6 days in culture ( $6.5 \pm 1.7$  vs  $19.0 \pm 4.6$ ,  $p=0.0055$ ). There was no significant difference in the total cell count in the fibroblast layer ( $6.6 \pm 0.8$  vs  $7.8 \pm 1.0$  respectively,  $p=0.35$ ). However, even in the 'responding' cultures, there was a non-significant trend towards a lower reticular layer cell count after 6 days in culture, when compared to the control discs ( $19.0 \pm 4.6$  vs  $31.6 \pm 1.7$ ,  $p=0.06$ ), suggesting that even within these cultures, cell loss was occurring.

#### **7.4.5. 'Edge' effects**

The effect of tissue damage was investigated by examining the cut edges of the fetal membrane discs. On the histological cross section of each disc two edges of the disc were available for examination (on occasion poor orientation of a disc within a wax block only allowed one disc edge to be visualised). Two fields were therefore analysed per disc, within the  $350\mu\text{m}$  edge zone of the disc (**section 7.3.4.**). No differences in the number of disc edges immunoreactive for  $\alpha$ -sma were observed in results for discs cultured in the presence or absence of 10% fetal bovine serum, and the results were therefore pooled. Cells immunoreactive for  $\alpha$ -sma were not observed within the fibroblast layer of the amnion in the disc edges.

On day 6 of culture, 40% of disc edges examined from whole fetal membrane discs (15 disc edges examined, cultures from **7.4.2.**) and 38% of disc edges from discs with decidua removed (21 disc edges examined, cultures from **7.4.3.**) were positive for  $\alpha$ -sma. The percentage of disc edges positive for  $\alpha$ -sma over time is demonstrated in **Figure 7.10**. 'Haloes' of tenascin-C were observed around reticular layer cells at some disc edges, although these did not always correlate with  $\alpha$ -sma positive disc edges (**Figure 7.11**). The Tn-C disc edges were not quantified due to the difficulty in detecting 'haloes' above the variable background matrix staining. Osteonectin positivity was not detected at disc edges.

#### **7.4.6. Addition of cytokines/additives**

Fetal membrane discs were cultured for 6 days in the presence and absence of endothelin-1, bFGF, GM-CSF, IL- $1\beta$ , IL-4, TGF- $\beta_1$ , angiotensin II and TNF- $\alpha$  (all in the absence of FBS; additive concentrations as in **Table 2.5**). Examination of slides immunostained with

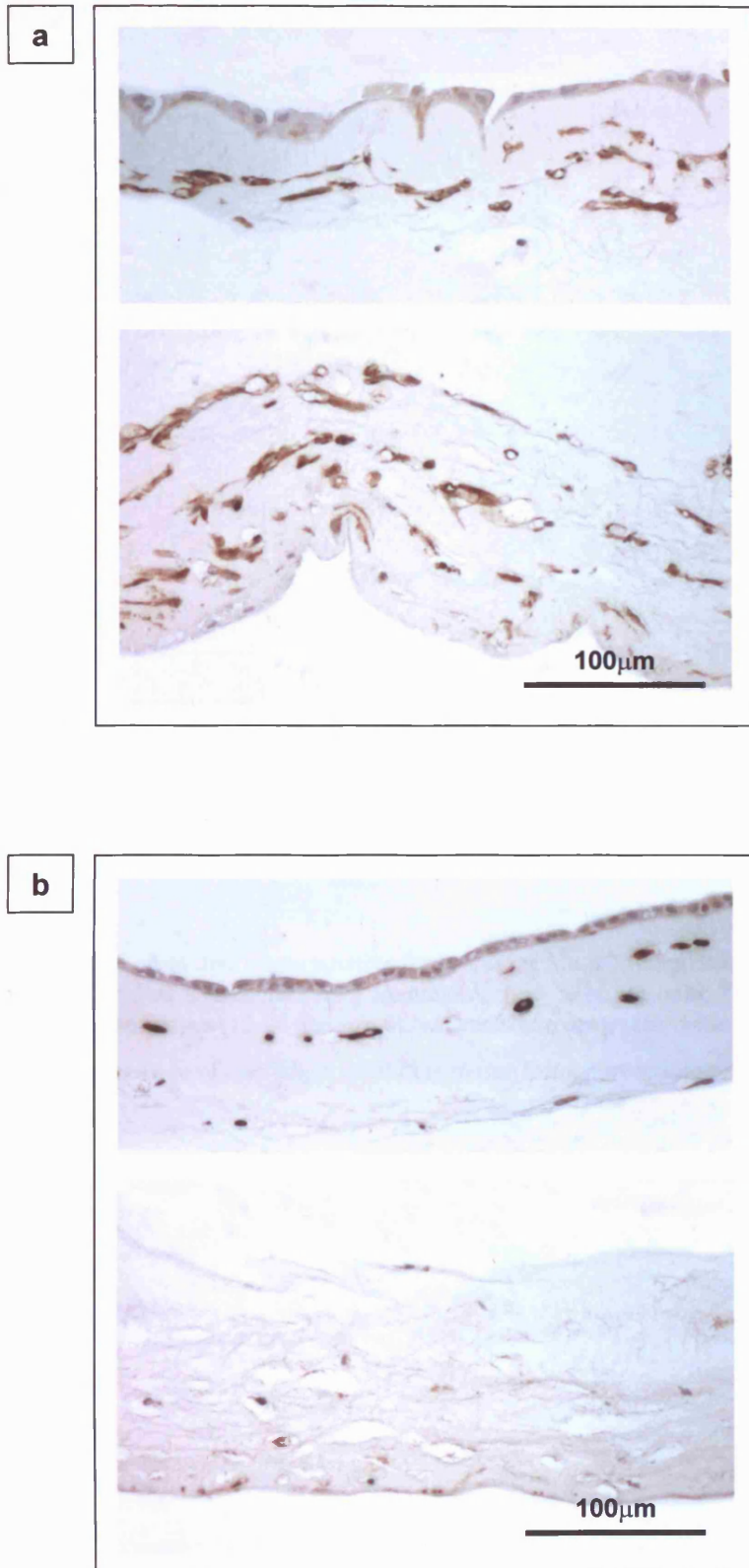


**Figure 7.9.** Immunohistochemistry for vimentin on 'superscraped' fetal membranes following 6 days in culture. In a 'responding' culture (a) numerous immunoreactive cells are detected in both the fibroblast layer and reticular layer. In a 'non-responding' culture (b), immunoreactive cells are detected in the fibroblast layer, but are virtually absent in the reticular layer. The upper picture in each pair illustrates the amnion, the lower picture the reticular layer.

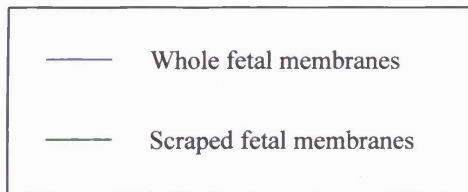
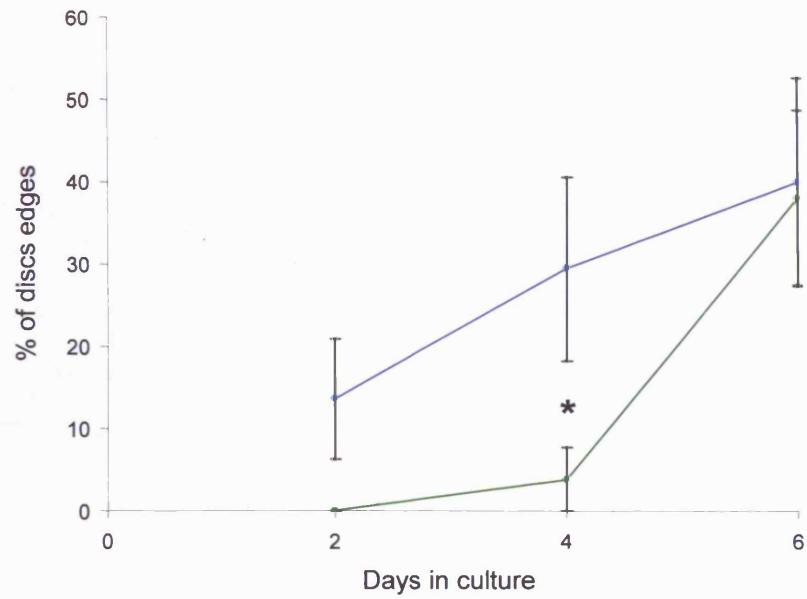


**Figure 7.10.** The proportion of disc edges positive for  $\alpha$ -sma within the reticular layer over time. Positivity for  $\alpha$ -sma was considered as a minimum of 5 immunoreactive cells per field. Each point represents the proportion of available disc edges (15-26 per group), with standard error also demonstrated.

Significantly greater proportion of disc edges exhibiting  $\alpha$ -sma immunoreactivity:

\*  $p < 0.05$

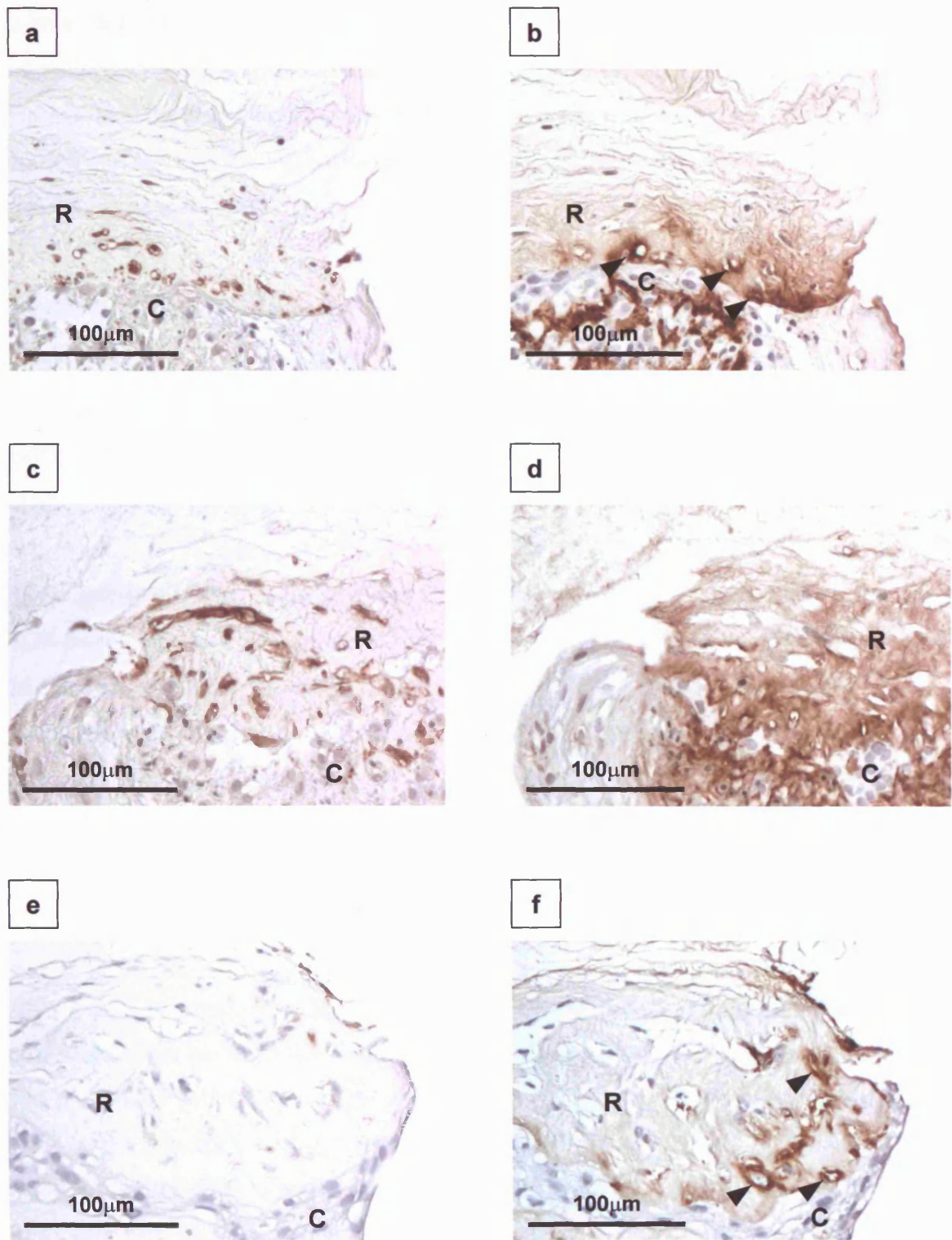


**Figure 7.11.** Immunohistochemistry for  $\alpha$ -sma (a, c & e) and tenascin-C (b, d & f) on the edges of fetal membrane discs after 6 days in culture. Large numbers of  $\alpha$ -sma immunoreactive cells are observed within the reticular layer close to the edge of the disc (a), corresponding to 'haloes' of tenascin-C around reticular layer cells on a serial section of the same disc (b). However, on another disc edge large numbers of  $\alpha$ -sma immunoreactive cells are detected (c), but no corresponding 'haloes' of tenascin-C on a serial section are observed (d), although this may be due to the greater background level of tenascin-C immunoreactivity. Examination of a further disc edge demonstrates absence of  $\alpha$ -sma immunoreactive cells (e), but the presence of 'haloes' of tenascin-C on a serial section (f). The reticular layer (R) and cytotrophoblast layer (C) are labelled, and 'haloes' of tenascin-C are indicated by arrowheads.

$\alpha$ -sma did not reveal any significant ( $> 2$  positive cells per field) numbers of immunoreactive cells with addition of any cytokine to the culture media except TGF $\beta_1$ . Further immunohistochemistry for tenascin-C, vimentin, and osteonectin was therefore carried out, and experiments to determine the dose-response and time course of response of myofibroblast activation.

#### 7.4.6.1. Response to TGF- $\beta_1$ in culture

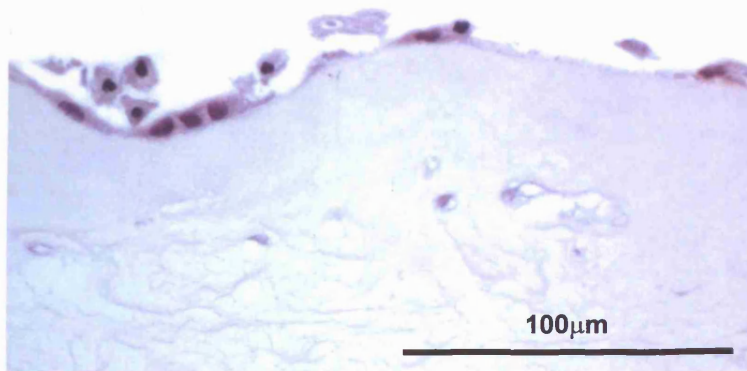
Fetal membrane discs cultured in the presence of TGF- $\beta_1$  developed extreme damage to the amniotic epithelium, with loss of large numbers of cells (Figure 7.12). After 6 days in culture, the thickness of the amniotic connective tissue of the fetal membrane discs cultured in the presence of 10ng/ml TGF- $\beta_1$  was 14% thicker than that of discs cultured in the absence of TGF- $\beta_1$  ( $p=0.03$ ). There were no other significant differences in fetal membrane morphology in fetal membrane discs cultured in the presence or absence of TGF- $\beta_1$ . There was a 54% higher total cell count within the reticular layer ( $40.21\pm 3.41$  vs  $26.10\pm 1.54$ ,  $p=0.0011$ ) in discs cultured for 6 days in the presence of 10ng/ml TGF- $\beta_1$ , compared to those cultured in the absence of TGF- $\beta_1$ . There was no significant difference in the total cell count in the fibroblast layer ( $6.58\pm 0.68$  vs  $5.19\pm 0.39$ ,  $p=0.084$ ). Discs cultured in the presence of 10ng/ml TGF- $\beta_1$  exhibited a mean reduction in disc diameter of 24% over 6 days in culture, not significantly different to the change in diameter of the control discs from the same experiments ( $p=0.71$ ).

After 6 days in culture significantly greater numbers of  $\alpha$ -sma immunoreactive cells were observed in both the fibroblast layer and reticular layer compared to control discs ( $p=0.002$  and  $p=0.00005$  respectively). These represented 52.2% and 27.3% of vimentin-positive cells in the fibroblast and reticular layers respectively (compared to 1.4-1.6% in the negative control discs, Figure 7.13a). Significantly higher numbers of cells within the fibroblast and reticular layers were immunoreactive for osteonectin ( $1.34\pm 0.36$  vs  $0.27\pm 0.10$ ,  $p=0.007$ ;  $9.12\pm 1.36$  vs  $2.48\pm 0.64$ ,  $p=0.0003$  respectively), representing 20.3% and 22.7% of vimentin-positive cells in these layers (compared to 5.2% and 9.5% of cells in negative control discs, Figure 7.13b). Immunoreactive tenascin-C appeared in discrete patches around cells of the fibroblast and reticular layers (Figure 7.13c).

a



b



c

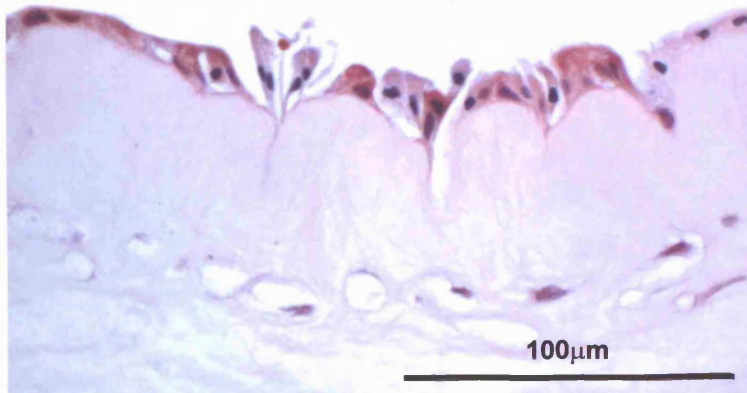


**Figure 7.12.** Haematoxylin and eosin stained sections of fetal membrane discs following 6 days in culture. The amniotic epithelium of a control disc is virtually intact (a), whereas those cultured in the presence of 10ng/ml TGF-β<sub>1</sub> exhibit varying degrees of epithelial damage, with marked loss of cells (b&c).

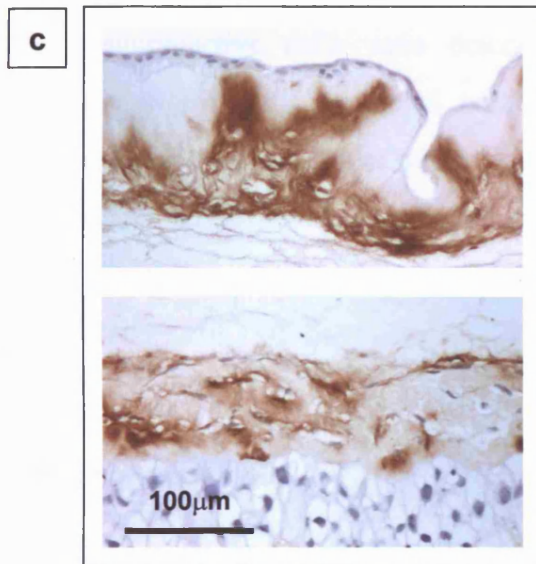
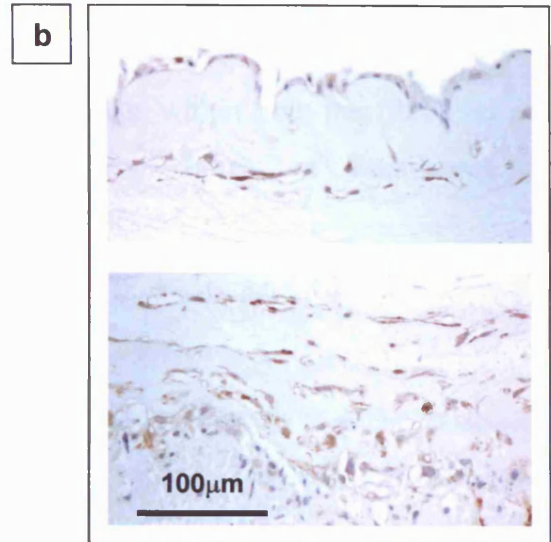
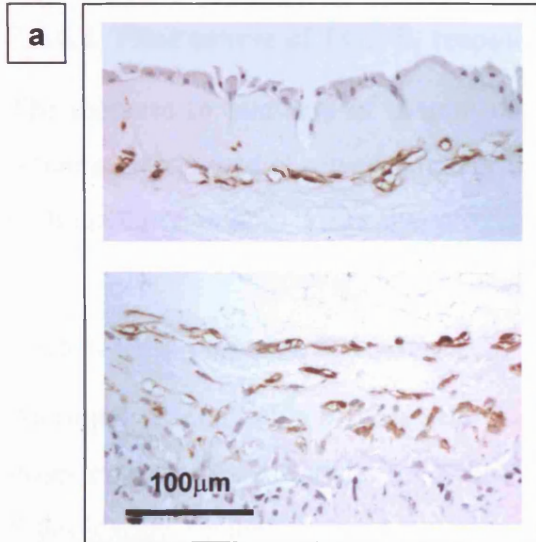


**Figure 7.13.** Immunohistochemistry for  $\alpha$ -sma (a), osteonectin (b) and tenascin-C (c) on fetal membrane discs cultured for 6 days in the presence of 10ng/ml TGF- $\beta_1$ . The upper picture of each pair is the amnion, the lower picture the reticular layer.

#### **7.4.6.2. Time course of TGF- $\beta_1$ response**

The increase in numbers of  $\alpha$ -sma immunoreactive cells within both the fibroblast and reticular layers was observed to occur by day 4 in culture (Figure 7.14). Immunoreactive cells appeared in both layers at approximately the same time.

#### **7.4.6.3. Dose-response for TGF- $\beta_1$**

An initial concentration of 10ng/ml was used to screen for response to TGF- $\beta_1$ . Subsequent dose-response experiments used concentrations of 1ng/ml, 10ng/ml and 100ng/ml. Significantly increased numbers of  $\alpha$ -sma immunoreactive cells were observed in the fibroblast layer of the amnion with 10ng/ml and 100ng/ml TGF- $\beta_1$  after 6 days in culture, in comparison to the control discs ( $p=0.013$  and  $p=0.006$  respectively). Increasing numbers of immunoreactive cells were detected with increasing concentrations of TGF- $\beta_1$ . Similarly significantly increased numbers of  $\alpha$ -sma immunoreactive cells were only observed in the reticular layer with 10ng/ml and 100ng/ml TGF- $\beta_1$  after 6 days in culture in comparison to the control discs ( $p=0.046$  and  $p=0.01$  respectively). As in the fibroblast layer, increasing numbers of  $\alpha$ -sma immunoreactive cells were observed with increased concentrations of TGF- $\beta_1$ .

### **7.5. Discussion**

This study has succeeded in upregulating the expression of  $\alpha$ -sma, osteonectin and tenascin-C in the fetal membranes *in vitro* by removal of both cytotrophoblast and decidua, and by addition of TGF- $\beta_1$ . The former technique induced  $\alpha$ -sma expression in 64% of reticular layer cells, the latter technique induced  $\alpha$ -sma expression in 27% of reticular layer cells (in comparison to 73% of reticular layer cells immunoreactive for  $\alpha$ -sma in 'extreme altered morphology' biopsies prior to labour at term, 4.4.2.1.). The pattern of induction of expression of these three proteins differed from the patterns observed *in vivo*.

Removal of the cytotrophoblast and decidual layers was performed to attempt to mirror the morphology of fetal membranes with extreme altered morphology, which have thin/absent decidua and a thin cytotrophoblast layer. This technique resulted in induction of  $\alpha$ -sma expression within the fibroblast and reticular layer, induction of osteonectin expression in the reticular layer, and induction of tenascin-C expression along the basement membrane

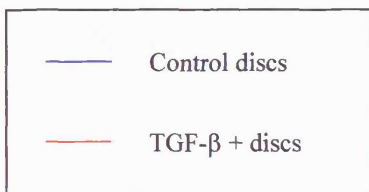
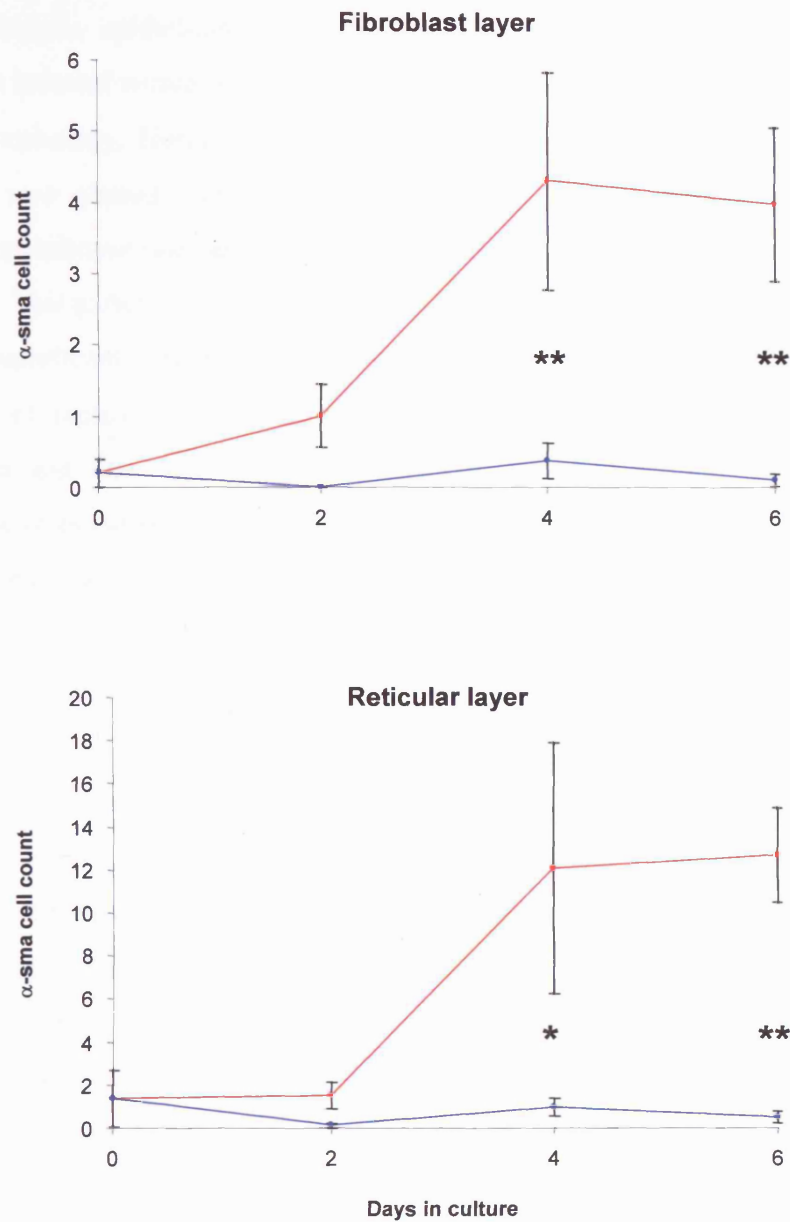


**Figure 7.14.** The number of  $\alpha$ -sma immunoreactive cells in the fibroblast layer (a) and reticular layer (b) over time, in the presence and absence of 10ng/ml TGF- $\beta_1$ . Each point represents the mean number of immunoreactive cells in the relevant layer in all discs examined at that time point (SEM also illustrated).

Significantly greater numbers of cells in TGF- $\beta_1$ + cultures:

\*\*  $p < 0.01$ ,

\*  $p < 0.05$

of the amniotic epithelium, and around cells of the reticular layer. The pattern of expression induced within the reticular layer mimics that observed in fetal membranes with altered morphology. However,  $\alpha$ -sma expression in the reticular layer was uncommon in the *ex-in vivo* altered morphology biopsies, and Tn-C expression along the amniotic basement membrane was only observed consistently in the amnion of the first and second trimesters. This pattern of expression was induced in 2 out of 6 cultures. In the remaining 4 cultures, significant cell death was observed, presumably due to tissue trauma from the technique of removal of the cellular layers. The mechanism of induction of  $\alpha$ -sma, osteonectin and Tn-C within these cultures may result from loss of paracrine signalling from the cytotrophoblast or decidual layers. It may alternatively result from the release of a local factor caused by the tissue trauma. The inconsistent induction of  $\alpha$ -sma and Tn-C expression at the edges of discs also supports the hypothesis that tissue damage may induce myofibroblast differentiation in the fetal membranes.

Addition of TGF- $\beta_1$  to the culture also induced expression of  $\alpha$ -sma, Tn-C and osteonectin. All three proteins were induced in both the fibroblast and reticular layers. Amniotic basement membrane staining for Tn-C was not observed. Again the pattern induced in the reticular layer mimic that observed in altered morphology fetal membranes, although  $\alpha$ -sma expression was induced in a lesser proportion of reticular layer cells in comparison to the removal of cytotrophoblast and decidua, and in comparison to the *ex-in vivo* biopsies. However, all three proteins were also induced in the fibroblast layer, which was rarely observed in *ex-in vivo* biopsies. Addition of TGF- $\beta_1$  also caused significant amniotic epithelial damage. The pattern induced by TGF- $\beta_1$  differs from that induced by removal of the cellular layers, suggesting that TGF- $\beta_1$  is not the factor released by tissue trauma in the latter technique, or if it is, then its response is modified by the release of other factors, or that its release is confined to specific layers of the membrane.

A number of morphological and histological changes were induced in the fetal membranes during 6 days in culture. The phenomenon of amniotic epithelium proliferating and growing over the cut edge of membrane has previously been described in fetal membrane organ culture (Devlieger *et al.*, 2000), when it was reported in 25% of cultures at Day 8 and 78.5% of cultures at Day 10, compared to 45% at Day 6 in this study. An associated loss of tissue architecture and increase in number of pyknotic cells at the cut membrane edge was also described (Devlieger *et al.*, 2000). Additionally, the current study has

described decidual necrosis, adjacent to the cytotrophoblast layer. This is the innermost part of the disc, and suggests insufficient diffusion of oxygen and nutrients into the central part of the disc. The morphological changes induced in the current work were induced in all cultures performed, and were characterised by increased thickness of the connective tissue layers of the amnion and chorion, and marked distension of the spongy layer. Reduction in the diameter of the disc was observed, although this did not explain the increase in connective tissue layer thickness. The increased connective tissue thickness was comparable to that observed in the 'Altered Morphology' membranes compared to midzone at term, yet the changes observed *in vitro* occurred in all cultures, and were not associated with culture conditions demonstrated to induce  $\alpha$ -sma expression. Additionally, there was no change in the thickness of the cellular layers of the discs. No additional morphological changes, or changes in the disc diameter, were observed in culture conditions demonstrated to induce  $\alpha$ -sma expression within the fetal membranes.

## 7.6. Conclusions

- $\alpha$ -sma, osteonectin and tenascin-C expression in the reticular layer of the chorion may be induced by tissue trauma, or by TGF- $\beta_1$ .
- $\alpha$ -sma, osteonectin and tenascin-C expression in the fibroblast layer is induced by TGF- $\beta_1$ . Tissue trauma induces  $\alpha$ -sma expression in the fibroblast layer and Tn-C expression along the amniotic basement membrane.
- The fetal membrane organ culture model employed in this study induced increased thickness of the connective tissue layers of the fetal membranes.
- It was not possible to induce morphological changes in the fetal membranes in association with induction of myofibroblast differentiation.

## **Chapter 8**

### **Myofibroblast differentiation, osteonectin and tenascin expression during fetal membrane development**

#### **8.1. Introduction**

The work in the previous chapters has established a cellular phenotype in the connective tissue layers of the fetal membranes overlying the cervix prior to labour at term, and within the rupture line following labour and delivery, associated with characteristic fetal membrane morphology:

- Extreme altered morphology, characterised by increased connective tissue layer thickness and decreased cellular layer thickness.
- Increased proportions of cells in the reticular layer of the chorion expressing  $\alpha$ -sma and osteonectin.
- Increased immunoreactive tenascin-C within the extracellular matrix of the reticular layer of the chorion.

It is therefore hypothesised that these changes develop within a restricted area of the fetal membranes, centred over the internal os of the cervix, during late pregnancy. Examination of the expression of these proteins and their relationship to the morphology and stage of development of the fetal membranes may provide evidence to support or refute this hypothesis.

#### **8.2. Aims**

- To examine the morphology of the fetal membranes throughout pregnancy.
- To determine the expression of  $\alpha$ -sma, osteonectin and tenascin-C in the connective tissue layers of the amnion and chorion throughout pregnancy.
- To examine the relationship between myofibroblast phenotype and fetal membrane morphology throughout pregnancy.

## **8.3. Materials and Methods**

### **8.3.1 Tissue samples**

Fetal membrane samples were obtained from first and second trimester surgical termination of pregnancy (n=12), and from preterm prelabour Caesarean sections (n=20) as previously described (2.1.2. & 2.1.3.). Midzone and 'extreme altered morphology' fetal membrane biopsies obtained prior to labour at term (n=10) were as previously used in Chapter 4.

### **8.3.2 Immunohistochemistry**

Immunohistochemistry was carried out on formalin-fixed wax-embedded tissue samples, using monoclonal antibodies to vimentin, desmin, osteonectin, tenascin-C, CD68, cytokeratin,  $\alpha$ -sma,  $\gamma$ -sma and smooth muscle myosin as previously described (2.3.).

### **8.3.3. *In situ* hybridisation**

*In situ* hybridisation was performed using probes to all isoforms of tenascin-C and to large isoforms of tenascin-C (2.6.).

### **8.3.4. Image analysis**

Haematoxylin and eosin stained tissue sections were examined by light microscopy, and the thickness of the constituent layers measured (2.8.1.1.). The number of immunoreactive cells was counted as previously described (2.8.1.2.).

### **8.3.5. Statistical analysis**

Statistical methods used to correlate the parameters measured, and to compare proportions of immunoreactive cells are described in section 2.9.

## **8.4. Results**

### **8.4.1. Fetal membrane morphology**

Examination of haematoxylin and eosin stained sections of the membrane biopsies demonstrated characteristic histological features of the amnion, chorion, amniochorion,

and amniochorio-decidua throughout gestation. Free amnion biopsies (n=5) were obtained at 8-13 weeks gestation. This may be because the amnion and chorion were still unfused in the pregnancy, or due to traumatic separation of amnion and chorion laeve during the termination of pregnancy. Significant variation in the histological appearance was observed. Some amnion biopsies (n=3, gestations 8, 9 and 10 weeks) had a 'tramline' appearance of amniotic epithelium, and a single layer of cells within the fibroblast layer, with an intervening very thin compact layer (**Figure 8.1a**). Other amnion biopsies (n=2, gestations 12 and 13 weeks) were thicker, with a multilayered fibroblast layer (**Figure 8.1b**). The single cell thickness appearance of the amniotic epithelium confirmed that this appearance is not artefact due to oblique sectioning.

Chorion laeve biopsies (n=5) were obtained at 9-13 weeks gestation. As for the amnion, the possibility of traumatic separation of amnion and chorion during the termination was considered. Particular care was taken to distinguish chorion laeve from chorionic plate. Chorionic plate was distinguished by the presence of blood vessels within the connective tissue, and by villi projecting from the cytotrophoblast layer (**Figure 8.2a**). Chorion laeve consisted of a layer of connective tissue, the reticular layer, with an attached cytotrophoblast layer. This varied from 1-3 cells thick, with occasional degenerate villi (**Figure 8.2b**). An apparent cleft within the cytotrophoblast layer was observed in one sample at 13 weeks gestation. Remnants of decidua capsularis were also identified on the same biopsy (**Figure 8.2c**).

Fused amniochorion (n=4) was obtained at 12, 15, 16 and 20 weeks gestation. This consisted of amnion, spongy layer, and chorion laeve, with cytotrophoblast layer and occasional degenerate villi (**Figure 8.3a&b**). The cytotrophoblast layer varied from 1-5 cells thick, with apparent 'clefts' within the layer observed in 3 out of 4 samples (12, 15 and 16 weeks gestation). Remnants of decidua capsularis were identified on all 4 samples, commonly necrotic in appearance (**Figure 8.3a&b**). Decidua parietalis was not observed on any of these samples.

Amniochoriodecidua, that is normally termed 'fetal membrane', was examined from 20 pregnancies from 25-36 weeks gestation. These all had attached decidua parietalis (**Figure 8.3c**).

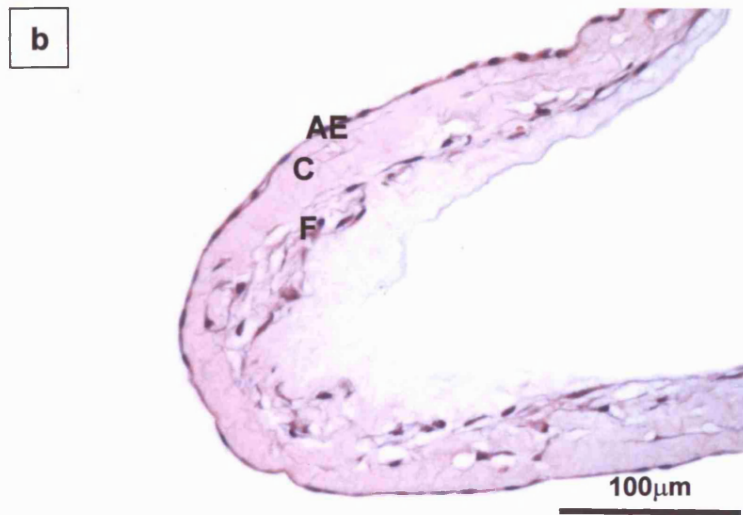
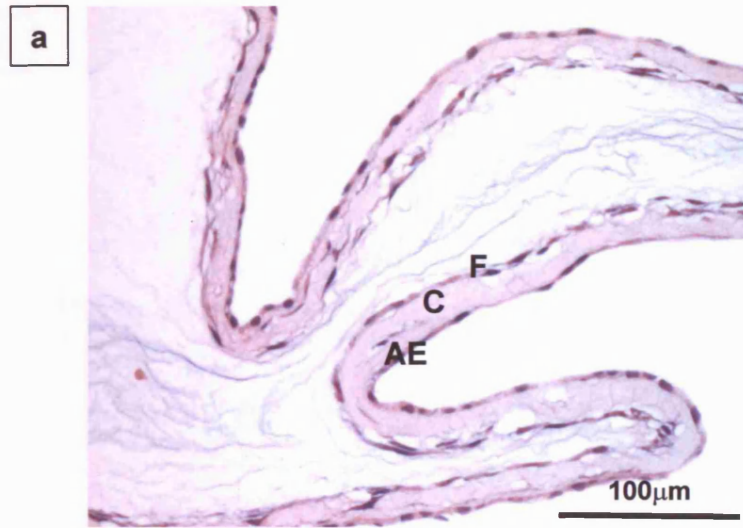


**Figure 8.1.** Haematoxylin and eosin stained sections of first trimester amnion, illustrating the range of morphology identified. The amniotic epithelium (AE), compact layer (C) and fibroblast layer (F) are highlighted.

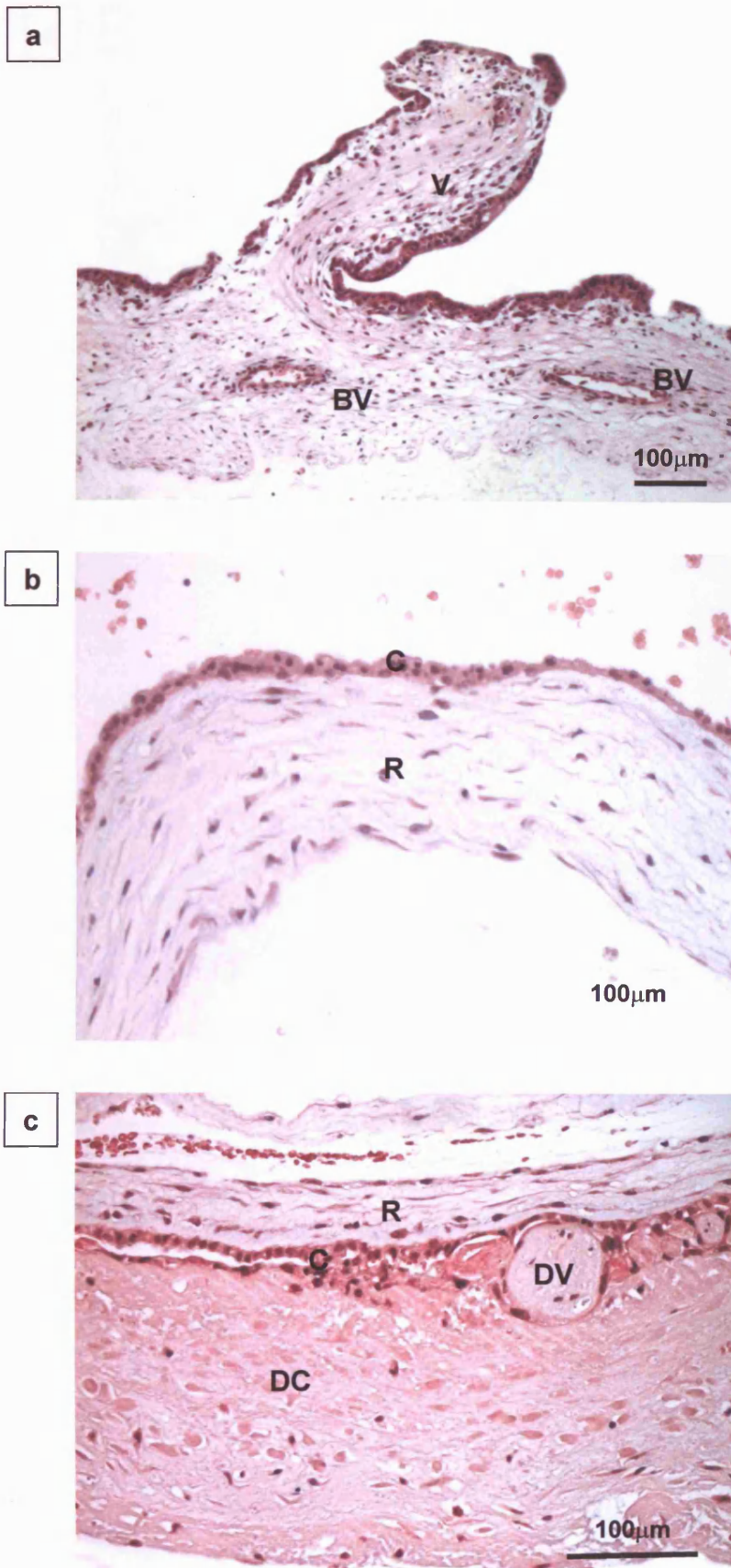


**Figure 8.2.** Haematoxylin and eosin stained sections of first trimester chorionic plate (a) and chorion laeve (b&c). The chorionic plate is characterised by the presence of blood vessels (BV) and villi (V). A range of morphology of chorion laeve was identified. The reticular layer (R), cytotrophoblast layer (C), a degenerate villus (DV) and decidua capsularis (DC) are illustrated.

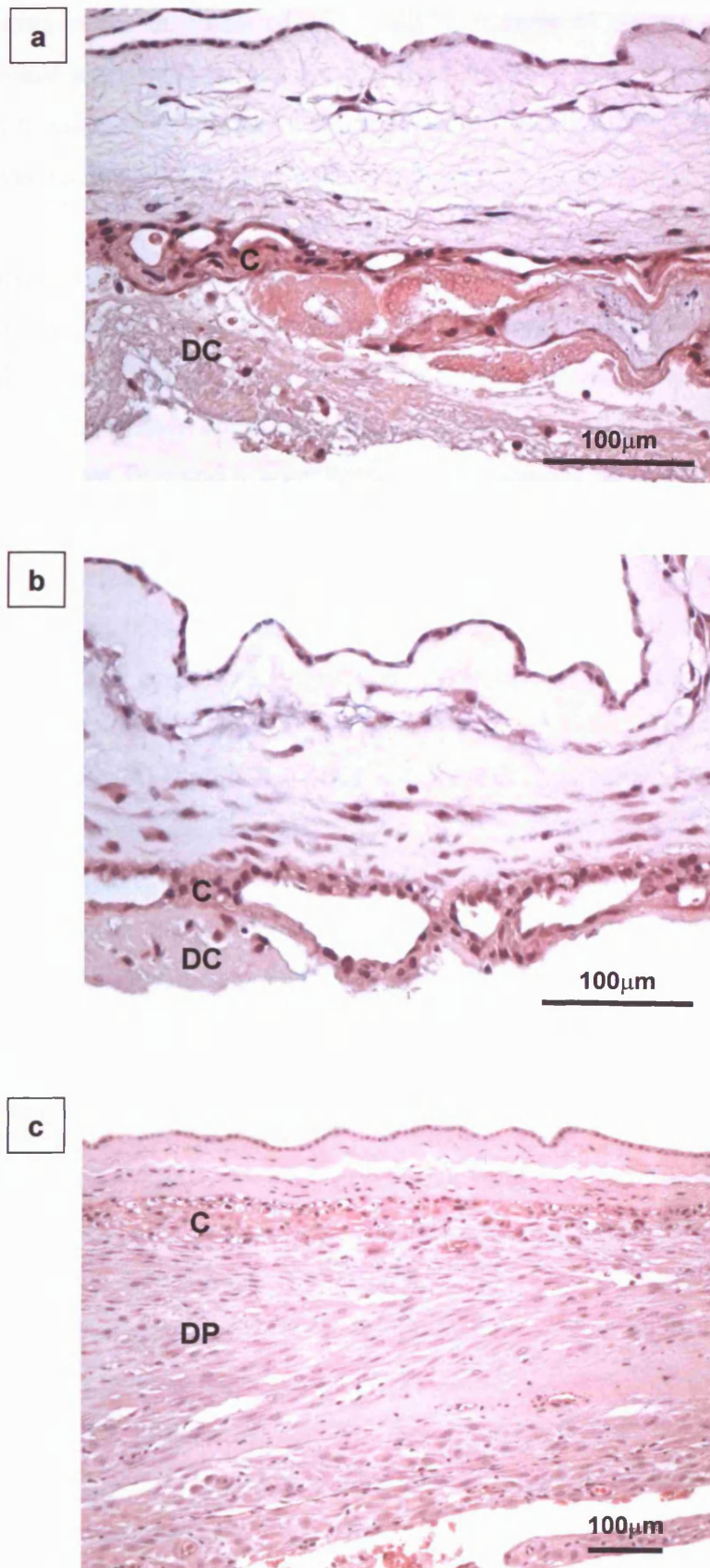


**Figure 8.3.** Haematoxylin and eosin stained sections of second trimester amniochorion (a&b) and preterm fetal membrane (c). Remnant of decidua capsularis (DC) are attached to the amniochorion. The amniochorion has fused to the decidua parietalis (DP) in the third trimester fetal membranes. The cytotrophoblast layer (C) is also illustrated.

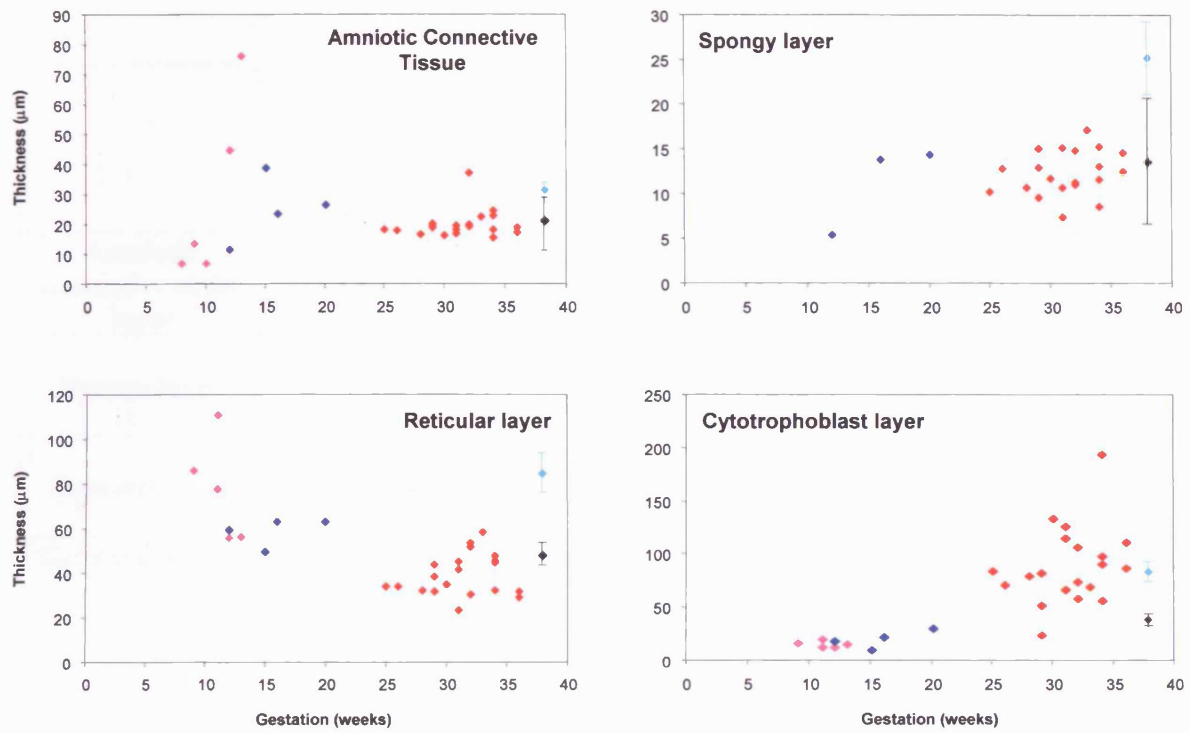
Measurements of the thickness of each individual layer of the membranes were plotted over the whole gestational period. Results from midzone and 'Altered Morphology' fetal membrane biopsies from elective Caesarean section (n=10) from Chapter 4 were used as reference values for 'normal' term fetal membranes.

The thicknesses of the amniotic connective tissue, spongy layer, reticular layer and cytotrophoblast layer are plotted in Figure 8.4. Although a gradual change in thickness of the individual layers with gestation is observed, fusion of the amnion with the chorion *per se* does not appear to exert an influence on the thickness. Comparison between morphology data obtained from first and second trimester membranes prior to and following amnio-chorial fusion did not reveal any significant differences. In contrast, fetal membranes obtained after fusion with the decidual parietalis appeared to exhibit different thickness characteristics than those prior to decidual fusion. Statistical comparisons were therefore made between 1<sup>st</sup>/2<sup>nd</sup> trimester samples, and 3<sup>rd</sup> trimester fetal membranes.

Results are shown in Table 8.1. The morphology measurements for the preterm 3<sup>rd</sup> trimester fetal membranes are very similar to term midzone fetal membranes, with no significant differences in the thickness of any layer between these two groups. The measurements for the preterm 3<sup>rd</sup> trimester samples thus have a similar relationship to term 'extreme altered morphology' fetal membranes as term midzone fetal membranes; the amniotic connective tissue layer, spongy layer and reticular layer are all significantly thinner, and the cytotrophoblast layer significantly thinner, than term 'extreme altered morphology' biopsies. The 1<sup>st</sup> /2<sup>nd</sup> trimester samples show mixed morphology characteristics. The thickness of the amniotic connective tissue layer varies widely. The spongy layer (found only in fused amniochorion samples) appears thin, comparable to term midzone samples. In contrast, the reticular layer is of comparable thickness to term 'extreme altered morphology' fetal membranes, and is thus significantly thicker than in both 3<sup>rd</sup> trimester preterm and term midzone fetal membranes. The cytotrophoblast layer in the 1<sup>st</sup>/2<sup>nd</sup> trimester samples is, however, significantly thinner than in the term 'extreme altered morphology' fetal membranes, and thus also than in 3<sup>rd</sup> trimester preterm and term midzone fetal membranes.

#### **8.4.2. Fetal membrane cellularity**

The number of cells within the amniotic epithelium, fibroblast layer, and reticular layer were counted, the cellular densities within the fibroblast and reticular layers calculated, and



#### Legend

- Free amnion/chorion laeve
- Amniochorion
- Preterm 'fetal membrane'
- Term 'midzone'
- Term 'extreme altered morphology'

**Figure 8.4.** Thickness measurements of the component layers of free amnion, free chorion, amniochorion, and 'fetal membrane' biopsies obtained throughout gestation. Each point represents the mean of 10 fields measured for each biopsy. All measurements are in  $\mu\text{m}$ . Mean ( $\pm\text{SEM}$ ) values for term 'extreme altered morphology' and 'midzone' fetal membranes (from Chapter 4) are shown for comparison.

	<b>1<sup>st</sup>/2<sup>nd</sup> trimester (n=9)</b>	<b>3<sup>rd</sup> trimester preterm 'FM' (n=20)</b>	<b>Term 'midzone' (n=10)</b>	<b>Term 'ZAM' (n=10)</b>
<b>Amniotic connective tissue layer</b>	27.80 ±7.57	20.04 <sup>a</sup> ±1.04	21.39 <sup>b</sup> ±9.04	31.57 <sup>a, b</sup> ±2.11
<b>Spongy layer</b>	11.26 ±2.90	12.38 <sup>c</sup> ±0.56	13.95 <sup>d</sup> ±7.32	25.67 <sup>c, d</sup> ±4.17
<b>Reticular layer</b>	69.22 <sup>e, f</sup> ±6.45	39.46 <sup>e, g</sup> ±2.09	47.39 <sup>f, h</sup> ±4.74	85.62 <sup>g, h</sup> ±9.21
<b>Cytotrophoblast layer</b>	18.00 <sup>i, j, k</sup> ±2.07	89.22 <sup>i, l</sup> ±8.14	83.01 <sup>j, m</sup> ±6.98	40.91 <sup>k, l, m</sup> ±4.93

**Table 8.1.** Thickness of the component layers of the amnion, chorion and amniochorion throughout gestation. All measurements are shown in  $\mu\text{m}$  (mean  $\pm$  SEM). Comparisons were made using t-tests, and significant differences are shown: **a, b, c, e, g, h, i, j, k, l, m**, all  $p < 0.01$ . **d, f**, both  $p < 0.05$

the relationship between the amniotic epithelial cells and fibroblast layer cells calculated (Table 8.2). The changes in the cellularity of the layers of the fetal membrane throughout gestation are shown in Figure 8.5. The number of fibroblast and reticular layer cells decreased throughout gestation such that the number of cells within these layers in the first and second trimesters was significantly higher than in the respective layers in term midzone fetal membranes. The thickness of the amniotic connective tissue layer also decreased through gestation (section 8.4.1.), although less so than the proportional decrease in the fibroblast layer cell count, as evidenced by the decrease in the fibroblast layer cell density through gestation. The number of amniotic epithelial cells per computer screen width increased between the 1<sup>st</sup>/2<sup>nd</sup> and 3<sup>rd</sup> trimesters (Table 8.2). The ratio of amniotic epithelial cells to fibroblast layer cells therefore increased markedly throughout gestation. The fall in the number of reticular layer cells throughout gestation matched the change in the thickness of the reticular layer (8.4.1.); thus the reticular layer cell density remained constant until term, when a significant fall was observed.

### **8.4.3. Cellular phenotype**

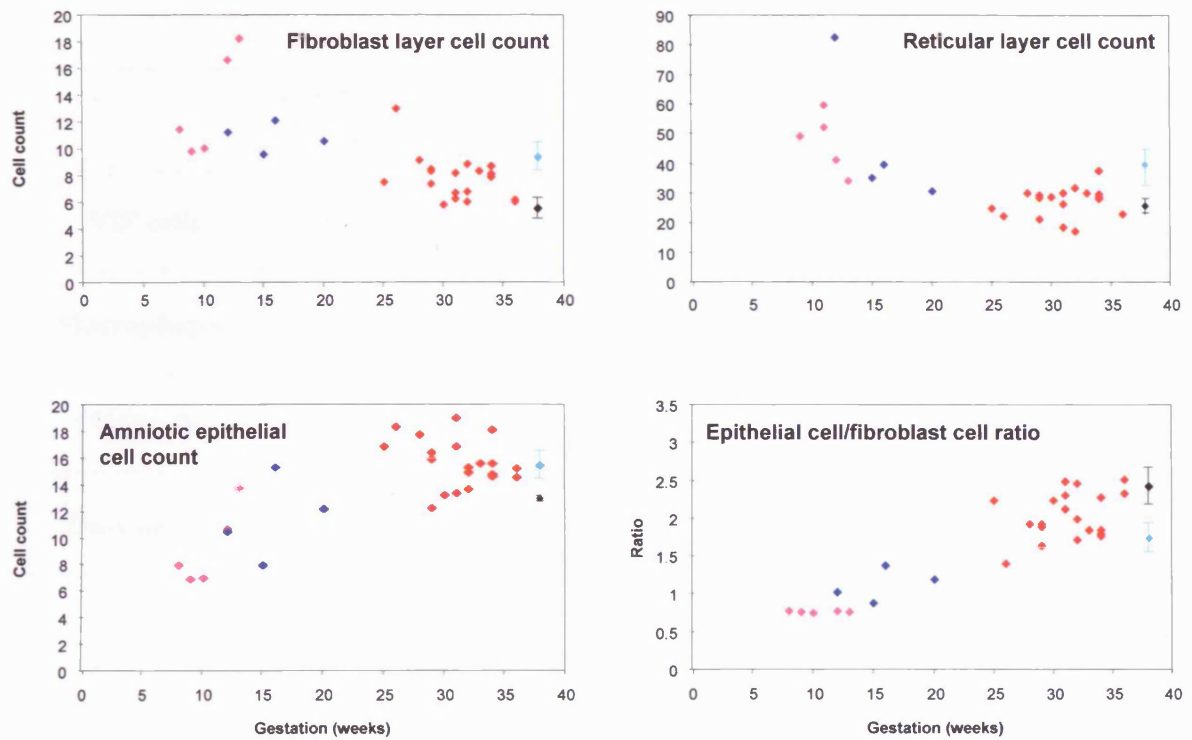
The total cell number within the fibroblast layer and reticular layer changed throughout gestation (8.4.2.), therefore expression of  $\alpha$ -sma, desmin and CD68 by cells within these layers was examined by looking at the percentage of the total cell number expressing the marker.

#### **8.4.3.1. Amnion**

The cellular population of the fibroblast layer of the amnion consisted of macrophages and fibroblasts ('V' cells), with a small proportion of cells which expressed either desmin ('VD' cells) or  $\alpha$ -sma ('VA' cells) (Table 8.3). The proportion of macrophages (CD68 immunoreactive) within the fibroblast layer was significantly lower in the 1<sup>st</sup> and 2<sup>nd</sup> trimester samples (7.15%), compared to the 3<sup>rd</sup> trimester preterm samples (19.77%). Rare cells expressed desmin within the fibroblast layer; the proportion was greatest in the 1<sup>st</sup> and 2<sup>nd</sup> trimester samples (9.16%). This represented a wide range of expression within this group, from 0-28% of cells. Throughout gestation rare cells within the fibroblast layer expressed  $\alpha$ -sma. The wide range of percentages, especially in the 1<sup>st</sup> and 2<sup>nd</sup> trimesters, is indicative of 3 samples (1 free amnion, 2 fused amniochorion) with high  $\alpha$ -sma expression (maximum 53.9% of cells). These three samples also had a high percentage of desmin expression (though there was no overall correlation between the proportion of desmin

	1 <sup>st</sup> /2 <sup>nd</sup> trimester (n=9)	3 <sup>rd</sup> trimester preterm 'FM' (n=20)	Term midzone (n=10)	Term 'ZAM' (n=10)
<b>Amniotic epithelial cells</b>	10.26 <sup>a, b, d</sup> ±1.02	15.64 <sup>a, c</sup> ±0.41	13.00 <sup>b, c</sup> ±0.32	15.42 <sup>d</sup> ±1.16
<b>Fibroblast layer cell count</b>	12.21 <sup>e, f</sup> ±1.04	7.83 <sup>e, g</sup> ±0.36	5.68 <sup>f, g, h</sup> ±0.71	9.47 <sup>h</sup> ±1.01
<b>Reticular layer cell count</b>	47.49 <sup>i, j</sup> ±5.43	27.29 <sup>i, k</sup> ±1.12	26.69 <sup>i, l</sup> ±2.35	39.78 <sup>k, l</sup> ±4.90
<b>AE/Fib cell ratio</b>	0.93 <sup>m, n, q</sup> ±0.08	2.04 <sup>m, o</sup> ±0.07	2.43 <sup>n, o, r</sup> ±0.72	1.77 <sup>q, r</sup> ±0.21
<b>Fibroblast layer cell density</b>	38.05 <sup>s, t, u</sup> ±6.53	24.66 <sup>s, v</sup> ±1.49	17.12 <sup>s, v</sup> ±1.63	19.72 <sup>u</sup> ±4.57
<b>Reticular layer cell density</b>	43.18 ±4.37	44.87 <sup>w, x</sup> ±2.00	37.32 <sup>w</sup> ±2.77	34.38 <sup>x</sup> ±4.19

**Table 8.2.** Cell counts of component layers of the fetal membrane throughout gestation. Fibroblast and reticular layer cell counts were assessed by immunoreactivity to vimentin. Figures given are mean ± SEM. Cell counts are expressed per computer screen width (176µm). Cell densities are per 0.01mm<sup>2</sup>. Comparisons were made using t-tests and significant differences are shown: a, c, d, e, f, g, h, i, j, k, m, n, p, s, t, v, all p<0.01. b, l, o, r, u, w, x, all p<0.05.



#### Legend

- Free amnion/chorion laeve
- Amniochorion
- Preterm 'fetal membrane'
- Term 'midzone'
- Term 'extreme altered morphology'

**Figure 8.5.** Cell counts of the component layers of the fetal membrane throughout gestation. Each point represents the mean of 10 fields measured for each biopsy. Cell counts are per computer screen width (176 $\mu$ m). Mean ( $\pm$ SEM) values for term 'extreme altered morphology' and 'midzone' fetal membranes (from Chapter 4) are shown for comparison.

	1 <sup>st</sup> /2 <sup>nd</sup> trimester (n=9)	3 <sup>rd</sup> trimester preterm 'FM' (n=20)	Term 'midzone' (n=10)	Term 'ZAM' (n=10)
'VD' cells	9.16 <sup>a</sup> ±3.57	1.81 <sup>a</sup> ±0.64	2.34 ±1.86	6.04 ±4.86
Macrophages	7.15 <sup>b</sup> ±1.19	19.77 <sup>b</sup> ±2.68	15.89 ±4.02	13.90 ±2.95
'VA' cells	9.78 <sup>c</sup> ±5.81	1.35 <sup>c, d</sup> ±0.66	1.55 ±1.15	9.88 <sup>d</sup> ±4.88
Osteonectin	17.21 <sup>e, f</sup> ±4.09	1.48 <sup>e, g</sup> ±0.51	3.01 <sup>f</sup> ±1.08	10.74 <sup>g</sup> ±4.56
'V' cells	79.23 ±6.34	77.48 ±2.67	80.66 ±3.50	75.19 ±5.85

**Table 8.3.** Percentage cell populations in the fibroblast layer of the amnion throughout gestation. Figures shown are mean ± SEM. The cell percentages calculated from counting the number of immunoreactive cells for the cell marker, and expressing that as a percentage of the vimentin immunoreactive cell count for the biopsy. The proportion of 'V' cells was deduced by subtraction of the proportion of macrophages and 'VD' or 'VA' cells (whichever is higher) from the total vimentin immunoreactive population. Comparisons were made using t-tests and significant differences are shown: a, b, e, f, g, all p<0.01. c, d, both p<0.05

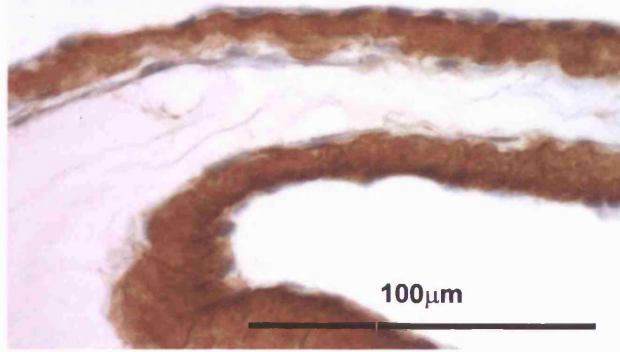
positive cells and the proportion of  $\alpha$ -sma positive cells). The single free amnion exhibiting a high level of  $\alpha$ -sma expression in the fibroblast layer (16.1%) was the biopsy with greatest connective tissue thickness. There were no consistent phenotypic or clinical features in common between these samples. The proportion of osteonectin immunoreactive cells also decreased with gestation. Preterm 3<sup>rd</sup> trimester samples had a similar proportion of osteonectin immunoreactive cells to term midzone samples.

A distinct and consistent pattern of tenascin-C immunoreactivity was observed in the 1<sup>st</sup> and 2<sup>nd</sup> trimester amnion, using a monoclonal antibody (BC-24) which detected all isoforms of tenascin-C. A thick band of immunoreactive tenascin-C was detected along the amniotic basement membrane, with some apparent diffusion of immunoreactive material into the adjacent compact layer and fibroblast layer (**Figure 8.6**). In preterm 3<sup>rd</sup> trimester fetal membranes, a fine line of tenascin-C immunoreactivity was detected along the amniotic basement membrane, varying from a continuous line to intermittent short patches of immunoreactivity (**Figure 8.6**). Amongst the term midzone and 'extreme altered morphology' fetal membrane biopsies, short patches of tenascin-C immunoreactivity were detected along the amniotic basement membrane in 9 out of 19 midzone and 10 out of 19 'extreme altered morphology' biopsies (**Figure 8.6**). The presence/absence of this immunoreactivity at term was largely patient specific, with 79% concordance in presence/absence of staining between paired midzone/'extreme altered morphology' biopsies. In order to identify the cell type which produced tenascin-C in the 1<sup>st</sup> and 2<sup>nd</sup> trimesters, *in situ* hybridisation was carried out on a 1<sup>st</sup> trimester amnion sample, and a 2<sup>nd</sup> trimester amniochorion sample, using probes to total tenascin-C, and to large isoform tenascin-C (2.6.). No positive cells could be identified.

#### **8.4.3.2. Chorion**

The cellular population of the reticular layer of the chorion consisted of macrophages (CD68 immunoreactive), myofibroblasts ('VD' cells and 'VDA' cells), and fibroblasts ('V' cells) (**Table 8.4**). The proportion of macrophages changed little through gestation. The highest proportion of macrophages was observed in the preterm 3<sup>rd</sup> trimester fetal membranes, significantly higher than in the 1<sup>st</sup>/2<sup>nd</sup> trimester and the term 'extreme altered morphology' fetal membranes (11.63%, 5.32% and 4.21% respectively). The proportion of fibroblasts ('V' cells) remained constant throughout gestation. The proportion of 'VD' myofibroblasts changed little through gestation. In contrast, 90% of cells in the 1<sup>st</sup> and 2<sup>nd</sup>

a



b

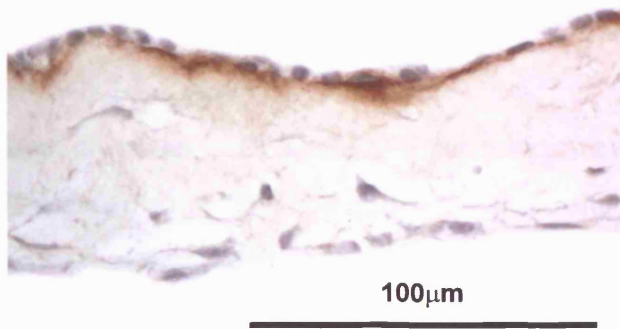


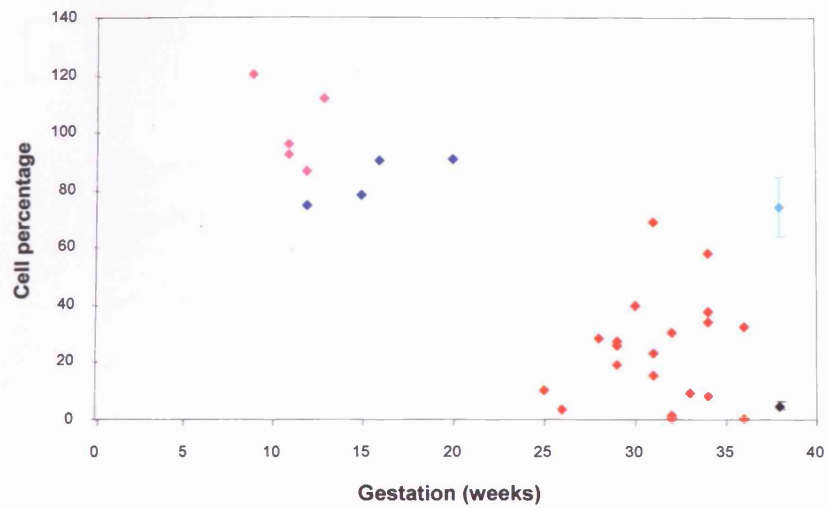
**Figure 8.6.** Tenascin-C immunoreactivity within first trimester free amnion. Immunoreactivity is observed along the amniotic basement membrane, diffusing into the underlying compact layer in (a).

	1 <sup>st</sup> /2 <sup>nd</sup> trimester (n=9)	3 <sup>rd</sup> trimester preterm 'FM' (n=20)	Term 'midzone' (n=10)	Term 'ZAM' (n=10)
'VD' cells	70.71 ±3.88	66.28 ±2.14	62.76 ±6.66	72.09 ±6.53
Macrophages	5.32 <sup>a</sup> ±1.36	11.63 <sup>a, b</sup> ±1.47	7.87 ±2.16	4.21 <sup>b</sup> ±0.74
'VDA' cells	93.43 <sup>c, d, e</sup> ±4.90	23.81 <sup>c, f</sup> ±4.19	5.20 <sup>d, g</sup> ±1.75	72.66 <sup>c, f, g</sup> ±10.00
Osteonectin	26.15 <sup>h, i, j</sup> ±3.86	3.21 <sup>h, k</sup> ±0.85	4.82 <sup>i, l</sup> ±1.48	43.90 <sup>h, k, l</sup> ±6.02
'V' cells	5.67 <sup>m, n, o</sup> ±2.34	22.09 <sup>m</sup> ±2.37	29.74 <sup>n</sup> ±6.35	26.12 <sup>o</sup> ±4.63

**Table 8.4.** Percentage cell populations in the reticular layer of the chorion throughout gestation. Figures shown are mean ± SEM. The cell percentages calculated from counting the number of immunoreactive cells for the cell marker, and expressing that as a percentage of the vimentin immunoreactive cell count for the biopsy. The proportion of 'V' cells was deduced by subtraction of the proportion of macrophages and 'VD' or 'VA' cells (whichever is higher) from the total vimentin immunoreactive population. Comparisons were made using t-tests and significant differences are shown: **b, c, d, e, f, g, h, i, k, l, m, n, o**, all  $p < 0.01$ . **a, j**, both  $p < 0.05$ .

trimesters were  $\alpha$ -sma positive, a proportion similar to the 'extreme altered morphology' biopsies at term. The proportion of  $\alpha$ -sma positive cells in the midzone at term was just 5%. The change in the proportion of  $\alpha$ -sma cells throughout gestation is illustrated in **Figure 8.7**. There was wide variation in the proportion of  $\alpha$ -sma cells in the early 3<sup>rd</sup> trimester, varying from 0-69%, although all biopsies in this group exhibited morphology comparable to 'midzone' biopsies at term. The proportion of osteonectin positive cells in the 1<sup>st</sup> and 2<sup>nd</sup> trimesters was also comparable to that in the 'extreme altered morphology' biopsies at term. As  $\alpha$ -sma immunoreactivity was detected in reticular layer cells, immunohistochemistry for  $\gamma$ -sma and smooth muscle myosin was performed, to compare the cellular phenotype to that detected at term in Chapter 3. Immunoreactivity for  $\gamma$ -sma was detected in the majority of cells of the reticular layer in all biopsies of chorion laeve prior to fusion with the amnion (5 out of 5), and in a single fused amniochorion only (1 out of 4; the earliest gestation amniochorion obtained) (**Figure 8.8**). Immunoreactivity for smooth muscle myosin was not detected in reticular layer cells of any biopsy.

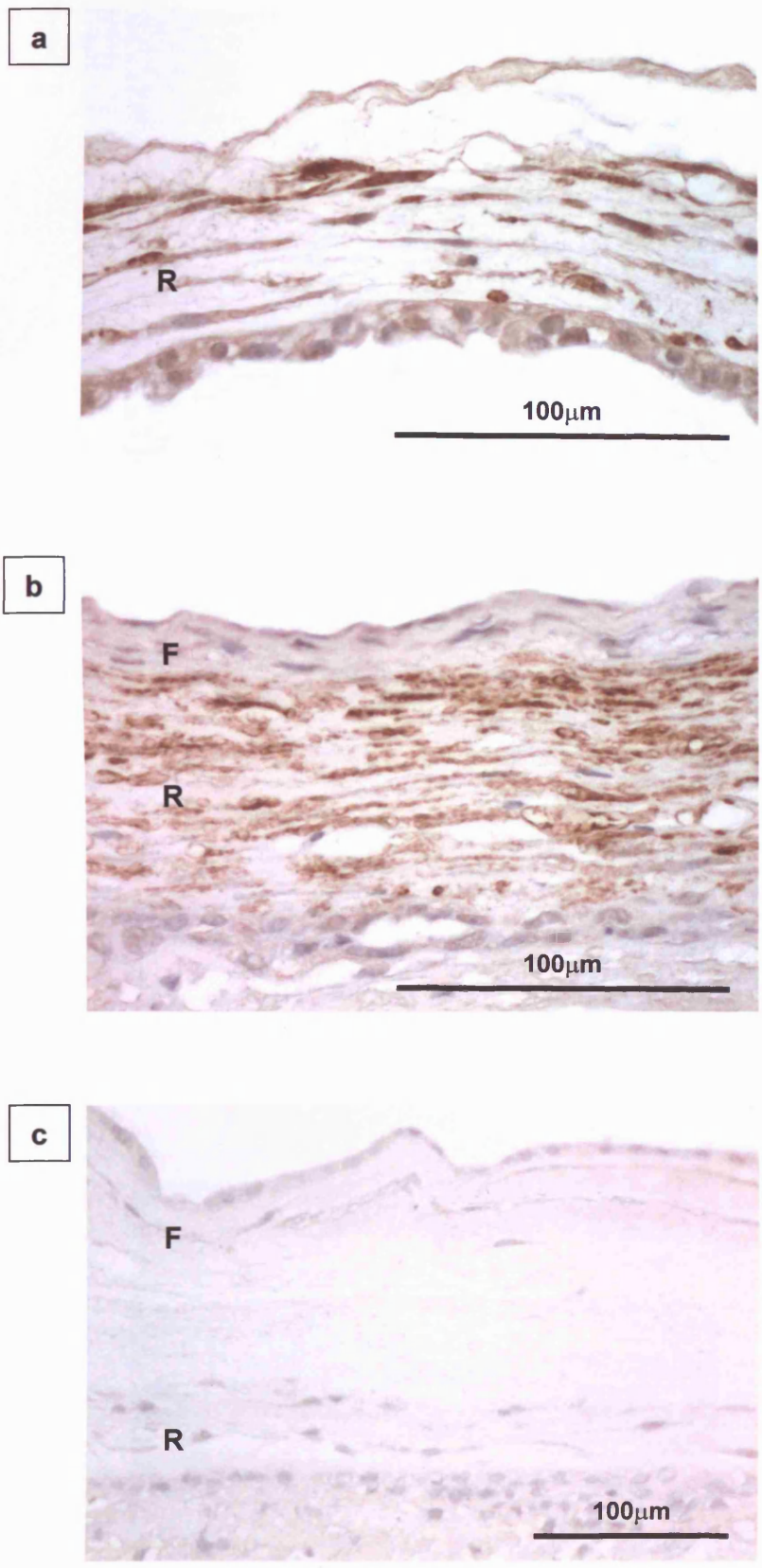
Tenascin-C immunoreactivity in the reticular layer of the chorion in the 1<sup>st</sup> and 2<sup>nd</sup> trimesters was detected in 7 out of 9 samples. It was completely absent from the reticular layer in 2 samples (9 weeks and 16 weeks gestation), restricted to small patches of immunoreactivity adjacent to the pseudobasement membrane in 6 samples, and was more extensive throughout the reticular layer in 1 sample (20 weeks gestation) (**Figure 8.9**). In 3<sup>rd</sup> trimester preterm fetal membrane samples, tenascin-C immunoreactivity within the reticular layer varied from complete absence, to intense immunoreactivity throughout the layer (**Figure 8.10**). This was assessed using a grading system validated on the results obtained by image analysis in Chapter 4. Thus a grade of 1 corresponded to a mean immunoreactivity of  $5.1 \pm 2.3\%$  (mean  $\pm$  SEM), grade 2  $15.1 \pm 4.3\%$ , grade 3  $31.5 \pm 3.7\%$  and grade 4  $53.2 \pm 3.5\%$  (totally absent, or grade 0, Tn-C immunoreactivity did not occur in any term fetal membrane samples), (**Figures 8.11 & 8.12a**). The first and second trimester samples consistently exhibited low immunoreactivity within the reticular layer, predominantly grade 0-2. Wide variation in immunoreactivity was exhibited by preterm midzone samples, comparable to term midzone samples (**Figure 8.12b**). The intensity of immunoreactivity did not correspond to the proportion of reticular layer cells immunoreactive for  $\alpha$ -sma (**Figure 8.12c**).



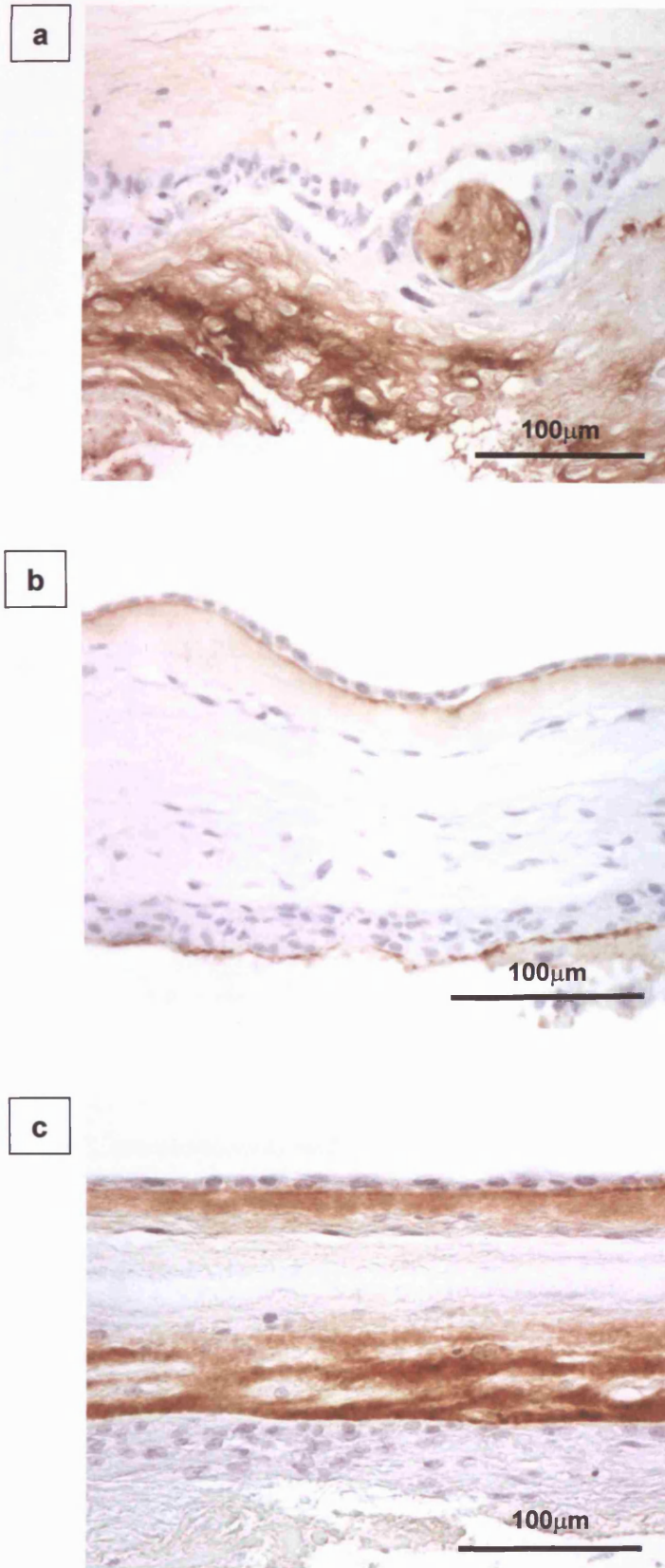
**Legend**

- Free amnion/chorion
- Amniochorion
- Preterm 'fetal membrane'
- Term 'midzone'
- Term 'extreme altered morphology'

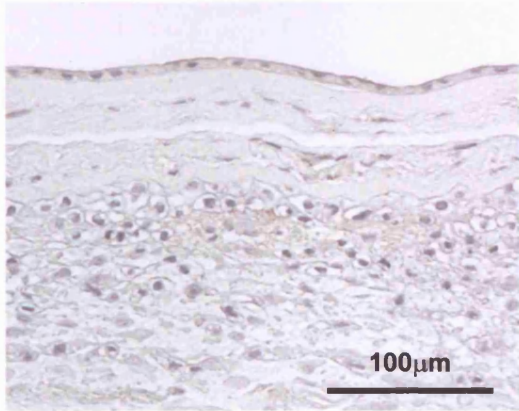
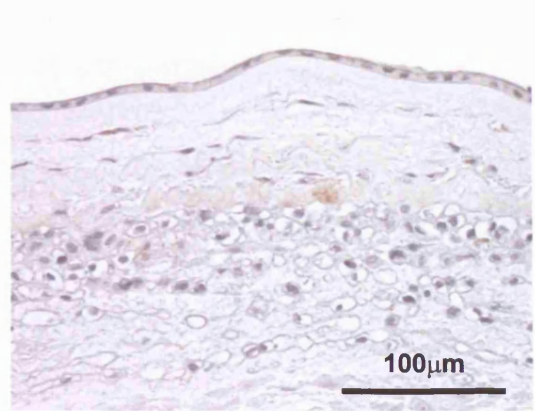
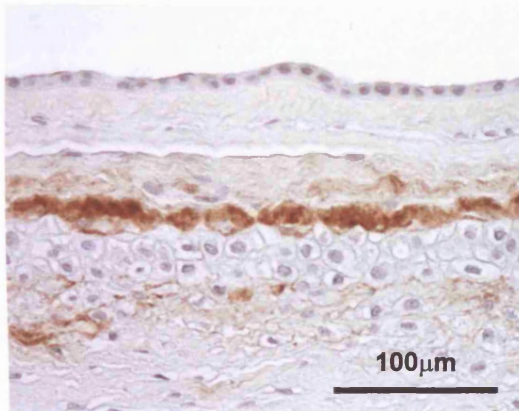
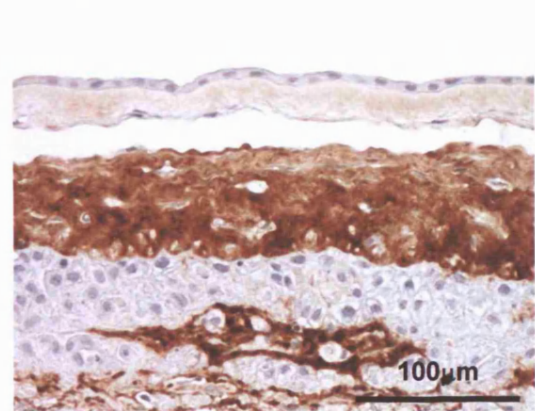
**Figure 8.7.** The changes in the percentage of 'VDA' cells within the reticular layer of the chorion throughout gestation. Each point represents the percentage of cells immunoreactive for  $\alpha$ -sma, calculated in relation to the number of cells in the reticular layer immunoreactive for vimentin. Mean ( $\pm$ SEM) values for term 'extreme altered morphology' and 'midzone' fetal membranes (from Chapter 4) are shown for comparison.



**Figure 8.8.** Immunoreactivity for  $\gamma$ -sma within first trimester free chorion (a), and second trimester amniochorion (b&c). Large numbers of immunoreactive cells were detected in the reticular layer (R) of all free chorion laeve biopsies (a) and in the earliest fused amniochorion biopsy (b) examined. Fibroblast layer (F) cells are negative for  $\gamma$ -sma. No immunoreactivity was detected in the remaining amniochorion biopsies (c).

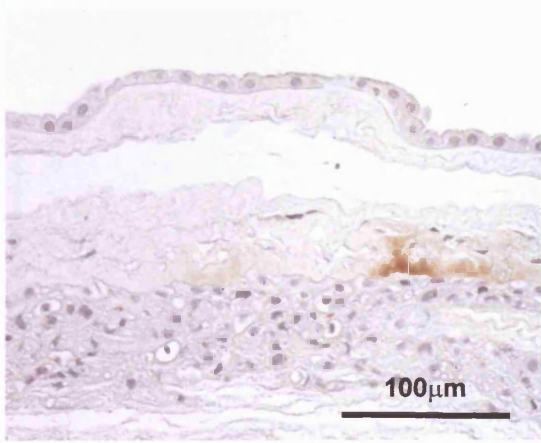


**Figure 8.9.** Tenascin-C immunoreactivity within pre-fusion free chorion laeve (**a**) and fused amniochorion (**b&c**). Minimal immunoreactivity is observed in the reticular layer of the free chorion laeve and 3 out of 4 samples of amniochorion (**a&b**). A single amniochorion biopsy at 20 weeks gestation exhibited intense reticular layer immunoreactivity (**c**). Immunoreactivity is also observed within a degenerate villus (**a**), and within the decidua capsularis (**a&b**).

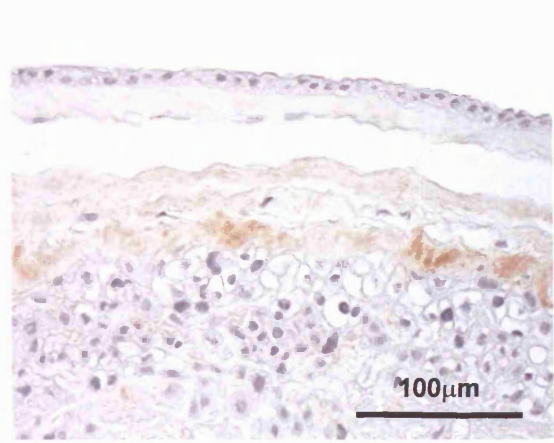
**a****b****c****d**

**Figure 8.10.** Tenascin-C immunoreactivity within preterm fetal membrane biopsies. A wide range of reticular layer immunoreactivity is observed, ranging from absent (**a**), through increasing levels (**b&c**) to intense (**d**).

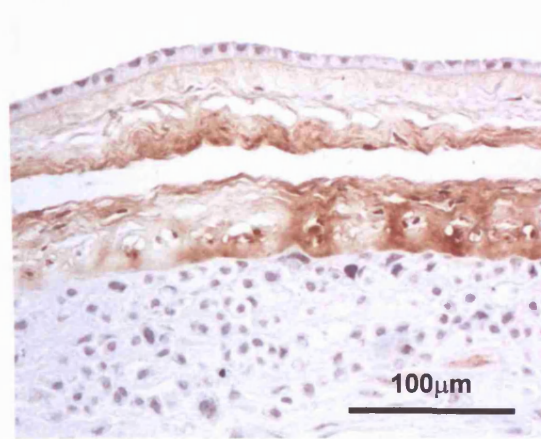
**a**



**b**



**c**



**d**

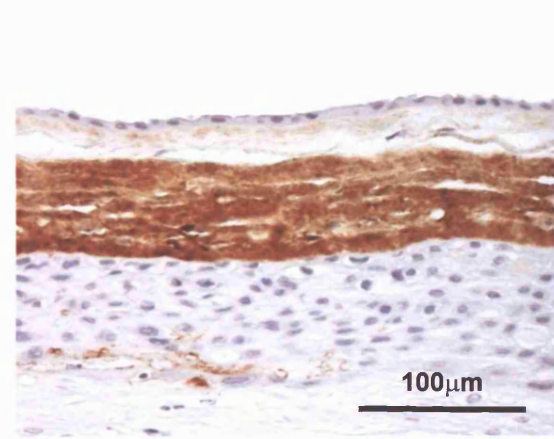


**Fig 8.11.** Tenascin-C immunoreactivity in term fetal membranes, demonstrating examples of Grade 1 (a), Grade 2 (b), Grade 3 (c), and Grade 4 (d) immunoreactivity within the reticular layer.



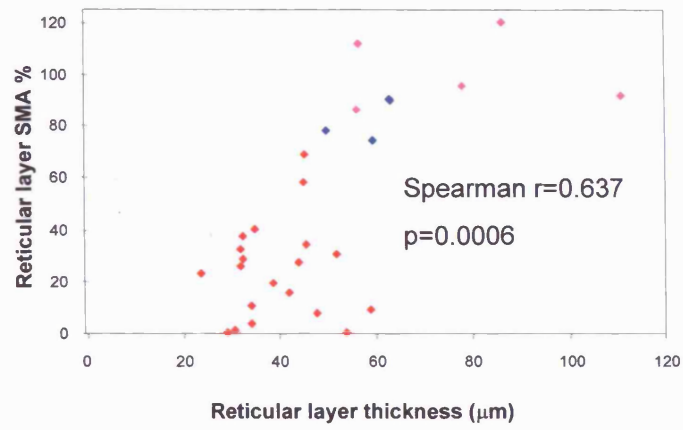
As no clear relationship between the proportion of  $\alpha$ -sma cells and gestation was observed between 25 weeks and 36 weeks, other parameters that may influence the cellular phenotype were considered. The proportion of  $\alpha$ -sma positive cells correlated with the thickness of the reticular layer, and inversely with the thickness of the cytotrophoblast layer (Figure 8.13).

## 8.5. Discussion

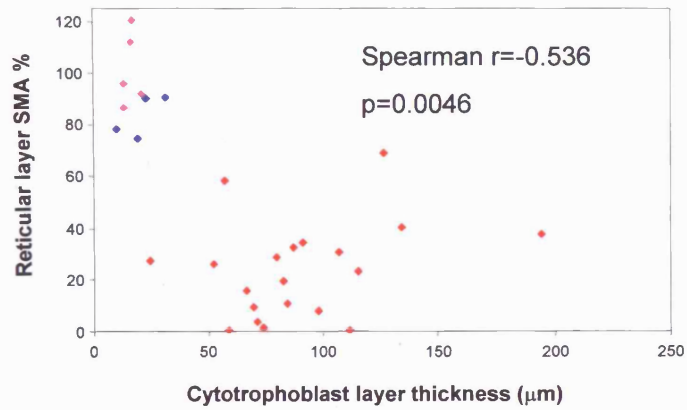
Studies on the ontogeny of any feature of the fetal membranes throughout gestation are limited by the range of tissue available. For this study, tissue was obtained from surgical termination of normal pregnancies during the first and second trimesters, up to 20 weeks gestation, although regional mapping of tissue was not possible. Tissue was not available between 20 and 25 weeks gestation from normal pregnancies. Elective Caesarean sections are performed at 38-39 weeks gestation in physiologically normal pregnancies, and tissue from term was therefore readily available. Prior to term, tissue was obtained from pre-labour Caesarean sections at 25-36 weeks gestation, performed for underlying fetal or maternal pathology. Regional mapping of fetal membrane biopsies was often not possible due to the technical difficulties in performing the Caesarean sections, especially at the earlier gestations. It is possible that the preterm fetal membranes obtained in this way may have been affected by the pathology that lead to the preterm delivery, although no consistent patterns were observed in association with any of the delivery groups (e.g. pre-eclampsia, intra-uterine growth restriction).

The literature is unclear with regards to the timing of fusion of amnion to chorion, and amniochorion to decidua. The earliest fused amniochorion observed in this study was at 12 weeks gestation. Free amnion and free chorion were obtained at 13 weeks of gestation, although this may have been due to traumatic separation of tissue during termination of pregnancy. Fused amniochorion was consistently obtained from 15 weeks onwards. These findings are compatible with amnio-chorial fusion at 12-14 weeks gestation, broadly in line with published estimates of 12 weeks (Benirschke & Kaufmann, 2000). No second trimester tissue was obtained with decidua parietalis attached, therefore the fusion of amniochorion with decidua is estimated at 20-25 weeks gestation from this study. This is later than one published estimate of 15-20 weeks (Benirschke & Kaufmann, 2000), and comparable to the alternative published estimate of 22-24 weeks (Moore & Persaud, 1998).

**a**



**b**



**Legend**

- Free amnion/chorion laeve
- Amniochorion
- Preterm 'fetal membrane'

**Figure 8.13.** The percentage of  $\alpha$ -sma immunoreactive cells within the reticular layer plotted against the thickness of the reticular layer (a) and the thickness of the cytotrophoblast layer (b). Each point represents the percentage of cells immunoreactive for  $\alpha$ -sma, calculated in relation to the number of cells in the reticular layer immunoreactive for vimentin.

The morphology and cellularity data obtained for the reticular layer demonstrates a reduction in the reticular layer thickness during gestation, with an accompanying decrease in cell number, thus giving a constant cell density. This is consistent with the occurrence of a stretch process throughout gestation. An early 'proliferation' phase followed by a late 'stretch' phase, has been previously suggested to occur within the amnion (Alger & Pupkin, 1986; Casey & MacDonald, 1996). The morphology data obtained from the amnion in this study did not support this. A very wide range of morphology data was observed during the first trimester, followed by little change in thickness during the remainder of pregnancy. A change in the amniotic epithelial: fibroblast cell ratio was observed throughout pregnancy, ranging from 0.7-0.8 in the first and second trimesters to 2.4 in the midzone at term. The methodology used within this study will inherently underestimate the amniotic epithelial: fibroblast cell ratio as it is based upon counting cytoplasmic staining for fibroblast cells, and nuclei of amniotic epithelial cells. This may explain the difference between the ratios obtained in this study and those quoted by Casey & MacDonald (1:1 in the first trimester, 10:1 at term) (Casey & MacDonald, 1996). The latter figure was based upon the numbers of cells extracted from the amniotic epithelial and fibroblast layers for cell culture experiments. Data examining the cell types within the fibroblast layer suggests an increase in the proportion of macrophages in the connective tissue layers of both amnion and chorion through gestation.

Overall, the chorion obtained during the first and second trimesters is similar to 'extreme altered morphology' fetal membranes at term, and not, as was anticipated, the midzone fetal membranes, both in terms of morphology (i.e. reticular layer and cytotrophoblast layer thickness) and cellular phenotype. During the first and second trimesters over 90% of cells express  $\alpha$ -sma and 26% express osteonectin, compared to 73% (Chapter 4) and 25-33% (Chapter 6) respectively in 'extreme altered morphology' fetal membranes at term. Critical differences between the chorion during 1<sup>st</sup> and 2<sup>nd</sup> trimesters compared to 'extreme altered morphology' at term are in expression of  $\gamma$ -sma (constitutive in the free chorion laeve only, mean 24% (range 2-61%) in rupture line fetal membranes following delivery at term), and in expression of Tn-C (low expression in 1<sup>st</sup> and 2<sup>nd</sup> trimesters, high expression in term 'extreme altered morphology'). During the third trimester, the morphology and cellular phenotype tend towards the feature of the midzone fetal membranes at term. The reticular layer thickness decreases, in conjunction with a reduction in  $\alpha$ -sma expression within the reticular layer, and an increase in the thickness of the cytotrophoblast layer.

The fetal membranes exist as free amnion and chorion prior to the first fusion at 12-15 weeks gestation, and subsequently fuse with the decidua parietalis at 20-25 weeks gestation. The hypothesis in 8.1., that the anatomically restricted morphological changes and cellular phenotype observed in the fetal membranes prior to the onset of labour at term develops during late pregnancy in the fetal membranes over the internal os of the cervix, would predict that all fetal membranes prior to this time would express a midzone phenotype (both in terms of morphology and cellular phenotype). However, the work within this chapter demonstrates that the morphology of the free amnion and chorion, and of the fused amniochorion, is analogous to that of 'extreme altered morphology' fetal membranes at term, and typical midzone morphology is only observed after fusion to the decidua parietalis. The cellular phenotype of the reticular layer of the free chorion laeve is 'VDAG', with a change to 'VDA' cells after fusion to the free amnion. The change to 'VD' cell only occurs after fusion of the amniochorion to the decidua parietalis. i.e. loss of differentiation of the myofibroblast occurs in the majority of the fetal membranes during gestation, with loss of expression of  $\gamma$ -sma and then  $\alpha$ -sma. Therefore the relationship between the cellular phenotypes, morphological changes, gestation and stage of fetal membrane development suggests that the process of fusion of amniochorion to decidua parietalis may play a role in modification of the cellular phenotype, specifically the loss of  $\alpha$ -sma and osteonectin expression. The loss of expression of  $\gamma$ -sma during gestation appears clearly related to amnio-chorial fusion in the samples examined in this study.

These results are consistent with failure of suppression of the constitutive activated myofibroblast phenotype observed in the 1<sup>st</sup>/2<sup>nd</sup> trimesters, leading to the presence of a region of myofibroblast activation within the lower uterine pole as demonstrated at term. This may result from relative failure of fusion of the amniochorion with the decidua parietalis in this region. Alternatively, complete suppression of the activated myofibroblast phenotype throughout the whole sac may occur, with subsequent reactivation of the phenotype due to lower uterine segment development and disruption of the feto-maternal interface during the late third trimester.

## 8.6. Conclusions

- 1<sup>st</sup> and 2<sup>nd</sup> trimester amnion and chorion have morphology and cellularity comparable to 'extreme altered morphology' fetal membranes at term.
- Preterm 3<sup>rd</sup> trimester fetal membranes have morphology and cellularity comparable to term 'midzone' fetal membranes.
- The cellularity of the connective tissue layers of the amnion and chorion decreases through gestation.
- The cellular phenotype of the 1<sup>st</sup> and 2<sup>nd</sup> trimester reticular layer is  $\alpha$ -sma and osteonectin positive, similar to the 'extreme altered morphology' fetal membrane at term.
- The  $\alpha$ -sma positive, osteonectin positive phenotype in the 1<sup>st</sup> and 2<sup>nd</sup> trimesters is not associated with tenascin-C expression, in contrast to the 'extreme altered morphology' fetal membrane at term.
- Although the  $\alpha$ -sma positive phenotype is associated with the thickness of the reticular layer and the cytotrophoblast layer, no clear 'switch-off' time of this phenotype could be determined during the 3<sup>rd</sup> trimester.

## **Chapter 9**

### **General Discussion**

This study examined the hypotheses that the previously described regional structural changes within the fetal membranes at term are present prior to the onset of labour, and are associated with myofibroblast differentiation. The nature of these structural changes, especially those of the connective tissue layers of the amnion and chorion and their ultrastructural features, are consistent with structural weakness (1.4.2.). The location of the structural changes corresponds to the site of fetal membrane rupture, thus if present prior to the onset of labour could predispose to subsequent fetal membrane rupture (1.5.1.). Additional evidence suggests that one of the cell populations present within the reticular layer are myofibroblasts (1.2.2.7.), cells with a key role in matrix degradation and synthesis in the 'wound response' (1.5.2.). Thus the activity of these cells and the relationship to fetal membrane structure in defined regions of the fetal membrane sac was sought, with particular reference to the onset of labour. Examination of the cellular populations of the connective tissue layers of the amnion and chorion was focussed upon the intermediate filament phenotype, and their expression of the key matricellular proteins tenascin-C and osteonectin. The changes in myofibroblast phenotype observed were examined in an *in vitro* organ culture model, and the ontogeny of the changes considered by examination of fetal membranes throughout the length of gestation.

#### **9.1. The Zone of Altered Morphology and its generation**

##### **9.1.1. Appearance prior to labour**

The Zone of Altered Morphology was described and defined as occurring within a restricted area of the rupture line following labour and delivery at term. The characteristic features were those of increased thickness of the connective tissue layers of both amnion and chorion, and thinning of the cytotrophoblast and attached decidua parietalis in comparison to fetal membranes obtained distal to this site (Malak & Bell, 1994b). The localisation of the ZAM was consistent with the site of the 'dependent membranes' described by Bourne, through which the rupture line of the fetal membrane sac always passes (Bourne, 1962; Malak & Bell, 1996). Ultrastructural features of extracellular matrix dispersal within the connective tissue layers of both amnion and chorion in the

ZAM were suggested to be consistent with structural weakness of the fetal membranes (Malak & Bell, 1994b; Malak & Bell, 1996). Therefore a key objective of this study was to identify whether structural alterations in the fetal membranes, as described in the ZAM, could be identified prior to the onset of labour.

This study confirms the hypothesis that the features of the ZAM are generated prior to the onset of labour. A region of fetal membranes exhibiting extreme altered morphology was identified in all fetal membranes examined prior to the onset of labour at 38-39 weeks. It was established that this region was located in the fetal membranes within the lower uterine segment, centred upon the internal os of the cervix.

Detailed studies of fetal membrane 'maps' obtained prior to the onset of labour describes a number of concentric zones of the fetal membrane, all centred upon the internal os of the cervix. An outer region of decidual thinning results in a region of fetal membranes exhibiting elevation of the Fetal Membrane Morphometric Index and affecting an average of 10.7% of the surface area of the fetal membranes. Within this region, gradual changes in the thickness of the connective tissue layers and of the cytotrophoblast layer were observed, resulting in an inner region exhibiting all of the characteristic features of the ZAM, described as 'extreme altered morphology'. The region of 'extreme altered morphology' is comparable in size with the ZAM identified by Malak (Malak & Bell, 1994b) in the fetal membranes following labour and delivery at term (4.5.). Within this region of extreme altered morphology, a region of 'mucus-associated' fetal membranes was identified in 6 out of 10 fetal membranes examined. These fetal membrane biopsies were characterised by thinner connective tissue layers than the surrounding extreme altered morphology fetal membrane biopsies (although not as thin as midzone fetal membranes), extreme thinning of the cytotrophoblast layer, minimal or absent decidua parietalis, and a layer of mucoid material attached to the cellular layers of the fetal membranes. These fetal membranes are hypothesised to lie directly over the internal os of the cervix, with attached cervical mucus. The variation in size of this inner region may represent variation in cervical effacement and dilatation at the time of membrane collection.

The location of the fetal membranes exhibiting extreme altered morphology within the uterus, overlying the internal os of the cervix, is consistent with a direct relationship to the subsequent rupture of the fetal membranes. It highlights the need to fully understand the

structural, cellular and biochemical features of the ZAM, and the factors leading to its generation, in order to understand the mechanisms of fetal membrane rupture.

### 9.1.2. Connective tissue layers

A key feature of the fetal membranes exhibiting extreme altered morphology prior to and during labour at term, is that of increased thickness of the connective tissue layers of both amnion and chorion. It has previously been interpreted as swelling of these layers (McLaren *et al.*, 1999a), but an alternative explanation is that it is a result of differential elasticity of the fetal membranes exhibiting extreme altered morphology in comparison to midzone fetal membranes. Millar *et al.* demonstrated the surface area of the fetal membranes *in vivo* to be 1.7-fold greater than the expelled *ex-in vivo* fetal membranes (Millar *et al.*, 2000). It has been assumed that the elastic recoil of the fetal membrane sac upon its expulsion from the uterus is evenly distributed throughout the gestation sac. However, it is possible that the increased thickness of the connective tissue layers of the amnion and chorion in the fetal membranes exhibiting extreme altered morphology reflects greater elastic recoil in comparison to the midzone fetal membranes. This is supported by examining the cellularity of the connective tissue layers of the fetal membranes. Fetal membranes exhibiting extreme altered morphology have an increased total cell count per computer screen width in both the amnion and reticular layer. When the thickness of the layer is corrected for by examining cellular density, there is no difference between fetal membranes with extreme altered morphology and midzone fetal membranes. This model is illustrated in Figure 9.1. The connective tissue layers of membranes exhibiting extreme altered morphology have a 1.7-fold greater thickness than midzone fetal membranes. This would equate to a 3-fold difference in the change in surface area resulting from elastic recoil upon expulsion of the membranes from the uterus in comparison to midzone fetal membranes. As is apparent by the illustration, this model would suggest that a greater amniotic epithelial cell count would be identified in fetal membranes exhibiting extreme altered morphology compared to midzone fetal membranes. Whilst a non-significant trend towards this was identified in this study, (1.2-fold greater number,  $p=0.06$ ) there are reasons why the expected 1.7-fold increase was not identified, including the possibility of increased cell loss in membranes with extreme altered morphology. Thus the lack of detection of the expected difference in amniotic epithelial cells does not invalidate the model.

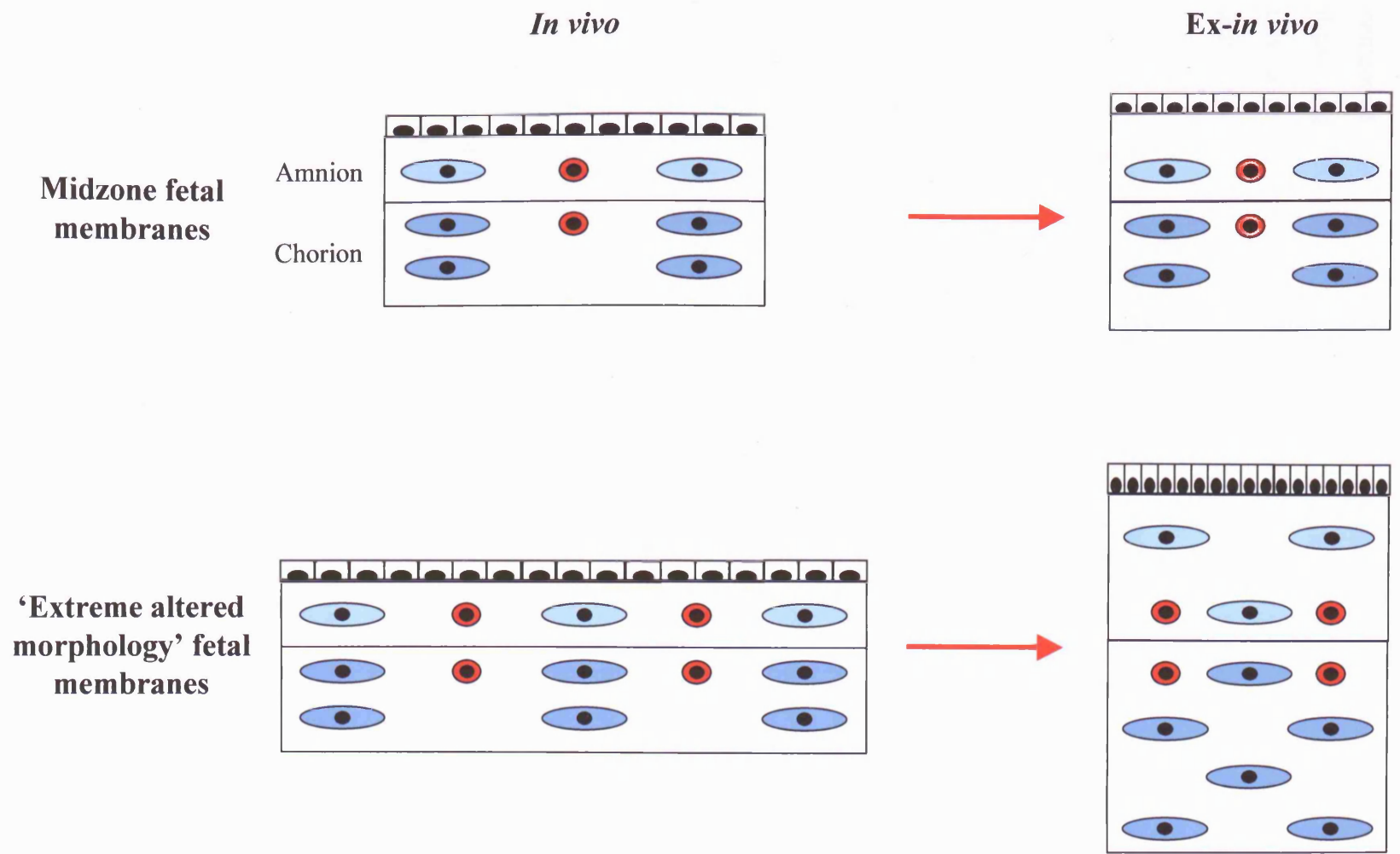


**Figure 9.1.** Diagrams illustrating how the detection of increased connective tissue thickness, increased cell number, but unchanged cell density, within fetal membrane biopsies exhibiting extreme altered morphology compared to midzone fetal membranes may arise due to differential elastic recoil of membranes from the two sites.

Therefore the increased connective tissue thickness in fetal membranes exhibiting extreme altered morphology, compared to midzone fetal membranes, may reflect a greater degree of elasticity of these membranes, either due to properties of the connective tissue (e.g. content of elastin or fibrillin) or due to properties of the mesenchymal cells. It does not discount the hypothesis that these membranes are structurally weak, as the evidence for this came primarily from ultrastructural studies. It is this finding which suggests that an active process is occurring within the fetal membranes with extreme altered morphology.

### **9.1.3. Generation of extreme altered morphology**

Examination of fetal membranes obtained during the 1<sup>st</sup>, 2<sup>nd</sup> and early 3<sup>rd</sup> trimesters may suggest how the region of fetal membranes with extreme altered morphology detected at term within the lower uterine segment arose. During the first and second trimesters the morphology and cellularity of the connective tissue layers of the amnion and chorion was comparable to that of the fetal membranes exhibiting extreme altered morphology at term. Following fusion of the amniochorion with the decidua parietalis, the fetal membrane morphology was more typical of midzone term fetal membranes. The cytotrophoblast layer is 1-2 cells thick prior to fusion with the decidua parietalis, and then becomes progressively thicker through the 3<sup>rd</sup> trimester.

The amnion and chorion in the first half of pregnancy are believed to increase in size by proliferation and growth, and during the second half of pregnancy by stretch, which is partly elastic in nature (Alger & Pupkin, 1986; Casey & MacDonald, 1996). The elastic properties of the fetal membranes in early pregnancy have not been reported, but if reflected by the growth and stretch of the fetal membranes, would be expected to commence in mid-pregnancy. Therefore the biopsies examined from the first and second trimesters may not exhibit elastic recovery as described above, and following fusion of amniochorion with decidua parietalis the amniochorion undergoes progressive stretch as the uterus expands, and the membrane thins.

Therefore there are two possible extreme mechanisms of the generation of the region of extreme altered morphology detected at term:

1. The fetal membranes throughout the whole sac exhibit typical midzone fetal membrane morphology and cellularity following fusion of the amniochorion to decidua parietalis. The features of extreme altered morphology are then generated centred upon the

internal os of the cervix in the late 3<sup>rd</sup> trimester. The lower uterine segment develops, cervical effacement and dilatation occurs, resulting in decidual thinning and loss of support (physical and nutritional) for the overlying fetal membranes. This results in loss of cytotrophoblast cells by apoptosis. i.e. the features of extreme altered morphology are generated by active processes in the late 3<sup>rd</sup> trimester of pregnancy.

2. Only the fetal membranes within the upper uterine segment become typical midzone fetal membranes following fusion of the amniochorion with decidua parietalis. A relative deficiency of decidua parietalis within the lower part of the uterus, and an absolute deficiency of the decidua parietalis directly over the internal os of the cervix limit cytotrophoblast proliferation and invasion. i.e. the features of extreme altered morphology are present from mid-pregnancy as a result of deficient fusion of the amniochorion with decidua parietalis.

The difference between these mechanisms depends upon the thickness of the underlying decidua parietalis within the lower uterine segment, and whether any decidua parietalis exists over the internal os of the cervix. The existence of a zone of fetal membranes with thin decidua parietalis, but without the other features of extreme altered morphology is supportive of the first of these options, as a first phase in the changes occurring (at the periphery of the region). However, it is more likely is a combination of both extreme models occurs, with fusion of amniochorion to all but a small region directly over the internal os of the cervix. Development of the lower uterine segment and cervical effacement leads to shearing and loss of decidual support over an increasing area during the 3<sup>rd</sup> trimester, with loss of cytotrophoblast cells through apoptosis (McLaren *et al.*, 1999b).

## **9.2. Myofibroblast phenotype in term fetal membranes**

Certain evidence would support that active processes are occurring within the connective tissue layers of the amnion and chorion in fetal membranes exhibiting altered morphology (9.1.), thus focussing attention upon the cells of these layers and their activity. The cells within the connective tissue layers of the amnion and chorion have been considered to be fibroblasts (1.2.2.4.) and fibroblasts or myofibroblasts (1.2.2.7.) respectively. The key question is therefore whether the fibroblastic phenotype in the connective tissue layers of the fetal membranes is associated with the features of altered morphology.

### 9.2.1. What is a myofibroblast?

During the course of this study, significant research has been published relating to the controversy surrounding the definition of a myofibroblast and to their relationship to fibroblasts and smooth muscle cells. Thus it is necessary firstly to review this evidence, prior to discussing the work carried out in the current study regarding the cellular populations of the amnion and chorion, their identity, activity, regulation, and relationship to the features of extreme altered fetal membrane morphology.

The myofibroblast was originally defined as a fibroblast exhibiting certain ultrastructural features of smooth muscle cells (Gabbiani *et al.*, 1971). Although myofibroblasts may be subclassified according to their expression of a number of intermediate filaments and myofilaments, and thus according to their immunohistochemical staining pattern (Serini & Gabbiani, 1999), they cannot be defined as a myofibroblast by immunohistochemical staining pattern alone (Schurch *et al.*, 1998). The key definition of a myofibroblast remains identification of ultrastructural features (Schurch *et al.*, 1998; Tomasek *et al.*, 2002).

More recently, a sub-classification of myofibroblasts has been proposed by Tomasek ((Tomasek *et al.*, 2002). He classified myofibroblasts into proto-myofibroblasts and differentiated myofibroblasts. The proto-myofibroblast has been defined as a myofibroblast that does not express  $\alpha$ -sma, and the differentiated myofibroblast as one that does express  $\alpha$ -sma. The proto-myofibroblast has stress fibres, however these contain cytoplasmic actin rather than  $\alpha$ -sma. They also contain focal adhesions, and connect to extracellular matrix fibronectin fibrils, including ED-A fibronectin (Tomasek *et al.*, 2002). It has been suggested that the proto-myofibroblast is always present in normal tissues where there is a need to generate mechanical tension (Serini & Gabbiani, 1999; Tomasek *et al.*, 2002). The differentiated myofibroblast expresses  $\alpha$ -sma, and exhibits increased expression of ED-A fibronectin, increased assembly of stress fibres, and focal adhesions with increased complexity (Dugina *et al.*, 2001; Tomasek *et al.*, 2002), and has dramatically increased ability to generate force (Tomasek *et al.*, 2002). Thus the expression of a key myofibroblast marker directly reflects the function of the cell.

It is unclear whether proto-myofibroblasts originate from fibroblasts, pericytes, or vascular smooth muscle cells (Schurch *et al.*, 1998; Powell *et al.*, 1999). It has been suggested that these cell types represent cellular isoforms of a common progenitor cell, which may

transform into myofibroblasts upon environmental stimulation and according to functional demand (Schurch *et al.*, 1998). Whilst the anatomical relationship in some tissues (e.g. umbilical cord (Nanaev *et al.*, 1997)) suggests that myofibroblasts may differentiate into smooth muscle cells, it remains unclear whether such a differentiation pathway really exists (Powell *et al.*, 1999; Tomasek *et al.*, 2002). Equally, whilst it has been demonstrated that myofibroblasts are lost from wounds by apoptosis (Darby *et al.*, 1990), it remains unclear whether de-differentiation of myofibroblasts back into fibroblasts can occur *in vivo* (Powell *et al.*, 1999; Tomasek *et al.*, 2002), although de-differentiation with loss of  $\alpha$ -sma expression by myofibroblasts has recently been demonstrated *in vitro* (Sohara *et al.*, 2002).

The relationship between myofibroblasts and smooth muscle cells, and the features that distinguish them has also been recently examined. What differentiates a myofibroblast from a smooth muscle cell? Myofibroblasts may express a number of markers considered typical of smooth muscle cells including  $\alpha$ -sma, smooth muscle myosin, SM22 and caldesmon (Gabbiani, 1998). The differentiation between the two cell types on an ultrastructural level may be subtle. The cytoplasm of smooth muscle cells is filled with microfilament bundles and associated dense bodies, and they therefore do not show the typical isolated stress fibres of myofibroblasts (Schurch *et al.*, 1998). However, the differentiated myofibroblast does not express smoothelin, considered a marker of contractile smooth muscle cells (van der Loop *et al.*, 1996; van der Loop *et al.*, 1997; Tomasek *et al.*, 2002).

### **9.2.2. Ultrastructural features of fetal membrane fibroblasts/myofibroblasts**

What is the ultrastructural evidence that the mesenchymal cells of the fetal membranes are fibroblasts or myofibroblasts?

The ultrastructural descriptions of the cells of the fibroblast layer are generally typical of fibroblasts (1.2.2.4.). However, two authors have noted the presence of intracellular bundles of filaments (Bourne, 1962; Hoyes, 1975). Hoyes considers the possibility that the cells are related to smooth muscle cells (Hoyes, 1975), although elsewhere in the literature the cells have still been considered to be fibroblasts (Bourne, 1962; Schmidt, 1992). An absence of communicating intercellular junctions has been observed in the fibroblast layer (Bartels & Wang, 1983). Thus the consensus in the literature is that the mesenchymal cell population of the fibroblast layer comprises fibroblasts.

There have been a number of ultrastructural descriptions of the cells of the reticular layer (1.2.2.7.). As the published literature is based on random fetal membrane biopsies, it is most likely that the descriptions are of  $\alpha$ -sma negative cells of the midzone. Ultrastructural features of stress fibres with dense bodies, nuclear indentation, incomplete basement membrane-like material on the cell surface and intercellular communicating junctions have all been described, thus leading to the conclusion that they are myofibroblasts (Bartels & Wang, 1983; Wang & Schneider, 1983; Malak, 1995).

The fibroblast and reticular layer share a common embryological origin with the mesenchyme of the placental villus and umbilical cord, the cells of both of which have been described as myofibroblasts (Feller *et al.*, 1985; Kohnen *et al.*, 1996; Nanaev *et al.*, 1997; Kobayashi *et al.*, 1998). However, one study examining the ultrastructural features of the Wharton's jelly cells of the umbilical cord noted an absence of fibronexus junctions, abundant myofilaments and the lack of development of the endoplasmic reticulum (Eyden *et al.*, 1994). The author therefore considered that these cells were more characteristic of a type of smooth muscle cell, and that they were not myofibroblasts.

Therefore the cells of the reticular layer, placental villus, and Wharton's jelly all have a number of the key ultrastructural features of a classical myofibroblast. However, fibronexi have not been described in any of these cell types. This is considered an absolute requirement for the definition of a myofibroblast by Eyden (Eyden, 2001). It is not clear whether this feature was sought in the published ultrastructural studies of the amnion and chorion, and whether the lack of reports of its presence can be considered to imply its absence.

The majority of ultrastructural studies of the fibroblast layer describe cells typical of fibroblasts, and therefore throughout this study they were considered as such. The cells of the reticular layer were considered throughout this study to be myofibroblasts due to the presence of the majority of the defining key ultrastructural features of myofibroblasts in reports in the literature. However, the regional variation in intermediate filament phenotype described in this study, in both fibroblast and reticular layers, opens the way for more detailed regional ultrastructural description of the different phenotypes, for clarification of the presence/absence of fibronexi, and for consideration that the cells of the fibroblast layer may include myofibroblasts.

### 9.2.3. Intermediate filament phenotype of fetal membrane myofibroblasts

Myofibroblasts have been classified according to their expression of the intermediate filaments and myofilaments vimentin, desmin,  $\alpha$ -sma,  $\gamma$ -sma and smooth muscle myosin (V, D, A, G, and M). This study demonstrates the cells within the fibroblast layer of the amnion of the midzone fetal membranes to be constitutively 'V' cells. However, 25% of the fetal membranes examined (2/10 mapped pre-labour 'cervical', Chapter 4; 0/5 labour 'cervical', Chapter 3; 3/5 post-labour rupture line, Chapter 3) exhibited expression of significant proportions of 'VA' cells (>20% of cells) within the fibroblast layer in the region of extreme altered morphology. 'VAG' cells were observed more rarely within the fibroblast layer: immunoreactive cells were only observed in a single post-labour rupture line sample, where 6.8% of cells were immunoreactive. The cells of the reticular layer of the chorion of the midzone fetal membranes are constitutively 'VD' cells, with regional expression of 'VDA' cells in association with extreme altered morphology. Regional detection of 'VDAG' cells (>10% of cells immunoreactive) was observed in the reticular layer in 35% of the fetal membranes examined (3/10 mapped prelabour 'cervical', Chapter 4; 1/5 labour 'cervical', Chapter 3; 3/5 post-labour rupture line, Chapter 3). 'VDAGM' cells were not observed within either the fibroblast or reticular layer. These results are illustrated in **Figure 9.2**.

Additionally, a gradient of differentiation is observed within the reticular layer; where present at low percentages 'VDA' cells tend to occur towards the cytotrophoblast layer with 'VD' cells occurring towards the spongy layer. Where greater proportions of 'VDA' cells were present, they extended throughout the reticular layer. However, where 'VDAG' cells occurred at low percentages within the reticular layer, they were detected closest to the interface with the spongy layer, in membranes already expressing  $\alpha$ -sma throughout their reticular layers. Again, where greater proportions of 'VDAG' cells were present, they extended throughout the reticular layer.

The reticular layer of the chorion and the fibroblast layer of the amnion share a common embryological origin with the mesenchyme of the placental villi and umbilical cord; all are derived from the extraembryonic mesoderm (1.2.1.). Thus the cells within these layers may be compared to the mesenchymal cells of the placental villus and the cord, both of which have been described as myofibroblasts, and whose intermediate filament and myofilament phenotype has been previously described (Feller *et al.*, 1985; Kohnen *et al.*, 1996; Nanaev *et al.*, 1997; Kobayashi *et al.*, 1998; Kacemi *et al.*, 1999).

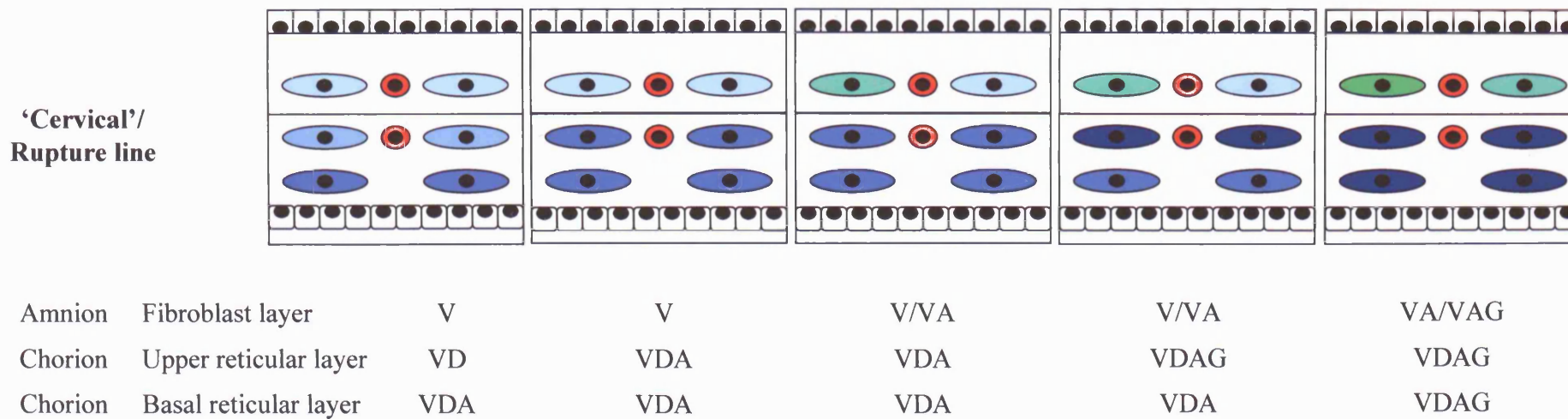
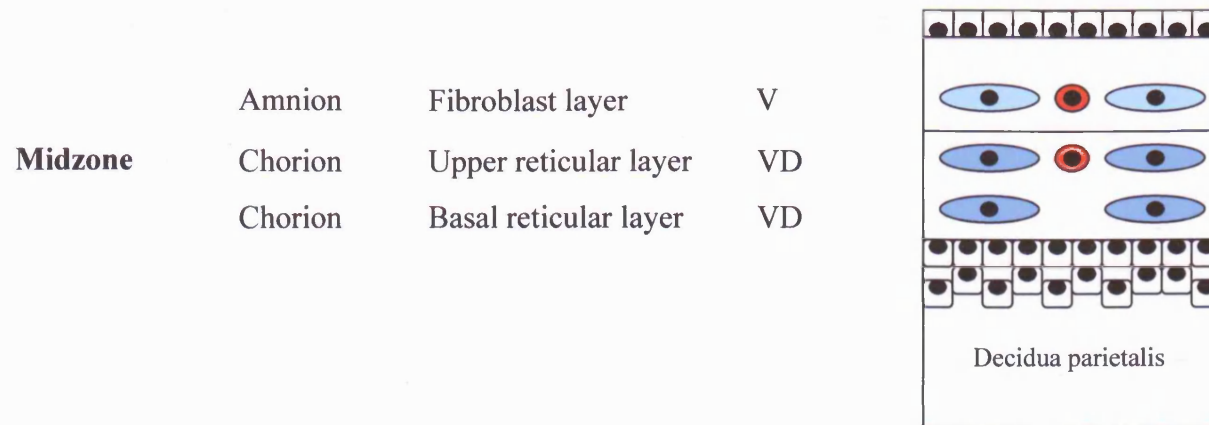


**Figure 9.2.** Diagrams illustrating the range of intermediate filament phenotypes detected in the fibroblast and reticular layers of midzone and 'cervical'/rupture line fetal membranes. The most common combinations of phenotypes between the fibroblast and reticular layers are illustrated. Only a single fetal membrane exhibited 'VAG' cells in the fibroblast layer, at a low percentage, and this was in association with 'VDAG' cells throughout the reticular layer.

The phenotypes of the umbilical cord (Nanaev *et al.*, 1997) and placental villus (Kohnen *et al.*, 1996) may therefore provide a model for that of the reticular layer and fibroblast layer. The models previously suggested for the umbilical cord and placental villus demonstrate a spatial distribution cells expressing desmin,  $\alpha$ -sma,  $\gamma$ -sma and smooth muscle myosin centred around the core blood vessel (Kohnen *et al.*, 1996; Nanaev *et al.*, 1997; Kobayashi *et al.*, 1998). This continuum has suggested to the authors that these phenotypes reflect a gradient of differentiation, with sequential acquisition of markers i.e. fibroblasts at the periphery of the villi and cord sequentially acquire the sequence of filaments D, A, G and M, and become 'VDAGM' cells, and finally vascular smooth muscle cells around the central blood vessel. However, cell proliferation was demonstrated within the peripheral 'V' and 'VD' cells within the villus, and also within the vascular smooth muscle cells. The authors therefore suggest that the differentiation of the vascular smooth muscle cells, and the differentiation of myofibroblasts, represent independent cell lines, and not a continuum (Kohnen *et al.*, 1996). The myofibroblasts within the placental villus and cord are reported to demonstrate increasing ultrastructural features of myofibroblast differentiation in association with acquisition of the intermediate filaments and myofilaments. The 'VDAGM' myofibroblast was described as ultrastructurally identical to a smooth muscle cell (Kohnen *et al.*, 1996; Nanaev *et al.*, 1997), placing a question over its separate identity from a smooth muscle cell. However, these were still thought to be myofibroblasts by their anatomical location and orientation, and their expression of dipeptidyl peptidase IV, a cell surface protease described in fibroblasts and myofibroblasts, but never by smooth muscle cells (Kohnen *et al.*, 1996).

The cells of the fibroblast layer and those of the reticular layer have a different constitutive intermediate filament phenotype in the midzone, and exhibit different behaviour patterns with respect to altered morphology, despite a common embryological origin from extraembryonic mesoderm. This different behaviour suggests a different lineage for the cells of the two layers. The key difference between the two cell types is the expression of desmin by the cells of the reticular layer. The fibroblast layer cells are constitutively 'V' cells, with potential to become 'VA' or 'VAG' cells rarely in association with altered morphology. The reticular layer cells are constitutively 'VD' cells (proto-myofibroblasts), which become 'VDA' cells (differentiated myofibroblasts), and occasionally 'VDAG' cells in association with altered morphology. A difference in behaviour may also be seen within the intermediate filament phenotype of the cord, where the subamniotic cells exhibit a greater degree of myofibroblast differentiation in comparison to the underlying cells of the

Wharton's jelly. This is in contrast to the analogous cells in the fibroblast layer, which exhibit a lesser degree of myofibroblast differentiation than those within the reticular layer. The amnion overlying the umbilical cord is in continuum with that in the gestation sac. The difference in behaviour between the amniotic fibroblasts in these two locations may be related to the pulsatility of the umbilical cord, placing the amniotic fibroblasts under repeated stretch.

### **9.3. Functions of differentiated myofibroblasts in the fetal membranes at term**

The discrete nature of the regional myofibroblast differentiation within the connective tissue layers of the fetal membranes overlying the cervix prior to labour suggests that these cells may play a specific and vital role in the function of the fetal membranes with respect to fetal membrane rupture and/or the onset of labour.

#### **9.3.1. Contractility**

One possible function of the differentiated ( $\alpha$ -sma positive) myofibroblast within the fetal membrane is that of contraction. It has long been recognised that myofibroblasts are contractile (Majno *et al.*, 1971; Gabbiani *et al.*, 1972), and that myofibroblast contractility is associated with  $\alpha$ -sma expression (Darby *et al.*, 1990). Myofibroblast contractility is apparent by their presence in normal and pathological healing wounds, and in fibrocontractive diseases such as Dupuytren's contracture (Tomasek *et al.*, 2002). Myofibroblasts connect with each other via gap junctions (Gabbiani *et al.*, 1978; Spanakis *et al.*, 1998), which would allow them to function as multicellular contractile units. Additionally, the intracellular stress fibres connect to extracellular fibronectin fibrils at fibronexi, also described as focal adhesions (Dugina *et al.*, 2001), permitting the force generated by the stress fibres to be transmitted to the extracellular matrix (Eyden, 1993; Tomasek *et al.*, 2002).

Although myofibroblasts may express smooth muscle myosin, the contractile function is related to the expression of  $\alpha$ -sma (Darby *et al.*, 1990; Hinz *et al.*, 2001), and is not dependent on smooth muscle myosin expression. In muscle cells contraction requires the presence of both actin and myosin. Several isoforms of myosin have been described, of both smooth muscle and non-muscle types (Loukianov *et al.*, 1997). In myofibroblasts, the

contractile apparatus is believed to contain  $\alpha$ -sma in association with non-muscle myosin (Benzonana *et al.*, 1988; Eddy *et al.*, 1988; Chiavegato *et al.*, 1995).

The expression of  $\alpha$ -sma by reticular layer cells overlying the cervix prior to the onset of labour and their contractile function may be the explanation for the 'differential elastic recoil' hypothesis proposed in 9.1.2. to explain the increased thickness of the connective tissue layers of fetal membranes exhibiting extreme altered morphology in comparison to midzone fetal membranes.

### 9.3.2. Secretion of matricellular proteins

Two further properties of differentiated myofibroblasts revealed in this study were production of tenascin-C and osteonectin. Production of these matricellular proteins was demonstrated by myofibroblasts and fibroblasts of the reticular layer and the fibroblast layer, and not by the macrophage population. Myofibroblast differentiation was not, though, a prerequisite for production of these proteins; they were not produced exclusively by  $\alpha$ -sma positive cells, although their expression was upregulated in association with the  $\alpha$ -sma phenotype in the chorion.

Tenascin-C and osteonectin are matricellular glycoproteins, and comprise two out of three such proteins considered as 'anti-adhesive'. The third glycoprotein within the group is thrombospondin-1 (Sage & Bornstein, 1991; Greenwood & Murphy-Ullrich, 1998). These proteins do not contribute significantly to extracellular matrix structure, but mediate cell-matrix interactions (Yan & Sage, 1999). They interfere with focal adhesions, promote cell rounding and detachment from the extracellular matrix, and are believed to act in an autocrine or paracrine fashion. Such changes are required for cells to undergo proliferation and migration. All of the anti-adhesive glycoproteins are expressed in tissues undergoing remodelling, such as in embryonic morphogenesis and in wound repair (Sage & Bornstein, 1991). Thrombospondin expression has been reported in the amniotic epithelium (Hao *et al.*, 2000), but its expression within the chorion has not been examined. Osteonectin exhibits specific binding to collagens I, II, III, IV, V and VIII, and the interaction between osteonectin and collagen is believed to contribute to its function of matrix remodelling (Yan & Sage, 1999). Although tenascin-C has been considered an 'anti-adhesive' protein, under certain culture conditions, especially culture on a collagen I substrate, Tn-C may

promote cell adhesion and spreading (Jones & Jones, 2000a). The response of the fibroblasts and myofibroblasts to the presence of Tn-C within the matrix is unknown.

### 9.3.3. Matrix degradation

It has been suggested that the ZAM as detected after labour and delivery, and its site of origin overlying the internal os of the cervix prior to labour, represents an area of structural weakness in the fetal membrane, which predisposes the membrane to rupture (Malak & Bell, 1994b; McLaren *et al.*, 1999a). The possibility of a degradative function of the differentiated myofibroblast therefore needs to be considered. Matrix metalloproteinases-1, -2, -3, and -9 are upregulated by osteonectin and/or tenascin-C *in vitro* (Tremble *et al.*, 1993; Tremble *et al.*, 1994; Khan & Falcone, 1997; Shankavaram *et al.*, 1997; Gilles *et al.*, 1998). Myofibroblasts have been demonstrated in other systems, including the wound response, to produce MMPs (Powell *et al.*, 1999). Upregulation of MMP-1, -2, -3, and -9 in the fetal membranes has been demonstrated with the onset of labour (Hulboy *et al.*, 1997; Bryant-Greenwood, 1998). However, only regional upregulation of MMP-9 expression in the fetal membranes has been demonstrated prior to labour (McLaren *et al.*, 2000a), with no regional differences detected in expression of MMP-1, -2, and -3 in the fetal membranes (McLaren *et al.*, 2000a; McLaren J, personal communication). Immunohistochemistry, suggests that the main site of MMP-9 production is the amniotic epithelium and cytotrophoblast layer, although some immunoreactivity is apparent in connective tissue cells (Vadillo-Ortega *et al.*, 1995; McLaren *et al.*, 2000a). Production of MMP-9 can be demonstrated *in vitro* in amniotic fibroblasts, although at low levels (Xu *et al.*, 2002). Capacity for production by reticular layer cells has not been investigated. So although Tn-C and osteonectin may potentially upregulate MMP-9 production by the myofibroblasts, the functional significance of this is uncertain, in the light of the greater level of epithelial production. The regulation of MMP-9 production by epithelial cells by Tn-C and osteonectin from the adjacent connective tissue layers is possible.

A degradative function for the differentiated myofibroblast within the fetal membranes may have two possible reasons. It is possible that matrix degradation is occurring in order to produce structural weakness in preparation for fetal membrane rupture. However, the majority of the strength of the fetal membrane lies in the amnion, rather than the chorion (Polishuk *et al.*, 1962; Meudt & Meudt, 1967). This would point away from myofibroblast differentiation within the reticular layer, where it was most commonly observed, playing a significant role in producing structural weakness of the fetal membranes. Alternatively it

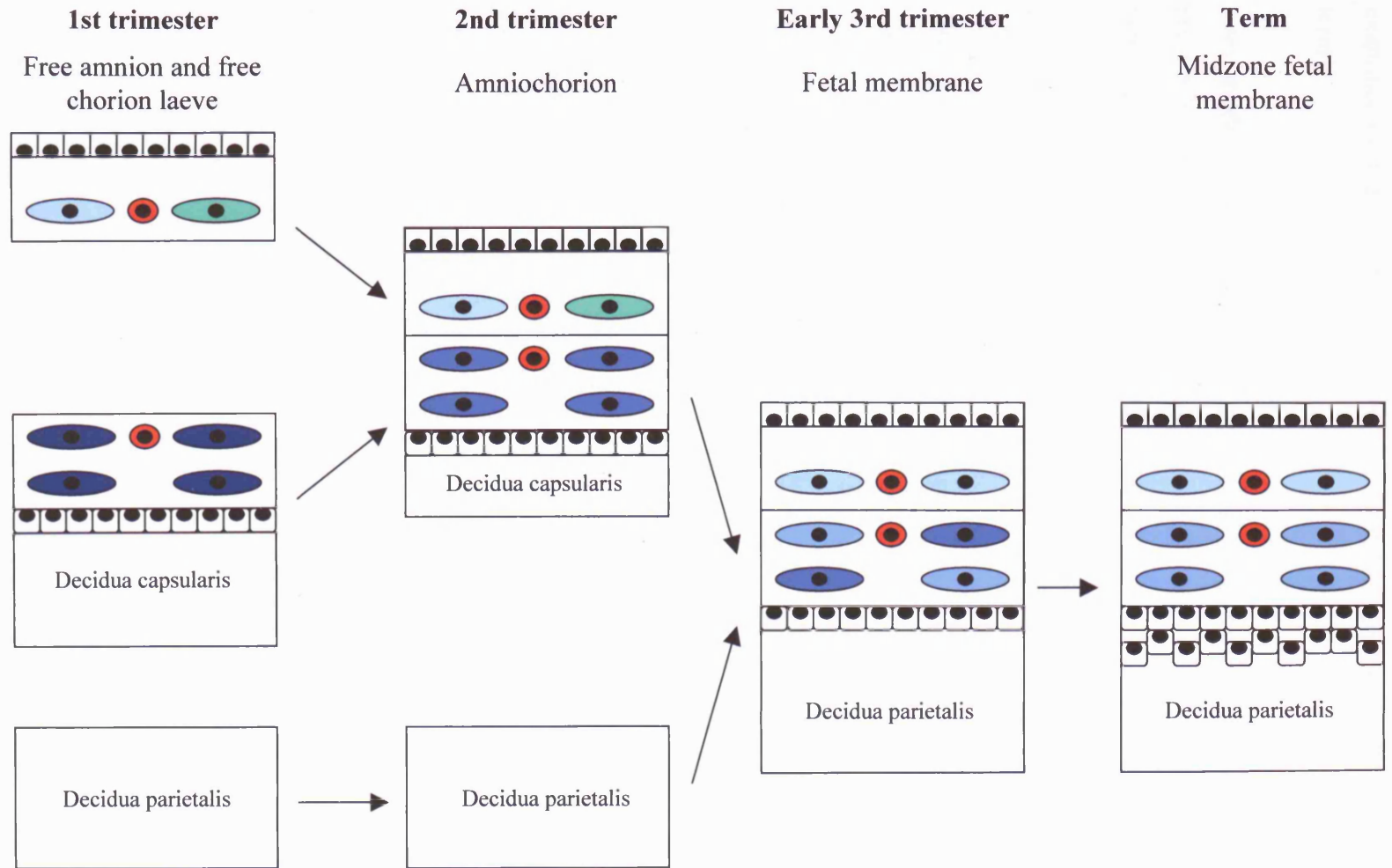
may be part of a process of tissue remodelling in the fetal membranes of the lower uterine pole, which is subject to differential stretch in comparison to the membrane in the upper pole of the uterus due to development of the lower uterine segment and cervical effacement in the latter part of pregnancy.

#### **9.3.4. Matrix synthesis**

The myofibroblast also plays a significant role in matrix synthesis in the wound response, as part of the process of remodelling (Powell *et al.*, 1999). It has been demonstrated that  $\alpha$ -sma positive myofibroblasts are the main producer of collagen during pulmonary fibrosis (Zhang *et al.*, 1994), and that  $\alpha$ -sma and collagen I expression are co-ordinately regulated in the myofibroblast (Desmouliere *et al.*, 1993). Expression of collagen I has also been demonstrated to be upregulated by osteonectin (Francki *et al.*, 1999). Collagen I is a major constituent of the connective tissue layers of the amnion and chorion (1.2.2.). Previous studies have demonstrated ultrastructural evidence of collagen disruption, but have also demonstrated evidence of increased synthesis of collagen, in fetal membranes of the ZAM in comparison to the midzone. It is therefore hypothesised that the differentiated myofibroblast promotes both matrix degradation (by osteonectin, tenascin-C and MMP-9 production) and matrix synthesis as part of a process of extracellular matrix remodelling in order to accommodate increasing differential stretch of the lower uterine pole fetal membranes in comparison to upper uterine pole fetal membranes without fetal membrane rupture occurring.

#### **9.4. Myofibroblast differentiation during gestation**

The pattern of myofibroblast differentiation, which has been deduced by examining fetal membranes obtained throughout gestation, is summarised in **Figure 9.3**. The non-macrophage cells of the reticular layer change from being constitutively 'VDAG' cells in the first and early second trimester, becoming 'VDA' and lastly 'VD' cells at term (in the midzone). The change from 'VDAG' to 'VDA' cells coincided with the fusion of amnion to chorion laeve. The timing of the change from 'VDA' to 'VD' cells occurred following fusion of the amniochorion to the decidua parietalis, although in some cases was not completed until the latter part of the third trimester. It had consistently occurred by 38 weeks gestation. The occurrence of 'VA' cells in the fibroblast layer was sporadic, and was observed in 11% (1 out of 9, with > 20% of cells  $\alpha$ -sma immunoreactive) of amnions



<b>Amnion</b>	Fibroblast layer	V/VA	V/VA	V	V
<b>Chorion</b>	Reticular layer	VDAG	VDA	VD/VDA	VD

**Figure 9.3.** The pattern of intermediate filament/myofilament phenotype in the fetal membranes throughout gestation.

examined during the first and second trimesters (compared to 25% of amnions examined at term).

Two models may be proposed for the development of the region of differentiated myofibroblasts observed in the reticular layer of the fetal membranes within the lower uterine pole at term:

1. The 'Switch off - switch on' model (**Figure 9.4a**).

This model proposes that the entire gestation sac contains differentiated myofibroblasts ('VDAG' cells) in the reticular layer in the first trimester. The cells progressively become 'VDA' and then 'VD' cells throughout the whole sac during gestation. There is then a separate 'switch-on' of myofibroblast differentiation in the reticular layer in a region of the fetal membranes centred over the internal os of the cervix, prior to labour at term.

2. The 'Switch off' model (**Figure 9.4b**).

This model proposes that the change from 'VDAG' to 'VDA' to 'VD' cells only occurs in the midzone fetal membranes during gestation. A residual region of fetal membranes containing differentiated myofibroblasts in the reticular layer is left centred over the internal os of the cervix.

Critical to both of these models is that the differentiated myofibroblast phenotype is suppressed by fusion of the amniochorion to decidua parietalis as demonstrated in Chapter 4. This must occur in order to generate the midzone phenotype detected over the majority of the gestation sac at term.

The lack of detailed fetal membrane maps during the critical time period of loss of  $\alpha$ -sma expression at 25-38 weeks gestation makes differentiating between these two models difficult. However, altered morphology with high reticular layer  $\alpha$ -sma expression typical of the ZAM at term, and typical midzone morphology and absent  $\alpha$ -sma expression have been observed in random fetal membrane biopsies from the same membrane sac from as early as 25 weeks gestation (unpublished data). This suggests the 'Switch off - switch on' model (**Figure 9.4a**) above is unlikely to be correct, and would be more suggestive of a 'Switch-off' (**Figure 9.4b**) model. The nature of the underlying decidua parietalis in the

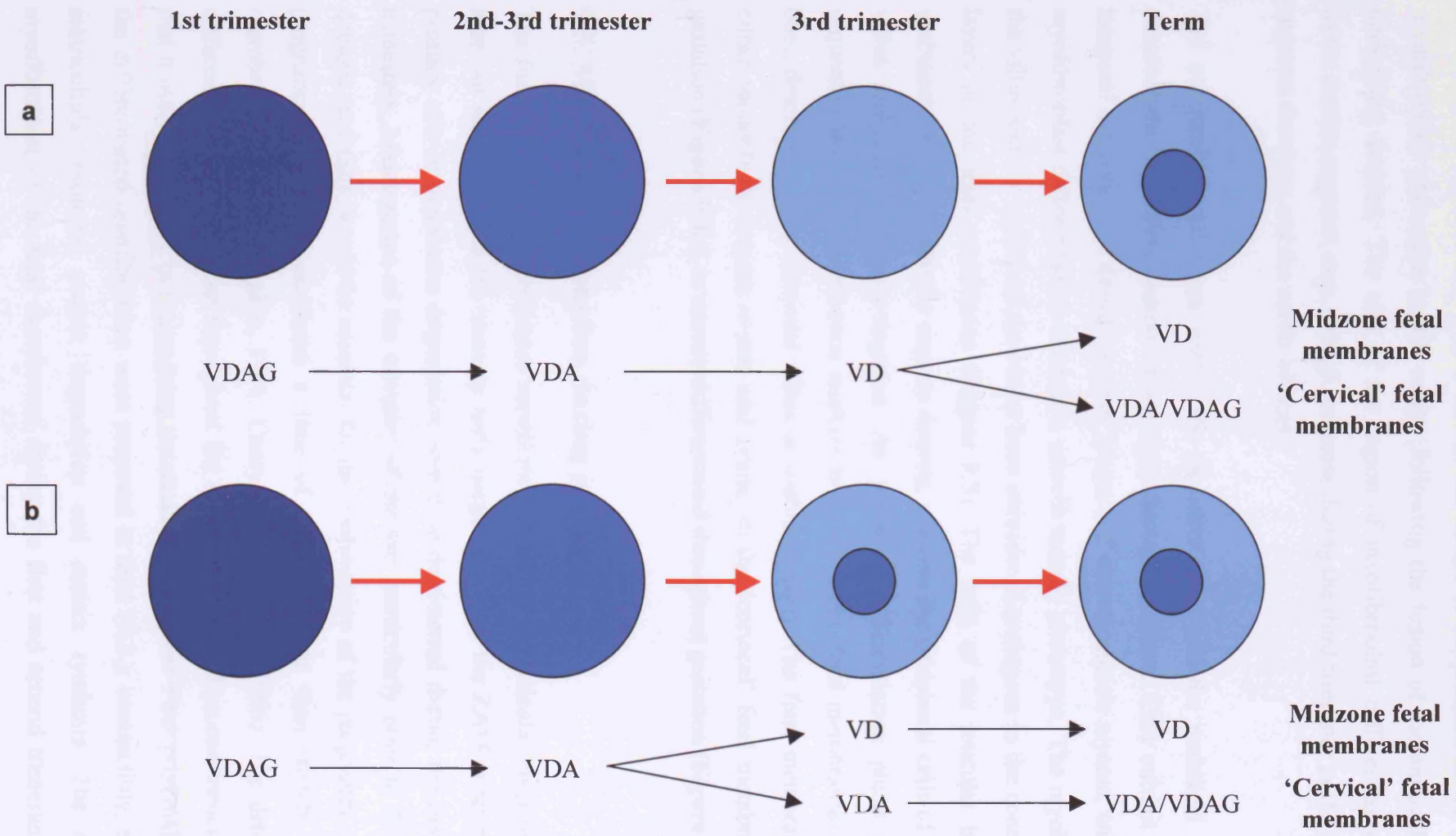


**Figure 9.4.** Alternative models of the generation of a region of myofibroblast differentiation in the reticular layer of the fetal membranes overlying the cervix at term. A representation of a sheet of fetal membrane is shown, with 'cervical' fetal membranes in the centre. Model (a) proposes that myofibroblast differentiation is lost in the whole fetal membrane sac, followed by a subsequent 'switch-on' in the 'cervical' fetal membranes at term. Model (b) proposes a 'switch-off' of myofibroblast differentiation in the midzone only, with myofibroblasts in the 'cervical' fetal membranes remaining differentiated throughout pregnancy.

lower uterine segment may play a role in the failure of suppression of the differentiated myofibroblast phenotype in this region following the fusion of the amniochorion to the underlying decidua. The size of the region of myofibroblast differentiation within the lower uterine segment may, though, increase during the third trimester as the lower uterine segment develops and the cervix effaces.

The comparable cell types within the placental villi and the umbilical cord do not demonstrate 'de-differentiation' at any time through gestation. They exhibit a spatial and temporal acquisition of desmin,  $\alpha$ -sma,  $\gamma$ -sma and smooth muscle myosin, with increasing myofibroblast differentiation towards a smooth muscle phenotype. The myofibroblasts of the villus and the umbilical cord have been considered analogous to the connective tissue layers of the fetal membranes (Figure 9.5). The cells of the reticular layer and the umbilical cord constitutively express desmin, whereas the peripheral cells of the placental villus are initially desmin-negative. An initial de-differentiation phase occurs, with sequential loss of differentiation markers in the midzone fetal membranes. This has not been described in the placental villus or umbilical cord. The fetal membrane cells then either sequentially acquire  $\alpha$ -sma and  $\gamma$ -sma, in the 'cervical' fetal membranes through gestation (Figure 9.4a), or remain differentiated throughout gestation (Figure 9.4b)

### **9.5. Myofibroblast function during gestation**

The function of the differentiated myofibroblast within the reticular layer of the chorion may not necessarily be the same in early pregnancy as in the ZAM at term. Certainly a primary role in membrane degradation would be detrimental during the first and second trimesters. Maintenance of the integrity of the sac, particularly prior to fusion with the decidua parietalis, would be essential for the continuation of the pregnancy. This stage of pregnancy has been considered a time of growth, rather than stretch, of the fetal membranes (Alger & Pupkin, 1986; Casey & MacDonald, 1996). The detection of the differentiated myofibroblast throughout the sac in the first and second trimesters suggests that it must play a role in maintaining the structure of the sac. Four principal functions of the differentiated myofibroblast were proposed at term (9.3.): contractility, expression of matricellular proteins, matrix degradation and matrix synthesis. The differentiated myofibroblast of the fetal membranes during the first and second trimesters may share some of these functions.

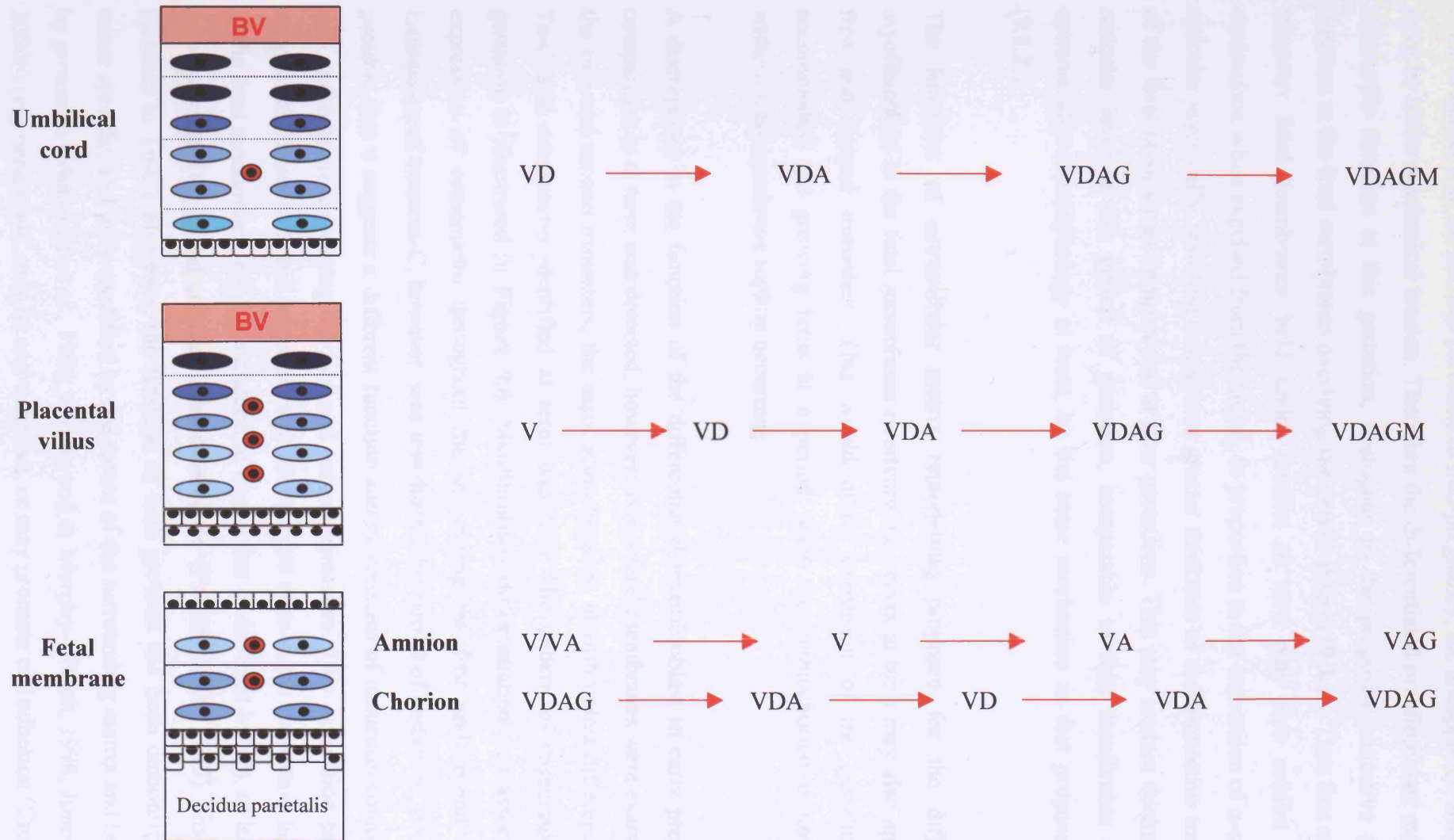


**Figure 9.5.** The differentiation pathways of the myofibroblasts of the umbilical cord, the myofibroblasts of the placental villus, the fibroblasts of the amnion, and the myofibroblasts of the chorion. The blood vessels (BV) of the umbilical cord and placental villus are labelled for orientation.

Prior to fusion with the decidua parietalis in mid-pregnancy, the unsupported amniochorion must be under mechanical tension. Therefore the differentiated myofibroblast may fulfill a contractile function at this gestation, analogous to the proposed protective contractile function in the fetal membranes overlying the cervix at term (9.3.1.). Thus first and second trimester fetal membranes held under tension *in vivo* may also exhibit increased contraction when expelled from the uterus, in proportion to the expression of  $\alpha$ -sma by the reticular layer cells, resulting in apparent greater thickness of the connective tissue layers of the fetal membranes compared to at later gestations. This may explain thickness of the reticular layer at this period of gestation, comparable to fetal membranes exhibiting extreme altered morphology at term, by the same mechanism as that proposed at term (9.1.2.).

The functions of extracellular matrix remodelling proposed for the differentiated myofibroblast in the fetal membranes overlying the cervix at term may also apply in the first and second trimesters. This would allow expansion of the gestation sac to accommodate the growing fetus at a period when the amniochorion is unsupported, without fetal membrane rupture occurring.

A discrepancy in the function of the differentiated myofibroblast in early pregnancy in comparison to at term was detected, however. When fetal membranes were examined from the first and second trimesters, the association between myofibroblast differentiation and Tn-C and osteonectin identified at term was lost. The pattern of expression through gestation is illustrated in Figure 9.6. Myofibroblast differentiation was associated with expression of osteonectin throughout the sac during the first and second trimesters. Expression of tenascin-C, however, was low during this period of gestation. It is therefore possible that it suggests a different function and mechanism of induction compared to  $\alpha$ -sma and osteonectin during the first and second trimesters. This expression pattern may suggest that tenascin-C and osteonectin fulfill different roles in the connective tissue layers of the fetal membranes (e.g. by induction of expression of different MMPs, or induction of expression of TGF- $\beta$  and collagen I by osteonectin (Francki *et al.*, 1999), properties not ascribed to Tn-C). However, the function of both proteins has been demonstrated to be tissue specific, and to be modified by the nature of the surrounding matrix and by cleavage by proteases (Motamed *et al.*, 1996; Greenwood & Murphy-Ullrich, 1998; Jones & Jones, 2000b) (e.g. tenascin-C may be anti-adhesive, or may promote cell adhesion (Crossin,

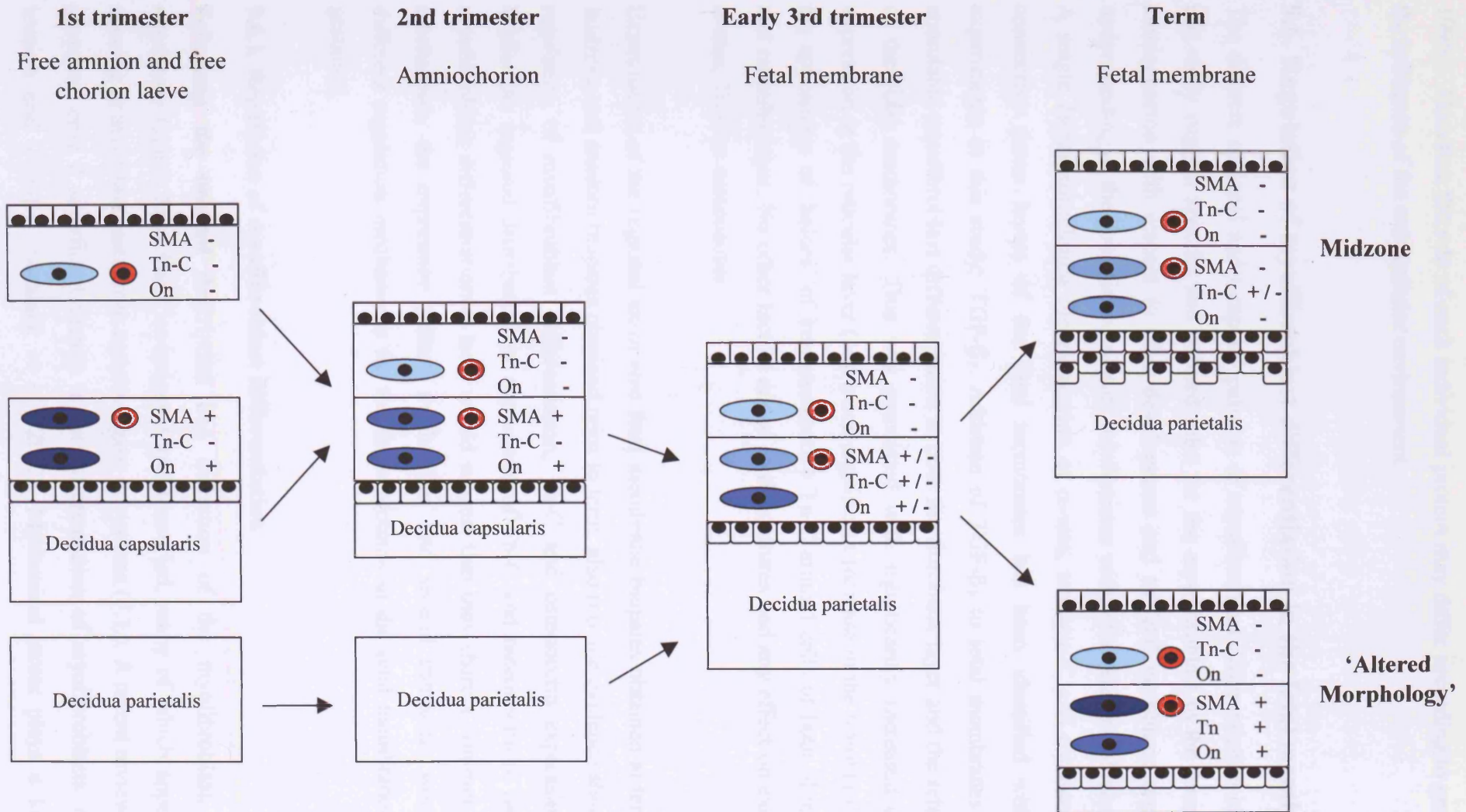


**Figure 9.6.** The major combinations of  $\alpha$ -sma (SMA), tenascin-C (Tn-C) and osteonectin (On) expression patterns in the connective tissue layers of the amnion and chorion in relation to the stages of fusion of the fetal membranes during gestation.

1996)). Therefore the role of each individual protein may differ according to gestation and the influence of the extracellular environment.

## **9.6. Regulation of myofibroblast differentiation in the fetal membranes**

The discrete regional and temporal patterns of myofibroblast differentiation identified in this study suggest specific and defined roles for the myofibroblast in the function of the amniochorion with respect to their development and to fetal membrane rupture. Thus understanding of the potential regulatory mechanisms within the fetal membrane is critical. A single factor stimulating the expression of  $\alpha$ -sma, tenascin-C and osteonectin in the connective tissue layers of the fetal membranes has been identified with *in vitro* experiments in this study: TGF- $\beta_1$ . Addition of TGF- $\beta_1$  to fetal membranes in culture stimulated myofibroblast differentiation in both the fibroblast layer and the reticular layer of the fetal membranes. This was associated with significantly increased osteonectin expression in the reticular layer (and a non-significant increase in the fibroblast layer), and the appearance of 'haloes' of immunoreactive Tn-C around cells of both fibroblast layer and reticular layer. No other factors added to the cultures had any effect on expression of  $\alpha$ -sma, Tn-C or osteonectin.

Examination of the regional *ex-in vivo* fetal membrane biopsies obtained at term, and the midzone and random biopsies obtained prior to term, also provide evidence about potential regulation of myofibroblast differentiation, Tn-C and osteonectin expression *in vivo*. Whilst the regional distribution of expression of Tn-C and osteonectin in parallel with myofibroblast differentiation at term would suggest that they share a common regulation mechanism, the expression pattern in the first and second trimesters would suggest different regulation mechanisms for the three proteins in the fetal membranes earlier in gestation.

### **9.6.1. Regulation of myofibroblast differentiation**

Following the original description and definition of the myofibroblast, numerous regulatory factors have been investigated and identified, many of which appeared to be specific to myofibroblasts from certain organs or systems (7.1.). A recent review, however, proposed only 2 significant factors in the differentiation of myofibroblasts: mechanical tension and TGF- $\beta_1$  (Tomasek *et al.*, 2002). Mechanical stress plays a key role in

myofibroblast differentiation (Hinz *et al.*, 2001), and modifies the induction of  $\alpha$ -sma in myofibroblasts by TGF- $\beta_1$  *in vitro* (Arora *et al.*, 1999; Narani *et al.*, 1999). This response requires the presence of the ED-A containing splice variant of fibronectin within the extracellular matrix (Serini *et al.*, 1998; George *et al.*, 2000). However, Tomasek *et al.* (Tomasek *et al.*, 2002) propose that mechanical stress stimulates fibroblast differentiation into cells termed 'proto-myofibroblasts' (Figure 9.7). These cells are present in normal tissues where there is a requirement to generate mechanical tension (Serini & Gabbiani, 1999; Tomasek *et al.*, 2002). The proto-myofibroblast is defined as a myofibroblast that does not express  $\alpha$ -sma, and thus the 'VD' myofibroblast of the reticular layer would be included in this definition. The proto-myofibroblast contains stress fibres, which terminate at fibronexi. Further differentiation and expression of  $\alpha$ -sma requires the presence of the ED-A containing splice variant of fibronectin, stimulation by TGF- $\beta_1$ , and ongoing mechanical tension. They then define the  $\alpha$ -sma expressing myofibroblast as a 'differentiated myofibroblast'. This cell contains organised stress fibres containing  $\alpha$ -sma, which connect to the extracellular fibronectin fibrils at fibronexi. Expression of TGF- $\beta_1$  is critical in the co-ordination of this process, as it has been demonstrated to stimulate expression of ED-A fibronectin and  $\alpha$ -sma (Tomasek *et al.*, 2002).

This model would implicate both stretch and TGF- $\beta_1$  as regulatory factors in the fetal membranes. The distribution of the differentiated myofibroblast, in the fetal membranes overlying the cervix prior to term, when cervical effacement and lower segment development would cause an increased stretch in these fetal membranes (in comparison to midzone fetal membranes), and in the unsupported chorion laeve and amniochorion of the first and second trimesters, is consistent with stretch playing a significant role in myofibroblast differentiation in the fetal membranes *in vivo*.

High extracellular tension (e.g. as must exist in the fetal membrane supported by the underlying uterine tissue) promotes alignment of microfilaments, formation of stress fibres, and differentiation into the proto-myofibroblast phenotype (the desmin-positive,  $\alpha$ -sma negative cells of the midzone fetal membrane). The proto-myofibroblast undergoes isometric contraction, which is transmitted to the surrounding matrix to maintain tension. Ongoing mechanical tension, with the addition of TGF- $\beta_1$ , in the presence of ED-A fibronectin stimulates  $\alpha$ -sma expression formation of the 'differentiated' myofibroblast, which significantly increased force generation by the cell (Tomasek *et al.*, 2002), (as

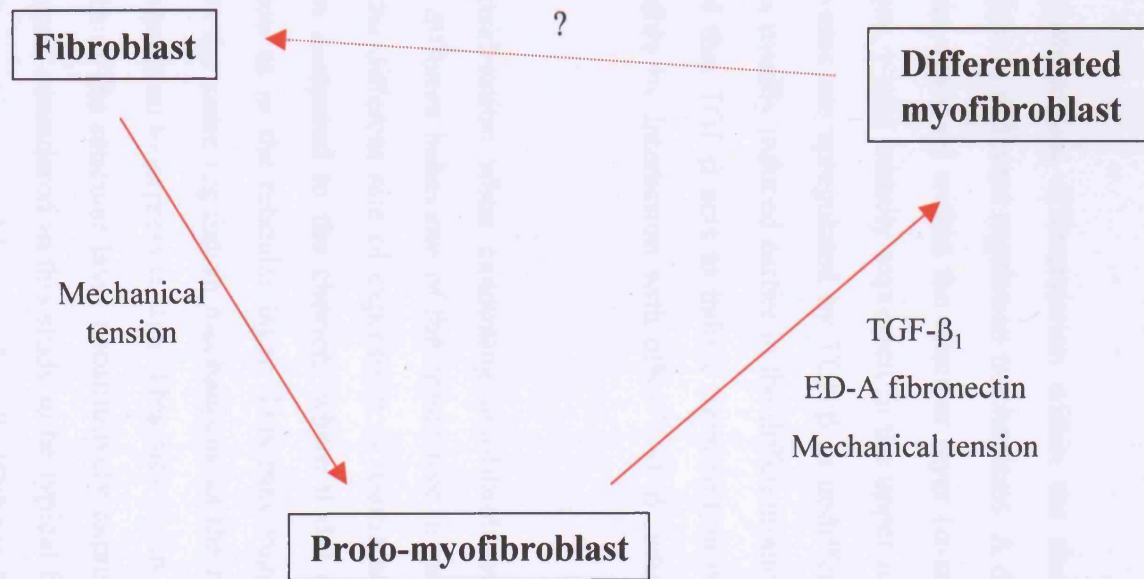


**Figure 9.7.** The relationship between the fibroblast, proto-myofibroblast and differentiated myofibroblast as proposed by Tomasek et al, 2002.

would be required in the unsupported chorion laeve, free amniochorion and 'cervical' fetal membranes).

Transforming growth factor- $\beta_1$  was the only factor studied *in vitro* in this study which stimulated  $\alpha$ -sma expression in the fibroblast and reticular layers of the term fetal membranes. This is consistent with the above model, and suggests that it plays a major role in myofibroblast differentiation in the fetal membranes *in vivo*.

The pattern of myofibroblast differentiation within the chorion suggests that different genes may be subject to different regulation mechanisms. A differentiation gradient for  $\alpha$ -sma and  $\gamma$ -sma was observed within the reticular layer ( $\alpha$ -sma initially expressed in the lower reticular layer,  $\gamma$ -sma initially expressed in the upper reticular layer). Expression of both  $\alpha$ -sma and  $\gamma$ -sma are upregulated by TGF- $\beta$  in undifferentiated mesenchymal cells. However,  $\alpha$ -sma is usually induced earlier in the differentiation pathway than  $\gamma$ -sma, it has been demonstrated that TGF- $\beta$  acts to induce transcription of the two genes by different mechanisms, possibly by interaction with other TGF- $\beta$  inducible factors (Hirschi *et al.*, 2002).

An important consideration when examining myofibroblast differentiation in the fetal membranes is the different behaviour of the connective tissue cells of the amnion and the chorion. Despite the different rate of expression of  $\alpha$ -sma among connective tissue cells within the amnion compared to the chorion, where it did occur, it exhibited the same regional distribution as in the reticular layer. This may suggest that the fibroblast layer cells are subject to the same regulation mechanisms as the reticular layer cells, although require greater stimulation to express  $\alpha$ -sma. This may be an intrinsic property of the cell. The myofibroblasts of the reticular layer constitutively express desmin, whereas the cells of the fibroblast layer, considered in this study to be typical fibroblasts, do not. Desmin is an intermediate filament expressed by muscle cells (Osborn & Weber, 1982), where it has been suggested that it acts to permit normal functioning of the contractile apparatus, and has been hypothesised, but not proven, that it may play a role in modulating signal transduction and gene expression (Paramio & Jorcano, 2002). Alternatively the different properties of fibroblast layer and reticular layer cells may be due to proximity to cytotrophoblast cells or amniotic fluid, or due to extracellular matrix signalling. The extracellular matrix of the amnion has been shown to down-regulate TGF- $\beta$  isoforms and

receptors, and also  $\alpha$ -sma expression, when used as a substrate for corneal and conjunctival fibroblast cell culture (Tseng *et al.*, 1999; Lee *et al.*, 2000). It is not known, however, how this property compares to the reticular layer extracellular matrix. The altered morphology of the fetal membranes may play a role in the different responses of the fibroblast layer and reticular layer cells. A key feature of altered morphology is thickening of the connective tissue layers, especially the spongy layer (Malak & Bell, 1994b). This may lead to a functional separation of the amnion and chorion, and impair the passage of factors such as TGF- $\beta_1$  from amnion to chorion and vice versa. Additionally, the spongy layer is rich in hyaluronic acid (Meinert *et al.*, 2001), which itself acts to inhibit expression of  $\alpha$ -sma by fibroblasts (Andreutti *et al.*, 1999).

The regulation of myofibroblast differentiation also requires consideration of the regulation of 'de-differentiation' of the myofibroblast, as loss of  $\alpha$ -sma expression in the reticular layer is apparent in the third trimester. The exact mechanism of the loss of  $\alpha$ -sma immunoreactivity in the cells of the reticular layer is unclear. The loss of  $\alpha$ -sma positive cells in the classical wound response occurs by apoptosis (Desmouliere *et al.*, 1995). TGF- $\beta_1$  is considered a pro-apoptotic factor in many cell types (Schuster & Krieglstein, 2002), but has been demonstrated to protect against apoptosis in the myofibroblast (Zhang & Phan, 1999). If this were the mechanism present in the reticular layer, the cellularity of the tissue would have to be maintained by proliferation of a sub-population of 'V' or 'VD' cells. The alternative mechanism for the reduction in the number of  $\alpha$ -sma positive cells is de-differentiation of the cells, changing from 'VDA' to 'VD' cells. Whilst the proto-myofibroblast phenotype may revert to that of a fibroblast upon the removal of mechanical tension (Tomasek *et al.*, 2002), de-differentiation of the differentiated myofibroblast, with loss of  $\alpha$ -sma expression, has only recently been described (Sohara *et al.*, 2002), and it is unclear whether the mechanism exists *in vivo*.

A reduction in mechanical stress on the amniochorion following fusion with the decidua parietalis is only one possible cause of the 'switch-off' of  $\alpha$ -sma expression in the midzone fetal membranes. The timing of the onset of the loss of  $\alpha$ -sma expression occurs after the time of fusion of the amniochorion to the decidua parietalis. Therefore nutrition of the fetal membrane may play a role. Prior to this time, nutrition of the avascular amniochorion must arise from the amniotic fluid and/or the secretions from decidual glands within uterine cavity (Burton *et al.*, 2001; Burton *et al.*, 2002). Following fusion, nutrition and

oxygenation of the amniochorion arises from the amniotic fluid, and from the vasculature of the decidua parietalis (Bourne, 1962).

### **9.6.2. Regulation of tenascin-C expression**

A large number of cytokines and growth factors have been demonstrated to regulate tenascin-C expression in different cell types (Chiquet-Ehrismann *et al.*, 1995), although TGF- $\beta_1$  has been demonstrated to consistently upregulate expression of Tn-C (Pearson *et al.*, 1988). This is the only cytokine demonstrated to upregulate Tn-C expression in term fetal membranes in this study, and is therefore proposed as a major regulator of Tn-C expression in term fetal membranes *in vivo*. However, low expression of Tn-C was observed in fetal membranes obtained from the first and second trimesters. This suggests that TGF- $\beta_1$  is not the major regulator of myofibroblast differentiation (i.e. expression of  $\alpha$ -sma) at this gestation (as virtually all reticular layer cells at this gestation express  $\alpha$ -sma), or that its effects are modulated by other factors, potentially related to the fusion of the amniochorion with the decidua parietalis.

Stretch is also a recognised factor known to upregulate expression of Tn-C (Feng *et al.*, 1999; Jarvinen *et al.*, 1999). It has been demonstrated that the control of Tn-C expression by mechanical factors acts at the level of a stress response element in the gene promoter (Chiquet-Ehrismann *et al.*, 1994). Although not examined *in vitro* as a regulatory factor in this study, the pattern of myofibroblast differentiation observed in the fetal membranes through gestation suggests that it may be a potential regulatory factor *in vivo*, warranting further study.

### **9.6.3. Regulation of osteonectin expression**

Osteonectin, like Tn-C, may be regulated by a number of growth factors and cytokines in different cell types *in vitro* (Motamed, 1999), including TGF- $\beta_1$  (Reed *et al.*, 1994). As a common regulatory factor of Tn-C,  $\alpha$ -sma and osteonectin, and as the only factor identified in this study to upregulate osteonectin expression in term fetal membranes, it is proposed, as for Tn-C, as a major regulatory factor of osteonectin in term fetal membranes *in vivo*.

The second major proposed regulatory factor of myofibroblast differentiation in the fetal membranes *in vivo* is stretch. The response of osteonectin expression to mechanical stress

is conflicting. *In vitro* models have demonstrated no change in osteonectin expression in cardiac myocytes (Yamamoto *et al.*, 1999), and reduced (Meyer *et al.*, 1999) and increased (Sato *et al.*, 1998) expression in osteoblasts in response to mechanical stress.

#### **9.6.4. TGF- $\beta_1$ in the fetal membranes**

Transforming growth factor- $\beta$  (TGF- $\beta$ ) is a cytokine, which exists in three isoforms ( $-\beta_1$ ,  $-\beta_2$  and  $-\beta_3$ ), which share a high degree of homology (Lawrence, 1996). It may be produced by most cell types, and is released as high molecular weight biologically inactive latent TGF- $\beta$ . This consists of the biologically active dimer, attached to a latency-associated protein (LAP). Additionally, the complex may be attached to latent TGF- $\beta$  binding protein (LTBP), which targets the complex to the extracellular matrix (Munger *et al.*, 1997). Latent TGF- $\beta$  may be activated by exposure to low pH, by plasmin, and by thrombospondin-1 (Lawrence, 1996; Munger *et al.*, 1997). The latent TGF- $\beta_1$  complexes are components of the extracellular matrix, where it associates with fibronectin and with unidentified microfibrils suggested to be fibrillin, and from which it could be released and activated by plasmin (Teipale *et al.*, 1996). The latent form of TGF- $\beta_1$  has a half-life of 90 minutes *in vivo*, compared to 2-3 minutes for the active form (Lawrence, 1996). The activity of TGF- $\beta$  may also be regulated by binding of the active form by soluble proteins, including decorin, betaglycan, heparin and  $\alpha_2$ -macroglobulin (Munger *et al.*, 1997).

TGF- $\beta$  acts via transmembrane receptors, and inhibits the growth of most cell types, and exerts an immunosuppressive effect. It plays a key role in wound healing, where it is a potent chemoattractant for monocytes, macrophages, lymphocytes, and neutrophils, and stimulates the release of cytokines from these cells (O'Kane & Ferguson, 1997). It enhances deposition of extracellular matrix components such as collagen, fibronectin and tenascin-C (Lawrence, 1996), inhibits proteases, and upregulates synthesis of protease inhibitors (O'Kane & Ferguson, 1997). Adult wound healing is characterised by TGF- $\beta_1$  expression, macrophage recruitment, and the formation of scar tissue. This is in contrast to fetal wound healing, characterised by expression of TGF- $\beta_3$ , absence of macrophage recruitment, and scarless wound healing (Adzick & Lorenz, 1994; Ferguson *et al.*, 1996; O'Kane & Ferguson, 1997).

TGF- $\beta_1$  protein and mRNA have been extracted in large amounts from fetal membranes at term (Kauma *et al.*, 1990), and may be secreted by fetal membranes in organ culture

(Brown *et al.*, 2000), but the cellular origin has not been identified. Expression has, however, been studied in the placenta with respect to its potential role in regulation of trophoblast-decidual interactions. TGF- $\beta_1$ , and its type I and type II receptors have been localised to the amniotic epithelium of the chorionic plate, the syncytiotrophoblast and extravillous trophoblast of the placenta, and to a lesser extent within the decidua (Dungy *et al.*, 1991; Graham *et al.*, 1992). It has maximal expression in syncytial sprouts in the placenta in the first trimester (Vuckovic *et al.*, 1992). It is therefore possible that TGF- $\beta_1$  within the fetal membrane originates from the cytotrophoblast, the amniotic epithelium, the myofibroblast or the macrophage, which produces TGF- $\beta_1$  as part of the wound response (Desmouliere & Gabbiani, 1996). The cellular origin of TGF- $\beta_1$  within the fetal membranes may therefore be the key to the understanding of the myofibroblast differentiation patterns observed.

#### **9.6.5. Integrated model of myofibroblast differentiation in the fetal membranes**

An integrated model of the many factors that may play a role in myofibroblast differentiation in the amnion and chorion throughout gestation is illustrated in **Figure 9.8**.

The pattern of myofibroblast differentiation within the fetal membranes throughout pregnancy is consistent with stretch playing a major role. The amniochorion is under tension throughout gestation. During the first half of pregnancy the amniochorion increases in size through growth, and is free within the uterine cavity. Maintenance of tension at this stage is critical for the integrity of the sac, and the contractile properties of the differentiated myofibroblast would fulfill this role. During the second half of pregnancy the amniochorion is fused to, and therefore supported by, the underlying decidua parietalis. The amniochorion over the majority of the sac, with the exception of that directly overlying the internal os of the cervix, therefore no longer requires a contractile function. The decidua parietalis within the lower uterine segment may be deficient, leading to defective fusion of the amniochorion at this site, and poor proliferation of the cytotrophoblast leading to a thinner layer in comparison to in the upper uterine pole.

During the latter half of pregnancy, the sac expands by stretch, and therefore remains under tension, maintaining the cells as proto-myofibroblasts. During the latter stages of the third trimester, lower segment develops and cervix effaces. The underlying decidual support is lost (both physical support, and nutritional support), and the tissue is subject to additional

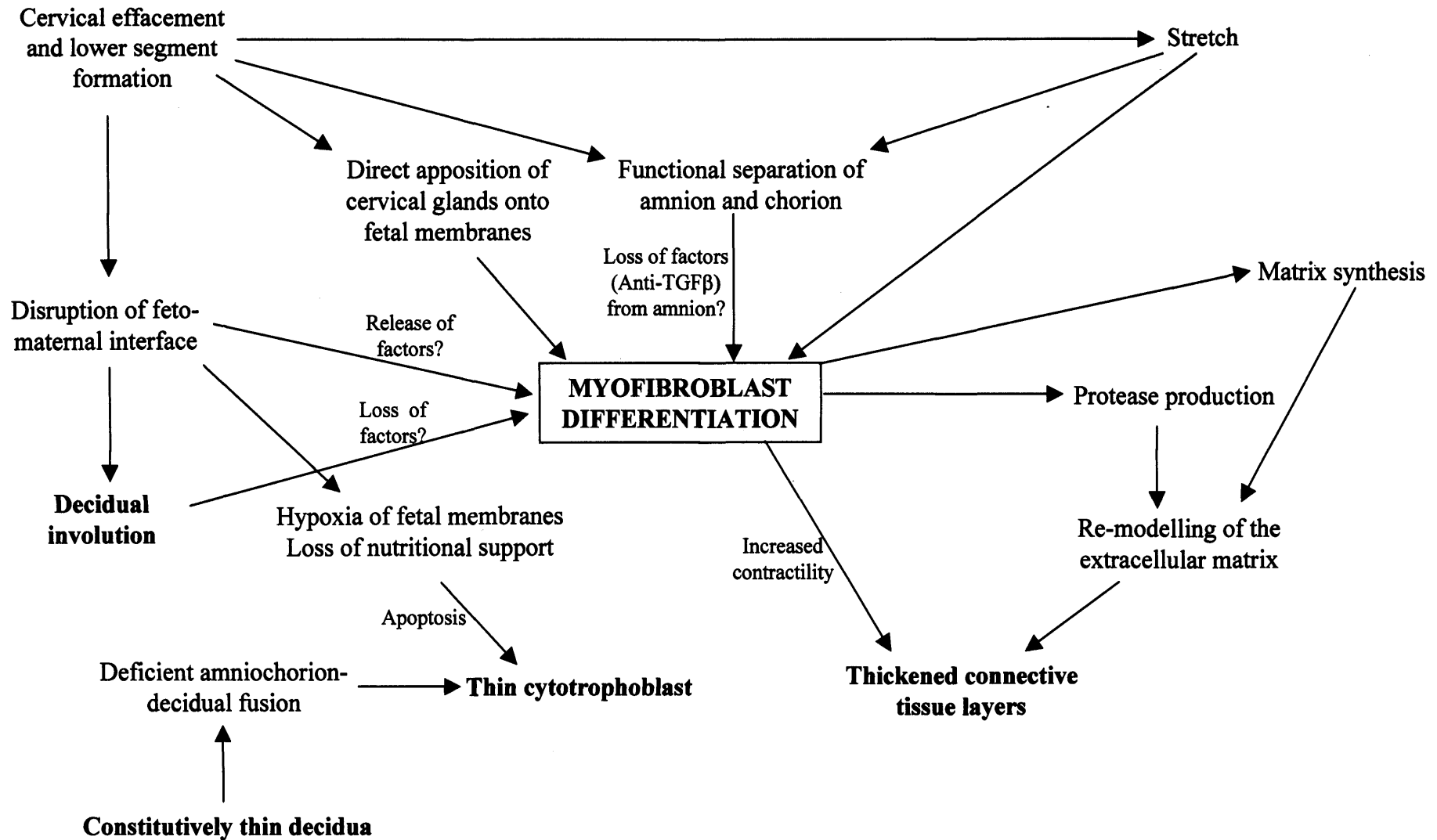


**Figure 9.8.** The potential factors involved in the regulation of myofibroblast differentiation in the fetal membranes during gestation, as discussed in 9.6.5. The key features of extreme altered morphology of the fetal membranes are highlighted.

stretch. Decidual thinning occurs, and loss of cytotrophoblast cells by apoptosis, with consequent thinning of the layer. Direct apposition of the cervical glands upon the fetal membranes may also play a role in myofibroblast differentiation. The contractile role of the differentiated myofibroblast is therefore required in the fetal membranes of the lower uterine segment to maintain integrity until the onset of labour.

Throughout gestation, where present, the differentiated myofibroblast plays an active role in matrix remodelling, through production of proteases and through synthesis of new matrix components, in order to accommodate the degree of stretch the fetal membrane is subjected to. The active processes of remodelling, and/or the contractile function and differential elastic recoil of the fetal membrane containing the differentiated myofibroblast, leads to an increased thickness of the connective tissue layers of amnion and chorion.

Throughout gestation, synthesis of TGF- $\beta_1$ , or release or activation of complexed TGF- $\beta_1$ , would be required to stimulate myofibroblast differentiation. The cellular origin of this within the fetal membranes is unclear, but its action may be modified by the action of proteases, and by structural changes in the fetal membranes, such as functional separation of amnion from chorion. There is also a potential role for regulatory growth factors or cytokines as yet unidentified.

### **9.7. Myofibroblast differentiation and fetal membrane rupture**

The fetal membranes within the lower uterine pole are theoretically subjected to a greater degree of stretch than those in the upper pole of the uterus during the latter part of the third trimester of pregnancy, as cervical effacement and lower uterine segment development occurs. All fetal membranes at 38 weeks express  $\alpha$ -sma within reticular layer cells in the lower uterine pole fetal membranes. Yet only 10% of fetal membranes rupture prior to labour at term (Duff, 1996). The differentiated myofibroblast may therefore act not to cause fetal membrane rupture over the cervix, but to maintain structural integrity in a region of membrane being subjected to extreme stretch. Their primary role may therefore be that of preventing premature membrane rupture, and acting to both degrade and synthesise extracellular matrix, permitting remodelling of the fetal membranes to accommodate differential stretch prior to the onset of labour. A similar role is proposed during the first and second trimesters, when the majority of the growth of the fetal membranes occurs (Alger & Pupkin, 1986; Casey & MacDonald, 1996).

The possibility that the differentiated myofibroblast within the reticular layer acts to maintain the structural integrity of the unsupported chorion during the first and second trimesters, and of a poorly supported region of the fetal membranes during a time of increasing stretch in the latter part of pregnancy (9.3.) contradicts the original hypothesis that these cells were responsible for generating a zone of weakened fetal membranes predisposed to rupture. This does not, however, discount the differentiated myofibroblast as a key cell in the process of fetal membrane rupture. Preterm prelabour fetal membrane rupture complicates 1-2% of all pregnancies (Major & Garite, 1997), and only a proportion of these cases is attributed to underlying infectious aetiology (Romero *et al.*, 1988). The aetiopathology of the remainder of cases of PPRM remains unclear. If the role of the myofibroblast as a supportive cell is correct, then defective regulation of myofibroblast differentiation may contribute to premature fetal membrane rupture, either at term or preterm gestations, or play a role in second trimester fetal loss. The greater understanding of the functions and regulation of these cells may lead to a therapeutic role for the modification of the myofibroblast phenotype in the prevention of untimely fetal membrane rupture.

## **9.8. Future research**

This study has examined the nature and functions of the fibroblastic and myofibroblastic cells of the connective tissue layers of the amniochorion and their potential role in fetal membrane rupture at term. Further research is required to determine whether the proposed models of their function are correct, and to model their activity *in vitro* to examine their regulation and methods of modifying their activity. Potential areas of research are:

1. Electron microscopic examination of regionally biopsied fetal membranes with and without  $\alpha$ -sma expression in the reticular layer, to determine whether features of myofibroblast differentiation correlate with  $\alpha$ -sma expression.
2. Examination of further detailed fetal membrane maps from preterm and term gestations, to identify whether a region of myofibroblast differentiation and altered fetal membrane morphology exists in the early third trimester, and to relate the size of any region identified to gestational age. The size of this area could be related to the degree of cervical effacement (both at term and preterm) as determined by measurement of cervical length by transvaginal ultrasound prior to Caesarean section.

3. Examination of the dividing membrane from twin pregnancies may help determine the influence of decidua upon the cellular phenotype of the overlying amniochorion.
4. Examination of regional fetal membrane biopsies from term and preterm gestations to look for evidence of apoptosis and cellular proliferation within the reticular layer, to determine whether apoptosis or de-differentiation of cells is the most likely mechanism of the loss of  $\alpha$ -sma expression. The relatively small number of cells examined in cross-sectional examination of this layer means that development of an 'en-face' method of examining the cells of this layer is required.
5. Biophysical determination of the relative strength and elastic properties of fetal membranes with and without myofibroblast differentiation in the reticular layer.
6. Microarray analysis on RNA extracted from the connective tissue layers of fetal membranes with altered morphology and midzone fetal membranes would identify other genes regulated in association with the altered morphology phenotype. Similar analysis could be performed on fetal membranes (or the dissected connective tissue layers) subjected to stretch *in vitro*.
7. *In vitro* organ culture models directed at induction of myofibroblast differentiation by mechanical stretch.
8. *In vitro* organ culture models directed at examining mechanisms of 'switch-off' of  $\alpha$ -sma expression in 'extreme altered morphology' fetal membrane biopsies with myofibroblast differentiation.
9. Development of methodology for isolation and culture of the connective tissue cells of the amnion and chorion will allow further examination of their regulation. To examine the response of cells to culture on a Tn-C-containing substrate. It would also permit development of an organotypic culture model – an 'artificial fetal membrane' to examine the role of the amniotic epithelium and cytotrophoblast layers.

## **Appendix**

### **Publications arising from this thesis**

#### **Papers**

1. McParland P. C., D. J. Taylor and S. C. Bell (2000).

Myofibroblast differentiation in the connective tissues of the amnion and chorion of term fetal membranes - implications for fetal membrane rupture and labour.

Placenta 21: 44-53

2. McParland P. C., S. C. Bell, J. H. Pringle and D. J. Taylor (2001).

Regional and cellular localization of osteonectin/SPARC expression in connective tissue and cytotrophoblastic layers of human fetal membranes at term.

Molecular Human Reproduction 7: 463-474

3. McParland P. C., D. J. Taylor and S. C. Bell.

Zones of altered morphology and chorionic connective tissue cellular phenotype in human fetal membranes (amniochorion and decidua) overlying the lower uterine pole and cervix prior to labour at term.

Submitted to American Journal of Obstetrics & Gynecology

#### **Abstracts**

4. McParland P. C. and S. C. Bell (1998).

Localisation of the extracellular matrix protein tenascin-C at the materno-fetal interface during pregnancy.

British Journal of Obstetrics and Gynaecology 105 (Suppl. 17): 75-76

5. McParland P. C. and S. C. Bell (1998).

Alteration in myofibroblastic phenotype in fetal membranes associated with the cervix and rupture site.

Prenatal and Neonatal Medicine 3 (Suppl. 2): 21

6. McParland P. C., J. H. Pringle and S. C. Bell (1998).  
Tenascin and the fetal membrane wound hypothesis - Programming for fetal membrane rupture?  
British Journal of Obstetrics and Gynaecology **105**: 1223-1224
  
7. McParland P. C., D. J. Taylor and S. C. Bell (1999).  
The association between myofibroblast differentiation in fetal membranes and parturition.  
British Journal of Obstetrics and Gynaecology **106**: 1322
  
8. McParland P. C., J. H. Pringle, D. J. Taylor and S. C. Bell (2000).  
Regional myofibroblast differentiation is associated with tenascin-C expression in the connective tissue layers of the human fetal membranes at term  
Journal of the Society for Gynecologic Investigation **7** (Suppl. 1): 126A
  
9. McParland P. C., D. J. Taylor and S. C. Bell (2000).  
Induction of myofibroblast differentiation in the connective tissue of the human fetal membranes by TGF- $\beta_1$  during organ culture  
Prenatal and Neonatal Medicine **5** (Suppl. 3): 26
  
10. McParland P. C., D. J. Taylor and S. C. Bell (2000).  
Regional expression of the matricellular protein osteonectin (SPARC/BM40) in the connective tissue layers of the human amniochorion at term  
Prenatal and Neonatal Medicine **5** (Suppl. 3): 26
  
11. McParland P. C., D. J. Taylor and S. C. Bell (2001).  
The presence of an area of fetal membranes overlying the lower uterine segment exhibiting morphological changes and myofibroblast activation is characteristic of fetal membranes obtained prior to the onset of labour at term.  
Journal of Obstetrics and Gynaecology **21**: 546

## References

- Adams M., J. L. Jones, R. A. Walker, J. H. Pringle and S. C. Bell (2002). Changes in tenascin-C isoform expression in invasive and preinvasive breast disease. Cancer Res **62**: 3289-3297.
- Adegboyega P. A., R. C. Mifflin, J. F. DiMari, J. I. Saada and D. W. Powell (2002). Immunohistochemical study of myofibroblasts in normal colonic mucosa, hyperplastic polyps, and adenomatous colorectal polyps. Arch Pathol Lab Med **126**: 829-836.
- Adzick N. S. and H. P. Lorenz (1994). Cells, matrix, growth factors, and the surgeon. The biology of scarless fetal wound repair. Annals Surg **220**: 10-18.
- Alger L. S. and M. J. Pupkin (1986). Etiology of preterm premature rupture of the membranes. Clin Obstet Gynecol **29**: 758-770.
- Al-Zaid N. S., K. A. Gumaa, M. N. Bou-Resli and M. E. A. Ibrahim (1986). Site variability in the solubility of collagen of human fetal membranes. J Reprod Fertil **77**: 665-668.
- Andreutti D., A. Geinoz and G. Gabbiani (1999). Effect of hyaluronic acid on migration, proliferation and  $\alpha$ -smooth muscle actin expression by cultured rat and human fibroblasts. J Submicrosc Cytol Pathol **31**: 173-177.
- Aplin J. D. and S. Campbell (1985). An immunofluorescence study of extracellular matrix associated with cytotrophoblast of the chorion laeve. Placenta **6**: 469-479.
- Aplin J. D., S. Campbell and T. D. Allen (1985). The extracellular matrix of human amniotic epithelium: Ultrastructure, composition and deposition. J Cell Sci **79**: 119-136.
- Arora P. D., N. Narani and C. A. G. McCulloch (1999). The compliance of collagen gels regulates transforming growth factor- $\beta$  induction of  $\alpha$ -smooth muscle actin in fibroblasts. Am J Pathol **154**: 871-882.
- Badouin C., G. Brignole, P. J. Pisella, F. Becquet and P. J. Philip (1997). Immunophenotyping of human dendriform cells from the conjunctival epithelium. Curr Eye Res **16**: 475-481.
- Balazs M. and A. Kovacs (1982). The 'transitional' mucosa adjacent to large bowel carcinoma - electron microscopic features and myofibroblast reaction. Histopathology **6**: 617-629.

- Bartels H. and T. Wang (1983). Intercellular junctions in the human fetal membranes. A freeze-fracture study. Anat Embryol **166**: 103-120.
- Bartsch U. (1996). The extracellular matrix molecule tenascin-C: expression in vivo and functional characterization in vitro. Prog Neurobiol **49**: 145-68.
- Basset P., J. P. Bellocq, C. Wolf, I. Stoll, P. Hutin, J. M. Limacher, O. L. Podhajcer, M. P. Chenard, M. C. Rio and P. Chambon (1990). A novel metalloproteinase gene specifically expressed in stromal cells of breast carcinomas. Nature **348**: 699-704.
- Beazley J. M. (1995). Natural labour and its active management. Dewhurst's textbook of obstetrics and gynaecology for postgraduates. C. R. Whitfield. Oxford, Blackwell Science: 293-311.
- Bell S. and T. Malak (1994). Formation of the chorio-decidual interface of human fetal membranes: is it analogous to anchoring villi development in the placenta? Ann NY Acad Sci **734**: 166-168.
- Bell S. C. and T. M. Malak (1997). Structural and cellular biology of the fetal membranes. Preterm labor. M. G. Elder, R. F. Lamont and R. Romero. New York, Churchill Livingstone. **401-430**.
- Bell S. C., J. H. Pringle, D. J. Taylor and T. M. Malak (1999). Alternatively spliced tenascin-C mRNA isoforms in human fetal membranes. Mol Hum Reprod **5**: 1066-76.
- Benirschke K. and P. Kaufmann (2000). Anatomy and pathology of the placental membranes. Pathology of the human placenta. New York, Springer-Verlag: 281-334.
- Benzonana G., O. Skalli and G. Gabbiani (1988). Correlation between the distribution of smooth muscle or non muscle myosins and  $\alpha$ -smooth muscle actin in normal and pathological soft tissues. Cell Motil Cytoskel **11**: 260-274.
- Berndt A., H. Kosmehl, D. Katenkamp and V. Tauchmann (1994). Appearance of the myofibroblastic phenotype in Dupuytren's disease is associated with a fibronectin, laminin, collagen type IV and tenascin extracellular matrix. Pathobiology **62**: 55-8.
- Blazejewski S., B. Le Bail, L. Boussarie, J. F. Blanc, L. Malaval, K. Okubo, J. Saric, P. Bioulac-Sage and J. Rosenbaum (1997). Osteonectin (SPARC) expression in human liver and in cultured human liver myofibroblasts. Am J Pathol **151**: 651-7.
- Blazejewski S., A.-M. Preaux, A. Mallat, I. Brocheriou, P. Mayes, D. Dhumeaux, D. Hartmann, D. Schuppan and J. Rosenbaum (1995). Human myofibroblastlike cells obtained by outgrowth are representative of the fibrogenic cells in the liver. Hepatology **22**: 788-797.

- Bogic L. V., S. Y. Yamamoto, L. K. Millar and G. D. Bryant-Greenwood (1997). Developmental regulation of the human relaxin genes in the decidua and placenta: Overexpression in the preterm premature rupture of the fetal membranes. Biol Reprod **57**: 908-920.
- Borsi L., E. Balza, P. Castellani, B. Carnemolla, M. Ponassi, G. Querze and L. Zardi (1994). Cell-cycle dependent alternative splicing of the tenascin primary transcript. Cell Adhes Commun **1**: 307-17.
- Borsi L., E. Balza, B. Gaggero, G. Allemanni and L. Zardi (1995). The alternative splicing pattern of the tenascin-C pre-mRNA is controlled by the extracellular pH. J Biol Chem **270**: 6243-5.
- Borsi L., B. Carnemolla, G. Nicolo, B. Spina, G. Tanara and L. Zardi (1992). Expression of different tenascin isoforms in normal, hyperplastic and neoplastic human breast tissues. Int J Cancer **52**: 688-92.
- Bou-Resli M. N., N. S. Al-Zaid and M. E. A. Ibrahim (1981). Full-term and prematurely ruptured fetal membranes. An ultrastructural study. Cell Tissue Res **220**: 263-278.
- Bourne G. L. (1962). The human amnion and chorion. London, Lloyd-Luke Ltd.
- Brown N. L., S. A. Alvi, M. G. Elder, P. R. Bennett and M. H. F. Sullivan (2000). The regulation of prostaglandin output from term intact fetal membranes by anti-inflammatory cytokines. Immunology **99**: 124-133.
- Bryant-Greenwood G. (1998). The extracellular matrix of the human fetal membranes: Structure and function. Placenta **19**: 1-11.
- Bryant-Greenwood G. and S. Y. Yamamoto (1995). Control of peripartal collagenolysis in the human chorion-decidua. Am J Obstet Gynecol **172**: 63-70.
- Bulmer J. N. and P. M. Johnson (1984). Macrophage populations in the human placenta and amniochorion. Clin Exp Immunol **57**: 393-403.
- Burton G. J., J. Hempstock and E. Jauniaux (2001). Nutrition of the human fetus during the first trimester - a review. Placenta **22 (Suppl A)**: S70-S76.
- Burton G. J., A. L. Watson, J. Hempstock, J. N. Skepper and E. Jauniaux (2002). Uterine glands provide histiotrophic nutrition for the human fetus during the first trimester of pregnancy. J Clin Endocrinol Metab **87**: 2954-2959.
- Bussolino F., M. Ziche, M. W. Wang, D. Alessi, L. Morbidelli, O. Cremona, A. Bosia, P. C. Marchisio and A. Mantovani (1991). In vitro and in vivo activation of endothelial cells by colony-stimulating factors. J Clin Invest **87**: 986-995.

- Campbell S. E. and L. C. Katwa (1997). Angiotensin II stimulated expression of transforming growth factor-beta1 in cardiac fibroblasts and myofibroblasts. J Mol Cell Cardiol **29**: 1947-58.
- Carnemolla B., L. Borsi, G. Bannikov, S. Troyanovsky and L. Zardi (1992). Comparison of human tenascin expression in normal, simian-virus-40-transformed and tumor-derived cell lines. Eur J Biochem **205**: 561-7.
- Carnemolla B., A. Siri, L. Borsi and L. Zardi (1996). Tenascin in disease. Tenascin and the counteradhesive molecules of the extracellular matrix. K. L. Crossin. Amsterdam, Harwood Academic: 89-108.
- Casey M. L. and P. C. MacDonald (1993). Human parturition: Distinction between the initiation of parturition and the onset of labor. Semin Reprod Endocrinol **11**: 272-284.
- Casey M. L. and P. C. MacDonald (1996). Interstitial collagen synthesis and processing in human amnion: a property of the mesenchymal cells. Biol Reprod **55**: 1253-60.
- Castellucci M., I. Classen-Linke, J. Muhlhauser, P. Kaufmann, L. Zardi and R. Chiquet-Ehrismann (1991). The human placenta: a model for tenascin expression. Histochemistry **95**: 449-58.
- Challis J. R. G. and W. Gibb (1996). Control of parturition. Prenat Neonat Med **1**: 283-291.
- Challis J. R. G., S. G. Matthews, W. Gibb and S. J. Lye (2000). Endocrine and paracrine regulation of birth at term and preterm. Endocrine Rev **21**: 514-550.
- Cheung P. Y. C., J. C. Walton, H.-H. Tai, S. C. Riley and J. R. G. Challis (1992). Localization of 15-hydroxyprostaglandin dehydrogenase in human fetal membranes, decidua, and placenta during pregnancy. Gynecol Obstet Invest **33**: 142-146.
- Chiavegato A., M. L. Bochaton-Piallat, E. D'Amore, S. Sartore and G. Gabbiani (1995). Expression of myosin heavy chain isoforms in mammary epithelial cells and in myofibroblasts from different fibrotic settings during neoplasia. Virchows Arch **426**: 77-86.
- Chibbar R., F. D. Miller and B. F. Mitchell (1993). Synthesis of oxytocin in amnion, chorion, and decidua may influence the timing of human parturition. J Clin Invest **91**: 185-192.
- Chiquet M., M. Matthisson, M. Koch, M. Tannheimer and R. Chiquet-Ehrismann (1996). Regulation of extracellular matrix synthesis by mechanical stress. Biochem Cell Biol **74**: 737-44.

- Chiquet-Ehrismann R., C. Hagios and S. Schenk (1995). The complexity in regulating the expression of tenascins. Bioessays 17: 873-878.
- Chiquet-Ehrismann R., E. J. Mackie, C. A. Pearson and T. Sakakura (1986). Tenascin: an extracellular matrix protein involved in tissue interactions during fetal development and oncogenesis. Cell 47: 131-139.
- Chiquet-Ehrismann R., M. Tannheimer, M. Koch, A. Brunner, J. Spring, D. Martin, S. Baumgartner and M. Chiquet (1994). Tenascin-C expression by fibroblasts is elevated in stressed collagen gels. J Cell Biol 127: 2093-101.
- Clark R. A. F. (1996). Wound repair: Overview and general considerations. The molecular and cellular biology of wound repair. R. A. F. Clark. New York, Plenum Press: 3-50.
- Copper R. L., R. L. Goldenberg, R. K. Creasy, M. B. DuBard, R. O. Davis, S. S. Entman, J. D. Iams and S. P. Cliver (1993). A multicenter study of preterm birth weight and gestational age-specific neonatal mortality. Am J Obstet Gynecol 168: 78-84.
- Cox S. M., M. R. King, M. L. Casey and P. C. MacDonald (1993). Interleukin-1b, -1a, and -6 and prostaglandins in vaginal/cervical fluids of pregnant women before and during labor. J Clin Endocrinol Metab 77: 805-815.
- Creasy R. K. (1993). Preterm birth prevention: Where are we? Am J Obstet Gynecol 168: 1223-1230.
- Crossin K. L. (1996). Tenascin: a multifunctional extracellular matrix protein with a restricted distribution in development and disease. J Cell Biochem 61: 592-8.
- Crossin K. L. (1996). Tenascin and the counteradhesive molecules of the extracellular matrix. Amsterdam, Harwood Academic Publishers.
- Damsky C. H., M. L. Fitzgerald and S. J. Fisher (1992). Distribution patterns of extracellular matrix components and adhesion receptors are intricately modulated during first trimester cytotrophoblast differentiation along the invasive pathway, in vivo. J Clin Invest 89: 210-22.
- Darby I., O. Skalli and G. Gabbiani (1990).  $\alpha$ -smooth muscle actin is transiently expressed by myofibroblasts during experimental wound healing. Lab Invest 63: 21-29.
- Desmouliere A. and G. Gabbiani (1996). The role of the myofibroblast in wound healing and fibrocontractive diseases. The molecular and cellular biology of wound repair. R. A. F. Clark. New York, Plenum Press: 391-423.
- Desmouliere A., A. Geinoz, F. Gabbiani and G. Gabbiani (1993). Transforming growth factor-beta 1 induces alpha-smooth muscle actin expression in granulation tissue

- myofibroblasts and in quiescent and growing cultured fibroblasts. J Cell Biol **122**: 103-11.
- Desmouliere A., M. Redard, I. Darby and G. Gabbiani (1995). Apoptosis mediates the decrease in cellularity during the transition between granulation tissue and scar. Am J Pathol **146**: 56-66.
- Desmouliere A., L. Rubbia-Brandt, A. Abdui, T. Walz, A. Macieira-Coelho and G. Gabbiani (1992).  $\alpha$ -Smooth muscle actin is expressed in a subpopulation of cultured and cloned fibroblasts and is modulated by  $\gamma$ -interferon. Exp Cell Res **201**: 64-73.
- Devlieger R., E. Gratacos, J. Wu, L. Verbist, R. Pijnenborg and J. A. M. Deprest (2000). An organ-culture for in vitro evaluation of fetal membrane healing capacity. Eur J Obstet Gynecol Reprod Biol **92**: 145-150.
- Duff P. (1996). Premature rupture of the membranes in term patients. Semin Perinatol **20**: 401-408.
- Dugina V., L. Fontao, C. Chaponnier, J. Vasiliev and G. Gabbiani (2001). Focal adhesion features during myofibroblastic differentiation are controlled by intracellular and extracellular factors. J Cell Sci **114**: 3285-3296.
- Dungy L. J., T. A. Siddiqi and S. Khan (1991). Transforming growth factor- $\beta_1$  expression during placental development. Am J Obstet Gynecol **165**: 853-857.
- Dziadek M., M. Paulsson, M. Aumailley and R. Timpl (1986). Purification and tissue distribution of a small protein (BM-40) extracted from a basement membrane tumor. Eur J Biochem **161**: 455-64.
- Economopoulos P., M. Sun, B. Purgina and W. Gibb (1996). Glucocorticoids stimulate prostaglandin H synthase type-2 (PGHS-2) in the fibroblast cells in human amnion cultures. Mol Cell Endocrinol **117**: 141-7.
- Eddy R. J., J. A. Petro and J. J. Tomasek (1988). Evidence for the nonmuscle nature of the "myofibroblast" of granulation tissue and hypertrophic scar. Am J Pathol **130**: 252-260.
- Egan D. and C. O'Herlihy (1988). Expectant management of spontaneous rupture of membranes at term. J Obstet Gynaecol **8**: 243-247.
- Ekblom M., R. Fassler, B. Tomasini-Johansson, K. Nilsson and P. Ekblom (1993). Downregulation of tenascin expression by glucocorticoids in bone marrow stromal cells and in fibroblasts. J Cell Biol **123**: 1037-45.
- El Maradny E., N. Kanayama, A. Halim, K. Maehara, K. Sumimoto and T. Terao (1994). Interleukin-8 induces cervical ripening in rabbits. Am J Obstet Gynecol **171**: 77-83.

- El Maradny E., N. Kanayama, A. Halim, K. Maehara and T. Terao (1996). Stretching of fetal membranes increases the concentration of interleukin-8 and collagenase activity. Am J Obstet Gynecol **174**: 843-849.
- Erickson H. P. and H. C. Taylor (1987). Hexabrachion proteins in embryonic chicken tissues and human tumours. J Cell Biol **105**: 1387-1394.
- Eyden B. (2001). The fibronexus in reactive and tumoral myofibroblasts: further characterisation by electron microscopy. Histol Histopathol **16**: 57-70.
- Eyden B. P. (1993). Brief review of the fibronexus and its significance for myofibroblastic differentiation and tumor diagnosis. Ultrastruct Pathol **17**: 611-612.
- Eyden B. P., J. Ponting, H. Davies, C. Bartley and E. Torgersen (1994). Defining the myofibroblast: normal tissues, with special reference to the stromal cells of Wharton's jelly in human umbilical cord. J Submicrosc Cytol Pathol **26**: 347-55.
- Fawthrop R. K. and C. D. Ockleford (1994). Cryofracture of human term amniochorion. Cell Tissue Res **277**: 315-323.
- Feinberg R. F., H. J. Kliman and C. J. Lockwood (1991). Is oncofetal fibronectin a trophoblast glue for human implantation? Am J Pathol **138**: 537-543.
- Feller A. C., H. Schneider, D. Schmidt and M. R. Parwaresch (1985). Myofibroblast as a major cellular constituent of villous stroma in human placenta. Placenta **6**: 405-415.
- Feng Y., J. H. Yang, H. Huang, S. P. Kennedy, T. G. Turi, J. F. Thompson, P. Libby and R. T. Lee (1999). Transcriptional profile of mechanically induced genes in human vascular smooth muscle cells. Circ Res **85**: 1118-23.
- Ferguson M. W. J., D. J. Whitby, M. Shah, J. Armstrong, J. W. Siebert and M. T. Longaker (1996). Scar formation: The spectral nature of fetal and adult wound repair. Plastic Reconstruct Surg **97**: 854-860.
- Fisher L. W., J. T. Stubbs and M. F. Young (1995). Antisera and cDNA probes to human and certain animal model bone matrix noncollagenous proteins. Acta Orthop Scand **66 (Suppl 266)**: 61-65.
- Fortunato S. J., R. Menon and S. J. Lombardi (1997). Collagenolytic enzymes (gelatinases) and their inhibitors in human amniochorionic membranes. Am J Obstet Gynecol **177**: 731-741.
- Fortunato S. J., R. Menon, K. F. Swan and T. W. Lyden (1994). I. Organ culture of amniochorionic membrane in vitro. Am J Reprod Immunol **32**: 184-187.
- Francki A., A. D. Bradshaw, J. A. Bassuk, C. C. Howe, W. G. Couser and E. H. Sage (1999). SPARC regulates the expression of collagen type I and transforming growth factor-beta 1 in mesangial cells. J Biol Chem **274**: 32145-32152.

- Freeman W. M., S. J. Walker and K. E. Vrana (1999). Quantitative RT-PCR: Pitfalls and potential. Biotechniques **26**: 112-125.
- French J. I. and J. A. McGregor (1996). The pathobiology of premature rupture of membranes. Semin Perinatol **20**: 344-368.
- Gabbiani G. (1992). The biology of the myofibroblast. Kidney Int **41**: 530-2.
- Gabbiani G. (1998). Evolution and clinical implications of the myofibroblast concept. Cardiovasc Res **38**: 545-8.
- Gabbiani G., C. Chaponnier and I. Huttner (1978). Cytoplasmic filaments and gap junctions in epithelial cells and myofibroblasts during wound healing. J Cell Biol **76**: 561-568.
- Gabbiani G., B. J. Hirschel, G. B. Ryan, P. R. Statkov and G. Majno (1972). Granulation tissue as a contractile organ. A study of structure and function. Exp Med **1972**: 719-734.
- Gabbiani G., G. B. Ryan and G. Majno (1971). Presence of modified granulation tissue and their possible role in wound contraction. Experientia **27**: 549-550.
- George J., S.-S. Wang, A.-M. Sevcsik, M. Sanicola, R. L. Cate, V. E. Koteliensky and D. M. Bissell (2000). Transforming growth factor- $\beta$  initiates wound repair in rat liver through induction of the EIIIA-fibronectin splice isoform. Am J Pathol **156**: 115-124.
- Germain A. M., P. C. MacDonald and M. L. Casey (1997). Endothelin receptor mRNAs in human fetal membranes, chorionic vessels, and decidua parietalis. Mol Cell Endocrinol **132**: 161-168.
- Germain A. M., J. Smith, M. L. Casey and P. C. MacDonald (1994). Human fetal membrane contribution to the prevention of parturition: Uterotonin degradation. J Clin Endocrinol Metab **78**: 463-470.
- Gilles C., J. A. Bassuk, H. Pulyaeva, E. H. Sage, J. M. Foidart and E. W. Thompson (1998). SPARC/osteonectin induces matrix metalloproteinase 2 activation in human breast cancer cell lines. Cancer Res **58**: 5529-36.
- Gomez R., R. Romero, M. Mazor, F. Ghezzi, C. David and B. H. Yoon (1997). The role of infection in preterm labor and delivery. Preterm labor. M. G. Elder, R. Romero and R. F. Lamont. New York, Churchill Livingstone: 85-125.
- Graham C. H., J. J. Lysiak, K. R. McCrae and P. K. Lala (1992). Localization of transforming growth factor- $\beta$  at the human fetal maternal interface: Role in trophoblast growth and differentiation. Biol Reprod **46**: 561-572.

- Greenwood J. A. and J. E. Murphy-Ullrich (1998). Signaling of de-adhesion in cellular regulation and motility. Microsc Res Tech **43**: 420-432.
- Grumet M., S. Hoffman, K. L. Crossin and G. M. Edelman (1985). Cytotactin, an extracellular matrix protein of neural and non-neural tissues that mediates glia-neuron interaction. Proc Natl Acad Sci U S A **82**: 8075-9.
- Hahn A. W., F. Kern, U. Jonas, M. John, F. R. Buhler and T. J. Resink (1995). Functional aspects of vascular tenascin-C expression. J Vasc Res **32**: 162-74.
- Hanssens M., L. Vercruyssen, M. J. N. C. Keirse, R. Pijnenborg and F. A. Van Assche (1995). Identification of 'renin'-containing cells in the choriodecidua. Placenta **16**: 517-525.
- Hao Y., D. H. Ma, D. G. Hwang, W. S. Kim and F. Zhang (2000). Identification of antiangiogenic and antiinflammatory proteins in human amniotic membrane. Cornea **19**: 348-352.
- Harger J. H., A. W. Hsing, R. E. Tuomala, R. S. Gibbs, P. B. Mead, D. A. Eschenbach, G. E. Knox and B. F. Polk (1990). Risk factors for preterm premature rupture of fetal membranes: a multicenter case-control study. Am J Obstet Gynecol **163**: 130-137.
- Harkonen E., I. Virtanen, A. Linnala, L. L. Laitinen and V. L. Kinnula (1995). Modulation of fibronectin and tenascin production in human bronchial epithelial cells by inflammatory cytokines in vitro. Am J Respir Cell Mol Biol **13**: 109-15.
- Helmig R. B., H. Oxlund, L. K. Petersen and N. Uldbjerg (1993). Different biomechanical properties of human fetal membranes obtained before and after delivery. Eur J Obstet Gynecol Reprod Biol **48**: 183-189.
- Hendricks C. H., W. E. Brenner and G. Kraus (1970). Normal cervical dilatation pattern in late pregnancy and labor. Am J Obstet Gynecol **106**: 1065-1082.
- Hieber A. D., D. Corcino, J. Motosue, L. B. Sandberg, P. J. Roos, S. Yeh Yu, K. Csiszar, H. M. Kagan, C. D. Boyd and G. Bryant-Greenwood (1997). Detection of elastin in the human fetal membranes: Proposed molecular basis for elasticity. Placenta **18**: 301-312.
- Hinz B., D. Mastrangelo, C. E. Iselin, C. Chapponier and G. Gabbiani (2001). Mechanical tension controls granulation tissue contractile activity and myofibroblast differentiation. Am J Pathol **159**: 1009-1020.
- Hirschi K. K., L. Lai, N. S. Belaguli, D. A. Dean, R. J. Schwartz and W. E. Zimmer (2002). Transforming growth factor-beta induction of smooth muscle cell phenotype requires transcriptional and post-translational control of serum response factor. J Biol Chem **277**: 6287-6295.

- Hotta O., H. Kitamura and Y. Taguma (1998). Detection of mature macrophages in urinary sediments: clinical significance in predicting progressive disease. Ren Fail **20**: 413-418.
- Hoyes A. D. (1971). Ultrastructure of the mesenchymal layers of the human chorion laeve. J Anat **109**: 17-30.
- Hoyes A. D. (1975). Structure and function of the amnion. Obstet Gynecol Annu **4**: 1-38.
- Hulboy D. L., L. A. Rudolph and L. M. Matrisian (1997). Matrix metalloproteinases as mediators of reproductive function. Mol Human Reprod **3**: 27-45.
- Ibrahim M. E. A., M. N. Bou-Resli, N. S. Al-Zaid and L. F. Bishay (1983). Intact fetal membranes. Morphological predisposition to rupture. Acta Obstet Gynecol Scand **62**: 481-485.
- Imai K., H. Kanzaki, H. Fujiwara, M. Maeda, M. Ueda, H. Suginami and T. Mori (1994). Expression and localization of aminoprptidase N, neutral endopeptidase, and dipeptidyl peptidase IV in the human placenta and fetal membranes. Am J Obstet Gynecol **170**: 1163-1168.
- Iruela-Arispe M. L., T. F. Lane, D. Redmond, M. Reilly, R. P. Bolender, T. J. Kavanagh and E. H. Sage (1995). Expression of SPARC during development of the chicken chorioallantoic membrane: Evidence for regulated proteolysis in vivo. Mol Biol Cell **6**: 327-343.
- Jarvinen T. A., L. Jozsa, P. Kannus, T. L. Jarvinen, M. Kvist, T. Hurme, J. Isola, H. Kalimo and M. Jarvinen (1999). Mechanical loading regulates tenascin-C expression in the osteotendinous junction. J Cell Sci **112 Pt 18**: 3157-66.
- Jester J. V., P. A. Barry-Lane, H. D. Cavanagh and W. M. Petroll (1996). Induction of alpha-smooth muscle actin expression and myofibroblast transformation in cultured corneal keratocytes. Cornea **15**: 505-16.
- Jones F. S. and D. W. Copertino (1996). The molecular biology of tenascin: structure, splice variants, and regulation of gene expression. Tenascin and counteradhesive molecules of the extracellular matrix. K. L. Crossin. Amsterdam, Harwood Academic Publishers: 1-22.
- Jones F. S. and P. L. Jones (2000a). The tenascin family of ECM glycoproteins: Structure, function, and regulation during embryonic development and tissue remodeling. Dev Dynamics **218**: 235-259.
- Jones P. L. and F. S. Jones (2000b). Tenascin-C in development and disease: gene regulation and cell function. Matrix Biol **19**: 581-596.

- Kacemi A., C. Vervelle, S. Uzan and J. C. Challier (1999). Immunostaining of vascular, perivascular cells and stromal components in human placental villi. Cell Mol Biol **45**: 101-113.
- Kaltreider D. F. and S. Kohl (1980). Epidemiology of preterm delivery. Clin Obstet Gynecol **23**: 17-31.
- Kamada S. and T. Kakunaga (1989). The nucleotide sequence of a human smooth muscle alpha-actin (aortic type) cDNA. Nucleic Acids Res **17**: 1767.
- Kanayama N. and H. Fukamizu (1989). Mechanical stretching increases prostaglandin E2 in cultured human amnion cells. Gynecol Obstet Invest **28**: 123-126.
- Kaplony A., D. R. Zimmermann, R. W. Fischer, B. A. Imhof, B. F. Odermatt, K. H. Winterhalter and L. Vaughan (1991). Tenascin Mr 220,000 isoform expression correlates with corneal cell migration. Development **112**: 605-14.
- Kauma S., D. Matt, S. Strom, D. Eierman and T. Turner (1990). Interleukin-1 $\beta$ , human leukocyte antigen HLA-DR $\alpha$ , and transforming growth factor- $\beta$  expression in endometrium, placenta, and placental membranes. Am J Obstet Gynecol **163**: 1430-1437.
- Keene D. R., L. Y. Sakai, G. P. Lunstrum, N. P. Morris and R. E. Burgeson (1987). Type VII collagen forms an extended network of anchoring fibrils. J Cell Biol **104**: 611-621.
- Keirse M. J. N. C. and A. C. Turnbull (1975). Metabolism of prostaglandins within the pregnant uterus. Br J Obstet Gynaecol **82**: 887-893.
- Khan K. M. and D. J. Falcone (1997). Role of laminin in matrix induction of macrophage urokinase-type plasminogen activator and 92-kDa metalloproteinase expression. J Biol Chem **272**: 8270-5.
- Khong T. Y., E. B. Lane and W. B. Robertson (1986). An immunocytochemical study of fetal cells at the maternal-placental interface using monoclonal antibodies to keratins, vimentin and desmin. Cell Tissue Res **246**: 189-195.
- Kobayashi K., T. Kubota and T. Aso (1998). Study on myofibroblast differentiation in the stromal cells of Wharton's jelly: expression and localization of alpha-smooth muscle actin. Early Hum Dev **51**: 223-33.
- Kohnen G., S. Kertschanska, R. Demir and P. Kaufmann (1996). Placental villous stroma as a model system for myofibroblast differentiation. Histochem Cell Biol **105**: 415-29.

- Koukoulis G. K., V. E. Gould, A. Bhattacharyya, J. E. Gould, A. A. Howedy and I. Virtanen (1991). Tenascin in normal, reactive, hyperplastic, and neoplastic tissues: biologic and pathologic implications. Hum Pathol **22**: 636-43.
- Laham N., S. P. Brennecke, K. Bendtzen and G. E. Rice (1994). Tumour necrosis factor alpha during human pregnancy and labour: maternal plasma and amniotic fluid concentrations and release from intrauterine tissues. Eur J Endocrinol **131**: 607-614.
- Lamireau T., B. Le Bail, L. Boussarie, M. Fabre, P. Vergnes, O. Bernard, F. Gautier, P. Bioulac-Sage and J. Rosenbaum (1999). Expression of collagens type I and IV, osteonectin and transforming growth factor beta-1 (TGFbeta1) in biliary atresia and paucity of intrahepatic bile ducts during infancy. J Hepatol **31**: 248-55.
- Lane T. F., M. L. Iruela-Arispe and E. H. Sage (1992). Regulation of gene expression by SPARC during angiogenesis in vitro. Changes in fibronectin, thrombospondin-1, and plasminogen activator inhibitor-1. J Biol Chem **267**: 16736-45.
- Lane T. F. and E. H. Sage (1994). The biology of SPARC, a protein that modulates cell-matrix interactions. Faseb J **8**: 163-73.
- Lankat-Buttgereit B., K. Mann, R. Deutzmann, R. Timpl and T. Krieg (1988). Cloning and complete amino acid sequences of human and murine basement membrane protein BM-40 (SPARC, osteonectin). FEBS Lett **236**: 352-6.
- Latijnhouwers M. A., G. J. de Jongh, M. Bergers, M. J. de Rooij and J. Schalkwijk (2000). Expression of tenascin-C splice variants by human skin cells. Arch Dermatol Res **292**: 446-54.
- Lavery J. P. and C. E. Miller (1977). The viscoelastic nature of chorioamniotic membranes. Obstet Gynecol **50**: 467-472.
- Lavery J. P. and C. E. Miller (1979). Deformation and creep in the human chorioamniotic sac. Am J Obstet Gynecol **134**: 366-375.
- Lawrence D. A. (1996). Transforming growth factor- $\beta$ : a general review. Eur Cytokine Netw **7**: 363-374.
- Le Bail B., S. Faouzi, L. Boussarie, J. Guirouilh, J. F. Blanc, J. Carles, P. Bioulac-Sage, C. Balabaud and J. Rosenbaum (1999). Osteonectin/SPARC is overexpressed in human hepatocellular carcinoma. J Pathol **189**: 46-52.
- Lee S.-B., D. Q. Li, D. T. H. Tan, D. Meller and S. C. G. Tseng (2000). Suppression of TGF- $\beta$  signaling in both normal conjunctival fibroblasts and pterygial body fibroblasts by amniotic membrane. Curr Eye Res **20**: 325-334.

- Lewis D. F., C. A. Major, C. V. Towers, J. A. Harding, T. Asrat and T. J. Garite (1992). Effects of digital vaginal exams on latency period in preterm premature rupture of membranes. Obstet Gynecol **80**: 630-634.
- Linnala A., E. Balza, L. Zardi and I. Virtanen (1993). Human amnion epithelial cells assemble tenascins and three fibronectin isoforms in the extracellular matrix. FEBS Lett **317**: 74-8.
- Linnala A., H. von Koskull and I. Virtanen (1994). Isoforms of cellular fibronectin and tenascin in amniotic fluid. FEBS Lett **337**: 167-70.
- Lockwood C. J., A. E. Senyei, M. R. Dische, D. Casal, K. D. Shah, S. N. Thung, L. Jones, L. Deligdisch and T. J. Garite (1991). Fetal fibronectin in cervical and vaginal secretions as a predictor of preterm delivery. New Engl J Med **325**: 669-674.
- Loukianov E., T. Loukianova and M. Periasamy (1997). Myosin heavy chain isoforms in smooth muscle. Comp Biochem Physiol **117B**: 13-18.
- Lu S., X. Gu, S. Hoestje and D. E. Epner (2002). Identification of an additional hypoxia responsive element in the glyceraldehyde-3-phosphate dehydrogenase gene promoter. Biochim Biophys Acta **1574**: 152-156.
- MacDonald P. C. and M. L. Casey (1993). The accumulation of prostaglandins (PG) in amniotic fluid is an aftereffect of labor and not indicative of a role for PGE2 or PGF2a in the initiation of human parturition. J Clin Endocrinol Metab **76**: 1323-1339.
- MacDonald P. C., S. Koga and M. L. Casey (1991). Decidual activation in parturition: examination of amniotic fluid for mediators of the inflammatory response. Ann NY Acad Sci **622**: 315-330.
- Mackie E. J., T. Scott-Burden, A. W. Hahn, F. Kern, J. Bernhardt, S. Regenass, A. Weller and F. R. Buhler (1992). Expression of tenascin by vascular smooth muscle cells. Alterations in hypertensive rats and stimulation by angiotensin II. Am J Pathol **141**: 377-88.
- Maehara K., N. Kanayama, E. E. Maradny, T. Uezato, M. Fujita and T. Terao (1996). Mechanical stretching induces interleukin-8 gene expression in fetal membranes: a possible role for the initiation of human parturition. Eur J Obstet Gynecol Reprod Biol **70**: 191-196.
- Majno G., G. Gabbiani, B. J. Hirschel, G. B. Ryan and P. R. Statkov (1971). Contraction of granulation tissue in vitro: Similarity to smooth muscle. Science **173**: 548-550.

- Major C. A. and T. J. Garite (1997). Preterm premature rupture of membranes. Preterm labor. M. G. Elder, R. F. Lamont and R. Romero. New York, Churchill Livingstone: 153-164.
- Malak T. M. (1995). Structural biology of the human fetal membranes. Obstetrics and Gynaecology. Leicester, University of Leicester.
- Malak T. M. and S. C. Bell (1994a). Distribution of fibrillin-containing microfibrils and elastin in human fetal membranes: a novel molecular basis for membrane elasticity. Am J Obstet Gynecol 171: 195-205.
- Malak T. M. and S. C. Bell (1994b). Structural characteristics of term human fetal membranes: a novel zone of extreme morphological alteration within the rupture site. Br J Obstet Gynaecol 101: 375-86.
- Malak T. M. and S. C. Bell (1996). Fetal membranes structure and prelabour rupture. Fetal Mat Med Rev 8: 143-164.
- Malak T. M., C. D. Ockleford, S. C. Bell, R. Dalgleish, N. Bright and J. Macvicar (1993). Confocal immunofluorescence localization of collagen types I, III, IV, V and VI and their ultrastructural organization in term human fetal membranes. Placenta 14: 385-406.
- Mattey D. L., P. T. Dawes, N. B. Nixon and H. Slater (1997). Transforming growth factor beta 1 and interleukin 4 induced alpha smooth muscle actin expression and myofibroblast-like differentiation in human synovial fibroblasts in vitro: modulation by basic fibroblast growth factor. Ann Rheum Dis 56: 426-31.
- McCachren S. S. and V. A. Lightner (1992). Expression of human tenascin in synovitis and its regulation by interleukin-1. Arthritis Rheum 35: 1185-96.
- McLaren J., T. M. Malak and S. C. Bell (1999a). Structural characteristics of term human fetal membranes prior to labour: identification of an area of altered morphology overlying the cervix. Human Reprod 14: 237-241.
- McLaren J., T. M. Malak, D. J. Taylor and S. C. Bell (1997). Extracellular matrix degradation in the connective tissue layers of the fetal membranes in the 'zone of altered morphology': Cellular populations and matrix metalloproteinases. J Soc Gynecol Inv 4: 220A.
- McLaren J., D. J. Taylor and S. C. Bell (1999b). Increased incidence of apoptosis in non-labour-affected cytotrophoblast cells in term fetal membranes overlying the cervix. Human Reprod 14: 895-900.
- McLaren J., D. J. Taylor and S. C. Bell (2000a). Increased concentration of pro-matrix metalloproteinase 9 in term fetal membranes overlying the cervix before labor:

- implications for membrane remodelling and rupture. Am J Obstet Gynecol **182**: 409-416.
- McLaren J., D. J. Taylor and S. C. Bell (2000b). Prostaglandin E(2)-dependent production of latent matrix metalloproteinase-9 in cultures of human fetal membranes. Mol Hum Reprod **6**: 1033-1040.
- Mead P. B. (1980). Management of the patient with premature rupture of the membranes. Clin Perinatol **7**: 243-255.
- Meinert M., G. V. Eriksen, A. C. Petersen, R. B. Helmig, C. Laurent, N. Uldbjerg and A. Malmstrom (2001). Proteoglycans and hyaluronan in human fetal membranes. Am J Obstet Gynecol **184**: 679-685.
- Meudt R. and E. Meudt (1967). Rupture of the fetal membranes: an experimental, clinical and histological study. Am J Obstet Gynecol **99**: 562-568.
- Meyer U., T. Meyer, J. Vosshans and U. Joos (1999). Decreased expression of osteocalcin and osteonectin in relation to high strains and decreased mineralization in mandibular distraction osteogenesis. J Craniomaxillofac Surg **27**: 222-227.
- Mighell A. J., J. Thompson, W. J. Hume, A. F. Markham and P. A. Robinson (1997). Human tenascin-C: identification of a novel type III repeat in oral cancer and of novel splice variants in normal, malignant and reactive oral mucosae. Int J Cancer **72**: 236-40.
- Mignatti P., D. B. Rifkin, H. G. Welgus and W. C. Parks (1996). Proteinases and tissue remodelling. The molecular and cellular biology of wound repair. R. A. F. Clark. New York, Plenum Press: 427-474.
- Millar L. K., J. Stollberg, L. DeBuque and G. Bryant-Greenwood (2000). Fetal membrane distension: Determination of the intrauterine surface area and distension of the fetal membranes preterm and at term. Am J Obstet Gynecol **182**: 128-134.
- Mitchell M. D., R. Romero, S. S. Edwin and M. S. Trautman (1995). Prostaglandins and parturition. Reprod Fertil Dev **7**: 623-632.
- Miwa T., Y. Manabe, K. Kurokawa, S. Kamada, N. Kanda, G. Bruns, H. Ueyama and T. Kakunaga (1988). Structure, chromosome location, and expression of the human smooth muscle (enteric type)  $\gamma$ -actin gene: Evolution of six human actin genes. Mol Cell Biol **11**: 3296-3306.
- Modesti A., T. Kalebic, S. Scarpa, S. Togo, G. Grotendorst, L. A. Liotta and T. J. Triche (1984). Type V collagen in human amnion is a 12nm fibrillar component of the pericellular interstitium. Eur J Cell Biol **35**: 246-255.

- Modesti A., S. Scarpa, G. D'Orazi, L. Simonelli and F. G. Caramia (1989). Localization of type IV and V collagens in the stroma of human amnion. Prog Clin Biol Res 296: 459-463.
- Moore K. L. and T. V. N. Persaud (1998). Before we are born. Essentials of embryology and birth defects. Philadelphia, W. B. Saunders Company.
- Morrison J. (1972). The development of the lower uterine segment. Aus N Z J Obstet Gynaecol 12: 182-185.
- Motamed K. (1999). SPARC (osteonectin/BM40). Int J Biochem Cell Biol 31: 1363-1366.
- Motamed M., J. A. Bassuk and E. H. Sage (1996). SPARC as a counteradhesive protein: structural and functional correlates. Tenascin and counteradhesive molecules of the extracellular matrix. K. L. Crossin, Harwood Academic: 127-144.
- Muchaneta-Kubara E. C. and A. M. Nahas (1997). Myofibroblast phenotypes expression in experimental renal scarring. Nephrol Dial Transplant 12: 904-915.
- Munger J. S., J. G. Harpel, P.-E. Gliezes, R. Mazziere, I. Nunes and D. B. Rifkin (1997). Latent transforming growth factor- $\beta$ : Structural features and mechanisms of activation. Kidney Int 51: 1376-1382.
- Nanaev A. K., G. Kohnen, A. P. Milovanov, S. P. Domogarsky and P. Kaufmann (1997). Stromal differentiation and architecture of the human umbilical cord. Placenta 18: 53-64.
- Narani N., P. D. Arora, A. Lew, L. Luo, M. Glogauer, B. Ganss and C. A. G. McCulloch (1999). Transforming growth factor- $\beta$  induction of  $\alpha$ -smooth muscle actin is dependent on the deformability of the collagen matrix. Curr Top Pathol 93: 47-60.
- Narvaez D., J. Kanitakis, M. Faure and A. Claudy (1996). Immunohistochemical study of CD34-positive dendritic cells of human dermis. Am J Dermatopathol 18: 283-288.
- Natali P. G., M. R. Nicotra, A. Bigotti, C. Botti, P. Castellani, A. M. Risso and L. Zardi (1991). Comparative analysis of the expression of the extracellular matrix protein tenascin in normal human fetal, adult and tumor tissues. Int J Cancer 47: 811-6.
- Nehemiah J. L., J. A. Schnitzer, H. Schulman and A. B. Novikoff (1981). Human chorionic trophoblasts, decidual cells, and macrophages: A histochemical and electron microscopic study. Am J Obstet Gynecol 140: 261-268.
- Nielsen B. S., M. Sehested, S. Timshel, C. Pyke and K. Dano (1996). Messenger RNA for urokinase plasminogen activator is expressed in myofibroblasts adjacent to cancer cells in human breast cancer. Lab Invest 74: 168-177.
- Nies D. E., T. J. Hemesath, J. H. Kim, J. R. Gulcher and K. Stefansson (1991). The complete cDNA sequence of human hexabrachion (Tenascin). A multidomain

- protein containing unique epidermal growth factor repeats. J Biol Chem **266**: 2818-23.
- Ockleford C. D., N. Bright, A. Hubbard, C. d'Lacey, J. Smith, L. Gardiner, T. Sheikh, M. Albentosa and K. Turtle (1993a). Micro-trabeculae, macro-plaques or mini-basement membranes in human term fetal membranes? Phil Trans R Soc Lond B **342**: 121-136.
- Ockleford C. D., T. Malak, A. Hubbard, K. Bracken, S.-A. Burton, N. Bright, G. Blakey, J. Goodliffe and C. d'Lacey (1993b). Confocal and conventional immunofluorescence and ultrastructural localisation of intracellular strength-giving components of human amniochorion. J Anat **183**: 483-505.
- Ockleford C. D., L. Mongan and A. R. D. Hubbard (1997). Techniques of advanced light microscopy and their applications to morphological analysis of human extra-embryonic membranes. Microsc Res Tech **38**: 153-164.
- O'Kane S. and M. W. J. Ferguson (1997). Transforming growth factor  $\beta$ s and wound healing. Int J Biochem Cell Biol **29**: 63-78.
- Osborn M. and K. Weber (1982). Intermediate filaments: Cell-type-specific markers in differentiation and pathology. Cell **31**: 303-306.
- Paramio J. M. and J. L. Jorcano (2002). Beyond structure: do intermediate filaments modulate cell signalling? Bioessays **24**: 836-844.
- Parry-Jones E. and S. Priya (1976). A study of the elasticity and tension of fetal membranes and of the relation of the area of the gestational sac to the area of the uterine cavity. Br J Obstet Gynaecol **83**: 205-212.
- Pearson C. A., D. Pearson, S. Shibahara, J. Hofsteenge and R. Chiquet-Ehrismann (1988). Tenascin: cDNA cloning and induction by TGF-beta. Embo J **7**: 2977-82.
- Polak J. M. and S. Van Noorden (1997). Introduction to immunocytochemistry. New York, Springer-Verlag.
- Polishuk W. Z., S. Kohane and A. Peranio (1962). The physical properties of fetal membranes. Obstet Gynecol **20**: 204-210.
- Polzin W. J. and K. Brady (1991). Mechanical factors in the etiology of premature rupture of the membranes. Clin Obstet Gynecol **34**: 702-714.
- Porter P. L., E. H. Sage, T. F. Lane, S. E. Funk and A. M. Gown (1995). Distribution of SPARC in normal and neoplastic human tissue. J Histochem Cytochem **43**: 791-800.

- Powell D. W., R. C. Mifflin, J. D. Valentich, S. E. Crowe, J. I. Saada and A. B. West (1999). Myofibroblasts. I. Paracrine cells important in health and disease. Am J Physiol **277**: C1-9.
- Pradet-Balade B., F. Boulme, H. Beug, E. W. Mullner and J. A. Garcia-Sanz (2001). Translation control: bridging the gap between genomics and proteomics. Trends Biochem Sci **26**: 225-229.
- Prieto A. L., F. S. Jones, B. A. Cunningham, K. L. Crossin and G. M. Edelman (1990). Localization during development of alternatively spliced forms of cytotoxic mRNA by in situ hybridization. J Cell Biol **111**: 685-98.
- Pringle J. H. (1995). Non-isotopic detection of RNA *in situ*. Non-isotopic methods in molecular biology. Oxford, Oxford University Press: 85-110.
- Reddy S., K. Ozgur, M. Lu, W. Chang, S. R. Mohan, C. C. Kumar and H. E. Ruley (1990). Structure of the human smooth muscle  $\alpha$ -actin gene. Analysis of a cDNA and 5' upstream region. J Biol Chem **265**: 1683-1687.
- Reed M. J., P. Puolakkainen, T. F. Lane, D. Dickerson, P. Bornstein and E. H. Sage (1993). Differential expression of SPARC and thrombospondin 1 in wound repair: immunolocalization and in situ hybridization. J Histochem Cytochem **41**: 1467-77.
- Reed M. J. and E. H. Sage (1996). SPARC and the extracellular matrix: implications for cancer and wound repair. Curr Top Microbiol Immunol **213**: 81-94.
- Reed M. J., R. B. Vernon, I. B. Abrass and E. H. Sage (1994). TGF- $\beta$ 1 induces the expression of type I collagen and SPARC, and enhances contraction of collagen gels, by fibroblasts from young and aged donors. J Cell Physiol **158**: 169-179.
- Rettig W. J., H. P. Erickson, A. P. Albino and P. Garin-Chesa (1994). Induction of human tenascin (neuronectin) by growth factors and cytokines: cell type-specific signals and signalling pathways. J Cell Sci **107**: 487-97.
- Roberts I. S. D., C. Burrows, J. H. Shanks, M. Venning and L. J. McWilliam (1997). Interstitial myofibroblasts: predictors of progression in membranous nephropathy. J Clin Pathol **50**: 123-127.
- Rocchi M., N. Archidiacono, G. Romeo, M. Saginati and L. Zardi (1991). Assignment of the gene for human tenascin to the region q32-q34 of chromosome 9. Hum Genet **86**: 621-3.
- Romero R., N. Athayde, E. Maymon, P. Pacora and R. Bahado-Singh (1999). Premature rupture of the membranes. Medicine of the fetus and mother. E. A. Reece and J. C. Hobbins. Philadelphia, Lippincott-Raven: 1581-1625.

- Romero R., R. Gonzalez, P. Baumann, E. Behnke, L. Rittenhouse, D. Barbiero, D. B. Cotton and M. D. Mitchell (1994). Topographic differences in amniotic fluid concentrations of prostanoids in women in spontaneous labor at term. Prostaglandin Leukotr Essent Fatty Acids **50**: 97-104.
- Romero R., R. Quintero, E. Oyarzun, Y. K. Wu, V. Sabo, M. Mazor and J. C. Hobbins (1988). Intraamniotic infection and the onset of labor in preterm premature rupture of the membranes. Am J Obstet Gynecol **159**: 661-666.
- Romero R., C. M. Salafia, A. P. Athanassiadis, S. Hanaoka, M. Mazor, W. Sepulveda and M. B. Bracken (1992). The relationship between acute inflammatory lesions of the preterm placenta and amniotic fluid microbiology. Am J Obstet Gynecol **166**: 1382-1388.
- Ronnov-Jessen L. and O. W. Petersen (1993). Induction of  $\alpha$ -smooth muscle actin by transforming growth factor- $\beta$ 1 in quiescent human breast gland fibroblasts. Lab Invest **68**: 696-707.
- Sadler T. W. (1985). Langman's medical embryology. Baltimore, Williams & Wilkins.
- Sage E. H. and P. Bornstein (1991). Extracellular proteins that modulate cell-matrix interactions. J Biol Chem **266**: 14831-14834.
- Sage E. H., C. Johnson and P. Bornstein (1984). Characterization of a novel serum albumin-binding glycoprotein secreted by endothelial cells in culture. J Biol Chem **259**: 3993-4007.
- Sangha R. K., J. C. Walton, C. M. Ensor, H.-H. Tai and J. R. Challis (1994). Immunohistochemical localization, messenger ribonucleic acid abundance, and activity of 15-hydroxyprostaglandin dehydrogenase in placenta and fetal membranes during term and preterm labor. J Clin Endocrinol Metab **78**: 982-989.
- Sappino A. P., W. Schurch and G. Gabbiani (1990). Differentiation repertoire of fibroblastic cells: Expression of cytoskeletal proteins as marker of phenotypic modulations. Lab Invest **63**: 144-161.
- Sato M., N. Yasui, T. Nakase, H. Kawahata, M. Sugimoto, S. Hirota, Y. Kitamura, S. Nomura and T. Ochi (1998). Expression of bone matrix proteins mRNA during distraction osteogenesis. J Bone Mineral Res **13**: 1221-1231.
- Savitz D. A., C. V. Ananth, E. R. Luther and J. M. Thorp (1997). Influence of gestational age on the time from spontaneous rupture of the chorioamniotic membranes to the onset of labor. Am J Perinatol **14**: 129-133.
- Schmidt W. (1992). The amniotic fluid compartment: the fetal habitat. Adv Anat Embryol Cell Biol **127**: 1-100.

- Schmitt-Graff A., A. Desmouliere and G. Gabbiani (1994). Heterogeneity of myofibroblast phenotypic features: an example of fibroblastic cell plasticity. Virchows Arch **425**: 3-24.
- Schurch W., T. A. Seemayer and G. Gabbiani (1998). The myofibroblast: a quarter century after its discovery. Am J Surg Pathol **22**: 141-147.
- Schurch W., T. A. Seemayer and R. Lagace (1981). Stromal myofibroblasts in primary invasive and metastatic carcinomas. A combined immunological, light and electron microscopic study. Virchows Arch A Pathol Anat Histol **391**: 125-139.
- Schuster N. and K. Krieglstein (2002). Mechanisms of TGF- $\beta$  mediated-apoptosis. Cell Tissue Res **307**: 1-14.
- Seemayer T. A., R. Legace, W. Schurch and G. M. Tremblay (1979). Myofibroblasts in the stroma of invasive and metastatic carcinoma. Am J Surg Pathol **3**: 525-533.
- Seemayer T. A., W. Schurch and R. Lagace (1982). The myofibroblast and defense against neoplasia: A hypothesis. Surv Immunol Res **1**: 268-273.
- Serini G., M. L. Bochaton-Piallat, P. Ropraz, A. Geinoz, L. Borsi, L. Zardi and G. Gabbiani (1998). The fibronectin domain ED-A is crucial for myofibroblastic phenotype induction by transforming growth factor-beta1. J Cell Biol **142**: 873-81.
- Serini G. and G. Gabbiani (1999). Mechanisms of myofibroblast activity and phenotypic modulation. Exp Cell Res **250**: 273-83.
- Shankavaram U. T., D. L. DeWitt, S. E. Funk, E. H. Sage and L. M. Wahl (1997). Regulation of human monocyte matrix metalloproteinases by SPARC. J Cell Physiol **173**: 327-34.
- Sharifi B. G., D. W. LaFleur, C. J. Pirola, J. S. Forrester and J. A. Fagin (1992). Angiotensin II regulates tenascin gene expression in vascular smooth muscle cells. J Biol Chem **267**: 23910-5.
- Singer I. I., D. W. Kawka, D. M. Kazazis and R. A. F. Clark (1984). In vivo co-distribution of fibronectin and actin fibers in granulation tissue: Immunofluorescence and electron microscope studies of the fibronexus at the myofibroblast surface. J Cell Biol **98**: 2091-2106.
- Siri A., B. Carnemolla, M. Saginati, A. Leprini, G. Casari, F. Baralle and L. Zardi (1991). Human tenascin: primary structure, pre-mRNA splicing patterns and localization of the epitopes recognized by two monoclonal antibodies. Nucleic Acids Res **19**: 525-31.

- Siri A., V. Knauper, N. Veirana, F. Caocci, G. Murphy and L. Zardi (1995). Different susceptibility of small and large human tenascin-C isoforms to degradation by matrix metalloproteinases. J Biol Chem **270**: 8650-4.
- Skalli O., P. Ropraz, A. Trzeciak, G. Benzonana, D. Gillessen and G. Gabbiani (1986). A monoclonal antibody against  $\alpha$ -smooth muscle actin: A new probe for smooth muscle differentiation. J Cell Biol **103**: 2787-2796.
- Skalli O., W. Schurch, T. Seemayer, R. Lagace, D. Montandon, B. Pittet and G. Gabbiani (1989). Myofibroblasts from diverse pathologic settings are heterogeneous in their content of actin isoforms and intermediate filament proteins. Lab Invest **60**: 275-285.
- Skinner S. J. M., G. A. Campos and G. C. Liggins (1981). Collagen content of human amniotic membranes: Effect of gestation length and premature rupture. Obstet Gynecol **57**: 487-489.
- Slater D. M., L. C. Berger, R. Newton, G. E. Moore and P. R. Bennett (1995). Expression of cyclooxygenase types 1 and 2 in human fetal membranes at term. Am J Obstet Gynecol **172**: 77-82.
- Smith W. L. and D. L. DeWitt (1996). Prostaglandin endoperoxide synthases-1 and -2. Adv Immunol **62**: 167-215.
- Sohara N., I. Znoyko, M. T. Levy, M. Trojanowska and A. Reuben (2002). Reversal of activation of human myofibroblast-like cells by culture on a basement membrane-like substrate. J Hepatol **37**: 214-221.
- Spanakis S. G., S. Petridou and S. K. Masur (1998). Functional gap junctions in corneal fibroblasts and myofibroblasts. Invest Ophthalmol Vis Sci **39**: 1320-1328.
- Sriramarao P. and M. A. Bourdon (1993). A novel tenascin type III repeat is part of a complex of tenascin mRNA alternative splices. Nucleic Acids Res **21**: 163-8.
- Steinman R. M., M. Pack and K. Inaba (1997). Dendritic cell development and maturation. Adv Exp Med Biol **417**: 1-6.
- Sun G., M. A. Stacey, A. Bellini, M. Marini and S. Mattoli (1997). Endothelin-1 induces bronchial myofibroblast differentiation. Peptides **19**: 1449-1451.
- Sutton L., D. Y. Mason and C. W. G. Redman (1983). HLA-DR positive cells in the human placenta. Immunology **49**: 103-112.
- Swaroop A., B. L. Hogan and U. Francke (1988). Molecular analysis of the cDNA for human SPARC/osteonectin/BM-40: sequence, expression, and localization of the gene to chromosome 5q31-q33. Genomics **2**: 37-47.

- Taccagni G., E. Rovere, M. Masullo, L. Christensen and B. Eyden (1997). Myofibrosarcoma of the breast. Review of the literature on myofibroblastic tumours and criteria for defining myofibroblastic differentiation. Am J Surg Pathol **21**: 489-496.
- Talts J. F., A. Weller, R. Timpl, M. Ekblom and P. Ekblom (1995). Regulation of mesenchymal extracellular matrix protein synthesis by transforming growth factor-beta and glucocorticoids in tumor stroma. J Cell Sci **108**: 2153-62.
- Tamm E. R., A. Siegner, A. Baur and E. Lutjen-Drecoll (1996). Transforming growth factor- $\beta$ 1 induces  $\alpha$ -smooth muscle-actin expression in cultured human and monkey trabecular meshwork. Exp Eye Res **62**: 389-397.
- Teipale J., J. Saharinen, K. Hedman and J. Keski-Oja (1996). Latent transforming growth factor- $\beta$ 1 and its binding protein are components of extracellular matrix microfibrils. J Histochem Cytochem **44**: 875-889.
- Termine J. D., H. K. Kleinman, S. W. Whitson, K. M. Conn, M. L. McGarvey and G. R. Martin (1981). Osteonectin, a bone-specific protein linking mineral to collagen. Cell **26**: 99-105.
- Tomasek J. J., G. Gabbiani, B. Hinz, C. Chapponier and R. A. Brown (2002). Myofibroblasts and mechano-regulation of connective tissue remodelling. Nature Rev Mol Cell Biol **3**: 349-363.
- Topozada M. K., N. A. Sallam, A. A. Gaafar and K. M. El-Kashlan (1970). Role of repeatedly stretching in the mechanism of timely rupture of the membranes. Am J Obstet Gynecol **108**: 243-249.
- Trautman M. S., S. S. Edwin, D. Collmer, D. J. Dudley, D. Simmons and M. D. Mitchell (1996). Prostaglandin H synthase-2 in human gestational tissues: Regulation in amnion. Placenta **17**: 239-245.
- Tremble P., R. Chiquet-Ehrismann and Z. Werb (1994). The extracellular matrix ligands fibronectin and tenascin collaborate in regulating collagenase gene expression in fibroblasts. Mol Biol Cell **5**: 439-53.
- Tremble P. M., T. F. Lane, E. H. Sage and Z. Werb (1993). SPARC, a secreted protein associated with morphogenesis and tissue remodeling, induces expression of metalloproteinases in fibroblasts through a novel extracellular matrix-dependent pathway. J Cell Biol **121**: 1433-44.
- Trimble C. L., M. H. Gray and N. S. McNutt (1992). The distribution of factor XIIIa-positive cells in the human fetus and placenta. Virchows Archiv A Pathol Anat **420**: 513-518.

- Tseng S. C., D. Q. Li and X. Ma (1999). Suppression of transforming growth factor-beta isoforms, TGF-beta receptor type II, and myofibroblast differentiation in cultured human corneal and limbal fibroblasts by amniotic membrane matrix. J Cell Physiol **179**: 325-335.
- Tucker R. P., J. A. Hammarback, D. A. Jenrath, E. J. Mackie and Y. Xu (1993). Tenascin expression in the mouse: in situ localization and induction in vitro by bFGF. J Cell Sci **104**: 69-76.
- Turnbull A. and A. Lopez Bernal (1994). Physiology and biochemistry of labour. Obstetrics. A. Turnbull and G. Chamberlain. Edinburgh, Churchill Livingstone: 701-711.
- Vadillo-Ortega F., G. Gonzalez-Avila, E. E. Furth, H. Lei, R. J. Muschel, W. G. Stetler-Stevenson and J. F. Strauss (1995). 92-kd type IV collagenase (matrix metalloproteinase-9) activity in human amniochorion increases with labour. Am J Pathol **146**: 148-156.
- Valentich J. D., V. Popov, J. I. Saada and D. W. Powell (1997). Phenotypic characterization of an intestinal subepithelial myofibroblast cell line. Am J Physiol **272**: C1513-24.
- van der Loop F. T. L., G. Gabbiani, G. Kohnen, F. C. S. Ramaekers and G. J. J. M. van Eys (1997). Differentiation of smooth muscle cells in human blood vessels as defined by smoothelin, a novel marker for the contractile phenotype. Arterioscler Thromb Biol **17**: 665-671.
- van der Loop F. T. L., G. Schaart, E. D. J. Timmer, F. C. S. Ramaekers and G. J. J. M. van Eys (1996). Smoothelin, a novel cytoskeletal protein specific for smooth muscle cells. J Cell Biol **134**: 401-411.
- van Herendael B. J., C. Oberti and I. Brosens (1978). Microanatomy of the human amniotic membranes. A light microscopic, transmission, and scanning electron microscopic study. Am J Obstet Gynecol **131**: 872-880.
- Van Meir C. A., M. M. Ramirez, S. G. Matthews, A. A. Calder, M. J. N. C. Keirse and J. R. G. Challis (1997). Chorionic prostaglandin catabolism is decreased in the lower uterine segment with term labour. Placenta **18**: 109-114.
- Vollmer G., M. I. Tan, W. Wunsche and K. Frank (1997). Expression of tenascin-C by human endometrial adenocarcinoma and stroma cells: heterogeneity of splice variants and induction by TGF-beta. Biochem Cell Biol **75**: 759-69.

- Vuckovic M., O. Genbacev and S. Kumar (1992). Immunohistochemical localisation of transforming growth factor- $\beta$  in first and third trimester human placenta. Pathobiology **60**: 149-150.
- Wang T. and J. Schneider (1983). Fine structure of the human chorionic membrane. Ultrastructural and histochemical examinations. Arch Gynecol **233**: 187-198.
- Watson A. L., M. E. Palmer and G. J. Burton (1996). An in vitro model for the study of wound healing in first trimester human placenta. Cell Tissue Res **286**: 431-8.
- Wewer U. M., R. Albrechtsen, L. W. Fisher, M. F. Young and J. D. Termine (1988). Osteonectin/SPARC/BM-40 in human decidua and carcinoma, tissues characterized by de novo formation of basement membrane. Am J Pathol **132**: 345-55.
- Wilson K. E., S. P. Langdon, A. M. Lessells and W. R. Miller (1996). Expression of the extracellular matrix protein tenascin in malignant and benign ovarian tumours. Br J Cancer **74**: 999-1004.
- Woessner J. F. (1991). Matrix metalloproteinases and their inhibitors in connective tissue remodeling. Faseb J **5**: 2145-2154.
- Wrana J. L., C. M. Overall and J. Sodek (1991). Regulation of the expression of a secreted acidic protein rich in cysteine (SPARC) in human fibroblasts by transforming growth factor  $\beta$ . Comparison of transcriptional and post-transcriptional control with fibronectin and type I collagen. Eur J Biochem **197**: 519-528.
- Xing Z., G. M. Tremblay, P. J. Sime and J. Gauldie (1997). Overexpression of granulocyte-macrophage colony-stimulating factor induces pulmonary granulation tissue formation and fibrosis by induction of transforming growth factor-beta 1 and myofibroblast accumulation. Am J Pathol **150**: 59-66.
- Xu P., N. Alfaidy and J. R. G. Challis (2002). Expression of matrix metalloproteinase (MMP)-2 and MMP-9 in human placenta and fetal membranes in relation to preterm and term labor. J Clin Endocrinol Metab **87**: 1353-1361.
- Yamamoto K., Q. N. Dang, S. P. Kennedy, R. Osathanondh, R. A. Kelly and R. T. Lee (1999). Induction of tenascin-C in cardiac myocytes by mechanical deformation. Role of reactive oxygen species. J Biol Chem **274**: 21840-21846.
- Yan J. S. and C.-S. Yin (1990). No decline in the preterm birth rate over three decades. Int J Gynecol Obstet **34**: 1-5.
- Yan Q. and E. H. Sage (1999). SPARC, a matricellular glycoprotein with important biological functions. J Histochem Cytochem **47**: 1495-506.
- Yeh I.-T., D. M. O'Connor and R. J. Kurman (1989). Vacuolated cytotrophoblast: A subpopulation of trophoblast in the chorion laeve. Placenta **10**: 429-438.

- Zhang H. Y., M. Gharaee-Kermani, K. Zhang, S. Karmioli and S. H. Phan (1996). Lung fibroblast alpha-smooth muscle actin expression and contractile phenotype in bleomycin-induced pulmonary fibrosis. Am J Pathol **148**: 527-37.
- Zhang H.-Y. and S. H. Phan (1999). Inhibition of myofibroblast apoptosis by transforming growth factor  $\beta_1$ . Am J Respir Cell Mol Biol **21**: 658-665.
- Zhang K., M. D. Rekhter, G. D. and S. H. Phan (1994). Myofibroblasts and their role in lung collagen gene expression during pulmonary fibrosis. A combined immunohistochemical and *in situ* hybridization study. Am J Pathol **145**: 114-145.
- Zhao Y. and S. L. Young (1995). TGF-beta regulates expression of tenascin alternative-splicing isoforms in fetal rat lung. Am J Physiol **268**: L173-80.
- Zingg H. H. (2001). Oxytocin and uterine activity. The endocrinology of parturition. Basic science and clinical application. R. Smith. Basel, Karger: 57-65.

## Myofibroblast Differentiation in the Connective Tissues of the Amnion and Chorion of Term Human Fetal Membranes—Implications for Fetal Membrane Rupture and Labour

P. C. McParland, D. J. Taylor and S. C. Bell<sup>a</sup>

Preterm Birth Research Group, Department of Obstetrics and Gynaecology, Faculty of Medicine and Biological Sciences, University of Leicester, Leicester LE2 7LX, UK

Paper accepted 2 July 1999

An area of the fetal membranes, within the rupture tear after spontaneous delivery at term, exhibits altered morphology compared to more distal sites. It is characterized by marked swelling of the amniotic and chorionic connective tissue layers, consistent with structural weakness, and a marked reduction of the thickness of both the cytotrophoblast and decidua layers. These features, albeit less extreme, have been identified in fetal membranes in the lower uterine pole in patients prior to labour. In this study of pre-labour, labour-affected and post-labour term fetal membranes, we report that these regions are associated with an alteration in the phenotype of the vimentin positive mesenchymal cell population of the chorionic connective tissue reticular layer, and are consistent with myofibroblastic differentiation, i.e.  $\alpha$ -smooth muscle actin ( $\alpha$ -sma) expression. In the reticular layer of the lower uterine pole biopsies in the labour-affected group the numbers and densities of  $\alpha$ -sma immunoreactive positive cells were 17-fold ( $P=0.04$ ) and 8.5-fold ( $P=0.02$ ) higher than in mid-zone biopsies. After delivery, in rupture line biopsies the numbers and densities were 50-fold ( $P=0.002$ ) and 36-fold ( $P=0.003$ ) higher compared to mid zone biopsies. The percentage of the vimentin positive population positive for  $\alpha$ -sma was 2–5 per cent in mid-zone biopsies compared to 49 per cent ( $P=0.03$ ) in the labour-affected 'cervical' biopsies and 69 per cent ( $P=0.05$ ) in the rupture line biopsies. Within the tear sites,  $\alpha$ -sma positive cells were also detected within the fibroblastic layer of the amniotic connective tissue. Although there was no significant difference between the numbers and density of  $\alpha$ -sma cells in the reticular layers between mid and lower uterine pole biopsies in the pre-labour group, in a proportion of patients the biopsies were similar to labour-affected biopsies indicating that this alteration occurs prior to clinically apparent labour in these patients. The incidence of  $\alpha$ -sma positive cells in the reticular layer correlated with morphological changes within the fetal membranes, for example thickness of reticular ( $r^2=0.349$ ,  $P=0.0006$ ) and amniotic connective tissue layers ( $r^2=0.389$ ,  $P=0.0002$ ). This suggests that cellular activities associated with myofibroblastic differentiation in the reticular layer of the chorion may be associated with the observed connective tissue changes, fetal membrane rupture and labour.

© 2000 Harcourt Publishers Ltd

Placenta (2000), 21, 44–53

### INTRODUCTION

Fetal membranes are still intact when labour begins at term in 90 per cent of pregnancies, and without intervention they spontaneously rupture near the end of the first stage of labour (Alger and Pupkin, 1986). However approximately 10 per cent of term pregnancies (Mead, 1980), and up to 60 per cent of preterm deliveries, are preceded by the pre-labour rupture of fetal membranes and therefore rupture is a direct antecedent of preterm birth (Kelly, 1995; French and McGregor, 1996). Although infection has been implicated in the aetiopathology of a proportion of pre-labour ruptures of fetal membranes (Gibbs et al., 1992; French and McGregor, 1996), the mechanisms in its absence (Malak and Bell, 1993; Kelly, 1995;

French and McGregor, 1996; Major and Garite, 1997; Parry and Strauss, 1998), and indeed the mechanisms underlying this spontaneous rupture during term labour, are unknown.

To account for the phenomenon of this spontaneous rupture during labour, studies have attempted to identify features of fetal membranes that may be uniquely associated with the rupture tear after spontaneous rupture and delivery at term (Bou-Resli, Al-Zaid and Ibrahim, 1981; Halaburt et al., 1989; Malak and Bell, 1994a). In the studies of Malak & Bell (1994a), involving comprehensive mapping of fetal membranes obtained after spontaneous labour and delivery, an area of the fetal membranes that exhibited unique morphological features, as compared to more distal regions, was demonstrated to be associated with the rupture tear. However, these features were restricted to a part of the rupture tear, and most commonly

<sup>a</sup> To whom correspondence should be addressed.

located at one end. This restricted area was termed the 'Zone of Altered Morphology' (ZAM), and its morphological features included marked swelling of the connective tissue layers of the amnion and chorion, consistent with its potential structural weakness, and marked reduction of the thickness of both the cytotrophoblast and decidua layers (Malak and Bell, 1994a). Subsequent studies have demonstrated similar, albeit less marked, changes prior to labour and rupture in the fetal membranes in the lower uterine pole overlying the cervix at term, as compared to membranes obtained from more distal regions, although in this situation marked patient-to-patient variation was detected (McLaren, Malak and Bell, 1999). This supports the view that this area in the lower uterine pole was generated prior to labour, producing an area of increased susceptibility to rupture and which, in response to the increased intra-amniotic pressures experienced during labour, represents the site of initial fetal membrane rupture and from which the tear, seen after delivery, would have been transmitted (Malak and Bell, 1993; Bell and Malak, 1997). That the region of the fetal membranes in the lower uterine pole would be ultimately represented by a region within the rupture tear after delivery is supported by Bourne (1962), who demonstrated that this site, visualized prior to delivery, was invariably detected within the rupture tear, and in most cases toward one end.

The connective tissues of the amnion and chorion include two layers containing mesenchymal cells, the fibroblast layer of the amnion and the reticular layer of the chorion. The exact cellular composition of the connective tissues of the amnion and chorion has been controversial. They have been reported to consist primarily of macrophages, based upon possession of specific cell markers (Sutton, Mason and Redman, 1983; Bulmer and Johnson, 1984), or HLA-DR/leucocyte common antigen positive dendritic cells (Sutton, Mason and Redman, 1983; Jenkins, O'Neill and Johnson, 1983). However they have also been reported to consist exclusively of fibroblasts (Schmidt, 1992), and to include myofibroblasts, as evidenced by the location of numerous cytoplasmic bundles of filaments in the amnion (Wang and Schneider, 1982) and chorion (Wang and Schneider, 1983) and the expression of the 'muscle-specific' intermediate filament desmin (Khong, Lane and Robertson, 1986). The morphological features in the connective tissue layers of the amnion and chorion in the 'Zone of Altered Morphology' were consistent with extracellular matrix degradation in this zone. Mesenchymal extracellular matrix degradation, detected during situations of tissue wounding, is associated with the activation or differentiation of resident mesenchymal fibroblastic cells into myofibroblasts, the hallmark of which is considered to be the acquisition of the intermediate filament  $\alpha$ -smooth muscle actin (Sappino, Schurch and Gabbiani, 1990; Schmitt-Graff, Desmouliere and Gabbiani, 1994; Schurch, Seemayer and Gabbiani, 1998). In the present study we have therefore examined the mesenchymal cells of the connective tissue layers in fetal membranes obtained from over the cervix, and more distally in patients at term prior to labour and during labour, and in the rupture tear

and distal from the rupture tear in patients after delivery, to determine whether the regional alterations in fetal membrane morphology could be correlated with myofibroblastic differentiation.

## MATERIALS AND METHODS

### Patient details

Fetal membranes unaffected by labour or delivery, were obtained from women ( $n=5$ ) undergoing elective caesarean sections between 38–39 weeks of pregnancy for repeat caesarean section or breech presentation. Fetal membranes affected by labour were obtained from women ( $n=5$ ) undergoing emergency caesarean sections between 38–39 weeks of pregnancy for breech presentation, fetal distress or dystocia. Fetal membranes ( $n=5$ ) were also collected after spontaneous delivery between 37–41 weeks. In these cases the fetal membranes ruptured spontaneously during labour. In all cases potentially infected membranes were excluded following identification of polymorphonuclear infiltration on histological examination.

### Tissue sampling

Fetal membranes were regionally biopsied according to our previous protocol. Specimens of  $1 \times 3$  cm were obtained from the following areas of the fetal membrane. (1) 'Cervical' (lower uterine pole) biopsies: following the delivery of the baby by caesarean section the fetal membranes overlying the cervix were located and marked by the application of Babcock tissue forceps. Areas adjacent to the clip were sampled. (2) Rupture tear biopsies: three biopsies were taken perpendicular to the rupture tear, at both ends and from the middle of the tear. After processing, morphology was assessed by light microscopy and the biopsy exhibiting features of the Zone of Altered Morphology (Malak and Bell, 1994a) was used for subsequent study and were referred to as the 'rupture site' biopsies. In selected patients the biopsies were taken sequentially from these sites to the placenta. (3) Mid-zone biopsies: these were obtained half-way between the cervical area and the placental edge in the case of caesarean sections and between the rupture line and the placental edge in patients after delivery. In all cases these biopsies were taken at least 10–12 cm from the cervical areas or rupture lines. Biopsies were rolled and fixed in buffered formalin (pH 7.6) for 48 h before processing and mounting in paraffin wax. Tissue sections were cut ( $4 \mu\text{m}$ ) and then stained with haematoxylin and eosin.

### Immunocytochemistry

Immunohistochemical staining for vimentin,  $\alpha$ -smooth muscle actin and smooth muscle myosin was performed on formalin fixed paraffin embedded tissue sections mounted on 3-aminopropyltriethoxysilane coated slides. Tissue sections

were de-waxed in xylene and hydrated gradually through graded alcohols. Sections employed for the detection of smooth muscle myosin were microwaved in 10 mM citric acid buffer, pH 6 for 30 min. Endogenous peroxidase activity was quenched following a 10 min incubation in a 6 per cent solution of H<sub>2</sub>O<sub>2</sub>. The slides were then treated with a 10 per cent solution of normal rabbit serum before this was removed and replaced with the appropriate primary monoclonal antibody. The antibodies anti-vimentin (Clone V9, Sigma, Poole, UK), anti- $\alpha$ -smooth muscle actin (Clone 1A4, Dako Ltd, Cambridge, UK) and anti-smooth muscle myosin (Clone SMMS-1, Dako Ltd, Cambridge, UK) were diluted in Tris-Buffered saline, pH 7.6 (TBS) and employed at 3.87, 1.9 and 4.26  $\mu$ g/ml respectively. The slides were incubated with anti-vimentin and anti-smooth muscle myosin overnight at 4°C or with anti- $\alpha$ -smooth muscle actin at 37°C for 1 h, and then washed in TBS for 20 min. Biotinylated rabbit anti-mouse Ig secondary antibody (Dako, Cambridge, UK) at 2.5  $\mu$ g/ml was then added and left for 20 min at room temperature. Subsequently slides were washed for 20 min and complexed with avidin-biotin peroxidase (Vector, Peterborough, UK) for 30 min. The complex was detected with a diaminobenzidine peroxidase substrate kit (Vector, Peterborough, UK). Negative controls involved omitting the primary antibody and replacing it with normal mouse IgG (Sigma, Poole, UK) at concentrations that matched that of the primary antibodies. The antibodies and techniques were validated by employing appropriate positive control tissues including umbilical cord, term placenta and myometrium.

### Histological and immunocytochemical assessment

Haematoxylin and eosin and immunocytochemical stained sections of membrane rolls from all biopsies were examined under light microscopy connected to an image capture system. This system comprised a Apple Macintosh Centris running Image<sup>®</sup> (version 1.51). Each section was divided into quadrants. For measurements of constituent layer thickness and for counting of immunoreactive cells 10 fields per roll were examined along the intersections of 0000 to 0600 hours and 0300 to 0900 hours. Measurements were taken only from sections cut vertically, showing a single layer of amniotic epithelium. The numbers of immunoreactive cells were counted in the whole thickness of each specified layer in a standard fetal membrane length as determined by the width of the computer screen at magnification of  $\times 40$ . The measurements of the thickness of constituent layers, compact together with the fibroblast layer (amniotic connective tissues), the reticular layer (chorionic connective tissue) and the cellular layers (cytotrophoblast and decidua layers) was taken from the same fields and each captured image was measured following calibration of the image with a internal scale slide and expressed in  $\mu$ m. In the case of separation of the connective tissue layers, the spaces were subtracted from the final

measurement in order to obtain the final connective tissue layer. The density of immunoreactive cells within fetal membrane layers was calculated from the data on immunoreactive cell number and thickness measurements on the same field and was expressed as cell number per 0.01 mm<sup>2</sup>. The FMMI (Fetal Membrane Morphometric Index) was calculated from the total cellular layer thickness (cytotrophoblast and decidua) and the connective tissue layer thickness i.e. amnion and chorionic reticular layers (Malak and Bell, 1994a).

### Statistical analysis

Two-way analysis of variance was used for the analysis of the number of immunoreactive cellular populations of the connective tissue layers and thickness measurements. Sampling from different subjects and from different zones of the fetal membranes were included as independent factors in the analysis. Scheffe's test was used for subsequent comparisons between different membrane zones and between patient groups. StatView<sup>®</sup> software, version 4.51 (Abacus Concepts, California, USA) was used for two-way analysis of variance and Scheffe's test. For comparisons between different membrane zones within individual patients Student's *t*-tests were employed.

## RESULTS

The major layers of the fetal membranes detectable in formalin-fixed sections are identified in Figure 1(a). The amnion is comprised of a single layer of cuboidal epithelium overlying the amniotic connective tissue layers, the acellular compact layer and the fibroblast layer. The chorion is comprised of the connective tissue reticular layer and the cytotrophoblast layer. The maternal-fetal interface is represented by the boundary between cytotrophoblast layer and the underlying maternal decidua layer.

Toluidine blue stained sections were initially employed to determine the total cell numbers within the connective tissue layers. However in a pilot study on serial sections the numbers of vimentin immunoreactive cells were 56 per cent higher than counts obtained from toluidine stained sections ( $r^2=0.86$ ,  $P=0.0001$ ), therefore vimentin immunoreactivity was employed to determine the total cell numbers within the tissue layers. Vimentin positive cells were detected in the fibroblast layer of the amnion and the reticular layer of the chorion in all biopsied zones from fetal membranes of all patients [Figure 1(b,c)]. There were no significant changes in the numbers of vimentin positive cell numbers per unit length of membrane in the connective tissue layers between any zones in any patient group or between patient groups (Table 1). Previous studies had reported regional changes in thickness of the constituent layers of the membranes, therefore we examined whether this had an effect upon cellular density. The thickness of the connective tissue layers of the amnion (the combined compact

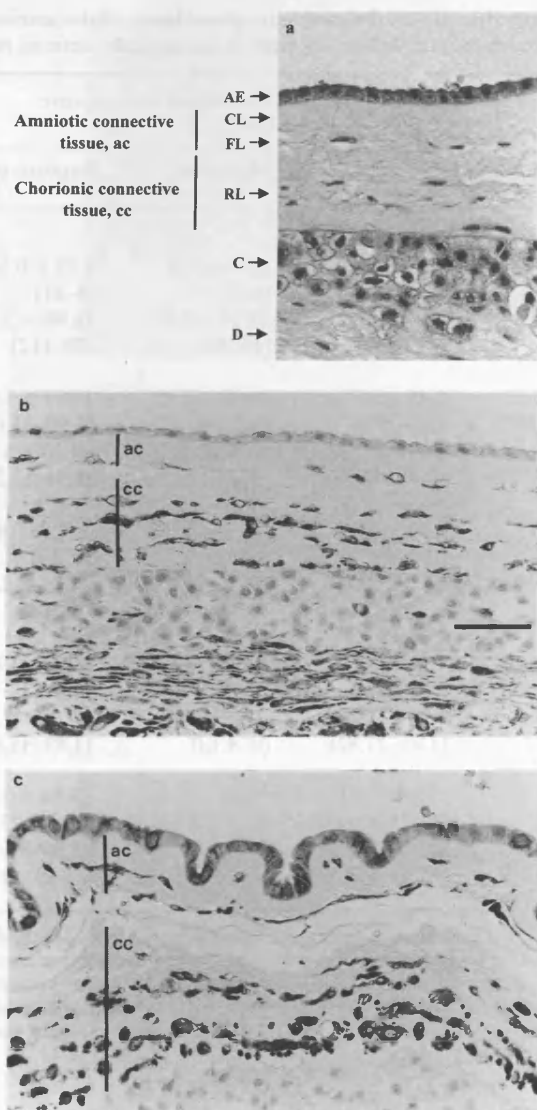


**Figure 1.** (a–c). Sections of fetal membrane biopsies obtained from a patient after spontaneous delivery at term stained with haematoxylin and eosin (a) and immunocytochemically stained for the presence of vimentin (b,c). Fetal membrane biopsies were obtained from the mid zone (a,b) and from the rupture tear (c). The haematoxylin and eosin stained section demonstrates the layers of the amnion, the amniotic epithelium (AE), the compact layer (CL), the fibroblast layer (FL), and of the chorion, the reticular layer (RL), the cytotrophoblast layer (C) and the attached maternal decidua (D). The amniotic connective tissue (ac) refers to the combined compact and fibroblast layer and the chorionic connective tissue (cc) to the reticular layer. Immunoreactive vimentin positive cells are seen in the fibroblast and reticular layers (b,c). Additionally, positive cells are detected in the decidua layer (b). The marked increase in thickness of the connective tissue layers of both amnion and chorion in the rupture line as compared to the mid zone biopsy is apparent by comparison of b with c. All photographs were taken at the same magnification. Scale bar: 50  $\mu$ m.

and fibroblast layers) and of the chorion (the reticular layer), were significantly thicker in biopsies associated with the rupture line compared to the mid-zones after delivery i.e. mean thickness of the amniotic connective tissue was 93 per cent higher ( $P=0.009$ ) and the reticular layer 74 per cent higher ( $P=0.013$ , Table 1). This is apparent by comparing the thickness of these layers in the biopsies obtained from the

mid-zone and rupture tear after delivery in Figure 1(b,c). This difference was also observed in the same layers between the 'cervical' biopsies and the mid-zone biopsies obtained prior to labour (36 per cent higher,  $P=0.025$ , and 30 per cent higher,  $P=0.023$ , respectively, Table 1). Although this difference did not reach significance in the labour-affected group the thickness of the amniotic connective tissue layers in 2/5 patients and the thickness of the reticular layer in 4/5 of patients was significantly thicker in the 'cervical' biopsies compared to their respective mid-zone biopsies (all  $P<0.0001$ ). There were no significant changes in the densities of vimentin positive cells in the connective tissue layers between any zones in any patient group or between patient groups. However within the patient groups vimentin positive cell density was significantly lower in the reticular layers of the 'cervical' biopsies compared to the mid-zones in 4/5 patients prior to labour ( $P\leq 0.01$ ), in 3/5 patients during labour ( $P\leq 0.002$ ) and in the rupture line biopsies in 3/5 patients after delivery compared to the mid-zone biopsies ( $P\leq 0.04$ ). When the data from all biopsies from all patients were combined there was a significant positive correlation between the absolute numbers of vimentin positive cells in the reticular layer and the thickness of this layer ( $r^2=0.349$ ,  $P=0.0006$ ) and the FMMI ( $r^2=0.465$ ,  $P=0.0001$ ), but a negative correlation between their density and the thickness of the reticular layer ( $r^2=0.431$ ,  $P=0.0001$ ) and of the amniotic connective tissue layer ( $r^2=0.308$ ,  $P=0.0014$ ).

Alpha-smooth muscle actin immunoreactive cells were identified in connective tissue layers but they exhibited a restricted distribution in that they were detected at high numbers principally in the reticular layer of 'cervical' and rupture line biopsies [Table 1, Figure 2(b,d,f)] and only rarely in their respective mid-zone biopsies [Table 1, Figure 2(a,c,e)]. In biopsies with lower numbers, it was noted that positive cells were detected toward the basal aspect of the reticular layer adjacent to the cytotrophoblastic layer [Figure 2(b)]. In biopsies with higher numbers, positive cells were distributed throughout the reticular layer [Figure 2(d)]. When they were also detected in the amniotic connective tissue layer the adjacent chorionic reticular layer always contained  $\alpha$ -smooth muscle actin positive cells, but not vice versa [Figure 2(f)]. The numbers expressed as unit length of membrane were 17-fold higher in the reticular layer of the 'cervical' compared to mid-zone biopsies in the labour affected group ( $P=0.04$ ) and 50-fold higher in the rupture line compared to mid-zone biopsies after delivery ( $P=0.002$ ) (Table 1). These changes were not affected by thickness of the connective tissue layers, since in the same sites mean densities of  $\alpha$ -smooth muscle actin cells were 8.5-fold ( $P=0.02$ ) and 36-fold ( $P=0.003$ ) higher, respectively (Table 1). When expressed as a percentage of the total vimentin positive population present, in the reticular layer of the mid-zone biopsies, the means ranged from only 2 to 5 per cent. In the labour affected 'cervical' biopsies this mean rose 9.8-fold to 49 per cent ( $P=0.03$ ) and in the rupture line biopsies 34.5-fold to 69 per cent ( $P=0.05$ ) (Table 2). There was no significant difference between the numbers and density of smooth muscle actin cells in the reticular layers

**Table 1.** Numbers and density of vimentin and  $\alpha$ -smooth muscle actin immunoreactive cells in the connective tissue layers of the amnion and chorion per unit length of the fetal membranes obtained prior to, during and after labour and delivery at term in anatomically defined regions

	Pre-labour ( <i>n</i> =5)		Labour ( <i>n</i> =5)		Post-labour and rupture ( <i>n</i> =5)	
	Mid-zone	'Cervical'	Mid-zone	'Cervical'	Mid-zone	Rupture site
<b>Vimentin numbers</b>						
Amnion	4.8 ± 0.25 (2–10)	6.06 ± 0.35 (2–14)	6.02 ± 0.29 (2–10)	5.92 ± 0.43 (1–18)	4.94 ± 0.22 (2–9)	8.28 ± 0.58 (3–21)
Chorion	26.08 ± 0.91 (14–45)	25.5 ± 0.81 (15–40)	22.42 ± 0.68 (16–34)	30.78 ± 1.87 (12–71)	24.64 ± 0.89 (14–40)	36.96 ± 3.2 (20–112)
<b>Vimentin density</b>						
Amnion	15.72 ± 0.9 (5.09–31.31)	15.35 ± 0.92 (4.62–30.85)	13.93 ± 0.81 (5.61–27.19)	9.48 ± 0.71 (2.3–24.1)	14.82 ± 1.02 (3.73–46.97)	14.97 ± 1.15 (3.98–35.63)
Chorion	33.27 ± 1.34 (16.8–53.53)	24.32 ± 1.46 (9.82–56.04)	27.35 ± 1.48 (11.73–59.39)	20.49 ± 1.42 (7.91–42.61)	31.11 ± 1.8 (12.03–88.56)	24.16 ± 1.48 (6.94–62.23)
<b><math>\alpha</math>-Smooth muscle actin numbers</b>						
Amnion	0	0.38 ± 0.11 (0–3)	0.04 ± 0.03 (0–1)	0.42 ± 0.13 (0–4)	0	1.96 ± 0.43 (0–13)
Chorion	0.42 ± 0.11 (0–4)	6.08 ± 1.3 (0–27)	1.02 ± 0.24 (0–7)	17.06 ± 2.21 (1–65)	0.5 ± 0.13 (0–4)	24.94 ± 2.39 (3–70)
<b><math>\alpha</math>-Smooth muscle actin density</b>						
Amnion	0	1.05 ± 0.35 (0–11.07)	0.09 ± 0.06 (0–3.01)	0.56 ± 0.19 (0–6.92)	0	3.42 ± 0.71 (0–18.2)
Chorion	0.46 ± 0.13 (0–4.62)	6.15 ± 1.43 (0–41.71)	1.17 ± 0.31 (0–9)	9.93 ± 1.05 (1.05–27.82)	0.46 ± 0.13 (0–4.13)	16.55 ± 1.56 (1.89–45.8)
<b>Thickness (<math>\mu</math>m)</b>						
Amnion	19.96 ± 0.69 (10.17–32.84)	27.15 ± 1.22 (13.29–58.65)	26.95 ± 1.59 (12.12–52)	37.78 ± 3.21 (11.34–111.04)	18.56 ± 0.76 (9.78–33.63)	35.84 ± 2.07 (10.17–77.81)
Chorion	52.98 ± 1.83 (26.2–85.63)	69.32 ± 4 (30.89–161.09)	57.8 ± 4.07 (28.54–139.98)	98.02 ± 5.25 (43.01–193.15)	54.98 ± 2.99 (22.68–115.74)	95.86 ± 5.48 (35.19–214.27)

Cells were counted in the full thickness of each layer along a specific length equal to the width of the computer screen at magnification of  $\times 40$ . Ten fields were examined in a fetal membrane biopsy from each zone in five patients and the minimum and maximum (in parentheses), mean and standard error values are derived from observations on 50 fields for each parameter. Statistical comparison of the number of the cells positively stained with antibodies against vimentin and  $\alpha$ -smooth muscle actin in the fibroblast and reticular layers between the selected zones within each patient group and between patient groups was performed using two-way analysis of variance and Scheffe's test. Densities, expressed as numbers per  $0.01 \text{ mm}^2$ , were determined from the measurements of thickness of the layers performed upon the same fields examined for immunoreactivity for each antibody.

between mid and 'cervical' biopsies in the prelabour patient group. However examination of individual patients revealed that in two patients both the numbers and densities were significantly higher (all  $P < 0.008$ ) in the 'cervical' biopsies compared to their mid-zones and were not significantly different to the levels observed in the 'cervical' biopsies from labour affected and rupture line biopsies (Figure 3). In the remaining three patients there was no difference between the numbers and densities at the two sites. In the amniotic connective tissue significant differences in numbers and densities were noted between the mid and 'cervical' biopsies in the labour affected patient group ( $P = 0.04$  and  $0.02$  respectively) but the differences in the cellular proportions were significant in this group and the post-labour group ( $P = 0.03$  and  $0.05$  respectively) (Table 2). When the data from all biopsies were combined there was a significant positive correlation between the absolute numbers of  $\alpha$ -smooth muscle actin positive cells in the reticular layer and its thickness ( $r^2 = 0.349$ ,  $P = 0.0006$ ), the number of vimentin positive cells in the reticular ( $r^2 = 0.595$ ,  $P = 0.0001$ ) and the amniotic connective tissue layers

( $r^2 = 0.389$ ,  $P = 0.0002$ ). There was also a correlation between both numbers and density of these cells in the reticular layer and the FMMI ( $r^2 = 0.576$ ,  $P = 0.0001$  and  $r^2 = 0.424$ ,  $P = 0.0001$  respectively).

In the fetal membrane obtained from a patient after rupture and delivery where multiple biopsies were obtained there was a correlation between  $\alpha$ -smooth muscle actin numbers in the reticular layers and the FMMI of the biopsies ( $r^2 = 0.679$ ,  $P = 0.0001$ ) (Figure 4).

No smooth muscle myosin positive cells were detected in the amniotic connective tissue and reticular layers of any biopsied zone of membranes, from any patient, although immunoreactive cells were associated with the walls of blood vessels in the maternal aspect of the decidual layers (Figure 5).

## DISCUSSION

In this study we have uniquely identified a specific alteration in the phenotype of mesenchymal cells in connective tissue layers

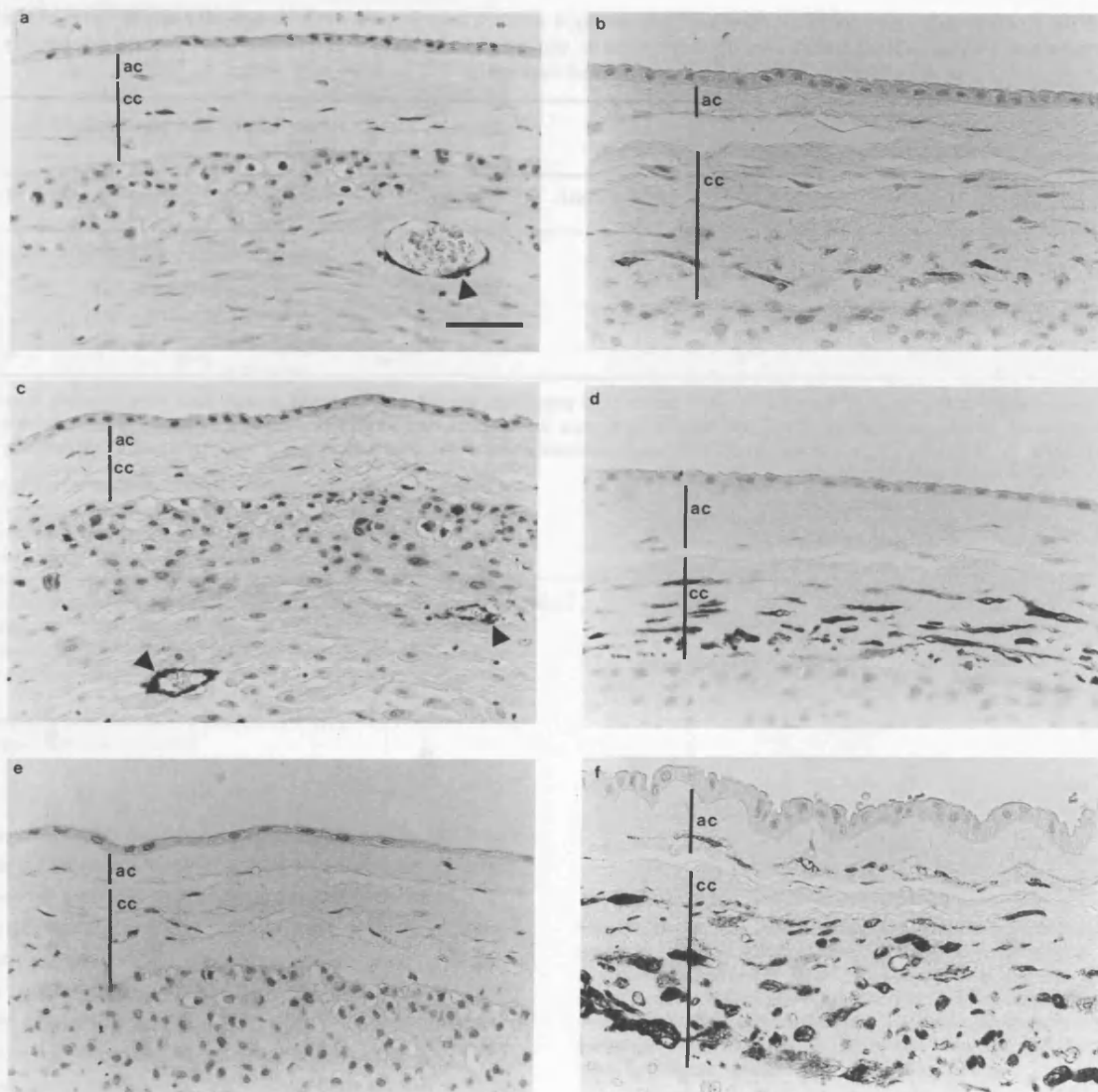


**Figure 2.** (a-f). Immunocytochemical staining for  $\alpha$ -smooth muscle actin in sections of fetal membrane biopsies obtained from the mid-zone (a) and membranes overlying the cervix (b) prior to labour, and from the mid-zone (c,e) and the rupture tear (d,f) after spontaneous delivery at term. Immunoreactive  $\alpha$ -smooth muscle actin positive cells were not detected within the reticular layer of the mid-zone biopsies (a,c,e). In a biopsy with only a small number of positive cells in the reticular layer, the cells are detected adjacent to the cytotrophoblast layer (b). In (d) positive cells are detected throughout the reticular layer. In (f) positive cells are also detected within the fibroblast layer. The amniotic connective tissue (ac) refers to the combined compact and fibroblast layer and the chorionic connective tissue (cc) to the reticular layer. Arrowheads in (a) and (c) indicate positive blood vessels within the maternal decidua. All photographs are taken at the same magnification. Scale bar: 50  $\mu$ m.

of the fetal membranes, consistent with the differentiation of myofibroblasts, in an anatomically defined region of the fetal membranes, i.e. membranes lying in the lower uterine pole, and associated with the process of parturition at term. The most dramatic alteration detected was the acquisition of  $\alpha$ -smooth muscle actin by mesenchymal cells of the reticular layer of biopsies obtained from over the cervix, in all patients during active labour, and within biopsies obtained in the rupture line after delivery. In this layer of the chorion in the 'cervical' biopsies obtained during labour 49 per cent of vimentin positive cells were  $\alpha$ -smooth muscle actin positive, and in biopsies from selected sites within the rupture tear after delivery this rose to 69 per cent. This was in contrast to biopsies obtained from the same fetal membranes, but at sites

more distal to the cervical area, where only 2-5 per cent of cells in the same reticular layer were vimentin and  $\alpha$ -smooth muscle actin positive, even after delivery. In the 'cervical' biopsies obtained prior to labour the percentage was also high i.e. 25 per cent. This was reflected by two patients whose mesenchymal phenotype in the 'cervical' biopsies were similar to labour-affected membranes, whereas in the remaining patients there was no significant  $\alpha$ -smooth muscle actin expression at this site, and was similar to all mid-zone biopsies.  $\alpha$ -Smooth muscle actin was also expressed by a significant proportion of mesenchymal cells in the fibroblastic layer of biopsies from the rupture line after delivery.

The definition of a myofibroblast is essentially one dependent upon the identification of certain ultrastructural features

**Table 2.** Percentage of vimentin positive cells possessing  $\alpha$ -smooth muscle actin in the connective tissue layers of the amnion and chorion of fetal membranes obtained prior to, during and after labour and delivery at term in anatomically defined regions

	Pre-labour (n=5)		Labour (n=5)		Post-labour and rupture (n=5)	
	Mid-zone	'Cervical'	Mid-zone	'Cervical'	Mid-zone	Rupture site
Amnion	0	6 $\pm$ 4 (0-19)	1 $\pm$ 0 (0-2)	6 $\pm$ 2 (0-12)	0	19 $\pm$ 8 (0-43)
Chorion	2 $\pm$ 1 (0-4)	25 $\pm$ 18 (0-93)	5 $\pm$ 2 (1-12)	49 $\pm$ 11 (33-90)	2 $\pm$ 1 (0-5)	69 $\pm$ 6 (52-86)

Estimations of the proportion of the total vimentin positive cell population stained with  $\alpha$ -smooth muscle actin were obtained from the mean values of immunoreactive cell numbers in each zone and patient, and statistical comparisons between the amniotic connective tissue layers and the reticular layers between the selected zones within each patient group was performed using two-way analysis of variance and Scheffe's test.

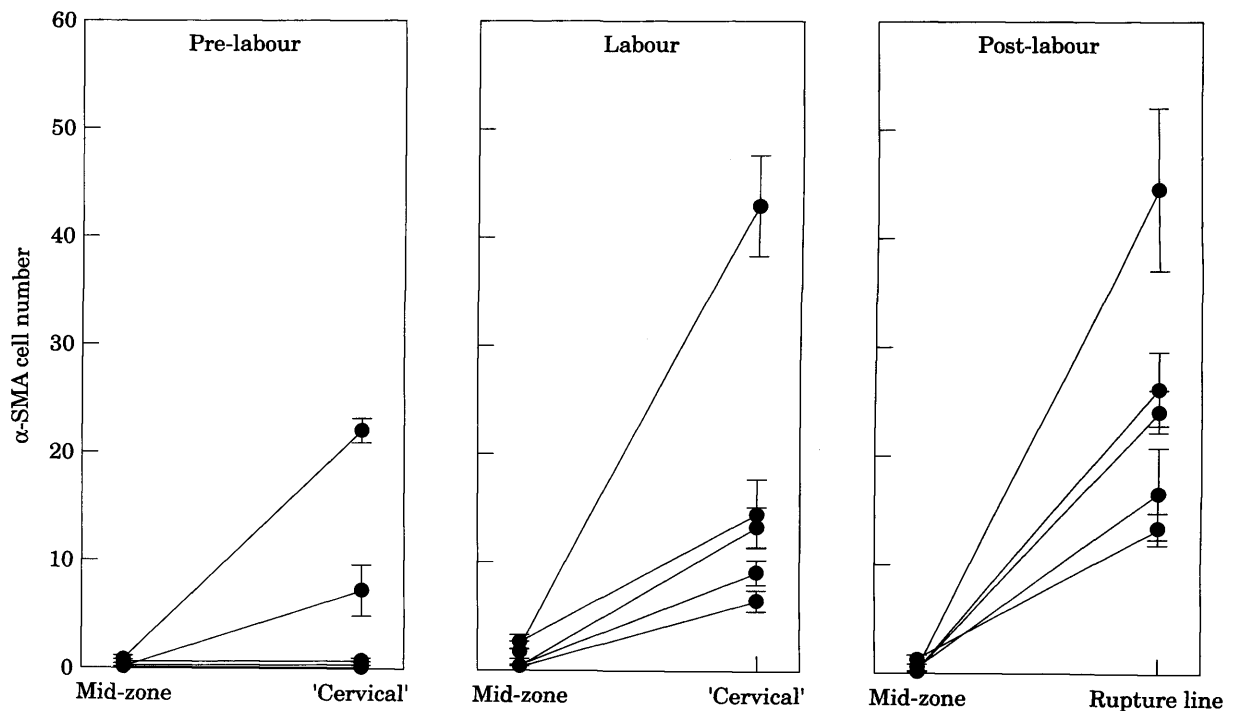


**Figure 3.** Numbers of  $\alpha$ -smooth muscle actin immunoreactive cells in the connective tissue layer of the chorion, the reticular layer, per unit length of the fetal membrane in biopsies obtained prior to, during and after labour and delivery at term in anatomically defined regions. Cells were counted in the full thickness of each layer along a specific length equal to the width of the computer screen at magnification of  $\times 40$  and the mean and standard error values are derived from observations on 10 fields per biopsy.

such as a well developed fibrillar cytoplasm, a cell to matrix fibronexus, gap junctions and an incomplete encapsulating basal lamina (Schurch, Seemayer and Gabbiani, 1998). Cells with such features have been described in the amniochorion (Wang and Schneider, 1982, 1983). However, myofibroblasts exhibit a variety of phenotypes (Schmitt-Graff, Desmouliere and Gabbiani, 1994) and have been classified according to their possession of particular subsets of intermediate filaments such as desmin and/or  $\alpha$ -smooth muscle actin, with the absence of smooth muscle myosin perhaps the only good marker distinguishing myofibroblasts from smooth muscle cells

(Sappino, Schurch and Gabbiani, 1990). The acquisition of  $\alpha$ -smooth muscle actin, but not smooth muscle myosin, by the mesenchymal cells in the reticular layer is analogous to the myofibroblast phenotype that differentiates during the early phase of a wound response and pathological conditions in other tissues (Desmouliere and Gabbiani, 1994). In these situations a number of functions have been ascribed to these cells, including turnover of the extracellular matrix, from initial degradation mediated by enzymes such as matrix metalloproteinases (MMPs), to synthesis during repair and scarring, and that of contraction.

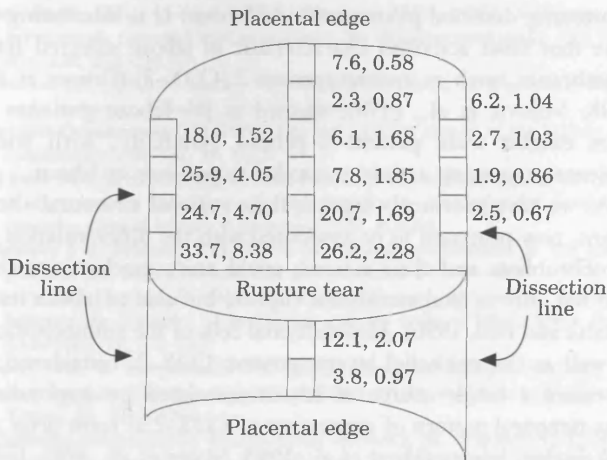


**Figure 4.** Map of biopsies obtained from a fetal membrane after spontaneous rupture and delivery at term. The fetal membrane was taken and cut along the specified dissection lines to allow the whole membrane to be placed flat and the biopsies were taken along the axis identified to the edge of the placenta. The first number refers to the mean values of the numbers of immunoreactive  $\alpha$ -smooth muscle actin cells in the reticular layer of a unit membrane length (one screen width at  $\times 40$ ) and the second the mean Fetal Membrane Morphometric Index (FMMI; Malak and Bell, 1994a) calculated from the width of the connective tissue and cellular layers in each biopsy. The means were calculated from 10 fields in each biopsy. The correlation equation between the immunoreactive  $\alpha$ -smooth muscle actin cell number and FMMI for all biopsies was  $y = 0.158x + 0.143$ .

The major cellular capacity for fibrillar collagen synthesis, which provides the major tensile strength of the membranes, appears to reside with the connective tissue cells of the fetal membranes and this declines to term (Casey and MacDonald, 1996). A number of MMPs and their inhibitors have been identified in the amniochorion (Bryant-Greenwood, 1998), although only an inhibitor, TIMP-1, appears to be preferentially expressed by the mesenchymal cells (Rowe et al., 1997). Thus, extracellular breakdown in the connective tissues of the membranes may principally reflect decreased expression of TIMP-1 and/or increased expression of MMPs. Whether myofibroblastic differentiation, reported in this study, is associated with these activities awaits further study. However, the fact that myofibroblastic differentiation correlated with the regional structural changes in the membranes in this study, including swelling of the connective tissue layers proposed to reflect matrix breakdown (Malak and Bell, 1994a), does suggest an association, if not causal, between myofibroblastic differentiation in the same layers and extracellular matrix breakdown.

Myofibroblasts also function to exert and transmit contractile forces and provide the force for wound contraction (Gabbiani et al., 1972). The expression of  $\alpha$ -smooth muscle actin in these cells appears to confer this contractile feature (Ronnov-Jessen and Peterson, 1996). Transmission of this force may be through the surrounding extracellular matrix. In the reticular layer this is rich in basal lamina components (Malak et al., 1993), demonstrated in smooth muscle to maintain intercellular connections and transmit contraction across the tissue (Eddy, Petro and Tomasek, 1988), and the extendible extracellular matrix protein fibrillin-1 (Reinhardt

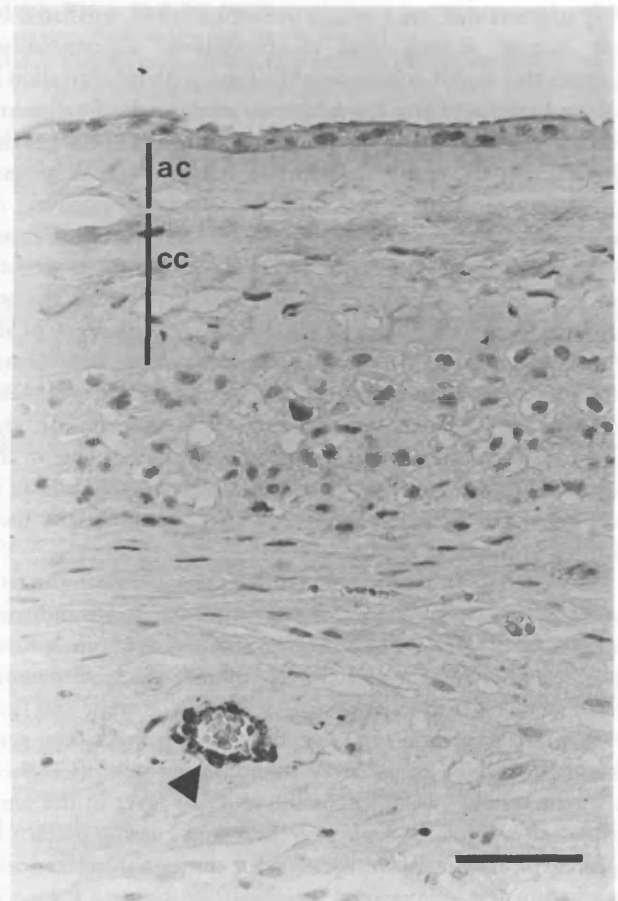


**Figure 5.** Immunocytochemical staining for smooth muscle myosin in a section of fetal membrane biopsied from the midzone in a patient after spontaneous delivery at term. No positive cells are seen in the connective tissue layers of either amnion or chorion. Arrowheads indicate positive blood vessel within the maternal decidua. The amniotic connective tissue (ac) refers to the combined compact and fibroblast layer and the chorionic connective tissue (cc) to the reticular layer. Scale bar: 50  $\mu$ m.

et al., 1996), present as long continuous cables intermeshing mesenchymal cells (Malak and Bell, 1994b). In the fetal membranes, which are under continuous and increasing stretch, particularly in the lower uterine pole, myofibroblasts may play a role in protection of the fetal membranes from overdistension and premature rupture.

The mechanisms responsible for myofibroblastic differentiation are unknown however three independent and interactive signals, cytokines, the extracellular matrix and mechanical forces, have been implicated (Sappino, Schurch and Gabbiani, 1990; Desmouliere and Gabbiani, 1994). Of these, cytokines appear to exert an essential role in modulation of cells to a myofibroblastic phenotype, and include granulocyte macrophage-colony stimulating factor (GM-CSF) and transforming growth factor beta-1 (TGF- $\beta$ 1) (Schurch, Seemayer and Gabbiani, 1998). Many of these factors are products of macrophages and the macrophage represents a subpopulation of the mesenchymal cells of the amniochorion (Bulmer and Johnson, 1984). The increase in immunoinflammatory cytokines associated with labour (Romero et al.,

1997) suggests that macrophage activation could, mediated by these factors, induce local myofibroblastic differentiation. However this would only be tenable if macrophage activation is also predominately anatomically restricted to the fetal membranes in the lower uterine pole. The mesenchymal cells of the amniochorion share the same developmental origin as mesenchymal cells of the umbilical cord and villous mesenchyme of the placenta. It has been proposed that at these sites myofibroblasts differentiate, by sequentially acquiring  $\alpha$ -smooth muscle actin and smooth muscle myosin, into the smooth muscle cells surrounding the fetal blood vessels (Kohnen et al., 1996; Nanaev et al., 1997). The signal at these sites is not known but is presumably influenced by growth of fetal capillaries into these tissues and angiogenic/vasculogenic signals which are absent on the avascularized mesenchyme of the fetal membranes. It appears that these cells may be plastic in their behaviour differentiating according to signals in their micro-environments.

A more tenable concept is that differential stretch in the fetal membranes in the lower uterine pole may provide the inducing stimulus, and since myofibroblasts provide traction, a functional response to that stretch. In support we have demonstrated an increase in tenascin-C (McParland, Pringle and Bell, 1998), whose expression is induced by stretch and whose gene contains a 'stretch-responsive' promoter element (Chiquet-Ehrismann et al., 1994), within the reticular layer in the same anatomical locations and physiological states as the pattern of appearance of smooth muscle actin immunoreactive cells described in this study. Fetal membranes subject to stretch in vitro also results in alterations in the production of activities of key molecules such as collagenase activity (El Maradny et al., 1996). It may be considered that stretch of the lower uterine pole could be provided by the formation of the lower uterine segment as part of labour, and indeed 'cervical' biopsies, in contrast to the mid-zone biopsies, from all patients in active labour possess high numbers of  $\alpha$ -smooth muscle actin immunoreactive cells. However, two patients exhibit the same phenomena in the pre-labour group and it is possible that myofibroblast differentiation is induced during a 'pre-clinical' phase of parturition corresponding to 'phase 1 of parturition' (Casey and MacDonald, 1993). These patients may have been further advanced in this phase and hence closer to clinical 'labour' if surgical intervention had not occurred. Given the localization of these changes to the fetal membranes over the lower uterine pole this phase could correspond to changes in the cervix and the lower uterine segment reflected by cervical

shortening detected prior to clinical labour. It is interesting to note that most activities characteristic of labour affected fetal membranes, such as cyclooxygenase-2 (COX-2) (Brown et al., 1998; Mijovic et al., 1998), studied in pre-labour patients at term exhibit wide patient-to-patient variability, with some patients possessing activities similar to patients in labour.

As we have previously argued, these regional structural alterations, now proposed to be associated with the differentiation of myofibroblasts and their actions, could unify mechanisms that lead not only to fetal membrane rupture but also to labour itself (Malak and Bell, 1996). Mesenchymal cells of the amniochorion, as well as the epithelial layers, possess COX-2, considered to represent a major source of labour-associated prostaglandins. The temporal pattern of expression of COX-2 at term prior to, and during, labour (Hirst et al., 1995; Slater et al., 1995; Gibb and Sun 1996; Mijovic et al., 1998) follows the same pattern of  $\alpha$ -smooth muscle acquisition by these cells reported in this study, therefore upregulation of COX-2 expression could be associated with this cellular phenotype. The parallel involution of the cytotrophoblastic layer in the fetal membranes overlying the cervix, another feature of the structural changes (Malak and Bell, 1994a; McLaren, Malak and Bell, 1999), would enable prostaglandins to escape degradation by the prostaglandin dehydrogenase, which is localized to this layer, allowing them to act upon the lower uterine segment and the cervix as part of parturition. This is supported by the report of decreased prostaglandin dehydrogenase in the fetal membranes in the lower uterine segment covering the cervix during term labour (van Meir et al., 1997a). In patients with idiopathic preterm labour we have also reported the premature appearance of structural alterations in their fetal membranes (Malak, Mulholland and Bell, 1994) and noted premature differentiation of the mesenchymal cells (McParland, Taylor and Bell, unpublished observations). This may also underlie the report of decreased prostaglandin dehydrogenase production in membranes from these patients (van Meir et al., 1997b), and in these cells as they undergo apoptosis (McLaren, Taylor and Bell, unpublished observations). Interestingly, in preterm labour COX activity is also prematurely induced, involving COX-1 and COX-2, and the mesenchymal cells of the amniochorion appear to be their sole site of the synthesis (Mijovic et al., 1998).

Further studies into the mechanism of induction of myofibroblast differentiation, in fetal membranes during term and preterm labour, and the possibility of its control may provide opportunities to inhibit their premature activation and preterm birth.

## ACKNOWLEDGEMENTS

The authors wish to thank technical members of staff of the academic Department of Obstetrics and Gynaecology for support and clinical members of the staff of the Leicester Royal Infirmary N.H.S. Trust for assistance with the collection of specimens. P. C. McParland was supported by grants from WellBeing and the Tommy's Campaign.

## REFERENCES

- Alger LS & Pupkin MJ (1986) Aetiology of preterm premature rupture of the membranes. *Clin Obstet Gynecol*, 29, 758-770.
- Bell SC & Malak TM (1997) Structural and Cellular Biology of the Fetal Membranes. In *Preterm Labor* (Ed.) Elder MG, Romero R & Lamont RF, pp. 401-428. New York: Churchill Livingstone.

- Bou-Resli MN, Al-Zaid NS & Ibrahim MEA (1981) Full-term and prematurely ruptured fetal membranes. An ultrastructural study. *Cell Tissue Res*, 220, 263–278.
- Bourne GL (1962) Premature rupture of membranes. In *The human amnion and chorion* pp. 175–192. London: Lloyds.
- Bryant-Greenwood GD (1998) The extracellular matrix of the human fetal membranes. *Placenta*, 19, 1–11.
- Brown NL, Alvi SA, Elder MG, Bennett PR & Sullivan, MHF (1998) A spontaneous induction of fetal membrane prostaglandin production precedes clinical labour. *J Endocrinol*, 157, R1–R6.
- Bulmer J & Johnson PM (1984) Macrophage populations in the human placenta and amniochorion. *Clin Exp Immunol*, 57, 393–403.
- Casey ML & MacDonald PC (1993) Human parturition: distinction between the initiation of parturition and the onset of labor. *Semin Reprod Endocrinol*, 11, 272–283.
- Casey ML & MacDonald PC (1996) Interstitial collagen synthesis and processing in human amnion: a property of the mesenchymal cells. *Biol Reprod*, 55, 1253–1260.
- Chiquet-Ehrismann R, Tannheimer M, Koch M, Brunner A, Spring J, Martin D, Baumgartner S & Chiquet M (1994) Tenascin-C expression by fibroblasts is elevated in stressed collagen gels. *J Cell Biol*, 127, 2093–2101.
- Desmouliere A & Gabbiani G (1994) Modulation of cytoskeletal features during pathological situations: the role of extracellular matrix and cytokines. *Cell Motil Cytoskeleton*, 29, 195–203.
- Eddy RJ, Petro JA & Tomasek JJ (1988) Evidence for the nonmuscle nature of the “myofibroblast” of granulation tissue and hypertrophic scar. *Am J Pathol*, 130, 252–260.
- El Maradny E, Kanayama N, Halim A, Maehara K & Terao T (1996) Stretching of fetal membranes increases the concentration of interleukin-8 and collagenase activity. *Am J Obstet Gynaecol*, 174, 843–849.
- French JI & McGregor JA (1996) The pathobiology of premature rupture of membranes. *Semin Perinatol*, 20, 344–368.
- Gabbiani G, Hirschel B, Ryan G, Statkov P & Majno G (1972) Granulation tissue as a contractile organ. *J Exp Med*, 135, 719–731.
- Gibb W & Sun M (1996) Localization of prostaglandin H synthase type 2 protein and mRNA in term human fetal membranes and decidua. *J Endocrinol*, 150, 497–503.
- Gibbs RS, Romero R, Hillier SL, Eschenbach DA & Sweet RL (1992) A review of premature birth and subclinical infection. *Am J Obstet Gynaecol*, 166, 1515–1528.
- Halaburt JT, Uldbjerg N, Helmig R & Ohlsson K (1989) The concentration of collagen and the collagenolytic activity in the amnion and the chorion. *Eur J Obstet Gynaecol Reprod Biol*, 31, 75–82.
- Hirst JJ, Teixeira F, Zakar T & Olson DM (1995) Prostaglandin endoperoxide-H-synthase-1 and -2 messenger ribonucleic acid levels in human amnion with spontaneous labor onset. *J Clin Endocrinol Metab*, 80, 517–523.
- Jenkins DM, O'Neill M & Johnson PM (1983) HLA-DR-positive cells in the human amniochorion. *Immunol Lett*, 6, 65–67.
- Kelly T (1995) The pathophysiology of premature rupture of the membranes. *Curr Opin Obstet Gynaecol*, 7, 140–145.
- Khong T, Lane E & Robertson W (1986) An immunocytochemical study of fetal cells at the maternal-placental interface using monoclonal antibodies to keratins, vimentin and desmin. *Cell Tissue Res*, 246, 189–195.
- Kohnen G, Kertschanska S, Demir R & Kaufmann P (1996) Placental villous stroma as a model system for myofibroblast differentiation. *Histochem Cell Biol*, 105, 415–429.
- Major CA & Garite TJ (1997) Preterm premature rupture of membranes. In *Preterm Labor* (Ed.) Elder MG, Romero R & Lamont RF, pp. 153–164. New York: Churchill Livingstone.
- Malak TM & Bell SC (1993) The structural characteristics of spontaneously ruptured fetal membranes: their relationship to membrane rupture and parturition. *Contemp Rev Obstet Gynaecol*, 5, 117–123.
- Malak TM & Bell SC (1994a) Structural characteristics of term human fetal membranes (amniochorion and decidua): a novel zone of extreme morphological alteration within the rupture site. *Br J Obstet Gynaecol*, 101, 375–386.
- Malak TM & Bell SC (1994b) Distribution of fibrillin-containing microfibrils and elastin in human fetal membranes: a novel molecular basis for membrane elasticity. *Am J Obstet Gynaecol*, 171, 195–205.
- Malak TM & Bell SC (1996) Fetal membranes structure and prelabour rupture. *Fetal Matern Med Rev*, 8, 143–164.
- Malak TM, Mulholland G & Bell SC (1994) Morphometric characteristics of the decidua, cytotrophoblast and connective tissue of the prelabour ruptured fetal membranes. *Ann NY Acad Sci*, 73, 430–433.
- Malak TM, Ockleford CD, Bell, SC, Dagleish, R, Bright N & MacVicar J (1993) Confocal immunofluorescence localization of collagen types I, III, IV, V and VI and their ultrastructural organization in term fetal membranes. *Placenta*, 14, 385–406.
- McLaren J, Malak TM & Bell SC (1999) Structural characteristics of term human fetal membranes prior to labour: identification of an area of altered morphology overlying the cervix. *Hum Reprod*, 14, 237–241.
- McParland, PC, Pringle, JH & Bell, SC (1998) Tenascin and the fetal membrane wound hypothesis—programming for fetal membrane rupture? *Br J Obstet Gynaecol*, 105, 1223–1224.
- Mead PB (1980) Management of the patient with premature rupture of the membranes. *Clin Perinatol*, 7, 243–255.
- Mijovic JE, Zakar T, Nairn TK & Olson DM (1998) Prostaglandin endoperoxide H synthase (PGHS) activity and PGHS -1 and -2 messenger ribonucleic acid abundance in human chorion throughout gestation and with preterm labor. *J Clin Endocrinol Metab*, 83, 1358–1367.
- Nanaev AK, Kohnen G, Milovanov AP, Domogatsky SP & Kaufmann P (1997) Stromal differentiation and architecture of the human umbilical cord. *Placenta*, 18, 53–64.
- Parry S & Strauss JF (1998) Premature rupture of the fetal membranes. *New Eng J Med*, 338, 663–670.
- Reinhardt DP, Keene DR, Corson GM, Poschl E, Bachinger HP, Gamber JE & Sakai LY (1996) Fibrillin-1: Organization in microfibrils and structural properties. *J Mol Biol*, 258, 104–116.
- Romero R, Gomez R, Mazor M, Ghezzi F & Yoon BH (1997) The preterm labor syndrome. In *Preterm Labor* (Ed.) Elder MG, Romero R & Lamont RF, pp. 29–49. New York: Churchill Livingstone.
- Ronnov-Jessen L & Peterson OW (1996) A function for filamentous  $\alpha$ -smooth muscle actin: retardation of motility in fibroblasts. *J Cell Biol*, 134, 67–80.
- Rowe TF, King LA, MacDonald PC & Casey ML (1997) Tissue inhibitor of metalloproteinase-1 and tissue inhibitor of metalloproteinase-2 expression in human amnion mesenchymal and epithelial cells. *Am J Obstet Gynaecol*, 176, 915–921.
- Sappino AP, Schurch W & Gabbiani G (1990) Differentiation repertoire of fibroblastic cells: expression of cytoskeletal proteins as marker of phenotypic modulations. *Lab Invest*, 63, 144–161.
- Schmidt W (1992) *The amniotic fluid compartment: The fetal habitat*. Berlin: Springer-Verlag.
- Schmitt-Graff A, Desmouliere A & Gabbiani G (1994) Heterogeneity of myofibroblast phenotype features: an example of fibroblastic cell plasticity. *Virchows Arch*, 425, 3–24.
- Schurch W, Seemayer T & Gabbiani G (1998) The myofibroblast: a quarter century after its discovery. *Am J Surg Pathol*, 22, 141–147.
- Slater DM, Berger LC, Newton R, Moore GE & Bennett PR (1995) Expression of cyclooxygenase types 1 and 2 in human fetal membranes at term. *Am J Obstet Gynaecol*, 172, 77–82.
- Sutton L, Mason DY & Redman CW (1983) HLA-DR positive cells in human placenta. *Immunology*, 49, 103–112.
- Van Meir CA, Matthews SG, Ramirez MM, Calder AA, Keirse MJNC & Challis JRG (1997a) Chorionic prostaglandin catabolism is decreased in the lower segment with term labor. *Placenta*, 18, 109–114.
- Van Meir CA, Matthews SG, Keirse MJNC, Ramirez MM, Bocking A & Challis JRG (1997b) 15-Hydroxyprostaglandin dehydrogenase: implications in preterm labor with and without ascending infection. *J Clin Endocrinol Metab*, 82, 969–976.
- Wang T & Schneider J (1982) Myofibroblast im bindegewebe des menschlichen amnions. *Z Geburtshilfe Perinatol*, 186, 164–169.
- Wang T & Schneider J (1983) Fine structure of human chorionic membrane: ultrastructural and histological examination. *Arch Gynecol*, 233, 187–198.

# Regional and cellular localization of osteonectin/SPARC expression in connective tissue and cytotrophoblastic layers of human fetal membranes at term

P.C.McParland<sup>1</sup>, S.C.Bell<sup>1,3</sup>, J.H.Pringle<sup>2</sup> and D.J.Taylor<sup>1</sup>

Preterm Birth Research Group, <sup>1</sup>Departments of Obstetrics and Gynaecology and <sup>2</sup>Department of Pathology, Leicester Warwick Medical School, Faculty of Medicine and Biological Sciences, University of Leicester, Leicester LE2 7LX, UK

<sup>3</sup>To whom correspondence should be addressed. E-mail: scb@leicester.ac.uk

**Fetal membranes overlying the cervix in patients prior to and during labour, and within the rupture tear after spontaneous delivery at term, exhibit altered morphology. In this study we report that in comparison to mid-zone fetal membranes biopsies, these regions are characterized by increased expression of the matricellular protein osteonectin or SPARC (Secreted Protein Acidic and Rich in Cysteine). In the reticular layer, the percentage of vimentin positive mesenchymal cells immunoreactive for osteonectin increased in these regions from 3–4% to 25–33% and represented a fraction of the  $\alpha$ -smooth muscle actin positive myofibroblasts elevated in the same regions. In the fibroblastic layer, the percentage of osteonectin positive cells increased from 1–5% to 8–13%; however, these did not exhibit the same relationship to the  $\alpha$ -smooth muscle actin positive myofibroblasts in this layer. In the cytotrophoblastic layer the percentage of cytotrophoblastic cells immunoreactive for osteonectin increased from 1% to 6–12%. Elevation of in-situ detectable mRNA was also observed in the same cellular populations in this region. The incidence of cells positive for osteonectin mRNA or protein in the reticular layer correlated with morphological changes. Osteonectin has been implicated in the regulation of extracellular matrix turnover, and its pattern of expression suggests a role in the regional connective tissue and cytotrophoblastic changes proposed to be involved in the cleavage and rupture of fetal membranes.**

*Key words:* amnion/chorion/cytotrophoblast/myofibroblast/osteonectin

## Introduction

In ~10% of term pregnancies and up to 60% of preterm deliveries, the fetal membranes, which encapsulate the fetus and amniotic fluid, rupture prior to labour. In the latter it is a direct antecedent of preterm birth (Alger and Pupkin, 1986; Keirse *et al.*, 1989; Kelly, 1995; French and McGregor, 1996; Romero *et al.*, 1999). Although infection has been implicated in the aetiopathology of a proportion of cases (Gibbs *et al.*, 1992; French and McGregor, 1996) the mechanisms of this pre-labour rupture in the absence of infection, and indeed the mechanisms underlying their spontaneous rupture during term labour, are essentially unknown (Kelly, 1995; French and McGregor, 1996; Major and Garite, 1997; Parry and Strauss, 1998; Romero *et al.*, 1999; Bell, 2000).

Previous studies have identified unusual morphological features of the fetal membranes within a restricted part of the rupture tear after labour and delivery at term (Bou-Resli *et al.*, 1981; Malak and Bell, 1993, 1994). These features include marked swelling of the connective tissue layers of the amnion and chorion (layers rich in fibrillar collagen types I and III

and which bestow the structural strength of the membranes) and thinning of the cellular layers, the cytotrophoblastic and decidua layers (Malak and Bell, 1994). Subsequent studies have demonstrated a similar altered morphology in single biopsies obtained from fetal membranes overlying the cervix in the lower uterine pole prior to, and during, labour at term, compared to biopsies distal to this site (McLaren *et al.*, 1999; McParland *et al.*, 2000). The rupture tear after delivery invariably involves the fetal membranes overlying the cervix in the lower uterine pole, suggesting that this area represents the site of initial membrane rupture. It has been proposed that the morphological features detected prior to, and during, labour at this site reflect a structural weakness, therefore indicating a localized site of increased susceptibility to rupture during the increased intra-amniotic pressures experienced during labour (Malak and Bell, 1993, 1994, 1996; Bell and Malak, 1997).

We recently reported that the morphological features at these anatomical sites, over the cervix prior to rupture and within the rupture line after delivery, were associated with an alteration in the phenotype of mesenchymal cells of the connective tissue

layers. This principally involved the reticular layer of the chorion, where a proportion of cells possessed  $\alpha$ -smooth muscle actin ( $\alpha$ -SMA) but not smooth muscle myosin (McParland *et al.*, 2000). This phenotype is considered the hallmark of the 'activated' or 'differentiated' myofibroblast (Sappino *et al.*, 1990; Schmitt-Graff *et al.*, 1994). A number of functions have been ascribed to these cells, including that of extracellular matrix synthesis and degradation, and that of contraction, and reflect their proposed central role in wound healing, fibro-contractive diseases and desmoplastic reactions to cancer (Schurch *et al.*, 1998; Powell *et al.*, 1999; Serini and Gabbiani, 1999).

Recently,  $\alpha$ -SMA positive myofibroblasts arising during human liver fibrogenesis have been demonstrated to express the matricellular protein osteonectin (Blazewski *et al.*, 1997). Osteonectin, also known as SPARC (Secreted Protein Acidic and Rich in Cysteine), BM-40 and 43K protein, is a 43 kDa  $\text{Ca}^{2+}$  and collagen binding glycoprotein (Termine *et al.*, 1981) considered to be a prototype of the matricellular proteins which include tenascin-C and thrombospondin (Sage and Bornstein, 1991; Lane and Sage, 1994; Motamed, 1999; Yan and Sage, 1999). In the adult its expression is limited but it has been identified in a variety of tissues undergoing cellular remodelling or renewal, and in sites exhibiting high cell proliferation and migration, extracellular matrix remodelling and active epithelial-mesenchymal interactions (Holland *et al.*, 1987; Sage *et al.*, 1989; Mundlos *et al.*, 1992; Reed *et al.*, 1993; Porter *et al.*, 1995). Osteonectin exhibits a diverse range of properties *in vitro*, including those that would support its suggested key role in wound repair and extracellular matrix turnover such as the regulation of the synthesis of plasminogen activator inhibitor-1 (Hasselaar *et al.*, 1991; Lane *et al.*, 1992) and of the matrix metalloproteinases (MMP)-1, -2, -3 and -9 (Tremble *et al.*, 1993; Shankavaram *et al.*, 1997; Gilles *et al.*, 1998).

In the present study we have therefore determined whether the anatomically defined regional alterations in fetal membrane morphology and myofibroblastic differentiation reported prior to, and during, labour and after membrane rupture at term, are associated with osteonectin expression.

## Materials and methods

### Patient details and tissue sampling

Fetal membranes were obtained prior to ( $n = 15$ ), during ( $n = 5$ ), and following ( $n = 5$ ) spontaneous labour at term as previously described (McParland *et al.*, 2000). Membranes were collected on an anonymous basis according to guidance from the local Ethics Committee. In all cases potentially infected membranes were excluded following identification of polymorphonuclear infiltration of the amniochorion on histological examination. Fetal membrane specimens of  $\sim 1 \times 3$  cm were regionally biopsied from the following areas of the fetal membrane: (i) 'cervical' (lower uterine pole) membrane biopsies from pre-labour (with intact membranes) and labour Caesarean sections; (ii) rupture tear biopsies following term vaginal delivery; (iii) mid-zone biopsies, obtained halfway between the cervical area and the placental edge in the cases of Caesarean sections and between the rupture line and the placental edge in patients after delivery. In all cases these biopsies were taken at least 10–12 cm

from the cervical areas or rupture lines. Sequential biopsies of  $\sim 1 \times 3$  cm were taken from the rupture line to the placental edge in a single patient following labour and delivery at term. Biopsies were rolled and fixed in 10% formal saline for 48 h before processing and mounting in paraffin wax. Tissue sections were cut (4  $\mu\text{m}$ ) and then stained with haematoxylin and eosin. For larger specimens to be used for protein and RNA extraction procedures, membranes were collected from an area within 5 cm of the Babcock, i.e. to include the 'cervical' area and at least 12 cm distally from the Babcock tissue forceps i.e. 'mid-zone'. The restricted area of tissue taken, to ensure accurate mapping, meant that in some cases different tissue samples were used for different techniques.

### Immunocytochemistry

Immunocytochemistry was performed on formalin-fixed paraffin-embedded tissue sections, as previously described (McParland *et al.*, 2000). The following murine monoclonal antibodies used were: anti-osteonectin (clone N50; Biodesign International, Kennebunk, USA, 7.5  $\mu\text{g}/\text{ml}$ ), anti-vimentin (clone V9; Sigma, Poole, UK; 3.87  $\mu\text{g}/\text{ml}$ ), anti- $\alpha$ -SMA (clone 1A4; Dako, Cambridge, UK; 1.9  $\mu\text{g}/\text{ml}$ ), anti-cytokeratin (clone MNF116; Dako; 0.93  $\mu\text{g}/\text{ml}$ ), and anti-CD68 (clone PG-M1; Dako; 3.6  $\mu\text{g}/\text{ml}$ ). Rabbit polyclonal antiserum against bovine osteonectin, BON-I, was a generous gift from L.W.Fisher (NIDCR; NIH, Bethesda, MA, USA; Fisher *et al.*, 1995) and was used at 1:4000. Tissue sections were microwaved in 10 mmol/l sodium citrate, pH 6.0, for 30 min prior to incubation with BON-I. Slides were incubated overnight at 4°C for anti-vimentin and BON-I or at 37°C for 1 h with other antibodies. Incubation with anti-osteonectin clone NSC was performed in the presence of 2 mmol/l  $\text{CaCl}_2$ . Negative controls were primary antibody omission and inclusion of mouse IgG (Sigma) or rabbit serum (Dako) at concentrations that matched that of the primary antibodies. Umbilical cord was used as a positive control tissue to validate the antibodies and techniques.

### Cell line and culture

Human melanoma cell line SK-MEL-28 was obtained from the American Type Culture Collection (Rockville, MD, USA). Cells were grown in  $\alpha$ -minimal essential medium containing 10% v/v fetal calf serum (Life Technologies Ltd, Paisley, UK) to 90% confluence. SK-MEL-28 cells were harvested with 0.25% trypsin-EDTA (Life Technologies) and lysed in 100 mmol/l Tris-HCl pH 8.0, 500 mmol/l LiCl, 10 mmol/l EDTA pH 8.0, 1% sodium dodecyl sulphate (SDS) and 5 mmol/l dithiothreitol.

### mRNA isolation

mRNA from SK-MEL-28 cells was captured onto Oligo d(T)<sub>25</sub> Dynabeads® (Dyna, Merseyside, UK), and washed in 10 mmol/l Tris-HCl pH 8.0, 0.15 mol/l LiCl, 1 mmol/l EDTA with and then without 0.1% SDS. Fresh fetal membrane samples were homogenized in Tri Reagent (Sigma), and stored at  $-80^\circ\text{C}$  until required. Total RNA extraction was performed according to the Tri Reagent extraction protocol from Sigma (Technical Bulletin MB-205).

### In-situ hybridization

A probe to detect osteonectin mRNA *in situ* was synthesized by reverse transcription-polymerase chain reaction (RT-PCR) amplification of a 325 bp region of the osteonectin gene, employing mRNA extracted from SK-MEL-28 cells. This template was then used in an 'asymmetric' PCR reaction incorporating digoxigenin to produce a single stranded antisense DNA probe.

Oligonucleotide primers were designed for osteonectin (forward primer 5'-GCTCCACCTGGACTACATCG-3', reverse primer 5'-GGAGAGGTACCCGTCATGG-3'), to amplify a 325 bp product span-

ning exons 6–9. Primers for  $\beta$ -actin were used as positive controls (forward 5'-GGAGACAAGCTTGCTCATCACCATTGGCAATGAGCG-3', reverse 5'-GCCAATTCGAGCTCTAGAAGCATTTGGCGGTGGACG-3'). Forward strand primers were synthesized with a 5' biotin group.

cDNA was prepared using 1  $\mu$ l SK-MEL-28 mRNA in RT buffer (50 mmol/l Tris-HCl pH 8.3, 50 mmol/l KCl, 10 mmol/l MgCl<sub>2</sub>, 10 mmol/l dithiothreitol, 0.5 mmol/l spermidine (Promega, Southampton, Hants), 1 mmol/l dNTPs (Roche Molecular Biochemicals, Lewes, East Sussex, UK), 25 IU RNasin<sup>®</sup> ribonuclease inhibitor (Promega), and 5 IU AMV reverse transcriptase (Promega) in a volume of 25  $\mu$ l. The reaction was incubated at 42°C for 1 h. cDNA was prepared from 0.5  $\mu$ g fetal membrane mRNA in the same manner, including 15 pmol oligo d(T)<sub>12–18</sub> (Amersham Pharmacia Biotech, St Albans, UK) in the reaction. Control reactions were prepared in the absence of AMV reverse transcriptase.

Templates for later synthesis of in-situ probes were produced by PCR, carried out in a Techne Genius<sup>®</sup> thermal cycler. The reaction was performed with 1  $\mu$ l SK-MEL-28 cDNA in the following reagents: 45 mmol/l Tris-HCl pH 8.8, 11 mmol/l (NH<sub>4</sub>)<sub>2</sub>SO<sub>4</sub>, 4.5 mmol/l MgCl<sub>2</sub>, 800  $\mu$ mol/l dNTPs, 110  $\mu$ g/ml bovine serum albumin, 6.7 mmol/l  $\beta$ -mercaptoethanol, 4.4  $\mu$ mol/l EDTA pH 8.0 and 10 pmol of forward and reverse primers in a reaction volume of 50  $\mu$ l. The DNA was denatured at 98°C for 5 min, and held at 62°C during the addition of 1 IU *Taq* polymerase (Promega), and heated to 72°C for 1 min. The following cycle profile was used: 98°C for 1 min, 62°C for 45 s, 72°C for 1 min, then the reaction held at 72°C at the end of the amplification. PCR for osteonectin was carried out for 25 cycles. PCR amplification from fetal membrane cDNA was carried out for 30 cycles. PCR products were loaded onto a 3% agarose gel containing 15  $\mu$ g/100 ml ethidium bromide, with 100 bp ladder (Life Technologies) in one lane as a size marker, and run at 100 V for 2 h. Bands were visualized on a UV transilluminator. One  $\mu$ l of the resultant product was used as a template for production of a probe for in-situ hybridization in an asymmetric PCR reaction including 70  $\mu$ mol/l digoxigenin-11-dUTP (Roche Molecular Biochemicals, Lewes, East Sussex, UK) and 100 pmol reverse primer in reaction buffer as described above. One IU *Taq* polymerase (Promega) was added after an initial denaturation to 98°C and amplification was carried out for 20 cycles. Double-stranded contaminant was removed by incubation with Streptavidin-Dynabeads<sup>®</sup> (Dyna), to give a single-stranded digoxigenin labelled probe. A positive control probe to  $\beta$ -actin was synthesized in the same manner. Probe concentration was titrated to eliminate background staining, whilst retaining good signal strength.

In-situ hybridization was carried out on de-waxed rehydrated tissue sections. Proteinase K pretreatment (2–10  $\mu$ g/ml) was optimized for each tissue section. Prehybridization, hybridization and post-hybridization washing were modified from the method of Pringle (1995) to include the presence of 50% formamide in these steps. Detection was carried out by incubation with anti-digoxigenin antibody (Roche Molecular Biochemicals) followed by BCIP/NBT (Sigma) containing 1 mmol/l levamisole (Sigma) (Pringle, 1995). Negative controls were carried out using sense probe to osteonectin, RNase pre-treatment of the tissue section, and by omission of the probe in the hybridization protocol. Umbilical cord was used as a positive control tissue.

#### **Histological, immunocytochemical and in-situ assessment**

Haematoxylin and eosin and immunocytochemical stained sections of membrane rolls from all biopsies were examined under light microscopy connected to an image capture system. This system comprised an Apple Macintosh Centris running NIH Image<sup>®</sup> (version 1.51). Each section was divided into quadrants. For measurements of

constituent layer thickness and for counting of immunoreactive and in-situ positive cells, 10 fields per roll were examined along the intersections of 12 o'clock to 6 o'clock and 3 o'clock to 9 o'clock. Measurements were taken only from sections cut vertically, showing a single layer of amniotic epithelium. The numbers of immunoreactive or in-situ positive cells were counted in the whole thickness of each specified layer in a standard fetal membrane length as determined by the width of the computer screen at magnification of  $\times 40$ . The derived fetal membrane morphometric index (FMMI) is the ratio of the total connective tissue layer thickness, i.e. amnion and chorionic reticular layers, and the total cellular layer thickness, i.e. cytotrophoblast and decidua (Malak and Bell, 1994). Fetal membrane morphology data, and vimentin and  $\alpha$ -SMA cell counting data for the majority of the samples in this study have been described previously (McParland *et al.*, 2000), and were used to derive osteonectin cell density and percentage data, and to relate osteonectin immunoreactivity to morphology and  $\alpha$ -SMA immunoreactivity.

#### **Protein extraction and Western blotting**

Fetal membrane samples were washed thoroughly in phosphate-buffered saline (PBS), and homogenized (50% w/v) in 0.2 mol/l 3-[cyclohexylamino]-1-propane-sulphonic acid, 150 mmol/l NaCl, 1 mmol/l EDTA with 1 mmol/l PMSF at pH 11.5. The homogenate was centrifuged at 100 000 g for 1 h and the supernatant stored at  $-80^{\circ}\text{C}$ . Proteins were separated under reducing conditions on 10% polyacrylamide gels with 0.1% SDS (Bio-Rad, Hemel Hempstead, Herts, UK). They were transferred to nitrocellulose in 25 mmol/l Tris, 192 mmol/l glycine, 20% methanol for 1 h at 100 V. The blots were blocked in 5% non-fat milk powder for 30 min and incubated in 0.2  $\mu$ g/ml mouse anti-osteonectin monoclonal antibody N50 or 1/2000 rabbit anti-bovine osteonectin, BON-I, overnight at 4°C. The blots were washed in 50 mmol/l Tris, 150 mmol/l NaCl, 0.1% Tween 20 (TBS-Tween), incubated in either horseradish peroxidase-conjugated sheep anti-mouse or donkey anti-rabbit antibody (Amersham Pharmacia Biotech), and washed in TBS-Tween. Detection was with enhanced chemiluminescence (Amersham Pharmacia Biotech). Bands were visualized by exposure to Kodak Biomax X-ray film. Films were scanned on a Umax Astra 1220P flatbed scanner and densitometry performed using Scion Image<sup>®</sup>. Control blots were incubated with equivalent concentration of mouse IgG or rabbit serum.

#### **Statistical analysis**

Two-way analysis of variance was used for the analysis of the number of immunoreactive cellular populations of the tissue layers and thickness measurements. Sampling from different subjects and from different zones of the fetal membranes were included as independent factors in the analysis. Scheffé's test was used for subsequent comparisons between different membrane zones and between patient groups. For comparison between cell counts for different zones for in-situ hybridization, and for protein densitometry results, Student's *t*-test was employed. Correlation coefficients were calculated using linear regression analysis. All statistical analysis was carried out using StatView<sup>®</sup> software, version 4.51 (Abacus Concepts, CA, USA).

## **Results**

#### **Localization of osteonectin immunoreactivity**

Osteonectin immunoreactive cells were identified in the amniotic epithelium, and in the fibroblast, reticular and cytotrophoblast layers in biopsies obtained from all zones and all patient groups studied with both monoclonal and polyclonal antibodies. Immunoreactive cells were also seen within degen-

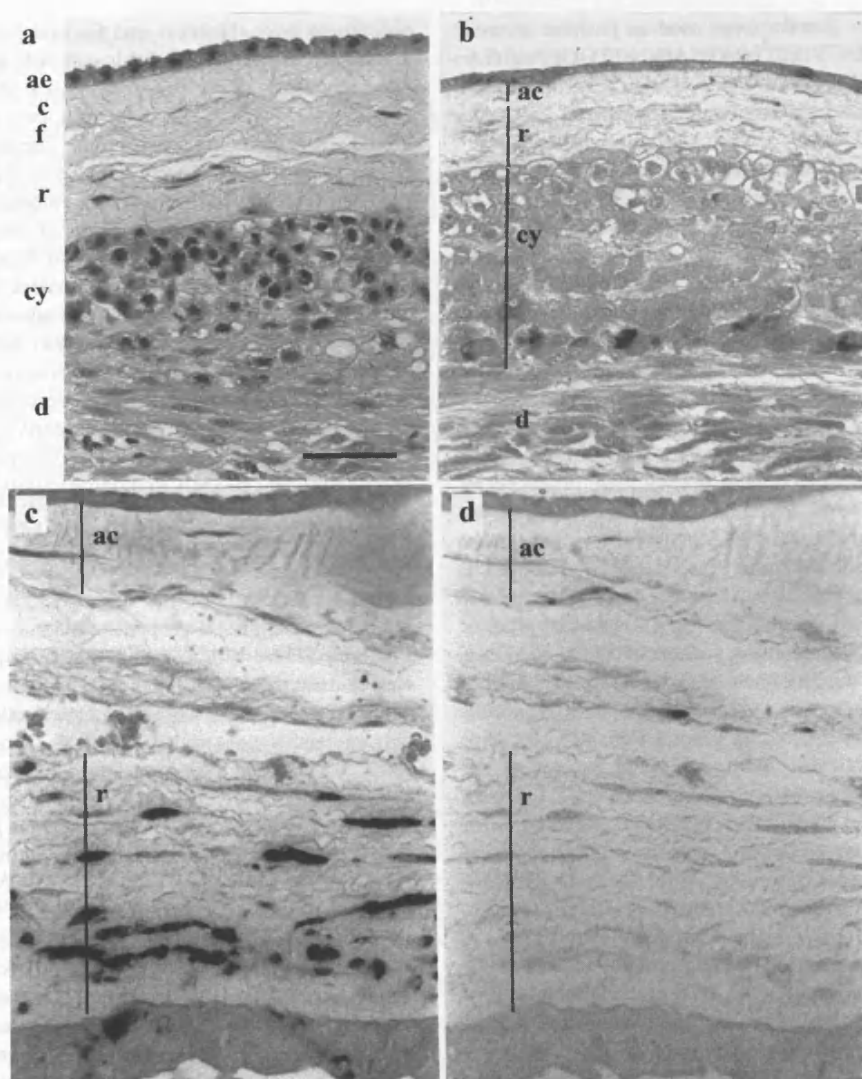


**Figure 1.** Sections of fetal membrane biopsies obtained prior to labour at term, stained with haematoxylin and eosin (a), and immunocytochemically stained for osteonectin (b, c) and CD68 (d). Fetal membrane biopsies were obtained from the mid-zone (a, b) and the region overlying the cervix (c, d). The haematoxylin and eosin-stained section demonstrates the layers of the amnion, the amniotic epithelium (ae), and the compact (c) and fibroblast (f) connective tissue layers, and of the chorion, the connective tissue reticular layer (r), the cytotrophoblast layer (cy) and the attached maternal decidua (d). The amniotic connective tissue (ac) refers to the combined compact and fibroblast layers. Immunoreactive osteonectin positive cells were detected in the amniotic epithelium and in the fibroblast, reticular and cytotrophoblast layers (b, c). Serial sections demonstrate that the osteonectin immunoreactive cells within the fibroblast and reticular layers do not co-express the macrophage marker CD68 (c, d). All photographs were taken at the same magnification. Scale bar = 50  $\mu$ m.

erate villi in the cytotrophoblast layer. No immunoreactivity was detected in the extracellular matrix. Serial sections stained with antibodies to CD68 or to cytokeratin and confirmed that the osteonectin positive cells seen within the fibroblast and reticular layers were fibroblasts, and not macrophages (Figure 1), and that those within the cellular layers of the membrane were cytotrophoblast cells (Figure 2). The latter cells were found predominantly within the superficial maternal aspect of the cytotrophoblast layer, although in membranes exhibiting significant thinning of the cytotrophoblast layer, immunoreactive cytotrophoblast cells were also seen adjacent to the pseudobasement membrane (Figure 2). Significant numbers of immunoreactive cells and regional differences in their incidence, were seen in the non-macrophage cells in the chorionic

reticular and amniotic fibroblastic layers, and in the cytotrophoblast cells of the cytotrophoblastic layer (Table I).

#### *Variation in distribution of osteonectin immunoreactivity*

The variation in the distribution of cells immunoreactive with the osteonectin monoclonal antibody was examined on sections of membrane biopsies obtained pre-labour, during labour and post-labour and delivery ( $n = 5$  per group). The numbers of osteonectin immunoreactive cells in the reticular layer expressed per unit length of membrane were 6.5-fold higher in the 'cervical' biopsies in the pre-labour group ( $P = 0.0073$ ), 10-fold higher in the 'cervical' biopsies in the labour-affected group ( $P = 0.0001$ ) and 12-fold higher in the post-labour rupture line biopsies after labour and delivery ( $P = 0.013$ ),

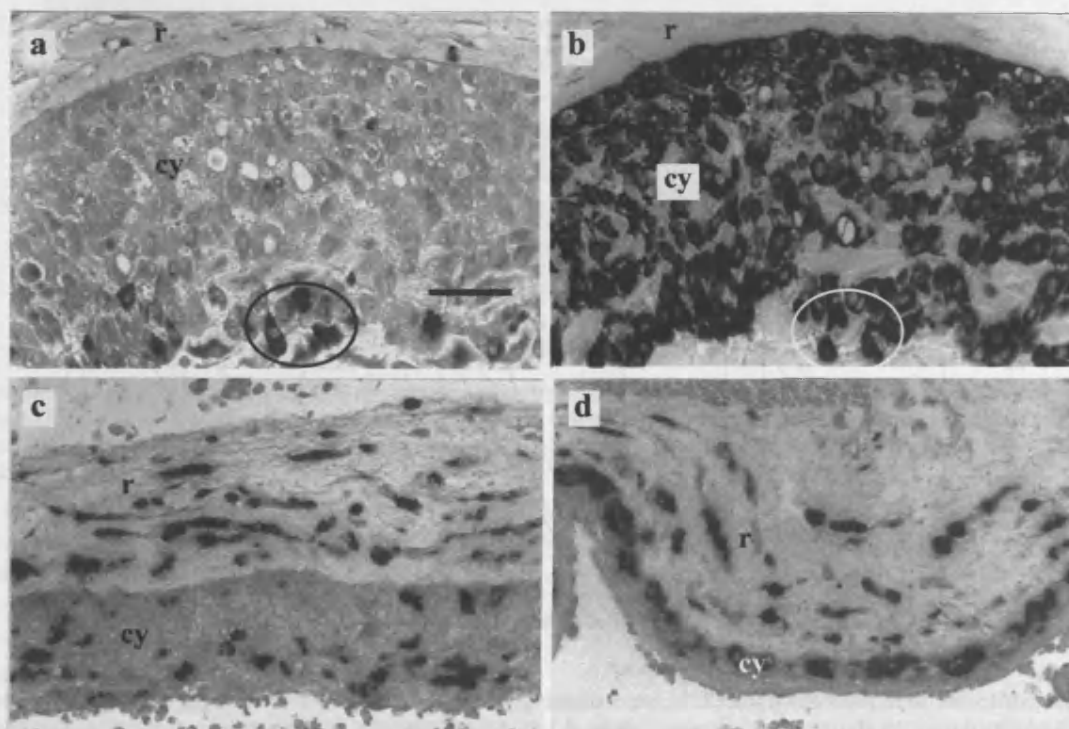


**Figure 2.** Sections of fetal membrane biopsies obtained from the mid-zone (a, b) and overlying the cervix (c, d) prior to the onset of labour at term, immunocytochemically stained for osteonectin (a, c, d) and cyokeratin (b). Osteonectin immunoreactive cells at the materno-fetal interface in the mid-zone biopsy co-express cyokeratin (a, b) (co-expressing cells circled). Within the 'cervical' biopsies, osteonectin immunoreactive cells within the cytotrophoblast layer are detected throughout the layer (c) or confined to adjacent to the pseudobasement membrane (d). The reticular layer (r) and the cellular cytotrophoblast (cy) are identified. All photographs are taken at the same magnification. Scale bar = 50  $\mu$ m.

**Table I.** Numbers of osteonectin immunoreactive cells in the tissue layers of the amnion and chorion per unit length of the fetal membranes obtained prior to, during and after labour and delivery at term in anatomically defined regions

	Pre-labour (n = 5)		Labour (n = 5)		Post-labour and rupture (n = 5)	
	Mid-zone	'Cervical'	Mid-zone	'Cervical'	Mid-zone	Rupture site
Amniotic epithelium	0.98 $\pm$ 0.26 (0-8)	1.12 $\pm$ 0.23 (0-6)	0.44 $\pm$ 0.15 (0-5)	0.46 $\pm$ 0.14 (0-4)	0.84 $\pm$ 0.20 (0-5)	1.26 $\pm$ 0.27 (0-8)
Fibroblast layer	0.18 $\pm$ 0.07 (0-2)	0.60 $\pm$ 0.12 (0-4)	0.06 $\pm$ 0.03 <sup>a</sup> (0-1)	0.76 $\pm$ 0.15 <sup>a</sup> (0-4)	0.28 $\pm$ 0.09 (0-3)	0.70 $\pm$ 0.17 (0-4)
Reticular layer	0.98 $\pm$ 0.21 <sup>b</sup> (0-7)	6.40 $\pm$ 0.66 <sup>b</sup> (0-17)	0.94 $\pm$ 0.19 <sup>c</sup> (0-6)	9.46 $\pm$ 0.73 <sup>c</sup> (1-20)	1.14 $\pm$ 0.22 <sup>d</sup> (0-6)	13.72 $\pm$ 1.47 <sup>d</sup> (2-57)
Cytotrophoblastic layer	0.74 $\pm$ 0.16 <sup>e</sup> (0-5)	4.26 $\pm$ 0.63 <sup>e</sup> (0-23)	0.54 $\pm$ 0.17 (0-7)	2.48 $\pm$ 0.51 (0-15)	0.72 $\pm$ 0.19 (0-6)	4.92 $\pm$ 0.86 (0-22)

Cells were counted in the full thickness of each layer along a specific length equal to the width of the computer screen at magnification of  $\times 40$ . Ten fields were examined each in fetal membrane biopsy from each zone in five patients and the minimum, maximum (in parentheses), mean and standard error values are derived from observations on 50 fields for each parameter. Statistical comparison of the number of the cells positively stained in the tissue layers between the selected zones within each patient group and between patient groups was performed using Two-way analysis of variance and Scheffé's test. Letters indicate significant differences between data: <sup>a,d,e</sup> $P < 0.05$ ; <sup>b</sup> $P < 0.01$ ; <sup>c</sup> $P = 0.0001$ .

compared to their respective mid-zone biopsies (Table I, Figure 3). These changes were not affected by thickness of the connective tissue layers since, in the same sites, the mean densities of osteonectin immunoreactive cells were increased in the pre-labour, labour-affected and post-labour groups 6.1-fold ( $P = 0.0091$ ), 5.3-fold ( $P < 0.0001$ ) and 7.5-fold ( $P = 0.0067$ ) respectively (data not shown). When expressed as a percentage of the total vimentin positive population present, in the reticular layer of the mid-zone biopsies the means ranged from only 3.51 to 4.03% (Table II). However, in the pre-labour 'cervical' biopsies, the labour-affected 'cervical' biopsies and in the post-labour rupture line biopsies, this was 7.1-fold higher at 24.85% ( $P = 0.002$ ), 8.2-fold higher at 33.00% ( $P = 0.003$ ,

and 9.3-fold higher at 33.00% ( $P = 0.0007$ ) respectively. There was no significant difference between the numbers of osteonectin immunoreactive cells, when expressed as a number or as a percentage of vimentin positive cells, in the reticular layers of the mid-zone biopsies between the patient groups, or between the 'cervical' biopsies and post-labour rupture line biopsies (Tables I and II).

In the amniotic connective fibroblast layer, significantly higher numbers of osteonectin immunoreactive cells were noted in the 'cervical' compared to the mid-zone biopsies in the labour-affected group (12.7-fold higher,  $P = 0.014$ , Table I), and in the proportion of vimentin positive cells immunoreactive for osteonectin in the 'cervical' compared to the mid-zone

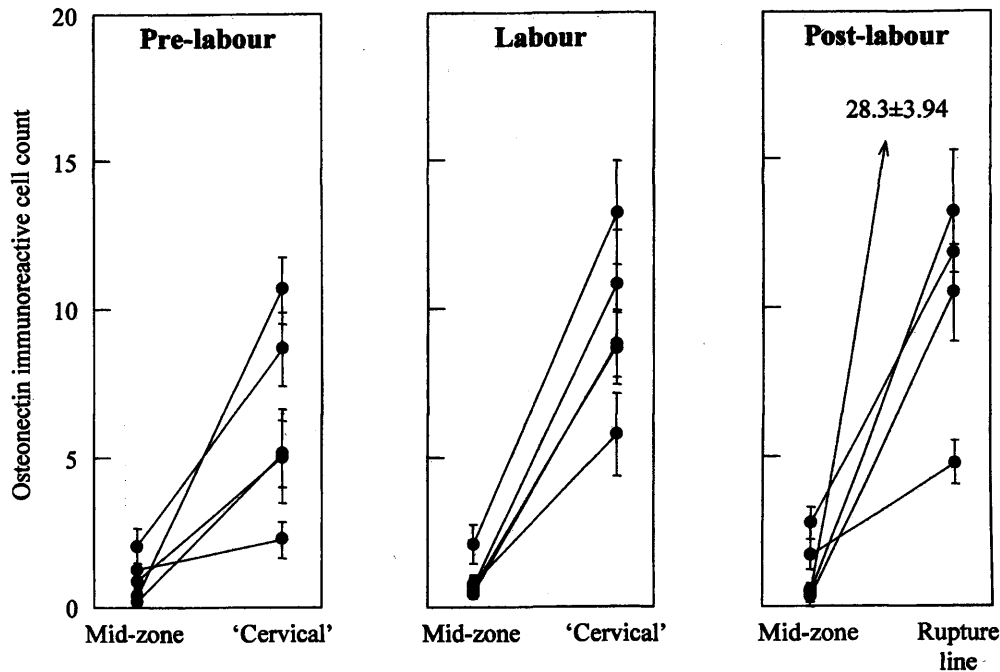


**Figure 3.** Numbers of osteonectin immunoreactive cells in the reticular layer of the chorion, per unit length of fetal membrane, in fetal membrane biopsies obtained prior to, during, and following labour at term in anatomically defined regions. Cells were counted in the full thickness of the reticular layer along a length of fetal membrane equal to the width of the computer screen at magnification of  $\times 40$ . The mean and standard error values are derived from observations on 10 fields per biopsy. Lines connect the data from the paired membrane samples from each patient.

**Table II.** Percentage of vimentin positive cells expressing osteonectin in the connective tissue layers of the amnion (the fibroblast layer), and chorion (the reticular layer), and of cytokeratin positive cells in the cellular layers (cytotrophoblast cells) of the fetal membranes obtained prior to, during and after labour and delivery at term in anatomically defined regions

	Pre-labour ( <i>n</i> = 5)		Labour ( <i>n</i> = 5)		Post-labour and rupture ( <i>n</i> = 5)	
	Mid-zone	'Cervical'	Mid-zone	'Cervical'	Mid-zone	Rupture site
Fibroblastic layer	1.44 ± 0.90 <sup>a</sup> (0-4.05)	10.36 ± 3.49 <sup>a</sup> (1.22-16.67)	0.81 ± 0.55 <sup>b</sup> (0-2.74)	13.43 ± 3.89 <sup>b</sup> (3.23-23.08)	4.46 ± 3.14 (0-16.92)	8.32 ± 1.88 (3.17-14.49)
Reticular layer	3.51 ± 1.10 <sup>c</sup> (0.81-6.56)	24.85 ± 4.60 <sup>c</sup> (11.66-38.91)	4.03 ± 1.60 <sup>d</sup> (2-10.4)	33.01 ± 6.84 <sup>d</sup> (17.9-50)	3.56 ± 1.20 <sup>e</sup> (1.24-7.57)	33.02 ± 5.42 <sup>e</sup> (12.66-41.9)
Cytotrophoblast layer	1.14 ± 0.38 <sup>f</sup> (0-0.63)	10.10 ± 3.61 <sup>f</sup> (0.52-10.26)	0.94 ± 0.25 (0.43-1.67)	6.29 ± 2.44 (1.32-12.70)	1.38 ± 0.36 <sup>g</sup> (0.50-2.38)	11.74 ± 4.25 <sup>g</sup> (4.87-28.03)

Estimations of the proportion of the total vimentin positive cell population in the connective tissue layer, and total cytokeratin positive cells in the cellular layers, stained with osteonectin were obtained from the mean values of immunoreactive cell numbers in each biopsy. Statistical comparison of the percentage of the cells positively stained in the tissue layers between the selected zones within each patient group and between patient groups was performed using two-way analysis of variance and Scheffé's test. Letters indicate significant differences between data: <sup>a,b,f,g</sup>*P* < 0.05; <sup>c,d</sup>*P* < 0.005; <sup>e</sup>*P* < 0.001.

biopsies in the pre-labour and the labour-affected groups (7.2-fold, *P* = 0.038, and 16.6-fold higher, *P* = 0.012 respectively; Table II). The failure to detect a difference in the post-labour group appeared to be due to increased numbers of immunoreactive cells in the mid-zone biopsy from one patient (16.9%), bringing the average for the group to 4.46%, compared to 1.44 and 0.81% in the pre-labour and labour-affected groups (Table II). Exclusion of the data from this patient brings the average for the group to 1.34%, significantly lower than the average for the rupture line biopsies, 8.32% (*P* = 0.015).

In the cytotrophoblast layer, there were 5.8-, 4.6- and 6.8-fold higher numbers of immunoreactive cells in the 'cervical' biopsies in the pre-labour, labour-affected, and in the post-labour rupture line biopsies compared to their respective

mid-zone biopsies, although this only achieved significance in the former group (*P* = 0.024, 0.078 and 0.11, Table I). The percentage of cytotrophoblast cells immunoreactive for osteonectin was significantly higher in the pre-labour and post-labour rupture line biopsies, compared to their respective mid-zone biopsies (8.8-fold *P* = 0.039, and 8.5-fold *P* = 0.041 respectively, Table II).

When the data from all biopsies were combined, there was a significant positive correlation between the absolute numbers of osteonectin positive cells in the reticular layer and the thickness of the reticular layer ( $r^2 = 0.434$ , *P* < 0.0001), the combined thickness of the amniotic and chorionic connective tissue layers ( $r^2 = 0.445$ , *P* < 0.0001), and the FMMI ( $r^2 = 0.868$ , *P* < 0.0001) and a negative correlation with the total thickness of the cellular layers ( $r^2 = 0.347$ , *P* = 0.0006).

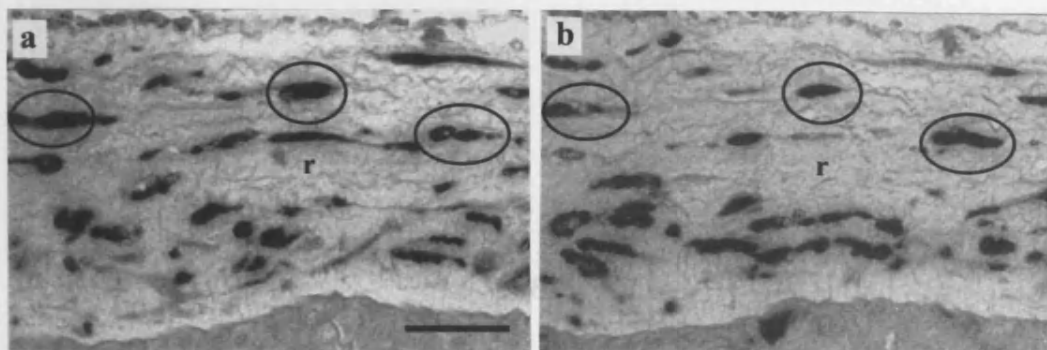


**Figure 4.** Serial sections of a fetal membrane biopsy obtained from overlying the cervix prior to the onset of labour at term, immunocytochemically stained with  $\alpha$ -smooth muscle actin ( $\alpha$ -SMA) (a), and monoclonal antibody to osteonectin, N50 (b). The reticular layer (r) is identified. A proportion of the cells immunoreactive for  $\alpha$ -SMA co-express osteonectin, examples are shown in circles. Both photographs are taken at the same magnification. Scale bar = 50  $\mu$ m.

There was also a significant positive correlation between the number of osteonectin positive cells in the fibroblast layer and in the reticular layer ( $r^2 = 0.436$ ,  $P < 0.0001$ ). The number of immunoreactive cells in the cytotrophoblast layer showed a weak but significant correlation with the number of immunoreactive cells in the reticular layer ( $r^2 = 0.137$ ,  $P = 0.044$ ), and a weak inverse correlation with the total thickness of the cellular layers ( $r^2 = 0.199$ ,  $P = 0.014$ ).

#### *Relationship to distribution of $\alpha$ -SMA immunoreactive cells*

Serial sections demonstrated that the majority of immunoreactive osteonectin cells within the reticular layer were also  $\alpha$ -SMA immunoreactive (Figure 4). However, not all  $\alpha$ -SMA immunoreactive cells contained immunoreactive osteonectin, e.g. in the reticular layer of post-labour rupture line biopsies  $57.7 \pm 11.4\%$  (mean  $\pm$  SEM) of  $\alpha$ -SMA positive cells were immunoreactive for osteonectin. However, in mid-zone biopsies, where the numbers of osteonectin positive cells in the reticular layers were low, these exceeded the numbers of  $\alpha$ -SMA positive cells. When the data from all biopsies were combined there was a significant positive correlation between the absolute numbers of osteonectin and  $\alpha$ -SMA positive cells in the reticular layer ( $r^2 = 0.630$ ,  $P < 0.0001$ ). On serial sections in the fibroblast layer, there was no apparent direct and consistent relationship between osteonectin and  $\alpha$ -SMA immunoreactive cells, with individual biopsies from cervical and rupture line fetal membranes possessing cells immunoreactive for either osteonectin or  $\alpha$ -SMA and for both. However, when data from all biopsies were combined, there was a significant correlation between the numbers of osteonectin and  $\alpha$ -SMA positive cells in the fibroblast layer ( $r^2 = 0.286$ ,  $P = 0.0023$ ). In a fetal membrane obtained from a patient after rupture and delivery, where multiple biopsies were obtained, there was a correlation between numbers of osteonectin immunoreactive cells in the reticular layer, the number of  $\alpha$ -SMA positive cells ( $r^2 = 0.86$ ,  $P < 0.0001$ ) and the FMMI of the biopsies ( $r^2 = 0.552$ ,  $P = 0.001$ ).

#### *Localization and distribution of osteonectin mRNA positive cells*

RT-PCR of mRNA from both fetal membranes and SK-MEL-28 cells demonstrated a single 325 bp band (Figure 5). In-situ

hybridization was performed on paired mid-zone and 'cervical' fetal membrane biopsies from five pre-labour patients. mRNA was detected in significant numbers of cells in both the reticular and fibroblast layers, and in smaller numbers of cells in the amniotic epithelial and cytotrophoblast layers (Figure 6). In the reticular layer the number of vimentin positive cells expressing osteonectin mRNA was 10.7-fold higher in the 'cervical' biopsies compared to the mid-zone biopsies ( $8.4 \pm 2.37$  compared to  $0.78 \pm 0.39$ ;  $P = 0.013$ ). In the fibroblast layer, the numbers of cells expressing osteonectin mRNA in the 'cervical' biopsies was 8.2-fold higher compared to those in the mid-zone biopsies ( $0.82 \pm 0.29$  compared to  $0.10 \pm 0.05$ ;  $P = 0.04$ ). This represented 9.27 and 25.44% of vimentin positive cells in the fibroblast and reticular layers of the 'cervical' biopsies respectively. As a group, 'cervical' biopsies exhibiting highest numbers of immunoreactive cells in the reticular and fibroblast layers also exhibited the highest numbers of in-situ positive cells. However, when serial sections were examined, areas found to contain the highest numbers of in-situ positive cells tended to contain low numbers of immunoreactive positive cells and vice versa. Within those areas positive for both, cells were detected that were positive for both protein and mRNA (Figure 6). On serial sections of 'cervical biopsies', in-situ positive cells in the reticular layer were immunoreactive for  $\alpha$ -SMA. In the 'cervical' biopsies of this group of patients, the percentages of cells immunoreactive for osteonectin and immunoreactive for  $\alpha$ -SMA were  $41.27 \pm 7.19\%$  and  $68.28 \pm 3.61\%$  in the reticular layer and  $14.73 \pm 3.67\%$  and  $18.35 \pm 11.13\%$  in the fibroblastic layers respectively (all results expressed as mean  $\pm$  SEM).

#### *Characterization of osteonectin protein in fetal membranes*

Western blotting of fetal membrane extracts obtained during and following labour ( $n = 9$ ) with monoclonal antibody revealed a single immunoreactive band with an apparent mol. wt of 43 000, consistent with that of authentic osteonectin (Figure 5). An identical band was detected with polyclonal antisera, with no evidence of any cleaved fragments (data not shown). Densitometry demonstrated significantly higher amounts of protein in the 'cervical'/rupture line biopsies compared to the mid-zone samples (2.9-fold higher,  $P = 0.0096$ ). The densitometry value correlated significantly with

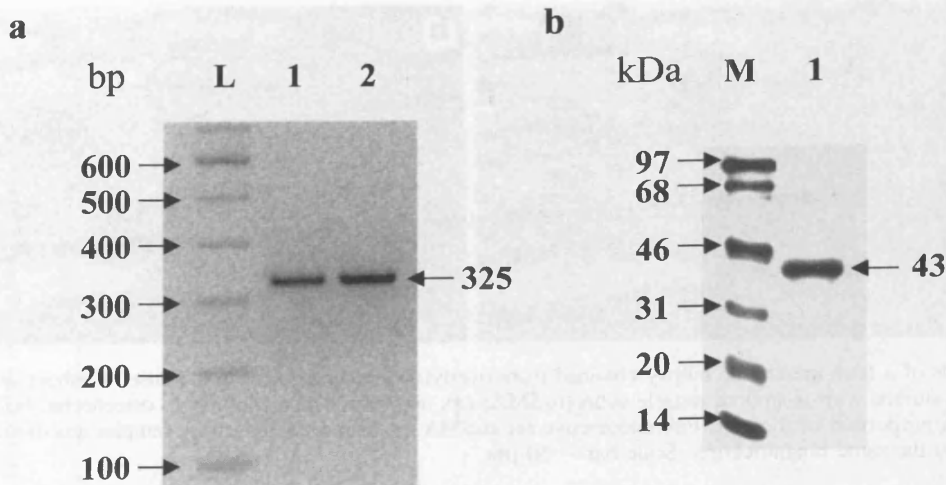


**Figure 5.** (a) Agarose gel electrophoresis of reverse transcriptase-polymerase chain reaction products from fetal membrane (lane 1, amplified for 30 cycles) and SK-MEL-28 mRNA (lane 2, amplified for 25 cycles). Lane L = 100 base pair ladder. (b) Western blot of a homogenate of a 'cervical' fetal membrane (lane 1) with monoclonal anti-osteonectin antibody N50. Lane M = size markers.

the total connective tissue thickness ( $r^2 = 0.403$ ,  $P = 0.0046$ ), and inversely with the total cellular thickness ( $r^2 = 0.381$ ,  $P = 0.0063$ ), and therefore also correlated with the derived FMMI of the membrane biopsies ( $r^2 = 0.50$ ,  $P = 0.001$ ). The densitometry value also correlated with the number of osteonectin immunoreactive cells within the reticular layer ( $r^2 = 0.394$ ,  $P = 0.0053$ ) and with the number of cells immunoreactive for  $\alpha$ -SMA within the reticular layer of the biopsies ( $r^2 = 0.25$ ,  $P = 0.037$ ).

## Discussion

In this study we have demonstrated the expression of osteonectin by specific mesenchymal populations within the connective tissue layers of human fetal membranes and, most importantly, that this pattern of expression was primarily restricted to specific anatomical regions, i.e. the 'cervical' membranes lying in the lower uterine pole before and during labour, and within the rupture line after delivery. This was particularly prominent within the chorionic connective tissue reticular layer where 25–33% of vimentin positive cells were immunoreactive for osteonectin at these sites in contrast to only 3–4% at distal sites. In the amniotic connective tissue fibroblastic layer obtained from the same sites, more mesenchymal cells expressed immunoreactive osteonectin compared to those at distal sites, albeit at a lower frequency, i.e. 8–13% and 1–4% respectively. A marked increase in the numbers of cells positive for osteonectin mRNA was detected in the same cellular populations in the same regions; however, a strict cellular colocalization between mRNA and protein was not observed, suggesting a transient increase in osteonectin transcription in these cells in these regions.

The anatomical distribution of expression of osteonectin in the connective tissue layers correlated with the reported distribution of  $\alpha$ -SMA positive cells (McParland *et al.*, 2000). However, in the present study we have noted that all patients in the pre-labour group exhibited higher expression of  $\alpha$ -SMA positive cells in the lower uterine pole 'cervical' biopsies.

Mesenchymal fibroblastic cells expressing  $\alpha$ -SMA are considered to represent 'activated'/'differentiated' myofibroblasts (Sappino *et al.*, 1990; Schmitt-Graff *et al.*, 1994) and the association of osteonectin expression with  $\alpha$ -SMA positive myofibroblasts has been previously reported in pathological conditions such as liver fibrosis (Blazejewski *et al.*, 1997) and tubulo-interstitial inflammation and fibrosis in the kidney (Pichler *et al.*, 1996). A similar association seems to apply to the  $\alpha$ -SMA positive 'activated' myofibroblastic cells in the reticular layer in the lower uterine pole 'cervical' biopsies. However, although its expression may be dependent upon this phenotype, the observation that only 58% of  $\alpha$ -SMA positive cells in the reticular layer expressed osteonectin suggests that other factors may be required to induce osteonectin in these cells. In the fibroblastic layer, however, although osteonectin and  $\alpha$ -SMA positive cells also increased in frequency in the cervical biopsies, these were not always co-localized indicating that osteonectin expression and the 'activated'/'differentiated' myofibroblast phenotype might not be intimately linked in the cells of this layer. This differential expression and, indeed, increased expression of osteonectin in the reticular layer compared to the fibroblastic layer, may relate to the normal phenotype of the mesenchymal cells present in these layers. Critically, mesenchymal cells of the reticular layer express desmin throughout the fetal membrane irrespective of anatomical location, and therefore represent a form of myofibroblast, albeit not expressing  $\alpha$ -SMA and hence not 'activated', whereas those in the fibroblastic layer are desmin negative and represent 'true' fibroblasts (Khong *et al.*, 1986). However, the fact that in both layers increased osteonectin expression and frequency of  $\alpha$ -SMA positive cells are detected in the same specific anatomical region indicates a common inducer(s) within this region prior to the onset of labour.

The factors and mechanisms involved in regulation of osteonectin have not been fully elucidated, and although there is evidence for positive regulation by transforming growth factor (TGF)- $\beta_1$ , interleukin-1, colony stimulating factor-1, progesterone and glucocorticoids and negative regulation by

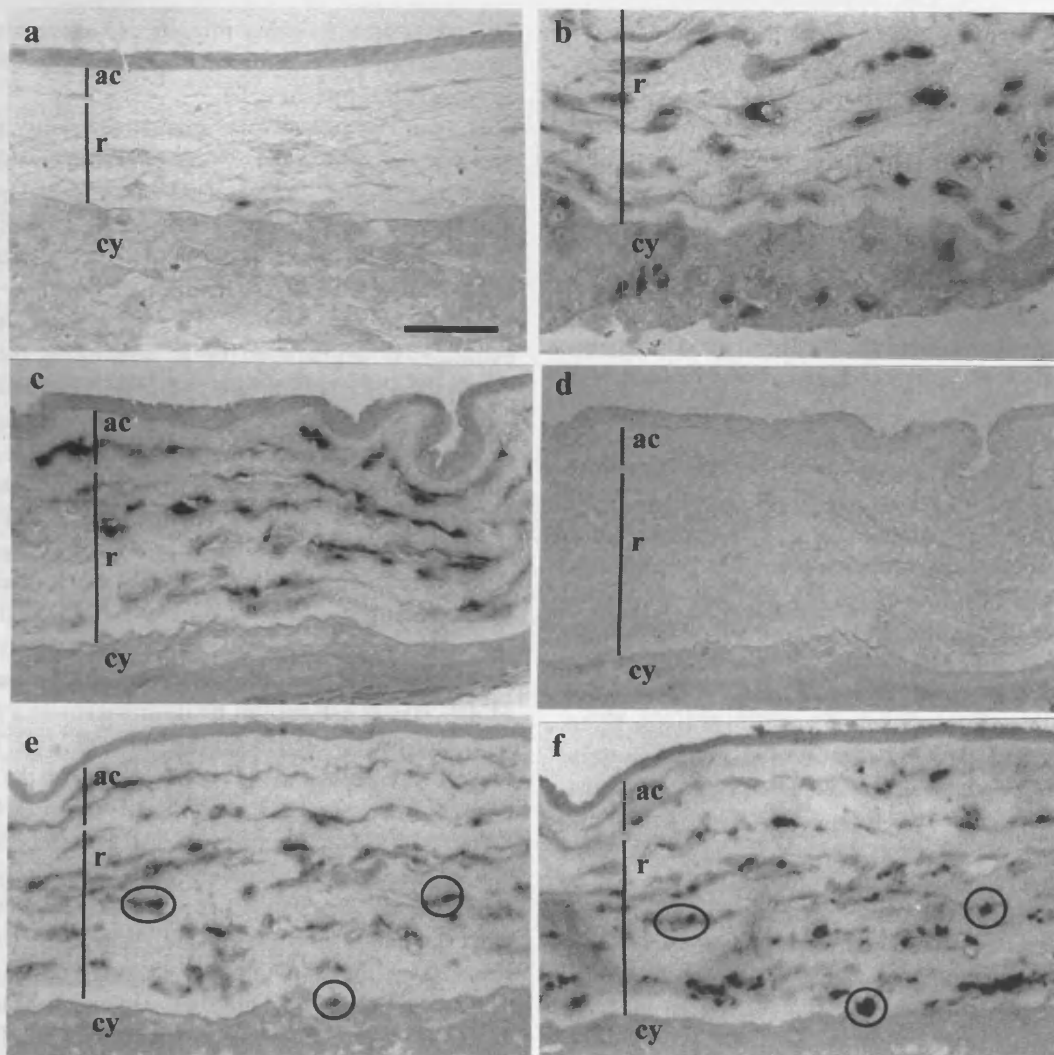


**Figure 6.** Fetal membrane biopsies obtained from the mid-zone (a) and from overlying the cervix (b-f) prior to the onset of labour at term. The amniotic connective tissue (ac), reticular (r) and cytotrophoblast (cy) layers are identified. In-situ hybridization with a probe to osteonectin mRNA shows very low numbers of positive cells within the mid-zone (a), with higher numbers of cells identified within the reticular layer (b, c, e), fibroblast layer (c, e) and cytotrophoblast layer (b) of the 'cervical' fetal membranes. Serial sections of in-situ hybridization against osteonectin mRNA on sections without (c) and with (d) pre-treatment with RNase demonstrates loss of signal with RNase pre-treatment. Serial section of in-situ hybridization (e) and immunocytochemistry (f) for osteonectin. Rare cells are seen to co-express mRNA and protein (circled). All photographs taken at the same magnification. Scale bar = 50  $\mu\text{m}$ .

NO, it has been proposed that other unidentified cytokines may act *in vivo* (Lane and Sage, 1994). Of these, TGF- $\beta$  has been demonstrated to increase osteonectin mRNA and protein in rabbit articular chondrocytes (Nakamura *et al.*, 1996), rat clonal pre-osteoblast-like cells (Zhou *et al.*, 1993), human gingival fibroblasts (Wrana *et al.*, 1991), dermal fibroblasts (Reed *et al.*, 1994) and pulp cells (Shiba *et al.*, 1998). Of the three independent and interactive signals that have been implicated in the induction of differentiation of  $\alpha$ -SMA-expressing myofibroblasts, i.e. cytokines, the extracellular matrix and mechanical forces, TGF- $\beta_1$  appears to exert an essential role (Desmouliere, 1995; Schurch *et al.*, 1998). In the connective tissues of the fetal membranes, high osteonectin expression and/or the appearance of the myofibroblastic phenotype are principally confined to a specific anatomical region, i.e. lower uterine pole, and are present prior to labour and

delivery. Labour or membrane rupture or delivery appear to have no effect upon expression, suggesting that this pattern is programmed into the fetal membranes during pregnancy. It has been suggested that the long-term differential stretch in the fetal membranes in the lower uterine pole, associated with the development of the lower uterine segment and/or cervical effacement during late pregnancy, may provide the inducing stimulus for myofibroblastic activation (McParland *et al.*, 2000). Since myofibroblasts provide traction, this possibly may represent a functional response to that stretch. Whether osteonectin gene transcription is also regulated by stretch is not known, but it did not appear after acute stretch of fetal membranes *in vitro* (Nemeth *et al.*, 2000). A direct role in contraction has been indicated by the identification of a keratocyte 'contraction-stimulating factor' as osteonectin (Mishima *et al.*, 1998). Osteonectin also enhances collagen

gel contraction by fibroblasts isolated from type I collagen-deficient mice (Iruela-Arispe *et al.*, 1996).

Previous studies of osteonectin expression have emphasized its presence in tissues that exhibit high rates of proliferation and morphological changes involving extracellular matrix turnover such as that during adult wound repair (Reed *et al.*, 1993). Amongst the in-vitro actions of this protein (Lane and Sage, 1994; Yan and Sage, 1999) many are indeed consistent with its role in rapid active turnover of the extracellular matrix. It inhibits the synthesis of certain components of the extracellular matrix such as laminin, fibronectin and thrombospondin (Kamihagi *et al.*, 1994), and increases the secretion of matrix metalloproteinase-1, -2, -3, -7 and -9 (Tremble *et al.*, 1993; Shankavaram *et al.*, 1997; Gilles *et al.*, 1998) and plasminogen activator inhibitor (PAI-1) (Hasselaar *et al.*, 1991). The anatomical region of the fetal membrane exhibiting altered morphology, i.e. the lower uterine pole, has been suggested to represent a site of structural weakness present at term prior to clinical labour. The dispersal of the fibrillar collagen type I/III-rich matrices, reflected by the thickened connective tissue layer in this region (Bell and Malak, 1997), is consistent with their degradation and/or increased turnover. The association of high osteonectin expression within connective tissue layers of this region, particularly within the chorion, and the correlation between osteonectin expression and layer thickness, suggests that these regions may be sites of active extracellular matrix remodelling mediated, in part, by the local action of osteonectin. The implication of this interpretation would be that the low osteonectin expression in the connective tissue layers of the mid-zone would be reflected by low extracellular matrix turnover and membrane stability in the upper uterine segment. The levels of the major enzyme activities involved in the intracellular processing and extracellular cross-linking of collagens indicates that the major active phase of synthesis and turnover of collagens by the mesenchymal cells of these layers in whole membranes is restricted to the first half of pregnancy (Casey and MacDonald, 1996, 1997). It will be of interest to determine whether osteonectin expression is detectable in the mesenchymal layers of the amnion and/or chorion during this early phase of pregnancy and indeed whether up-regulation of these enzymes occurs in the lower uterine pole at term in parallel with osteonectin expression.

Osteonectin expression was also detected within cytotrophoblasts, and in the mid-zone biopsies positive cells were concentrated at the maternal aspect adjacent to the decidua. In the regions of altered morphology, 6-9-fold higher percentages of immunoreactive cells were recorded. Since a characteristic of these regions is a thin cytotrophoblastic layer, this could simply reflect the smaller numbers of osteonectin negative cells beneath the interface. However, absolute numbers of immunoreactive cells were higher in this region and positive cells were apparent adjacent to the pseudobasement membrane in the basal aspect of the layer suggesting that there was additional expression induced at these sites. Whether osteonectin expression is a reflection of a function of these cells during differential attachment of the cytotrophoblastic layer to the decidua during early pregnancy and/or of differential breakdown of the maternal-fetal interface at these sites remains to

be investigated. In either role, its expression may again relate to aspects of extracellular matrix stability and turnover at the maternal-fetal interface.

Despite the intracellular immunoreactivity, no osteonectin was ever detected in the extracellular matrix. This was consistent with previous reports of its almost exclusive intracellular localization in other tissues (Sage *et al.*, 1989; Porter *et al.*, 1995) in spite of evidence supporting its secretion and its putative functions in the extracellular matrix. This paradox has been suggested to be due to either its susceptibility to extracellular degradation or to binding in the extracellular matrix resulting in epitope masking. Osteonectin is readily degraded by cathepsins, neutral metalloproteinases, elastases and serine proteases (Lane and Sage, 1994). If this occurs *in vivo* it could have significant functional consequences since the domains and sequences of the protein linked to specific activities can be conserved in proteolytically generated peptides, e.g. modulation of cell shape, modulation of proliferation metal binding, collagen binding etc. (Lane and Sage, 1994). Indeed in some instances the peptide may even be more active than the native protein, for example, endogenous protease- or MMP-cleaved osteonectin binds collagens at a higher affinity than does native osteonectin (Sasaki *et al.*, 1997). Additionally they may possess activities not evidenced in the intact protein, as seen with the angiogenic KGHK motif (Motamed and Sage, 1997). Osteonectin may also be incorporated into the extracellular matrix. It has recently been reported that the immunoreactive negative basement membrane underlying the lens epithelium is a 'virtual repository' for osteonectin, as revealed by immunoblotting of extracts (Yan and Sage, 1999). This may relate to the ability of osteonectin to bind collagens, especially type III, via its C-terminal extracellular calcium-binding module (Sage *et al.*, 1989; Yan and Sage, 1999). Although both interpretations may apply to the connective tissues of the amnion and chorion, their rich fibrillar collagen type I and III matrices (Bell and Malak, 1997; Bryant-Greenwood, 1998) and the lack of evidence of any degradation of the readily extractable osteonectin may support an analogy to the situation in the eye (Yan and Sage, 1999).

Further studies are required to determine the nature of osteonectin produced by the mesenchymal cells at these anatomical areas of the fetal membranes, particularly its regulation and function. This will determine whether it has a role in the generation of the morphological features at the site linked with labour induced rupture, and whether its abnormal expression may be associated with situations where the fetal membrane rupture occurs prior to labour.

### Acknowledgements

We wish to thank Dr L.W.Fisher (NIDCR, NIH, Bethesda, MA, USA) who generously donated the immunoreagent described in Materials and methods. We also thank Mrs S.Spurling and J.Ashmore for expert technical assistance and the clinical members of the staff of the University Hospitals of Leicester NHS Trust for assistance with the collection of specimens. P.C.McParland was supported by a grant from Tommy's Campaign.

## References

- Alger, L.S. and Pupkin, M.J. (1986) Etiology of preterm premature rupture of the membranes. *Clin. Obstet. Gynecol.*, **29**, 758–770.
- Bell, S.C. (2000) Mechanisms underlying prelabour rupture of the fetal membranes. In Kingdom, J., Jauniaux, E. and O'Brian, S. (eds), *The Placenta: Basic Sciences and Clinical Practice*. RCOG Press, London. pp. 187–204.
- Bell, S.C. and Malak, T.M. (1997) Structural and cellular biology of the fetal membranes. In Romero, R., Elder, M.G. and Lamont, R.F. (eds), *Preterm Labor*. Churchill Livingstone, New York and London, pp. 401–428.
- Blazewski, S., Le Bail, B., Boussarie, L. et al. (1997) Osteonectin (SPARC) expression in human liver and in cultured human liver myofibroblasts. *Am. J. Pathol.*, **151**, 651–657.
- Bou-Resli, M.N., Al-Zaid, N.S. and Ibrahim, M.E.A. (1981) Full-term and prematurely ruptured fetal membranes. An ultrastructural study. *Cell Tiss. Res.*, **220**, 263–278.
- Bryant-Greenwood, G.D. (1998) The extracellular matrix of the human fetal membranes: structure and function. *Placenta*, **19**, 1–11.
- Casey, M.L. and MacDonald, P.C. (1996) Interstitial collagen synthesis and processing in human amnion: a property of the mesenchymal cells. *Biol. Reprod.*, **55**, 1253–1260.
- Casey, M.L. and MacDonald, P.C. (1997) Lysyl oxidase (ras resection gene) expression in the human amnion: ontogeny and cellular localization. *J. Clin. Endocrinol. Metab.*, **82**, 167–172.
- Desmoulière, A. (1995) Factors influencing myofibroblast differentiation during wound healing and fibrosis. *Cell Biol. Int.*, **19**, 471–476.
- Fisher, L.W., Stubbs, J.T. and Young, M.F. (1995) Antisera and cDNA probes to human and certain animal model bone matrix non-collagenous proteins. *Acta Orthop. Scand.*, **61**, 61–65.
- French, J.I. and McGregor, J.A. (1996) The pathobiology of premature rupture of membranes. *Semin. Perinatol.*, **20**, 344–368.
- Gibbs, R.S., Romero, R., Hillier, S.L. et al. (1992) A review of premature birth and subclinical infection. *Am. J. Obstet. Gynecol.*, **166**, 1515–1528.
- Gilles, C., Bassuk, J.A., Pulyaeva, H. et al. (1998) SPARC/osteonectin induces matrix metalloproteinase 2 activation in human breast cancer cell lines. *Cancer Res.*, **58**, 5529–5536.
- Hasselaar, P., Loskutoff, D.J., Sawdey, M. et al. (1991) SPARC induces the expression of type 1 plasminogen activator inhibitor in cultured bovine aortic endothelial cells. *J. Biol. Chem.*, **266**, 13178–13184.
- Holland, P.W., Harper, S.J., McVey, J.H. et al. (1987) *In vivo* expression of mRNA for the Ca<sup>++</sup>-binding protein SPARC (osteonectin) revealed by *in situ* hybridization. *J. Cell Biol.*, **105**, 473–482.
- Iruela-Arispe, M.L., Vernon, R.B., Wu, H. et al. (1996) Type I collagen-deficient Mov-13 mice do not retain SPARC in the extracellular matrix: implications for fibroblast function. *Dev. Dyn.*, **207**, 171–183.
- Kamihagi, K., Katayama, M., Ouchi, R. et al. (1994) Osteonectin/SPARC regulates cellular secretion rates of fibronectin and laminin extracellular matrix proteins. *Biochem. Biophys. Res. Commun.*, **200**, 423–428.
- Keirse, M.J., Ohlsson, A., Treffers, P. et al. (1989) Prelabour rupture of the membranes at preterm. In Chalmers, I., Enkin, M. and Keirse, M.J. (eds), *Effective Care in Pregnancy and Childbirth*. Oxford University Press, Oxford, pp. 666–693.
- Kelly, T. (1995) The pathophysiology of premature rupture of the membranes. *Curr. Opin. Obstet. Gynecol.*, **7**, 140–145.
- Khong, T.Y., Lane, E.B. and Robertson, W.B. (1986) An immunocytochemical study of fetal cells at the maternal-fetal interface using monoclonal antibodies to keratins, vimentin and desmin. *Cell Tissue Res.*, **246**, 189–195.
- Lane, T.F. and Sage, E.H. (1994) The biology of SPARC, a protein that modulates cell-matrix interactions. *FASEB J.*, **8**, 163–173.
- Lane, T.F., Iruela-Arispe, M.L. and Sage, E.H. (1992) Regulation of gene expression by SPARC during angiogenesis *in vitro*. Changes in fibronectin, thrombospondin-1, and plasminogen activator inhibitor-1. *J. Biol. Chem.*, **267**, 16736–16745.
- Major, C.A. and Garite, T.J. (1997) Preterm premature rupture of membranes. In Romero, R., Elder, M.G. and Lamont, R.F. (eds), *Preterm Labor*. Churchill Livingstone, New York and London, pp. 153–164.
- Malak, T.M. and Bell, S.C. (1993) The structural characteristics of spontaneously ruptured fetal membranes: their relationship to membrane rupture and parturition. *Contemp. Rev. Obstet. Gynecol.*, **5**, 117–123.
- Malak, T.M. and Bell, S.C. (1994) Structural characteristics of term human fetal membranes (amniochorion and decidua): a novel zone of extreme morphological alteration within the rupture site. *Br. J. Obstet. Gynaecol.*, **101**, 375–386.
- Malak, T.M. and Bell, S.C. (1996) Fetal membranes structure and prelabour rupture. *Fetal Mat. Med. Rev.*, **8**, 143–164.
- McLaren, J., Malak, T.M. and Bell, S.C. (1999) Structural characteristics of term human fetal membranes prior to labour: identification of an area of altered morphology overlying the cervix. *Hum. Reprod.*, **14**, 237–241.
- McParland, P.C., Taylor, D.J. and Bell, S.C. (2000) Myofibroblast differentiation in the connective tissues of the amnion and chorion of term human fetal membranes: implications for fetal membrane rupture and labour. *Placenta*, **21**, 44–53.
- Mishima, H., Hibino, T., Hara, H. et al. (1998) SPARC from corneal epithelial cells modulates collagen contraction by keratocytes. *Invest. Ophthalmol. Vis. Sci.*, **39**, 2547–2553.
- Motamed, K. (1999) SPARC (osteonectin/BM-40) *Int. J. Biochem. Cell Biol.*, **31**, 1363–1366.
- Motamed, K. and Sage, E.H. (1997) Regulation of vascular morphogenesis by the matricellular protein SPARC. *Kidney Int.*, **51**, 1383–1387.
- Mundos, S., Schwahn, B., Reichert, T. et al. (1992) Distribution of osteonectin mRNA and protein during human embryonic and fetal development. *J. Histochem. Cytochem.*, **40**, 283–291.
- Nakamura, S., Kamihagi, K., Satakeda, H. et al. (1996) Enhancement of SPARC (osteonectin) synthesis in arthritic cartilage. *Arth. Rheum.*, **39**, 539–551.
- Nemeth, E., Millar, L.K. and Bryant-Greenwood, G. (2000) Fetal membrane distension. II. Differentially expressed genes regulated by acute distension *in vitro*. *Am. J. Obstet. Gynecol.*, **186**, 60–67.
- Parry, S. and Strauss, J.F. (1998) Premature rupture of the fetal membranes. *New Eng. J. Med.*, **338**, 663–670.
- Pichler, R.H., Hugo, C., Shankland, S.J. et al. (1996) SPARC is expressed in renal interstitial fibrosis and in renal vascular injury. *Kidney Int.*, **50**, 1978–1989.
- Porter, P.L., Sage, E.H., Lane, T.F. et al. (1995) Distribution of SPARC in normal and neoplastic human tissue. *J. Histochem. Cytochem.*, **43**, 791–800.
- Powell, D.W., Miffilin, R.C., Valentich, J.D. et al. (1999) Myofibroblasts I. Paracrine cells important in health and disease. *Am. J. Physiol.*, **277**, C1-C19.
- Pringle, J.H. (1995) Non-isotopic detection of RNA *in situ*. In Levey E.R. and Herrington, C.S. (eds), *Non-isotopic Methods in Molecular Biology: A Practical Approach*. IRL Press, Oxford, UK, pp. 85–110.
- Reed, M.J., Puolakkainen, P., Lane, T.F. et al. (1993) Differential expression of SPARC and thrombospondin 1 in wound repair: immunolocalization and *in situ* hybridization. *J. Histochem. Cytochem.*, **41**, 1467–1477.
- Reed, M.J., Vernon, R.B., Abrass, I.B. et al. (1994) TGF-beta 1 induces the expression of type I collagen and SPARC, and enhances contraction of collagen gels, by fibroblasts from young and aged donors. *J. Cell. Physiol.*, **158**, 169–179.
- Romero, R., Athayde, N., Maymon, E. et al. (1999) Premature rupture of the membranes. In Reece, E.A. and Hobbins, J.C. (eds), *Medicine of the Fetus and Mother*, 2nd edn. Lippincott-Raven, Philadelphia, pp. 1581–1625.
- Sage, E.H. and Bornstein, P. (1991) Extracellular proteins that modulate cell-matrix interactions. SPARC, tenascin, and thrombospondin. *J. Biol. Chem.*, **266**, 14831–14834.
- Sage, H., Vernon, R.B., Decker, J. et al. (1989) Distribution of the calcium-binding protein SPARC in tissues of embryonic and adult mice. *J. Histochem. Cytochem.*, **37**, 819–829.
- Sappino, A.P., Schurch, W. and Gabbiani, G. (1990) Differentiation repertoire of fibroblastic cells: expression of cytoskeletal proteins as marker of phenotypic modulations. *Lab. Invest.*, **63**, 144–161.
- Sasaki, T., Göhring, W., Mann, K. et al. (1997) Limited cleavage of extracellular matrix protein BM-40 by matrix metalloproteinases increases its affinity for collagens. *J. Biol. Chem.*, **272**, 9237–9243.
- Schmitt-Gräff, A., Desmoulière, A. and Gabbiani, G. (1994) Heterogeneity of myofibroblast phenotypic features: an example of fibroblastic cell plasticity. *Virch. Archiv.*, **425**, 3–24.
- Schurch, W., Seemayer, T. and Gabbiani, G. (1998) The myofibroblast: a quarter century after its discovery. *Am. J. Surg. Pathol.*, **22**, 141–147.
- Serini, G. and Gabbiani, G. (1999) Mechanisms of myofibroblast activity and phenotypic modulation. *Exp. Cell Res.*, **250**, 273–283.
- Shankavaram, U.T., DeWitt, D.L., Funk, S.E. et al. (1997) Regulation of human monocyte matrix metalloproteinases by SPARC. *J. Cell. Physiol.*, **173**, 327–334.
- Shiba, H., Fujita, T., Doi, N. et al. (1998) Differential effects of various growth factors and cytokines on the syntheses of DNA, type I collagen, laminin, fibronectin, osteonectin/secreted protein, acidic and rich in cysteine (SPARC), and alkaline phosphatase by human pulp cells in culture. *J. Cell. Physiol.*, **174**, 194–205.

- Termin, J.D., Kleinman, H.K., Whitson, S.W. *et al.* (1981) Osteonectin, a bone-specific protein linking mineral to collagen. *Cell*, **26**, 99–105.
- Tremble, P.M., Lane, T.F., Sage, E.H. *et al.* (1993) SPARC, a secreted protein associated with morphogenesis and tissue remodeling, induces expression of metalloproteinases in fibroblasts through a novel extracellular matrix-dependent pathway. *J. Cell Biol.*, **121**, 1433–1444.
- Wrana, J.L., Overall, C.M. and Sodek, J. (1991) Regulation of the expression of a secreted acidic protein rich in cysteine (SPARC) in human fibroblasts by transforming growth factor beta. Comparison of transcriptional and post-transcriptional control with fibronectin and type I collagen. *Eur. J. Biochem.*, **197**, 519–528.
- Yan, Q. and Sage, E.H. (1999) SPARC, a matricellular glycoprotein with important biological functions. *J. Histochem. Cytochem.*, **47**, 1495–1505.
- Zhou, H., Hammonds, R.G.J., Findlay, D.M. *et al.* (1993) Differential effects of transforming growth factor-beta 1 and bone morphogenetic protein 4 on gene expression and differentiated function of preosteoblasts. *J. Cell. Physiol.*, **155**, 112–119.

Received on December 29, 2000; accepted on February 27, 2001